



**HAL**  
open science

# Cubic and higher order equations of state for fluid mixtures: development, parameterization and validation through industrial energy conversion applications

Andrés Piña-Martinez

## ► To cite this version:

Andrés Piña-Martinez. Cubic and higher order equations of state for fluid mixtures: development, parameterization and validation through industrial energy conversion applications. Chemical and Process Engineering. Université de Lorraine, 2021. English. NNT : 2021LORR0170 . tel-03456951

**HAL Id: tel-03456951**

**<https://hal.univ-lorraine.fr/tel-03456951v1>**

Submitted on 21 Jun 2022

**HAL** is a multi-disciplinary open access archive for the deposit and dissemination of scientific research documents, whether they are published or not. The documents may come from teaching and research institutions in France or abroad, or from public or private research centers.

L'archive ouverte pluridisciplinaire **HAL**, est destinée au dépôt et à la diffusion de documents scientifiques de niveau recherche, publiés ou non, émanant des établissements d'enseignement et de recherche français ou étrangers, des laboratoires publics ou privés.



## AVERTISSEMENT

Ce document est le fruit d'un long travail approuvé par le jury de soutenance et mis à disposition de l'ensemble de la communauté universitaire élargie.

Il est soumis à la propriété intellectuelle de l'auteur. Ceci implique une obligation de citation et de référencement lors de l'utilisation de ce document.

D'autre part, toute contrefaçon, plagiat, reproduction illicite encourt une poursuite pénale.

Contact : [ddoc-theses-contact@univ-lorraine.fr](mailto:ddoc-theses-contact@univ-lorraine.fr)

## LIENS

Code de la Propriété Intellectuelle. articles L 122. 4

Code de la Propriété Intellectuelle. articles L 335.2- L 335.10

[http://www.cfcopies.com/V2/leg/leg\\_droi.php](http://www.cfcopies.com/V2/leg/leg_droi.php)

<http://www.culture.gouv.fr/culture/infos-pratiques/droits/protection.htm>

# THESE

Présentée par

**Andrés David PIÑA-MARTINEZ**

Ingénieur de l'Ecole Nationale Supérieure des Industries Chimiques

pour l'obtention du grade de

**DOCTEUR DE L'UNIVERSITÉ DE LORRAINE**

**Spécialité : Génie des Procédés, des Produits et des Molécules**

**Cubic and higher order equations of state for fluid mixtures: Development, parameterization and validation through industrial energy conversion applications**

*Équations d'état cubiques et modèles d'ordre supérieur pour décrire les mélanges fluides : Développement, paramétrage et validation sur des procédés industriels de conversion d'énergie*

Thèse soutenue publiquement le 07 octobre 2021 devant la commission d'examen :

**Rapporteurs :**

Mme. Claire ADJIMAN      Professeur à l'Imperial College London, Londres, Royaume Uni  
M. Paolo STRINGARI      Chargé de Recherche (HDR), Mines ParisTech, Paris, France

**Examineurs :**

M. Ioannis ECONOMOU      Professeur à l'Université Texas A&M au Qatar, Doha, Qatar  
M. Jean-Noël JAUBERT      Professeur à l'Université de Lorraine, Nancy, France (directeur de thèse)

**Membres invités :**

Mme. Véronique FALK      Professeur à l'Université de Lorraine, Nancy, France  
M. Laurent AVAULLEE      Docteur, TOTAL ENERGIES, Pau, France  
Mme. Silvia LASALA      Maître de conférences à l'Université de Lorraine, Nancy, France  
M. Romain PRIVAT      Maître de conférences à l'Université de Lorraine, Nancy, France (co-directeur de thèse)

---

Laboratoire Réactions et Génie des Procédés (LRGP)

1 rue Grandville, 54000, Nancy, France



*Satisfaction lies in the effort, not in the attainment.  
Full effort is full victory.*

*- Mohandas Gandhi*



## Acknowledgments

This work was carried out at the Laboratoire Réactions et Génie des Procédés (LRGP) at the École Nationale Supérieure des Industries Chimiques (ENSIC) in Nancy. I would like to thank Dr. Laurent Falk, director of the LRGP, for having welcomed me in this laboratory.

I would like to express special and sincere gratitude to my supervisor: Professor Jean-Noël Jaubert. Thanks for trusting me from the very beginning. I would like to thank you for your kind attitude and extensive knowledge guidance. During our discussions, you always showed your pedagogy skills, and used a precise and simple language to express me your advices. Your guidance all along my journey has been irreplaceable.

I would also like to express sincere gratitude to my co-supervisor: Dr. Romain Privat. Thanks for allowing me to learn from your invaluable expertise. You provided precious advices and remarks for the progression of my research. Thanks for all the discussions, contributions and efforts dedicated to my thesis.

Jean-Noël, Romain: it has been an honor for me to work with you. You treated me as a peer since the early stages of my journey. Thanks for inspiring and helping me all these years. I really appreciated all the Thermodynamics Masterclasses. We have shared extraordinary moments all the way through, thus giving me, beyond a professional relation, a friendship. Without a doubt, I can say that I could not have had any better supervisors.

Special thanks to Dr. Silvia Lasala for your active participation and critical feedbacks on my thesis. The opportunity of working with you enriched me from scientific and human points of view.

Thanks to Prof. Claire Adjiman and Dr. Paolo Stringari for reviewing this work and evaluate my dissertation. I extend my sincere gratitude to Prof. Ioannis Economou for accepting to preside the defense committee, and for your strong words of appreciation. Our productive collaboration has enhanced and expanded the perspectives of my research.

Dr. Laurent Avaullée, thermodynamic expert from the French energy company TotalEnergies, is gratefully acknowledged for sponsoring this research. Thanks for the questions and advices during the defense. I would like to thanks Prof. Véronique Falk for advising and helping me to better understand critical aspects of the product design framework. I would also want to add special acknowledgments to my follow-up committee members, Prof. Mauricio Camargo and Dr. Stéphane Vitu.

At this point, I want to say that back to my undergraduate thermodynamics' courses, I always heard about the equations of state proposed by Dr. Giorgio Soave or Prof. Ding-Yu Peng, as well as the  $\alpha$ -functions developed by Dr. Paul Mathias. I would like to use this occasion to extend my deepest gratitude to them for giving me the opportunity to pursue advances in thermodynamics together during my thesis. Collaborating and publishing with you has been an honor for me.

Special thanks go to all the members (researchers, technicians and PhD fellows) of the ThermE group for all the moments we shared together. In particular, my very good friend Dr. Edouard Moine. Thanks for sending the message that brought me back to France.

## Acknowledgments

---

During my PhD, I had the opportunity to teach at ENSIC and EEIGM. I would like to thank the colleagues that I had the pleasure to work with over these years.

My whole hearted thanks to my friends that I met at ENSIC, Johan and Steph, for being always there when I needed. My warmest thanks for the PhD fellows from the “Team Colombie”: Michu, Camila, Pipe and Diego. Thanks for all the support and countless coffee and lunch breaks, and “*planes tranqui*”, “*dos polas y nos vamos*”...

Thanks to all the friends I found at LRGP, especially Alexis, Cristian (Banguera) and Iliàs for the *billard breaks* and all the unforgettable moments we spent together. Thanks to the *Bureau de Jeunes Chercheurs* with whom I have had countless funny moments. Thank you Maïa, Pauline, Mathilde, Zeinab, Ludivine and Jonathan. I have to thank all my friends that I met in France: Taty, Nata, Nico (Comandante), David, Adrián, Dana, Sasha (and the many other dear friends near and far).

A big thanks to all the members of the Jaguars Baseball Softball SLUC Nancy, especially to Leni, Eme, Ewan, Killian, Chris, David (Papy), Erwan, François, Julien and Jorel for all the moments we had as a team inside and outside the field. I remember you that we were “champions du monde du Grand Est” and I am looking forward to clinch this title again. I also want to thank all my friends and colleagues from Colombia. Special mentions to John (El Pocaluz) and Camilo (Migic). Thank you for sharing stories and friendship for more than 10 years.

J’ai une pensée pour ma deuxième famille, celle que j’ai rencontrée en France. Françoise et Antoine, merci de m’avoir accueilli si chaleureusement dans le sein de votre famille. Raphaël, Nouche et Bernard, merci pour tous les moments que l’on a partagés ensemble. Vous comptez énormément pour moi.

Je remercie du fond du cœur ma chère, ma précieuse Camille. Merci pour ton soutien inconditionnel au quotidien, ton sourire et tes mots bienveillants. Tu as énormément contribué à la réussite de ma thèse.

Finalmente, agradezco de todo corazón a mi familia. Sin ustedes nada de esto habría sido posible. Ocupan un lugar inmenso en mi vida y pueden sentir como suyo este logro. Aunque nos separen miles de kilómetros, su cariño y apoyo incondicionales me han acompañado siempre.

A mis padres, Stella y Jorge, les doy infinitas gracias por haber tenido tanta confianza en mí. Siempre, en todas las decisiones que he tomado, han estado ahí para brindarme todo su apoyo y amor. Nunca tendré cómo retribuir la educación y los valores que me inculcaron, y que me han traído hasta aquí. Nosotros los hijos no podemos escoger nuestros padres, pero, si tuviera que elegir, los escogería a ustedes una y mil veces.

Quiero dedicarles unas letras a mis abuelos. Primero, a mi abuela paterna, Saturnina Leal Ponce, una mujer de un temple y pujanza sin igual. Gracias por todas tus enseñanzas. Agradezco a mi abuela materna, Gladys Flórez de Martínez, mi segunda madre. Nunca podré devolverle todo el tiempo que dedicó a mi crianza, todos los esfuerzos para que nunca me faltara nada. Por último, este manuscrito se lo dedico especialmente a mi abuelo paterno, Don Venancio Martínez Otálvarez, que ya no está con nosotros y a quien extraño profundamente.

*Nancy, November 16, 2021.*

*Andrés David Piña Martínez*

---

# Contents

List of figures .....	xv
List of tables .....	xxi
List of publications .....	xxvii
Nomenclature .....	xxix
Introduction .....	3
Context .....	3
Motivation and objectives .....	4
Outline .....	6
Chapter 1 : The phase-equilibrium problem.....	9
1.1 Introduction .....	9
1.2 Nature of the problem.....	9
1.3 Application of thermodynamics to phase-equilibrium problems .....	10
1.4 Equations of state .....	12
1.4.1 The virial equation of state .....	12
1.4.2 Analytical equations of state .....	13
1.4.3 Nonanalytic equations of state.....	13
1.5 Activity-coefficient models .....	18
1.6 Concluding remarks .....	22
Chapter 2 : Equations of state for pure compounds.....	25
2.1 Introduction .....	25
2.2 Generalities of cubic equations of state for pure compounds.....	25
2.2.1 Modifications of the $\alpha$ -function .....	28
2.2.2 Modifications of the volumetric function .....	33
2.3 Translated and consistent CEoS .....	33
2.3.1 The consistency concept.....	33
2.3.2 The volume-translation concept .....	34
2.3.3 Translated-consistent version of the Peng-Robinson EoS.....	36
2.4 Towards a highly accurate cubic equation of state.....	36
2.5 Concluding remarks .....	40
Chapter 3 : Equations of state for mixtures .....	43

3.1	Introduction .....	43
3.2	Classical Van der Waals mixing rules.....	43
3.3	EoS/ $g^E$ mixing rules.....	45
3.3.1	The infinite pressure reference .....	45
3.3.2	The zero-pressure reference .....	49
3.4	Proposed EoS/ $a^E$ mixing rules .....	51
3.5	Reference database for the comparison of thermodynamic models .....	53
3.6	Extension of the $\tau$ -PR model to mixtures.....	55
3.7	Concluding remarks .....	56
Chapter 4 : Combined Heating, Cooling and Power .....		61
4.1	Introduction .....	61
4.2	Electricity, heating and cooling in modern society .....	61
4.3	Conventional CCHP configurations .....	63
4.4	Novel CCHP configuration .....	63
4.5	Chemical product design .....	64
4.5.1	Classes of chemical products.....	64
4.5.2	Definition of chemical product design .....	65
4.5.3	Framework for product design .....	65
4.5.4	Retained approach .....	66
4.6	Results .....	67
4.7	Concluding remarks .....	68
Conclusions .....		71
Main findings and contributions.....		71
Perspectives and future research .....		73
Publications .....		75
Publication I : <i>I</i> -PC-SAFT: an Industrialized version of the volume-translated PC-SAFT equation of state for pure components, resulting from experience acquired all through the years on the parameterization of SAFT-type and cubic models.....		77
PI.I	Introduction .....	79
PI.II	Part 1: parameterization of the PC-SAFT and SRK EoS with parameterization methods P1 and P2 that involve three input parameters. ....	83
PI.II.I	Parameterization of the PC-SAFT EoS .....	83
PI.II.II	Parameterization of the SRK EoS .....	85

PI.III	Comparison of SRK and PC-SAFT EoS at fixed parameterization methods (P1 and P2)	86
PI.IV	Part 2: parameterization of the PC-SAFT and SRK EoS with parameterization method P1t that involves four input parameters [ $T_{c,exp}$ , $P_{c,exp}$ , $\omega_{exp}$ and $v_{liq,exp}^{sat}(T_r = 0.8)$ ]	94
PI.V	Conclusion	98
Publication II : Analysis of the combinations of property data that are suitable for a safe estimation of consistent Twu $\alpha$ -function parameters. Updated parameter values for the translated-consistent tc-PR and tc-RK cubic equations of state		
PII.I	Introduction	103
PII.II	Overview of the DIPPR database	106
PII.II.I	Error evaluation of the DIPPR correlations	106
PII.II.II	Drawing up of a list of compounds potentially suitable for parameter fitting	108
PII.III	Suitable combinations of property data for the safe estimation of consistent Twu91 $\alpha$ -function parameters	109
PII.III.I	Fitting procedure	110
PII.III.II	Results	111
PII.IV	Updated consistent Twu91 $\alpha$ -function parameters	113
PII.IV.I	Constitution of a pure-compound database	113
PII.IV.II	Results	113
PII.V	Updated volume-translation parameters (c)	115
PII.V.I	Results	115
PII.VI	Updated generalized Twu88 $\alpha$ -functions suitable for the tc-PR and tc-RK EoS	117
PII.VII	Conclusion	119
Publication III : Updated versions of the generalized Soave $\alpha$ -function suitable for the Redlich-Kwong and Peng-Robinson equations of state		
PIII.I	Introduction	123
PIII.II	Updated Soave $m$ parameter	125
PIII.III	Results	128
PIII.IV	Conclusion	131
Publication IV : Search for the optimal expression of the volumetric dependence of the attractive contribution in cubic equations of state		
PIV.I	Introduction	135
PIV.II	Historical background	136
PIV.II.I	Selection of constant ( $u, w$ ) values	136

PIV.II.II	Selection of component-dependent $(u, w)$ pairs.....	138
PIV.III	On the interest to combine $\omega$ -dependent $(u, w)$ parameters and a volume-translation parameter in a CEoS.....	141
PIV.III.I	On the interest to select $\omega$ -dependent $(u, w)$ pairs in untranslated CEoS .....	141
PIV.III.II	On the interest to select $\omega$ -dependent $(u, w)$ pairs in translated CEoS .....	143
PIV.III.III	Search for $\omega$ -dependent $(u, w)$ parameters to be used with untranslated CEoS that lead to the same performance as $(u_o, w_o)$ universal constants used in translated CEoS .....	144
PIV.IV	Search for the optimal $(u, w)$ set from a map reporting deviations between EoS predictions and experimental properties in the $(u, w)$ space.....	146
PIV.IV.I	Exploration of map reporting deviations between EoS predictions and experimental properties in the $u - w$ space .....	146
PIV.IV.II	Optimal $(u, w)$ values for untranslated CEoS .....	149
PIV.IV.III	Optimal $(u, w)$ values for translated CEoS .....	151
PIV.IV.IV	Optimal translated and consistent CEoS .....	153
PIV.V	Conclusion.....	155
Publication V	: Use of 300 000 experimental data over 1800 pure fluidsto assess the performance of 4 CEoS: SRK, PR, $tc$ -RK, $tc$ -PR. ....	157
PV.I	Introduction .....	159
PV.II	Description of the guidelines to constitute a pure-component reference database.....	160
PV.II.I	Existing pure-fluid databases .....	160
PV.II.II	Key properties .....	161
PV.II.III	Assessment of correlations' accuracy.....	162
PV.II.IV	Molecules to be incorporated in the database.....	165
PV.II.V	Associating character.....	165
PV.II.VI	Temperature ranges and deviations .....	166
PV.II.VII	Guidelines summary and data points.....	166
PV.III	Benchmark of the SRK, PR, $tc$ -RK and $tc$ -PR EoS.....	169
PV.III.I	Models .....	169
PV.III.II	Results and discussion.....	170
PV.IV	Conclusion.....	173
Publication VI	: A benchmark database containing binary-system-high-quality-certified data for cross-comparing thermodynamic models and assessing their accuracy .....	177
PVI.I	Introduction .....	179
PVI.II	Criterion to build a benchmark database .....	180

PVI.II.I	Literature review .....	180
PVI.II.II	Which thermophysical properties should be included? .....	181
PVI.II.III	Which binary systems should be included? .....	182
PVI.II.IV	How many systems and how many data should be included? .....	188
PVI.II.V	The built database .....	188
PVI.III	Grading of a thermodynamic model by means of the proposed database in order to assess its accuracy .....	211
PVI.III.I	Evaluation of the deviations between model predictions and experimental data ...	211
PVI.III.II	Treatment of “out-of-model” data points .....	213
PVI.III.III	Grading of a thermodynamic model .....	215
PVI.IV	Illustration: grading and discussion around the accuracy of the Peng-Robinson EoS with classical mixing rules and a temperature-dependent BIP .....	220
PVI.IV.I	The model .....	220
PVI.IV.II	The fitting procedure .....	221
PVI.IV.III	System-by-system results of the fitting procedure .....	224
PVI.IV.IV	Grading of the model: PR EoS + classical mixing rules with a T-dependent $k_{ij}$ ..	225
PVI.IV.V	Discussion around the accuracy of the model: PR EoS + classical mixing rules with a T-dependent $k_{ij}$ .....	229
PVI.V	Conclusions .....	231
Publication VII : What is the optimal activity coefficient model to be combined with the translated-consistent Peng-Robinson (tc-PR) equation of state through advanced mixing rules? Cross-comparison and grading of the Wilson, UNIQUAC and NRTL $a^E$ models against a benchmark database involving 200 binary systems. ....		
		233
PVII.I	Introduction .....	235
PVII.II	Implementation of the <i>tc</i> -PR model coupled with $EoS/a_{res}^{E,\gamma}$ mixing rules .....	237
PVII.II.I	Quadratic Van der Waals mixing rules .....	238
PVII.II.II	$EoS/a_{res}^{E,\gamma}$ mixing rules .....	238
PVII.II.III	Implementation of the <i>tc</i> -PR- $a_{res}^{E,\gamma}$ models .....	242
PVII.II.IV	Implementation of the PR-Van Laar model .....	244
PVII.III	Grading of the <i>tc</i> -PR-Wilson, <i>tc</i> -PR-UNIQUAC and <i>tc</i> -PR-NRTL models .....	245
PVII.III.I	Grading procedure .....	246
PVII.III.II	Grading results .....	250
PVII.III.III	Discussion .....	261

PVII.IV	Conclusions .....	270
Publication VIII : Design of promising working fluids for emergent combined cooling, heating and power (CCHP) systems. ....		277
PVIII.I	Introduction .....	279
PVIII.II	Product design framework applied to the selection of working fluids .....	280
PVIII.II.I	Working-fluid design for vapor-compression refrigeration applications .....	282
PVIII.II.II	Working-fluid design for ORC applications .....	282
PVIII.II.III	Strengths and weaknesses.....	283
PVIII.III	CCHP cycle description .....	283
PVIII.III.I	From power to combined heating and power .....	284
PVIII.III.II	CCHP configuration .....	287
PVIII.III.III	Actual CCHP configuration and degrees of freedom .....	290
PVIII.IV	Working-fluid selection methodology.....	293
PVIII.IV.I	Target properties.....	294
PVIII.IV.II	Chemical design space. Data curation and preparation.....	297
PVIII.IV.III	Thermodynamic model.....	299
PVIII.IV.IV	Screening procedure .....	300
PVIII.IV.V	Performance evaluation.....	301
PVIII.V	Case studies and operating specifications .....	303
PVIII.V.I	Case study 1: Residential/Commercial user .....	303
PVIII.V.II	Case study 2: Food industry .....	304
PVIII.VI	Results .....	306
PVIII.VI.I	Screening results.....	306
PVIII.VI.II	Performance results .....	308
PVIII.VII	Conclusions .....	310
Bibliography.....		317
Appendix .....		377
Appendix A : Supporting Information of Publication I.....		379
Appendix B : Supporting Information of Publication II .....		379
Appendix C : Supplementary data of Publication III .....		379
Appendix D : Supporting Information of Publication V .....		379
Appendix E : Supporting Information of Publication VI .....		379
Appendix F : Supporting Information of Publication VII .....		380

Appendix G : Supporting Information of Publication VIII .....	380
Résumé en français des travaux menés et des résultats obtenus .....	381
Contexte .....	383
Motivations et objectifs .....	384
Plan de la thèse .....	386
Principaux résultats obtenus .....	387
Perspectives .....	392
Résumé .....	393



## List of figures

<b>Figure I.1.</b> Evolution of the share of EU energy consumption coming from renewable sources since 2005. Data provided by the European Environment Agency [5]. .....	4
<b>Figure I.2.</b> Scheme of the organization of this manuscript.....	6
<b>Figure 1-1.</b> Illustration of the phase-equilibrium problem. ....	9
<b>Figure 1-2.</b> Schematic representation of the procedure that forms a SAFT model molecule [38]: (a) the reference fluid consists of hard spheres; (b) dispersion forces are added; (c) chain sites are added and chain molecules appear; (d) hydrogen bonding is added and molecules form association complexes through association sites.....	15
<b>Figure 2-1.</b> Graphical illustration of the P�eneloux–type volume translation concept. ....	35
<b>Figure 4-1.</b> a) Schematic view of a CCHP system with an electric/engine-driven cooling system. b) Schematic view of a CCHP system with a thermally-activated cooling system. (*) VC stands for vapor compression.....	63
<b>Figure 4-2.</b> a) Schematic view of an ideal CCHP cycle as proposed by Briola [6]. b) Sketch of the corresponding temperature-entropy diagram. ....	64
<b>Figure 4-3.</b> Scheme of the product-design approach adopted in this work for the selection of suitable working fluids for CCHP applications. ....	67
<b>Figure PI.1.</b> Generalized charts of the PC-SAFT EoS: plot of $\omega$ , $T_c^*$ and $P_c^*$ as a function of $m$ . ....	84
<b>Figure PI.2.</b> MAPE on several thermodynamic properties as predicted by the SRK and PC-SAFT EoS. Parameterization P1 (red): the three input parameters are constrained to the exact reproduction of ( $T_{c,exp}$ , $P_{c,exp}$ , $\omega_{exp}$ ). Parameterization P2 (blue): the three input parameters are fit to saturation properties ( $P^{sat}$ , $\Delta_{vap}H$ , $c_{P,liq}^{sat}$ , $v_{liq}^{sat}$ ).....	89
<b>Figure PI.3.</b> Vaporization curve with respect to temperature predicted by PC-SAFT (left) and SRK (right) EoS. Parameterization P1 (red): the three input parameters are constrained to the exact reproduction of ( $T_{c,exp}$ , $P_{c,exp}$ , $\omega_{exp}$ ). Parameterization P2 (blue): the three input parameters are fit to saturation properties ( $P^{sat}$ , $\Delta_{vap}H$ , $c_{P,liq}^{sat}$ , $v_{liq}^{sat}$ ).....	90
<b>Figure PI.4.</b> (Pressure, volume) plane predicted by PC-SAFT (left) and SRK (right) EoS. Parameterization P1 (red): the three input parameters are constrained to the exact reproduction of ( $T_{c,exp}$ , $P_{c,exp}$ , $\omega_{exp}$ ). Parameterization P2 (blue): the three input parameters are fit to saturation properties ( $P^{sat}$ , $\Delta_{vap}H$ , $c_{P,liq}^{sat}$ , $v_{liq}^{sat}$ ).....	91
<b>Figure PI.5.</b> MAPE on $v_{liq}^{sat}$ wrt. MAPE on $P_c$ obtained with the PC-SAFT EoS. Parameterization P2 is used and (from right to left) the weight given to the critical pressure is successively increased. ....	92
<b>Figure PI.6.</b> MAPE on several thermodynamic properties as predicted by the ( $t$ -)PC-SAFT and ( $t$ -)SRK EoS. Parameterization P1 (red): the three input parameters are constrained to the exact reproduction of ( $T_{c,exp}$ , $P_{c,exp}$ , $\omega_{exp}$ ). Parameterization P2 (blue): the three input parameters are fit to saturation	

properties ( $P^{\text{sat}}$ , $\Delta_{\text{vap}}H$ , $c_{P,\text{liq}}^{\text{sat}}$ , $v_{\text{liq}}^{\text{sat}}$ ). Parameterization P1t (yellow): the four input parameters of the translated EoS are constrained to the exact reproduction of [ $T_{c,\text{exp}}$ , $P_{c,\text{exp}}$ , $\omega_{\text{exp}}$ , $v_{\text{liq,exp}}^{\text{sat}}(T_r = 0.8)$ ].	96
.....	96
<b>Figure PI.7.</b> (Pressure, volume) plane predicted by ( $t$ -)PC-SAFT (left) and ( $t$ -)SRK (right) EoS. Parameterization P1 (red): the three input parameters are constrained to the exact reproduction of ( $T_{c,\text{exp}}$ , $P_{c,\text{exp}}$ , $\omega_{\text{exp}}$ ). Parameterization P1t (yellow): the four input parameters of the translated EoS are constrained to the exact reproduction of [ $T_{c,\text{exp}}$ , $P_{c,\text{exp}}$ , $\omega_{\text{exp}}$ , $v_{\text{liq,exp}}^{\text{sat}}(T_r = 0.8)$ ].	97
<b>Figure PIII.1.</b> Correlation of optimized $m$ parameter against $\omega_{\text{exp}}$ for both the PR and RK EoS. Comparison between the original correlation and the one determined in this work. Each of the 1720 open circles represent a pure compound.	128
<b>Figure PIV.1.</b> Deviation on saturated liquid molar volume up to $T_r = 0.9$ as a function of the acentric factor $\omega$ , calculated by the SRK and PR EoS. The 14 substances are by order of $\omega$ : CH <sub>4</sub> , C <sub>2</sub> H <sub>4</sub> , C <sub>2</sub> H <sub>6</sub> , C <sub>3</sub> H <sub>6</sub> , C <sub>3</sub> H <sub>8</sub> , but-1-ene, n-butane, benzene and the n-alkanes from n-pentane to n-decane.	142
<b>Figure PIV.2.</b> Deviation on saturated liquid molar volume ( $v_{\text{liq}}^{\text{sat}}$ ) up to $T_r = 0.9$ as a function of the acentric factor $\omega$ , calculated by the <i>translated</i> -SRK and <i>translated</i> -PR EoS. The scale has intentionally been kept identical to the one of Figure PIV.1 and the 14 substances are those of Figure PIV.1.	143
<b>Figure PIV.3.</b> Plot of $u_t$ (●) and $w_t$ (●) stemming from the $t$ -PR EoS as a function of the acentric factor $\omega$ . With such $u$ and $w$ parameters, the MAPE on $v_{\text{liq}}^{\text{sat}}$ is about 2% (see Figure PIV.2) so that such pairs can be considered as <i>optimal</i> values. The 14 substances are those of Figure PIV.1. The two straight lines ( $w = -3\omega$ and $u = 1 + 3\omega$ ) recall the values recommended by Schmidt and Wenzel.	145
<b>Figure PIV.4.</b> Representation of the feasible and unfeasible regions of CEoS in the $u - w$ space.	147
<b>Figure PIV.5.</b> Values of the <i>global mean percentage error per property</i> (see Eq.(PIV.24)) as a function of the parameters $u$ and $w$ for untranslated CEoS.	150
<b>Figure PIV.6.</b> Values of the <i>global mean percentage error per property</i> (see Eq. (PIV.25)) as a function of the parameters $u$ and $w$ for translated CEoS.	152
<b>Figure PV.1.</b> Ratio of well and badly modeled molecules by the SRK EoS classified into non-self-associating (NSA) and self-associating (SA) fluids. Green: well-modeled molecules. Red: Badly-modeled molecules.	176
<b>Figure PV.2.</b> Ratio of well and badly modeled molecules by the PR EoS classified into non-self-associating (NSA) and self-associating (SA) fluids. Green: well-modeled molecules. Red: Badly-modeled molecules.	176
<b>Figure PV.3.</b> Ratio of well and badly modeled molecules by the $tc$ -RK EoS classified into non-self-associating (NSA) and self-associating (SA) fluids. Green: well-modeled molecules. Red: Badly-modeled molecules.	176
<b>Figure PV.4.</b> Ratio of well and badly modeled molecules by the $tc$ -PR EoS classified into non-self-associating (NSA) and self-associating (SA) fluids. Green: well-modeled molecules. Red: Badly-modeled molecules.	176
<b>Figure PVI.1.</b> (a) Illustration of the definition of a hydrogen bond (red dashed line). The arrows indicate the more electronegative atom, i.e., the direction in which the shared pair of electrons (of the covalent bond) is shifted. (b) case of the pentafluoroethane-dimethyl ether system.	183

<b>Figure PVI.2.</b> Procedure followed to build the proposed database. ....	187
<b>Figure PVI.3.</b> Notation used in the files <i>database.xlsx</i> and <i>BACi_with visualization of the data.xlsx</i> (i=1 to 9) when the experimental pressure is not mentioned. ....	213
<b>Figure PVI.4.</b> Illustration of all the cases in which <i>out of model</i> data points can appear. For such exp. data points, the MAPE cannot be evaluated. (a): experimentally 2-phase data points that are found to be 1-phase by the model. (b) An azeotropic system is predicted as a zeotropic system so that the homogeneous azeotrope is declared out of model. In addition, for small mole fractions, $y_{1,\text{exp}} > x_{1,\text{exp}}$ whereas the model predicts the opposite. (c) A homogeneous azeotrope is predicted as heterogeneous. (d) A 3-phase line is not predicted by the model. (e) 2 critical points that are not predicted by the model are experimentally observed. (f) The model predicts 2 critical points whereas only one is experimentally observed. ....	214
<b>Figure PVI.5.</b> Overview of the accuracy of the model: {PR EoS + classical mixing rules with a T-dependent $k_{ij}$ } by plotting the marks in ten properties for the four categories of binary systems based on the type of association they exhibit. ....	229
<b>Figure PVI.6.</b> Marks in 10 properties calculated for five categories of binary systems based on how they deviate from ideality (marks on VLLE data are not shown due to a lack of information for some categories of binary systems). ....	231
<b>Figure PVII.1.</b> a) Calculated and experimental isothermal pressure - composition VLE phase diagram that does not exhibit <i>out-of-model</i> points. b) Phase diagrams exhibiting <i>out-of-model</i> points due to an underestimation of the experimental azeotropic pressure by the model. (*): experimental dew points. (+): experimental bubble points. (-): calculated dew curve. (-): calculated bubble curve. $P_{az}$ : calculated azeotropic pressure. $x_{az}$ : calculated azeotropic composition. ....	249
<b>Figure PVII.2.</b> Overview of the accuracy of the <i>tc</i> -PR-Wilson, <i>tc</i> -PR-UNIQUAC, <i>tc</i> -PR-NRTL and PR-van Laar by plotting the overall marks per property ( $prop \in \{x, y, P_{LLV}, z_{LLV}, P_c, x_c, P_{azeo}, x_{azeo}, h^M, c_P^M\}$ ) as returned by Eq. (PVII.35). The complete database, i.e., the 200 binary systems are considered here. ....	251
<b>Figure PVII.3.</b> Overview of the accuracy of the <i>tc</i> -PR-Wilson, <i>tc</i> -PR-UNIQUAC, <i>tc</i> -PR-NRTL and PR-Van Laar by plotting the average marks for the four categories of binary systems based on the type of association they exhibit. ....	261
<b>Figure PVII.4.</b> Overview of the accuracy of the <i>tc</i> -PR-Wilson, <i>tc</i> -PR-UNIQUAC, <i>tc</i> -PR-NRTL and PR-Van Laar by plotting the marks on ten properties for the category including mixtures without association (BACs 1 to 4). ....	262
<b>Figure PVII.5.</b> Pressure – composition VLE phase diagrams (left) and mixing heat capacity – composition diagrams (right) for the binary system Cyclohexane (1) + Monochlorobenzene calculated with the <i>tc</i> -PR-Wilson (a, b), <i>tc</i> -PR-UNIQUAC (c, d), <i>tc</i> -PR-NRTL (e, f) and PR-Van Laar (g, h) models. Phase equilibrium diagrams convention: (*): experimental dew points. (+): experimental bubble points. (-): calculated dew curve. (-): calculated bubble curve. Caloric properties diagrams convention: (+): experimental data. (-): calculated curve. ....	263
<b>Figure PVII.6.</b> Pressure – composition VLE phase diagrams for the binary system N <sub>2</sub> (1) + n-pentane calculated with the <i>tc</i> -PR-Wilson (a, b), <i>tc</i> -PR-UNIQUAC (c, d), <i>tc</i> -PR-NRTL (e, f) and PR-Van Laar (g, h) models. Phase equilibrium diagrams convention: (*): experimental dew points. (+): experimental	

---

bubble points. (●): experimental critical point. (–): calculated dew curve. (–): calculated bubble curve. .....	264
<b>Figure PVII.7.</b> Global Phase-Equilibrium Diagrams (GPEDs) (left), pressure – composition VLE phase diagrams (center) and mixing heat capacity – composition diagrams (right) for the binary system N <sub>2</sub> (1) + Methane calculated the <i>tc</i> -PR-Wilson (a, b, c), <i>tc</i> -PR-UNIQUAC (d, e, f), <i>tc</i> -PR-NRTL (g, h, i) and PR-Van Laar (j, k, l) models. GPED convention: (✱) experimental critical points. (–) calculated critical line. (–) calculated vapor-pressure curves of pure components. Phase equilibrium diagrams convention: (✱): experimental dew points. (+): experimental bubble points. (–): calculated dew curve. (–): calculated bubble curve. ....	265
<b>Figure PVII.8.</b> Overview of the accuracy of the <i>tc</i> -PR-Wilson, <i>tc</i> -PR-UNIQUAC, <i>tc</i> -PR-NRTL and PR-Van Laar by plotting the marks on ten properties for the category including mixtures in which cross-association takes place alone. ....	266
<b>Figure PVII.9.</b> Pressure – composition VLE phase diagrams (left) and mixing heat capacity – composition diagrams (right) for the binary system Methyl acetate (1) + Chloroform calculated with the <i>tc</i> -PR-Wilson (a, b), <i>tc</i> -PR-UNIQUAC (c, d), <i>tc</i> -PR-NRTL (e, f) and PR-Van Laar (g, h) models. Phase equilibrium diagrams convention: (✱): experimental dew points. (+): experimental bubble points. (▲): experimental azeotropic point. (–): calculated dew curve. (–): calculated bubble curve. Caloric properties diagrams convention: (+): experimental data. (–): calculated curve. ....	267
<b>Figure PVII.10.</b> Pressure – composition VLE phase diagrams (left) and mixing heat capacity – composition diagrams (right) for the binary system Ethyl acetate (1) + 1, 1, 2, 2-tetrachloroethane calculated with the <i>tc</i> -PR-Wilson (a, b), <i>tc</i> -PR-UNIQUAC (c, d), <i>tc</i> -PR-NRTL (e, f) and PR-Van Laar (g, h) models. Phase equilibrium diagrams convention: (✱): experimental dew points. (+): experimental bubble points. (–): calculated dew curve. (–): calculated bubble curve. Caloric properties diagrams convention: (+): experimental data. (–): calculated curve. ....	268
<b>Figure PVII.11.</b> Overview of the accuracy of the <i>tc</i> -PR-Wilson, <i>tc</i> -PR-UNIQUAC, <i>tc</i> -PR-NRTL and PR-Van Laar by plotting the marks on ten properties for the category including mixtures in which self-association tends to be broken. ....	269
<b>Figure PVII.12.</b> Pressure – composition VLE phase diagrams (left) and mixing enthalpy – composition diagrams (right) for the binary system Methanol (1) + Benzene calculated with the <i>tc</i> -PR-Wilson (a, b), <i>tc</i> -PR-UNIQUAC (c, d), <i>tc</i> -PR-NRTL (e, f) and PR-Van Laar (g, h) models. Phase equilibrium diagrams convention: (✱): experimental dew points. (+): experimental bubble points. (▲): experimental azeotropic point. (–): calculated dew curve. (–): calculated bubble curve. (–): calculated three-phase line. Caloric properties diagrams convention: (+): experimental data. (–): calculated curve. ....	272
<b>Figure PVII.13.</b> Pressure – composition VLE phase diagrams for the binary system Ethane (1) + Water calculated with the <i>tc</i> -PR-Wilson (a, b), <i>tc</i> -PR-UNIQUAC (c, d), <i>tc</i> -PR-NRTL (e, f) and PR-Van Laar model (g, h) models. Phase equilibrium diagrams convention: (✱): experimental dew points. (+): experimental bubble points. (●): experimental critical point. (–): calculated dew curve. (–): calculated bubble curve. ....	273
<b>Figure PVII.14.</b> Overview of the accuracy of the <i>tc</i> -PR-Wilson, <i>tc</i> -PR-UNIQUAC, <i>tc</i> -PR-NRTL and PR-Van Laar by plotting the marks on ten properties for the category including mixtures in which both cross- and self-association take place (BACS 7 to 9). ....	274

<b>Figure PVII.15.</b> Pressure – composition VLE phase diagrams for the binary system Dimethyl ether (1) + Water calculated with the <i>tc</i> -PR-Wilson (a, b), <i>tc</i> -PR-UNIQUAC (c, d), <i>tc</i> -PR-NRTL (e, f) and PR-Van Laar model (g, h) models. Phase equilibrium diagrams convention: (✱): experimental dew points. (+): experimental bubble points. (●): experimental critical point. (▲): experimental three-phase line compositions. (–): calculated dew curve. (–): calculated bubble curve. (–): calculated three-phase line. ....	275
<b>Figure PVIII.1.</b> a) Schematic view of an ideal Rankine cycle. b) Sketch to the corresponding temperature-entropy diagram. ....	284
<b>Figure PVIII.2.</b> a) Schematic view of an ideal CHP cycle. b) Sketch of the corresponding temperature-entropy diagram. ....	285
<b>Figure PVIII.3.</b> Sketch of the temperature-entropy diagram of two CHP cycles: cycle A (1-2-2'-3-4-5-6-1), cycle B (1-2-2'-3-4-5'-6'-1). ....	286
<b>Figure PVIII.4.</b> Enlarged temperature-entropy diagram for the CHP cycles considered in Figure PVIII.3. ....	286
<b>Figure PVIII.5.</b> Enlarged temperature-entropy diagram for two CHP cycles providing heat at different temperatures. ....	288
<b>Figure PVIII.6.</b> a) Schematic view of an ideal CCHP cycle. b) Sketch of the corresponding temperature-entropy diagram. ....	289
<b>Figure PVIII.7.</b> Scheme of the product-design approach adopted in this work for the selection of suitable working fluids for CCHP applications. ....	294
<b>Figure PVIII.8.</b> GHS classification of n-pentane. Obtained from the public-domain PubChem database of the National Institutes of Health [1308]. ....	296
<b>Figure PVIII.9.</b> Pre-screening on DDB-2020 database. ....	298
<b>Figure PVIII.10.</b> Pre-screening on DIPPR-2020 database. ....	298
<b>Figure PVIII.11.</b> Pre-screening on the NIST TDE 103b database. ....	299
<b>Figure PVIII.12.</b> Illustration of the comparison between a conventional generation and trigeneration systems. ....	302
<b>Figure PVIII.13.</b> Saturation pressure at $T_C = 10\text{ }^\circ\text{C}$ versus critical temperature for the 1568 molecules remaining after filter 2 for case study 1. ....	307
<b>Figure PVIII.14.</b> Inverse of volumetric capacity versus inverse of energy utilization factor for the 9 molecules remaining after the screening procedure: a) Case study 1. b) Case study 2. The numbers correspond to the ranking of each molecule as shown in Table PVIII.8. ....	310
<b>Figure F.1 .</b> Évolution de la part de la consommation énergétique de l'UE provenant de sources renouvelables depuis 2005. Données fournies par l'Agence européenne pour l'environnement [5]. ..	384
<b>Figure F.2 .</b> a) Vue schématique d'un cycle CCHP idéal. b) Esquisse du diagramme température-entropie correspondant. ....	391



## List of tables

<b>Table 2-1.</b> Classification of $\alpha$ -functions commonly implemented in process simulation software. ....	31
<b>Table 2-2.</b> Possible combinations of accurate pseudo-experimental data available in the DIPPR database for a given pure component. The pure fluid type is an arbitrary index that indicates which properties among $P^{sat}$ , $\Delta_{vap}H$ and $c_{P,liq}^{sat}$ are associated with accurate data and can thus be used to fit $\alpha$ -function parameters. ....	37
<b>Table 2-3.</b> Comparison of the mean absolute percentage errors (MAPEs) calculated with the $tc$ -PR EoS and the PR EoS armed with the updated Soave $\alpha$ -function determined in Publication III. ....	38
<b>Table 3-1.</b> Definition of the 9 groups of binary systems identified each by a BAC (binary association code) and the 4 categories used for the grading of a model. ....	54
<b>Table PI.1.</b> Average MAPE on several thermodynamic properties as predicted by the PC-SAFT EoS calculated over 587 non-associating pure components. ....	87
<b>Table PI.2.</b> Average MAPE on several thermodynamic properties as predicted with the SRK EoS calculated over 587 non-associating pure components. ....	87
<b>Table PI.3.</b> Average MAPE on several thermodynamic properties as predicted by the $t$ -PC-SAFT and $t$ -SRK EoS calculated over 587 non-associating pure components. In both cases parameterization method P1 $t$ was followed so that the $t$ -PC-SAFT EoS is named $I$ -PC-SAFT. ....	95
<b>Table PI.4.</b> Average MAPE on speeds of sound in $n$ -pentane as predicted by the $I$ -PC-SAFT and $t$ -SRK EoS. ....	98
<b>Table PII.1.</b> Possible combinations of accurate pseudo-experimental data available in the DIPPR database for a given pure component. The pure fluid type is an arbitrary index that indicates which properties among $P^{sat}$ , $\Delta_{vap}H$ and $c_{P,liq}^{sat}$ are associated with accurate data and can thus be used to fit $\alpha$ -function parameters. ....	106
<b>Table PII.2.</b> Acceptance thresholds for the different property correlations and types of error. ....	108
<b>Table PII.3.</b> Comparison of the number of molecules included in the database by Le Guennec et al. <sup>3</sup> and this work. ....	109
<b>Table PII.4.</b> Arrangements of the properties for Twu91 $\alpha$ -function parameter fitting. ....	110
<b>Table PII.5.</b> MAPE on $P^{sat}$ , $\Delta_{vap}H$ and $c_{P,liq}^{sat}$ according to the property considered for parameter fitting. ....	112
<b>Table PII.6.</b> Number of molecules for which at least the pseudo-experimental data of $P^{sat}$ can be accurately generated. ....	112
<b>Table PII.7.</b> Number of <i>non-quantum</i> compounds for which the experimental properties can be accurately estimated. ....	113
<b>Table PII.8.</b> Rejection thresholds for molecule selection. ....	114
<b>Table PII.9.</b> Distribution of the 1721 retained molecules according to the available accurate property data. ....	114
<b>Table PII.10.</b> MAPE on $P^{sat}$ , $\Delta_{vap}H$ and $c_{P,liq}^{sat}$ as predicted from the updated <i>consistent</i> PR and RK EoS. ....	115

<b>Table PII.11.</b> Distribution of the 1489 molecules for which at least $P^{sat}$ and $v_{liq}^{sat}$ can be accurately generated from the DIPPR database.....	116
<b>Table PII.12.</b> MAPE on $v_{liq}^{sat}$ as predicted by the <i>consistent</i> PR and RK EoS on an updated database. Effect of the volume translation. ....	116
<b>Table PII.13.</b> MAPE on $v_c$ as predicted by the <i>consistent</i> PR and RK EoS. Effect of the selected volume translation. ....	117
<b>Table PII.14.</b> MAPE on $P^{sat}$ , $\Delta_{vap}H$ , $c_{P,liq}^{sat}$ , $v_{liq}^{sat}$ , $v_c$ , $T_c$ , and $P_c$ as predicted by the <i>translated-consistent</i> PR and RK EoS with the updated parameters determined in this study.....	117
<b>Table PII.15.</b> Comparison of the MAPEs calculated with the 3-parameter Twu91, generalized Twu88 and Soave $\alpha$ -functions for the translated PR and RK EoS. ....	119
<b>Table PIII.1.</b> Distribution of the 1720 retained compounds according to the accurate property data available in the DIPPR database.....	126
<b>Table PIII.2.</b> Comparison of the MAPEs calculated with the original and the updated Soave $\alpha$ -functions. Application to the PR and RK EoS. ....	128
<b>Table PIII.3.</b> Comparison of the MAPEs on $v_{liq}^{sat}$ calculated with the original and the updated Soave $\alpha$ -functions. Application to the translated and untranslated PR and RK EoS.....	129
<b>Table PIII.4.</b> Comparison of the MAPEs on the molar critical volume ( $v_c$ ) calculated with the original and the updated Soave $\alpha$ -functions. Application to the translated and untranslated PR and RK EoS. ....	130
<b>Table PIV.1.</b> Selected values of $u$ and $w$ for the volume function of the attractive term in cubic equations of state. ....	141
<b>Table PIV.2.</b> Available properties for the 1525 components that are used to determine the optimum values of $u$ and $w$ .....	148
<b>Table PIV.3.</b> Comparison of the main untranslated CEoS (VdW, SRK, PR) with the optimized untranslated CEoS developed in this work. Note that all EoS are combined with a Soave-type $\alpha$ -function. ....	151
<b>Table PIV.4.</b> Comparison of the main translated CEoS ( <i>t</i> -VdW, <i>t</i> -SRK, <i>t</i> -PR) with the optimized translated CEoS developed in this work and called <i>t</i> -OptiM. All EoS use a Soave-type $\alpha$ -function..	153
<b>Table PIV.5.</b> Comparison of the most famous <i>translated-consistent</i> CEoS (tc-VdW, tc-RK, tc-PR, tc-SW) with the optimized one developed in this work and called tc-OptiM. All EoS are combined with the Twu 91 $\alpha$ -function. ....	154
<b>Table PV.1.</b> MAPE and SD obtained with the <i>generalized</i> version of the <i>tc</i> -PR model used for this work.....	163
<b>Table PV.2.</b> Acceptance thresholds for the different property correlations and types of error. ....	164
<b>Table PV.3.</b> Overview of the data available in the proposed database.....	166
<b>Table PV.4.</b> Expressions of the SRK, PR, <i>tc</i> -RK and <i>tc</i> -PR EoS.....	167
<b>Table PV.5.</b> MAPE on $P^{sat}$ , $v_{liq}^{sat}$ , $\Delta_{vap}H$ , $c_{P,liq}^{sat}$ , $v_c$ , $T_c$ and $P_c$ as predicted by the SRK, PR, <i>tc</i> -RK and <i>tc</i> -PR EoS. ....	170
<b>Table PV.6.</b> MAPE on $P^{sat}$ , $v_{liq}^{sat}$ , $\Delta_{vap}H$ , $c_{P,liq}^{sat}$ and $v_c$ depending on the associating character as predicted by the SRK, PR, <i>tc</i> -RK and <i>tc</i> -PR EoS. ....	171

---

<b>Table PV.7.</b> Distribution of well-modeled compounds across different chemical groups for the SRK, PR, <i>tc</i> -RK and <i>tc</i> -PR EoS.....	175
<b>Table PVI.1.</b> Definition of the ten families of binary systems and their corresponding BAC ( <i>binary association code</i> ).....	184
<b>Table PVI.2.</b> Overview of how the deviations from ideality are distributed among the nine binary association codes (BACs) for the 200 binary systems of the proposed database (the abbreviations used for the <i>associating character</i> of a pure compound are: NA for “Non-Associating”, HA for “Hydrogen-Acceptor”, HD for “Hydrogen-Donor” and SA for “Self-Associating”). .....	191
<b>Table PVI.3.</b> Overview of the distribution of the different types of experimental data among the nine binary association codes (BACs) for the 200 binary systems of the proposed database (the abbreviations used for the <i>associating character</i> of a pure compound are: NA for “Non-Associating”, HA for “Hydrogen-Acceptor”, HD for “Hydrogen-Donor” and SA for “Self-Associating”). .....	192
<b>Table PVI.4.</b> List of the 26 binary systems for which the binary association code is: BAC=1 (NA-NA). Such a BAC corresponds to a binary system involving a “Non-Associating” (NA) molecule + another “Non-Associating” (NA) molecule. Corresponding origin of the deviations from ideality and list of the references in which the experimental data can be found. By convention, <i>Molecule 1</i> refers to the more volatile component. ....	193
<b>Table PVI.5.</b> List of the 24 binary systems for which the binary association code is: BAC=2 (HA-NA). Such a BAC corresponds to a binary system involving a “Hydrogen-Acceptor” (HA) molecule + a “Non-Associating” (NA) molecule. Corresponding origin of the deviations from ideality and list of the references in which the experimental data can be found. By convention, <i>Molecule 1</i> refers to the more volatile component. ....	195
<b>Table PVI.6.</b> List of the 20 binary systems for which the binary association code is: BAC=3 (HD-NA). Such a BAC corresponds to a binary system involving a “Hydrogen-Donor” (HD) molecule + a “Non-Associating” (NA) molecule. Corresponding origin of the deviations from ideality and list of the references in which the experimental data can be found. By convention, <i>Molecule 1</i> refers to the more volatile component. ....	197
<b>Table PVI.7.</b> List of the 22 binary systems for which the binary association code is: BAC=4 (HA-HA or HD-HD). Such a BAC corresponds to a binary system involving two “Hydrogen-Acceptor” (HA) molecules or two “Hydrogen-Donor” (HD) molecules. Corresponding origin of the deviations from ideality and list of the references in which the experimental data can be found. By convention, <i>Molecule 1</i> refers to the more volatile component. ....	199
<b>Table PVI.8.</b> List of the 18 binary systems for which the binary association code is: BAC=5 (SA-NA). Such a BAC corresponds to a binary system involving a “Self-Associating” (SA) molecule + a “Non-Associating” (NA) molecule. Corresponding origin of the deviations from ideality and list of the references in which the experimental data can be found. By convention, <i>Molecule 1</i> refers to the more volatile component. ....	201
<b>Table PVI.9.</b> List of the 25 binary systems for which the binary association code is: BAC=6 (HD-HA). Such a BAC corresponds to a binary system involving a “Hydrogen-Donor” (HD) molecule + a “Hydrogen-Acceptor” (HA) molecule. Corresponding origin of the deviations from ideality and list of the references in which the experimental data can be found. By convention, <i>Molecule 1</i> refers to the more volatile component. ....	203

---

---

<b>Table PVI.10.</b> List of the 16 binary systems for which the binary association code is: BAC=7 (SA-HD). Such a BAC corresponds to a binary system involving a “Self-Associating” (SA) molecule + a “Hydrogen-Donor” (HD) molecule. Corresponding origin of the deviations from ideality and list of the references in which the experimental data can be found. By convention, <i>Molecule 1</i> refers to the more volatile component. ....	205
<b>Table PVI.11.</b> List of the 26 binary systems for which the binary association code is: BAC=8 (SA-HA). Such a BAC corresponds to a binary system involving a “Self-Associating” (SA) molecule + a “Hydrogen-Acceptor” (HA) molecule. Corresponding origin of the deviations from ideality and list of the references in which the experimental data can be found. By convention, <i>Molecule 1</i> refers to the more volatile component. ....	206
<b>Table PVI.12.</b> List of the 23 binary systems for which the binary association code is: BAC=9 (SA-SA). Such a BAC corresponds to a binary system involving a “Self-Associating” (SA) molecule + another “Self-Associating” (SA) molecule. Corresponding origin of the deviations from ideality and list of the references in which the experimental data can be found. By convention, <i>Molecule 1</i> refers to the more volatile component. ....	208
<b>Table PVI.13.</b> Specified and calculated variables for the different binary-system properties involved in the database. ....	212
<b>Table PVI.14.</b> Overview of the MAPE between experimental data and values calculated with the model: $\{PR\ EoS + \text{classical mixing rules with a } T\text{-dependent } k_{ij}\}$ for the 200 binary systems included in the proposed database that are classified in 9 binary association codes (BACs). The abbreviations used for the <i>associating character</i> of a pure compound are: NA for “Non-Associating”, HA for “Hydrogen-Acceptor”, HD for “Hydrogen-Donor” and SA for “Self-Associating”.....	227
<b>Table PVI.15.</b> Rating of the 9 binary association codes in order to finally grade the model: $\{PR\ EoS + \text{classical mixing rules with a } T\text{-dependent } k_{ij}\}$ . The abbreviations used for the <i>associating character</i> of a pure compound are: NA for “Non-Associating”, HA for “Hydrogen-Acceptor”, HD for “Hydrogen-Donor” and SA for “Self-Associating”. ....	228
<b>Table PVII.1.</b> Parameters $r_1$ and $r_2$ for some classical cubic equations of state.....	237
<b>Table PVII.2.</b> Final marks and corresponding success ratios of the <i>tc</i> -PR-Wilson, <i>tc</i> -PR-UNIQUAC, <i>tc</i> -PR-NRTL and PR-Van Laar models using the grading procedure described by Jaubert et al. [130] and slightly updated in Section PVII.III.I. x: liquid phase composition data ( $x_1$ or $x_1^\alpha$ ). y: gas phase (or 2 <sup>nd</sup> liquid phase) composition data ( $y_1$ or $x_1^\beta$ ). LLV: three-phase lines data. Crit: critical point data. Az: azeotropic data.....	250
<b>Table PVII.3.</b> Overview of the MAPEs between experimental data and model predictions along with the corresponding success ratios ( <i>tc</i> -PR-Wilson) for the 200 binary systems included in the benchmark database proposed by Jaubert et al. [130]. The mixtures are classified in 9 BACs as proposed by Jaubert et al. [130]. The abbreviations used for the associating character of a pure compound are: NA for “Non-Associating”, HA for “Hydrogen-Acceptor”, HD for “Hydrogen-Donor” and SA for “Self-Associating”. Dots (-) indicate that no experimental data are available in the database for the respective properties. ....	253
<b>Table PVII.4.</b> Rating of the 9 binary association codes in order to obtain the final grade of the <i>tc</i> -PR-Wilson model. ....	254

---

<b>Table PVII.5.</b> Overview of the MAPEs between experimental data and model predictions along with the corresponding success ratios ( <i>tc</i> -PR-UNIQUAC) for the 200 binary systems included in the benchmark database proposed by Jaubert et al. [130]. The mixtures are classified in 9 BACs as proposed by Jaubert et al. [130]. The abbreviations used for the associating character of a pure compound are: NA for “Non-Associating”, HA for “Hydrogen-Acceptor”, HD for “Hydrogen-Donor” and SA for “Self-Associating”. Dots (-) indicate that no experimental data are available in the database for the respective properties.....	255
<b>Table PVII.6.</b> Rating of the 9 binary association codes in order to obtain the final grade of the <i>tc</i> -PR-UNIQUAC model.....	256
<b>Table PVII.7.</b> Overview of the MAPEs between experimental data and model predictions along with the corresponding success ratios ( <i>tc</i> -PR-NRTL) for the 200 binary systems included in the benchmark database proposed by Jaubert et al. [130]. The mixtures are classified in 9 BACs as proposed by Jaubert et al. [130]. The abbreviations used for the associating character of a pure compound are: NA for “Non-Associating”, HA for “Hydrogen-Acceptor”, HD for “Hydrogen-Donor” and SA for “Self-Associating”. Dots (-) indicate that no experimental data are available in the database for the respective properties.....	257
<b>Table PVII.8.</b> Rating of the 9 binary association codes in order to obtain the final grade of the <i>tc</i> -PR-NRTL model.....	258
<b>Table PVII.9.</b> Overview of the MAPEs between experimental data and model predictions along with the corresponding success ratios (PR-Van Laar) for the 200 binary systems included in the benchmark database proposed by Jaubert et al. [130]. The mixtures are classified in 9 BACs as proposed by Jaubert et al. [130]. The abbreviations used for the associating character of a pure compound are: NA for “Non-Associating”, HA for “Hydrogen-Acceptor”, HD for “Hydrogen-Donor” and SA for “Self-Associating”. Dots (-) indicate that no experimental data are available in the database for the respective properties.....	259
<b>Table PVII.10.</b> Rating of the 9 binary association codes in order to obtain the final grade of the PR-Van Laar model.....	260
<b>Table PVIII.1.</b> Summary of the specified variables and specifications equations for the CCHP system studied in this work. ....	291
<b>Table PVIII.2.</b> Screening order retained for this work. ....	301
<b>Table PVIII.3.</b> Summary of filtering criteria. ....	304
<b>Table PVIII.4.</b> Summary of operating specifications. ....	305
<b>Table PVIII.5.</b> Progress of the number of compounds passing the successive filters from the initial pool of 2540 candidates for the two considered case studies. ....	306
<b>Table PVIII.6.</b> Minimum operating pressures ( $P^{sat}(T_C)$ ) of four reference fluids for the two considered case studies.....	308
<b>Table PVIII.7.</b> List of 9 candidates passing the screening filters for the two considered case studies. Note: Filter on $P_{min}$ for case study 2 is relaxed.....	313
<b>Table PVIII.8.</b> CCHP cycle performances for the nine candidates passing the screening filters. Ranking is based on EUF.....	314

**Table PVIII.9.** Parameters corresponding to the tc-PR model and the mean absolute percentage average (MAPE) on the properties of interest for the nine candidates passing the screening filters. The calculation of MAPEs is described in reference [184]. ..... 315

## List of publications

The research work of this thesis resulted in the 12 publications and a book chapter presented hereafter. However, only Publications I to VIII are included in this manuscript since they were essential for the achievement of the objective of this thesis. The four remaining publications and the book chapter are the result of side research activities.

### **Publication I**

Moine, E.; Piña-Martinez, A.; Jaubert, J.-N.; Sirjean, B.; Privat, R. I-PC-SAFT: An Industrialized Version of the Volume-Translated PC-SAFT Equation of State for Pure Components, Resulting from Experience Acquired All through the Years on the Parameterization of SAFT-Type and Cubic Models. *Ind. Eng. Chem. Res.* 2019, 58 (45), 20815–20827. DOI: <https://doi.org/10.1021/acs.iecr.9b04660>.

### **Publication II**

Piña-Martinez, A.; Le Guennec, Y.; Privat, R.; Jaubert, J.-N.; Mathias, P. M. Analysis of the Combinations of Property Data That Are Suitable for a Safe Estimation of Consistent Two  $\alpha$ -Function Parameters: Updated Parameter Values for the Translated-Consistent  $tc$ -PR and  $tc$ -RK Cubic Equations of State. *J. Chem. Eng. Data* 2018, 63 (10), 3980–3988. DOI: <https://doi.org/10.1021/acs.jced.8b00640>.

### **Publication III**

Piña-Martinez, A.; Privat, R.; Jaubert, J.-N.; Peng, D.-Y. Updated Versions of the Generalized Soave  $\alpha$ -Function Suitable for the Redlich-Kwong and Peng-Robinson Equations of State. *Fluid Phase Equilibria* 2019, 485, 264–269. DOI: <https://doi.org/10.1016/j.fluid.2018.12.007>.

### **Publication IV**

Piña-Martinez, A.; Privat, R.; Lasala, S.; Soave, G.; Jaubert, J.-N. Search for the Optimal Expression of the Volumetric Dependence of the Attractive Contribution in Cubic Equations of State. *Fluid Phase Equilibria* 2020, 522, 112750. DOI: <https://doi.org/10.1016/j.fluid.2020.112750>.

### **Publication V**

Piña-Martinez, A.; Privat, R.; Jaubert, J.-N. Use of 300,000 experimental data over 1 800 pure fluids to assess the performance of 4 CEoS: SRK, PR,  $tc$ -RK,  $tc$ -PR. *AIChE J.* 2021. DOI: <https://doi.org/10.1002/aic.17518>.

### **Publication VI**

Jaubert, J.-N.; Le Guennec, Y.; Piña-Martinez, A.; Ramirez-Velez, N.; Lasala, S.; Schmid, B.; Nikolaidis, I. K.; Economou, I. G.; Privat, R. A Benchmark Database Containing Binary-System-High-Quality-Certified Data for Cross-Comparing Thermodynamic Models and Assessing Their Accuracy. *Ind. Eng. Chem. Res.* 2020, 59 (33), 14981–15027. DOI: <https://doi.org/10.1021/acs.iecr.0c01734>.

### **Publication VII**

Piña-Martinez, A.; Privat, R.; Nikolaidis, I. K.; Economou, I. G.; Jaubert, J.-N.; Use of a reliable benchmark database for the assessment of the *translated-consistent* Peng-Robinson (*tc-PR*) equation of state armed with EoS/ $a_{res}^{E,\gamma}$  mixing rules embedding three different  $g^E$  models: Wilson, UNIQUAC and NRTL. *Ind. Eng. Chem. Res.* 2021. DOI: <https://doi.org/10.1021/acs.iecr.1c03003>.

### **Publication VIII**

Piña-Martinez, A.; Lasala, S.; Privat, R.; Falk, V.; Jaubert, J.-N. Design of promising working fluids for emergent combined cooling, heating and power (CCHP) systems. *ACS Sustain. Chem. Eng.* 2021, 9 (35), 11807–11824. DOI: <https://doi.org/10.1021/acssuschemeng.1c03362>.

### **Publication IX**

Ramirez-Velez, N.; Piña-Martinez, A.; Jaubert, J.N.; Privat, R. Parameterization of SAFT models: analysis of different parameter estimation strategies and application to the development of a comprehensive database of PC-SAFT molecular parameters. *J. Chem. Eng. Data* 2020, 65, 5920–5932. DOI: <https://doi.org/10.1021/acs.jced.0c00792>.

### **Publication X**

Vitu, S.; Piña-Martinez, A.; Privat, R.; Debacq, M.; Havet, J.L.; Daridon, J.L.; Jaubert, J.N. Experimental determination and modelling of high-pressure phase behavior for the binary system CO<sub>2</sub> + cyclooctane. *J. Supercrit. Fluids* 2021, 174, 105249. DOI: <https://doi.org/10.1016/j.supflu.2021.105249>.

### **Publication XI**

Zid, S.; Bazile, J.P.; Daridon, J.L.; Piña-Martinez, A.; Jaubert, J.N.; Vitu, S. Fluid phase equilibria for the CO<sub>2</sub> + 2,3-dimethylbutane binary system from 291.9 K to 373.1 K. *J. Supercrit. Fluids* 2021, 179, 105387. DOI: <https://doi.org/10.1016/j.supflu.2021.105387>.

### **Publication XII**

Ramirez-Velez, N.; Privat, R.; Piña-Martinez, A.; Jaubert, J.N. Assessing the performance of non-associating SAFT-type EoS to reproduce  $P^{sat}$ ,  $v_{liq}^{sat}$ ;  $\Delta_{vap}H$  and  $c_{P,liq}^{sat}$  of 1 800 pure fluids. *AIChE J.* 2021. (Submitted).

### **Book chapter I**

Lasala, S.; Piña-Martinez, A.; Jaubert, J.N. Organic Rankine Cycles for Waste Heat Recovery - Analysis and Applications. Chapter : A predictive equation of state to perform an extending screening of working fluids for power and refrigeration cycles. (14 pages). ISBN : 978-953-51-6692-4 (April 2020). DOI: <https://dx.doi.org/10.5772/intechopen.77463>.

# Nomenclature

## Acronyms

Acronym	Description
ACM	Activity Coefficient Model
ARD	Absolute Relative Deviation
BAC	Binary Association Code
BIP	Binary Interaction Parameter
BWR	Benedict-Webb-Rubin
CCHP	Combined Cooling, Heating and Power
CEoS	Cubic Equation of State
CHP	Combined Heat and Power
DDB	Dortmund Data Bank
DES	Distributed Energy Systems
DIPPR	Design Institute for Physical Properties
EoS	Equation of State
EU	European Union
HV	Huron-Vidal
IEA	International Energy Agency
LCVM	Linear Combination of the Vidal and Michelsen mixing rules
LJ-SAFT	Lennard-Jones-Statistical Associating Fluid Theory
LLE	Liquid-Liquid Equilibrium
MAPE	Mean Absolute Percentage Error
MBWR	Modified Benedict-Webb-Rubin
MHV	Modified Huron-Vidal
MR	Mixing Rule
NIST	National Institute of Standards and Technology
NRTL	Non-Randomness Two-Liquid
NSA	Non-Self-Associating
PC-SAFT	Perturbed-Chain-Statistical Associating Fluid Theory
PPR78	Predictive Peng-Robinson 1978
PR	Peng-Robinson
PR2SRK	Peng-Robinson to Soave-Redlich-Kwong
PSRK	Predictive Soave-Redlich-Kwong
REFPROP	Reference Fluid Thermodynamic and Transport Properties Database
RES	Renewable Energy Source
RK	Redlich-Kwong
RQ	Research Question
SA	Self-Associating
SAFT	Statistical Associating Fluid Theory
SAFT-VR	Variable Range Statistical Associating Fluid Theory
SRK	Soave-Redlich-Kwong
<i>tc</i> -PR	translated-consistent Peng-Robinson
<i>tc</i> -RK	translated-consistent Redlich-Kwong

Acronym	Description
TPT	Thermodynamic Perturbation Theory
UMR	Universal Mixing Rule
UNIFAC	UNIversal quasi-chemical Functional group Activity Coefficient
UNIQUAC	UNIversal QUAsi Chemical
VdW	Van der Waals
VLE	Vapor-Liquid Equilibrium
VLLE	Vapor-Liquid-Liquid Equilibrium
VTPR	Volume-Translated Peng-Robinson

## Greek symbols

Symbol	Description	Units
$\alpha$	Alpha function	-
$\alpha$	Non-randomness parameter	-
$\gamma$	Activity coefficient	-
$\Gamma$	Reduced energetic parameter	-
$\delta$	Solubility parameter	-
$\theta$	Surface area fraction	-
$\Lambda$	Binary interaction parameter	J.mol <sup>-1</sup> or K
$\mu$	Chemical potential	-
$\rho$	Density	kg.m <sup>-3</sup>
$\rho$	Molar liquid density	mol.m <sup>-3</sup>
$\tau$	Binary interaction parameter	J.mol <sup>-1</sup> or K
$\varphi$	Fugacity coefficient	-
$\omega$	Acentric factor	-

## Latin symbols

Symbol	Description	Units
a	Attractive parameter	Pa.m <sup>6</sup> .mol <sup>-2</sup>
a	Molar Helmholtz free energy	J.mol <sup>-1</sup>
b	Covolume	m <sup>3</sup> .mol <sup>-1</sup>
c	Volume-translation parameter	m <sup>3</sup> .mol <sup>-1</sup>
C	Huron-Vidal universal parameter	-
$c_p$	Isobaric molar heat capacity	J.mol <sup>-1</sup> .K <sup>-1</sup>
$c_v$	Isochoric molar heat capacity	J.mol <sup>-1</sup> .K <sup>-1</sup>
f	fugacity	Pa
g	Molar Gibbs energy	J.mol <sup>-1</sup>
h	Molar enthalpy	J.mol <sup>-1</sup>
k	Binary interaction parameter	J.mol <sup>-1</sup> or K
L, M, N	Two a-function parameters	-
m	Soave a-function polynomial	-
n	Number of moles	mol
P	Pressure	Pa

<b>Symbol</b>	<b>Description</b>	<b>Units</b>
q	Van der Waals area	$\text{m}^2 \cdot \text{mol}^{-1}$
R	Universal gas constant	$\text{J} \cdot \text{mol}^{-1} \cdot \text{K}^{-1}$
r	Van der Waals volume	$\text{m}^3 \cdot \text{mol}^{-1}$
$r_1, r_2$	CEoS universal parameters	-
s	Molar entropy	$\text{J} \cdot \text{mol}^{-1} \cdot \text{K}^{-1}$
T	Temperature	K
u	Molar internal energy	$\text{J} \cdot \text{mol}^{-1}$
u, w	CEoS universal parameters	-
v	Molar volume	$\text{m}^3 \cdot \text{mol}^{-1}$
V	Volume	$\text{m}^3$
w	Sound speed	$\text{m} \cdot \text{s}^{-1}$
x, y, z	Molar fraction	-
Z	Compressibility factor	-

### Subscript/Superscript

<b>Symbol</b>	<b>Description</b>
O	Reference
*	Pure compound
C	Critical
comb	Combinatorial
Crit	Critical
E	Excess
Exp	Experimental
G	Group
i, j	Component index
Id	Ideal
M	Mixture
R	Reduced
Res	Residual
Sat	Saturation
T	Translated
U	Untranslated



# **Introduction**



# Introduction

## Context

According to the International Energy Agency (IEA), “modern economies depend on the reliable and affordable delivery of electricity” [1]. Furthermore, heating arises as the largest energy end-use, since it accounts for the half of the total energy consumption in the world. Refrigeration and especially cooling demand have been growing steadily since the half of the last century. Therefore, it is undeniable that society on these days depends deeply on electricity, heating and cooling supply, to such an extent that the way to make it more efficient, environmentally friendly and sustainable constitutes one of the major challenges of this century.

In general, electricity is generated at centralized power plants. They use a variety of energy resources such as coal, nuclear power and natural gas. In addition, renewable energy sources (RES) (or simply *renewables*) such as hydropower, wind, solar and geothermal are also included. A much smaller but growing amount of electricity is produced through distributed generation, which refers to a variety of technologies that generate electricity at or near where it will be used.

In turn, heating and cooling are supplied mostly by on-site technologies. Although the size of installations can vary from industrial to residential purposes, the heating and cooling systems are at the same place that end-users.

The most part of the primary energy required for the supply of electricity, heating and cooling comes from non-renewable sources. This represents a major obstacle in the way of achieving carbon neutrality in the future. In recent years, the European Union (EU) legislation on promotion of RES has evolved significantly [2]. Back in 2009, EU policymakers set a target of a 20% share of EU energy consumption coming from RES by 2020. Recently, in 2018, the target of a 32% share of EU energy consumption coming from RES by 2030 was agreed [3].

As shown in [Figure I.1](#), the share of EU energy consumption coming from renewable sources in 2019 was 19.7%. One of the strategies to achieve the target of 32% in 2030 is to increase the use of distributed energy systems (DES). This type of systems not only helps to the reduction of electricity losses along transmission and distribution lines that appear when the electricity generation is centralized; but are suitable for the inclusion of RES in the energetic mix of a country or region. Distributed generation may serve a single structure, such as a home or business, or it may be part of a microgrid (a smaller grid that is also tied into the larger electricity delivery system), such as at a major industrial facility, a military base, or a large college campus [4].

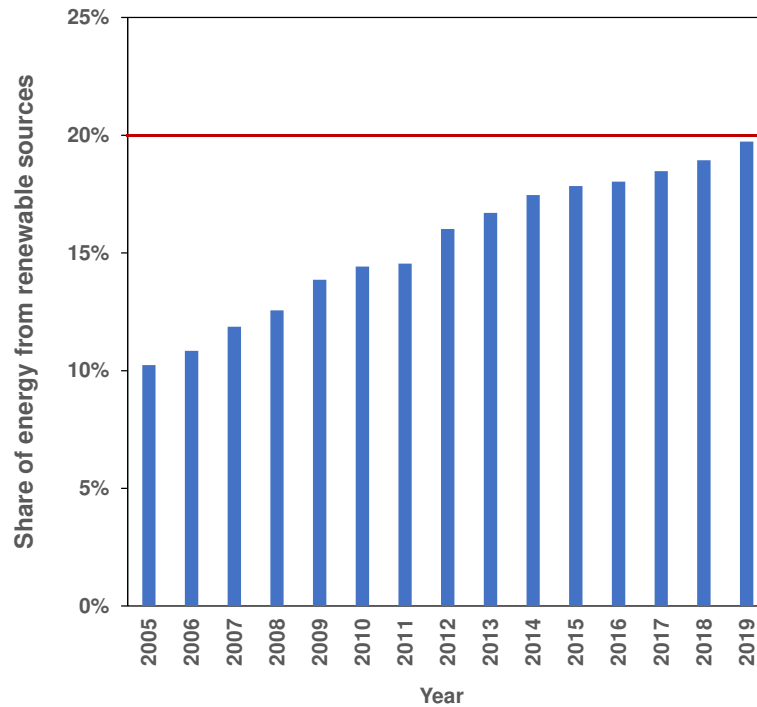


**Figure I.1.** Evolution of the share of EU energy consumption coming from renewable sources since 2005. Data provided by the European Environment Agency [5].

The promotion of DES has opened the way to different technologies such as combined heat and power (CHP) or combined cooling, heating and power (CCHP) systems. Conventional CHP/CCHP systems consist of different subsystems (prime mover, heat recovery system, cooling system) for each objective, which, in turn, contain different working fluids and do not operate on the same thermodynamic cycle. Moreover, CHP/CCHP systems operate with single-phase expanders and/or compressors. Recently, Briola [6] and Briola et al. [7] presented a novel CCHP cycle, inspired by the patents of Mokadam [8] and Fabris [9], operating with two-phase expanders and compressors. Such a cycle enables the development of an all-in-one device capable of producing electric, heating and cooling power with a single working fluid. Among the design challenges of this novel CCHP system, the working fluid selection appears as a key stage of its development.

The research work of this thesis is devoted to address this challenge by proposing a methodology of the selection of working fluids for all-in-one CCHP systems.

## Motivation and objectives

Several works have been focused on the selection of working fluids for conventional and novel CCHP systems [10–14]. Nevertheless, it is possible to identify the following shortcomings in the previous CCHP working fluid design works:

- the number of investigated working fluids is rather small and/or influenced by previous studies on Organic Rankine Cycle (ORC) configurations;
- a systematic evaluation of thermodynamic and constructional along with toxicological, flammability and environmental criteria has not been conducted for CCHP systems (by

constructional criteria, it is here referred to technical limitations due to the practical construction of operation units; in the present, this is essentially the maximum allowed pressure before material failure and the management of air entry in low-pressure systems).

The main objective of this thesis was to develop a product-design approach with a large space exploration of working fluids for the selection of suitable candidates for CCHP applications. This approach considers thermodynamic, process-related, environmental, flammability and toxicity aspects in the selection process as well as performance assessment.

In order to design or assess the performances of thermodynamic cycles, it is necessary to establish mass, energy and exergy balances. For instance, the application of the first law of thermodynamics (also named *energy rate balance*) to an open multi-component system at steady state can be written as:

$$\dot{W} + \dot{Q} = \sum \dot{m}_{out} \left( h_{out} + \frac{v_{out}^2}{2} + gz_{out} \right) - \sum \dot{m}_{in} \left( h_{in} + \frac{v_{in}^2}{2} + gz_{in} \right)$$

where  $\dot{W}$  and  $\dot{Q}$  are the net rates of energy transfer by work and by heat;  $\dot{m}$  is the mass flowrate; and  $h$ ,  $v$  and  $z$  denote the specific enthalpy, velocity and position of a stream, respectively. Subscripts *in* and *out* resp. mean *inlet* and *outlet* streams. From the energy balance, it is possible to observe that the whole design relies on the accurate estimation of enthalpies and implicitly, entropies involved in exergy balances and the isentropic-efficiency definitions of certain operations, which, in turn, requires the knowledge of the physical state of the stream. It implies that a phase-equilibrium problem should be solved and that vapor pressures of pure components must be estimated with high accuracy. Least but not last, density is a key property involved in the design of the piping system and device such as expanders, compressors, pumps and heat exchangers.

In summary, the key properties of a working fluid that should be properly predicted for the purpose of this thesis are: vapor pressure, density, enthalpy and entropy. This task is ensured by a thermodynamic model. In this thesis, cubic equations of state are retained due to their accuracy, the low number of required experimental parameters and their availability as well, ease of implementation, and robustness.

In order to ensure the accuracy of any model and its applicability in the whole fluid region (i.e., in the sub- and supercritical domains), it is necessary to compare its predictions against experimental data. In the context of this thesis, four properties are considered to assess the accuracy of the thermodynamic model: vapor pressure ( $P^{sat}$ ), liquid density ( $\rho_{liq}^{sat}$ ), enthalpy of vaporization ( $\Delta_{vap}H$ ) and saturated-liquid heat capacity ( $c_{P,liq}^{sat}$ ).

Since prior to the implementation of the product design methodology it is necessary to develop an accurate and efficient cubic equation of state, this work was developed in three stages, as shown in [Figure I.2](#), and addressed three fundamental research questions (RQs):

**RQ1:** Which modifications should be made to cubic equations of state in order to accurately reproduce vapor pressures, liquid densities, enthalpies of vaporizations and heat capacities of pure compounds?

**RQ2:** What is the best approach to extend pure-component cubic equations of state to mixtures?

**RQ3:** Which approach from the product-design framework is the most appropriate for the inclusion of thermodynamic, constructional, toxicological, flammability and environmental criteria in the selection of working fluids for CCHP applications?

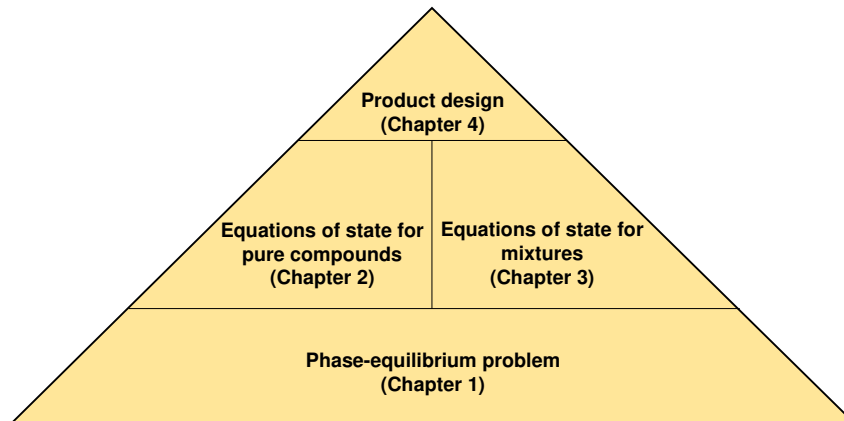


**Figure I.2.** Scheme of the organization of this manuscript.

## Outline

This dissertation consists of four chapters, which present the background of the research work and a summary of the key findings of the publications supporting this thesis. The content of the chapters is summarized as follows:

- Chapter 1** Provides a brief overview of the phase-equilibrium problem, as well as the tools that chemical engineering thermodynamics disposes to solve it, such as equations of state and excess Gibbs energy models.
- Chapter 2** Presents the research work devoted to address RQ1, i.e., the study and improvement of cubic equations of state (CEoS) for pure compounds. In this chapter, the modifications applied to CEoS over the years in order to improve their accuracy are discussed. Finally, the *translated-consistent* Peng-Robinson (*tc*-PR) model is introduced, as well as the suitable parameterization method that should be used in order to obtain a robust and accurate CEoS.
- Chapter 3** Describes the extension of cubic equations of state to mixtures (RQ2). In particular, the extension of the *tc*-PR EoS to mixtures is described. Three different options are studied for this purpose. The performance of the three resulting models is compared against a reference database containing binary-system data for the assessment of their accuracy.
- Chapter 4** Addresses RQ3. The CCHP cycle that has been retained for this thesis is presented. Then, the product-design framework is described as well as the approaches that can be implemented. The results of the selection of promising working fluids for CCHP applications are discussed.

Finally, this manuscript is closed by the general conclusions about the research work carried out in this thesis, as well as some perspectives concerning further work related to cubic equations of state, and the application of the proposed working-fluid selection methodology to more sophisticated energy systems.

# **Chapter 1: The phase-equilibrium problem**



# Chapter 1 : The phase-equilibrium problem

## 1.1 Introduction

Phase-equilibrium thermodynamics aims at setting the relations among various properties such as temperature, pressure and composition that ultimately prevail when two or more phases reach a state of equilibrium wherein all tendency for further change has ceased. It is a subject that is crucial and necessary in order to understand and obtain reliable designs of phase-contacting unit operations such as distillation, absorption, extraction, adsorption and leaching, which are essential unit operations in chemical industry.

In the case of CCHP systems, phase-equilibrium thermodynamics provides information about the state of a stream and establishes the way for the estimation of properties such as enthalpy or entropy, required for the solution of energy balances and the calculation of performance indicators such as thermal efficiency.

In this chapter, a brief overview of the phase-equilibrium problem is presented as well as the tools that chemical engineering thermodynamics disposes to solve it such as equations of state and excess Gibbs energy models. A complete description of the phase-equilibrium problem can be found on references [15–18].

## 1.2 Nature of the problem

The type of problem that phase-equilibrium thermodynamics seeks to solve is illustrated schematically in Figure 1-1.

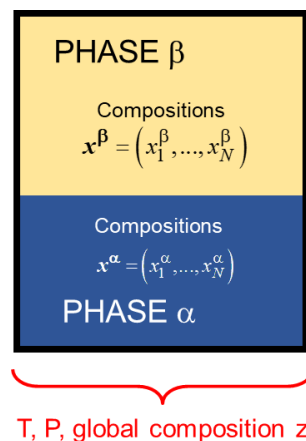


**Figure 1-1.** Illustration of the phase-equilibrium problem.

Consider that two multicomponent phases,  $\alpha$  and  $\beta$ , have reached an equilibrium state at a given temperature  $T$  and mole fractions  $x_1^\alpha, x_2^\alpha, \dots$ , of phase  $\alpha$ . The task, then, could be to find pressure  $P$  of the system and  $x_1^\beta, x_2^\beta, \dots$ , of phase  $\beta$ . The alternative case would be to know pressure  $P$  and  $x_1^\alpha, x_2^\alpha, \dots$ , and search for  $x_1^\beta, x_2^\beta, \dots$ , and  $T$ . The number of intensive properties, i.e., those that are

independent of mass, size, or shape of the phase, that must be specified to fix unambiguously the state of equilibrium is given by the *Gibbs phase rule*. In the absence of chemical reactions, the phase rule writes:

$$\text{Number of independent intensive properties} = \text{Number of components} - \text{Number of phases} + 2 \quad (1.1)$$

For example, for a two-phase system containing two components, the number of independent intensive properties is equal to two. In general, the properties of interest of such a system are reduced to  $x_1^\alpha$ ,  $x_1^\beta$ ,  $T$  and  $P$ <sup>1</sup>. In consequence, two of these variables, any two, must be specified in order to find the remaining ones. At this stage, several questions arise. How can the problem illustrated in [Figure 1-1](#) be solved? What theoretical framework is available to provide a basis for finding a solution? The answers to these questions are given by thermodynamics.

### 1.3 Application of thermodynamics to phase-equilibrium problems

As any other science, in thermodynamics, most of the problems in the real life are solved by describing them in abstract, mathematical terms. In such a way, it is sometimes possible to obtain a simple solution to the problem not in terms of physical reality, but in terms of mathematical variables issued from the abstract description of the real problem. In the case of the phase-equilibrium problem, thermodynamics provides the mathematical framework necessary to obtain an abstract solution to it.

Prausnitz et al. [15] explained that the solution of a phase-equilibrium problem using thermodynamics requires three steps:

- I. The real problem is translated into an abstract, mathematical problem.
- II. A solution is found to the mathematical problem.
- III. The mathematical solution is translated back into physically meaningful terms.

In the paper “On the Equilibrium of Heterogeneous Substances”, published in 1876, J. W. Gibbs [19] introduces the phase rule and thoroughly analysed the phenomenon of equilibrium. He defined the *chemical potential* ( $\mu_i$ ) function and made it possible to achieve the goal of steps I and II. The starting point of Gibbs was the resulting statement of the combination of the first and second law of thermodynamics for an open static system:

$$dU = TdS - PdV + \sum_i \mu_i dn_i \quad (1.2)$$

where  $dU$ ,  $dS$ ,  $dV$  and  $dn_i$  are infinitesimal changes in energy, entropy, volume and the number of moles of component  $i$ , respectively.

The function  $\mu_i$  is an intensive quantity and depends on temperature, pressure and composition. It was expected to consider  $\mu_i$  as a chemical potential since it is the coefficient of  $dn_i$ , just as  $T$  (the coefficient of  $dS$ ) is a thermal potential governing heat transfer and  $-P$  (the coefficient of  $dV$ ) is a

---

<sup>1</sup> Since  $\sum_i x_i = 1$  for each phase,  $x_2^\alpha$  and  $x_2^\beta$  can be expressed with respect to  $x_1^\alpha$  and  $x_1^\beta$ . They are thus non-independent variables.



## 1.4 Equations of state

Formal thermodynamics for calculating fugacities from volumetric data yields to two key equations:

$$\ln \varphi_i = \frac{1}{RT} \int_0^P \left[ \left( \frac{\partial V}{\partial n_i} \right)_{T,P,n_{j \neq i}} - \frac{RT}{P} \right] dP \quad (1.10)$$

and

$$\ln \varphi_i = \frac{1}{RT} \int_V^\infty \left[ \left( \frac{\partial P}{\partial n_i} \right)_{T,V,n_{j \neq i}} - \frac{RT}{V} \right] dV - \ln \left( \frac{Pv}{RT} \right) \quad (1.11)$$

where the fugacity coefficient is defined by

$$\varphi_i \equiv \frac{f_i}{y_i P} \quad (1.12)$$

and  $v = V/n$ . The algebraic relations relating variables  $P$ ,  $T$ ,  $v$  and  $x$  or  $y$  are known as equations of state [16].

The volumetric properties of a pure fluid in a given state are commonly expressed with the molar compressibility factor  $z$ , which can be written as a function of  $T$  and  $P$  or  $T$  and  $v$

$$z \equiv \frac{Pv}{RT} = F_P(T, P) \quad (1.13)$$

$$z = F_v(T, v) \quad (1.14)$$

where  $v$  is the molar volume,  $P$  is the absolute pressure,  $T$  is the absolute temperature, and  $R$  is the universal gas constant. A well-known family of relations  $F_P(T, P)$  or  $F_v(T, v)$  is that of equations of state (EoS). They are classified into pressure- or volume-explicit. Commonly, a user specifies the gas state with  $T$  and  $P$  since these are most easily measured and so Eq. (1.13) is considered most convenient. Nevertheless, if the objective is to describe both gaseous and liquid phases with the same parameters, the required multiplicity of volume roots demands a function of the form (1.14).

The discussion presented hereafter is not comprehensive but aims at presenting the most popular types of EoS.

### 1.4.1 The virial equation of state

The virial equation of state, usually applied for gaseous phases, is a polynomial series in pressure or in inverse volume whose coefficients are functions only of  $T$  for a pure fluid. The consistent forms for the initial terms are

$$z(T, P) = 1 + B(T) \left( \frac{P}{RT} \right) + \left[ C(T) - B(T)^2 \right] \left( \frac{P}{RT} \right)^2 + \dots \quad (1.15)$$

$$z(T, v) = 1 + \frac{B(T)}{v} + \frac{C(T)}{v^2} + \dots \quad (1.16)$$

where coefficient  $B(T)$  is the second virial coefficient,  $C(T)$  is the third virial coefficient, and so on. The second virial coefficient  $B$  is properly evaluated from low-pressure P-V-T data by the definition

$$B(T) = \lim_{\rho \rightarrow 0} \left( \frac{\partial z}{\partial \rho} \right)_T \quad (1.17)$$

where  $\rho = 1/v$ . Similarly, the third virial coefficient must also be evaluated from P-V-T data at low pressures and it is defined by

$$C(T) = \lim_{\rho \rightarrow 0} \frac{1}{2!} \left( \frac{\partial^2 z}{\partial \rho^2} \right)_T \quad (1.18)$$

### 1.4.2 Analytical equations of state

In order to employ the term “analytical” to define an equation of state, it is necessary that the function  $F_v(T, v)$  has powers of  $v$  no higher than quartic. Then, when  $T$  and  $P$  are specified, it is possible to solve for  $v$  analytically. In this dissertation, cubic EoS (CEoS) has special attention because of their widespread use and simple form. In a general form, CEoS can be written as follows

$$P = \frac{RT}{v-b} - \frac{a(T)}{v^2 + ubv + wb^2} \quad (1.19)$$

Or analogously whether the condition  $u^2 - 4w > 0$  is satisfied:

$$P = \frac{RT}{v-b} - \frac{a(T)}{(v-r_1b)(v-r_2b)} \quad (1.20)$$

with

$$\begin{cases} r_1 = \frac{-u - \sqrt{u^2 - 4w}}{2} \\ r_2 = \frac{-u + \sqrt{u^2 - 4w}}{2} \end{cases} \quad (1.21)$$

where parameter  $a$  is a measure of the attractive forces between molecules; parameter  $b$  is the so-called covolume, which attempts to correct the perfect-gas law for the fact that molecules have a non-zero effective volume; and the constants  $u$  and  $w$  are either universal constants (the same values apply to all compounds) or substance-dependent quantities. Cubic equations of state are described in detail in [Chapter 2](#) and [Chapter 3](#).

### 1.4.3 Nonanalytic equations of state

Although the simplicity and robustness of cubic equations of state, there exists property behaviors that cannot be described with high accuracy by them. In order to try to overcome such limitations, different

approaches were considered. Three of them are the BWR/MBWR models, Wagner formulations and Statistical Associating Fluid Theory (SAFT) family of equations of state. Their common characteristic is that they are nonanalytic equations of state.

### **BWR/MBWR and Wagner models**

These equations of state are specific to particular pure substances (or mixtures). They have multiple parameters and are frequently based on expansions of the Helmholtz energy (Span-Wagner, GERG ...); they are applicable to a liquid, a gas or a system in vapor-liquid equilibrium. They are not universal and not adaptable to a specific compound; they generally contain a very high number of component parameters. For example, the NIST (National Institute of Standards and Technology) developed a software program known as REFPROP (Reference Fluid Thermodynamic and Transport Properties Database) which contains specific equations of state for 147 pure substances. In this category of models, it is possible to cite for example the Benedict-Webb-Rubin (BWR) equations of state, Bender, Span-Wagner, GERG-2008.

It should be noted that the great strength of these models is their accuracy whereas their weakness lies in the necessity of disposing of a high number of non-predictable and component-specific input parameters to describe a single species: each pure substance is represented by an equation of state that involves a large number of fitted parameters (generally several dozens). Processing of mixtures also requires knowledge of multiple additional interaction parameters. The use of these models is therefore limited to pure substances and a few mixtures that have previously been extensively measured, which remains an obstacle to their development.

### **Statistical associating fluid theory**

Since the late 1980's, The Statistical Associating Fluid Theory (SAFT) family of equations of state, which has been developed based on the Thermodynamic Perturbation Theory (TPT) has gained considerable popularity in both academia and industry. A large amount of research work has been done over the last almost three decades towards the improvement of SAFT, in order to become more accurate for different types of systems such as strongly polar mixtures, polymers, electrolytes, while last years many applications of SAFT in the oil and gas industry have been reported [20–28].

By extending Wertheim's [29–33] theory, [34,35] and [36,37] developed the Statistical Associating Fluid Theory (SAFT) equation of state. Although SAFT derived equations of state are mathematically complex, the underlying concepts are straightforward. SAFT based equations are constructed by summing intra and inter molecular contributions to the Helmholtz energy. The expression for the  $Tv$ -residual Helmholtz energy ( $a^{res}$ ) is given by:

$$a^{res} = a^{hs} + a^{chain} + a^{disp} + a^{assoc} \quad (1.22)$$

where  $a^{hs}$  is the hard sphere contribution,  $a^{chain}$  is the contribution for chain formation,  $a^{disp}$  is the contribution from dispersion forces, and  $a^{assoc}$  is the contribution coming from association, e.g. hydrogen bonding. Figure 1-2, shows schematically the procedure followed to form a SAFT model molecule.

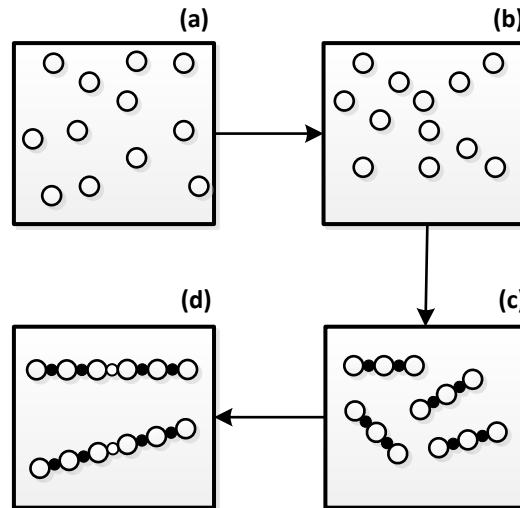


**Figure 1-2.** Schematic representation of the procedure that forms a SAFT model molecule [38]: (a) the reference fluid consists of hard spheres; (b) dispersion forces are added; (c) chain sites are added and chain molecules appear; (d) hydrogen bonding is added and molecules form association complexes through association sites.

Huang and Radosz [36] were the first to propose an engineering formulation of SAFT EoS and used this equation to correlate vapor-liquid equilibria of over 100 real pure fluids. They demonstrated that SAFT was applicable to small, large, polydisperse, and associating molecules over the whole density range. Furthermore, they [37] extended SAFT to mixtures by testing 60 phase equilibrium data sets for both symmetric and asymmetric binary systems, with respect to the size of the molecules, as well as for binary mixtures containing associating compounds. They concluded that the mixing rules for the hard sphere, chain and association terms were not required when using rigorous statistical mechanical expressions. Only the dispersion term required mixing rules, and only one binary temperature-independent parameter was necessary for the representation of the experimental data.

### *The original SAFT EoS*

In the original SAFT [36,37], the hard sphere term is calculated as proposed by Carnahan and Starling [39]:

$$\frac{a^{hs}}{RT} = m \frac{4\eta - 3\eta^2}{(1-\eta)^2} \quad (1.23)$$

where  $m$  is the number of spherical segments per molecule and  $\eta$  is the reduced density.

The chain and association terms are calculated from the following expressions proposed by Chapman et al. [35]:

$$\frac{a^{chain}}{RT} = (1-m) \ln \left[ \frac{1-0.5\eta}{(1-\eta)^3} \right] \quad (1.24)$$

$$\frac{a^{assoc}}{RT} = \sum_{A=1}^M \left[ \ln(X^A) - 0.5X^A \right] + 0.5M \quad (1.25)$$

where  $M$  is the number of association sites per molecule and  $X^A$  is the mole fraction of molecules not bonded at site  $A$ . In Eq. (1.25), the summation is taken over all association sites of the molecule. The quantity  $X^A$  is calculated from the expression:

$$X^A = \left( 1 + N_{Av} \sum_B \rho X^B \Delta^{AB} \right)^{-1} \quad (1.26)$$

where the summation is taken over all sites.  $N_{Av}$  is Avogadro's number,  $\rho$  is the molar density and  $\Delta^{AB}$  is the association strength that is calculated from:

$$\Delta^{AB} = \frac{1 - 0.5\eta}{(1 - \eta)^3} \left( \exp \frac{\varepsilon^{AB}}{kT} - 1 \right) (\sigma^3 \kappa^{AB}) \quad (1.27)$$

where  $\sigma$  is the temperature-independent segment diameter that is calculated by:

$$\sigma = \left( \frac{6\tau}{\pi N_{Av}} u^\infty \right)^{1/3} \quad (1.28)$$

In Eq. (1.28),  $u^\infty$  is the segment volume and  $\tau$  is equal to 0.74048, which corresponds to the packing fraction of a face centered cubic (FCC) lattice. Also,  $\varepsilon^{AB}$  and  $\kappa^{AB}$  in Eq. (1.27) are the association energy and volume parameters.

For the dispersion term, a number of different expressions have been proposed in the various SAFT versions. In the original SAFT of Huang and Radosz [36] the following expression is used:

$$\frac{a^{disp}}{RT} = m \sum_{i=1}^4 \sum_{j=1}^9 D_{ij} \left( \frac{u}{kT} \right)^i \left( \frac{\eta}{0.74048} \right)^j \quad (1.29)$$

where  $u$  is the temperature-dependent dispersion energy of interaction between segments calculated as:

$$u = u^o \left( 1 + \frac{e}{kT} \right) \quad (1.30)$$

where  $u^o$  is the temperature-independent dispersion energy of interaction between segments, and  $e/k$  was set equal to 10 K for all molecules except a few small molecules.

For pure non-associating compounds, three pure-component parameters are utilized in SAFT:  $m$ ,  $u^o/k$ , and  $u^\infty$ , while for self-associating compounds two additional parameters are utilized for each pair of donor-acceptor sites:  $\varepsilon^{AB}$  and  $\kappa^{AB}$ . The resulting (three or more) pure-component parameters are determined by fitting pure compound properties, usually vapor pressures and saturation liquid densities.

For the extension of original SAFT to mixtures, the equation of Mansoori et al. [40] is used for the hard-sphere mixtures, whereas the chain and the association terms are extended to mixtures rigorously [39]. The dispersion term is extended to mixtures by assuming the Van der Waals one-fluid theory approximation. Mixing rules are only needed for  $u/k$  in the dispersion term and they are the following:

$$\frac{u}{k} = \frac{\sum_i \sum_j x_i x_j m_i m_j \left( \frac{u_{ij}}{kT} \right) (u^o)_{ij}}{\sum_i \sum_j x_i x_j m_i m_j (u^o)_{ij}} \quad (1.31)$$

$$(u^o)_{ij} = \left[ \frac{(u^o)_i^{1/3} + (u^o)_j^{1/3}}{2} \right]^3 \quad (1.32)$$

$$u_{ij} = (u_{ii} u_{jj})^{1/2} (1 - k_{ij}) \quad (1.33)$$

where  $k_{ij}$  is a binary adjustable parameter that is determined by fitting binary phase equilibrium data.

For mixtures containing associating compounds [36], the number and type of association sites, i.e., the association scheme of the compound, should be firstly established. For the association term only combining rules for the association parameters are needed when two associating species are present in the mixture:

$$\varepsilon_{ij} = (\varepsilon_{ii} \varepsilon_{jj})^{1/2} \quad (1.34)$$

$$\kappa_{ij}^{AB} = \left[ \frac{(\kappa_{ii}^{AB})^{1/3} + (\kappa_{jj}^{AB})^{1/3}}{2} \right]^3 \quad (1.35)$$

### ***Modifications of the SAFT equation***

Since the original development of SAFT, numerous modifications have been proposed. Excellent reviews on the different variations of SAFT are presented by Economou [41] and Kontogeorgis and Folas [42].

Some of these variations include: the simplified-SAFT [43] that uses a simplification for the dispersion term; the LJ-SAFT [44,45] that accounts explicitly for the repulsive and dispersion interactions using the Lennard-Jones equation as well as for dipole-dipole interactions; the soft-SAFT [46] that uses a Lennard-Jones reference fluid instead of the hard-sphere fluid in the original SAFT as in LJ-SAFT; the SAFT-VR [47] that uses for the dispersion term a square-well potential instead of the hard-sphere and the SAFT-VR-Mie [48,49] that incorporates the variable Mie potential rather than the square-well or Lennard-Jones potentials.

PC-SAFT [50,51] is one of the most successful modifications of the SAFT theory. The main difference between original SAFT and PC-SAFT is on the reference fluid used. Specifically, PC-SAFT uses the hard-chain reference fluid to account for the dispersion interactions unlike SAFT that uses the hard-sphere reference fluid.

## 1.5 Activity-coefficient models

According to the  $\gamma - \phi$  approach (Eq. (1.7)) can be rewritten as

$$x_i \cdot \gamma_{i,liq}(T, P, \mathbf{x}) \cdot P_i^{sat}(T) = P \cdot y_i \cdot \frac{\phi_{i,vap}(T, P, \mathbf{y})}{\phi_i^*(T, P_i^{sat}(T))} \exp\left(\frac{1}{RT} \int_P^{P_i^{sat}(T)} v_{i,liq}^*(T, P) \cdot dP\right) \quad (1.36)$$

This approach can only be implemented at temperatures and pressures lower than the minimal critical temperature and pressure of the components in the mixture since it is necessary to define the vapor pressure  $P_i^{sat}(T)$  for each of them.

Classical thermodynamics provides an expression relating  $\gamma_i$  with  $T$ ,  $P$  and  $\mathbf{z}$ . Such an expression relates the excess molar Gibbs energy of a mixture to the activity coefficient:

$$g^E = RT \sum_i x_i \ln \gamma_i \quad (1.37)$$

It is worth recalling that an excess property,  $m^E$ , is the difference between the property of the real mixture,  $m$ , and the property of the ideal mixture,  $m^{id}$ , at the same temperature, pressure, composition and state of aggregation:

$$m^E \equiv m - m^{id} \quad (1.38)$$

In consequence, excess Gibbs energy of an ideal solution is zero and activity coefficients are equal to unity. The excess Gibbs energy can be represented as the sum of an energetic part, accounting for interactions between molecules, the so-called *residual contribution*  $g_{res}^E$ , and of a term which accounts for molecular size and shape, the combinatorial contribution  $g_{comb}^E$ :

$$g^E = g_{comb}^E + g_{res}^E \quad (1.39)$$

The combinatorial part requires only pure-component parameters, while the residual part contains adjustable parameters, which, at least in principle, are temperature dependent.

Many expressions relating  $g^E$  to composition have been proposed. They are called classically  $g^E$  models or activity-coefficient models. A common feature of such models is that they are pressure-independent. Indeed, all excess Gibbs energy models should theoretically depend on pressure but our current knowledge on liquid theory still lacks of enough accuracy to estimate the influence of the pressure on  $g^E$  models.

$g^E$  models can be classified into purely empirical models and theoretical-based models. The first family of models includes the one- and two-parameter Margules model and the Redlich-Kister model. For binary mixtures, they write:

**One-parameter Margules [52]:**

$$\frac{g^E(T, \mathbf{z})}{RT} = A(T) \cdot z_1 \cdot z_2 \quad (1.40)$$

**Two-parameter Margules [52]:**

$$\frac{g^E(T, \mathbf{z})}{RT} = z_1 z_2 [A_{21}(T)z_1 + A_{12}(T)z_2] \quad (1.41)$$

**Redlich-Kister [53]:**

$$\frac{g^E(T, \mathbf{z})}{RT} = z_1 z_2 \sum_{k=0}^N A_k (z_1 - z_2)^k \quad (1.42)$$

where  $N$  is the polynomial order, and  $A_k$  are adjustable parameters.

The theoretical-based models, in turn, may be purely residual models, purely combinatorial models and models with both the combinatorial and residual contributions. The first category includes the Van Laar, Scatchard-Hildebrand and NRTL models.

**Van Laar [54]:**

For a binary mixture:

$$\frac{g^E(T, \mathbf{z})}{RT} = z_1 z_2 \frac{A_{12}(T)A_{21}(T)}{A_{12}(T)z_1 + A_{21}(T)z_2} \quad (1.43)$$

**Scatchard-Hildebrand [55,56]:**

For a binary mixture:

$$\frac{g^E(T, \mathbf{z})}{RT} = \frac{z_1 v_1^* z_2 v_2^* (\delta_1 - \delta_2)^2}{RT(z_1 v_1^* + z_2 v_2^*)} \quad (1.44)$$

where  $\delta_i$  is the solubility parameter for component  $i$ .

**N.R.T.L (non-randomness two-liquid) [57]:**

The general expression is:

$$\frac{g^E(T, \mathbf{z})}{RT} = \sum_i^{n_c} z_i \frac{\sum_j^{n_c} \tau_{ji} G_{ji} z_j}{\sum_k^N G_{ki} z_k} \quad (1.45)$$

with  $\tau_{ij} = \frac{\Delta g_{ij}}{RT}$  and  $G_{ij} = -\alpha \cdot \tau_{ij}$ , where  $\tau_{ij}$ ,  $\tau_{ji}$  are adjustable parameters and  $\alpha$  accounts for the fact that, due to intermolecular forces, the mixing of molecules is never entirely random.

For a binary mixture:

$$\frac{g^E(T, \mathbf{z})}{RT} = z_1 z_2 \left[ \frac{\tau_{21} G_{21}}{z_1 + z_2 G_{21}} + \frac{\tau_{12} G_{12}}{z_2 + z_1 G_{12}} \right] \quad (1.46)$$

An example of purely combinatorial models is the Flory-Huggins  $g^E$  model.

**Flory-Huggins [58,59]:**

For a binary mixture:

$$\frac{g^E(T, \mathbf{z})}{RT} = z_1 \ln \left( \frac{\phi_1}{z_1} \right) + z_2 \ln \left( \frac{\phi_2}{z_2} \right) \quad (1.47)$$

where  $\phi_i = \frac{z_i v_i^*}{\sum_j z_j v_j^*}$ .

Finally, the  $g^E$  models that consist of combinatorial and residual contributions are:

**Wilson [60]:**

The general expression is:

$$\frac{g^E}{RT} = - \sum_i z_i \ln \left( \sum_j z_j \Lambda_{ij} \right) \quad (1.48)$$

with  $\Lambda_{ij} = \frac{v_j^*}{v_i^*} \exp \left( - \frac{A_{ij}}{RT} \right)$ , and  $\Lambda_{ii} = \Lambda_{jj} = 1$ .

For a binary mixture:

$$\frac{g^E(T, \mathbf{z})}{RT} = -z_1 \ln \left[ z_1 + z_2 \frac{v_2^*}{v_1^*} \exp \left( - \frac{A_{12}}{T} \right) \right] - z_2 \ln \left[ z_2 + z_1 \frac{v_1^*}{v_2^*} \exp \left( - \frac{A_{21}}{T} \right) \right] \quad (1.49)$$

where:

$$\frac{g_{comb}^E(\mathbf{z})}{RT} = z_1 \ln \left( \frac{v_1^*}{z_1 v_1^* + z_2 v_2^*} \right) + z_2 \ln \left( \frac{v_2^*}{z_1 v_1^* + z_2 v_2^*} \right) \quad (1.50)$$

and

$$\begin{aligned} \frac{g_{res}^E(T, \mathbf{z})}{RT} = & -z_1 \ln \left[ \frac{z_1 v_1^*}{z_1 v_1^* + z_2 v_2^*} + \frac{z_2 v_2^*}{z_1 v_1^* + z_2 v_2^*} \exp \left( - \frac{A_{12}}{T} \right) \right] \\ & - z_2 \ln \left[ \frac{z_2 v_2^*}{z_1 v_1^* + z_2 v_2^*} + \frac{z_1 v_1^*}{z_1 v_1^* + z_2 v_2^*} \exp \left( - \frac{A_{21}}{T} \right) \right] \end{aligned} \quad (1.51)$$

**UNIQUAC (UNIversal QUAsi Chemical) [61]:**

The general expression is:

$$\frac{g^E(T, \mathbf{z})}{RT} = \sum_i z_i \ln \left( \frac{\Phi_i}{z_i} \right) + \frac{z}{2} \sum_i q_i z_i \ln \left( \frac{\theta_i}{\Phi_i} \right) - \sum_i q_i z_i \ln \left( \sum_j \theta_j \tau_{ji} \right) \quad (1.52)$$

with  $\theta_i = \frac{x_i q_i}{\sum_{j=1}^{n_c} x_j q_j}$ ,  $\varphi_i = \frac{x_i r_i}{\sum_{j=1}^{n_c} x_j r_j}$ .  $r_i$  and  $q_i$  are the molecular volume and surface area (called Van der

Waals volume and area).

The combinatorial contribution is expressed as

$$\frac{g_{comb}^E(\mathbf{z})}{RT} = \sum_i^{n_c} z_i \ln \left( \frac{\Phi_i}{z_i} \right) + \frac{z}{2} \sum_i^{n_c} q_i z_i \ln \left( \frac{\theta_i}{\Phi_i} \right) \quad (1.53)$$

and the residual part is given by

$$\frac{g_{res}^E(T, \mathbf{z})}{RT} = - \sum_i^{n_c} q_i z_i \ln \left( \sum_j^{n_c} \theta_j \tau_{ji} \right) \quad (1.54)$$

### **UNIFAC (UNIversal quasi-chemical Functional group Activity Coefficient) [62]:**

The general expression is:

$$\frac{g^E(T, \mathbf{z})}{RT} = \sum_i^{n_c} z_i \ln \left( \frac{\Phi_i}{z_i} \right) + \frac{z}{2} \sum_i^{n_c} q_i z_i \ln \left( \frac{\theta_i}{\Phi_i} \right) + \sum_i^{n_c} z_i \ln \gamma_{i,res} \quad (1.55)$$

The combinatorial contribution has the same form as that of the UNIQUAC model (Eq. (1.53)). In addition,  $\theta_i$  and  $\varphi_i$  are calculated identically as done for the UNIQUAC model. In contrast, the pure-component parameters  $r_i$  and  $q_i$  are calculated by a group-contribution method [16]:

$$r_i = \sum_k^{N_g} \nu_k^{(i)} R_k \quad (1.56)$$

$$q_i = \sum_k^{N_g} \nu_k^{(i)} Q_k \quad (1.57)$$

where  $N_g$  is the number of functional groups of molecule  $I$ ,  $\nu_k^{(i)}$  is the number of functional groups of type  $k$  in molecule  $I$ , and  $R_k$  and  $Q_k$  are the volume and surface area parameters of each functional group  $k$ .

The residual part is given by

$$\frac{g_{res}^E(T, \mathbf{z})}{RT} = \sum_i^{n_c} z_i \ln \gamma_{i,res} \quad (1.58)$$

with:

$$\left\{ \begin{array}{l}
\ln \gamma_{i,res} = \sum_k^{N_g} v_k^{(i)} \left[ \ln \Gamma_k - \ln \Gamma_k^{(i)} \right] \\
\ln \Gamma_k = Q_k \left[ 1 - \ln \left( \sum_j^{N_g} \Theta_j \Psi_{kj} \right) - \sum_j^{N_g} \frac{\Theta_j \Psi_{kj}}{\sum_l^{N_g} \Theta_l \Psi_{lj}} \right] \\
\Theta_j = \frac{X_j Q_j}{\sum_l^{N_g} X_l Q_l} \\
X_j = \frac{\sum_i^{n_c} z_i v_j^{(i)}}{\sum_i^{n_c} z_i \sum_l^{N_g} v_l^{(i)}} \\
\Psi_{kj} = \exp \left( -\frac{a_{kj}}{RT} \right)
\end{array} \right. \quad (1.59)$$

where  $a_{kj}$  and  $a_{jk}$  are obtained from a database using a wide range of experimental results.

## 1.6 Concluding remarks

This chapter on the phase-equilibrium problem has presented no more than a brief introduction to a very broad subject. The objective was to show the crucial role of equations of state and  $g^E$  models in phase-equilibrium calculations since they link abstract, mathematical terms with experimentally measurable quantities such as temperature or pressure, which are much closer to our physical senses than the abstract concept of chemical potential.

Among the available models, EoS with a high number of parameters such as EoS explicit in Helmholtz energy or the modified Benedict-Webb-Rubin (MBWR) EoS as used by the NIST, lead to the highly accurate reproduction of thermodynamic properties. Nevertheless, they are available only for 147 pure fluids.

Since one of the main objectives of this dissertation is to screen a large number of fluids suitable for CCHP applications, cubic equations of state are retained for the estimation of saturation and caloric properties required for the selection of the working fluid of CCHP systems and the calculation of performance indicators since their main advantage is their capacity to accurately correlate (with a few-percent deviation, as shown in next chapters) saturated vapor pressures, liquid densities, enthalpies of vaporization and heat capacities of pure substances.

Finally,  $g^E$  models will receive special attention since they are incorporated in advanced mixing rules for the extension of cubic equation of state to mixtures.

## **Chapter 2: Equations of state for pure compounds**



## Chapter 2 : Equations of state for pure compounds

### 2.1 Introduction

Commonly, equations of state are developed initially for pure substances. Then, they are extended to mixtures by using proper mixing and combining rules. In this dissertation, it was decided to follow the same methodology. This chapter is thus devoted to the study and improvement of cubic equations of state (CEoS) for pure compounds. The question of mixtures is addressed in [Chapter 3](#).

This chapter provides the description of the modifications that have been introduced into CEoS over the years in order to improve the prediction of vapor pressures, liquid densities, enthalpies of vaporization and saturated-liquid heat capacities. Finally, the research work of this thesis devoted to address RQ1 is presented.

### 2.2 Generalities of cubic equations of state for pure compounds

The Van der Waals (VdW) equation of state [63], proposed in 1873, is the first, simplest and best-known cubic equation of state. It is written:

$$P(T, v) = \frac{RT}{v-b} - \frac{a_c}{v^2} \quad \text{with:} \quad \begin{cases} a_c = \frac{27 R^2 T_{c,\text{exp}}^2}{64 P_{c,\text{exp}}} \\ b = \frac{1}{8} \frac{RT_{c,\text{exp}}}{P_{c,\text{exp}}} \end{cases} \quad (2.1)$$

where  $a_c$  is the constant attractive parameter and parameter  $b$  is the so-called covolume, which attempts to correct the perfect-gas law for the fact that molecules have a non-zero effective volume. It is a so-called 2-parameter CEoS because its application to a pure component requires the preliminary knowledge of two experimental component-dependent parameters (the critical temperature  $T_{c,\text{exp}}$  and pressure  $P_{c,\text{exp}}$ ).

One of the strengths of the theory proposed by Van der Waals is the independent treating of **repulsive** and **attractive** forces, identified in Eq. (2.1) by the terms  $P_{rep}$  and  $P_{att}$ , respectively. Moreover, the VdW EoS is capable of representing vapor-liquid coexistence. This equation is able to predict fluid behavior above and below the critical point, as well as mixture phenomena such as critical azeotropy or retrograde condensation.

Although all the qualitatively capabilities of the vdW EoS, it was not considered as accurate enough for process design applications. In consequence, different modifications have been introduced into the VdW EoS over the years. In a general form, the CEoS resulting from such modifications can be written as follows:

$$P = \frac{RT}{v-b} - \frac{a(T)}{v^2 + ubv + wb^2} \quad (2.2)$$

where the constants  $u$  and  $w$  are either universal constants (the same values apply to all compounds) or substance-dependent quantities. The temperature-dependent  $a(T)$  parameter is classically written as:

$$a(T) = a_c \cdot \alpha(T) \quad (2.3)$$

It is the product of the value of the attractive parameter at the critical temperature ( $a_c$ ) multiplied by a so-called  $\alpha$ -function, which is dimensionless. Such an  $\alpha$ -function has a great influence on the calculated vapor-liquid equilibrium properties like vapor pressure, enthalpy of vaporization and saturated-liquid heat capacity. On the other hand, the volume function of the attractive term ( $v^2 + ubv + wb^2$ ) and, in particular, the numerical values assigned to  $u$  and  $w$ , govern essentially the accuracy of the predicted volumetric properties.

As a matter of fact, the two EoS which received most attention in the last 50 years are those proposed by Soave [64] (he introduced the so-called Soave-Redlich-Kwong EoS denoted SRK) and Peng-Robinson [65–67] (PR). For a given pure component, such modern EoS require the specification of three macroscopic properties ( $T_{c,\text{exp}}$ ,  $P_{c,\text{exp}}$  and  $\omega_{\text{exp}}$ ) and they thus obey a 3-parameter corresponding states principle [68,69]. In this dissertation, they are simply referred as 3-parameter EoS.

The SRK EoS is characterized by  $u = 1$ ,  $w = 0$  and the use of the so-called Soave  $\alpha$ -function [64]. It is defined by:

$$P(T, v) = \frac{RT}{v-b} - \frac{a_c \cdot \alpha(T)}{v(v+b)} \left\{ \begin{array}{l} \alpha(T) = \left[ 1 + m \left( 1 - \sqrt{T/T_c} \right) \right]^2 \\ m = 0.480 + 1.574\omega_{\text{exp}} - 0.176\omega_{\text{exp}}^2 \\ a_c = \Omega_a \frac{R^2 T_{c,\text{exp}}^2}{P_{c,\text{exp}}} \\ b = \Omega_b \frac{RT_{c,\text{exp}}}{P_{c,\text{exp}}} \\ \Omega_a = \frac{1}{9(\sqrt[3]{2}-1)} \approx 0.42748 \\ \Omega_b = \frac{\sqrt[3]{2}-1}{3} \approx 0.08664 \\ z_c = 1/3 \end{array} \right. \quad (2.4)$$

In turn, Peng and Robinson [65] selected  $u = 2$  and  $w = -1$ . The PR EoS expression is:

$$P(T, v) = \frac{RT}{v-b} - \frac{a_c \cdot \alpha(T)}{v(v+b) + b(v-b)} \quad \left\{ \begin{array}{l} \alpha(T) = \left[ 1 + m \left( 1 - \sqrt{T/T_c} \right) \right]^2 \\ m = 0.37464 + 1.54226\omega_{\text{exp}} - 0.26992\omega_{\text{exp}}^2 \\ a_c = \Omega_a \frac{R^2 T_{c,\text{exp}}^2}{P_{c,\text{exp}}} \\ b = \Omega_b \frac{RT_{c,\text{exp}}}{P_{c,\text{exp}}} \\ X = \left[ 1 + \sqrt[3]{4 - 2\sqrt{2}} + \sqrt[3]{4 + 2\sqrt{2}} \right]^{-1} \approx 0.25308 \\ \Omega_a = \frac{8(5X + 1)}{49 - 37X} \approx 0.45724 \\ \Omega_b = \frac{X}{X + 3} \approx 0.07780 \\ z_c = 1/(X + 3) \approx 0.3074 \end{array} \right. \quad (2.5)$$

After Soave's and Peng and Robinson's contribution, the trends in research on cubic EoS have followed two main routes: 1) modifications of the  $\alpha$ -function, and 2) modifications of the volumetric function included in the attractive term. Such modifications are discussed in Sections 2.2.1 and 2.2.2. It is worth noting that the review by Valderrama [70] provides a wide overview of the CEoS modifications.

A less discussed point in literature but extremely important for the performances of EoS is the *parameterization method*. Equations of state (EoS) for pure fluids contain two types of parameters: those fixed by the theoretical foundations and those that are component-dependent. Typically, the pure-component parameters are either evaluated by regression on vapor-pressure and saturated liquid density data or are determined from critical coordinates and acentric factor data. The parameterization method consists in attributing numerical values to component-dependent parameters.

In the case of CEoS, the covolume ( $b$ ) and the critical value of the attractive parameter ( $a_c$ ) of cubic EoS (CEoS) for pure compounds are conventionally determined from the knowledge of the experimental critical temperature ( $T_{c,\text{exp}}$ ) and pressure ( $P_{c,\text{exp}}$ ) in order the model exactly reproduces such values. The acentric factor ( $\omega_{\text{exp}}$ ) is usually added as a third parameter in order to improve the correlation of vapor pressures. The open literature highlights that other parameterization methods are only used on rare occasions so that their influence on model performances has seldom been assessed. However, it is possible to cite Ting et al. [20], Voutsas et al. [71] or Alfradique and Castier [72] who fit the three pure-component parameters ( $b$ ,  $a_c$  and  $m_{\text{Soave}}$ ) for the Peng-Robinson [65,67] EoS to saturated liquid densities and vapor pressures. They got accurate correlation of pure fluid properties and were able to satisfactorily describe mixtures of alkanes. More recently, Segura et al. [73] proposed a more sophisticated technique for parameterizing CEoS. They demonstrated that accurate densities can be obtained with CEoS but the price to pay is an overestimation by the model of the experimental critical pressure and temperature. Llovel et al. [74] explained that such an overestimation is opportune for predicting the critical region by means of the crossover correction [75–77].

The impact of the parameterization method on the performances of CEoS and SAFT-type EoS is discussed in [Publication I](#). Two parameterization methods were tested:

- **Parameterization method 1 (P1):** the three input parameters are constrained to exactly reproduce  $T_{c,\text{exp}}$ ,  $P_{c,\text{exp}}$  and a second point of the vapor-pressure curve by means of the acentric factor (i.e., the vapor pressure at a reduced temperature equal to 0.7).
- **Parameterization method 2 (P2):** the three input parameters are fit to vapor-pressure ( $P^{\text{sat}}$ ), enthalpy of vaporization ( $\Delta_{\text{vap}}H$ ), saturated-liquid heat-capacity ( $c_{p,\text{liq}}^{\text{sat}}$ ) and liquid molar volume ( $v_{\text{liq}}^{\text{sat}}$ ) data so that the model is not constrained to pass through the experimental critical coordinates ( $T_{c,\text{exp}}$ ,  $P_{c,\text{exp}}$ ).

In [Publication I](#), it is shown that vapor pressures, enthalpies of vaporization and saturated-liquid heat capacities are not impacted by the change of parameterization method. Nevertheless, it is impossible to obtain simultaneously accurate prediction of the critical coordinates (especially critical pressure) and liquid densities with a CEoS or a SAFT-type EoS. In particular, it is possible to highlight the antagonism between the reproduction of the critical pressure and liquid densities. Therefore, this duality imposes a choice. One option is to have an accurate reproduction of liquid densities by using the parameterization method P2 and try to correct the calculation of critical pressures. The other option is to exactly reproduce the critical point by using the parameterization method P1 and try to correct liquid densities.

Solution 1 can be considered but a crossover approach for the correction of the critical temperature and pressure should be used. For its implementation, at least two additional parameters per pure component are required. In order to determine them experimental data near the critical region must be available. On the contrary, concepts such as volume translation make the improvement of liquid densities possible when parameterization P1 (the classical one for CEoS) is implemented. In the case of this dissertation, it was decided to force  $a_c$  and  $b$  parameters to exactly reproduce  $T_{c,\text{exp}}$ ,  $P_{c,\text{exp}}$ . Then, our work was devoted to study of the influence of  $\alpha$ -functions and the volumetric function and their parameterization on the performances of CEoS. This is summarized in [Publication II](#) to [Publication IV](#).

### 2.2.1 Modifications of the $\alpha$ -function

One of the most influential contributions in the prediction of vapor pressures of non-polar and slightly polar compounds was the introduction in 1972 of the Soave  $\alpha$ -function [64]. For a given pure compound (characterized by its acentric factor  $\omega_{\text{exp}}$  and its critical temperature  $T_{c,\text{exp}}$ ), it is expressed as:

$$\alpha_{\text{Soave}}(T_r, \omega_{\text{exp}}) = \left[ 1 + m(\omega_{\text{exp}}) \cdot (1 - \sqrt{T_r}) \right]^2 \quad (2.6)$$

with

$$m = A + B\omega_{\text{exp}} + C\omega_{\text{exp}}^2 \quad (2.7)$$

$T_r = T/T_{c,\text{exp}}$  is the reduced temperature;  $A$ ,  $B$  and  $C$  are universal constants which depend on the selected EoS.

Over the years, different expressions of the  $\alpha$ -functions have been introduced. They can be classified depending on their:

- 1) mathematical form (polynomial or exponential);
- 2) the unicity of their formulation (piecewise or overall temperature domain);
- 3) and their scope (generalized or component-dependent).

Table 2-1 contains the classification according to these three criteria of a dozen of  $\alpha$ -functions implemented in commercial process simulation software.

Based on the first criterion,  $\alpha$ -functions inspired by the Soave formulation are called polynomial functions as they are polynomials of the square-root of the reduced temperature. Such functions present a drawback related to the fact that they may diverge at very high temperatures [16]. To overcome this limitation, some authors proposed exponential  $\alpha$ -functions characterized by being positive and decreasing functions throughout the whole temperature domain.

Concerning the unicity criterion, an overall  $\alpha$ -function is valid for the whole temperature range. On the contrary, a piecewise  $\alpha$ -function consists of two sub-functions, one for the subcritical domain and another one for the supercritical region. Although this approach improves accuracy on vapor pressure predictions, it raises a non-negligible issue related with the fact that continuity of the first and second derivatives of the  $\alpha$ -function at the critical temperature must be enforced [78]. This is necessary to guarantee that calculated residual enthalpies and heat capacities are continuous functions at the critical temperature.

Finally, the criterion related to the scope of  $\alpha$ -functions refers to the universality of their parameters, i.e., such parameters are universal (or generalized) constants or component-dependent values. The coefficients of the generalized  $\alpha$ -functions are usually determined using correlations that only depend on the acentric factor ( $\omega$ ), while the parameters of the component-dependent  $\alpha$ -functions must be regressed, component by component, from experimental data. It is worth noting that the generalized  $\alpha$ -functions, although less accurate than the component-dependent  $\alpha$ -functions, are extremely useful when experimental data to fit the specific parameters of a given  $\alpha$ -function are not available. Moreover, generalized  $\alpha$ -functions are easy to implement because the acentric factor is known for thousands of pure components or can be estimated by well-established correlations or group-contribution methods.



**Table 2-1.** Classification of  $\alpha$ -functions commonly implemented in process simulation software.

		<b>Polynomial</b>	<b>Exponential</b>	<b>Polynomial &amp; Exponential</b>
<b>Generalized <math>\alpha</math>-functions</b>	<b>T-overall formulation</b>	Soave (1972) [64] $\alpha(T) = [1 + m(\omega) \cdot (1 - \sqrt{T_r})]^2$ $m_{RK}(\omega) = 0.480 + 1.574\omega - 0.176\omega^2$ $m_{PR}(\omega) = 0.37464 + 1.54226\omega - 0.26992\omega^2$	Trebble-Bishnoi [79] $\alpha(T) = \exp[L(1 - T_r)]$ For alkanes, water and CO <sub>2</sub> : If $\omega \leq 0.4$ ; $L = 0.418 + 1.58\omega - 0.580\omega^2$ If $\omega > 0.4$ ; $L = 0.212 + 2.20\omega - 0.831\omega^2$	N.A.
	<b>Piecewise</b>	N.A.	Twu (1995) [80,81] $\alpha(T) = \alpha^{(0)} + \omega[\alpha^{(1)} - \alpha^{(0)}]$ $\alpha^{(0)} = T_r^{N^{(0)}} [M^{(0)} - 1] \exp\left[L^{(0)}(1 - T_r^{M^{(0)}N^{(0)}})\right]$ $\alpha^{(1)} = T_r^{N^{(1)}} [M^{(1)} - 1] \exp\left[L^{(1)}(1 - T_r^{M^{(1)}N^{(1)}})\right]$ where $L^{(i)}$ , $M^{(i)}$ , $N^{(i)}$ are domain-specific parameters.	
<b>Component-dependent <math>\alpha</math>-functions</b>	<b>T-overall formulation</b>	Soave (1984) [82] $\alpha(T) = 1 + (1 - T_r) \left( a + \frac{b}{T_r} \right)$	Twu (1988) [83] $\alpha(T) = T_r^{2(M-1)} \exp[L(1 - T_r^{2M})]$	Melhem-Saini-Goodwin [84] $\alpha(T) = \exp\left[m(1 - T_r) + n(1 - \sqrt{T_r})^2\right]$
		Gibbons-Laughton [85] $\alpha(T) = 1 + X(T_r - 1) + Y(\sqrt{T_r} - 1)$	Twu (1991) [86] $\alpha(T) = T_r^{N(M-1)} \exp[L(1 - T_r^{MN})]$	
			Trebble-Bishnoi [87] $\alpha(T) = \exp[L(1 - T_r)]$	

<b>Component-dependent <math>\alpha</math>-functions</b>	<b>Piecewise</b>	<p>Stryjek-Vera [88]</p> $\alpha(T) = \left[1 + \kappa \cdot (1 - \sqrt{T_r})\right]^2$ $\kappa = \kappa_0 + \kappa_1 (1 + \sqrt{T_r})(0.7 - T_r)$ $\kappa_0 = 0.378893 + 1.4897153\omega - 0.17131848\omega^2 + 0.0196554\omega^3$ $\begin{cases} \kappa_1(T \leq 0.7T_c) \neq 0 \\ \kappa_1(T > 0.7T_c) = 0 \end{cases}$	N.A.	<p>Boston-Mathias [89]</p> $\begin{cases} \alpha_{sub}(T) = \alpha(T_r \leq 1) = \alpha_{Soave} \left[1 + m \cdot (1 - \sqrt{T_r})\right]^2 \\ \alpha_{sup}(T) = \alpha(T_r > 1) = \exp\left[L(1 - T_r^\gamma)\right] \end{cases}$ <p>with <math>\begin{cases} L = \frac{2m}{1+m} \\ \gamma = 1 + \frac{m}{2} \end{cases}</math></p>
		<p>Mathias-Copeman [90]</p> $\alpha(T) = \left[ \begin{array}{l} 1 + c_1(1 - \sqrt{T_r}) + c_2(1 - \sqrt{T_r})^2 \\ + c_3(1 - \sqrt{T_r})^3 \end{array} \right]^2$ $\begin{cases} \text{if } T_r \leq 1, \text{ then } c_1 \neq 0; c_2 \neq 0; c_3 \neq 0 \\ \text{if } T_r > 1, \text{ then } c_1 \neq 0; c_2 = c_3 = 0 \end{cases}$		<p>Mathias [91]</p> $\begin{cases} \alpha_{sub}(T) = \alpha(T_r \leq 1) = \alpha_{Soave} \left[ \begin{array}{l} 1 + m \cdot (1 - \sqrt{T_r}) - \\ p(1 - T_r)(0.7 - T_r) \end{array} \right]^2 \\ \alpha_{sup}(T) = \alpha(T_r > 1) = \left[ \exp\left[L(1 - T_r^\gamma)\right] \right]^2 \end{cases}$ <p>with <math>\begin{cases} L = 1 + \frac{m}{2} + 0.3p \\ \gamma = \frac{L-1}{L} \end{cases}</math></p>

### 2.2.2 Modifications of the volumetric function

To parameterize the volumetric function of CEoS, two options are on the table. The first option is to consider  $u$  and  $w$  as universal (component-independent) constants. By doing so, the critical compressibility factor returned by the EoS ( $z_c^{EoS}$ ) is the same for all components. However, known experimental values of  $z_c$  range between 0.0144 (for magnesium oxide) and 0.637 (for triethyl phosphate); therefore, by selecting this first option, the predicted saturated liquid densities, and particularly those in the critical region, are inevitably going to deviate from their experimental values. However, to the best of our knowledge, a systematic study of how the selection of  $u$  and  $w$  values (that can be chosen in a very large range of values) influence the accuracy of CEoS for property predictions was never conducted. The second option is to consider  $u$  and  $w$  as component-dependent factors. A first possibility is to correlate  $u$  and  $w$  to a readily available property like the acentric factor. Alternatively, the volume-translation concept, as initially developed by P eneloux et al. [92], can be used: the addition of a component-specific volume translation parameter entails that the  $u$  and  $w$  parameters become component-specific themselves.

An overview of the various modifications operated on the volume function of the attractive term of CEoS is presented in [Publication IV](#).

## 2.3 Translated and consistent CEoS

As stated before, this chapter is devoted to the study and improvement of cubic equations of state (CEoS) for pure compounds. To achieve this, two concepts have been integrated to the classic definition of CEoS: the consistency and the volume-translation concepts. This section deals with the inclusion of these concepts in CEoS, such as Peng-Robinson, yielding to the *translated-consistent* PR model.

### 2.3.1 The consistency concept

As seen in [Section 2.2.1](#),  $\alpha$ -functions may have different formulations or include more parameters in order to reach higher accuracy on the reproduction of vapor pressures. Nevertheless, as stated by Poling et al. [16], most of the  $\alpha$ -functions presented in the literature have been developed without evaluating their predictive capability in the supercritical domain. Moreover, as studied by Le Guennec et al. [93], some  $\alpha$ -functions may lead to low-accuracy prediction of binary phase diagrams involving at least one supercritical compound, as well as improper variations of pure-component supercritical properties with respect to temperature. To overcome these problems, Le Guennec et al. defined a “consistency test” with the requirements that are absolutely necessary to get physically meaningful behaviors in both the subcritical and supercritical domains. The consistency test imposes that  $\alpha$ -functions must:

- I. Be of class  $C^2$ , i.e., their first  $(d\alpha/dT)$  and second  $(d^2\alpha/dT^2)$  derivatives must exist and must be continuous at any temperature.
- II. Be positive at any temperature  $(\alpha(T) \geq 0)$ .
- III. Be monotonically decreasing for any temperature value  $(d\alpha/dT \leq 0)$ .
- IV. Be convex for any temperature value  $(d^2\alpha/dT^2 \geq 0)$ .
- V. Verify  $d^3\alpha/dT^3 \leq 0$  at any temperature.

Le Guennec et al. [93] tested whether 12  $\alpha$ -functions, generally available in process simulation software, were or not able to pass the proposed consistency test in Eq. (2.8). They found that eight over twelve of these well-known  $\alpha$ -functions (Soave 1972 [64], Soave 1984 [82], Gibbons-Laughton [85], Stryjek-Vera [88], Boston-Mathias [89], Mathias-Copeman [90], Mathias [91], Twu 1995 [80,81]) failed the consistency test whichever the values of their parameters. The four remaining  $\alpha$ -functions (Trebble-Bishnoi [79], Melhem-Saini-Goodwin [84], Twu 1988 [83], Twu 1991 [86]) passed the test but only if constraints were added to their parameters. Among them, the 3-parameter Twu91  $\alpha$ -function

$$\alpha(T_r) = T_r^{N(M-1)} \exp\left[L(1 - T_r^{MN})\right] \quad (2.9)$$

was judged to exhibit the best tradeoff between complexity and flexibility. For these reasons, Le Guennec et al. [94] decided to implement it in the development of the *translated-consistent* version of the PR EoS (*tc-PR*).

### 2.3.2 The volume-translation concept

As stated in the previous section, the volume-translation concept is a way to make  $u$  and  $w$  parameters component-specific. Jaubert et al. [95] explained that by solving a Van der Waals (VdW)-type EoS (SRK, PR ...) at given T and P, the calculated molar volume, noted  $v_o$ , is generally notably different from the corresponding experimental value. As a first example, it is known by experience that the volumes returned by the SRK EoS are generally too large and they thus need to be reduced by a quantity  $c$  (the volume correction) in order to get a new volume  $v_t$  closer to the experimental value than  $v_o$ . The subscripts  $o$  and  $t$  refer to *original* (i.e. untranslated) and to *translated* equations of state, respectively. As a second example, depending on the studied component, molar volumes returned by the PR EoS are either too large or too small: they thus need to be either reduced or enlarged and the volume correction  $c$  is either positive or negative.

By definition of the volume translation  $c$ , the original and translated molar volumes are linked by:

$$v_t = v_o - c \quad (2.10)$$

Consequently, it is possible to assert that obtaining a consistent translated EoS from an original untranslated equation just consists in replacing  $v_o$  by  $(v_t + c)$  within the untranslated expression.

Mathematically speaking, this translation is thus defined by the following equation:

$$\underbrace{P_t(T, v_t)}_{\substack{\text{mathematical} \\ \text{expression of} \\ \text{the translated EoS}}} = P_o(T, v_t + c) \quad (2.11)$$

Since the original and translated states of the considered pure fluid have the same pressure and temperature (the two states only differ by the value of the molar volume), one has:

$$\left\{ \begin{array}{l} P = \underbrace{P_t(T, v_t)}_{\substack{\text{value of the pressure} \\ \text{returned by the translated} \\ \text{EoS (the temperature is T} \\ \text{and the molar volume } v_t)}} = \underbrace{P_o(T, v_o)}_{\substack{\text{value of the pressure} \\ \text{returned by the original} \\ \text{EoS (the temperature is T} \\ \text{and the molar volume } v_o)}} \\ v_t = v_o - c \end{array} \right. \quad (2.12)$$

Let us take as an example, the Van der Waals EoS. The original equation writes:

$$P_o(T, v_o) = \frac{RT}{v_o - b_o} - \frac{a}{v_o^2} \quad (2.13)$$

Consequently, the translated form is:

$$P_t(T, v_t) = \frac{RT}{(v_t + c) - b_o} - \frac{a}{(v_t + c)^2} \quad (2.14)$$

According to Eq. (2.12) and as illustrated in Figure 2-1, the Péneloux-type volume correction corresponds to a translation of the whole original P-v isotherm (of the amount  $-c$ ) along the volume axis.

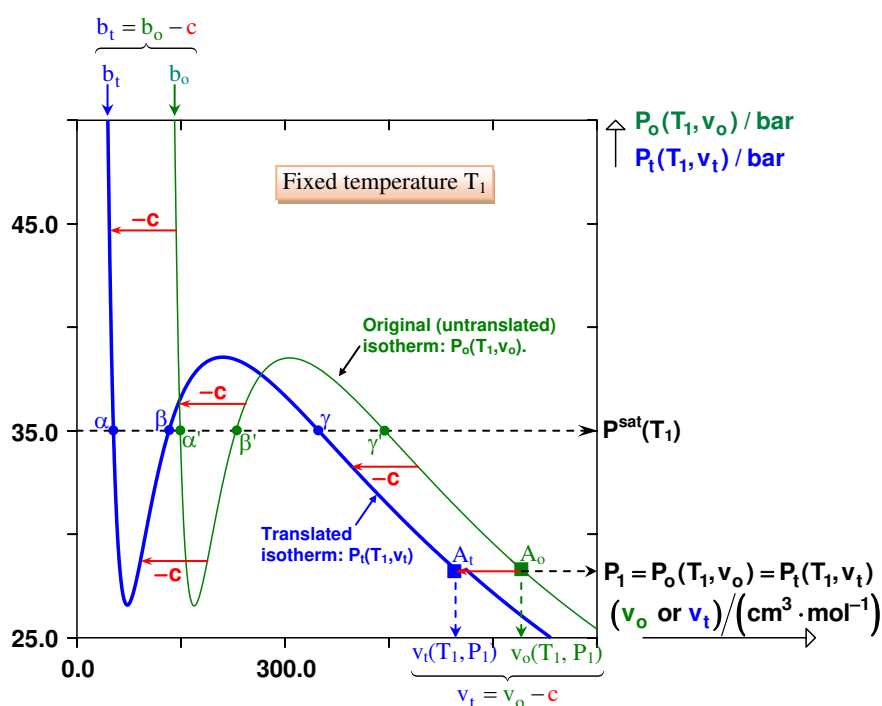


**Figure 2-1.** Graphical illustration of the Péneloux-type volume translation concept.

One of the key assets of the volume-translation concept is that if it is temperature-independent, the calculation of vapor pressures, enthalpies of vaporization and saturated-liquid heat capacities remains unaffected [95]. In consequence, the problem of reproducing  $P^{sat}$ ,  $\Delta_{vap}H$  and  $c_{P,liq}^{sat}$  by modifying the  $\alpha$ -function can be uncoupled from that of reproducing experimental liquid density data.

### 2.3.3 Translated-consistent version of the Peng-Robinson EoS

As presented in Section 2.2, Peng and Robinson selected  $u = 2$ ,  $w = -1$  and a Soave-type  $\alpha$ -function. Such an equation of state has constant ( $u, w$ ) values and a generalized  $\alpha$ -function. From the standpoint of the  $\alpha$ -function, instead of using the Soave-type function, consider the highly flexible and component-dependent Twu91  $\alpha$ -function (Eq. (2.9)).

If parameters ( $L, M, N$ ) are regressed in order to fulfill all of the conditions reported in Eq. (2.8), the Twu91  $\alpha$ -function becomes *consistent*. In addition, consider that the substance-dependent volume-translation parameter,  $c$ , is determined, component by component, in order that the *translated* EoS exactly reproduces the experimental saturated liquid volume at a reduced temperature of 0.8, [ $v_{liq,exp}^{sat}(T_r = 0.8)$ ], that is:

$$c = v_{liq}^{sat,u-CEoS}(T_r = 0.8) - v_{liq,exp}^{sat}(T_r = 0.8) \quad (2.15)$$

where  $v_{liq}^{sat,u-CEoS}(T_r = 0.8)$  is the molar volume calculated with the original (*untranslated*) CEoS at  $T_r = 0.8$ . The implementation of these concepts along with the Peng-Robinson EoS gave birth to the *translated-consistent* Peng-Robinson (*tc-PR*) model:

$$P(T, v) = \frac{RT}{v + c - b} - \frac{a_c \cdot \alpha(T_r)}{(v + c)(v + c + b) + b(v + c - b)}$$

$$\text{with: } \begin{cases} \alpha(T_r) = T_r^{N(M-1)} \exp[L(1 - T_r^{MN})] \\ c = v_{liq}^{sat,u-PR}(T_r = 0.8) - v_{liq,exp}^{sat}(T_r = 0.8) \\ \eta_c = \left[1 + \sqrt[3]{4 - 2\sqrt{2}} + \sqrt[3]{4 + 2\sqrt{2}}\right]^{-1} \approx 0.25308 \\ a_c = \frac{40\eta_c + 8}{49 - 37\eta_c} \frac{R^2 T_{c,exp}^2}{P_{c,exp}} \approx 0.45724 \frac{R^2 T_{c,exp}^2}{P_{c,exp}} \\ b = \frac{\eta_c}{\eta_c + 3} \frac{RT_{c,exp}}{P_{c,exp}} \approx 0.07780 \frac{RT_{c,exp}}{P_{c,exp}} \end{cases} \quad (2.16)$$

Such a model was the culminating point of years of research on the field of cubic equations of state. The detailed development of the model is presented in the work of Le Guennec et al. [96]. They determined the  $L, M, N$  parameters for 1116 compounds by minimizing an objective function which considered the deviations on either vapor pressures or enthalpies of vaporization or saturated liquid heat capacities.

## 2.4 Towards a highly accurate cubic equation of state

After the inclusion of the consistency and volume-translation concepts to a CEoS such as *tc-PR*, the way towards a highly accurate model had been opened. Nevertheless, some points had to be further deepened.

At this point, it is known that the Twu91  $\alpha$ -function is consistent if the  $L, M, N$  parameters are regressed in order to fulfill all of the conditions reported in Eq. (2.8). It is worth noting that these conditions guarantee a proper qualitatively behavior. Nevertheless, Le Guennec et al. [94] had no guarantee that by

regressing parameters on any of the combinations of  $P^{sat}$ ,  $\Delta_{vap}H$  and  $c_{P,liq}^{sat}$ , the quantitative quality of the model was ensured.

Indeed, it was observed that depending on the experimental data on which parameters were fitted, results were not satisfactory. For this reason, [Publication II](#) dealt with the analysis of the combinations of property data among vapor pressure, enthalpy of vaporization and saturated-liquid heat capacity that are suitable for a safe estimation of consistent Twu  $\alpha$ -function parameters. Depending on the availability of these 3 properties, it is possible to arbitrarily define seven types of pure compounds, as shown in [Table 2-2](#).

**Table 2-2.** Possible combinations of accurate pseudo-experimental data available in the DIPPR database for a given pure component. The pure fluid type is an arbitrary index that indicates which properties among  $P^{sat}$ ,  $\Delta_{vap}H$  and  $c_{P,liq}^{sat}$  are associated with accurate data and can thus be used to fit  $\alpha$ -function parameters.

Type of pure fluid	Properties for which accurate data are available (that were considered in the fitting procedure of $\alpha$ -function parameters by Le Guennec et al. [94])
1	( $P^{sat}$ )
2	( $\Delta_{vap}H$ )
3	( $c_{P,liq}^{sat}$ )
4	( $P^{sat} + \Delta_{vap}H$ )
5	( $P^{sat} + c_{P,liq}^{sat}$ )
6	( $\Delta_{vap}H + c_{P,liq}^{sat}$ )
7	( $P^{sat} + \Delta_{vap}H + c_{P,liq}^{sat}$ )

The methodology used in [Publication II](#) was to work with fluids for which  $P^{sat}$ ,  $\Delta_{vap}H$  and  $c_{P,liq}^{sat}$  experimental data were simultaneously available. The interest of choosing these pure compounds was that if it was decided to fit the (L, M, N) parameters using not three but one or two of the selected properties, it became possible to predict the remaining ones and to compare them with experimental values. It was thus possible to determine whether taking specific combinations of 1 or 2 properties into account for parameter fitting could lead to unreliable sets of (L, M, N) parameters. The conclusion of the study is that reliable parameters are obtained on the condition that they are – at least – fitted to vapor-pressure data and that it is strongly advised to not exclusively fit  $\alpha$ -function parameters to enthalpy of vaporization and/or saturated-liquid heat capacity data.

Concerning SAFT-type EoS, a similar study was carried out in [Publication IX](#). It was concluded that it is necessary and sufficient to fit PC-SAFT EoS parameters using both vapor-pressure and density data. Moreover, including  $\Delta_{vap}H$  and/or  $c_{P,liq}^{sat}$  data in the regression procedure is not a necessity and only marginally improves the reproduction of these properties.

Back to the study of CEoS, the next stage was to assess the difference in their accuracy if a generalized or a component-dependent  $\alpha$ -function such as the Twu91  $\alpha$ -function was implemented. For this purpose,

the Soave 1972  $\alpha$ -function was retained for comparison since it has been demonstrated over the years to be a safe, robust and soundly developed function. It is worth noting that Soave came up with the form of the  $\alpha$ -function by using experimental data. However, the  $m$  polynomial was determined by correlating different values of  $\omega$  and the corresponding  $m$  values enabling to exactly reproduce reduced vapor pressures at  $T_r = 0.7$  calculated as:  $P_r^{sat}(T_r = 0.7) = 10^{-\omega-1}$ .

In [Publication III](#), it was decided to propose an updated version of the Soave  $\alpha$ -function, and specifically of the  $m$  polynomial, suitable for the PR and SRK EoS considering molecules for which at least accurate vapor-pressure data are available in the DIPPR database (which contains a large amount of experimental data that were not available at the time of Soave's proposal). The approach retained in [Publication III](#) differs from that of Soave in the fact that the  $m$  values were no longer obtained in order to ensure the reproduction of the reduced vapor pressures at  $T_r = 0.7$ , but by minimizing an objective function containing deviations on at least  $P^{sat}$ , and/or  $\Delta_{vap}H$  and/or  $c_{P,liq}^{sat}$ .

By updating the Soave  $\alpha$ -function, the comparison between it and the Twu91  $\alpha$ -function would be fairer. By comparing the original and updated versions of the Soave  $\alpha$ -function, it was possible to conclude that significant improvement on the reproduction of vapor pressures was obtained for the PR EoS with respect to the original version. Updated SRK EoS achieved similar results for the three properties of interest ( $P^{sat}$ ,  $\Delta_{vap}H$  and  $c_{P,liq}^{sat}$ ), in comparison with the original SRK equation.

At this point, it was possible to compare the impact of implementing the updated generalized Soave or the component-dependent Twu91  $\alpha$ -functions along with CEoS. [Table 2-3](#) highlights the improvement on the prediction of  $P^{sat}$ ,  $\Delta_{vap}H$  and  $c_{P,liq}^{sat}$  by implementing a component-dependent  $\alpha$ -function with the Peng-Robinson EoS. The basis of comparison corresponds to the 1721 molecules for which at least vapor pressure data were available in the DIPPR database.

**Table 2-3.** Comparison of the mean absolute percentage errors (MAPEs) calculated with the  $tc$ -PR EoS and the PR EoS armed with the updated Soave  $\alpha$ -function determined in [Publication III](#).

EoS	MAPE on $P^{sat}$ (1721 fluids)	MAPE on $\Delta_{vap}H$ (1453 fluids)	MAPE on $c_{P,liq}^{sat}$ (829 fluids)
$tc$ -PR	1.0%	1.9%	2.0%
PR with the updated Soave $\alpha$ -function determined in <a href="#">Publication III</a>	1.8%	2.8%	6.8%

After the study of  $\alpha$ -functions parameterization and the advantage of implementing a consistent and component-dependent expression instead of a generalized one for the reproduction of  $P^{sat}$ ,  $\Delta_{vap}H$  and  $c_{P,liq}^{sat}$ , it is time to discuss about the volumetric function and its impact on liquid densities. In [Publication IV](#), it was analyzed through a systematic methodology how parameters  $u$  and  $w$  influence the accuracy of predicted volumetric and vapor-liquid equilibrium properties, both for untranslated and translated cubic equations of state. The methodology consisted of exploring the  $(u - w)$  space, i.e., defining a mesh

and testing every point ( $u$ ,  $w$ ) in order to look for such points (or zones) for which the reproduction of  $P^{sat}$ ,  $\Delta_{vap}H$  and  $\rho_{liq}^{sat}$  was the best as possible.

On the light of results obtained in [Publication IV](#), it was concluded that:

- The unique solution to predict accurate volumetric properties is to make  $u$  and  $w$  component-dependent.
- The volume translation technique is probably the best option to make  $u$  and  $w$  component-dependent. Such a technique indeed avoids the development of a correlation between ( $u$ ,  $w$ ) and  $\omega$ . Moreover, its application is straightforward.
- The optimal values of  $u$  and  $w$  for both untranslated and translated CEoS are ( $u_{opt} = 2.16$ ,  $w_{opt} = -0.86$ ). The choice of Peng and Robinson ( $u = 2$  ;  $w = -1$ ) was thus a very good one. Moreover, if both pairs of parameters are coupled with the consistent Twu91  $\alpha$ -function (Eq. (2.9)) and the volume-translation parameter, as defined in Eq. (2.15), the resulting models *tc*-Optim (with  $u_{opt} = 2.16$ ,  $w_{opt} = -0.86$ ) and *tc*-PR (with  $u = 2$  ;  $w = -1$ ) are able to correlate vapor pressures with an error of 1% whereas errors on  $\Delta_{vap}H$ ,  $c_{P,liq}^{sat}$  and  $v_{liq}^{sat}$  are close to 2%.

At this point and based on the conclusions of [Publication II](#) to [Publication IV](#), the *tc*-PR model arises as one of the most accurate CEoS ever published. Nevertheless, an important point had not been analysed yet: the influence of the associating character of the molecules, i.e., their ability to be involved in a hydrogen bond. How a model performs with non-self-associating (NSA) and self-associating (SA) molecules gives a deeper insight of its performance. In particular, for the *tc*-PR model, having such an insight could open the way to further improvement. This is one of the main motivations of [Publication V](#), which is devoted to the constitution of a database suitable for the identification of the strengths and weaknesses of a given thermodynamic model for pure compounds. 1800 molecules for which, in addition to the critical coordinates ( $T_c$ ,  $P_c$  and  $v_c$ ), accurate correlations for  $P^{sat}$  and  $\rho_{liq}^{sat}$  are available. Among them, 1536 fluids also possess an accurate correlation for  $\Delta_{vap}H$  and 890 for  $c_{P,liq}^{sat}$ , resulting in a database containing 306 700 high-quality pseudo-experimental data points. The proposed database was used to assess the performance of 4 CEoS: Peng-Robinson (PR), Soave-Redlich-Kwong (SRK), and the *translated-consistent* versions of PR (*tc*-PR) and RK (*tc*-RK). Results obtained over 1800 compounds and more than 306 000 data points highlight:

- The use of the highly flexible, component-dependent Twu91  $\alpha$ -function drastically improves the reproduction of vapor pressures, enthalpies of vaporization and liquid heat capacities.
- The spectacular improvement in the reproduction of liquid molar volumes when a substance-dependent volume-translation parameter is used.
- The impressive accuracy of the *tc*-PR EoS that got an average overall deviation lower than 2% over the 306 700 available experimental data points. Excellent results are obtained for all the properties, except the molar critical volumes.
- The striking fact that not all the non-self-associating molecules are well modeled by the studied CEoS and that almost 2/3 of the self-associating compounds of the database are represented with high accuracy by CEoS. At this step, one might wonder whether the addition of an association term is the right solution to improve the accuracy of EoS.

Finally, in Publication XII, the performance of the PC-SAFT [50,51] and the I-PC-SAFT EoS (Publication I) without an association term was evaluated over the non-associating and self-associating molecules contained in the database proposed in Publication V by determining their capacity at correlating the following properties:  $P^{sat}$ ,  $\rho_{liq}^{sat}$ ,  $\Delta_{vap}H$ ,  $c_{P,liq}^{sat}$ ,  $T_c$ ,  $P_c$  and  $v_c$ . It was found that the PC-SAFT equation is able to reproduce  $P^{sat}$  and  $\rho_{liq}^{sat}$  data with a deviation close to 1% what is really excellent. The price to pay is however a large deviation on the critical pressure. The I-PC-SAFT EoS exactly reproduces the critical pressure and temperature but at the expense of a larger liquid density deviation. The key conclusion is that there is no correlation between the strength of association and the accuracy with which the experimental data were correlated. Poor results are obtained for more than 15% of the non-self-associating compounds but 70% of the self-associating compounds are accurately correlated although no association term was included in the considered equations of state.

## 2.5 Concluding remarks

This chapter on cubic equations of state for pure compounds presented the variety of modifications implemented since the time of Van der Waals until our days in order to improve the accuracy on the reproduction of key properties in the chemical engineering domain such as vapor pressure and density. Such modifications have been focused on the  $\alpha$ -function and the volumetric functions of the attractive term of the CEoS. In addition, independently of the modifications, a key point that defines the capabilities of any EoS is the parameterization, i.e., the attribution of numerical values to component-dependent parameters. For this reason, the research work of this thesis got started by evaluating the impact of the parameterization method on the performances of CEoS and SAFT-type EoS.

Chapter 2 introduced two major concepts for the development of accurate CEoS: the consistency and volume-translation concepts. The implementation of these concepts along with the Peng-Robinson EoS gave birth to the *translated-consistent* Peng-Robinson (*tc*-PR) model. In order to pursue the quest for the best CEoS, the following studies were carried out in this thesis:

- Determining the properties absolutely necessary for a reliable parameterization of  $\alpha$ -functions implemented in CEoS, and particularly, the Twu  $\alpha$ -function used in the *tc*-PR model.
- Assessing the impact of using sophisticated and consistent  $\alpha$ -functions instead of generalized ones.
- Looking for the optimal expression of the volumetric function included in CEoS, and studying of the capabilities of the volume-translation concept when coupled with CEoS.
- Investigating how CEoS perform depending on the associating character of molecules.

This work showed that the *tc*-PR model had the capacity to accurately correlate saturated vapor pressures, liquid densities, enthalpies of vaporization and heat capacities. In consequence, such a model is suitable for implementation in the selection of pure working fluids for the CCHP applications studied in this dissertation. As discussed in the introduction, the development of EoS can be divided into two stages: 1) the formulation of a model for pure components and 2) its extension to mixtures. Since the pure-component stage of the development of the *tc*-PR EoS was completed, the next step was thus to extend it to mixtures. This is addressed in Chapter 3.

## **Chapter 3: Equations of state for mixtures**



## Chapter 3 : Equations of state for mixtures

### 3.1 Introduction

The second stage of the development of an EoS is its extension to mixtures. For this purpose, Van der Waals proposed the one-fluid theory, which considers that the properties of a fluid mixture are assumed identical to those of a hypothetical pure fluid, at the same temperature and pressure, whose EoS parameters also depend on mole fractions of species. Based on the one-fluid theory, cubic equations of state can be expressed with the following generic formulation:

$$P(T, v, z) = \frac{RT}{v - b_m} - \frac{a_m}{(v - r_1 b_m)(v - r_2 b_m)} \quad (3.1)$$

where  $r_1$  and  $r_2$  are two universal constants which just depend on the selected equation of state, and  $a_m$  and  $b_m$  are the energy and covolume parameters of the mixture, related to the composition of the mixture  $\mathbf{z}$ , to the energy ( $a_i(T)$ ) and covolume ( $b_i$ ) parameters of a given number of pure components by means of properly defined functions, the so-called *mixing rules*.

When applied to a mixture, the *tc*-PR EoS thus writes:

$$P(T, v, z) = \frac{RT}{v + c_m - b_m} - \frac{a_m}{(v + c_m)(v + c_m + b_m) + b_m(v + c_m - b_m)} \quad (3.2)$$

where  $c_m$  is the volume-translation parameter of the mixture, for which, as well as for  $a_m$  and  $b_m$ , a mixing rule should be defined.

This chapter presents the strengths and weaknesses of the most relevant mixing rules that are classically implemented to extend CEoS to mixtures. Then, the approach retained in this work in order to overcome such weaknesses is described. Finally, the question of the extension of the *tc*-PR model to mixtures is addressed.

### 3.2 Classical Van der Waals mixing rules

Classical Van der Waals (VdW) mixing rules have been constructed under the assumption that the mixture of molecules (1) and (2) of a binary system is random, which implies that using a *molecule pin*, the probability of selecting a molecule (1) is equal to its molar fraction  $z_1$  in the mixture. As an example, let us determine a mixing rule for the parameter  $a_m$  which represents the attractive interactions. In all binary mixtures, there are 3 types of possible interactions between the 2 molecules: interactions (1)+(1), (2)+(2) or (1)+(2). The probability that a molecule (1) will interact with another molecule (1) is equal to  $z_1^2$  because for independent events, the probability of an intersection is the product of the probabilities. Similarly the probability of a (2)+(2) interaction is equal to  $z_2^2$  and the probability of a (1)+(2) or (2)+(1) interaction is equal to  $2z_1z_2$ . If  $a_{11}$ ,  $a_{22}$  and  $a_{12}$  represent respectively the contributions made by interactions (1)+(1), (2)+(2) and (1)+(2) to the interactions of the mixture, the

mixing rule for  $a_m$  – which sets the mathematical method used to sum the contributions of the interactions – is written (for a random mixture):

$$a_m = z_1^2 a_{11} + 2z_1 z_2 a_{12} + z_2^2 a_{22} = \sum_{i=1}^2 \sum_{j=1}^2 z_i z_j a_{ij} \quad (3.3)$$

$a_{11}$  and  $a_{22}$  are the attractive parameters of the pure substances (1) and (2) and here it is implied that  $a_{12}$  is identical to  $a_{21}$ . Thus, classic mixing rules stipulate that the parameters  $a_m$  and  $b_m$  are quadratic functions of the composition:

$$\begin{cases} a_m = \sum_{i=1}^{n_c} \sum_{j=1}^{n_c} z_i z_j a_{ij} \\ b_m = \sum_{i=1}^{n_c} \sum_{j=1}^{n_c} z_i z_j b_{ij} \end{cases} \quad (3.4)$$

The *combining rules* define the expressions for coefficients  $a_{ij}$  and  $b_{ij}$  of Eq. (3.4).

$$\begin{cases} a_{ij} = \sqrt{a_i a_j} (1 - k_{ij}) \\ b_{ij} = \frac{b_i + b_j}{2} (1 - l_{ij}) \end{cases} \quad (3.5)$$

In Eq. (3.5),  $k_{ij}$  and  $l_{ij}$  are binary interaction parameters (BIP). The absolute values of binary interaction parameters  $|k_{ij}|$  and  $|l_{ij}|$  are generally small compared to unity. For simple mixtures of nonpolar components,  $l_{ij}$  is systematically set to zero and  $k_{ij}$  is fitted to binary vapor-liquid equilibrium (VLE) data. Several authors developed correlations for the estimation of  $k_{ij}$ . Chueh et Prausnitz [97], for instance, came up with a correlation for mixtures of light alkanes. Gao et al. [98], in turn, proposed an expression for light-hydrocarbon mixtures. Such correlations were temperature independent. On the other hand, Stryjek [99], Kordas et al. [100], and Valderrama et al. [101,102] proposed temperature-dependent correlations for  $k_{ij}$ . It is worth noting that  $k_{ij}$  and  $l_{ij}$  may be temperature dependent without affecting the cubic character of the EoS. On the contrary, if they depend on pressure or density, the complexity of the resulting equation would rather increase.

VdW1f mixing rules are useful for the extension of pure-fluid equations of state to mixtures of nonpolar (or slightly polar) components [103–105]. However, for highly nonideal mixtures quadratic mixing rules are inadequate as shown by Voros and Tassios [106] or Anderko [107]. In order to overcome this problem, the original mixing rules have been modified in several ways. Most of the approaches included composition-dependent binary interaction parameters, such as the modifications proposed by Panagiotopoulos and Reid [108], Adachi and Sugi [109], Stryjek and Vera [110], Sandoval et al. [111], or Schwartzentruber et al. [112].

### 3.3 EoS/ $g^E$ mixing rules

Cubic EoS with Van der Waals one-fluid mixing rules lead to very accurate results at low and high pressures for *simple* mixtures (slightly polar, hydrocarbons, gases). They also allow the prediction of many more properties than phase equilibria (e.g. excess properties, heat capacities, etc.). Such mixing rules can however not be applied with success to polar mixtures. On the contrary,  $g^E$  models (activity-coefficient models) are applicable to low pressures and are able to correlate polar mixtures. It thus seems a good idea to combine the strengths of both approaches, i.e. the cubic EoS and the activity coefficient models and thus to have a single model suitable for phase equilibria of polar and non-polar mixtures and at both low and high pressures. This combination of EoS and  $g^E$  models is possible via the so-called EoS/ $g^E$  models which are essentially mixing rules for the energy parameter of cubic EoS. As explained in the book by Kontogeorgis and Folas [42], the starting point for deriving EoS/ $g^E$  models is the equality of the excess Gibbs energies from an EoS and from an explicit activity coefficient model at a suitable reference pressure. The activity coefficient model may be chosen among the classical forms of molar excess Gibbs energy functions (Redlich-Kister, Margules, Wilson, Van Laar, NRTL, UNIQUAC, UNIFAC...). Such models are pressure-independent (they only depend on temperature and composition) but the same quantity from an EoS depends on pressure, temperature and composition explaining why a reference pressure needs to be selected before equating the two quantities. In order to avoid confusion, the selected activity coefficient model will be expressed as  $g^{E,\gamma}$ , while  $g^{E,EoS}$  will represent the excess Gibbs energy calculated from an EoS by:

$$\frac{g^{E,EoS}}{RT} = \sum_{i=1}^{n_c} z_i \cdot \ln \left[ \frac{\hat{\varphi}_i^{EoS}(T, P, \mathbf{z})}{\varphi_{pure i}^{EoS}(T, P)} \right] \quad (3.6)$$

where  $\hat{\varphi}_i^{EoS}$  is the fugacity coefficient of component  $i$  in the mixture and  $\varphi_{pure i}^{EoS}$  the fugacity coefficient of the pure compound at the same temperature, pressure and in the same aggregation state as the mixture. The starting equation to derive EoS/ $g^E$  models is thus:

$$g^{E,EoS}(T, P_{ref}, \mathbf{z}) = g^{E,\gamma}(T, \mathbf{z}) \quad (3.7)$$

#### 3.3.1 The infinite pressure reference

The basic assumption of the method is the use of the infinite pressure as the reference pressure.

##### The Huron-Vidal mixing rules

The first systematic successful effort in developing an EoS/ $g^E$  mixing rule is that of Huron and Vidal [113]. Starting from Eq. (3.7), they obtained:

$$\begin{cases} \frac{a_m(T, \mathbf{x})}{b_m(\mathbf{x})} = \sum_{i=1}^{n_c} z_i \frac{a_i(T)}{b_i} + \frac{g^{E,\gamma}}{\Lambda_{EoS}} \\ b_m(\mathbf{x}) = \sum_{i=1}^{n_c} z_i b_i \end{cases} \quad (3.8)$$

where  $\Lambda_{EoS}$  is defined by:

$$\Lambda_{EoS} = \frac{1}{r_2 - r_1} \cdot \ln\left(\frac{1 - r_2}{1 - r_1}\right) \text{ if } r_1 \neq r_2 \text{ and } \Lambda_{EoS} = \frac{1}{r_1 - 1} \text{ if } r_1 = r_2 \quad (3.9)$$

A positive feature of the Huron-Vidal (HV) mixing rule includes an excellent correlation of binary systems, especially with the NRTL  $g^{E,\gamma}$  model. A limitation is that it does not permit the use of the large collections of interaction parameters of  $g^{E,\gamma}$  models which are based on low-pressure VLE data (e.g. the UNIFAC tables). Indeed, the excess Gibbs energy at high pressures is, in general, different from the value at low pressures at which the parameters of the  $g^{E,\gamma}$  models are typically estimated.

### **From the Van der Waals one-fluid (VdW1f) mixing rules with T-dependent $k_{ij}$ to the HV mixing rules**

It is possible to show that the classical VdW1f mixing rules with T-dependent  $k_{ij}$  used in the PPR78 [114] and PR2SRK models are strictly equivalent to the Huron-Vidal mixing rules if a van-Laar type  $g^{E,\gamma}$  model is selected in Eq. (3.8).

$$a_m(T, \mathbf{x}) = \sum_{j=1}^{n_c} z_j z_j \sqrt{a_i a_j} [1 - k_{ij}(T)] \quad \text{and} \quad b_m(\mathbf{x}) = \sum_{i=1}^{n_c} z_i b_i \quad (3.10)$$

Indeed, by sending Eq. (3.10), i.e., the classical vdW mixing rules, in Eq. (3.8), one has:

$$\begin{aligned} \frac{g^{E,\gamma}}{\Lambda_{EoS}} &= \frac{a_m(T, \mathbf{z})}{b_m(\mathbf{z})} - \sum_{i=1}^{n_c} z_i \frac{a_i(T)}{b_i} = \frac{\sum_{i=1}^{n_c} \sum_{j=1}^{n_c} z_i \cdot z_j \sqrt{a_i \cdot a_j} \cdot [1 - k_{ij}(T)]}{\sum_{j=1}^{n_c} z_j \cdot b_j} - \sum_{i=1}^{n_c} z_i \cdot \frac{a_i(T)}{b_i} \\ &= \frac{\sum_{i=1}^{n_c} \sum_{j=1}^{n_c} z_i \cdot z_j \sqrt{a_i \cdot a_j} \cdot [1 - k_{ij}(T)] - \sum_{i=1}^{n_c} z_i \cdot \frac{a_i(T)}{b_i} \times \sum_{j=1}^{n_c} z_j \cdot b_j}{\sum_{j=1}^{n_c} z_j \cdot b_j} \end{aligned} \quad (3.11)$$

It is possible to write:

$$\sum_{i=1}^{n_c} z_i \cdot \frac{a_i(T)}{b_i} \times \sum_{j=1}^{n_c} z_j \cdot b_j = \sum_{i=1}^{n_c} \sum_{j=1}^{n_c} z_i \cdot z_j \frac{a_i \cdot b_j}{b_i} = \frac{1}{2} \sum_{i=1}^{n_c} \sum_{j=1}^{n_c} z_i \cdot z_j \frac{a_i \cdot b_j}{b_i} + \frac{1}{2} \sum_{i=1}^{n_c} \sum_{j=1}^{n_c} z_i \cdot z_j \frac{a_j \cdot b_i}{b_j} \quad (3.12)$$

Thus,

$$\begin{aligned} \frac{g^{E,\gamma}}{\Lambda_{EoS}} &= \frac{\sum_{i=1}^{n_c} \sum_{j=1}^{n_c} z_i \cdot z_j \left[ \sqrt{a_i \cdot a_j} \cdot [1 - k_{ij}(T)] - \frac{1}{2} \frac{a_i \cdot b_j}{b_i} - \frac{1}{2} \frac{a_j \cdot b_i}{b_j} \right]}{\sum_{j=1}^{n_c} z_j \cdot b_j} \\ &= \frac{\sum_{i=1}^{n_c} \sum_{j=1}^{n_c} z_i \cdot z_j \cdot b_i \cdot b_j \left[ \frac{\sqrt{a_i}}{b_i} \cdot \frac{\sqrt{a_j}}{b_j} \cdot [1 - k_{ij}(T)] - \frac{1}{2} \frac{a_i}{b_i^2} - \frac{1}{2} \frac{a_j}{b_j^2} \right]}{\sum_{j=1}^{n_c} z_j \cdot b_j} \end{aligned} \quad (3.13)$$

At this step, we introduce for clarity:  $\delta_i = \sqrt{a_i}/b_i$  which has the Scatchard-Hildebrand solubility parameter feature, and the parameter  $E_{ij}$  is defined by:

$$E_{ij} = \delta_i^2 + \delta_j^2 - 2\delta_i\delta_j [1 - k_{ij}(T)] \quad (3.14)$$

Eq. (3.13) thus writes:

$$\frac{g^{E,\gamma}}{\Lambda_{EoS}} = -\frac{1}{2} \cdot \frac{\sum_{i=1}^{n_c} \sum_{j=1}^{n_c} z_i \cdot z_j \cdot b_i \cdot b_j \cdot E_{ij}(T)}{\sum_{j=1}^{n_c} z_j \cdot b_j} \quad (3.15)$$

Eq. (3.15) is the mathematical expression of a Van Laar-type  $g^{E,\gamma}$  model. Therefore, it has been demonstrated that it is rigorously equivalent to use a Van Laar-type  $g^{E,\gamma}$  model in the Huron-Vidal mixing rules or to use classical mixing rules with temperature-dependent  $k_{ij}$ . From Eq. (3.14) one has:

$$k_{ij}(T) = \frac{E_{ij}(T) - (\delta_i - \delta_j)^2}{2\delta_i\delta_j} \quad (3.16)$$

Eq. (3.16) thus establishes a connection between  $E_{ij}$  of the Van Laar-type  $g^{E,\gamma}$  model and  $k_{ij}$  of the classical mixing rules.

### **The Wong-Sandler mixing rules**

It can be demonstrated that the Huron Vidal mixing rules violate the imposed by statistical thermodynamics quadratic composition dependency of the second virial coefficient:

$$B = \sum_{i=1}^{n_c} \sum_{j=1}^{n_c} z_i z_j B_{ij} \quad (3.17)$$

To satisfy Eq. (3.17), Wong and Sandler [115] decided to revisit the Huron-Vidal mixing rules. Since they made use of the infinite pressure as the reference pressure, like Huron and Vidal, they obtained:

$$a_m(T, \mathbf{z}) = b_m(\mathbf{z}) \left[ \sum_{i=1}^{n_c} z_i \frac{a_i(T)}{b_i} + \frac{g^{E,\gamma}}{\Lambda_{EoS}} \right] \quad (3.18)$$

However, knowing that the second virial coefficient from a cubic EoS is given as:

$$B = b_m - \frac{a_m}{RT} \quad (3.19)$$

The combination of Eqs. (3.17) and (3.19) gives:

$$b_m(\mathbf{z}) = \frac{a_m(T, \mathbf{z})}{RT} + \sum_{i=1}^{n_c} \sum_{j=1}^{n_c} z_i z_j B_{ij} \quad (3.20)$$

Substituting Eq. (3.18) in Eq. (3.20), one obtains:

$$b_m(\mathbf{z}) = \frac{\sum_{i=1}^{n_c} \sum_{j=1}^{n_c} z_i z_j B_{ij}}{1 - \frac{g^{E,\gamma}}{RT \Lambda_{EoS}} - \sum_{i=1}^{n_c} x_i \frac{a_i(T)}{RT b_i}} \quad (3.21)$$

The following choice for the cross virial coefficient is often used:

$$B_{ij} = \frac{1}{2} (B_i + B_j) (1 - k_{ij}) \quad (3.22)$$

Eq. (3.22) makes unfortunately appear an extra binary interaction parameter ( $k_{ij}$ ), the value of which can be estimated through various approaches.

Substituting Eq. (3.19) in Eq. (3.22), one has:

$$B_{ij} = \frac{\left(b_i - \frac{a_i}{RT}\right) + \left(b_j - \frac{a_j}{RT}\right)}{2} (1 - k_{ij}) \quad (3.23)$$

The Wang-Sandler mixing rules thus write:

$$\left\{ \begin{array}{l} b_m(T, \mathbf{z}) = \frac{\sum_{i=1}^{n_c} \sum_{j=1}^{n_c} z_i z_j \frac{\left(b_i - \frac{a_i}{RT}\right) + \left(b_j - \frac{a_j}{RT}\right)}{2} (1 - k_{ij})}{1 - \frac{g^{E,\gamma}}{RT \Lambda_{EoS}} - \sum_{i=1}^{n_c} z_i \frac{a_i(T)}{RT b_i}} \\ a_m(T, \mathbf{z}) = b_m(\mathbf{z}) \left[ \sum_{i=1}^{n_c} z_i \frac{a_i(T)}{b_i} + \frac{g^{E,\gamma}}{\Lambda_{EoS}} \right] \end{array} \right. \quad (3.24)$$

It is thus possible to conclude that the Wong-Sandler mixing rules differ from the Huron-Vidal mixing rules in the way of estimating the covolume. In Eq. (3.24),  $b_m$  has become temperature-dependent. Many papers illustrate the key success of the Wong-Sandler mixing rules to predict VLE using existing low-pressure parameters from activity coefficient models.

### 3.3.2 The zero-pressure reference

The zero-pressure reference should permit a direct use of  $g^{E,\gamma}$  interaction parameter tables (e.g. DECHEMA). Starting from Eq. (3.7) and by setting  $P = 0$ , one obtains:

$$\left\{ \begin{array}{l} \frac{g^{E,\gamma}}{RT} = Q(\Gamma) - \sum_{i=1}^{n_c} z_i \cdot Q(\Gamma_i) + \sum_{i=1}^{n_c} z_i \cdot \ln\left(\frac{b_i}{b_m}\right) \text{ with } \left\{ \begin{array}{l} \Gamma = \frac{a_m}{b_m RT} \\ \Gamma_i = \frac{a_i}{b_i RT} \end{array} \right. \\ Q(\Gamma) = -\ln\left(\frac{1-\eta_0(\Gamma)}{\eta_0(\Gamma)}\right) - \frac{\Gamma}{r_1-r_2} \ln\left(\frac{1-\eta_0(\Gamma) \cdot r_2}{1-\eta_0(\Gamma) \cdot r_1}\right) \\ Q(\Gamma_i) = -\ln\left(\frac{1-\eta_0(\Gamma_i)}{\eta_0(\Gamma_i)}\right) - \frac{\Gamma_i}{r_1-r_2} \ln\left(\frac{1-\eta_0(\Gamma_i) \cdot r_2}{1-\eta_0(\Gamma_i) \cdot r_1}\right) \end{array} \right. \quad (3.25)$$

with

$$\left\{ \begin{array}{l} \eta_0(\Gamma) = \frac{r_1 + r_2 + \Gamma + \sqrt{(r_1 + r_2 + \Gamma)^2 - 4(r_1 r_2 + \Gamma)}}{2(r_1 r_2 + \Gamma)} \text{ subject to: } \Gamma \geq \Gamma_{\text{lim}} \\ \eta_0(\Gamma_i) = \frac{r_1 + r_2 + \Gamma_i + \sqrt{(r_1 + r_2 + \Gamma_i)^2 - 4(r_1 r_2 + \Gamma_i)}}{2(r_1 r_2 + \Gamma_i)} \text{ subject to: } \Gamma_i \geq \Gamma_{\text{lim}} \\ \Gamma_{\text{lim}} = -r_1 - r_2 + 2 + 2\sqrt{1 - r_1 - r_2 + r_1 r_2} \end{array} \right. \quad (3.26)$$

After selecting a mixing rule for the covolume, Eq. (3.25) becomes an implicit mixing rule for the energy parameter, which means that an iterative procedure is needed for calculating the energy parameter.

#### **The MHV-1 mixing rule**

In order to obtain an explicit mixing rule and to address the limitation introduced by the presence of  $\alpha_{\text{lim}}$ , Michelsen [116] proposed to define a linear approximation of the  $Q$  function by:

$$Q(\Gamma) = q_0 + q_1 \cdot \Gamma \quad (3.27)$$

Doing so, Eq. (3.25) can be written:

$$\Gamma = \sum_{i=1}^{n_c} z_i \cdot \Gamma_i + \frac{1}{q_1} \left[ \frac{g^{E,\gamma}}{RT} - \sum_{i=1}^{n_c} z_i \cdot \ln\left(\frac{b_i}{b_m}\right) \right] \quad (3.28)$$

Eq. (3.28) is the so called MHV-1 (modified Huron-Vidal first order) mixing rule, sometimes used with a linear mixing rule for the covolume parameter. Michelsen advices to use  $q_1 = -0.593$  for the SRK EoS,  $q_1 = -0.53$  for the PR EoS and  $q_1 = -0.85$  for the VdW EoS.

#### **The PSRK model**

Holderbaum and Gmehling [117] proposed the PSRK (predictive SRK) model based on the MHV-1 mixing rule. These authors however used a slightly different  $q_1$  value than the one proposed by

Michelsen. They selected:  $q_1 = -0.64663$ . In order to make their model predictive, Holderbaum and Gmehling combine the SRK EoS with a predictive  $g^{E,\gamma}$  model (the original or the modified Dortmund UNIFAC). Moreover, they developed extensive parameter tables, including parameters for gas-containing mixtures. The PSRK model may thus be used to model petroleum fluids.

### **The UMR-PRU and VTPR models**

The UMR-PRU (universal mixing rule-Peng Robinson UNIFAC) and the VTPR (volume translated Peng Robinson) models, both use the MVH-1 mixing rule. They were respectively developed by Voutsas et al. [118] and by Ahlers and Gmehling [119,120]. In both cases, the same translated form of the PR EoS is used. The Twu  $\alpha$ -function is however used in the VTPR model whereas the Mathias-Copeman expression is used in the UMR-PRU model. Both models incorporate the UNIFAC  $g^{E,\gamma}$  model in Eq. (3.28). However, in order to be able to properly correlate asymmetric systems, only the residual part of UNIFAC is used in the VTPR model. These authors indeed assume that the combinatorial part of UNIFAC and  $\sum x_i \cdot \ln(b_i/b_m)$  in Eq. (3.28) cancel each other. In the UMR-PR model the residual part of UNIFAC but also the Staverman-Guggenheim contribution of the combinatorial term is used. These authors also assume that the Flory-Huggins combinatorial part of UNIFAC and  $\sum x_i \cdot \ln(b_i/b_m)$  in Eq. (3.28) cancel each other. A novel aspect of these models is the mixing rule used for the covolume parameter. Both models give better results than PSRK. After noting  $\Gamma = \frac{a_m}{b_m RT}$ , the equations to be used are:

VTPR:

$$\Gamma = \sum_{i=1}^{n_c} z_i \cdot \Gamma_i + \frac{1}{q_1} \left[ \frac{g^{E,UNIFAC}_{residual}}{RT} \right] \quad (3.29)$$

$$b_m = \sum_{i=1}^{n_c} \sum_{j=1}^{n_c} z_i z_j b_{ij} \quad \text{with: } b_{ij} = \left( \frac{b_i^{1/s} + b_j^{1/s}}{2} \right)^s \quad \text{and } s = \frac{4}{3}$$

UMP-PR:

$$\alpha = \sum_{i=1}^{n_c} z_i \cdot \alpha_i + \frac{1}{q_1} \left[ \frac{g^{E,UNIFAC}_{residual}}{RT} + \frac{g^{E,UNIFAC}_{Staverman-Guggenheim \text{ combinatorial contribution}}}{RT} \right] \quad (3.30)$$

$$b = \sum_{i=1}^{n_c} \sum_{j=1}^{n_c} z_i z_j b_{ij} \quad \text{with: } b_{ij} = \left( \frac{b_i^{1/s} + b_j^{1/s}}{2} \right)^s \quad \text{and } s = 2$$

The mixing rule described by Eq. (3.29), was also applied to the SRK EoS by Chen et al. [121] in order to define a new version of the PSRK model. In this latter case, the SRK EoS was combined with a Mathias-Copeman  $\alpha$ -function.

### **The LCVM model**

The LCVM model by Boukouvalas et al. [122] is based on a mixing rule which is a Linear Combination of the Vidal and Michelsen (MHV-1) mixing rules:

$$\Gamma_{LCVM} = \lambda \cdot \Gamma_{Huron-Vidal} + (1 - \lambda) \cdot \Gamma_{Michelsen} \quad (3.31)$$

From Eq. (3.8), one has:

$$\Gamma_{Huron-Vidal} = \sum_{i=1}^{n_c} z_i \cdot \Gamma_i + \frac{g^{E,\gamma}}{R \cdot T \cdot \Lambda_{EoS}} \quad (3.32)$$

whereas  $\Gamma_{Michelsen}$  is given by Eq. (3.28). The LCVM as used today is based on the original UNIFAC  $g^{E,\gamma}$  model and the value  $\lambda = 0.36$  should be used in all applications. Their authors use a translated form of the PR EoS and obtain accurate results especially for asymmetric systems.

### **The MHV-2 mixing rule**

In order to increase the accuracy of the MHV-1 mixing rule, Dahl and Michelsen [123] proposed in 1990 a quadratic approximation of the  $Q$  function by:

$$Q(\Gamma) = q_0 + q_1 \cdot \Gamma + q_2 \cdot \Gamma^2 \quad (3.33)$$

thus defining the MHV-2 model. It is advised to use  $q_1 = -0.4783$  and  $q_2 = -0.0047$  for the SRK EoS;  $q_1 = -0.4347$  and  $q_2 = -0.003654$  for the PR EoS. Doing so, Eq. (3.25) can be written as:

$$\frac{g^{E,\gamma}}{RT} = q_1 \left( \Gamma - \sum_{i=1}^{n_c} z_i \cdot \Gamma_i \right) + q_2 \left( \Gamma^2 - \sum_{i=1}^{n_c} z_i \cdot \Gamma_i^2 \right) + \sum_{i=1}^{n_c} z_i \cdot \ln \left( \frac{b_i}{b_m} \right) \quad (3.34)$$

Eq. (3.34) does not yield anymore to an explicit mixing rule but instead has to be solved in order to determine  $\Gamma$ . For such a mixing rule, parameter tables are available for many gases. As a general rule, MHV-2 provides a better reproduction of the low-pressure VLE data than MHV-1.

## **3.4 Proposed EoS/ $a^E$ mixing rules**

Although HV and MHV mixing rules have been widely used since their initial proposal, over the last decades various studies have shown that:

- in the case of HV mixing rules, researchers could not explain why satisfactory results were obtained with  $g^{E,\gamma}$  models that contained only a residual (enthalpic) contribution such as the NRTL  $g^{E,\gamma}$  model. This is supported by the fact that the combinatorial term from the EoS cancels out. In consequence, it would not be pertinent to use a  $g^{E,\gamma}$  model with both a combinatorial and a residual contribution.

in the case of MHV mixing rules, the presence of two types of combinatorial terms in the MR, i.e., from the  $g^{E,\gamma}$  model and from the EoS, which are of the same type but are not quantitatively equivalent, penalizes the accuracy of the model [124,125]. This phenomenon is referred as the **presence of a double combinatorial term**. To increase the accuracy of their model, the authors of the UMR-PRU and VTPR mixing rules thus decided to arbitrarily cancel the two combinatorial contributions.

For these reasons, in this dissertation it was decided to propose a modification to the way that has been classically used to derive advanced mixing rules. This resulted in the formulation of EoS/ $a_{res}^{E,\gamma}$  mixing

rules that were used in this thesis. In this section, the details of the motivations to propose EoS/ $a_{res}^{E,\gamma}$  mixing rules are discussed.

First of all, it is worth recalling that the idea of combining the cubic EoS and the activity coefficient models and thus to have a single model suitable for phase equilibria of polar and non-polar mixtures and at both low and high pressures was an excellent idea. It also should be noted that when one refers to activity coefficient models, thousands of fitted binary interaction parameters are hidden behind. Indeed, another motivation of the development of EoS/ $g^E$  mixing rules was to be able to use the BIPs available in the DECHEMA books. It could be said that the EoS/ $g^E$  approach was driven by the weight of history.

In order to use available BIPs for  $g^{E,\gamma}$  models such as Van Laar, Wilson, NRTL or UNIQUAC, as discussed in the previous section, the starting point must be equality of the excess Gibbs energies from an EoS and from an explicit activity coefficient model at a suitable reference pressure. However, both  $g^E$  coming from the EoS and the activity coefficient model are the result of the sum of a combinatorial and a residual contribution.

To illustrate this, consider the following example. From Eq. (3.7), the equality of  $g^E$  is respected, as done by all the approaches presented in the previous section. Nevertheless, any of the EoS/ $g^E$  approaches imposed the equality of both the residual and combinatorial contributions. It implies that for a non-athermal and non-regular solution it may happen that Eq. (3.7) was verified by a compensation of errors from the two contributions.

$$\underbrace{g^{E,EoS}}_{10u} = \underbrace{g^{E,\gamma}}_{10u} \quad (3.35)$$

$$\underbrace{g_{comb}^{E,EoS}}_{5u} + \underbrace{g_{res}^{E,EoS}}_{5u} = \underbrace{g_{comb}^{E,\gamma}}_{7u} + \underbrace{g_{res}^{E,\gamma}}_{3u} \quad (3.36)$$

The problem is even more clear when athermal and regular solutions are studied. In the case of an athermal solution such as methane + n-tetracosane, in which departure from ideality is only due to size and shape effects, the residual contribution vanishes. However, we know that the expressions of the combinatorial parts do not yield the same numerical values, which leads to an inconsistency. Similarly, the problem appears for regular solutions, such as methanol + ethanol, since the residual contributions from the  $g^{E,\gamma}$  model and the EoS are not equal, either.

Therefore, one may think that the solution to this problem is to define the system of two equations and two unknowns given by Eq. (3.37):

$$F(x) = \begin{pmatrix} g_{comb}^{E,EoS} - g_{comb}^{E,\gamma} \\ g_{res}^{E,EoS} - g_{res}^{E,\gamma} \end{pmatrix} = 0 \quad \text{with} \quad x = \begin{pmatrix} a_m \\ b_m \end{pmatrix} \quad (3.37)$$

Unfortunately, the problem described in Eq. (3.37) does not have solution. Indeed, no  $g^{E,\gamma}$  model contains a combinatorial term identical to the one provided by the EoS. Therefore, a sound starting point for advanced mixing rules could be:

$$g_{res}^{E,EoS} = g_{res}^{E,\gamma} \quad (3.38)$$

Nevertheless, as pointed out by Wong and Sandler [126] and Jaubert and Privat [127], no consistent mathematical expression for  $g^{E,\gamma}$  is known. Indeed, all excess Gibbs energy models should theoretically depend on pressure but our current knowledge on liquid theory still lacks of enough accuracy to estimate the influence of the pressure on  $g^{E,\gamma}$  models. In consequence, all activity-coefficient models predict:  $v^{E,\gamma} = -\left(\partial g^{E,\gamma} / \partial P\right)_{T,\mathbf{z}} = 0$ . Although the experimental values of  $v^E$  are often small, such a result is thermodynamically inconsistent ( $g^E$  should indeed be a function of composition, temperature and pressure) and must be seen as a theoretical weakness. Since  $g^{E,\gamma} = a^{E,\gamma} + P \cdot v^{E,\gamma}$ , the developers of  $g^{E,\gamma}$  models (UNIQUAC, Wilson...) decided to construct expressions for  $a^{E,\gamma}$  and to use them to determine activity coefficients. As an illustration, in their paper relative to the derivation of UNIQUAC [128], Abrams and Prausnitz write: “*For liquid mixtures at ordinary pressures, the effect of pressure is negligible*”. In conclusion, all  $g^{E,\gamma}$  are in fact  $a^{E,\gamma}$  models and some of them, like NRTL or Van Laar, that do not contain a combinatorial term are even only  $a_{residual}^{E,\gamma}$  models. At low pressures, it is reasonable to assume that  $g^E \approx a^E$ . However, to define mixing rules for EoS that are used under high pressures, we see no reason to keep such an approximation and we find much more appropriate to equate the excess Helmholtz energies from an EoS and from a low-pressure  $a^{E,\gamma}$  model than the excess Gibbs energies. In consequence, Eq. (3.38) becomes:

$$g_{res}^{E,EoS} = g_{res}^{E,\gamma} \quad (3.39)$$

which is the starting point for the derivation of the EoS/ $a_{res}^{E,\gamma}$  mixing rules implemented for the extension of the  $tc$ -PR model to mixtures. The derivation of EoS/ $a_{res}^{E,\gamma}$  mixing rules is treated in detail in Publication VII. The resulting mixing rule for  $a_m/b_m$  seems particularly appropriate since the result is independent of the reference pressure (zero or infinite). It writes:

$$\left\{ \begin{array}{l} b_m : \text{any mixing rule} \\ \frac{a_m}{b_m} = \sum_i^{n_c} z_i \frac{a_i}{b_i} + \frac{a_{res}^{E,\gamma}}{\Lambda_{EoS}} \\ \text{with } \Lambda_{EoS} = \frac{1}{r_2 - r_1} \ln \left( \frac{1 - r_2}{1 - r_1} \right) \end{array} \right. \quad (3.40)$$

### 3.5 Reference database for the comparison of thermodynamic models

After the presentation of the most relevant approaches to define mixing rules, one could imagine that the number of thermodynamic models resulting from different EoS armed with different types of mixing rules is not small. In the last twenty years, hundreds of publications were devoted to the development of sophisticated models or to the improvement of already existing EoS [129]. Chemical engineering thermodynamics is thus a field under steady development and to assess the accuracy of a thermodynamic model or to cross-compare two models, it is necessary to confront model predictions with experimental data. Moreover, for the extension of the  $tc$ -PR EoS to mixtures, different strategies were tested and a reliable way of comparison was required.

For these reasons, [Publication VI](#) was focused on the development of a high-quality reference database containing binary-system data for the cross-comparison of thermodynamic models and the assessment of their accuracies. With such a database, it is possible to determine how well a thermodynamic model predicts the behavior of binary mixtures according to the associating character of their components. Indeed, a specific procedure for the calculation of the deviations between model calculations and experimental data was discussed in detail, as well as a methodology for grading a thermodynamic model was proposed. In total, 200 non-electrolytic binary mixtures were selected to cover all categories of mixtures. They were divided into 9 groups (characterized each by a so-called *binary association code*, BAC) according to the associating character of the two components, i.e., to their ability to be involved in a hydrogen bond (see [Table 3-1](#)). In addition, during the grading of a thermodynamic model, only four categories of binary systems are retained based on the type of association they (see the last column of [Table 3-1](#)) exhibit.

**Table 3-1.** Definition of the 9 groups of binary systems identified each by a BAC (binary association code) and the 4 categories used for the grading of a model.

Component 1	Component 2	Binary association code (BAC)	Type of exhibited association
NA (Non-Associating) <i>nonpolar</i>	NA (Non-Associating) <i>nonpolar</i>	1	Mixtures without association
HA (Hydrogen-Acceptor) <i>polar but non-associating</i>	NA (Non-Associating) <i>nonpolar</i>	2	
HD (Hydrogen-Donor) <i>polar but non-associating</i>	NA (Non-Associating) <i>nonpolar</i>	3	
HA (Hydrogen-Acceptor) <i>polar but non-associating</i>	HA (Hydrogen-Acceptor) <i>polar but non-associating</i>	4	
SA (Self-Associating) <i>polar and associating</i>	NA (Non-Associating) <i>nonpolar</i>	5	Mixtures in which self-association takes place (but tends to be broken)
HD (Hydrogen-Donor) <i>polar but non-associating</i>	HA (Hydrogen-Acceptor) <i>polar but non-associating</i>	6	Mixtures in which cross-association takes place alone
SA (Self-Associating) <i>polar and associating</i>	HD (Hydrogen-Donor) <i>polar but non-associating</i>	7	Mixtures in which both cross-association and self-association take place
SA (Self-Associating) <i>polar and associating</i>	HA (Hydrogen-Acceptor) <i>polar but non-associating</i>	8	
SA (Self-Associating) <i>polar and associating</i>	SA (Self-Associating) <i>polar and associating</i>	9	

In general, for each binary system of the database, ten properties were experimentally determined: liquid phase composition  $x$ , gas phase composition (or second liquid phase composition)  $y$ , three-phase pressure  $P_{LLV}$ , three-phase composition  $z_{LLV}$ , critical pressure  $P_c$ , critical composition  $x_c$ , azeotropic pressure  $P_{azeo}$ , azeotropic composition  $x_{azeo}$ , mixing enthalpy  $h^M$  and mixing heat capacity  $c_P^M$ .

The database developed in [Publication VI](#) could be used to assess the impact of mixing-rules selection and the number of parameters included within. Models such as the Peng-Robinson (PR) EoS armed with classical mixing rules and temperature-dependent binary interaction parameters (BIPs), as well as the

PC-SAFT EoS with classical mixing rules, no induced association scheme and no regressed BIPs have been graded following the proposed procedure, recently [130,131].

### 3.6 Extension of the $tc$ -PR model to mixtures

As stated in the introduction, in order to apply the  $tc$ -PR model to mixtures it is necessary to define mixing rules for  $a_m$ ,  $b_m$  and  $c_m$ . For the covolume of the mixture ( $b_m$ ), it has been applied the classical quadratic mixing rule with the generalized formulation of the combining rule proposed by Lorentz for  $b_{ij}$  [124]:

$$\begin{cases} b_m = \sum_i^{n_c} \sum_j^{n_c} z_i z_j b_{ij} \\ b_{ij} = \left( \frac{b_i^{1/s} + b_j^{1/s}}{2} \right)^s \end{cases} \quad (3.41)$$

where the parameter  $s$  has been set to  $3/2$ . In addition, a linear MR has been chosen for the volume-translation parameter:  $c_m(\mathbf{z}) = \sum_i z_i \cdot c_i$ . To sum up, when applied to a mixture, the  $tc$ -PR EoS writes:

$$P(T, v, \mathbf{z}) = \frac{RT}{v + c_m - b_m} - \frac{a_m(T, \mathbf{z})}{(v + c_m)(v + c_m + b_m) + b_m(v + c_m - b_m)}$$

$$\text{with: } \begin{cases} b_m = \sum_i^{n_c} \sum_j^{n_c} z_i z_j \left( \frac{b_i^{2/3} + b_j^{2/3}}{2} \right)^{3/2} \\ a_m = b_m \left[ \sum_i^{n_c} z_i \frac{a_i}{b_i} + \frac{a_{res}^{E,\gamma}}{\Lambda_{PR}} \right] \text{ with } \Lambda_{PR} = -\sqrt{2}/2 \cdot \ln(1 + \sqrt{2}) \\ c_m = \sum_i^{n_c} z_i \cdot c_i \end{cases} \quad (3.42)$$

Concerning the choice of  $c_m$ , it is worth recalling that, in the case of pure compounds, a temperature-independent volume-translation parameter does not affect the calculation of vapor pressures, enthalpies of vaporization and saturated-liquid heat capacities, as shown by Jaubert et al. [95]. This allowed for a separated treatment between those properties and liquid densities. In the case of mixtures, a similar distinction between the treatment of phase equilibria and properties of mixing, and volumetric properties is desirable. It would imply that parameter  $b_m$  and, particularly, the binary interaction parameters embedded in the  $a_{res}^{E,\gamma}$  models have the duty of improving the accuracy on phase equilibria predictions and properties of mixing, such as enthalpy ( $h^M$ ), entropy ( $s^M$ ) or heat capacity ( $c_P^M$ ). On the other hand, volumetric properties will be corrected thanks to the volume-translation parameter. This question was addressed by Privat et al. [132], and they proved that the calculation of phase equilibria and properties of mixing remains unaffected only when a linear mixing rule for  $c_m$  is implemented and

temperature-independent pure-compound volume-translation parameters are used, which is already the case of the  $tc$ -PR model for pure compounds.

In order to test the best approach to extend the  $tc$ -PR model to mixtures, it was decided to include three different  $a_{res}^{E,\gamma}$  models in the mixing rule for  $a_m/b_m$ . Such models were the residual part of the Wilson and UNIQUAC models and the  $a_{res}^{E,\gamma}$  NRTL model. The resulting models were called  $tc$ -PR-Wilson,  $tc$ -PR-UNIQUAC and  $tc$ -PR-NRTL, respectively. The implementation of such models is explained in [Publication VII](#). The performance of the three resulting models was compared against the experimental data of the benchmark database, presented in [Publication VI](#). Indeed, the binary interaction parameters for each model and for each of the 200 binary systems included in the database were fitted over available experimental data.

In the light of the obtained results, it is possible to conclude that the best choice to extend the  $tc$ -PR EoS to mixtures along with EoS/ $a_{res}^{E,\gamma}$  mixing rules is to use the residual part of the Wilson  $a_{res}^{E,\gamma}$  model, named  $tc$ -PR-Wilson. This conclusion is supported by the fact that the  $tc$ -PR-Wilson reaches the best results from the quantitative and qualitative standpoints. Nevertheless, improvements have to be made in terms of the behavior correlation of systems in which hydrogen bonds are broken without the possibility to form new ones, as well as in the reproduction of energetic properties for systems in which self-association does not take place. All the grading results, as well as the representation of some binary mixtures' behavior are summarized in [Publication VII](#).

### 3.7 Concluding remarks

In this chapter, the extension of the translated-consistent Peng-Robinson ( $tc$ -PR) EoS to mixtures has been introduced. For this purpose, the research work of this thesis consisted of:

- developing a benchmark database to enable a standardized assessment of the performance of a given thermodynamic model or to compare two models. To classify database's systems on the base of their thermodynamic complexity, the binary systems were classified according to the type of association they exhibit. In the end, the proposed database embeds 200 binary mixtures and includes for each system both phase equilibrium data (VLE, LLE, VLLE, azeotropic data, critical data) and energetic data ( $h^M$  and  $c_p^M$  data). For each property, a detailed procedure explaining how deviations between model predictions and experimental data have to be estimated was provided.
- Using such a benchmark database for the assessment of the  $tc$ -PR EoS armed with EoS/ $a_{res}^{E,\gamma}$  mixing rules embedding three different  $g^{E,\gamma}$  models: Wilson, UNIQUAC and NRTL. It has been shown that the best choice to extend the  $tc$ -PR EoS to mixtures along with EoS/ $a_{res}^{E,\gamma}$  mixing rules is to use the residual part of the Wilson  $a_{res}^{E,\gamma}$  model, named  $tc$ -PR-Wilson.

Although further work should be focused on the study of the influence of the temperature dependence of the binary interaction parameters of the  $tc$ -PR-Wilson model on the reproduction of phase-equilibria and energetic properties data; or on the development of a group-contribution-based predictive  $tc$ -PR-

Wilson model; in the context of this thesis, the work devoted to cubic equations of state for pure compounds and mixtures was considered as achieved since RQ1 and RQ2 were satisfactorily addressed.

Then, in the next chapter, the *tc*-PR model is implemented in the working-fluid design methodology developed for CCHP systems.



## **Chapter 4: Combined Cooling, Heating and Power**



## Chapter 4 : Combined Heating, Cooling and Power

### 4.1 Introduction

As stated in the introduction of this manuscript, the main objective of this thesis was to develop a product-design approach with a large space exploration of working fluids for the selection of suitable candidates for CCHP applications. This approach should consider thermodynamic, process-related, environmental, flammability and toxicity aspects in the selection process as well as performance assessment. In order to ensure that the performance of CCHP fluids is computed reliably, a great part of the research work of this thesis was devoted to the study of cubic equations of state for pure compounds and mixtures with the purpose of enhancing their accuracy on the estimation of saturation and caloric properties.

In [Chapter 2](#), it was shown that the *tc*-PR model has the capacity to accurately correlate (with a few-percent deviation) saturated vapor pressures, liquid densities, enthalpies of vaporization and heat capacities of pure substances. In [Chapter 3](#), the *tc*-PR-Wilson model for mixtures was introduced and its promising capabilities were demonstrated. Nevertheless, improvements have to be made in terms of the behavior predictions of systems in which hydrogen bonds are broken without the possibility to form new ones, as well as in the prediction of energetic properties for systems in which self-association does not take place. Since the *tc*-PR-Wilson is still in development, it was decided to develop the product design approach for the selection of pure working fluids.

This chapter presents the context of cooling, heating and power needs. Then, the CCHP cycle retained in this thesis is described. It is worth noting that a detailed explanation of the conception of a CCHP cycle is provided in [Publication VIII](#). Next, a brief description of the product design framework is presented. Finally, the resulting working fluids from the database search and screening procedure, as well as their performances are summarized.

It is worth noting that in the context of this thesis, in the [Book chapter I](#), the capabilities of the Enhanced-Predictive-PR78 EoS (E-PPR78) to be used for mixture screening in power and refrigeration cycles were assessed. The E-PPR78 EoS is a variant of the PPR78 EoS [\[114\]](#), which enables both the predictive determination of binary interaction parameters and the accurate calculation of pure-fluid and mixture thermodynamic properties.

### 4.2 Electricity, heating and cooling in modern society

Concerning electricity, it is basically consumed by the industry, residential, commercial and agricultural sectors. Generally, electric power demand is categorized into two types: *baseload* and *peaking* power. The former corresponds to the minimum amount of electric power needed to be supplied to the electrical grid at any given time; while the latter refers to the energy provided to meet fluctuations in electricity demand. Baseload power must be supplied by constant and reliable primary energy sources. According to the Global Energy Review presented by the IEA [\[1\]](#), the most common baseload stations are coal-fired and nuclear steam power plants, with 39% and 10.6% of the world electricity production,

respectively. Both types of plants operate on different configurations of the Hirn cycle with superheat and reheat and have long turn-on times (few hours), not suitable to guarantee peak dispatchable generation. On the other hand, peaking power must be provided by fast acting plants running on dispatchable primary energy sources. These include: oil & gas, dispatchable renewable and variable (or intermittent) renewable sources. Among oil-&-gas-based peaking plants, gas turbines and reciprocating engines are the leading technologies for such purposes. Gas-turbine based plants are one of the most important peaking power stations; those are based on simple gas cycle (Brayton cycle) and combined cycle (Brayton + Hirn cycles) power plants. Additionally, reciprocating engines, mostly based on the Diesel cycle, provide stationary electrical power in remote locations. Among dispatchable renewable plants, hydroelectric facilities play an important role in the balance of peaking generation on grid systems since they can be turned on in just a few seconds. Hydropower-based plants are followed by biomass, solar thermal and geothermal power plants, operating on the Organic Rankine Cycle (ORC), as the back-up peaking supply systems. Finally, variable renewable power systems include mainly wind turbines and solar photovoltaic devices.

In terms of heat, the largest demand comes from three main sectors: industrial, commercial and residential. Industry consumes over a half of heat produced for process heat, drying and industrial hot water uses. Most of the rest of the produced heating power is used for space heating, water heating and cooking in the residential sector. The remainder is used in agriculture. The heating equipment, contrarily to energy power plants, is often on site and is largely dominated by fossil fuel-based and conventional electric systems, such as water boilers and electric resistance heaters. Heating technologies are completed by heat pumps, district heating and other renewables-based technologies.

Regarding cooling needs, they can be classified into two major applications: refrigeration and air-conditioning. Firstly, the refrigeration sector includes the following subsectors: residential, commercial, food processing and cold storage, industrial, and transport. Residential refrigeration encompasses refrigerators and freezers used for food storage in domestic units. Commercial refrigeration, in turn, refers to the cooling power required by retail outlets for holding and displaying frozen and fresh food for customer purchase. Food processing and cold storage cover the cooling needs for preserving, processing and storing food from its source to the distribution point. Industrial refrigeration deals with the larger cooling power and equipment required for chemical processing, cold storage, food processing and district cooling. Finally, transport refrigeration consists of systems for transporting chilled or frozen goods. On the other hand, in terms of air conditioning, it is possible to define three types of applications: residential, commercial and mobile. Residential and commercial air-conditioning are related to space cooling in houses or small rooms, and large buildings (i.e. supermarkets, hospitals), respectively. Mobile air-conditioning (MAC) refers to cooling systems used in cars, light commercial vehicles and truck cabins. The cooling power supply relies upon vapor-compression (VC) systems, and thermally-driven chillers based on absorption and adsorption technologies [133].

### 4.3 Conventional CCHP configurations

COGEN Europe, the European Association for the Promotion of Cogeneration, defines CHP as the simultaneous production of useful heat and electricity from a single primary energy source [134]. It is worth noting that CHP (also named cogeneration) systems are more than 100 years-old and can achieve efficiencies ranging from 70% to 90% [135]. They consist of a prime mover, which produces electric power, and a heat recovery system enabling the supply of heating power at different temperatures. Now, if part of the produced mechanical/electrical power (see Figure 4-1a) or the residual heat (see Figure 4-1b) from a CHP system is further utilized for space or process cooling, it becomes a CCHP system. The prime-mover technologies for typical CHP/CCHP applications are gas turbines and reciprocating engines for large facilities or districts, and micro-turbines, ORC, Stirling engines and even fuel cells for small-scale end-users. Cooling technologies, in turn, include thermally-activated units such as absorption chillers or desiccant humidifiers; as well as electric- and engine-driven chillers [136,137].

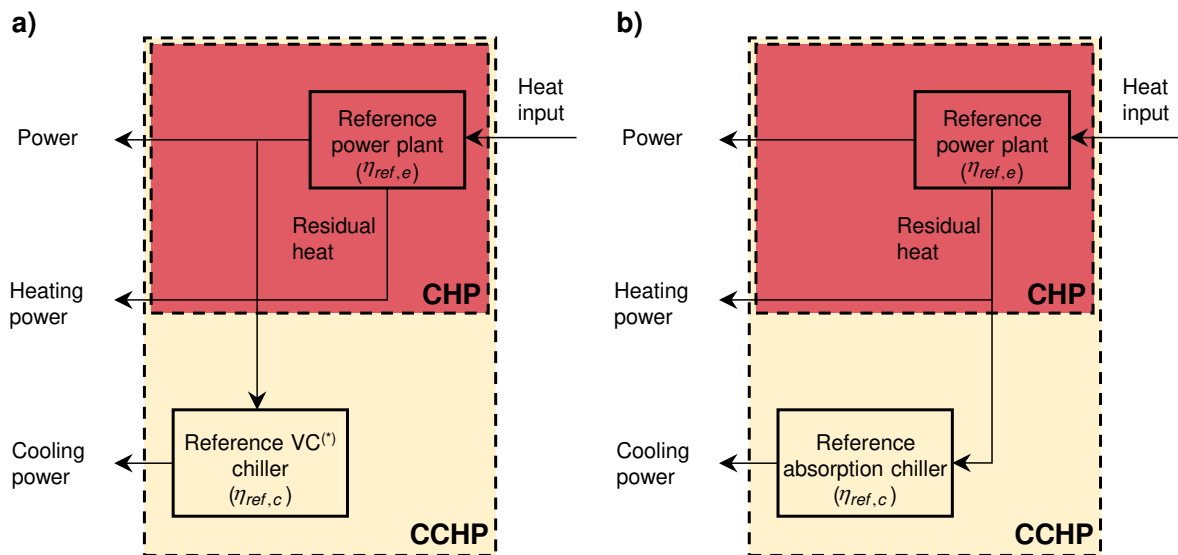


**Figure 4-1.** a) Schematic view of a CCHP system with an electric/engine-driven cooling system. b) Schematic view of a CCHP system with a thermally-activated cooling system. (\*) VC stands for vapor compression.

### 4.4 Novel CCHP configuration

In this thesis, a simplified version of the CCHP cycle proposed by Briola [6] in his patent is considered. This cycle operates with a single working fluid and allows expansions and compressions to take place in the single-phase regions as well as in the two-phase domain. To illustrate this, the operation of the ideal CCHP system is presented. The CCHP configuration is shown in Figure 4-2.

The working fluid in a liquid state is compressed isentropically by a pump (1-2), heated at constant pressure in an evaporator (2-3) until partial or total vaporization is reached, and expanded isentropically in a turbine (3-4). Then, the process (4-5) is intended to provide the required specific heating power ( $q_M$ ) at  $T_M$ . This is followed by an isentropic expansion (5-6) and condensation at constant pressure (6-7). Then, the fluid is expanded isentropically (7-8), heated at constant pressure in an evaporator (8-9), compressed isentropically (9-10), and, finally condensed at constant pressure (10-1) to the initial

state. The amount of specific heat absorbed isothermally by the working fluid from the low-temperature source at  $T_C$  represents a cooling effect ( $q_C$ ) in the surroundings.

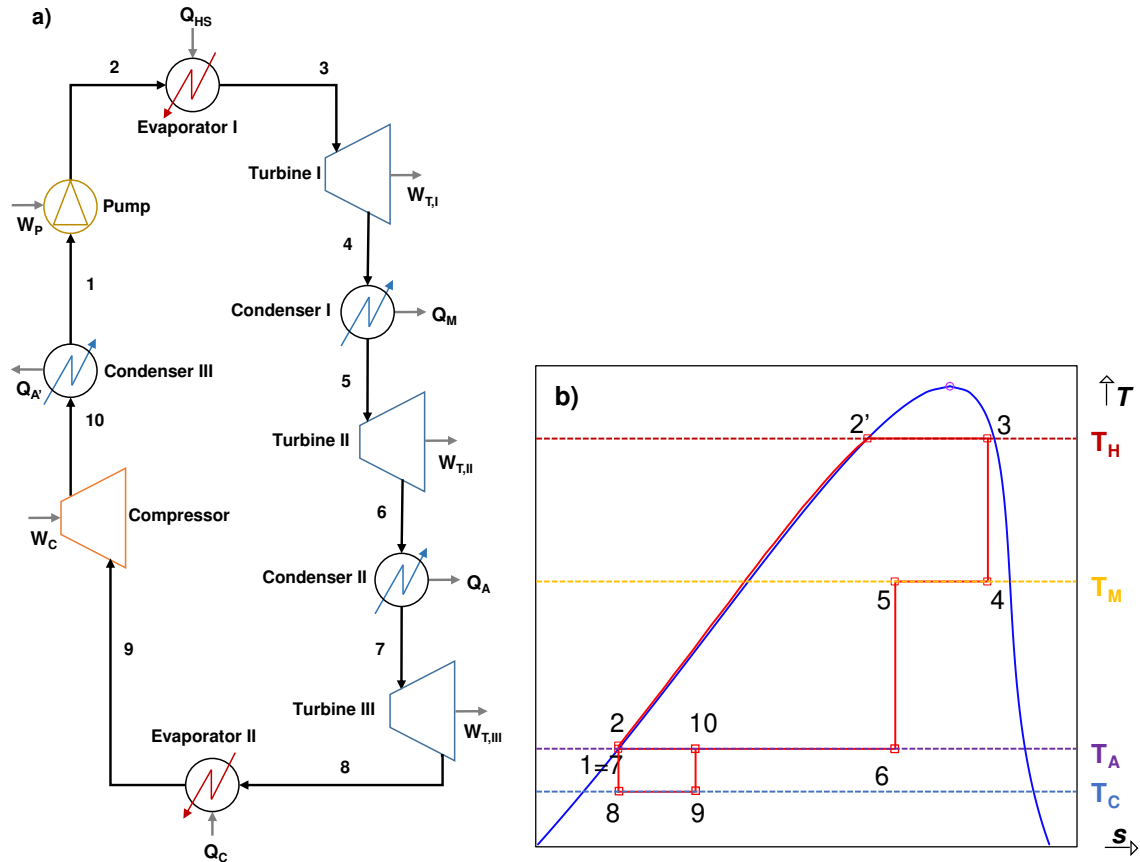


**Figure 4-2.** a) Schematic view of an ideal CCHP cycle as proposed by Briola [6]. b) Sketch of the corresponding temperature-entropy diagram.

## 4.5 Chemical product design

Through the human history, the impact of chemical products in human life has been crucial. The use of fuels for electricity and transportation, pharmaceuticals, plastics, pesticides, perfumes, soap, and a broad array of products is a proof of that. Samudra and Sahinidis [138] stated that a product can be defined as any chemical entity that enables a device or process to perform a desired function. In order to identify such chemical entities, the product design framework has emerged. In the next sections, the definition of chemical product design is presented as well as the classification of chemical products.

### 4.5.1 Classes of chemical products

Seader et al. [139] suggest that chemical products can be classified as: (1) basic chemical products, (2) industrial products, and (3) configured consumer products. Basic chemical products are normally well-defined molecules and mixtures of molecules characterized by thermophysical and transport properties. Examples include: polymers, refrigerants, solvents, lubricants, proteins, solutes or ceramics. These products are also known as commodity chemicals, which are produced in large volumes at small profit margins in dedicated equipment.

Industrial chemicals are often characterized by their microstructure, particle-size distribution, functional (e.g., cleansing, adhesion, shape), sensorial, rheological and physical properties rather than their molecular structure. These chemicals are the focus of engineered materials such as fibers, plastics, monolayer and multilayer films, creams and pastes, glass substrates, and many others.

Configured consumer chemical products are sold directly to the consumer. In this category, chemical products are often devices which effect chemical change. A blood oxygenator used in open-heart surgery, a dialysis device, drug delivery patches are examples of such type of products.

#### 4.5.2 Definition of chemical product design

According to Moggridge and Cussler [140], product design is the process of identifying the best set of candidates that fit desired product functional criteria. This process can be represented by four principal steps as follows:

1. Needs. What needs should the product fill?
2. Ideas. What different solutions/formulations could fill this need?
3. Selection. Which products are the most promising?
4. Manufacture. How can the product be made and critically tested?

#### 4.5.3 Framework for product design

In turn, Gani [141] proposes a modified version of Moggridge and Cussler's main stages of product design, well adapted to molecular products:

1. Needs and goals. What needs/target properties should the product fill?
2. Generation. What different feasible molecules can be tested?
3. Selection. Which candidates are the most promising?
4. Manufacture. How can the product be made?
5. Performance. Does the product actually satisfy the desired performances?

In the first step, the requirements and the functionalities of the product must be defined. Moreover, it is necessary, and sometimes a hard task, to convert these requirements into quantitative specifications. After this stage, a list of candidates, usually referred to as "design space", that could satisfy these needs is generated. Then the best candidates are selected in stage 3, and finally, in 'manufacture', a process design stage is implemented to determine how the product will be made. Performances can be studied using experimental trials or mathematical models. The most common chemical product design methods consist of:

- Experiment-based trial and error: this approach is used when mathematical models for the estimation of the target (desired) properties are not available. It is often required past knowledge and experience to define the design space. Experimental design approach is frequently used then. This procedure is limited frequently by a fixed amount of chemical, time, and financial resources.

- **Model-based search techniques:** this approach is used when reliable and validated mathematical models for the estimation of all the target properties are available. Such models have contributed to the development of the computer-aided molecular design (CAMD) framework. The design space can be quite wide; however, to reduce this space (i.e., the number of candidate molecules), past knowledge and experience may be invoked.
- **Hybrid experiment-model based techniques:** this approach is used when only certain properties can be estimated by mathematical models. The most common option is to use models to reduce the list of candidates to a small number of molecules, which may be further evaluated by means of the experiment-based trial and error approach. In such a way, by reducing the design space, the time and resources spent on the experimental effort are reduced.

**Databases:** Database search is suitable for designing simple molecular products and ingredients selection for some formulated products. Using databases often ensures property reliability and allow a fast generation of the feasible candidates list [142]. Usually, databases are used for preselection of candidates and, in a further stage, their performances are assessed with model-based techniques or experiments.

- **Heuristics:** this approach is supported by heuristic rules (i.e., empirical rules easing the convergence process but are not necessarily optimal) that help to make design decisions, as well as reliable selections. Such rules result from a combination of experience and available knowledge.

#### 4.5.4 Retained approach

In [Publication VIII](#), the methodologies with large-space exploration of working fluids for ORC and vapor-compression (VC) refrigeration configurations are introduced.

The CAMD framework offers the largest design space in terms of candidates and the possibility to find global optimal solutions. Nevertheless, the lack of reliable property models implemented in CAMD tools, for all the potentially considered chemical families, may lead to the exclusion of environmental or safety targets, which are extremely important for the working-fluid design. On the other hand, database search does not provide the largest possible design spaces and, thus, may miss potential candidates but enables the fast generation of feasible candidate lists. Moreover, by combining different databases, it is possible to include more target properties in the design approach.

Recognizing the forces and limitations of CAMD and database search methodologies, it was considered nevertheless that, for the purpose of this thesis, the latter offered the best trade-off between design space and considered target properties. The database search methodology has been implemented to screen about 60 000 species included in the DDB, the DIPPR and the NIST TDE 103b databases. The screening approach considered thermodynamic, process-related, constructional, safety and environmental constraints.

The proposed methodology follows the main stages defined by Gani [141]: 1) Needs and goals; 2) Generation; 3) Selection; 4) Manufacture; 5) Performance. A scheme of the product-design approach adopted in this work for the selection of suitable working fluids for CCHP applications is presented in Figure 4-3.

The needs and goals are defined according to the target properties. Then, the initial set of candidates is defined by means of database search. Next, the screening is applied and followed by the performance evaluation, which is supported by the  $tc$ -PR equation of state. It is worth noting that Gani et al. [143] explained that in the case of basic chemicals, such as refrigerants or solvents, for which the end-use properties are often directly related to their molecular structure, the manufacturing process does not affect product properties, and, therefore, stage 4 (manufacture) can be excluded from the design procedure.

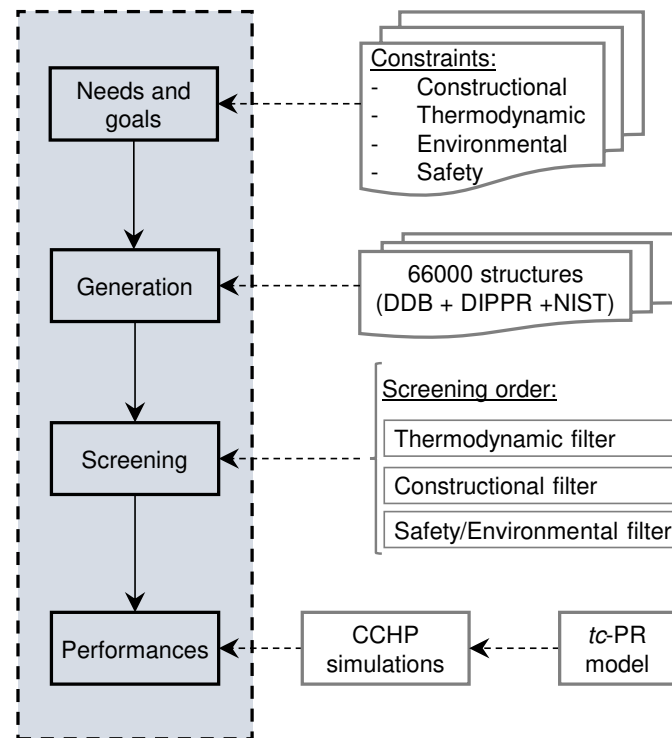


**Figure 4-3.** Scheme of the product-design approach adopted in this work for the selection of suitable working fluids for CCHP applications.

## 4.6 Results

In [Publication VIII](#), two case studies related to different CCHP end-users are investigated to assess the impact of operating conditions on the list of promising working fluids. For both case studies, the heat source temperature is 160 °C. For the sake of simplicity, it is assumed that the overall required duty by the end-users is equal to 100 kW ( $|\dot{W}_{net}| + |\dot{Q}_M| + \dot{Q}_C = \dot{m}(|w_{net}| + |q_M| + q_C)$ ). In addition, the cooling, heating and electric needs are quantified as a percentage of the total duty requirements. It is worth noting that the overall required duty of 100 kW is a calculation basis.

For case study 1, it is assumed that for the residential/commercial users:

- The cooling needs include air-conditioning, and they represent 30 % of the total duty. Comfort temperatures in summer range between 20 and 25 °C. To reach such temperatures, the working fluid should enter the evaporator II at 10 °C, i.e., at 20 °C decreased by the pinch point temperature.

- The heating needs account for the 40 % of the total duty and are related to space heating or hot water requirements. Heating power is commonly required at 90 °C.
- The electric power required to drive machines, devices and essential equipment reaches the remaining 30 % of the total duty.

For case study 2, it is assumed that for the food industry:

- The cooling needs include food storage and preservation, and they represent 20 % of the total duty. The set-point temperature within fridges is usually maintained between 2 and 5 °C. To reach such temperatures, the working fluid should enter the evaporator II at -10 °C.
- The heating needs, in turn, represent 60 % of the total duty and are related to the production of low-pressure steam or to specific processes such as pasteurization. Heating power is commonly required at 130 °C.
- The electric power required to drive machines, devices and essential equipment reaches the remaining 20 % of the total duty.

The results of the screening procedure coupled with the performance evaluation have demonstrated that flammable fluids such as vinylacetylene or HFC-152 have a good potential for CCHP applications. In the case where highly constraining safety restrictions are imposed, HCFO-1233zd(E) could be an interesting candidate since it is non-flammable and non-toxic. This is described in detail in the Results section of [Publication VIII](#). Moreover, the well-known tradeoff between flammability and environmental impact is observed [144,145]. In order to reduce the GWP and ODP, molecules should be less halogenated, which implies that flammability increases. In addition, among these fluids, none of them are toxic or fatal substances.

## 4.7 Concluding remarks

In this chapter, the development of a product-design approach with a large space exploration of working fluids for the selection of suitable candidates for CCHP systems have been described. This approach allows for the consideration of thermodynamic, process-related, environmental, flammability and toxicity aspects in the selection process as well as performance assessment. In order to ensure that the performance of CCHP fluids is computed reliably, the *tc*-PR model for pure compounds was implemented.

## **Conclusions**



## Conclusions

In this thesis a methodology for the selection of promising working fluids for Combined Cooling, Heating and Power (CCHP) applications has been presented. This study has intended to provide an insight about working fluids that should be considered for further theoretical and experimental investigations. A key stage of the development of the proposed methodology relied on the study of cubic equations of state for pure compounds and mixtures in with the purpose of enhancing their accuracy on the estimation of saturation and caloric properties.

### Main findings and contributions

#### **RQ1. Which modifications should be made to cubic equations of state in order to accurately reproduce vapor pressures, liquid densities, enthalpies of vaporizations and heat capacities for pure compounds?**

Throughout this work it has been showed that two major concepts are necessary for the development of CEoS: the consistency and volume-translation concepts. The implementation of these concepts along with a sound parameterization method leads to highly accurate CEoS such as the *translated-consistent* Peng-Robinson (*tc*-PR) EoS.

The research work of this thesis resulted in the enhancement of the capabilities of the *tc*-PR model, developed by Le Guennec et al. [146], to yield to a highly accurate cubic equation of state that not only could be used in the field of energy-related applications but in the computer-aided design of fluid-fluid phase-contacting unit operations. Prior to this study the *tc*-PR model had shown a promising potential in terms of accuracy on vapor pressures, liquid densities, enthalpies of vaporization and heat capacities. Nevertheless, there was no guarantee that by regressing parameters on any of the combinations of  $P^{sat}$ ,  $\Delta_{vap}H$  and  $c_{P,liq}^{sat}$ , the quantitative quality of the model was ensured. This thesis contributed to show that reliable parameters are obtained on the condition that they are – at least – fitted to vapor-pressure data.

This thesis also contributed to the constitution of a reference database suitable for the identification of the strengths and weaknesses of a given thermodynamic model for pure compounds. 1800 molecules for which, in addition to the critical coordinates ( $T_c$ ,  $P_c$  and  $v_c$ ), accurate correlations for  $P^{sat}$  and  $\rho_{liq}^{sat}$  are available. Among them, 1536 fluids also possess an accurate correlation for  $\Delta_{vap}H$  and 890 for  $c_{P,liq}^{sat}$ , resulting in a database containing 306 700 high-quality pseudo-experimental data points.

The studies presented in [Publication I](#) to [Publication V](#) highlight that the use of the highly flexible, component-dependent Twu91  $\alpha$ -function drastically improves the reproduction of vapor pressures, enthalpies of vaporization and liquid heat capacities. In addition, such studies show the spectacular improvement in the reproduction of liquid densities when a substance-dependent volume-translation parameter is used. Finally, these publications also highlight the impressive accuracy of the *tc*-PR EoS that got an average overall deviation lower than 2% over the 306 700 available experimental data points.

In particular, such a model is able to correlate vapor pressures with an error of 1% whereas errors on  $\Delta_{\text{vap}}H$ ,  $c_{P,\text{liq}}^{\text{sat}}$  and  $v_{\text{liq}}^{\text{sat}}$  are close to 2%.

### **RQ2. Which is the best approach to extend cubic equations of state to mixtures?**

In order to safely extend CEoS to mixtures addressing the question of mixing rules is capital. The research work of this thesis introduced advanced mixing rules (EoS/ $a_{\text{res}}^{E,\gamma}$ ) derived by equating the residual part of the excess Helmholtz energy from an EoS and from an explicit activity-coefficient model (ACM). The implementation of such mixing rules seems particularly appropriate since the result is independent of the reference pressure at which both contributions are equated.

The next step was to extend the *tc*-PR model to mixtures implementing EoS/ $a_{\text{res}}^{E,\gamma}$  mixing rules. For this purpose, three activity coefficient models were tested: Wilson, UNIQUAC and NRTL. In the light of the obtained results, it is possible to conclude that the best choice to extend the *tc*-PR EoS to mixtures along with EoS/ $a_{\text{res}}^{E,\gamma}$  mixing rules is to use the residual part of the Wilson  $a_{\text{res}}^{E,\gamma}$  model, named *tc*-PR-Wilson. It yields a remarkable percentage of 4% of “out-of-model” data points. The *tc*-PR-Wilson model distinguishes especially in the prediction of liquid and gas phase compositions, azeotropic points and three-phase pressures.

In the same way as for pure compounds, a high-quality reference database was built that can be used for assessing the accuracy of a thermodynamic model or to cross-compare the performances of different models when applied to mixtures. A specific procedure for the calculation of the deviations between model calculations and experimental data was discussed in detail, as well as a methodology for grading a thermodynamic model was proposed. In total, 200 non-electrolytic binary mixtures were selected to cover all categories of mixtures. They were divided into 9 groups according to the associating character of the two components, i.e., to their ability to be involved in a hydrogen bond. In general, for each binary system of the database, ten properties were experimentally determined: liquid phase composition  $x$ , gas phase composition (or second liquid phase composition)  $y$ , three-phase pressure  $P_{LLV}$ , three-phase composition  $z_{LLV}$ , critical pressure  $P_c$ , critical composition  $x_c$ , azeotropic pressure  $P_{\text{azeo}}$ , azeotropic composition  $x_{\text{azeo}}$ , mixing enthalpy  $h^M$  and mixing heat capacity  $c_P^M$ .

### **RQ3. Which approach from the product-design framework is the most appropriate for the inclusion of thermodynamic, constructional, toxicological, flammability and environmental criteria in the selection of working fluids for CCHP applications?**

The Computer-Aided Molecular Design (CAMD) framework offers the largest design space in terms of candidates and the possibility to find global optimal solutions. Nevertheless, the lack of reliable property models implemented in CAMD tools, for all the potentially considered chemical families, may lead to the exclusion of environmental or safety targets, which are extremely important for the working-fluid design. On the other hand, database search does not provide the largest possible design spaces and, thus, may miss potential candidates but enables the fast generation of feasible candidate lists. Moreover, by combining different databases, it is possible to include more target properties in the design approach.

Recognizing the forces and limitations of CAMD and database search methodologies, it was considered nevertheless that, for the purpose of this thesis, the latter offered the best trade-off between design space

and considered target properties. The database search methodology has been implemented to screen about 60 000 species included in the DDB, the DIPPR and the NIST TDE 103b databases. The screening approach considered thermodynamic, process-related, constructional, safety and environmental constraints. The screening coupled with the performance evaluation have demonstrated that flammable fluids such as vinylacetylene or HFC-152 have a good potential for CCHP applications. In the case where highly constraining safety restrictions are imposed, HCFO-1233zd(E) could be an interesting candidate since it is non-flammable and non-toxic.

## Perspectives and future research

During the development of this thesis, several assumptions were made and different questions have been raised. Therefore, the different future lines of research are proposed for more detailed study and analysis.

- **Study of the inclusion of an association term for pure compounds:** The following striking fact was demonstrated: not all the non-self-associating molecules are well modeled by CEoS, such as SRK, PR, *tc*-RK and *tc*-PR, and that almost 2/3 of the self-associating compounds of the database are represented with high accuracy by CEoS. At this step, one might wonder whether the addition of an association term is the right solution to improve the accuracy of EoS.
- **Study of the self-association phenomenon for mixtures:** Although the promising potential of the *tc*-PR-Wilson model, improvements have to be made in terms of the behavior predictions of systems in which hydrogen bonds are broken without the possibility to form new ones.
- **Study of the temperature dependence of binary interaction parameters of the *tc*-PR-Wilson model:** The next step is to study the influence of the temperature dependence of the binary interaction parameters of the *tc*-PR-Wilson model on the reproduction of VLE, LLE, VLLE and energetic property data.

**Development of a group-contribution-based predictive *tc*-PR-Wilson model:** Even if the proposed binary-system database contains 200 systems and about 48 000 experimental data points, more experimental measurements are required for some molecules belonging to specific chemical families. For this reason, recent work has been devoted to the experimental determination and modeling of high-pressure phase behavior for binary systems such as CO<sub>2</sub> + cyclooctane ([Publication X](#)), and CO<sub>2</sub> + 2,3-dimethylbutane ([Publication XI](#)).

**Implementation of a holistic approach with process and product design:** following the methodology proposed by Bowskill et al. [147], it would be interesting to develop a computer-based method for the integrated process and working-fluid design for CCHP applications. Along with thermo-physical calculations performed with the *tc*-PR model, it would be desirable to implement reliable methods for the estimation of flammability or toxicity for such molecules for which these properties are still missing.



## **Publications**



# **Publication I : *I*-PC-SAFT: an Industrialized version of the volume-translated PC-SAFT equation of state for pure components, resulting from experience acquired all through the years on the parameterization of SAFT-type and cubic models.**

Edouard Moine<sup>1</sup>, Andrés Piña-Martinez<sup>1</sup>, Jean-Noël Jaubert<sup>1(\*)</sup>, Baptiste Sirjean<sup>1</sup>, Romain Privat<sup>1(\*)</sup>

<sup>(1)</sup> *Université de Lorraine, École Nationale Supérieure des Industries Chimiques, Laboratoire Réactions et Génie des Procédés (UMR CNRS 7274), 1 rue Grandville, 54000, Nancy, France*

## **Abstract**

The SAFT and cubic models are often compared in the open literature. Usually, limitations and strengths of both types of equations of state (EoS) are ascribed to their theoretical foundations. Little attention has been paid until now to the influence of parameterization choices on the performance of these EoS. By parameterization, it is here meant the way or method used to attribute values to EoS component-dependent parameters. SAFT-type and cubic EoS for pure compounds use two different parameterization methods: SAFT parameters are generally regressed on vapor-pressure and liquid-density data while cubic models use as input parameters experimental values of the critical temperature, pressure and acentric factor and are generally parameterized in order to exactly reproduce these three properties. As a consequence of these parameterization methods, SAFT EoS overestimate critical pressures while cubic EoS fail in reproducing accurately liquid-density data.

In order to discuss the influence of parameterization methods on EoS performances, three different parameterization methods are considered and applied to both SAFT and cubic models. It is shown that at a fixed parameterization method, SAFT and cubic EoS are equivalent as they exhibit similar accuracies for the correlation of vapor-pressure, enthalpy of vaporization, heat capacity and liquid-density data. This study led us to conclude that EoS requiring three component-dependent parameters cannot provide simultaneous accurate prediction for all the properties of a pure fluid. It is highlighted that the key point to get high accuracy (for non-associating pure compounds) is to work with an EoS equivalent to a four-parameter corresponding-states principle, i.e., that requires the specification of four macroscopic properties for a given pure compound.

Eventually, we have considered a volume-translated PC-SAFT EoS version involving 4 input parameters: the three classical ones ( $m$ ,  $\sigma$ ,  $\varepsilon$ ) and a volume-translation parameter ( $c$ ). Such an EoS shows excellent performances: for no less than 587 non-associating compounds vapor-pressure data are predicted with an error of 1.5 %, liquid-heat capacity and enthalpy of vaporization are predicted with an error of 3 % while liquid density data are predicted with an error of 4 %; critical temperatures and pressures are exactly reproduced.



## PI.I Introduction

Equations of state (EoS) for pure fluids contain two types of parameters: those fixed by the theoretical foundations and those that are component-dependent. Typically, the pure-component parameters are either evaluated by regression on vapor-pressure and saturated liquid density data or are determined from critical coordinates and acentric factor data. The procedure that consists in attributing numerical values to component-dependent parameters is called *parameterization method* hereafter.

Usually, the *parameterization method* is implicitly associated with the model itself:

as a first example, the covolume ( $b$ ) and the critical value of the attractive parameter ( $a_c$ ) of cubic EoS (CEoS) for pure compounds are conventionally determined from the knowledge of the experimental critical temperature ( $T_{c,exp}$ ) and pressure ( $P_{c,exp}$ ) in order the model exactly reproduces such values. The acentric factor ( $\omega_{exp}$ ) is usually added as a third parameter in order to improve the correlation of vapor pressures. The open literature highlights that other parameterization methods are only used on rare occasions so that their influence on model performances has seldom been assessed. We can however cite Ting et al. [20], Voutsas et al. [71] or Alfradique and Castier [72] who fit the three pure-component parameters ( $b$ ,  $a_c$  and  $m_{Soave}$ ) for the Peng-Robinson [65,67] EoS to saturated liquid densities and vapor pressures. They got accurate correlation of pure fluid properties and were able to satisfactorily describe mixtures of alkanes. More recently, Segura et al. [73] proposed a more sophisticated technique for parameterizing CEoS. They demonstrated that accurate densities can be obtained with CEoS but the price to pay is an overestimation by the model of the experimental critical pressure and temperature. Llovel et al. [74] explained that such an overestimation is opportune for predicting the critical region by means of the crossover correction [75–77].

As a second example, non-associating SAFT-type EoS are typically parameterized by fitting the component-dependent parameters to vapor pressure and liquid density data [148–154] whereas other procedures are scarcely applied. As an exception, we can cite Pfohl et al. [155] who enforced the PC-SAFT EoS to reproduce the experimental critical temperature and pressure in order to avoid the disadvantage of the conventional parameterization that leads to a significant overestimation of  $T_c$  and  $P_c$  and thus results in erroneous phase splitting in solute + solvent mixtures at temperatures and pressures slightly above the critical point of the solvent. In order to improve the description of systems in the critical region with EoS that are based on mean-field theories, it is necessary to rescale molecular-based EoS parameters since these theories do not take into account the inherent fluctuations in the critical region. In the case of the SAFT-VR EoS, McCabe et al. [156] and Galindo and Blas [157,158] rescaled the size and energy parameters to improve the critical region representation while maintaining the third parameter from the original set. In fact, such authors defined two sets of parameters: one to get accurate liquid densities and one to get accurate critical points. It was indeed impossible to obtain an accurate prediction of all pure fluid properties with a unique set. Similar conclusions were drawn by Blas and Vega [159] and by Pàmies and Vega [160] with the Soft-SAFT EoS. Cismondi et al. [161], Bouza et al. [162] and Privat et al. [68] rescaled the PC-SAFT EoS in order to exactly

reproduce  $T_{c,exp}$ ,  $P_{c,exp}$  and  $\omega_{exp}$  as is done with CEoS. The proposed parameters reproduce vapor pressures with high accuracy and assure an exact representation of the critical coordinates. However, this is achieved at the expense of underestimated liquid densities. Similar conclusion was drawn by Vinhal et al. [163] in the case of the CPA [164–166] (Cubic Plus Association) EoS. Since 2014, Ilya Polishuk [167–171] is developing the accurate critical-point based PC-SAFT EoS (CP-PC-SAFT) in which the three parameters are determined in order to reproduce the experimental critical temperature and pressure and the triple point liquid density. Its implementation necessitated a reevaluation of part of the PC-SAFT universal parameters matrix and additional revisions as well.

This short bibliographical review outlines that parameterization is a key issue – unfortunately not systematically addressed by model developers – because the accuracy of a model is the result of both its theoretical foundations and its parameterization. Thanks to this first analysis, we acquired the conviction that a comparison of the ‘real’ capacities of the SAFT and cubic EoS is fair if the same parameterization method is used for both models.

Still according to this bibliographic study (and, in particular, following Polishuk [167]), the adjective *industrialized* will be solely used to describe EoS models such that:

- the method used to derive the compound-specific parameters follows an entirely transparent and universal protocol
- and (ii) the numerical inputs for each pure component (e.g.  $T_{c,exp}$  or  $P_{c,exp}$ ) are either easily available in databases or can be estimated from predictive correlations.

### What can be said about the industrialization degree of well-known cubic and SAFT-type EoS?

(i) Regarding non-associating SAFT-type EoS, the input parameters (they are generally three) are most often fit to vapor pressure, liquid density, and, sometimes, speed of sound data [153,172]. However, the considered properties may vary from one developer to another. In addition:

- For each property data, the temperature ranges and the number of regressed data points are not defined unambiguously: it is observed that they are selected depending on data availability and developer’s habits.
- The fitting procedure is sometimes implemented by using only one type of experimental property (e.g., for ionic liquids, some authors only consider liquid-density data since the small vapor pressures of ionic liquids are rarely known at low to moderate temperatures) and the consequence of such a practice on the determination of EoS parameters and thus, on EoS performances remains unknown.

In the same spirit, the consequence of using one set of properties (e.g.,  $P^{sat} + \rho_{liq}$ ) over another one (e.g.,  $P^{sat} + \rho_{liq} + \text{speed of sound}$ ) in the fitting procedure is rarely discussed and questioned. As an exception, we can however cite the papers by Liang et al. [173,174] in which these two approaches are deeply discussed.

As a consequence, it can be claimed that the classical parameterization method for SAFT EoS is far from being standardized and is sometimes vague, explaining why there is currently (at the exception of the CP-PC-SAFT EoS by Ilya Polishuk [167]) no industrialized version of this family of EoS.

(ii) Regarding cubic models, their transparent and universal parameterization by the exact reproduction of the experimental critical temperature and pressure and the vapor pressure at a reduced temperature of 0.7 by means of the acentric factor has been imposed by the industrial needs and, in particular, by the oil & gas industry throughout the 20<sup>th</sup> century. Industrialized versions of the Peng-Robinson [65,66,175] and SRK [176] EoS became very popular in particular because they provide accurate estimations of vapor pressures, critical point coordinates and energetic properties (mainly, heat capacity and enthalpy). Liquid densities are not accurately predicted but this deficiency was compensated by the development of specific correlations for that purpose [177,178].

From the above, it appears that the parameterization of SAFT and cubic models are notably different. Nevertheless, the reasons for such choices are not often discussed by model developers. This leads us to think that most of parameterization practices seem to result from the weight of history. On the one hand, the industrial needs imposed the parameterization of CEoS at the pure-compound critical point. On the other hand, the parameterization proposed by the authors of the first SAFT model has been kept throughout the years. As discussed above, the parameterization method generally used for SAFT EoS suffers from a lack of standardization and transparent implementation leading to the absence of an industrialized version. The unavailability of the fluid-specific parameters is today an obstacle for a wide implementation of SAFT models in industrial simulators. As an illustration in 2010, the working party on thermodynamic and transport properties of the European Federation of Chemical Engineering (EFCE) [179] pointed out the “lack of standardization, reference data, and correct and transparent implementations, especially in commercially available simulation programs” and noticed that even if “the use of new methods, such as SAFT, is increasing, they are not yet in position to replace traditional methods such as cubic EoS”. Moreover, even if most of commercial chemical-engineering simulation software contain different SAFT versions, parameter libraries are not always provided and rarely contain association parameters. In addition, the correlation or prediction of SAFT EoS parameters remains an important issue. As a very rare exception, some authors have proposed predictive methods for estimating pure-component PC-SAFT EoS parameters [180–182].

### **What can be learnt from the open literature regarding the compared performances of SAFT-type and cubic EoS?**

When SAFT and cubic EoS are compared in literature studies, it is often stated that:

- SAFT-type EoS provide very accurate predictions of liquid density and vapor-pressure data until  $T_r$  close to 1 but highly overestimate the critical pressure.
- Cubic EoS provide accurate vapor-pressure predictions and an exact reproduction of the experimental critical coordinates in the (pressure, temperature) plane. Nevertheless, liquid-density data are not accurately estimated.

Usually, limitations and strengths of both types of EoS are immediately related to their theoretical foundations. For cubic EoS, it is said that their limitations are assigned to the not-sophisticated enough Van der Waals theory, while their success is largely attributed to the cancellation of errors of both repulsive and attractive term. For SAFT-like EoS, in turn, it is stated that their good performance can be explained by the advanced degree of the underlying theory (the SAFT).

Nevertheless, as mentioned above, not enough attention has been paid to the influence of the chosen parameterization. One may wonder which of these limitations result from the models (and their theoretical background) and which ones are due to the parameterization.

In this paper, the influence of the parameterization on the performance of the models is studied. For each model type (SAFT and cubic), two parameterization methods are first tested:

- Parameterization method 1 (P1): the three input parameters are constrained to exactly reproduce  $T_{c,exp}$ ,  $P_{c,exp}$  and a second point of the vapor-pressure curve by means of the acentric factor (i.e., the vapor pressure at a reduced temperature equal to 0.7).
- Parameterization method 2 (P2): the three input parameters are fit to vapor-pressure ( $P^{sat}$ ), enthalpy of vaporization ( $\Delta_{vap}H$ ), saturated-liquid heat-capacity ( $c_{P,liq}^{sat}$ ) and liquid molar volume ( $v_{liq}^{sat}$ ) data so that the model is not constrained to pass through the experimental critical coordinates ( $T_{c,exp}$ ,  $P_{c,exp}$ ).

To provide global and significant results and to be totally fair when comparing the EoS and their parameterization, it is decided to work on a basis of 587 non-self-associating pure compounds, belonging to various chemical families. Non-self-associating compounds means that they do not have both a lone pair of electrons and a labile hydrogen so that hydrogen bonding cannot occur. These 587 components were selected in the DIPPR database (Design Institute for Physical Properties) because all the desired properties:  $P^{sat}$ ,  $\Delta_{vap}H$ ,  $c_{P,liq}^{sat}$ ,  $v_{liq}^{sat}$ , the critical coordinates ( $T_c$ ,  $P_c$ ) and acentric factor  $\omega$  were available and presented an error  $\leq 5\%$ .

When parameterization method P1 is used, it is possible to translate the EoS by means of a temperature-independent volume translation [92,132,183] in order to improve the accuracy of the prediction of liquid molar volumes. Doing so, a fourth input parameter (the so-called volume-translation parameter) is added to the model. This parameter, denoted  $c$  hereafter, is selected in order to exactly reproduce the experimental saturated liquid volume at a reduced temperature of 0.8. Such a third parameterization is a variation of parameterization P1 and will thus be noted P1 $t$  (where  $t$  stands for translated). It will be applied to both SAFT and cubic EoS. In such a case, the four input parameters become:  $T_{c,exp}$ ,  $P_{c,exp}$ ,  $\omega_{exp}$  and  $v_{liq,exp}^{sat}(T_r = 0.8)$ . As a major result of this study, it will be shown that the successive application of the three parameterization methods (P1, P2 and P1 $t$ ) mentioned above and the analysis of the resulting deviations made it possible to derive an industrialized version of the PC-SAFT EoS for non-associating pure components. The performances of this model in terms of vapor pressure, liquid-density, heat-capacity and vaporization enthalpy data reproduction are evaluated and compared to industrialized cubic models.

This paper is organized in two parts: part 1 is dedicated to the parameterization of the PC-SAFT and SRK EoS using parameterization methods P1 and P2. The comparison of both EoS at fixed parameterization method is then discussed. Parameterization method P1t is treated in a second part for both SAFT and cubic models.

## PI.II Part 1: parameterization of the PC-SAFT and SRK EoS with parameterization methods P1 and P2 that involve three input parameters.

In the following sections, EoS that require 3 component-dependent parameters (also called input parameters) will be simply denoted *3-parameter EoS*.

### PI.II.I Parameterization of the PC-SAFT EoS

#### 2.1.1 Use of parameterization method P2 (classical parameterization of SAFT-type EoS) in which the

3 input parameters are fit to saturation properties ( $P^{\text{sat}}$ ,  $\Delta_{\text{vap}}H$ ,  $c_{P,\text{liq}}^{\text{sat}}$ ,  $v_{\text{liq}}^{\text{sat}}$ )

The PC-SAFT EoS has been selected here as a reference SAFT-type EoS. When applied to a non-associating pure component, the PC-SAFT EoS requires 3 input parameters that are denoted: ( $m_i$ ,  $\sigma_i$ ,  $\varepsilon_i/k$ ), a segment number, a segment diameter and an energy parameter, respectively. In the original version of PC-SAFT, Gross and Sadowski [152] regressed these parameters on vapor-pressure ( $P^{\text{sat}}$ ) and liquid density ( $\rho_{\text{liq}}^{\text{sat}}$ ) data. In this work, the three input parameters are fit to  $P^{\text{sat}}$ ,  $\Delta_{\text{vap}}H$ ,  $c_{P,\text{liq}}^{\text{sat}}$ ,  $v_{\text{liq}}^{\text{sat}}$  by minimizing the objective function defined by Eq. (PI.1). A detailed description of the fitting procedure is given in our previous papers [184,185]. More information about the considered temperature range in order to estimate the deviations on each property can be found in the Supporting Information (Appendix A) (see Table S5).

$$OF = \sum_{i=1}^{50} \left[ \left| \frac{P^{\text{sat,DIPPR}}(T_i^{P^{\text{sat}}}) - P^{\text{sat,EoS}}(T_i^{P^{\text{sat}}})}{P^{\text{sat,DIPPR}}(T_i^{P^{\text{sat}}})} \right| + \left| \frac{\Delta_{\text{vap}}H^{\text{DIPPR}}(T_i^{\Delta_{\text{vap}}H}) - \Delta_{\text{vap}}H^{\text{EoS}}(T_i^{\Delta_{\text{vap}}H})}{\Delta_{\text{vap}}H^{\text{DIPPR}}(T_i^{\Delta_{\text{vap}}H})} \right| + \left| \frac{c_{P,\text{liq}}^{\text{sat,DIPPR}}(T_i^{c_{P,\text{liq}}^{\text{sat}}}) - c_{P,\text{liq}}^{\text{sat,EoS}}(T_i^{c_{P,\text{liq}}^{\text{sat}}})}{c_{P,\text{liq}}^{\text{sat,DIPPR}}(T_i^{c_{P,\text{liq}}^{\text{sat}}})} \right| + \left| \frac{v_{\text{liq}}^{\text{sat,DIPPR}}(T_i^{v_{\text{liq}}^{\text{sat}}}) - v_{\text{liq}}^{\text{sat,EoS}}(T_i^{v_{\text{liq}}^{\text{sat}}})}{v_{\text{liq}}^{\text{sat,DIPPR}}(T_i^{v_{\text{liq}}^{\text{sat}}})} \right| \right] \quad (\text{PI.1})$$

#### 2.1.2 Use of parameterization method P1 in which $T_{c,\text{exp}}$ , $P_{c,\text{exp}}$ and $\omega_{\text{exp}}$ are exactly reproduced

The main feature of parameterization method P1 is that the ( $m_i$ ,  $\sigma_i$ ,  $\varepsilon_i/k$ ) parameters are constrained to exactly reproduce the experimental critical temperature and pressure and the vapor pressure at a reduced temperature equal to 0.7. As highlighted by Cismondi et al. [161] and recently by Privat et al. [68], it is straightforward to determine  $m_i$ ,  $\sigma_i$  and  $\varepsilon_i/k$  from the mere knowledge of  $T_{c,\text{exp}}$ ,  $P_{c,\text{exp}}$  and

$\omega_{exp}$ . Indeed, not only the acentric factor  $\omega$ , but also dimensionless quantities  $T_c^*$  and  $P_c^*$  defined by Eq. (PI.2) can be expressed as univocal functions of the segment number  $m$ .

$$\begin{cases} T_c^* = \frac{T_{c,i}}{\varepsilon_i/k} \\ P_c^* = \frac{P_{c,i} \cdot \sigma_i^3}{k \cdot (\varepsilon_i/k)} \end{cases} \quad (\text{PI.2})$$

Such functions are plotted in Figure PI.1.

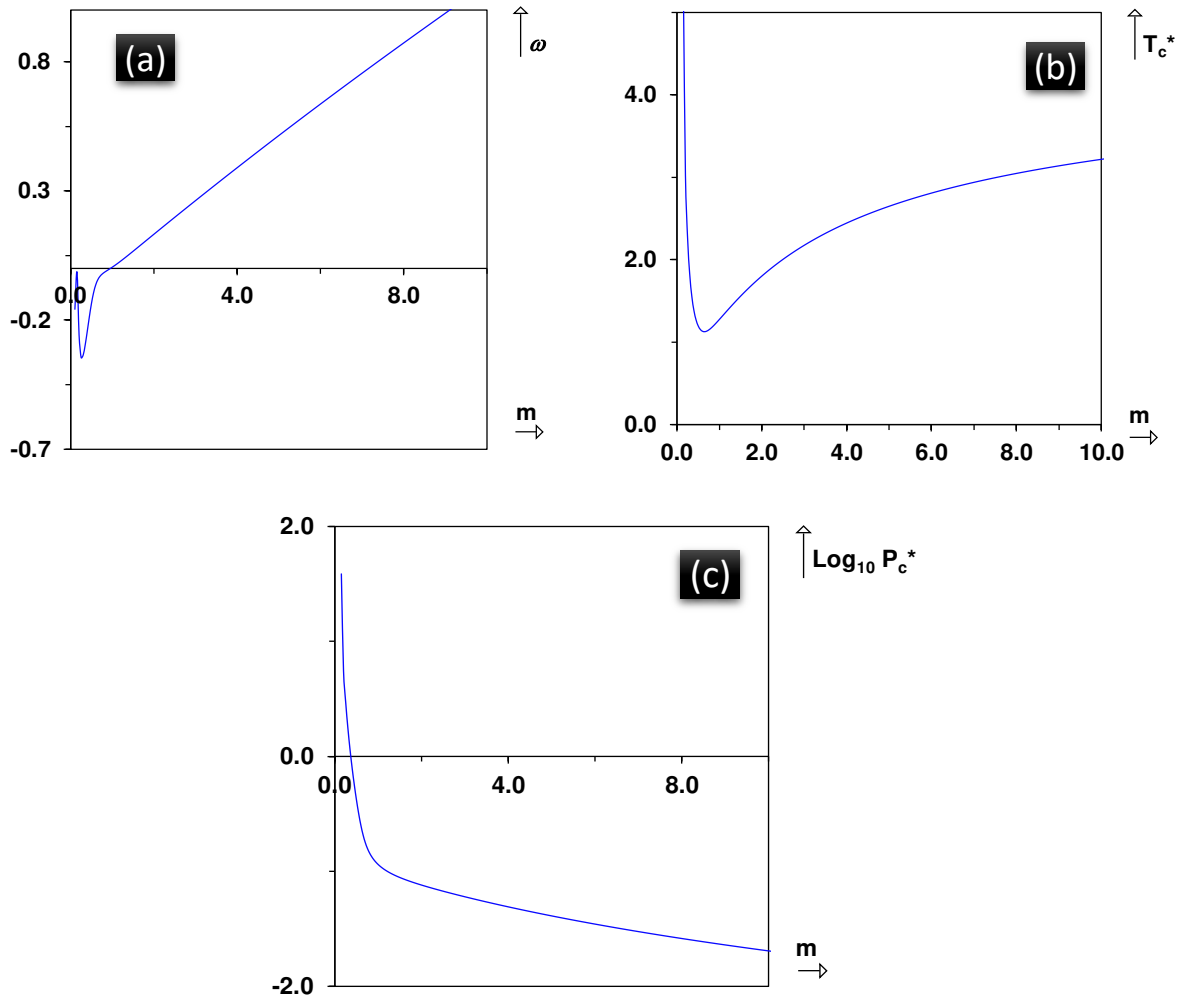


**Figure PI.1.** Generalized charts of the PC-SAFT EoS: plot of  $\omega$ ,  $T_c^*$  and  $P_c^*$  as a function of  $m$ .

In practice, knowing  $\omega_{i,exp}$ , Figure PI.1a makes it possible to estimate univocally the  $m_i$  parameter. Once  $m_i$  is known, Figure PI.1b provides the value of  $T_c^*$  and according to Eq. (PI.2), parameter  $\varepsilon_i/k$  is given by :

$$\varepsilon_i/k = \frac{T_{c,i,exp}}{T_c^*} \quad (\text{PI.3})$$

Then, knowing  $m_i$ , [Figure PI.1c](#) provides the value of  $P_c^*$ . Knowing both the values of  $m_i$  and  $\varepsilon_i/k$ , the last input parameter  $\sigma_i$  is obtained from the following formula also deduced from Eq. (PI.2):

$$\sigma_i = \left[ \frac{\varepsilon_i}{k} \cdot \frac{k \cdot P_c^*}{P_{c,i,exp}} \right]^{1/3} \quad (\text{PI.4})$$

Since experimental values of  $T_c$ ,  $P_c$  and  $\omega$  are known for most of usual chemicals or can be estimated from correlations, this parameterization method takes the advantage of being universal (i.e., applicable to any pure species) and entirely transparent.

In practice, it is advised to use the following polynomial correlations (established for  $m$  ranging from 1 to 20) to approximate the relations between  $(m_i, \sigma_i, \varepsilon_i/k)$  and  $(T_{c,i,exp}, P_{c,i,exp}, \omega_{i,exp})$ :

$$\begin{cases} m_i \approx 0.5959\omega_{i,exp}^2 + 7.5437\omega_{i,exp} + 0.9729 \\ \varepsilon_i/k \approx T_{c,i,exp} \left( 4.7968 \cdot 10^{-6} m_i^5 - 3.0895 \cdot 10^{-4} m_i^4 + 7.8649 \cdot 10^{-3} m_i^3 - 0.10215 m_i^2 + 0.75358 m_i + 0.63659 \right) \\ \sigma_i \approx \left[ \varepsilon_i/k \cdot \frac{k}{P_{c,i,exp}} 10^{(1.6345 \cdot 10^{-7} m_i^6 - 1.1346 \cdot 10^{-5} m_i^5 + 3.1389 \cdot 10^{-4} m_i^4 - 4.4618 \cdot 10^{-3} m_i^3 + 3.6282 \cdot 10^{-2} m_i^2 - 0.22498 m_i - 0.77655)} \right]^{1/3} \end{cases} \quad (\text{PI.5})$$

## PI.II.II Parameterization of the SRK EoS

Use of parameterization method P1 (classical parameterization of CEoS) in which  $T_{c,exp}$ ,  $P_{c,exp}$  and  $\omega_{exp}$  are exactly reproduced

In this work, the Soave-Redlich-Kwong (SRK) EoS [\[176\]](#) is used as reference cubic EoS. For a pure fluid, such an EoS writes:

$$P(T, v) = \frac{RT}{v-b} - \frac{a_c \cdot \alpha(T)}{v(v+b)} \quad \text{with} \quad \alpha(T) = \left[ 1 + m_{Soave} \left( 1 - \sqrt{T/T_{c,exp}} \right) \right]^2 \quad (\text{PI.6})$$

Using parameterization method P1, the covolume ( $b$ ), the critical value of the attractive parameter ( $a_c$ ) and  $m_{Soave}$  are fixed by the exact reproduction of the experimental critical coordinates ( $T_{c,exp}$ ,  $P_{c,exp}$ ) and a second point of the vaporization curve by means of the acentric factor ( $\omega_{exp}$ ). The following equations apply:

$$\begin{cases} a_c = \Omega_a \frac{R^2 T_{c,exp}^2}{P_{c,exp}} \quad \text{with:} \quad \Omega_a = \frac{1}{9(\sqrt[3]{2}-1)} \\ b = \Omega_b \frac{RT_{c,exp}}{P_{c,exp}} \quad \text{with:} \quad \Omega_b = \frac{\sqrt[3]{2}-1}{3} \end{cases} \quad (\text{PI.7})$$

It was also decided to use the Soave's correlation [see Eq. (PI.8)], because (i) it was developed to reproduce the vapor pressure at a reduced temperature of 0.7 and (ii) it is available in all commercially available simulation programs.

$$m_{Soave} = 0.480 + 1.574\omega_{exp} - 0.176\omega_{exp}^2 \quad (\text{PI.8})$$

To be extremely precise, let us recall that such a correlation does not exactly reproduce  $\omega_{exp}$ . However, the difference between  $\omega_{exp}$  and the calculated value of  $\left[-\log_{10} P_r^{sat}(T_r = 0.7) - 1\right]$  was assumed to be negligible.

Use of parameterization method P2 in which the three input parameters are fit to saturation properties ( $P^{sat}$ ,  $\Delta_{vap}H$ ,  $c_{P,liq}^{sat}$ ,  $v_{liq}^{sat}$ )

The three component-dependent parameters of the SRK EoS ( $b_i$ ,  $a_{c,i}$  and  $m_{Soave,i}$ ) are fit to vapor-pressure, enthalpy of vaporization, saturated-liquid heat-capacity and liquid density data by minimizing the objective function defined in Eq. (PI.1). It is worth recalling that using this parameterization method, the critical temperature and pressure predicted by the EoS are different from the experimental ones. With the three input parameters fit to experimental data, it is thus possible to calculate the new critical coordinates [see Eq. (PI.9)], to compare them with experimental ones, and to assess the impact of this parameterization.

$$\begin{cases} T_{c,i,EoS} = \frac{\Omega_b}{\Omega_a} \times \frac{a_{c,i}}{Rb_i} \neq T_{c,i,exp} \\ P_{c,i,EoS} = \frac{R\Omega_b}{b_i} T_{c,i,EoS} \neq P_{c,i,exp} \end{cases} \quad (\text{PI.9})$$

### PI.III Comparison of SRK and PC-SAFT EoS at fixed parameterization methods (P1 and P2)

In this section, a comparison between SAFT and cubic models at a fixed parameterization method is proposed. For a given pure fluid, the mean absolute percentage error (MAPE) on each thermodynamic property ( $P^{sat}$ ,  $\Delta_{vap}H$ ,  $c_{P,liq}^{sat}$ ,  $v_{liq}^{sat}$ ,  $T_c$ ,  $P_c$ ,  $v_c$ ) is calculated as:

$$MAPE_{prop} (\%) = \frac{100}{N_T} \sum_{i=1}^{N_T} \left| \frac{prop_{i,exp} - prop_{i,calc}}{prop_{i,exp}} \right| \quad (\text{PI.10})$$

where  $prop_{i,calc}$  and  $prop_{i,exp}$  denote the property calculated using an EoS and the experimental property extracted from the DIPPR database, respectively. For temperature-dependent properties ( $P^{sat}$ ,  $\Delta_{vap}H$ ,  $c_{P,liq}^{sat}$ ,  $v_{liq}^{sat}$ ),  $N_T$  is the number of temperatures at which the property was evaluated (in this study,  $N_T = 50$ ). For the critical coordinates ( $T_c$ ,  $P_c$ ,  $v_c$ ),  $N_T$  is unity. The average results yielded for both models using the two proposed parameterization methods P1 and P2 are presented in [Table PI.1](#), [Table PI.2](#) and [Figure PI.2](#). Detailed compound-by-compound results and values of all the corresponding parameters are reported in the Supporting Information ([Appendix A](#)) (see Tables S1, S2, S3 and S4).

**Table PI.1.** Average MAPE on several thermodynamic properties as predicted by the PC-SAFT EoS calculated over 587 non-associating pure components.

Property	Parameterization method P1	Parameterization method P2 (classical parameterization of SAFT-type EoS)
$v_{\text{liq}}^{\text{sat}}(T_r < 0.9)$	17 %	1.5 %
$v_c$	19 %	4.4 %
$P^{\text{sat}}$	1.5 %	1.7 %
$\Delta_{\text{vap}}H$	3.2 %	2.4 %
$c_{P,\text{liq}}^{\text{sat}}$	2.9 %	2.3 %
$T_c$	0.0 %	1.8 %
$P_c$	0.0 %	17 %

**Table PI.2.** Average MAPE on several thermodynamic properties as predicted with the SRK EoS calculated over 587 non-associating pure components.

Property	Parameterization method P1 (classical parameterization of cubic EoS)	Parameterization method P2
$v_{\text{liq}}^{\text{sat}}(T_r < 0.9)$	16 %	1.7 %
$v_c$	29 %	14 %
$P^{\text{sat}}$	1.7 %	1.1 %
$\Delta_{\text{vap}}H$	2.6 %	3.3 %
$c_{P,\text{liq}}^{\text{sat}}$	4.7 %	5.5 %
$T_c$	0.0 %	2.2 %
$P_c$	0.0 %	16 %

First of all, it is possible to highlight that  $P^{\text{sat}}$ ,  $\Delta_{\text{vap}}H$ ,  $c_{P,\text{liq}}^{\text{sat}}$  deviations are more or less the same regardless of the model considered (PC-SAFT or SRK) and regardless of the parameterization method used. It can thus be claimed that the theoretical foundations of both EoS classes enables to reproduce satisfactorily  $P^{\text{sat}}$ ,  $\Delta_{\text{vap}}H$  and  $c_{P,\text{liq}}^{\text{sat}}$  data.

On the other hand, it is observed that when the parameterization P1 is used, the experimental critical pressure is exactly reproduced, while a very poor reproduction of liquid molar volume data is observed (this statement applies both to the PC-SAFT and the SRK EoS). Conversely, whatever the EoS is (PC-SAFT or SRK), the use of parameterization P2 leads to an accurate reproduction of  $v_{\text{liq}}^{\text{sat}}$  and to a significant overestimation of  $P_c$ . Such observations totally agree with those already published by many

---

authors (see the introduction of this paper) but by considering more than 500 fluids, this study makes it possible to conclude that these observations are completely general.

As a conclusion, it can be claimed that:

- Cubic and SAFT models exhibit the same behavior provided they are parameterized using the same procedure. The very similar accuracy observed is certainly a consequence of (i) the same number (three) of required component-dependent parameters (ii) the comparable physical meaning of the 3 input parameters embedded in each EoS. The segment number  $m$  is, somehow, the molecular equivalent of the acentric factor  $\omega$ ; it explicitly takes into account the chain length or non-sphericity of the molecules. In the same manner,  $\sigma$ , the segment diameter is clearly related to the covolume  $b$  that is proportional to the molecular volume. Last,  $\varepsilon$ , an energy parameter is the molecular equivalent of  $a_c$ , the critical value of the attractive parameter.
- Whatever the EoS (cubic or SAFT), the parameterization modifies dramatically the model performances (especially the capability to predict  $v_{\text{liq}}^{\text{sat}}$  and  $P_c$  properties) and thus, plays a major role in that respect.
- It is impossible to obtain simultaneously accurate predictions for  $v_{\text{liq}}^{\text{sat}}$  and  $P_c$ .

These results are also graphically illustrated in [Figure PI.3](#) and [Figure PI.4](#) in which an hydrocarbon (n-decane), a ketone (3-pentanone) and a permanent gas (nitrogen) are selected to highlight the impact of the parameterization method on the EoS accuracy for both SAFT and cubic models. It is possible to observe that for a small molecule like nitrogen,  $P_c$  is only slightly overestimated when parameterization P2 is selected, regardless of the EoS type. Similarly, liquid molar volumes are also only slightly overestimated when parameterization P1 is chosen. We can thus conclude that for spherical molecules like  $\text{N}_2$ , the impact of the parameterization is negligible and that accurate results are obtained for all the properties whatever being the 3-parameter EoS considered (PC-SAFT or SRK). For non-spherical molecules (like n-decane) or polar molecules (like 3-pentanone), regardless of the EoS, a good reproduction of liquid density data induces a significant overestimation of the critical pressure. Symmetrically, an exact reproduction of the critical pressure leads to a substantial overestimation of liquid densities.

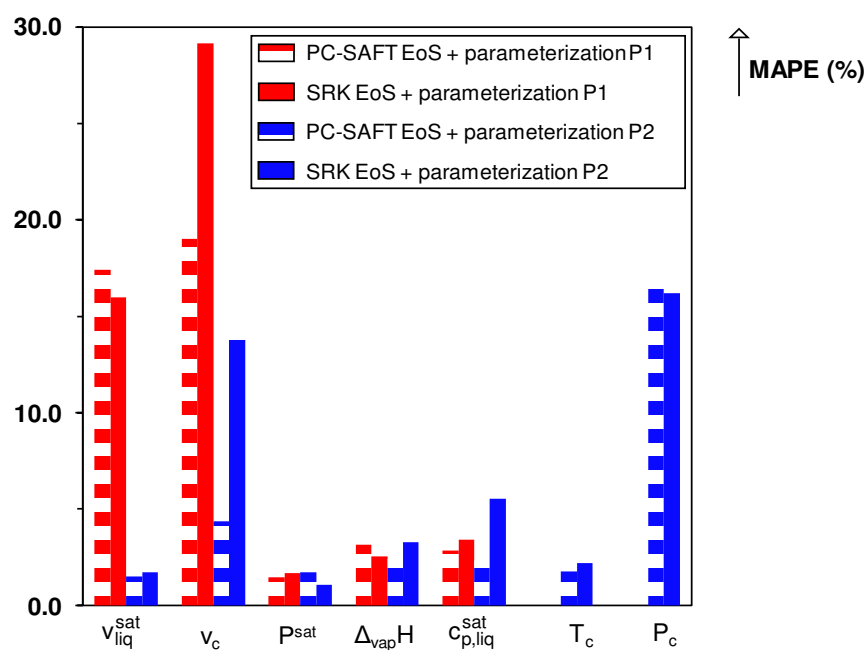


**Figure PI.2.** MAPE on several thermodynamic properties as predicted by the SRK and PC-SAFT EoS. Parameterization P1 (red): the three input parameters are constrained to the exact reproduction of  $(T_{c,exp}, P_{c,exp}, \omega_{exp})$ . Parameterization P2 (blue): the three input parameters are fit to saturation properties  $(P^{sat}, \Delta_{vap}H, c_{p,liq}^{sat}, v_{liq}^{sat})$ .

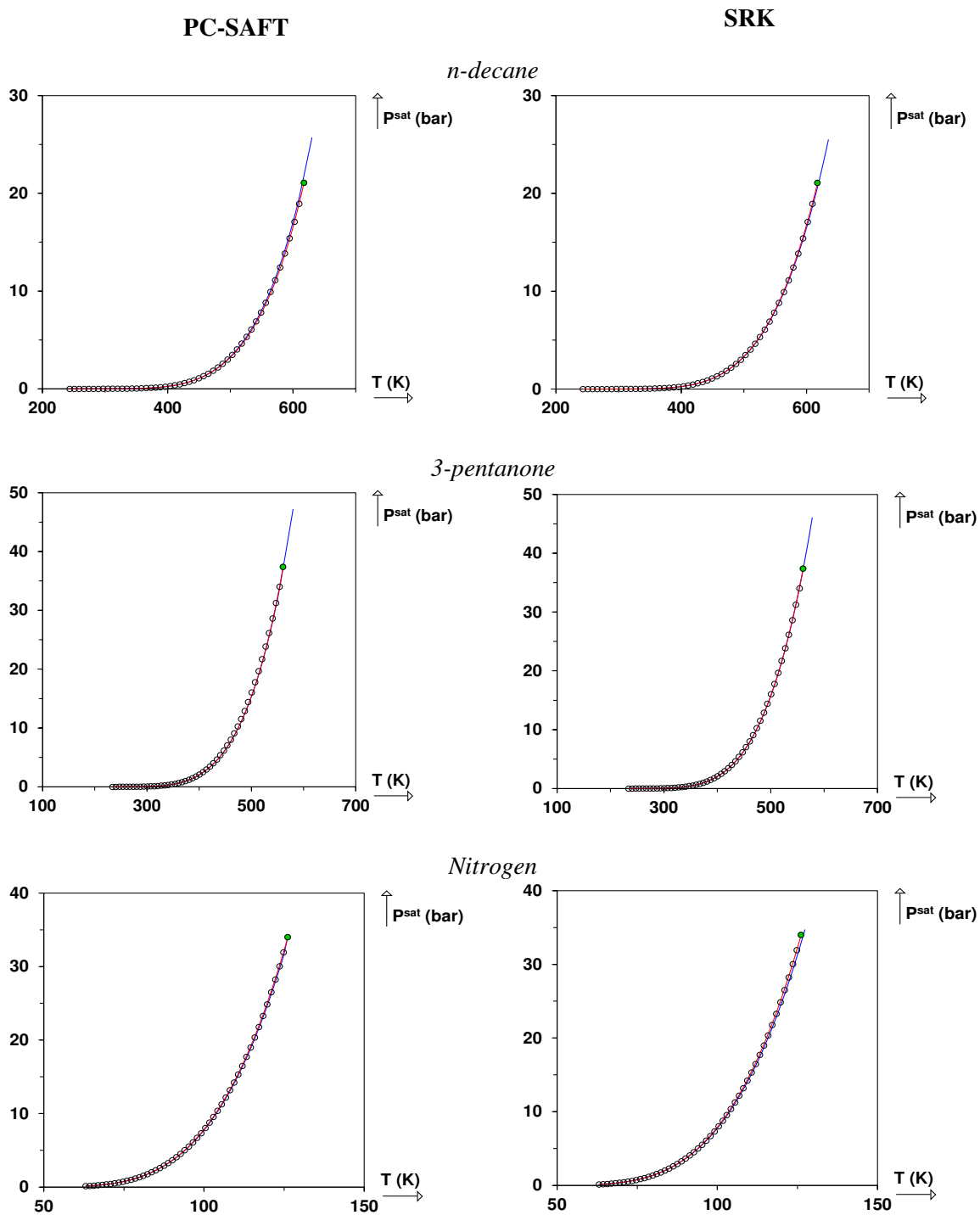


**Figure PI.3.** Vaporization curve with respect to temperature predicted by PC-SAFT (left) and SRK (right) EoS. Parameterization P1 (red): the three input parameters are constrained to the exact reproduction of  $(T_{c,\text{exp}}, P_{c,\text{exp}}, \omega_{\text{exp}})$ . Parameterization P2 (blue): the three input parameters are fit to saturation properties  $(P^{\text{sat}}, \Delta_{\text{vap}}H, c_{P,\text{liq}}^{\text{sat}}, v_{\text{liq}}^{\text{sat}})$ .

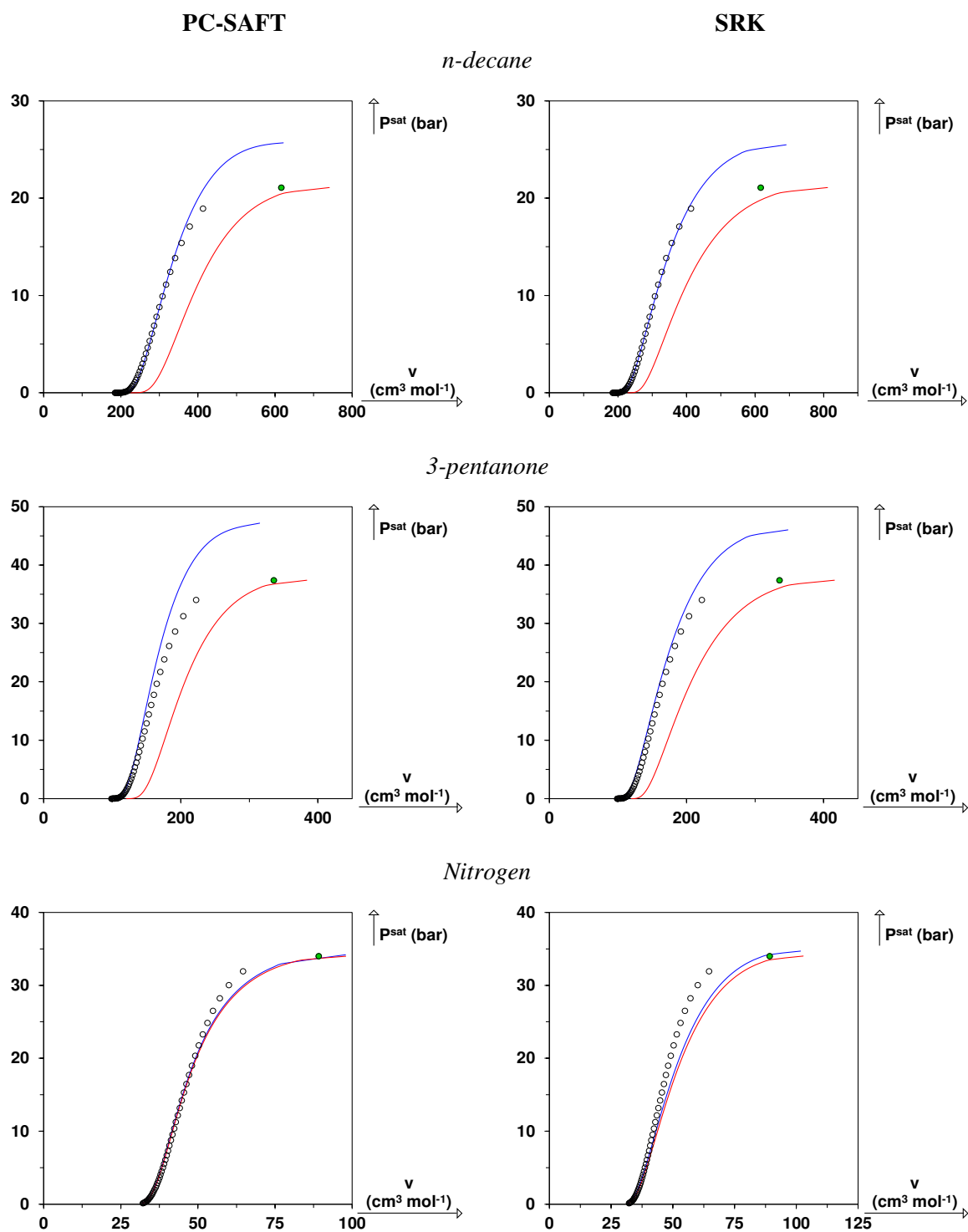


**Figure PI.4.** (Pressure, volume) plane predicted by PC-SAFT (left) and SRK (right) EoS. Parameterization P1 (red): the three input parameters are constrained to the exact reproduction of  $(T_{c,\text{exp}}, P_{c,\text{exp}}, \omega_{\text{exp}})$ . Parameterization P2 (blue): the three input parameters are fit to saturation properties  $(P^{\text{sat}}, \Delta_{\text{vap}}H, c_{P,\text{liq}}^{\text{sat}}, v_{\text{liq}}^{\text{sat}})$ .

For non-spherical molecules, there is a real antagonism between the exact reproduction of the experimental critical pressure, on the one side, and an accurate reproduction of liquid molar volume data, on the other side. This observation applies both for SAFT and cubic models. To highlight this antagonism, it was decided to use parameterization method P2 but to give an increasing weight to the critical pressure (through the objective function defined in Eq. (PL.1)). Results obtained with the PC-SAFT EoS can be seen in Figure PL.5 (a similar plot would be observed with the SRK EoS) for 4 compounds. Such a figure shows unambiguously that the better the prediction of  $P_c$  is, the more deteriorated the liquid molar volumes are (and vice-versa). Although scarcely discussed, such an antagonism was noticed by Vinhal et al. [163] in their attempt to rescale the pure-component parameters of the CPA EoS for methanol.

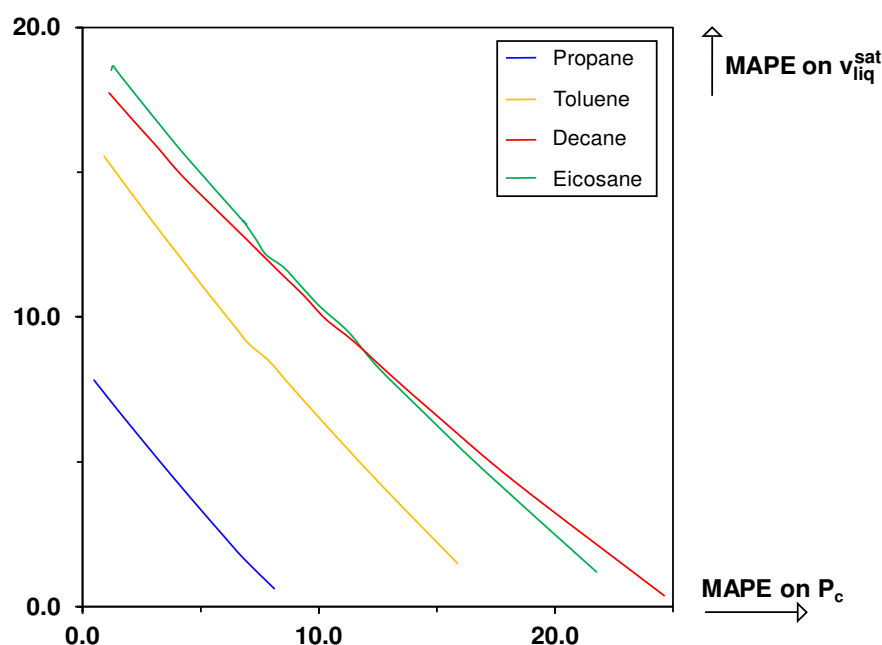


**Figure PL.5.** MAPE on  $v_{\text{liq}}^{\text{sat}}$  wrt. MAPE on  $P_c$  obtained with the PC-SAFT EoS. Parameterization P2 is used and (from right to left) the weight given to the critical pressure is successively increased.

The key conclusion of the above section (part 1) is that, except for spherical molecules, the 3-parameter corresponding-states law is not accurate enough to model the behavior of non-associating pure compounds. Therefore, we consider that EoS requiring only three component-dependent parameters are not accurate enough for practical applications. Note that this observation does not depend on the theoretical background underlying the EoS: 3-parameter cubic or molecular-based EoS cannot provide simultaneously an accurate prediction of volumetric, critical, energetic and phase transition properties of a pure fluid. Switching from one parameterization method to another only modifies the list of properties that are or are not accurately correlated. As an example, parameterization method P1 leads to huge deviations on liquid densities but makes it possible to perfectly match the critical pressure whereas parameterization method P2 leads to small deviations on liquid densities but in turn, strongly overestimates critical pressures. This paper makes it possible to conclude that the number of compound-

specific parameters must be larger than 3, what corroborates the conclusions by Bouza et al. [162] and Pfohl et al. [155] who explained that the 4-parameter BACK [186] (Boublik–Alder–Chen–Kreglewski) EoS is the unique one (among the many equations they tested) capable of providing excellent predictions of many properties for various pure fluids. In particular, Bouza et al. [162] parameterized the BACK EoS in terms of  $T_c$ ,  $P_c$ ,  $\omega$  and critical compressibility factor ( $z_c$ ). Similarly, not only Patel and Teja [187] but also Cismondi and Mollerup [188] highlighted that the addition of a fourth component-dependent parameter like  $z_c$  (the critical compressibility factor) significantly improved the performances of CEoS.

Although it is sometimes believed that 4 component-dependent parameters are only necessary to estimate the properties of strongly polar or hydrogen-bonded compounds (see, e.g., the papers by Xiang [189,190]), the excellent review on the corresponding-states principle (CSP) by Leland and Chappellear [191] also concludes that it is necessary to use a 4-parameter CSP to catch the behavior of molecules which have moderate polarity and which are not spherical (as most of the 587 compounds we considered in this paper). In view of improving EoS, it seems interesting to recall which parameters are most often used by developers of corresponding-states interrelationships. A brief literature review makes it possible to conclude that the many papers devoted to the development of 4-parameter corresponding-state methods for the prediction of thermodynamic properties always use  $T_c$  and  $P_c$  as first 2 parameters. The most used third parameters are the radius of gyration [192–194], the acentric factor [195,196] or the normal boiling point [197]. The fourth parameter is usually the critical compressibility factor [195] ( $z_c$ ) or a liquid density data point [192,193,196]. It was indeed observed that liquid densities are very sensitive to polar interactions.

At this step, some may wonder why the SAFT-VR EoS [151] which contains 4 component-dependent parameters behaves like the PC-SAFT EoS. Indeed, as explained in the introduction of this paper, a unique set of SAFT-VR parameters cannot correlate all pure fluid properties [156–158]. We believe that such a behavior can be explained by the use of 2 SAFT-VR parameters ( $\varepsilon$  and  $\lambda$ ) to describe the same square-well potential. We are indeed convinced that the four parameters in a four-parameter CS approach cannot be freely chosen: each of them must contribute to a particular description of the physics of the molecule.

At first sight, a dead end is reached: cubic and molecular-based EoS contain generally 3 component-specific parameters and we demonstrated that more than 3 (probably 4) parameters are necessary for non-associating pure compounds. A new issue thus arises: how a fourth parameter could be introduced in any 3-parameter SAFT or cubic EoS?

The previous sections highlighted that, regardless of the considered EoS, small deviations on  $P^{\text{sat}}$ ,  $\Delta_{\text{vap}}H$  and  $c_{P,\text{liq}}^{\text{sat}}$  could be obtained with parameterization method P1 whereas large deviations on liquid densities are observed. Another key point – visible in Figure PI.4 – is that the molar volumes calculated by PC-SAFT or SRK are effectively too large when parameterization method P1 is used but this overestimation is more or less constant along the bubble curve (it does not strongly depend on temperature). The use of the volume translation concept coupled to parameterization method P1 could thus strongly improve the results. By doing so, i.e., by translating an EoS (cubic or SAFT), a new

parameter (the volume shift or volume translation) appears and a translated 3-parameter EoS becomes a 4-parameter EoS. In this study the volume translation,  $c$ , was selected in order to exactly reproduce the experimental saturated liquid molar volume at a reduced temperature of 0.8. It is thus calculated as:

$$c = v_{\text{liq,calc}}^{\text{sat}}(T_r = 0.8) - v_{\text{liq,exp}}^{\text{sat}}(T_r = 0.8) \quad (\text{PI.11})$$

The four macroscopic properties that must be specified are thus:  $T_{c,\text{exp}}$ ,  $P_{c,\text{exp}}$ ,  $\omega_{\text{exp}}$  and  $v_{\text{liq,exp}}^{\text{sat}}(T_r = 0.8)$ . It is noticeable that they are similar to those used in the very accurate 4-parameter corresponding-states methods developed by Wilding and Rowley [192,193] and by Wu and Stiel [196].

Although frequently used with CEoS (see, e.g., our recent papers on translated and consistent [185,198,199] CEoS), the volume-translation concept has been used for the first time with SAFT EoS by Palma et al. [200] only very recently. These authors highlighted how the use of a volume shift in PC-SAFT improved the description of speed of sound and other derivative properties. Fifteen years ago, Cismondi et al. [161] wrote that “a temperature-independent volume translation would provide much better results with PC-SAFT in all cases” but surprisingly they did not perform calculations with a translated form of the PC-SAFT EoS. Working with CPA, Vinhal et al. [163] also explain that a volume translation technique can be used to improve liquid-density predictions.

Similarly, is it possible to improve the accuracy of 3-parameter EoS when parameterization method P2 is used? It is recalled that the reason why critical pressures are overestimated when parameterization method P2 is used is that the EoS (SAFT or cubic) rely both on a mean field theory (density fluctuations close to the critical point have not been taken into account). To eliminate this drawback, a crossover treatment could be added, as McCabe and Kiselev made for the SAFT-VR EoS [201]. However, by doing so, several new component-dependent parameters would be added making difficult the definition of an industrialized version of the EoS of interest. Consequently, this approach was disregarded in this study.

## PI.IV Part 2: parameterization of the PC-SAFT and SRK EoS with parameterization method P1t that involves four input parameters [ $T_{c,\text{exp}}$ ,

$P_{c,\text{exp}}$ ,  $\omega_{\text{exp}}$  and  $v_{\text{liq,exp}}^{\text{sat}}(T_r = 0.8)$ ]

Following the conclusions drawn in the previous section, it is now decided to work with *translated* versions of the PC-SAFT and SRK EoS. Such translated forms are obtained by replacing – in the original (untranslated) EoS – the molar volume  $v$  by  $(v + c)$  where  $c$  is the volume correction. As an example, the translated SRK EoS (*t*-SRK) writes:

$$P(T, v) = \frac{RT}{(v+c)-b} - \frac{a_c \cdot \alpha(T)}{(v+c)(v+c+b)} \quad \text{with} \quad \begin{cases} a_c = \frac{1}{9(\sqrt[3]{2}-1)} \frac{R^2 T_{c,\text{exp}}^2}{P_{c,\text{exp}}} \\ b = \frac{\sqrt[3]{2}-1}{3} \frac{RT_{c,\text{exp}}}{P_{c,\text{exp}}} \end{cases} \quad (\text{PI.12})$$

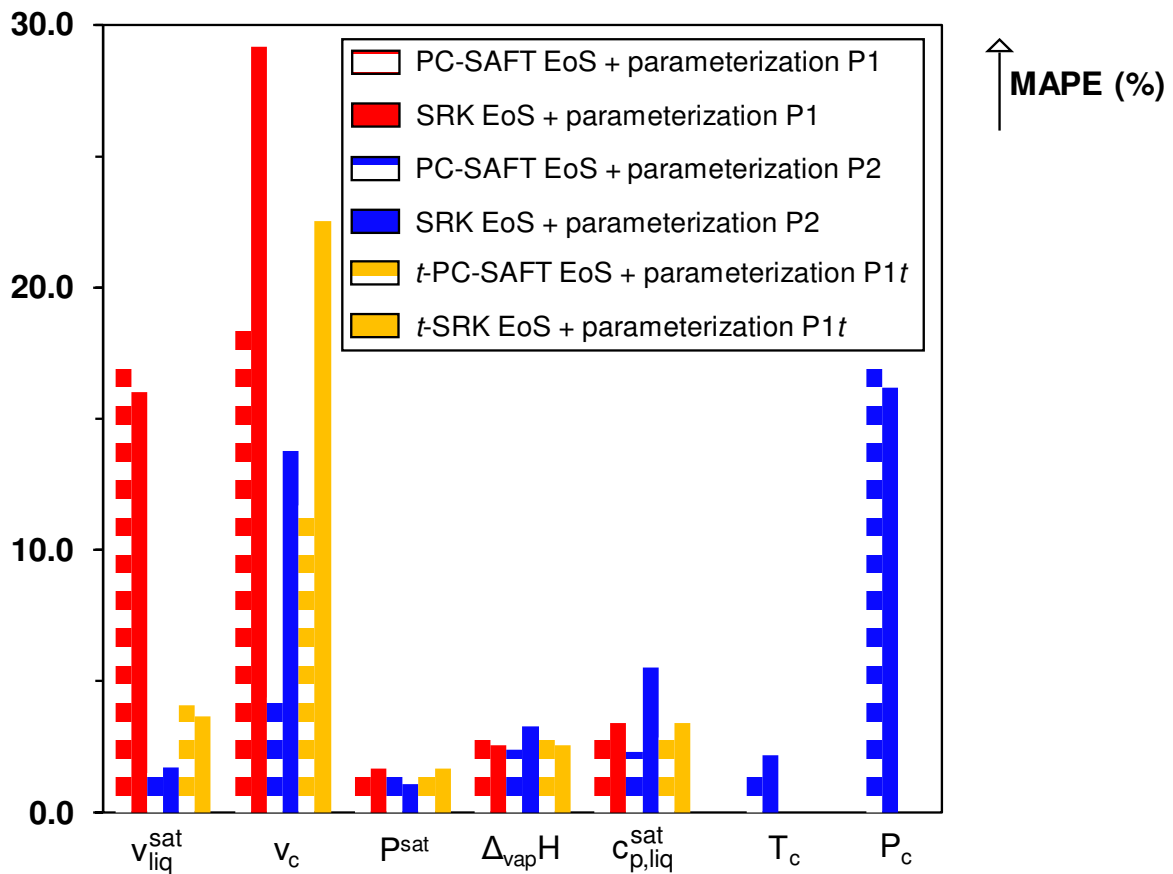
As previously stated, the *t*-PC-SAFT and the *t*-SRK (where *t* stands for “translated”) EoS are parameterized with method P1*t* that imposes an exact reproduction of  $T_{c,exp}$ ,  $P_{c,exp}$ ,  $\omega_{exp}$  and the experimental saturated liquid density at  $T_r = 0.8$ . Doing so, four macroscopic properties must be specified; it can be claimed that the *t*-PC-SAFT and *t*-SRK EoS rely now on a four-parameter corresponding-states principle. Such EoS will be simply denoted *4-parameter EoS* in the following sections. The procedure used in section 2.1.2 to determine  $m_i$ ,  $\sigma_i$  and  $\varepsilon_i/k$  from the mere knowledge of  $T_{c,exp}$ ,  $P_{c,exp}$  and  $\omega_{exp}$  remains exactly the same: the three parameters  $m_i$ ,  $\sigma_i$  and  $\varepsilon_i/k$  are not affected by volume translation and Eq. (PI.5) still applies. Indeed, a temperature-independent volume translation leaves unaffected the vapor pressures [183], so that the critical coordinates in the (P,T) plane and the acentric factor (that depends solely on the reduced vapor pressure at  $T_r = 0.7$ ) remain the same. Consequently, the parameterization procedures for the 3 parameters common to 3-parameter and 4-parameter EoS can be kept. Jaubert et al. also demonstrated [183] that not only the vapor pressures but also the vaporization enthalpies and the heat capacities were unaffected by a temperature-independent volume translation. As a direct consequence, the original and the translated forms of any EoS lead to the same calculated values of  $P^{sat}$ ,  $\Delta_{vap}H$ , and  $c_{P,liq}^{sat}$ . We can thus assert that the small deviations on  $P^{sat}$ ,  $\Delta_{vap}H$ , and  $c_{P,liq}^{sat}$  obtained with parameterization method P1 and reported in Table PI.1 and Table PI.2 still apply in this section. Obviously, the deviations on  $P_c$  and  $T_c$  are still equal to zero. However, as expected, the addition of a volume-translation parameter spectacularly lowers the MAPE on  $v_{liq}^{sat}(T_r < 0.9)$  and, to a less extent, the deviation on the critical molar volume. With the *t*-PC-SAFT EoS, the deviations on  $v_{liq}^{sat}(T_r < 0.9)$  are decreased from 17 % to 4.1 % and with the *t*-SRK EoS they are reduced from 16.8 % to 3.7 %. Such results are graphically illustrated in Figure PI.6 and Figure PI.7. Deviations obtained with the *t*-PC-SAFT and *t*-SRK EoS can be quantitatively assessed in Table PI.3. Detailed compound-by-compound results and values of all the corresponding parameters are reported in the Supporting Information (Appendix A) (see Tables S1 and S2).

**Table PI.3.** Average MAPE on several thermodynamic properties as predicted by the *t*-PC-SAFT and *t*-SRK EoS calculated over 587 non-associating pure components. In both cases parameterization method P1*t* was followed so that the *t*-PC-SAFT EoS is named *I*-PC-SAFT.

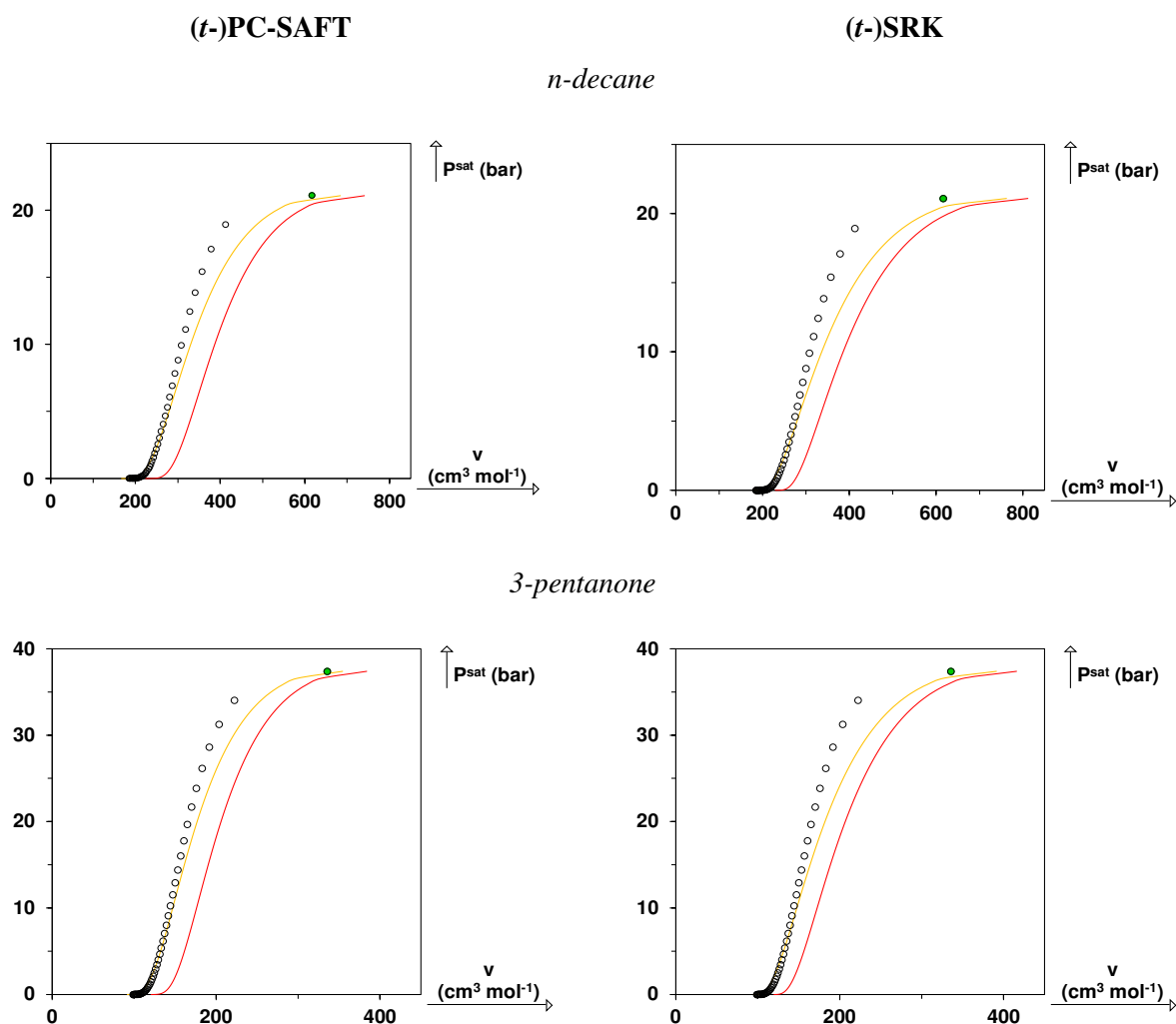
Property	<i>I</i> -PC-SAFT (parameterization method P1 <i>t</i> )	<i>t</i> -SRK (parameterization method P1 <i>t</i> )
$v_{liq}^{sat}(T_r < 0.9)$	4.1 %	3.7 %
$v_c$	12 %	23 %
$P^{sat}$	1.5 %	1.7 %
$\Delta_{vap}H$	3.2 %	2.6 %
$c_{P,liq}^{sat}$	2.9 %	4.7 %
$T_c$	0.0 %	0.0 %
$P_c$	0.0 %	0.0 %

Table PI.3 accentuates – once again – that both EoS show very similar accuracies: all the deviations (except for the critical molar volume) are lower than 5 % what seems reasonable for most of industrial applications. It is however noticeable that all the deviations only concern saturation properties so that it would be interesting to better investigate – in a next paper – how both models behave at extremely high pressures.

The methods used to derive the component-specific parameters of both the  $t$ -PC-SAFT and  $t$ -SRK EoS follow an entirely transparent and universal protocol and the numerical inputs for each pure fluid are easily accessible in databases. Following Polishuk [167] and Hendricks et al. [179], such EoS are thus ready to be implemented in industrial simulators. For this reason, it is proposed to baptize the  $t$ -PC-SAFT EoS coupled with the parameterization method P1 $t$  that exactly reproduces:  $T_{c,\text{exp}}$ ,  $P_{c,\text{exp}}$ ,  $\omega_{\text{exp}}$  and  $v_{\text{liq,exp}}^{\text{sat}}$  ( $T_r = 0.8$ ):  $I$ -PC-SAFT EoS (for *Industrialized*-PC-SAFT).



**Figure PI.6.** MAPE on several thermodynamic properties as predicted by the ( $t$ -)PC-SAFT and ( $t$ -)SRK EoS. Parameterization P1 (red): the three input parameters are constrained to the exact reproduction of ( $T_{c,\text{exp}}$ ,  $P_{c,\text{exp}}$ ,  $\omega_{\text{exp}}$ ). Parameterization P2 (blue): the three input parameters are fit to saturation properties ( $P^{\text{sat}}$ ,  $\Delta_{\text{vap}} H$ ,  $C_{p,\text{liq}}^{\text{sat}}$ ,  $v_{\text{liq}}^{\text{sat}}$ ). Parameterization P1 $t$  (yellow): the four input parameters of the translated EoS are constrained to the exact reproduction of [ $T_{c,\text{exp}}$ ,  $P_{c,\text{exp}}$ ,  $\omega_{\text{exp}}$ ,  $v_{\text{liq,exp}}^{\text{sat}}$  ( $T_r = 0.8$ )].



**Figure PI.7.** (Pressure, volume) plane predicted by (*t*-)PC-SAFT (left) and (*t*-)SRK (right) EoS. Parameterization P1 (red): the three input parameters are constrained to the exact reproduction of  $(T_{c,\text{exp}}, P_{c,\text{exp}}, \omega_{\text{exp}})$ . Parameterization P1 $t$  (yellow): the four input parameters of the translated EoS are constrained to the exact reproduction of  $[T_{c,\text{exp}}, P_{c,\text{exp}}, \omega_{\text{exp}}, v_{\text{liq,exp}}^{\text{sat}}(T_r = 0.8)]$ .

Before conclusion and in order to follow the recommendations of one of the reviewers of this paper, we found interesting to compare the predictions for speeds of sound in a *n*-alkane like *n*-pentane. With the help of the Dortmund Data Bank, it was possible to collect 58 experimental data points of speed of sound in gaseous pentane [202] and 940 values in liquid *n*-pentane [203–215]. For such data, the experimental temperature varies from 263 to 437 K and the pressure from 1.5 kPa to 810 MPa. The corresponding deviations are reported in Table PI.4 for both the *I*-PC-SAFT and *t*-SRK EoS. It is clear that both models are able to perfectly catch the speeds of sound in the gas domain. The calculated deviations ( $< 0.1\%$ ) are definitively lower than the experimental uncertainty. For both models, the predicted speeds of sound in the liquid region are not acceptable ( $> 20\%$ ) but it is important to explain that the calculated speeds of sound are systematically lower than the experimental ones. Moreover, the deviations are more or less constant whatever the temperature so that by decreasing the value of the volume translation, such deviations are immediately reduced to 4% (the prize to pay is however the worsening of liquid

densities). It would be risky to draw conclusions on results obtained on a unique *n*-alkane and the prediction of speeds of sound will be analyzed in details in a following article.

**Table PI.4.** Average MAPE on speeds of sound in *n*-pentane as predicted by the *I*-PC-SAFT and *t*-SRK EoS.

Property	<i>I</i> -PC-SAFT (parameterization method <i>P1t</i> )	<i>t</i> -SRK (parameterization method <i>P1t</i> )
Speed of sound in gaseous <i>n</i> -pentane (58 exp. data points)	0.04 %	0.09 %
Speed of sound in liquid <i>n</i> -pentane (940 exp. data points)	22.1 %	20.6 %

## PI.V Conclusion

This paper was aimed at explaining which of the physical background or the parameterization of SAFT and cubic models was responsible for their well-documented limitations. Consequently, a large part of this paper was devoted to test the influence of the parameterization method on model performance. In this study, working on 587 non-associating compounds for which many experimental data were available in the DIPPR database, it has been shown that:

- three-parameter equations of state (or equivalently the 3-parameter CSP) cannot provide simultaneous accurate predictions for all the properties of non-associating pure fluids except for the so-called *simple* fluids like CH<sub>4</sub> or N<sub>2</sub>. Consequently, by describing the behavior of a pure fluid with 3 macroscopic properties only, a choice has to be made on the list of properties that are or are not accurately correlated. In any 3-parameter EoS (molecular-based or cubic), such a choice can be governed by changing the parameterization method.
- The modern statistical mechanical basis of 3-parameter molecular-based EoS does not increase their accuracy in comparison to 3-parameter cubic EoS. We here mean that a complex theoretical background of an EoS does not necessarily guarantee a better description of pure-component behavior (for pure fluids, it was observed that complexity did not boost EoS performances).

The key point to get high accuracy with non-associating compounds is to work with an EoS (cubic or molecular-based) deriving from a four-parameter corresponding-states principle, i.e., that requires the specification of 4 macroscopic properties for a given pure fluid. The adaptation of SAFT-type EoS, to associating compounds can be classically made by adding an association term. The estimation and prediction of the association parameters remain an issue that requires further developments. When dealing with CEoS, self-associating compounds can be described by using a consistent [184,185,198,199] sophisticated  $\alpha$ -function (like the one developed by Twu [216]) or by adding an association term (this is the CPA approach).

- Translating a molecular-based or a cubic EoS makes it possible to switch from a 3-parameter EoS to a 4-parameter EoS. This study highlighted that the translated *t*-PC-SAFT and the *t*-SRK EoS show accurate (and sometimes, very accurate) results when the four parameters ( $m_i$ ,  $\sigma_i$ ,  $\varepsilon_i/k$  and  $c_i$  for *t*-PC-SAFT ;  $b_i$ ,  $a_{c,i}$ ,  $m_{Soave,i}$  and  $c_i$  for *t*-SRK) are determined in order to exactly reproduce the 4 macroscopic properties:  $T_{c,exp}$ ,  $P_{c,exp}$ ,  $\omega_{exp}$  and  $v_{liq,exp}^{sat}$  ( $T_r = 0.8$ ).

Last but not least, the proposed parameterization of the *t*-PC-SAFT EoS follows an entirely transparent and universal protocol. Moreover the four numerical inputs per pure compound are easily accessible in usual databases. Consequently, following Polishuk [167] and Hendricks [179] recommendations, it is proposed to call the translated version of PC-SAFT presented in this article: the *I*-PC-SAFT EoS (for *Industrialized* PC-SAFT EoS). Such an EoS shows excellent performances : for the 587 non-associating compounds that were considered, vapor-pressure data are predicted with an error of 1.5 %, liquid-heat capacity and enthalpy of vaporization are predicted with an error of 3 % while liquid density data are predicted with an error of 4 %; critical temperatures and pressures are exactly reproduced.



## **Publication II : Analysis of the combinations of property data that are suitable for a safe estimation of consistent Twu $\alpha$ -function parameters. Updated parameter values for the translated-consistent tc-PR and tc-RK cubic equations of state.**

Andrés Pina-Martinez<sup>1</sup>, Yohann Le Guennec<sup>1</sup>, Romain Privat<sup>1(\*)</sup>, Jean-Noël Jaubert<sup>1(\*)</sup>, Paul M. Mathias<sup>2</sup>

<sup>1</sup> Université de Lorraine, École Nationale Supérieure des Industries Chimiques, Laboratoire Réactions et Génie des Procédés (UMR CNRS 7274), 1 rue Grandville, 54000, Nancy, France

<sup>2</sup> Fluor Corporation, 3 Polaris Way, Aliso Viejo, California 92698, United States

### **Abstract**

The suitability of different combinations of property data among vapor-pressure ( $P^{sat}$ ), enthalpy of vaporization ( $\Delta_{vap}H$ ) and saturated-liquid heat-capacity ( $c_{P,liq}^{sat}$ ) data for fitting consistent Twu  $\alpha$ -function parameters is evaluated. A given combination is declared to be suitable if the obtained fitted parameters produce acceptable predictions for the 3 considered properties for the 783 molecules included in the *reference* database. Calculations are carried out using the *translated-consistent* versions of the Peng-Robinson (*tc*-PR) and Redlich-Kwong (*tc*-RK) cubic equations of state (CEoS). It is demonstrated that reliable parameters are obtained on the condition that they are – at least – fitted to vapor-pressure data. It is strongly advised to not exclusively fit  $\alpha$ -function parameters to enthalpy of vaporization and/or saturated-liquid heat capacity data.

Finally, Twu  $\alpha$ -function parameters (L, M, N) suitable for the *tc*-PR and *tc*-RK CEoS are determined for the 1721 molecules, for which at least accurate vapor-pressure data are available in the DIPPR database. The volume-translation parameter  $c$  has also been determined but for only 1489 pure fluids. In addition, the generalized versions of the *tc*-PR and *tc*-RK CEoS ('generalized' means that the input parameters of these models are the experimental critical temperature, critical pressure and acentric factor) are updated.



## PII.I Introduction

Most of the 2-parameter cubic equations of state (CEoS) obey the general formulation:

$$P(T, v) = \frac{RT}{v-b} - \frac{a(T)}{(v-r_1b)(v-r_2b)} \quad (\text{PII.1})$$

where parameter  $a$  is a measure of the attractive forces between molecules; parameter  $b$  is the so-called covolume, which attempts to correct the perfect-gas law for the fact that molecules have a finite volume; and  $r_1$  and  $r_2$  are two universal constants that depend on the selected EoS. The temperature-dependent  $a$  parameter of any CEoS is classically written as:

$$a(T) = a_c \cdot \alpha(T) \quad (\text{PII.2})$$

that is, as the product of the value of the attractive parameter at the critical temperature ( $a_c$ ) multiplied by a so-called  $\alpha$ -function, which is dimensionless. It is possible to distinguish two types of  $\alpha$ -functions: *generalized* and *component-dependent*. The coefficients of the generalized  $\alpha$ -functions are usually determined using correlations that only depend on the acentric factor ( $\omega$ ), while the parameters of the component-dependent  $\alpha$ -functions must be regressed, component by component, from experimental data. It is worth noting that the generalized  $\alpha$ -functions, although less accurate than the component-dependent  $\alpha$ -functions, are extremely useful when experimental data to fit the specific parameters of a given  $\alpha$ -function are not available. Moreover, generalized  $\alpha$ -functions are easy to implement because the acentric factor is known for thousands of pure components or can be estimated by well-established correlations or group-contribution methods [217].

As recently highlighted by Le Guennec et al. [218,219],  $\alpha$ -functions cannot be freely chosen. The temperature dependence of  $\alpha$ -functions must indeed obey the following list of constraints to guarantee safe property predictions in both subcritical and supercritical domains:

$$\alpha(T_c) = 1 \text{ and for all T: } \begin{cases} \alpha \geq 0 & \text{and } \alpha(T_r) \text{ continuous} \\ \frac{d\alpha}{dT_r} \leq 0 & \text{and } \frac{d\alpha}{dT_r} \text{ continuous} \\ \frac{d^2\alpha}{dT_r^2} \geq 0 & \text{and } \frac{d^2\alpha}{dT_r^2} \text{ continuous} \\ \frac{d^3\alpha}{dT_r^3} \leq 0 \end{cases} \quad (\text{PII.3})$$

An  $\alpha$ -function that fulfills all of the conditions reported in Eq. (PII.3) was described as *consistent* by Le Guennec et al. These authors also demonstrated that the highly flexible 3-parameter  $\alpha$ -function developed by Twu et al. in 1991 [220] (denoted hereafter as Twu91):

$$\alpha(T_r) = T_r^{N(M-1)} \exp\left[L(1 - T_r^{MN})\right] \quad (\text{PII.4})$$

became consistent if the following constraints were added to the 3 parameters:

$$\left\{ \begin{array}{l} \delta < 0 \\ L\gamma > 0 \\ \gamma < 1 - \delta \end{array} \right. \quad \text{or} \quad \left\{ \begin{array}{l} \delta < 0 \\ L\gamma > 0 \\ \gamma < 1 - 2\delta + 2\sqrt{\delta(\delta-1)} \\ 4Y^3 + 4ZX^3 + 27Z^2 - 18XYZ - X^2Y^2 > 0 \end{array} \right.$$

$$\text{with: } \left\{ \begin{array}{l} \delta = N(M-1) \\ \gamma = MN \\ X = -3(\gamma + \delta - 1) \\ Y = \gamma^2 + 3\delta\gamma - 3\gamma + 3\delta^2 - 6\delta + 2 \\ Z = -\delta(\delta^2 - 3\delta + 2) \end{array} \right. \quad (\text{PII.5})$$

Le Guennec et al. coupled this noteworthy  $\alpha$ -function to the volume translation concept [221,222] discovered by P eneloux et al. [223] in 1982 to define the *translated-consistent* versions of the Peng-Robinson [224] (PR) and Redlich-Kwong [225] (RK) EoS. The volume correction, denoted hereafter as  $c$ , was selected to exactly reproduce the experimental saturated liquid volume at a reduced temperature of 0.8 [ $v_{\text{liq,exp}}^{\text{sat}}(T_r = 0.8)$ ], that is:

$$c = v_L^{\text{sat,u-CEoS}}(T_r = 0.8) - v_{L,\text{exp}}^{\text{sat}}(T_r = 0.8) \quad \text{with} \quad T_r = \frac{T}{T_c} \quad (\text{PII.6})$$

where  $v_L^{\text{sat,u-CEoS}}(T_r = 0.8)$  is the molar volume calculated with the original (*untranslated*) CEoS at  $T_r = 0.8$ .

These EoS, for which safe property predictions are guaranteed in both subcritical and supercritical domains because the  $\alpha$ -function passes the consistency test proposed by Le Guennec et al. are also almost certainly the most accurate 3-parameter CEoS ever published. They can be expressed as:

tc - PR:

$$P(T, v) = \frac{RT}{v-b} - \frac{a_c \cdot \alpha(T_r)}{(v+c)(v+b+2c) + (b+c)(v-b)} \quad \text{with: } \left\{ \begin{array}{l} \alpha(T_r) = T_r^{N(M-1)} \exp\left[L(1 - T_r^{MN})\right] \\ c = v_{\text{liq}}^{\text{sat,u-PR}}(T_r = 0.8) - v_{\text{liq,exp}}^{\text{sat}}(T_r = 0.8) \\ \eta_c = \left[1 + \sqrt[3]{4 - 2\sqrt{2}} + \sqrt[3]{4 + 2\sqrt{2}}\right]^{-1} \approx 0.25308 \\ a_c = \frac{40\eta_c + 8}{49 - 37\eta_c} \frac{R^2 T_{c,\text{exp}}^2}{P_{c,\text{exp}}} \approx 0.45724 \frac{R^2 T_{c,\text{exp}}^2}{P_{c,\text{exp}}} \\ b = \frac{\eta_c}{\eta_c + 3} \frac{RT_{c,\text{exp}}}{P_{c,\text{exp}}} - c \approx 0.07780 \frac{RT_{c,\text{exp}}}{P_{c,\text{exp}}} - c \end{array} \right. \quad (\text{PII.7})$$

*tc - RK* :

$$P(T, v) = \frac{RT}{v-b} - \frac{a_c \cdot \alpha(T)}{(v+c)(v+b+2c)} \quad \text{with:} \quad \begin{cases} \alpha(T_r) = T_r^{N(M-1)} \exp\left[L(1-T_r^{MN})\right] \\ c = v_{liq}^{sat, u-RK}(T_r = 0.8) - v_{liq,exp}^{sat}(T_r = 0.8) \\ a_c = \frac{1}{9(\sqrt[3]{2}-1)} \frac{R^2 T_{c,exp}^2}{P_{c,exp}} \\ b = \frac{\sqrt[3]{2}-1}{3} \frac{RT_{c,exp}}{P_{c,exp}} - c \end{cases} \quad (\text{PII.8})$$

By working with 1116 pure fluids, Le Guennec et al. [94] not only published a library of consistent parameters that are suitable for the *tc*-PR and *tc*-RK EoS but also developed a generalized version of the Twu  $\alpha$ -function for both CEoS (RK and PR). Recently, Bell et al. [226] also published consistent Twu parameters for more than 2500 pure fluids. While the overall aims of these studies were similar, a noticeable difference should be highlighted: Bell et al. [226] directly employed experimental data from the ThermoDataEngine (TDE) database of NIST, while Le Guennec et al. [94] fitted the 3 parameters of the  $\alpha$ -function on pseudo-experimental data generated from correlations available in the DIPPR database. Indeed, the DIPPR database provides a set of temperature-dependent correlations, the coefficients of which are fit to actual experimental data, making it possible to estimate, among other properties, vapor pressures, enthalpies of vaporization and saturated-liquid heat capacities of pure components. Note that for each component and each property, an experimental error is provided. The benefit of using DIPPR correlations instead of raw experimental data is the ability to carry out fitting procedures on pseudo-experimental data that are regularly distributed between the triple point and critical point. By doing so, the optimization results (i.e.,  $\alpha$ -function parameters) are not biased by experimental data points that are concentrated in a specific temperature range. The approach also eliminates the opportunity for independent evaluation of the raw data.

It is worth noting that Le Guennec et al. [94] determined  $\alpha$ -function parameters for 1116 pure compounds by minimizing an objective function accounting for deviations between calculated and pseudo-experimental vapor pressure ( $P^{sat}$ ) and/or enthalpy of vaporization ( $\Delta_{vap}H$ ) and/or saturated-liquid heat capacity ( $c_{P,liq}^{sat}$ ) data. For many components, thanks to the DIPPR correlations, it was possible to generate accurate pseudo-experimental data for all 3 properties, whereas for other components, only 2 or even 1 accurate property could be generated. Therefore, each set of  $\alpha$ -function parameters was fitted on one out of the seven different possible combinations of the pseudo-experimental data properties shown in Table PII.1.

In view of this situation, the key questions we address in this paper are:

Are all of the possible arrangements of the properties listed in Table PII.1 suitable for parameter fitting? If not, some of the parameters we published in 2016 [94] should not be used.

- Which property combinations are the most appropriate for parameter fitting?

As previously explained, Bell et al. [226] published Twu parameters for more than 2500 pure fluids, while the library published by Le Guennec [94] contains parameters for less than half the number of pure components. This is because Le Guennec et al. only considered a DIPPR correlation to be

acceptable if its experimental error (reported in the DIPPR database) was lower or equal to 5%. However, it is believed that, in many cases, this error is overestimated. Thus, another objective of this paper is to review the uncertainty of the correlations reported in the DIPPR database and to develop a new procedure to evaluate error of DIPPR correlations. This new procedure makes it possible to notably increase the number of compounds for which the Twu parameters can be determined.

**Table PII.1.** Possible combinations of accurate pseudo-experimental data available in the DIPPR database for a given pure component. The pure fluid type is an arbitrary index that indicates which properties among  $P^{sat}$ ,  $\Delta_{vap}H$  and  $c_{P,liq}^{sat}$  are associated with accurate data and can thus be used to fit  $\alpha$ -function parameters.

Type of pure fluid	Properties for which accurate data are available (that were considered in the fitting procedure of $\alpha$ -function parameters by Le Guennec et al. [94])
1	$(P^{sat})$
2	$(\Delta_{vap}H)$
3	$(c_{P,liq}^{sat})$
4	$(P^{sat} + \Delta_{vap}H)$
5	$(P^{sat} + c_{P,liq}^{sat})$
6	$(\Delta_{vap}H + c_{P,liq}^{sat})$
7	$(P^{sat} + \Delta_{vap}H + c_{P,liq}^{sat})$

In the first section of this study, an error evaluation of DIPPR correlations is performed in order to draw up a list of compounds for which accurate data of interest ( $P^{sat}$  and/or  $\Delta_{vap}H$  and/or  $c_{P,liq}^{sat}$ ) are available in the DIPPR database. The next section presents the combinations of the property data that are suitable for parameter regression. Finally, an update of the Twu91  $\alpha$ -function and volume-translation parameters with respect to Le Guennec et al.'s initial study is proposed. Component-dependent parameters are determined for 1721 pure fluids. The updated versions of the generalized Twu88  $\alpha$ -functions and volume-translation correlations for both the PR and RK EoS are also provided.

## PII.II Overview of the DIPPR database

### PII.II.I Error evaluation of the DIPPR correlations

As previously stated, this paper addresses the fitting of consistent Twu91  $\alpha$ -function parameters on vapor pressure ( $P^{sat}$ ), enthalpy of vaporization ( $\Delta_{vap}H$ ) and saturated-liquid heat capacity ( $c_{P,liq}^{sat}$ ) data. It is thus decided to draw up the list of pure components for which the DIPPR database has reasonable experimental error for at least one out of the three aforementioned properties.

At this step, it should be noted that only the residual part of the isobaric heat capacity can be estimated from a CEoS. The  $c_P$  of the fluid is obtained by adding the heat capacity of the corresponding perfect gas to the residual contribution expressed from the EoS:

$$c_P(T, v) = c_{P, perfect\ gas}(T) + c_{P, residual}(T, v) \quad (\text{PII.9})$$

The heat capacities of perfect gases can be estimated from DIPPR correlations. Consequently, the error of four correlations per compound must be taken into account when evaluating a pure component:  $P^{sat}$ ,  $\Delta_{vap}H$ ,  $c_{P, liq}^{sat}$  and  $c_{P, perfect\ gas}$ . Henceforth, in this work, when it is stated that  $c_{P, liq}^{sat}$  data can be accurately generated, it is implied that both the  $c_{P, liq}^{sat}$  and  $c_{P, perfect\ gas}$  pseudo-experimental data can be accurately generated.

In this study, the 11.1.0 version (May 2016) of the DIPPR database is used. It should be noted that in the DIPPR database:

- for a series of experimental data, the single attribute ERROR that is reported is the experimental uncertainty of the measured values. This uncertainty can either be provided by the source or calculated by the DIPPR staff.
- for a temperature-dependent correlation, the way that the attribute ERROR is calculated is not known with certainty. Generally, ERROR is equal to the maximum error among those of the data series used to fit correlation parameters.

For certain compounds it is found that the ERROR reported in the DIPPR was overestimated. Indeed, for such cases, the DIPPR reported uncertainty (henceforth called type I error), set to the maximum uncertainty among the data series, was much higher than the average uncertainty value and did not reflect the confidence we could have on the experimental data. Therefore, the actual average uncertainty is calculated (henceforth called type II error) for each of the four temperature-dependent properties ( $P^{sat}$ ,  $\Delta_{vap}H$ ,  $c_{P, liq}^{sat}$  and  $c_{P, perfect\ gas}$ ) and for all pure compounds in the DIPPR database. For a given property and a given pure fluid, a type II error is calculated as:

$$\text{Type II error} = \frac{\sum_{j=1}^{n_{series}} N_{data, j} \times Error_j}{\sum_{j=1}^{n_{series}} N_{data, j}} \quad (\text{PII.10})$$

where  $N_{data, j}$  is the number of experimental data points available in the series  $j$  and  $Error_j$  the corresponding experimental error.

A third strategy to evaluate the correlation errors is to compare pseudo-experimental data with calculated values obtained using the *generalized* version of the *tc*-PR model, which was developed by Le Guennec et al. [94]. Based on the predictive performance of the model, it is possible to state that if a correlation is well represented by the generalized model, it is implied that there is no reason to reject the pseudo-experimental data, and the correlation is considered to be accurate.

For type III errors, the threshold of acceptance (noted *TH*) for each property is defined as:

For  $P^{sat}$ : the mean absolute percentage error (MAPE) on  $P^{sat}$  calculated by the generalized *tc*-PR EoS (see **Table 6** in Le Guennec et al. [94]) from a database including 980 compounds + one standard deviation:

$$TH_{P^{sat}}^{type III} = 2.0\% + 1.2\% = 3.2\% \quad (\text{PII.11})$$

For  $\Delta_{vap}H$ : the mean absolute percentage error (MAPE) on  $\Delta_{vap}H$  calculated by the generalized *tc*-PR EoS (see **Table 6** in Le Guennec et al. [94]) from a database including 805 compounds + one standard deviation:

$$TH_{\Delta_{vap}H}^{type III} = 2.8\% + 1.5\% = 4.3\% \quad (\text{PII.12})$$

For  $c_{P,liq}^{sat}$ : the mean absolute percentage error (MAPE) on  $c_{P,liq}^{sat}$  calculated by the generalized *tc*-PR EoS (see **Table 6** in Le Guennec et al. [94]) from a database including 529 compounds + one standard deviation – 5% (maximum allowed error for  $c_{P,perfect\ gas}$ ). The maximum error of the perfect gas heat capacity was subtracted to focus on the deviation on the residual heat capacity, which is the sole property calculable from the EoS:

$$TH_{c_{P,liq}^{sat}}^{type III} = 6.7\% + 4.3\% - 5\% = 6\% \quad (\text{PII.13})$$

The thresholds of the three types of error are reported in **Table PII.2**.

**Table PII.2.** Acceptance thresholds for the different property correlations and types of error.

Error type	Acceptance thresholds for each property			
	$P^{sat}$	$\Delta_{vap}H$	$c_{P,liq}^{sat}$	$c_{P,perfect\ gas}$
Type I (error reported in the DIPPR database)	5%	5%	5%	5%
Type II (average exp. error calculated by Eq. (PII.10))	5%	5%	5%	5%
Type III (deviation calculated by the gen. <i>tc</i> -PR EoS)	3.2%	4.3%	6%	-

Finally, it is considered that a property can be accurately estimated by a DIPPR correlation if at least one out of the three types of error is less than or equal to its respective threshold.

### PII.II.II Drawing up of a list of compounds potentially suitable for parameter fitting

First, the use of cubic equations of state requires critical temperature ( $T_c$ ) and critical pressure ( $P_c$ ) data. Whether a generalized  $\alpha$ -function is used, the acentric factor ( $\omega$ ) is also needed. Therefore, the first criterion that suitable molecules must meet is that the three experimental constants,  $T_c$ ,  $P_c$  and  $\omega$ , are simultaneously reported in the DIPPR database. Additionally, molecules for which none of the three saturation properties of interest ( $P^{sat}$ ,  $\Delta_{vap}H$ ,  $c_{P,liq}^{sat}$ ) can be accurately generated are removed. Application of these criteria results in 1887 suitable molecules among 2162 available in the DIPPR database. The properties of some compounds, especially metals with a critical temperature higher than 2000 K (Li, K, Ca, LiI) or quantum fluids (He-3 and p-H<sub>2</sub>) that are not of industrial interest, were removed from the database, leaving 1881 compounds. In comparison to the work by Le Guennec et al.,

who only considered type I errors, the definition of two new types of error (type II and type III) makes it possible to significantly increase the number of potentially suitable components for parameter fitting. Let us recall that 1116 pure fluids were considered by Le Guennec et al., whereas 1881 pure fluids are considered in this study.

In [Table PII.3](#), these 1881 molecules are distributed along the 7 fluid types defined in [Table PII.1](#) (i.e., according to the number and type of accurate properties that can be generated for each of them), and a comparison is made with the previous work of Le Guennec et al. Among the 1116 molecules considered by Le Guennec et al., 684 kept the same fluid *type*, whereas 432 moved to a new fluid type. For instance, if type I error is solely considered to evaluate the uncertainty of the correlations (as in Le Guennec et al.), only  $c_{P,liq}^{sat}$  can be estimated for 1-hexene, and consequently, it belongs to type 3 (as defined by [Table PII.1](#) and [Table PII.3](#)). If type II and III errors are also considered, all three of the temperature-dependent properties,  $P^{sat}$ ,  $\Delta_{vap}H$  and  $c_{P,liq}^{sat}$ , can be estimated and 1-hexene moves to type 7.

**Table PII.3.** Comparison of the number of molecules included in the database by Le Guennec et al.<sup>3</sup> and this work.

Type of pure fluid	Accurate property data available	Le Guennec et al.	This work
1	( $P^{sat}$ )	166	217
2	( $\Delta_{vap}H$ )	20	25
3	( $c_{P,liq}^{sat}$ )	98	53
4	( $P^{sat} + \Delta_{vap}H$ )	401	705
5	( $P^{sat} + c_{P,liq}^{sat}$ )	47	80
6	( $\Delta_{vap}H + c_{P,liq}^{sat}$ )	18	18
7	( $P^{sat} + \Delta_{vap}H + c_{P,liq}^{sat}$ )	366	783
TOTAL		1116	1881

### PII.III Suitable combinations of property data for the safe estimation of consistent Twu91 $\alpha$ -function parameters

[Table PII.1](#) indicates that it was possible to define 7 types of pure fluids depending on the availability of accurate pseudo-experimental data. As explained in the introduction, our key concern is to determine which of these 7 types are suitable for safely fitting consistent Twu91  $\alpha$ -function parameters and to order these types. To answer this question, the approach proposed in this section is aimed at fitting Twu91  $\alpha$ -function parameters for type 7 pure-compounds, such that all three temperature-dependent properties,  $P^{sat}$ ,  $\Delta_{vap}H$  and  $c_{P,liq}^{sat}$ , can be accurately estimated from DIPPR correlations. The interest in choosing these pure-compounds is that if it is decided to fit the (L, M, N) parameters using not three but one or two of the selected properties, it becomes possible to predict the remaining ones and to compare them with pseudo-experimental values. It is thus possible to determine whether taking specific combinations of 1 or 2 properties into account for parameter fitting may lead to non-reliable sets of (L, M, N)

parameters. Consequently, for the 783 type 7 fluids (see [Table PII.3](#)), seven different fittings were carried out, as shown in [Table PII.4](#). In the second column, the properties that were taken into account for each fitting are presented. In the third column, the properties predicted by the CEoS with the fitted (L, M, N) parameters are provided.

**Table PII.4.** Arrangements of the properties for Twu91  $\alpha$ -function parameter fitting.

Fitting procedure index	Property data included in the Twu parameter fitting procedure	Properties predicted with the optimized Twu parameter set
1	$(P^{sat})$	$(\Delta_{vap}H + c_{P,liq}^{sat})$
2	$(\Delta_{vap}H)$	$(P^{sat} + c_{P,liq}^{sat})$
3	$(c_{P,liq}^{sat})$	$(P^{sat} + \Delta_{vap}H)$
4	$(P^{sat} + \Delta_{vap}H)$	$(c_{P,liq}^{sat})$
5	$(P^{sat} + c_{P,liq}^{sat})$	$(\Delta_{vap}H)$
6	$(\Delta_{vap}H + c_{P,liq}^{sat})$	$(P^{sat})$
7	$(P^{sat} + \Delta_{vap}H + c_{P,liq}^{sat})$	-

### PII.III.I Fitting procedure

In this study, generation of the pseudo-experimental data obeys the following rules:

1. Regardless of the considered property among  $P^{sat}$ ,  $\Delta_{vap}H$  and  $c_{P,liq}^{sat}$ , 50 equidistant pseudo-experimental data points are generated in their valid temperature range,  $[T_{min}; T_{max}]$ .
2. For the  $\Delta_{vap}H$  and  $c_{P,liq}^{sat}$  correlations, in the case that  $T_{max}$  exceeds  $0.98T_c$ ,  $T_{max} = 0.98T_c$  is set. The reason for this choice is simple:  $\Delta_{vap}H$  goes to zero at the critical temperature and the calculation of the relative deviation with the experimental data induces a division by zero. Similarly,  $c_{P,liq}^{sat}$  goes to infinity at the critical temperature so that, once again, the relative deviation with the experimental value cannot be calculated.
3. For the  $P^{sat}$  correlations,  $T_{max} = T_c$  is set. However, in the case where  $P^{sat}(T_{min}) < 0.1 \text{ bar}$ , the value of  $T_{min}$  is increased to enforce that  $P^{sat}(T_{min}) = 0.1 \text{ bar}$  (considering that most industrial processes operate at higher values of pressure and that  $P^{sat}$  is highly uncertain at low pressures, say less than 1 torr).

The optimal set of (L, M, N) parameters is the one which minimizes the generic objective function depicted in Eq. [\(PII.14\)](#), which is a ponderation of the Mean Absolute Percentage Error (MAPE) on  $P^{sat}$ ,  $\Delta_{vap}H$  and  $c_{P,liq}^{sat}$ . The objective function is obviously adapted according to the fitting procedure index defined in [Table PII.4](#). As an example, for fitting procedure number 1, the objective function only considers the MAPE on  $P^{sat}$ . The fitting procedure is conducted by imposing the mathematical constraints necessary to obtain consistent parameters, as explained by Le Guennec et al. and recalled from the introduction.

$$\begin{aligned}
OF = \frac{100}{50} \sum_{i=1}^{50} \left[ \right. & \left. \frac{\left| P^{sat,DIPPR} \left( T_i^{P^{sat}} \right) - P^{sat,EoS} \left( T_i^{P^{sat}} \right) \right|}{P^{sat,DIPPR} \left( T_i^{P^{sat}} \right)} \right. \\
& + \frac{\left| \Delta_{vap} H^{DIPPR} \left( T_i^{\Delta_{vap} H} \right) - \Delta_{vap} H^{EoS} \left( T_i^{\Delta_{vap} H} \right) \right|}{\Delta_{vap} H^{DIPPR} \left( T_i^{\Delta_{vap} H} \right)} \\
& \left. + WF \frac{\left| c_{P,liq}^{sat,DIPPR} \left( T_i^{c_{P,liq}^{sat}} \right) - c_{P,liq}^{sat,EoS} \left( T_i^{c_{P,liq}^{sat}} \right) \right|}{c_{P,liq}^{sat,DIPPR} \left( T_i^{c_{P,liq}^{sat}} \right)} \right] \quad (P11.14)
\end{aligned}$$

For fitting procedure 6, the weighting factor on  $c_{P,liq}^{sat}$  (denoted as  $WF$  in Eq. (P11.14)) is set to 1. In turn, for fitting procedures 5 and 7, special attention is devoted to the estimation of  $WF$ ; as an initial choice, it is set to 1. Nevertheless, for certain compounds, deviations on  $c_{P,liq}^{sat}$  are found to be much smaller than those on  $P^{sat}$ . In these cases, the deviation on  $c_{P,liq}^{sat}$  is reduced to better correlate  $P^{sat}$  (i.e., to obtain smaller deviations on  $P^{sat}$ ). This goal is made possible by carrying out successive minimizations by changing the value of  $WF$  from 1 to 0.1, with a step of 0.1. In practice, this procedure is run for a considered compound if:

- The MAPE on  $P^{sat}$  is larger than 2% (which corresponds to the average MAPE plus one standard deviation calculated for the 782 considered compounds when  $WF = 1$ ) **and** the MAPE on  $c_{P,liq}^{sat}$  is smaller than that on  $P^{sat}$ .
- The MAPE on  $c_{P,liq}^{sat}$  is considerably smaller (two times) than that on  $P^{sat}$  **and** the MAPE on  $c_{P,liq}^{sat}$  is larger than 1%.

These conditions are summarized in Eq. (P11.15) :

$$\begin{aligned}
& MAPE \text{ on } P^{sat} > 2\% \text{ **and** } MAPE \text{ on } c_{P,liq}^{sat} < MAPE \text{ on } P^{sat} \\
& 2 \times MAPE \text{ on } c_{P,liq}^{sat} < MAPE \text{ on } P^{sat} \text{ **and** } MAPE \text{ on } c_{P,liq}^{sat} > 1\%
\end{aligned} \quad (P11.15)$$

In a second step, the weighing factor is selected on a case by case basis to obtain what we consider to be the best compromise between the MAPE on the vapor pressures and MAPE on the saturated-liquid heat capacities.

### P11.III.II Results

The Mean Absolute Percentage Error (MAPE) on  $P^{sat}$ ,  $\Delta_{vap} H$  and  $c_{P,liq}^{sat}$  is reported in Table P11.5 for the seven fitting procedures described in Table P11.4. Procedure 7, for which the 3 properties are simultaneously considered, serves as a reference. It is observed that fitting procedures that are carried out when only considering  $c_{P,liq}^{sat}$  (procedure 3) yield extremely high deviations: 24.8% and 16.0% for the predicted properties  $P^{sat}$  and  $\Delta_{vap} H$ , respectively. Conversely, it is crucial to include experimental

$c_{P,liq}^{sat}$  data in the fitting procedure to obtain a MAPE on  $c_{P,liq}^{sat}$  lower than 5% (see procedures 1, 2 and 4 in Table PII.5). Procedures 2 and 6, for which no vapor pressure data are considered, seem to yield acceptable average deviations for the predicted properties. However, the deviations on  $P^{sat}$  are higher than the average deviation plus one standard deviation of the reference case (procedure 7). Moreover, for certain molecules, the average deviation on  $P^{sat}$  unfortunately reaches 20%. We thus strongly recommend against fitting  $\alpha$ -function parameters when experimental  $P^{sat}$  data are not available.

**Table PII.5.** MAPE on  $P^{sat}$ ,  $\Delta_{vap}H$  and  $c_{P,liq}^{sat}$  according to the property considered for parameter fitting.

Fitting N° procedure	Property taken into account for fitting	MAPE on $P^{sat}$ (783 compounds)	MAPE on $\Delta_{vap}H$ (783 compounds)	MAPE on $c_{P,liq}^{sat}$ (783 compounds)
1	( $P^{sat}$ )	0.7%	2.7%	6.8%
2	( $\Delta_{vap}H$ )	2.1%	1.4%	5.1%
3	( $c_{P,liq}^{sat}$ )	24.8%	16.0%	0.6%
4	( $P^{sat} + \Delta_{vap}H$ )	0.9%	1.6%	5.1%
5	( $P^{sat} + c_{P,liq}^{sat}$ )	1.3%	2.8%	1.7%
6	( $\Delta_{vap}H + c_{P,liq}^{sat}$ )	3.1%	2.3%	1.7%
7	( $P^{sat} + \Delta_{vap}H + c_{P,liq}^{sat}$ )	1.1%	2.2%	2.3%

For procedure 5, very accurate predictions are achieved. To sum up, if we accept deviations on  $c_{P,liq}^{sat}$  higher than 5%, it is recommended to only estimate consistent Twu91  $\alpha$ -functions parameters for molecules for which at least the pseudo-experimental data of  $P^{sat}$  can be accurately generated (procedures 1, 4, 5 and 7 in Table PII.6).

**Table PII.6.** Number of molecules for which at least the pseudo-experimental data of  $P^{sat}$  can be accurately generated.

Type of pure fluid	Accurate property data available	This work
1	( $P^{sat}$ )	217
4	( $P^{sat} + \Delta_{vap}H$ )	705
5	( $P^{sat} + c_{P,liq}^{sat}$ )	80
7	( $P^{sat} + \Delta_{vap}H + c_{P,liq}^{sat}$ )	783
TOTAL:		<b>1785</b>

After the reference case for which the 3 experimental properties are available, the most favorable case is that for which  $P^{sat}$  and  $c_{P,liq}^{sat}$  are available (procedure 5), followed by procedure 4, for which  $P^{sat}$  and  $\Delta_{vap}H$  are experimentally known, and procedure 1, for which only  $P^{sat}$  is known. The grading of

the 4 procedures is as follows: procedure 7 > procedure 5 > procedure 4 > procedure 1. The number of molecules belonging to each of these 4 categories of fluids for which vapor pressure data are available are summarized in [Table PII.6](#).

Among the 1116 molecules studied by Le Guennec et al. [94] for which L,M,N parameters are published, it is recommended not to use these values for 34 molecules (see the Supporting Information - Appendix A) since they were estimated by only taking experimental  $\Delta_{vap}H$  data or experimental  $c_{P,liq}^{sat}$  data, or both of them, into account (fluids of types 2, 3 or 6 in Table PII.3).

## PII.IV Updated consistent Twu91 $\alpha$ -function parameters

Following the conclusion of the previous section, a safe estimation of consistent Twu91  $\alpha$ -functions parameters is carried out only for molecules for which at least  $P^{sat}$  pseudo-experimental data can be accurately generated from DIPPR correlations. The objective function, imposed constraints and data generation rules used in this section are identical to those used previously.

### PII.IV.I Constitution of a pure-compound database

As highlighted in [Table PII.6](#), among the 2162 molecules available in the DIPPR database, it is possible to accurately generate at least experimental  $P^{sat}$  data for 1785 of them.

It should be noted that among these 1785 molecules, there are 4 quantum fluids (He, H<sub>2</sub>, Ne and deuterium), which require special treatment [94]. The (L, M, N) parameters for these fluids are presented in the Supporting Information section ([Appendix B](#)), but are identical to those published by Le Guennec et al. [94].

In this paper, deviations are thus calculated for 1781 non-quantum fluids for which accurate  $P^{sat}$  and/or  $\Delta_{vap}H$  and/or  $c_{P,liq}^{sat}$  data are available (see [Table PII.7](#)).

**Table PII.7.** Number of *non-quantum* compounds for which the experimental properties can be accurately estimated.

Property	Number of compounds
( $P^{sat}$ )	1781
( $\Delta_{vap}H$ )	1487
( $c_{P,liq}^{sat}$ )	863

### PII.IV.II Results

Among the 1781 studied molecules, it is found that by working with the *tc*-PR EoS, 61 reach a mean deviation on at least one property among  $P^{sat}$ ,  $\Delta_{vap}H$  or  $c_{P,liq}^{sat}$  greater than the average MAPE ( $\bar{x}$ ) calculated for the 1781 compounds plus 3 times the standard deviation ( $\sigma$ ). These thresholds are provided in [Table PII.8](#).

These molecules are considered to be outliers, and it is decided not to publish the corresponding values of the L, M, N parameters (i.e., to remove them from the consolidated database) except for mercury, which is considered to be a molecule of interest as shown by a number of recent research articles. Among these 60 molecules, 14 were unfortunately considered as reliable by Le Guennec et al. and  $\alpha$ -function parameters should not have been published [94]. These large deviations are justified as follows:

1. Some of these 60 molecules do not obey the 3-parameter corresponding-state theorem, so that their properties cannot be modeled with an EoS from the mere knowledge of  $T_c$ ,  $P_c$  and  $\alpha(T)$ . This behavior is detected when the acentric factor does not reflect at all the size of the molecule. As an example, the acentric factor of trimethylolpropane ( $C_6H_{14}O_3$ ) is 1.6; by comparison, a similar value is reached in the alkane family for n-hexatriacontane (n- $C_{36}$ ) (its acentric factor is equal to 1.5).
2. There is a problem with the experimental data that was not detected by the correlation selection procedure.

**Table PII.8.** Rejection thresholds for molecule selection.

Property	Average MAPE over 1781 fluids ( $\bar{x}$ )	Standard deviation over 1781 fluids ( $\sigma$ )	Threshold ( $\bar{x} + 3\sigma$ )
( $P^{sat}$ )	1.2%	1.6%	<b>6%</b>
( $\Delta_{vap}H$ )	2.0%	2.0%	<b>8%</b>
( $c_{P,liq}^{sat}$ )	2.3%	3.4%	<b>13%</b>

**Table PII.9.** Distribution of the 1721 retained molecules according to the available accurate property data.

Type of pure fluid	Accurate property data available	This work
1	( $P^{sat}$ )	198
4	( $P^{sat} + \Delta_{vap}H$ )	694
5	( $P^{sat} + c_{P,liq}^{sat}$ )	70
7	( $P^{sat} + \Delta_{vap}H + c_{P,liq}^{sat}$ )	759
<b>TOTAL</b>		<b>1721</b>

The regressed parameters of the 1721 remaining molecules (Table PII.9) are reported in the Supporting Information (Appendix B) for both the PR and the RK EoS. The MAPE on  $P^{sat}$ ,  $\Delta_{vap}H$  and  $c_{P,liq}^{sat}$  are reported in Table PII.10 for both *consistent*-PR and *consistent*-RK EoS.

It can be stated that the PR or RK EoS, coupled with a consistent Twu91  $\alpha$ -function, are capable of accurately reproducing the properties of interest. The MAPE on vapor pressures for more than 1700

compounds is only 1 %, while the deviations on  $\Delta_{vap}H$  and  $c_{P,liq}^{sat}$  are approximately 2%. It is possible to observe that the addition of up to 600 compounds with respect to that used in Le Guennec et al. [94] did not affect the mean deviations on the studied properties.

Furthermore, it is possible to compare the MAPE on  $P^{sat}$ ,  $\Delta_{vap}H$  and  $c_{P,liq}^{sat}$  obtained in this work with those calculated by Bell et al. [226]. It is observed that the average deviation on  $P^{sat}$  in this work is five-fold lower than that obtained by Bell et al. (see Table PII.10). Conversely, the MAPE on  $c_{P,liq}^{sat}$  is two-fold greater than that obtained by Bell et al. [226]. This difference is probably due to the mathematical expressions of the objective functions, which are different in the two studies and to the fact that vapor pressures considered in this work were cut off at 0.1 bar whereas Bell et al. accepted – as part of the fitting exercise – much lower vapor pressures for which it is not scarce to get large relative deviations.

**Table PII.10.** MAPE on  $P^{sat}$ ,  $\Delta_{vap}H$  and  $c_{P,liq}^{sat}$  as predicted from the updated *consistent* PR and RK EoS.

Source	EoS	MAPE on $P^{sat}$	MAPE on $\Delta_{vap}H$	MAPE on $c_{P,liq}^{sat}$
This work (1721 fluids)		<b>(1721 compounds)</b>	<b>(1453 compounds)</b>	<b>(829 compounds)</b>
	<i>consistent</i> -PR	1.0%	1.9%	2.0%
	<i>consistent</i> -RK	1.2%	1.9%	2.2%
Le Guennec et al. [94] (1116 fluids)		<b>(980 compounds)</b>	<b>(805 compounds)</b>	<b>(529 compounds)</b>
	<i>consistent</i> -PR	0.9%	2.0%	2.0%
	<i>consistent</i> -RK	1.1%	2.1%	2.2%
Bell et al. [226] (2571 fluids)		<b>(2571 compounds)</b>	<b>(764 compounds)</b>	<b>(414 compounds)</b>
	<i>consistent</i> -PR	4.9%	1.5%	0.9%

## PII.V Updated volume-translation parameters (c)

To calculate the volume-translation parameter, it is imposed to exactly reproduce the pseudo-experimental saturated-liquid molar volume returned by the DIPPR correlation at a reduced temperature of 0.8, as described by Le Guennec et al. [94]. The volume translation parameter is thus calculated as:

$$c = v_{liq}^{sat,u-CEoS}(T_r = 0.8) - v_{liq,exp}^{sat}(T_r = 0.8) \quad (\text{PII.16})$$

where  $v_{liq}^{sat,u-CEoS}(T_r = 0.8)$  is the molar volume calculated with the original (*untranslated*) CEoS at  $T_r = 0.8$ .

### PII.V.I Results

To estimate the MAPE on the liquid molar volumes, it is necessary to identify the molecules for which the pseudo-experimental liquid densities can be accurately generated following the procedure described in Section PII.III.I (i.e., error reported in the DIPPR database or average experimental error calculated

by Eq. (PII.10) is lower than 5%). As highlighted in Table PII.11, among the 1721 compounds included in the database, 1489 have accurate correlations for the liquid molar volume data.

**Table PII.11.** Distribution of the 1489 molecules for which at least  $P^{sat}$  and  $v_{liq}^{sat}$  can be accurately generated from the DIPPR database.

Type of pure fluid	Accurate property data available	This work	Accurate property data available	This work
1	$(P^{sat})$	198	$(P^{sat} + v_{liq}^{sat})$	164
4	$(P^{sat} + \Delta_{vap}H)$	694	$(P^{sat} + \Delta_{vap}H + v_{liq}^{sat})$	543
5	$(P^{sat} + c_{P,liq}^{sat})$	70	$(P^{sat} + c_{P,liq}^{sat} + v_{liq}^{sat})$	65
7	$(P^{sat} + \Delta_{vap}H + c_{P,liq}^{sat})$	759	$(P^{sat} + \Delta_{vap}H + c_{P,liq}^{sat} + v_{liq}^{sat})$	717
<b>TOTAL</b>		<b>1721</b>		<b>1489</b>

As previously done for the  $P^{sat}$ ,  $\Delta_{vap}H$  and  $c_{P,liq}^{sat}$  properties, for each of these 1489 compounds, the DIPPR correlation was used to generate 50 equidistant liquid molar volume data points between  $T_{min}$  and  $T_{max} = 0.9T_c$ . Here,  $T_{min}$  is the minimum temperature at which  $v_{liq}^{sat}$  can be estimated from the DIPPR correlation, whereas  $T_{max} = 0.9T_c$  is the highest temperature at which the volume-translation concept has beneficial effect. By denoting  $v_{liq}^{sat,t-CEoS}$ , the molar volume calculated with the translated EoS, the MAPE on  $v_{liq}^{sat}$  is calculated as:

$$MAPE = \frac{100}{50} \sum_{i=1}^{50} \left| \frac{v_{liq}^{sat,DIPPR} \left( T_i^{v_{liq}^{sat}} \right) - v_{liq}^{sat,t-CEoS} \left( T_i^{v_{liq}^{sat}} \right)}{v_{liq}^{sat,DIPPR} \left( T_i^{v_{liq}^{sat}} \right)} \right| \quad (\text{PII.17})$$

These MAPE are reported in Table PII.12 for both the PR and RK EoS in their translated and original versions. The calculated volume-translation parameters are reported in the Supporting Information (Appendix B) for both the PR and RK EoS. It is observed that the reproduction of the  $v_{liq}^{sat}$  data is dramatically improved for both models.

**Table PII.12.** MAPE on  $v_{liq}^{sat}$  as predicted by the *consistent* PR and RK EoS on an updated database. Effect of the volume translation.

EoS	MAPE on $v_{liq}^{sat}$ ( $T_r < 0.9$ ) (1489 compounds)	
	Untranslated EoS	Translated EoS
<i>consistent</i> -PR	8.7%	2.2%
<i>consistent</i> -RK	19.2%	3.7%

In addition, the average deviations on the molar critical volume are reported in Table PII.13. At the critical point, the volume-translation parameter  $c$  has too weak an influence on the calculated critical

volume ( $v_c$ ) to obtain a good match with the experimental value. Although the influence of the volume translation concept is more visible on the RK EoS, the PR CEoS yields better predictions of  $v_c$ .

**Table PII.13.** MAPE on  $v_c$  as predicted by the *consistent* PR and RK EoS. Effect of the selected volume translation.

EoS	MAPE on $v_c$ (1489 compounds)	
	Untranslated EoS	Translated EoS
<i>consistent</i> -PR	21%	20%
<i>consistent</i> -RK	31%	24%

In [Table PII.14](#), the accurate results obtained with the *tc*-PR and *tc*-RK CEoS using the updated parameters determined in this study are summarized. This table highlights that the accuracies of both EoS are very similar, with the exception of the molar volumes, which are better correlated with the PR EoS.

**Table PII.14.** MAPE on  $P^{sat}$ ,  $\Delta_{vap}H$ ,  $c_{P,liq}^{sat}$ ,  $v_{liq}^{sat}$ ,  $v_c$ ,  $T_c$ , and  $P_c$  as predicted by the *translated-consistent* PR and RK EoS with the updated parameters determined in this study.

EoS	MAPE on $P^{sat}$ (1721 fluids)	MAPE on $\Delta_{vap}H$ (1453 fluids)	MAPE on $c_{P,liq}^{sat}$ (829 fluids)	MAPE on $v_{liq}^{sat}$ (1489 fluids) ( $T_r < 0.9$ )	MAPE on $v_c$ (1489 fluids)	MAPE on $T_c$ (1721 fluids)	MAPE on $P_c$ (1721 fluids)
<i>tc</i> -PR	1.0%	1.9%	2.0%	2.2%	20%	0%	0%
<i>tc</i> -RK	1.2%	2.0%	2.2%	3.7%	24%	0%	0%

In [Table PII.14](#), the MAPEs on the critical temperature and critical pressure, which are necessarily zero, are reported to remind the reader that these errors are not null with EoS that do not satisfy the critical constraints, e.g., SAFT-type EoS. A proper prediction of the pure-component critical coordinates is, however, a prerequisite to accurately predict the global phase equilibrium diagrams (GPED) of binary systems [\[227,228\]](#).

## PII.VI Updated generalized Twu88 $\alpha$ -functions suitable for the *tc*-PR and *tc*-RK EoS

This section aims to update the generalized formulations for the *tc*-PR and *tc*-RK EoS. It is recalled that the interest of these formulations is that they can be applied to components for which consistent Twu91  $\alpha$ -function parameters cannot be determined from experimental data since no vapor pressure data are available in the literature.

As explained in our previous paper [\[94\]](#), parameter N is set to 2 in order to work with the so-called Twu88 [\[229\]](#)  $\alpha$ -function whereas L and M are correlated as second order polynomials with respect to the acentric factor  $\omega$  (see Eq. [\(PII.18\)](#)):

$$\begin{cases} \alpha(T_r) = T_r^{2(M-1)} \exp[L(1 - T_r^{2M})] \\ L(\omega) = L_1\omega^2 + L_2\omega + L_3 \\ M(\omega) = M_1\omega^2 + M_2\omega + M_3 \end{cases} \quad (\text{PII.18})$$

To update the polynomial expressions for parameters L and M, the 759 molecules that have simultaneously accurate correlations for the  $P^{sat}$ ,  $\Delta_{vap}H$  and  $c_{P,liq}^{sat}$  properties are used (see [Table PII.11](#)). The resulting expressions, for both the PR and RK CEoS, are:

$$PR\ CEoS: \begin{cases} L(\omega) = 0.0925\omega^2 + 0.6693\omega + 0.0728 \\ M(\omega) = 0.1695\omega^2 - 0.2258\omega + 0.8788 \end{cases} \quad (\text{PII.19})$$

$$RK\ CEoS: \begin{cases} L(\omega) = 0.0611\omega^2 + 0.7535\omega + 0.1359 \\ M(\omega) = 0.1709\omega^2 - 0.2063\omega + 0.8787 \end{cases} \quad (\text{PII.20})$$

As proposed by Le Guennec et al., a comparison of the MAPEs obtained with the following three  $\alpha$ -functions is performed:

- i. the component-dependent Twu91  $\alpha$ -function with the updated parameters determined in this paper,
- ii. the updated generalized Twu88  $\alpha$ -function, and the Soave  $\alpha$ -function.

[Table PII.15](#) highlights that the 2 generalized  $\alpha$ -functions, namely “generalized Twu88” and Soave have similar accuracy with, however, an advantage to the first one, especially when predicting  $P^{sat}$  and  $c_{P,liq}^{sat}$  with the PR EoS. Conversely, it is observed that the results are strongly improved if the deviations calculated for the gen. Twu88  $\alpha$ -function are compared with those calculated for the component-dependent Twu91  $\alpha$ -function. The conclusions are identical to those drawn previously and with the exception of molar volumes which are better correlated with the PR EoS, [Table PII.15](#) does not make it possible to conclude which of the PR or RK EoS is the most accurate. Working with the Soave  $\alpha$ -function, the RK EoS is the best-suited but the reverse situation occurs when considering the Twu88 or Twu91  $\alpha$ -functions.

Many process simulation software programs however express  $c \cdot P_c / (RT_c)$  as a linear function of the Rackett compressibility factor ( $z_{RA}$ ), appearing in the improvement of the original Rackett equation [230] proposed by Spencer and Danner [231]. In this study, it was decided to work with the 1489 compounds, for which  $v_{liq}^{sat}$  can be accurately estimated. The obtained correlations are:

$$\begin{cases} c_{PR} = \frac{RT_c}{P_c} (0.1975 - 0.7325z_{RA}) \\ c_{RK} = \frac{RT_c}{P_c} (0.2150 - 0.7314z_{RA}) \end{cases} \quad (\text{PII.21})$$

With such correlations, MAPEs on  $v_{liq}^{sat}$  data, over 1489 compounds modeled with the gen. Twu88  $\alpha$ -function, in a temperature range so that  $T_r \leq 0.9$ , coupled with the PR and RK EoS, are 3.0% and 4.0%, respectively.

To conclude this section, the updated correlations of volume-translation parameters to  $\omega$  are presented below:

$$\begin{cases} c_{PR} = \frac{RT_c}{P_c} (0.0096 + 0.0048\omega) \\ c_{RK} = \frac{RT_c}{P_c} (0.0227 + 0.0093\omega) \end{cases} \quad (\text{PII.22})$$

We know by experience that these correlations are not very accurate but can be useful in the case where  $T_c$ ,  $P_c$  and  $\omega$  are the unique data available for a given compound, which is often the case for the pseudo-components encountered in the oil and gas industry.

**Table PII.15.** Comparison of the MAPEs calculated with the 3-parameter Twu91, generalized Twu88 and Soave  $\alpha$ -functions for the translated PR and RK EoS.

$\alpha$ -function	Peng-Robinson			Redlich-Kwong		
	Twu91	gen. Twu88	Soave	Twu91	gen. Twu88	Soave
MAPE on $P^{sat}$ (1721 compounds)	1.0%	1.8%	2.8%	1.2%	2.1%	2.3%
MAPE on $\Delta_{vap}H$ (1453 compounds)	1.9%	2.7%	3.1%	1.9%	2.9%	2.9%
MAPE on $c_{P,liq}^{sat}$ (829 compounds)	2.0%	4.1%	7.1%	2.2%	4.3%	5.3%
MAPE on $v_{liq}^{sat}$ (1489 compounds) ( $T_r < 0.9$ )	2.2%	2.2%	2.2%	3.7%	3.8%	3.8%

## PII.VII Conclusion

In this study, the suitable combinations of properties among vapor pressures, enthalpies of vaporization and saturated liquid heat capacities for fitting Twu91  $\alpha$ -function parameters were investigated. The study reveals that reliable (L, M, N) parameters are obtained if the fitting includes at least vapor pressure data. Fitting with only the enthalpies of vaporization and/or saturated liquid heat capacities are wholly inadvisable.

One thousand seven hundred twenty-one compounds, for which at least accurate vapor-pressure data could be generated, were found in the DIPPR database, and the 3 (L, M, N) parameters were determined for these fluids. Using these parameters, the  $tc$ -PR EoS leads to the following very small average deviations:  $\Delta P^{sat} = 1\%$ ,  $\Delta_{vap}H = \Delta c_{P,L}^{sat} = 2\%$  and  $\Delta v_L^{sat}(T_r < 0.9) = 2.2\%$ . Moreover, for the  $tc$ -PR and  $tc$ -RK CEoS to be applied to components not included in the DIPPR database, a generalized version of these models was developed. The 3-parameter Twu91  $\alpha$ -function was substituted by the 2-parameter Twu88 function, and the parameters L and M were correlated to the acentric factor.

In comparison with the previous work of Le Guennec et al. and as explained notably in [Sections PII.III.II](#) and [PII.IV.II](#), 52 molecules that were considered to be suitable by these authors for fitting  $\alpha$ -function parameters were declared non-reliable in this study. The reject of these 52 molecules is justified as follows:

- for 34 molecules, no vapor pressure data were available (see [Section PII.III.II](#)).
- For 14 molecules, the deviations between experimental and calculated properties were abnormally high so that such molecules were considered to be outliers (see [Section PII.IV.II](#))
- 4 molecules (Ca, K, Li and LiI) are metals with critical temperature higher than 2000 K which we believe can not be seriously modeled by a CEoS.

In return, 661 new molecules were added to the library developed in this work.

# Publication III : Updated versions of the generalized Soave $\alpha$ -function suitable for the Redlich-Kwong and Peng-Robinson equations of state.

Andrés Pina-Martinez<sup>1</sup>, Romain Privat<sup>1(\*)</sup>, Jean-Noël Jaubert<sup>1(\*)</sup>, Ding-Yu Peng<sup>2</sup>

<sup>(1)</sup>Université de Lorraine, École Nationale Supérieure des Industries Chimiques, Laboratoire Réactions et Génie des Procédés (UMR CNRS 7274), 1 rue Grandville, 54000, Nancy, France

<sup>(2)</sup>University of Saskatchewan, Department of Chemical and Biological Engineering, Engineering Building, Saskatoon, Saskatchewan, S7N 5A9, Canada

## Abstract

More than 40 years after their publication, updated versions of the generalized Soave  $\alpha$ -function  $\left( \alpha(T_r, \omega) = \left[ 1 + m(\omega)(1 - T_r^{0.5}) \right]^2 \right)$  suitable for the Redlich-Kwong (RK) and Peng-Robinson (PR) equations of state (EoS) are proposed in this work. The new mathematical expressions of  $m_{RK}(\omega)$  and  $m_{PR}(\omega)$  have been determined by correlating optimal  $m$  values, fitted on vapor pressures ( $P^{sat}$ ) and/or enthalpies of vaporization ( $\Delta_{vap}H$ ) and/or saturated-liquid heat capacities ( $c_{P,liq}^{sat}$ ) against the acentric factor  $\omega$ . The correlations determined in this study can be considered as broad-based and sound since they were established on 1720 pure compounds belonging to many different chemical families (hydrocarbons, halogenated, oxygenated, sulfur, nitrogen compounds ...) for which experimental data were available. Significant improvement on the reproduction of vapor pressures was obtained for the PR EoS with respect to the original version. Updated SRK EoS achieved similar results for the three properties of interest ( $P^{sat}$ ,  $\Delta_{vap}H$  and  $c_{P,liq}^{sat}$ ), in comparison with the original SRK equation.



## PIII.I Introduction

As stated by Valderrama [232], the Soave-Redlich-Kwong (SRK) [233] and the Peng-Robinson [234] equations of state (EoS) are the most popular cubic equations used currently in research, simulation and optimization in which thermodynamics and VLE properties are required. These two equations have been considered for all types of calculations, from simple estimations of pure-fluid volumetric properties and vapor pressures to descriptions of complex multicomponent systems. As a direct consequence, all the commercially available process simulation packages (ProSim, Pro/II, Aspen, UniSim ...) include the SRK and PR EoS among their thermodynamic models. Such EoS are usually used in their *translated* form [221–223] in order to improve their abilities to predict liquid densities. They can be summarized as follows:

*t* – SRK:

$$P(T, v) = \frac{RT}{v-b} - \frac{a_c \cdot \alpha(T_r, \omega_{\text{exp}})}{(v+c)(v+b+2c)} \quad \text{with:} \quad \begin{cases} a_c = \frac{1}{9(\sqrt[3]{2}-1)} \frac{R^2 T_{c,\text{exp}}^2}{P_{c,\text{exp}}} \\ b = \frac{\sqrt[3]{2}-1}{3} \frac{RT_{c,\text{exp}}}{P_{c,\text{exp}}} - c \end{cases} \quad (\text{PIII.1})$$

*t* – PR:

$$P(T, v) = \frac{RT}{v-b} - \frac{a_c \cdot \alpha(T_r, \omega_{\text{exp}})}{(v+c)(v+b+2c) + (b+c)(v-b)} \quad \text{with:} \quad \begin{cases} \eta_c = \left[ 1 + \sqrt[3]{4-2\sqrt{2}} + \sqrt[3]{4+2\sqrt{2}} \right]^{-1} \approx 0.25308 \\ a_c = \frac{40\eta_c + 8}{49 - 37\eta_c} \frac{R^2 T_{c,\text{exp}}^2}{P_{c,\text{exp}}} \approx 0.45724 \frac{R^2 T_{c,\text{exp}}^2}{P_{c,\text{exp}}} \\ b = \frac{\eta_c}{\eta_c + 3} \frac{RT_{c,\text{exp}}}{P_{c,\text{exp}}} - c \approx 0.07780 \frac{RT_{c,\text{exp}}}{P_{c,\text{exp}}} - c \end{cases} \quad (\text{PIII.2})$$

where  $c$  is the component-dependent volume-translation factor. It is usually [94] selected in order to exactly reproduce the experimental saturated liquid volume at a reduced temperature of 0.8. The temperature-dependent function  $\alpha(T_r, \omega_{\text{exp}})$  in the attraction term of both the SRK and PR equations is the one developed by Soave. For a given pure compound (characterized by its acentric factor  $\omega_{\text{exp}}$  and its critical temperature  $T_{c,\text{exp}}$ ), it is expressed as:

$$\alpha_{\text{Soave}}(T_r, \omega_{\text{exp}}) = \left[ 1 + m(\omega_{\text{exp}}) \cdot (1 - \sqrt{T_r}) \right]^2 \quad (\text{PIII.3})$$

with,

$$m = A + B\omega_{\text{exp}} + C\omega_{\text{exp}}^2 \quad (\text{PIII.4})$$

$T_r = T/T_{c,\text{exp}}$  is the reduced temperature;  $A$ ,  $B$  and  $C$  are universal constants which depend on the selected EoS.

In 1972, Soave [233] assumed  $\omega$  values ranging from zero to 0.5 with a step of 0.05. For each of these eleven  $\omega$  values, he determined the corresponding  $m$  values enabling to exactly reproduce reduced

vapor pressures at  $T_r = 0.7$  calculated as:  $P_r^{sat}(T_r = 0.7) = 10^{-\omega^{-1}}$ . Such  $m$  values were correlated against  $\omega$  with the following second order polynomial:

$$m_{RK} = 0.480 + 1.574\omega - 0.176\omega^2 \quad (\text{PIII.5})$$

In 1976, Peng and Robinson [234], determined for 14 hydrocarbons (methane, ethane, propane, i-butane, n-butane, cyclohexane, benzene, i-pentane, n-pentane, n-hexane, n-heptane, n-octane, n-nonane and n-decane) and 3 permanent gases ( $N_2$ ,  $CO_2$ ,  $H_2S$ )  $m$  values suitable for their EoS by minimizing deviations between calculated and experimental vapor pressures. They used vapor pressure data from the normal boiling point to the critical point. These optimized  $m$  values were correlated against the acentric factor and the resulting equation was:

$$m_{PR} = 0.37464 + 1.54226\omega - 0.26992\omega^2 \quad (\text{PIII.6})$$

As recently recalled by Lopez-Echeverry et al. [235], since 1976 many papers were devoted to improving the Soave  $\alpha$ -function. The most recent is probably the one published by Yang et al. [236] a few weeks ago. We will only cite a few of them, essentially written by Soave himself or by Peng and Robinson. As a first example, in 1978 Graboski and Daubert [237] refit the constants in Eq. (PIII.5). The regression was based on a detailed set of hydrocarbon vapor pressure data compiled by the American Petroleum Institute. The regression equation for  $m_{RK}$  based on such data was derived to be:

$$m_{RK} = 0.48508 + 1.55171\omega - 0.15613\omega^2 \quad (\text{PIII.7})$$

As a second example, in 1993 Soave [238] correlated vapor pressures generated by the Lee-Kesler equation in order to derive – for the RK EoS – the following two-parameter  $\alpha$ -function particularly suitable for heavy hydrocarbons:

$$\alpha(T_r) = 1 + m(1 - T_r) + n(1 - \sqrt{T_r})^2 \quad \text{with:} \quad \begin{cases} m = 0.484 + 1.515\omega - 0.044\omega^2 \\ n = 2.756m - 0.700 \end{cases} \quad (\text{PIII.8})$$

Soave [238] also explains that the 2 parameters  $m$  and  $n$  in Eq. (PIII.8) can be adjusted separately to correlate accurately experimental vapor pressures of polar substances. A few months later, Soave [239] advises to divide  $m$  values returned by Eq. (PIII.5) by a factor 1.18 in order the translated SRK EoS accurately predicts fugacity coefficients of pure gaseous fluids at high temperature and high pressure.

As a third example, in 1978, Robinson and Peng [240] proposed a piecewise expression of  $m$ . They recommended to generate  $m$  values for substances whose acentric factors are lower or equal to that of n-decane by Eq. (PIII.6) which was published in 1976. For heavier molecules, they advised to estimate  $m$  by a third order polynomial of the acentric factor:

$$\begin{cases} m_{PR} = 0.37464 + 1.54226\omega - 0.26992\omega^2 & \omega \leq \omega_{n\text{-decane}} \\ m_{PR} = 0.379642 + 1.48503\omega - 0.164423\omega^2 + 0.016666\omega^3 & \omega > \omega_{n\text{-decane}} \end{cases} \quad (\text{PIII.9})$$

Eq. (PIII.9) received a considerable acclaim and is used in particular in the well-acknowledged PPR78 model [228,241,242].

This short bibliographic review makes it possible to conclude that the correlations of  $m$  parameters against  $\omega$  have always been conducted on a small number of hydrocarbons in order to either exactly reproduce the vapor pressure at  $T_r = 0.7$  or to minimize the deviations between calculated and experimental vapor pressures. In this paper, we decided to follow the conclusions of one of our recent studies [243] in which we demonstrated that safe  $\alpha$ -function parameters can only be obtained if the fittings are carried out considering at least vapor pressure ( $P^{sat}$ ) data. As was done in our previous paper [243] and thanks to the DIPPR database, we were able to find 1720 compounds for which accurate vapor pressures were available. Moreover, for 1522 out of these 1720 compounds, the DIPPR database also provided enthalpies of vaporization ( $\Delta_{vap}H$ ) and/or saturated liquid heat capacity ( $c_{P,liq}^{sat}$ ) data.

For each of these 1720 compounds,  $m_{RK}$  and  $m_{PR}$  were determined in order to minimize the deviations between calculated and available experimental data that include  $P^{sat}$  and/or  $\Delta_{vap}H$  and/or  $c_{P,liq}^{sat}$ . To the best of our knowledge,  $\Delta_{vap}H$  and  $c_{P,liq}^{sat}$  data were never used to calibrate the Soave  $\alpha$ -function and no fittings were conducted on a so huge number of components. Eventually, these optimized  $m$  values were correlated against the acentric factor in order to update the generalized Soave  $\alpha$ -function suitable for the RK and PR EoS.

At this step, it is worth noting that the Soave  $\alpha$ -function does not pass the consistency test proposed by Le Guennec et al. [218,219] which stipulates that  $\alpha$ -functions must obey the following list of constraints to guarantee safe property predictions in both subcritical and supercritical domains:

$$\alpha(T_c) = 1 \text{ and for all T: } \begin{cases} \alpha \geq 0 & \text{and } \alpha(T_r) \text{ continuous} \\ \frac{d\alpha}{dT_r} \leq 0 & \text{and } \frac{d\alpha}{dT_r} \text{ continuous} \\ \frac{d^2\alpha}{dT_r^2} \geq 0 & \text{and } \frac{d^2\alpha}{dT_r^2} \text{ continuous} \\ \frac{d^3\alpha}{dT_r^3} \leq 0 \end{cases} \quad (\text{PIII.10})$$

However as explained by Le Guennec et al. [218], the 1972 Soave  $\alpha$ -function is consistent i.e. satisfies the constraints given in Eq. (PIII.10) up to a temperature which is generally higher than 1500 K. This is the reason why this study was conducted and the reason why the Soave  $\alpha$ -function is certainly the most used  $\alpha$ -function in chemical industries.

## PIII.II Updated Soave $m$ parameter

As stated in the introduction, thanks to the DIPPR database we were able to find 1720 compounds belonging to many different chemical families (hydrocarbons, halogenated, oxygenated, sulfur, nitrogen compounds ...) for which at least vapor pressure data could be accurately generated from a temperature-dependent correlation (see the Supplementary Material section (Appendix C) for the whole listing of the 1720 compounds). In addition, for 1522 compounds among these 1720, other experimental data like enthalpy of vaporization ( $\Delta_{vap}H$ ) and/or saturated liquid heat capacity ( $c_{P,liq}^{sat}$ ) were also available.

Table PIII.1 summarizes the available property data for the 1720 compounds considered in this study.

**Table PIII.1.** Distribution of the 1720 retained compounds according to the accurate property data available in the DIPPR database.

Accurate property data available in the DIPPR database	Number of compounds
$(P^{sat} + \Delta_{vap}H + c_{P,liq}^{sat})$	758
$(P^{sat} + \Delta_{vap}H)$	694
$(P^{sat} + c_{P,liq}^{sat})$	70
$(P^{sat})$	198
<b>TOTAL:</b>	<b>1720</b>

First of all, optimal  $m$  parameters for each of the 1720 considered compounds have been determined. Our first task was thus to generate pseudo-experimental data thanks to the correlations available in the DIPPR database. Generation of the pseudo-experimental data obeyed the following rules:

- 1) Regardless of the considered property among  $P^{sat}$ ,  $\Delta_{vap}H$  and  $c_{P,liq}^{sat}$ , 50 equidistant pseudo-experimental data points were generated in their valid temperature range,  $[T_{min}; T_{max}]$ .
- 2) For the  $\Delta_{vap}H$  and  $c_{P,liq}^{sat}$  correlations, in the case that  $T_{max}$  exceeds  $0.98T_c$ ,  $T_{max} = 0.98T_c$  was set. The reason for this choice is simple:  $\Delta_{vap}H$  goes to zero at the critical temperature and the calculation of the relative deviation with the experimental data induces a division by zero. Similarly,  $c_{P,liq}^{sat}$  goes to infinity at the critical temperature so that, once again, the relative deviation with the experimental value cannot be calculated.
- 3) For the  $P^{sat}$  correlation,  $T_{max} = T_c$  was set. However, in the case where  $P^{sat}(T_{min}) < 0.1 \text{ bar}$ , the value of  $T_{min}$  was increased to enforce that  $P^{sat}(T_{min}) = 0.1 \text{ bar}$  (considering that most industrial processes operate at higher values of pressure and that  $P^{sat}$  data can be highly uncertain at very-low pressures, say less than 1 torr).

The optimal  $m$  parameter was the one which minimized the generic objective function given by Eq. (PIII.11), which is a weighting of the Mean Absolute Percentage Error (MAPE) between calculated and experimental  $P^{sat}$ ,  $\Delta_{vap}H$  and  $c_{P,liq}^{sat}$ . The objective function was obviously adapted according to the available experimental data.

$$\begin{aligned}
OF_{\alpha} = \frac{100}{50} \sum_{i=1}^{50} & \left[ \left| \frac{P^{sat,DIPPR}(T_i^{P^{sat}}) - P^{sat,EoS}(T_i^{P^{sat}})}{P^{sat,DIPPR}(T_i^{P^{sat}})} \right| \right. \\
& + \left| \frac{\Delta_{vap}H^{DIPPR}(T_i^{\Delta_{vap}H}) - \Delta_{vap}H^{EoS}(T_i^{\Delta_{vap}H})}{\Delta_{vap}H^{DIPPR}(T_i^{\Delta_{vap}H})} \right| \\
& \left. + WF \left| \frac{c_{P,liq}^{sat,DIPPR}(T_i^{c_{P,liq}^{sat}}) - c_{P,liq}^{sat,EoS}(T_i^{c_{P,liq}^{sat}})}{c_{P,liq}^{sat,DIPPR}(T_i^{c_{P,liq}^{sat}})} \right| \right] \quad (PIII.11)
\end{aligned}$$

When experimental saturated liquid heat capacities were available, a special attention was devoted to the estimation of the weighting factor on  $c_{P,liq}^{sat}$  [denoted as  $WF$  in Eq. (PIII.11)]. As an initial choice, it was set to 1. Nevertheless, for certain compounds, deviations on  $c_{P,liq}^{sat}$  were found to be much smaller than those on  $P^{sat}$ . In these cases, the accuracy on  $c_{P,liq}^{sat}$  was deteriorated to gain accuracy on  $P^{sat}$  (i.e., to obtain smaller deviations on  $P^{sat}$ ). This goal was made possible by carrying out successive minimizations by changing the value of  $WF$  from 1 to 0.1, with a step of 0.1. In practice, this procedure was run for a considered compound if:

- The MAPE on  $P^{sat}$  was larger than 2% **and** the MAPE on  $c_{P,liq}^{sat}$  was smaller than that on  $P^{sat}$ ,
- or
- the MAPE on  $c_{P,liq}^{sat}$  was considerably smaller (two times) than that on  $P^{sat}$  **and** the MAPE on  $c_{P,liq}^{sat}$  was larger than 1%.

These conditions are summarized in Eq. (PIII.12):

$$\begin{aligned}
& MAPE \text{ on } P^{sat} > 2\% \text{ **and** } MAPE \text{ on } c_{P,liq}^{sat} < MAPE \text{ on } P^{sat} \\
& \text{or} \\
& 2 \times MAPE \text{ on } c_{P,liq}^{sat} < MAPE \text{ on } P^{sat} \text{ **and** } MAPE \text{ on } c_{P,liq}^{sat} > 1\%
\end{aligned} \quad (PIII.12)$$

In a second step, the weighting factor was selected following a case-by-case analysis to obtain what we considered the best compromise between the MAPE on the vapor pressures and MAPE on the saturated-liquid heat capacities.

### PIII.III Results

Optimized  $m$  parameters for each of the 1720 compounds considered in this study are reported in the Supplementary material section (Appendix C) for both the PR and the RK EoS. As illustrated in Figure PIII.1, they have been correlated against  $\omega_{\text{exp}}$  for both cubic EoS. The resulting expressions are the following second order polynomials:

$$m_{PR} = 0.4062 + 1.3988\omega - 0.0778\omega^2 \quad (\text{PIII.13})$$

$$m_{RK} = 0.4976 + 1.4796\omega - 0.0722\omega^2 \quad (\text{PIII.14})$$

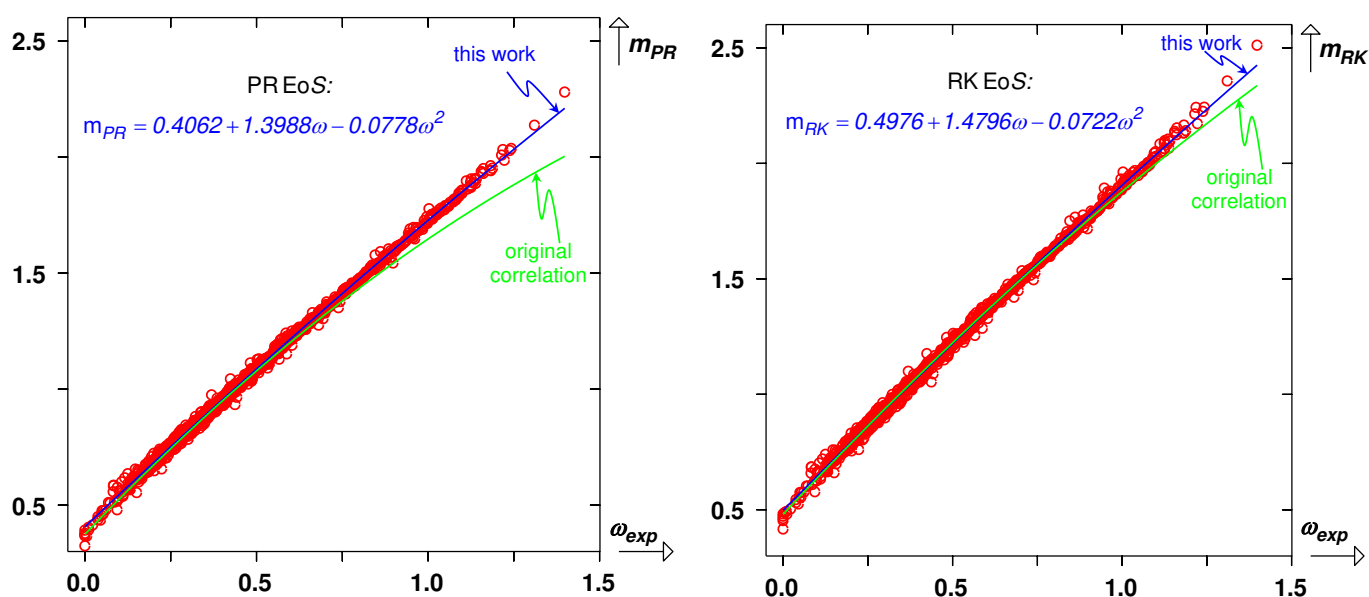


**Figure PIII.1.** Correlation of optimized  $m$  parameter against  $\omega_{\text{exp}}$  for both the PR and RK EoS. Comparison between the original correlation and the one determined in this work. Each of the 1720 open circles represent a pure compound.

**Table PIII.2.** Comparison of the MAPEs calculated with the original and the updated Soave  $\alpha$ -functions. Application to the PR and RK EoS.

	Peng-Robinson		Redlich-Kwong	
	Original Soave $\alpha$ -function [Eq. (PIII.6)]	Updated Soave $\alpha$ -function in this work [Eq. (PIII.13)]	Original Soave $\alpha$ -function [Eq. (PIII.5)]	Updated Soave $\alpha$ -function in this work [Eq. (PIII.14)]
<b>MAPE on <math>P^{\text{sat}}</math> (1720 compounds)</b>	2.7%	<b>1.8%</b>	2.2%	<b>2.2%</b>
<b>MAPE on <math>\Delta_{\text{vap}}H</math> (1452 compounds)</b>	3.1%	<b>2.8%</b>	2.9%	<b>2.9%</b>
<b>MAPE on <math>c_{P,\text{liq}}^{\text{sat}}</math> (828 compounds)</b>	7.1%	<b>6.8%</b>	5.3%	<b>5.3%</b>

In order to have an overview of the capabilities of these two new expressions, they are compared with original polynomials for both the PR and RK equations. The Mean Absolute Percentage Error (MAPE) on  $P^{sat}$ ,  $\Delta_{vap}H$  and  $c_{P,liq}^{sat}$  calculated with the original and the updated Soave  $\alpha$ -functions are reported in [Table PIII.2](#) (the detailed results obtained with the updated  $\alpha$ -functions for each of the 1720 compounds are available in the Supplementary material section - [Appendix C](#)). A graphical comparison of the original and updated polynomials can be found in [Figure PIII.1](#).

It is first observed that there is no difference between the original and updated Soave  $\alpha$ -functions coupled with the RK EoS. All the three properties of interest ( $P^{sat}$ ,  $\Delta_{vap}H$  and  $c_{P,liq}^{sat}$ ) are reproduced with the same accuracy. This demonstrates the worldwide recognized pertinence of the approach used by Soave for correlating  $m$  values against  $\omega$ . It is however worth noting that the updated  $\alpha$ -function is more accurate than the original  $\alpha$ -function for very heavy molecules having an acentric factor larger than 1. Such an improvement is not reflected in the average deviations given in [Table PIII.2](#) because the number of very heavy compounds is small in comparison to the total number of compounds. The significant divergence between the 2 polynomials when  $\omega_{exp}$  is larger than 1 is however prominent in [Figure PIII.1](#).

On the other hand, it is possible to highlight the decrease of 0.9% of MAPE on  $P^{sat}$  when the updated Soave  $\alpha$ -function, instead of the original version, is coupled with the PR EoS. Above all, [Table PIII.2](#) highlights that the accuracies of both EoS are very similar. This is especially true with the updated Soave  $\alpha$ -functions (the use of the original Soave  $\alpha$ -functions gives indeed an advantage to the SRK EoS). It is also possible to conclude that the use of a one-parameter  $\alpha$ -function (like the one developed by Soave) makes it impossible to simultaneously catch  $P^{sat}$ ,  $\Delta_{vap}H$  and  $c_{P,liq}^{sat}$ . Indeed, for both EoS, the MAPE on  $c_{P,liq}^{sat}$  is larger than 5%.

**Table PIII.3.** Comparison of the MAPEs on  $v_{liq}^{sat}$  calculated with the original and the updated Soave  $\alpha$ -functions. Application to the translated and untranslated PR and RK EoS.

	Peng-Robinson		Redlich-Kwong	
	Original Soave $\alpha$ -function [Eq. <a href="#">(PIII.6)</a> ]	Updated Soave $\alpha$ -function in this work [Eq. <a href="#">(PIII.13)</a> ]	Original Soave $\alpha$ -function [Eq. <a href="#">(PIII.5)</a> ]	Updated Soave $\alpha$ -function in this work [Eq. <a href="#">(PIII.14)</a> ]
	<i>Untranslated</i>		<i>Untranslated</i>	
<b>MAPE on <math>v_{liq}^{sat}</math> (1488 compounds) (<math>T_r &lt; 0.9</math>)</b>	8.8%	<b>8.7%</b>	19%	<b>19%</b>
	<i>Translated</i>		<i>Translated</i>	
	2.2%	<b>2.2%</b>	3.8%	<b>3.8%</b>

At this step, it was also decided to estimate the MAPE on the liquid molar volumes. Among the 1720 compounds considered in this paper, the DIPPR database has accurate correlations to estimate liquid molar volumes at saturation ( $v_{liq}^{sat}$ ) for 1488 of them. As previously done for the  $P^{sat}$ ,  $\Delta_{vap}H$  and  $c_{P,liq}^{sat}$  properties, for each of these 1488 compounds, the DIPPR correlation was used to generate 50

equidistant liquid molar volume data points between  $T_{\min}$  and  $T_{\max} = 0.9T_c$ . In this case,  $T_{\min}$  is the minimum temperature at which  $v_{liq}^{sat}$  can be estimated from the DIPPR correlation, whereas  $T_{\max} = 0.9T_c$  is the highest temperature at which the volume-translation concept has beneficial effect. By denoting  $v_{liq}^{sat,t-CEoS}$ , the molar volume calculated with the translated EoS [see Equations (PIII.1) and (PIII.2)], the MAPE on  $v_{liq}^{sat}$  is calculated as:

$$MAPE = \frac{100}{50} \sum_{i=1}^{50} \left| \frac{v_{liq}^{sat,DIPPR} \left( T_i^{v_{liq}^{sat}} \right) - v_{liq}^{sat,t-CEoS} \left( T_i^{v_{liq}^{sat}} \right)}{v_{liq}^{sat,DIPPR} \left( T_i^{v_{liq}^{sat}} \right)} \right| \quad (PIII.15)$$

These MAPEs are reported in Table PIII.3 for both the PR and RK EoS in their translated and untranslated versions (the detailed results obtained with the updated  $\alpha$ -functions for each of the 1488 compounds are available in the Supplementary material section - Appendix C).

Such a table highlights that the reproduction of the experimental  $v_{liq}^{sat}$  data is dramatically improved for both EoS when a volume translation is applied. Another key conclusion is that the choice of the  $\alpha$ -function (original or updated) has a negligible impact on the MAPE on  $v_{liq}^{sat}$ . In addition, for completing our analysis, the average deviations on the molar critical volume are reported in Table PIII.4 (the detailed results obtained with the updated  $\alpha$ -functions for each of the 1488 compounds are available in the Supplementary material section - Appendix C).

**Table PIII.4.** Comparison of the MAPEs on the molar critical volume ( $v_c$ ) calculated with the original and the updated Soave  $\alpha$ -functions. Application to the translated and untranslated PR and RK EoS.

	Peng-Robinson		Redlich-Kwong	
	Original Soave $\alpha$ -function [Eq. (PIII.6)]	Updated Soave $\alpha$ -function in this work [Eq. (PIII.13)]	Original Soave $\alpha$ -function [Eq. (PIII.5)]	Updated Soave $\alpha$ -function in this work [Eq. (PIII.14)]
	<i>Untranslated</i>		<i>Untranslated</i>	
<b>MAPE on <math>v_c</math> (1488 compounds)</b>	21%	<b>21%</b>	31%	<b>31%</b>
	<i>Translated</i>		<i>Translated</i>	
	20%	<b>20%</b>	24%	<b>24%</b>

At the critical point, the volume-translation parameter  $c$  has too small influence on the calculated critical volume ( $v_c$ ) to obtain a good match with the experimental value. Although the influence of the volume translation concept is more visible on the RK EoS, the PR CEoS yields better predictions of  $v_c$ . Table PIII.3 and Table PIII.4 definitively demonstrate the superiority of the PR EoS to correlate molar volumes in comparison to the SRK EoS.

To conclude this section, we need to say a few words about VLE calculations for binary systems when classical vdW one-fluid mixing rules that involve a temperature-independent interaction parameter ( $k_{12}$ )

are considered. A prerequisite for successful correlation of binary systems is accurate knowledge of the vapor pressure of each pure component; this is certainly the dominant factor whereas the second most important factor is the  $k_{12}$ . Consequently, by improving the prediction of vapor pressure data, the updated correlations developed in this study contribute doubtless to a better correlation of binary systems. A key question we also need to address is: how much change in the interaction parameter is needed when we switch from the original to the updated correlation? It is indeed acknowledged that numerical values of  $k_{12}$  are specific to the considered  $\alpha$ -function. To answer this question, we decided to refer to the work by Jaubert and Privat [244] who developed an equation making possible to calculate the  $k_{12}$  suitable for a desired  $\alpha$ -function (e.g., the updated  $\alpha$ -function developed in this work) knowing the corresponding  $k_{12}$  value for another  $\alpha$ -function (e.g., the original Soave  $\alpha$ -function). Such an equation writes:

$$k_{12}^{updated} = \frac{2k_{12}^{original} \delta_1^{original} \delta_2^{original} + (\delta_1^{original} - \delta_2^{original})^2 - (\delta_1^{updated} - \delta_2^{updated})^2}{2\delta_1^{updated} \delta_2^{updated}} \quad (\text{PIII.16})$$

$$\text{with: } \delta_i^{original} = \frac{\sqrt{a_{c,i} \cdot \alpha_i^{original}}}{b_i} \quad \text{and} \quad \delta_i^{updated} = \frac{\sqrt{a_{c,i} \cdot \alpha_i^{updated}}}{b_i}$$

Eq. (PIII.16) was used for several binary systems and the change in  $k_{12}$  was found to be small after switching from the original to the updated correlation. Consequently, it is possible to continue use of the numerical values of  $k_{12}$  available in commercial process simulation softwares for hundreds of binary systems when the updated correlations developed in this paper are used. It is however obviously advised to update  $k_{12}$  values thanks to Eq. (PIII.16).

### PIII.IV Conclusion

In this study, updated versions of the generalized Soave  $\alpha$ -function suitable for the RK and PR EoS have been proposed. Significant improvement on the reproduction of vapor pressure data have been obtained for the PR EoS with respect to the original version. The modified SRK EoS achieved similar results for the three properties of interest, in comparison with the original SRK equation. A significant difference however appears for very heavy molecules having an acentric factor larger than 1. This paper makes it also possible to conclude that the accuracies of the PR and SRK EoS are very similar, except for molar volumes, which are better predicted with the PR EoS.

To conclude, we do encourage developers of commercial process simulation softwares to update the parameters of the  $m(\omega_{\text{exp}})$  function involved in Soave  $\alpha$ -functions as reported in Eqs. (PIII.13) and (PIII.14) of the present study.



## **Publication IV : Search for the optimal expression of the volumetric dependence of the attractive contribution in cubic equations of state.**

Andrés Piña-Martinez<sup>1</sup>, Romain Privat<sup>1(\*)</sup>, Silvia Lasala<sup>1</sup>, Giorgio Soave<sup>2</sup>, Jean-Noël Jaubert<sup>1(\*)</sup>

*(<sup>1</sup>) Université de Lorraine, École Nationale Supérieure des Industries Chimiques, Laboratoire Réactions et Génie des Procédés (UMR CNRS 7274), 1 rue Grandville, 54000, Nancy, France*

*(<sup>2</sup>) Via Europa 7, I-20097 San Donato Milanese, Italy*

### **Abstract**

The 2<sup>nd</sup> degree polynomial volume function ( $v^2 + ubv + wb^2$ ), involved in the attractive term of cubic equations of state, has a strong influence on the calculated volumetric properties and, to a lesser extent, influences the calculated vapor-liquid equilibrium properties such as vapor pressure and enthalpy of vaporization. This function contains two parameters ( $u$  and  $w$ ) that were either selected constant or constituent-dependent in the literature. In this work, it is analyzed through a systematic methodology how parameters  $u$  and  $w$  influence the accuracy of predicted volumetric and vapor-liquid equilibrium properties, both for untranslated and translated cubic equations of state. It was thus possible to determine the optimum values of such parameters and to discuss if the values selected in well-known cubic equations of state are the most relevant.



## PIV.I Introduction

Today, computer-aided-process-design software allow virtually any engineer to simulate large flowsheets with considerable detail. Such simulators embed many thermodynamic models, and among these, equations of state (EoS) play a major role. The proper selection of these latter determines in large part the accuracy of the simulation. Indeed, as explained by Agarwal et al. [245], *if we have an equation of state (EoS) and the ideal-gas heat capacities, we can calculate not only phase equilibria, but also all the needed thermodynamic properties for a comprehensive model of an entire flowsheet*. Among these properties, vapor pressures are paramount, liquid densities are fundamental for mass balances whereas enthalpies, entropies and heat capacities are key properties for energy and exergy balances. Among different types of equations of state, the so-called cubic equations of state (CEoS), usually written in pressure-explicit form, arise as a widespread choice due to their accuracy, the low number of required experimental parameters and their availability as well, ease of implementation, ability to provide reasonable estimation of enthalpies and entropies and robustness. In a generalized form, CEoS can be expressed as:

$$P(T, v) = \frac{RT}{v-b} - \frac{a(T)}{v^2 + ubv + wb^2} \quad (\text{PIV.1})$$

where parameter  $a$  is a measure of the attractive forces between molecules; parameter  $b$  is the so-called covolume, which attempts to correct the perfect-gas law for the fact that molecules have a non-zero effective volume; and the constants  $u$  and  $w$  are either universal real numbers (the same values apply to all compounds) or substance-dependent quantities. The temperature-dependent  $a(T)$  parameter is classically written as:

$$a(T) = a_c \cdot \alpha(T) \quad (\text{PIV.2})$$

It is the product of the value of the attractive parameter at the critical temperature ( $a_c$ ) multiplied by a so-called  $\alpha$ -function, which is dimensionless. Such an  $\alpha$ -function has a great influence on the calculated vapor-liquid equilibrium properties like vapor pressure, enthalpy of vaporization and saturated-liquid heat capacity. On the other hand, the volume function of the attractive term ( $v^2 + ubv + wb^2$ ) and, in particular, the numerical values assigned to  $u$  and  $w$ , govern essentially the accuracy of the predicted volumetric properties. To parametrize this function, two options are on the table. The first option is to consider  $u$  and  $w$  as universal (component-independent) constants. By doing so, the critical compressibility factor returned by the EoS ( $z_c^{EoS}$ ) is the same for all components. However, known experimental values of  $z_c$  range between 0.0144 (for magnesium oxide) and 0.637 (for triethyl phosphate); therefore, by selecting this first option, the predicted saturated liquid densities, and particularly those in the critical region, are inevitably going to deviate from their experimental values. However, to the best of our knowledge, a systematic study of how the selection of  $u$  and  $w$  values (that can be chosen in a very large range of values) influence the accuracy of CEoS for property predictions was never conducted. The second option is to consider  $u$  and  $w$  as component-dependent factors. A first possibility is to correlate  $u$  and  $w$  to a readily available property like the acentric factor. Alternatively, the volume-translation concept, as initially developed by P eneloux et al. [92], can be used: the addition of a component-specific volume translation parameter entails that the  $u$  and  $w$  parameters

become component-specific themselves. But, are these two alternatives equivalent? Would it be an interest to combine them? (i.e., to use component-dependent  $u$  and  $w$  parameters and to simultaneously translate the EoS). Here again, we did not find in the literature any systematic study comparing the usefulness to correlate  $u$  and  $w$  to  $\omega$  or to use of a volume-translated EoS.

Bearing this in mind, the first part of this paper presents a historical background of the most popular modifications of the volume function proposed to improve the ability of CEoS to predict volumetric properties. The second part of this paper explores the possibility to correlate  $u$  and  $w$  to the acentric factor and to simultaneously translate the EoS. In the last part of this paper, a map reporting deviations between EoS predictions and experimental properties in the  $u-w$  space is screened in order to deem how such parameters influence the accuracy of the predicted volumetric and vapor-liquid equilibrium properties, both for untranslated and translated CEoS. This map made it possible to determine the optimal  $(u, w)$  values and to discuss the parametrization of the volume function in the attractive term of well-known cubic equations of state.

## PIV.II Historical background

An overview of the various modifications operated on the volume function of the attractive term of CEoS is presented below. A particular attention is devoted to the choice for the  $u$  and  $w$  parameters.

### PIV.II.I Selection of constant $(u, w)$ values

In 1873, J.D. Van der Waals [63] proposed the first, simplest and best known cubic equation of state:

$$P(T, v) = \frac{RT}{v-b} - \frac{a_c}{v^2} \quad \text{with:} \quad \begin{cases} a_c = \frac{27 R^2 T_{c,\text{exp}}^2}{64 P_{c,\text{exp}}} \\ b = \frac{1 RT_{c,\text{exp}}}{8 P_{c,\text{exp}}} \end{cases} \quad (\text{PIV.3})$$

It is a so-called 2-parameter CEoS because its application to a pure component requires the preliminary knowledge of two experimental (exp) component-dependent parameters (the critical temperature  $T_{c,\text{exp}}$  and pressure  $P_{c,\text{exp}}$ ). In Eq. (PIV.3),  $R$  is the gas constant,  $T$ , the temperature,  $P$ , the pressure and  $v$ , the molar volume. The Van der Waals EoS gives a qualitatively correct description of fluid properties and phase behavior [246], but it predicts a too large critical compressibility factor of  $3/8$  and thus leads to very poor correlation of densities in the critical region. By identification with Eq. (PIV.1), it is noticeable that  $u$  and  $w$  were set to  $u=w=0$ . Although numerous modifications of the Van der Waals equation were proposed, very few different  $(u, w)$  pairs were tested out.

As a matter of fact, the two EoS which received most attention in the last 50 years are those proposed by Soave [64] (he introduced the so-called Soave-Redlich-Kwong EoS denoted SRK) and Peng-Robinson [65–67] (PR). For a given pure component, such modern EoS require the specification of three macroscopic properties ( $T_{c,\text{exp}}$ ,  $P_{c,\text{exp}}$  and  $\omega_{\text{exp}}$ ) and they are thus equivalent to a 3-parameter corresponding states principle [68,69]. In this paper, they are simply referred as 3-parameter EoS. The

equation developed by Harmens [247] (Ha) to predict the properties of air also received substantial attention.

Without clear explanation or theoretical foundations, all these authors assumed that  $u$  and  $w$  are subject to the constraint:  $u + w = 1$ . As a first example, the SRK EoS is characterized by  $u = 1$  and  $w = 0$  and the corresponding critical compressibility factor is equal to  $1/3$ . The SRK EoS is defined by:

$$P(T, v) = \frac{RT}{v-b} - \frac{a_c \cdot \alpha(T)}{v(v+b)} \left\{ \begin{array}{l} \alpha(T) = \left[ 1 + m(1 - \sqrt{T/T_c}) \right]^2 \\ m = 0.480 + 1.574\omega_{\text{exp}} - 0.176\omega_{\text{exp}}^2 \\ a_c = \Omega_a \frac{R^2 T_{c,\text{exp}}^2}{P_{c,\text{exp}}} \\ b = \Omega_b \frac{RT_{c,\text{exp}}}{P_{c,\text{exp}}} \\ \Omega_a = \frac{1}{9(\sqrt[3]{2} - 1)} \approx 0.42748 \\ \Omega_b = \frac{\sqrt[3]{2} - 1}{3} \approx 0.08664 \\ \text{corresponds to: } u = 1 ; w = 0 \text{ and } z_c = 1/3 \end{array} \right. \quad (\text{PIV.4})$$

In 1976, Peng and Robinson selected  $u = 2$  and  $w = -1$  so that the corresponding critical compressibility factor is equal to  $0.3074$ . The PR EoS expression is:

$$P(T, v) = \frac{RT}{v-b} - \frac{a_c \cdot \alpha(T)}{v(v+b) + b(v-b)} \left\{ \begin{array}{l} \alpha(T) = \left[ 1 + m(1 - \sqrt{T/T_c}) \right]^2 \\ m = 0.37464 + 1.54226\omega_{\text{exp}} - 0.26992\omega_{\text{exp}}^2 \\ a_c = \Omega_a \frac{R^2 T_{c,\text{exp}}^2}{P_{c,\text{exp}}} \\ b = \Omega_b \frac{RT_{c,\text{exp}}}{P_{c,\text{exp}}} \\ X = \left[ 1 + \sqrt[3]{4 - 2\sqrt{2}} + \sqrt[3]{4 + 2\sqrt{2}} \right]^{-1} \approx 0.25308 \\ \Omega_a = \frac{8(5X + 1)}{49 - 37X} \approx 0.45724 \\ \Omega_b = \frac{X}{X + 3} \approx 0.07780 \\ \text{corresponds to: } \begin{cases} u = 2 ; w = -1 \\ z_c = 1/(X + 3) \approx 0.3074 \end{cases} \end{array} \right. \quad (\text{PIV.5})$$

In 1977, focusing on the reproduction of vapor-liquid equilibria (VLE) of the nitrogen-argon-oxygen system, Harmens selected  $u = 3$  and  $w = -2$ . He claimed that the strength of the equation lied in the fact that for nitrogen  $z_c = 0.2883$ , which is very close to the value returned by his model:  $z_c = 0.2862$ .

## PIV.II.II Selection of component-dependent ( $u, w$ ) pairs

As previously stated, assigning universal values to  $u$  and  $w$  entails the prediction by the EoS of a unique  $z_c$  value for all components. In order to improve the prediction of liquid densities in the critical region, the  $z_c$  parameter must be made component-dependent and no longer universal. One way to reach this goal is to use component-dependent values for  $u$  and  $w$ . A possibility is to correlate  $u$  and  $w$  to a readily available property. This is exactly what Schmidt and Wenzel [248] decided to do in 1980 after noticing that the SRK EoS better describes liquid molar volumes (at  $T_r = 0.7$ ) of spherical molecules like methane (for which  $\omega = 0$ ) than the PR EoS while, conversely, the PR EoS yields better results for n-heptane (the acentric factor of which is about 0.35) than the SRK EoS. Both the SRK ( $u = 1 ; w = 0$ ) and PR ( $u = 2 ; w = -1$ ) EoS satisfy  $u + w = 1$  so that Schmidt and Wenzel kept this relationship. Moreover, in order to find back the SRK EoS ( $w = 0$ ) when  $\omega = 0$  and the PR ( $w = -1$ ) EoS when  $\omega \approx 0.35$ , they set:  $w = -3\omega$ . This led them to the following expression:

$$P(T, v) = \frac{RT}{v-b} - \frac{a_c \cdot \alpha(T)}{v^2 + (1+3\omega)bv - 3\omega b^2} \quad (\text{PIV.6})$$

The same year, a similar methodology was applied by Harmens and Knapp [249]. They also kept  $u + w = 1$  and, following Schmidt and Wenzel, they developed a complex correlation to estimate  $u$  from the mere knowledge of the acentric factor. They proposed:

$$\begin{cases} u = 1 + \frac{1 - 3z_c}{0.10770z_c + 0.76405z_c^2 - 1.24282z_c^3 + 0.96210z_c^4} \\ \text{with: } z_c = 0.3211 - 0.080\omega_{\text{exp}} + 0.0384\omega_{\text{exp}}^2 \end{cases} \quad (\text{PIV.7})$$

For small-size molecules characterized by  $z_c = 1/3$ , Eq. (PIV.7) returns  $u = 1$  and  $w = 0$  corresponding to the SRK EoS. Similarly, by setting  $z_c = 0.3074$  (corresponding to intermediate-size molecules like n-hexane), the PR EoS constants are obtained ( $u = 2$  and  $w = -1$ ).

In 1982, Patel and Teja [187] also followed the footsteps of Schmidt and Wenzel and selected  $u + w = 1$ . For non-polar molecules,  $w$  was correlated to the acentric factor and a Soave-type  $\alpha$ -function was used. In particular, in order to determine  $w$ , it is first necessary to calculate the smallest positive root (noted  $x_{\min}$ ) of the following cubic equation:

$$\begin{cases} x^3 + (2 - 3z_c)x^2 + (3z_c^2)x - z_c^3 = 0 \\ \text{with: } z_c = 0.329032 - 0.076799\omega_{\text{exp}} + 0.0211947\omega_{\text{exp}}^2 \end{cases} \quad (\text{PIV.8})$$

Once done: 
$$w = \frac{3z_c - 1}{x_{\min}} \quad (\text{PIV.9})$$

For a light non-polar substance characterized by  $\omega = 0$ , Eq. (PIV.9) returns a value of  $w$  close to zero so that the new equation is comparable to the SRK equation and, for components whose acentric factors are close to 0.3, we get  $w \approx -1$  so that the proposed equation is comparable to the PR EoS. As previously observed with the works by Schmidt and Wenzel or Harmens and Knapp, characteristics of both the SRK and PR equation are implicit in the new formulation by Patel and Teja.

For polar molecules, Patel and Teja failed to correlate  $w$  and the shape parameter  $m$  of the  $\alpha$ -function (see, e.g., Eq. (PIV.4)) with the acentric factor. They thus decided to work with a 4-parameter CEoS.  $m$  and  $w$  were considered as adjustable parameters and were fitted component by component on experimental vapor-pressure and liquid-density data. In the end, their EoS requires the knowledge of  $T_{c,\text{exp}}$ ,  $P_{c,\text{exp}}$ ,  $m$  and  $w$ .

In 1976, Fuller [250] published a 5-parameter EoS that requires the knowledge of  $T_{c,\text{exp}}$ ,  $P_{c,\text{exp}}$ ,  $v_{c,\text{exp}}$ ,  $\omega_{\text{exp}}$  and  $\bar{P}_{\text{exp}}$  (the experimental value of the parachor) for a given pure component. With the aim of accurately correlating the liquid densities of polar and non-polar components, he decided to set  $w=0$  and to make  $u$  component and temperature-dependent. Fuller also selected a temperature-dependent covolume and we know today that such a choice is thermodynamically inconsistent since it leads to the crossing of isotherms in a (P,v) plane and to negative heat capacities [251–253]. His final equation takes the form:

$$P(T, v) = \frac{RT}{v-b(T)} - \frac{a_c \cdot \alpha(T)}{v^2 + u(T, T_{c,\text{exp}}, P_{c,\text{exp}}, v_{c,\text{exp}}, \omega_{\text{exp}}, \bar{P}_{\text{exp}}) \cdot bv} \quad (\text{PIV.10})$$

In 1992, Twu *et al.* [254] carried out an analysis of the CEoS on a  $u-w$  diagram with the aim of discussing the representation of volumetric properties. 21 possible combinations of  $u$  and  $w$  were checked for a number of alkanes, alcohols and glycols. They established that the relationship between  $u$  and  $w$  should be:  $u-w=4$  for the best representation of saturated-liquid densities. The following expression was obtained:

$$P(T, v) = \frac{RT}{v-b} - \frac{a_c \cdot \alpha(T)}{v^2 + (w+4)bv + wb^2} \quad (\text{PIV.11})$$

In Eq. (PIV.11),  $w$  is treated – component by component – as an adjustable parameter. It is obtained by minimizing the deviations between calculated and experimental liquid densities. In order to simultaneously get accurate vapor pressures, Twu used a 3-parameter (noted  $L$ ,  $M$ , and  $N$ )  $\alpha$ -function [216] so that in the end, each pure component is characterized by 6 parameters ( $T_{c,\text{exp}}$ ,  $P_{c,\text{exp}}$ ,  $w$ ,  $L$ ,  $M$ ,  $N$ ).

At this step, we believe it is important to recall that the brilliant concept to make  $u$  and  $w$  substance-dependent in order to get better liquid densities was first introduced by Clausius who proposed the following equation in 1880 [255]:

$$P(T, v) = \frac{RT}{v-b} - \frac{a_c \cdot \alpha(T_r)}{(v+c)^2} \quad \text{with: } \alpha(T_r) = \frac{1}{T_r} \quad (\text{PIV.12})$$

where  $c$  is a component-dependent parameter. For such an EoS, we immediately get:  $u = 2\frac{c}{b}$  and  $w = \left(\frac{c}{b}\right)^2$ .

Another method to obtain component-dependent  $u$  and  $w$  parameters (and thus to get  $z_c$  component-dependent in order to achieve better representation of volumetric properties) is to translate the EoS. This simple and ingenious concept, proposed by P eneloux [92], corresponds to a translation of the whole P-v isotherm (of the amount  $-c$ ) along the volume axis. Indeed, for a given component, the saturated-liquid volume calculated by a CEoS at a given temperature is usually notably different from the experimental value but the difference between the calculated and the experimental volume is approximately constant when varying the temperature. Consequently, a temperature-independent volume translation (all the calculated molar volumes are translated by a constant amount  $c$ ) significantly improves the description of saturated-liquid densities. Assuming that subscripts  $o$  and  $t$  refer to the original (i.e. untranslated) and translated equations of state, respectively, the shifted volume  $v_t$  (closer to the experimental value than  $v_o$ ) is linked to  $v_o$  by:

$$v_t = v_o - c \quad (\text{PIV.13})$$

In Eq. (PIV.13), the substance-dependent volume-translation parameter,  $c$ , is often determined in order that the translated EoS exactly reproduces the experimental saturated liquid volume at  $T_r = 0.8$ . At this step it is possible to determine the relationship between  $u_o$  and  $w_o$  stemming from the untranslated EoS and  $u_t$  and  $w_t$  from the translated EoS.

Starting with a non-translated EoS with the form of Eq. (PIV.1) in which  $u_o$  and  $w_o$  are constant:

$$P_o(T, v_o) = \frac{RT}{v_o - b_o} - \frac{a_c \cdot \alpha(T)}{v_o^2 + u_o b_o v_o + w_o b_o^2} \quad (\text{PIV.14})$$

the expression of the translated EoS is obtained by replacing in Eq. (PIV.14)  $v_o$  by  $(v_t + c)$  and  $b_o$  by  $(b_t + c)$  [132,183]. This gives the form:

$$P_t(T, v_t) = \frac{RT}{v_t - b_t} - \frac{a_c \cdot \alpha(T)}{(v_t + c)^2 + u_o(b_t + c)(v_t + c) + w_o(b_t + c)^2} \quad (\text{PIV.15})$$

By rearranging Eq. (PIV.15), in the form of Eq. (PIV.1), we get:

$$P_t(T, v_t) = \frac{RT}{v_t - b_t} - \frac{a_c \cdot \alpha(T)}{v_t^2 + u_t b_t v_t + w_t b_t^2} \quad \text{with:} \quad \begin{cases} u_t = u_o + (2 + u_o) \left( \frac{c}{b_t} \right) \\ w_t = w_o + (u_o + 2w_o) \left( \frac{c}{b_t} \right) + (1 + u_o + w_o) \left( \frac{c}{b_t} \right)^2 \end{cases} \quad (\text{PIV.16})$$

Depending on the component-dependent parameters  $c$  and  $b_t$ , the  $u_t$  and  $w_t$  parameters are now component-dependent, and thus  $z_{c,t}$ , the critical compressibility factor of the translated CEoS, is component dependent too. Indeed, as a direct consequence of having translated the critical volume ( $v_{c,t} = v_{c,o} - c$ ), we immediately get:  $z_{c,t} = z_{c,o} - \frac{P_{c,\text{exp}}}{RT_{c,\text{exp}}} c$ .

Finally, in Table PIV.1, the values of  $u$  and  $w$  are reported for all the CEoS previously mentioned.

**Table PIV.1.** Selected values of  $u$  and  $w$  for the volume function of the attractive term in cubic equations of state.

EoS	$u$	$w$
Van der Waals (1873) [63]	0	0
Clausius (1880) [255]	$2\frac{c}{b}$	$\left(\frac{c}{b}\right)^2$
Soave-Redlich-Kwong (1972) [64]	1	0
Peng and Robinson (1976) [65]	2	-1
Harmens (1977) [247]	3	-2
Schmidt and Wenzel (1980) [248]	$1 + 3\omega$	$-3\omega$
Harmens and Knapp (1980) [249]	component-dependent	$1 - u$
Patel and Teja (1982) [187]	$1 - w$	component-dependent
Fuller (1976) [250]	component-dependent	0
Twu, et al. (1992) [254]	$4 + w$	component-dependent
<i>translated</i> EoS (1982) [92]	$u_o + (2 + u_o)\left(\frac{c}{b_t}\right)$	$w_o + (u_o + 2w_o)\left(\frac{c}{b_t}\right) + (1 + u_o + w_o)\left(\frac{c}{b_t}\right)^2$

This table highlights that very few  $(u, w)$  pairs of constant parameters were explored. It is however well-established that the SRK and PR EoS predict the saturated liquid volumes with an average deviation of about 16% and 8% respectively. This means that by changing the  $(u, w)$  pair from  $(1; 0)$  to  $(2; -1)$ , the deviations are divided by 2. Thus, by screening all the possible  $(u, w)$  pairs, the optimal one, leading to the most accurate reproduction of volumetric data, could be determined. This table also shows that the volume-translation concept was never applied to an EoS expressing  $u$  and  $w$  as generalized functions of the acentric factor. For all these reasons, in the next sections the usefulness of using functions of the acentric factor for the  $(u, w)$  parameters in a translated EoS is first discussed. Then, a large screening of  $(u, w)$  pairs for both untranslated and translated CEoS will be performed to identify the optimal one.

### PIV.III On the interest to combine $\omega$ -dependent $(u, w)$ parameters and a volume-translation parameter in a CEoS

#### PIV.III.I On the interest to select $\omega$ -dependent $(u, w)$ pairs in untranslated CEoS

In order to highlight the interest of selecting  $\omega$ -dependent  $(u, w)$  parameters for a better correlation of liquid-density data, let us illustrate that the selection of universal  $(u, w)$  constants entails that smallest deviations over liquid-density data are solely obtained for molecule having a specific acentric factor. To do so, the SRK ( $u = 1, w = 0$ ) and PR ( $u = 2, w = -1$ ) EoS, that embed a generalized  $\alpha$ -function, are

considered. Note that a similar study was conducted by Schmidt and Wenzel 40 years ago but these authors only calculated the deviation over one kind of datum: the molar volume at  $T_r = 0.7$ . Here, our plan is to consider a larger range of temperatures to get more reliable conclusions. Following Schmidt and Wenzel, 14 hydrocarbons ranging from  $\text{CH}_4$  ( $\omega = 0.01$ ) to n-decane ( $\omega = 0.49$ ) were selected. For each of them, the correlation reported by the DIPPR database to estimate the molar liquid volume at saturation was used to generate 50 equidistant data points between  $T_{\min}$  and  $T_{\max} = 0.9T_c$ . Here,  $T_{\min}$  is the minimum temperature at which  $v_{liq}^{sat}$  can be estimated from the DIPPR correlation. Once done, the MAPE (Mean Absolute Percentage Error) on  $v_{liq}^{sat}$  was calculated as:

$$MAPE = \frac{100}{50} \sum_{i=1}^{50} \left| \frac{v_{liq}^{sat, DIPPR} \left( T_i^{v_{liq}^{sat}} \right) - v_{liq}^{sat, CEoS} \left( T_i^{v_{liq}^{sat}} \right)}{v_{liq}^{sat, DIPPR} \left( T_i^{v_{liq}^{sat}} \right)} \right| \quad (\text{PIV.17})$$

The results shown in [Figure PIV.1](#) highlight that, for a given acentric factor value, deviations on  $v_{liq}^{sat}$  are strongly impacted by the choice of the EoS i.e. by the values assigned to  $u$  and  $w$ . [Figure PIV.1](#), in which a large range of temperature was considered, differs significantly from the one published by Schmidt and Wenzel but leads to similar conclusions: the SRK EoS ( $u = 1$ ,  $w = 0$ ) describes well the liquid volume at low values of  $\omega$ ; while the PR EoS ( $u = 2$ ,  $w = -1$ ) yields the best results around  $\omega = 0.30$  (for n-hexane).

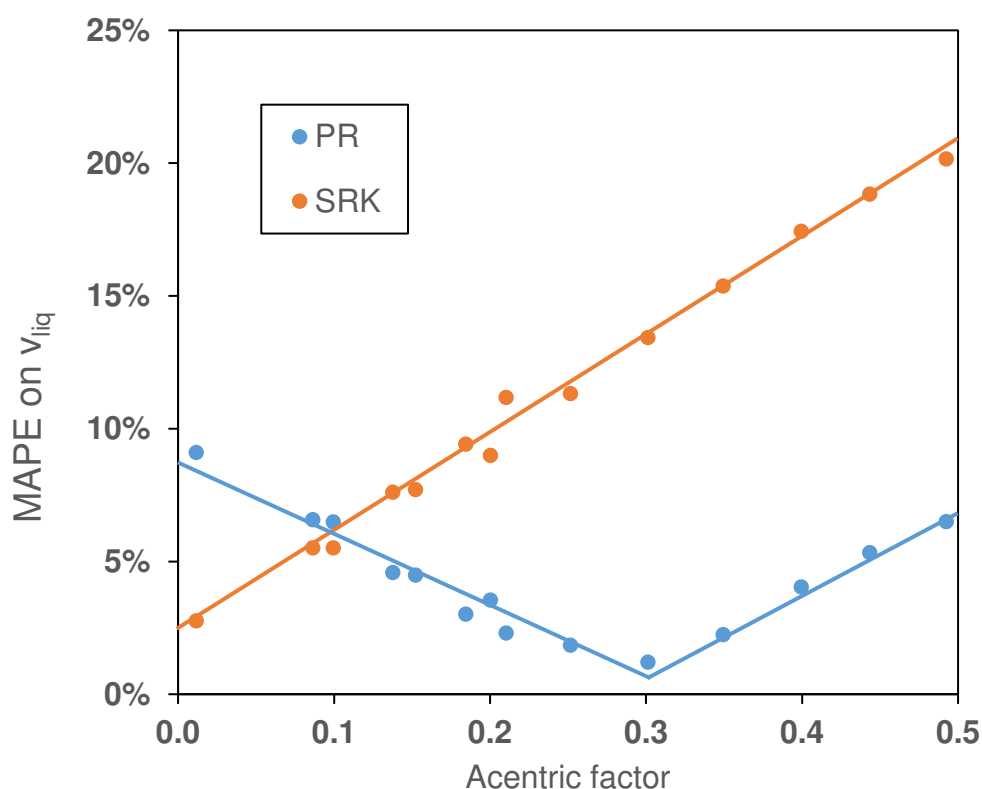


**Figure PIV.1.** Deviation on saturated liquid molar volume up to  $T_r = 0.9$  as a function of the acentric factor  $\omega$ , calculated by the SRK and PR EoS. The 14 substances are by order of  $\omega$ :  $\text{CH}_4$ ,  $\text{C}_2\text{H}_4$ ,  $\text{C}_2\text{H}_6$ ,  $\text{C}_3\text{H}_6$ ,  $\text{C}_3\text{H}_8$ , but-1-ene, n-butane, benzene and the n-alkanes from n-pentane to n-decane.

What can be said for  $\omega$  values different from 0 and 0.3? For sure, [Figure PIV.1](#) does not help to determine which  $(u, w)$  pair is suitable when, e.g.,  $\omega = 0.5$ . Schmidt and Wenzel assumed  $w = -3\omega$  and  $u = 1 + 3\omega$  although they had no argument justifying that  $u$  and  $w$  should be linear functions of  $\omega$ .

### PIV.III.II On the interest to select $\omega$ -dependent $(u, w)$ pairs in translated CEoS

The second possibility to make  $z_c$  component-dependent is to translate the EoS explaining why it was now decided to check the influence of the acentric factor on the correlation of saturated-liquid volumes with translated versions of the SRK and PR EoS. In this study, the substance-dependent volume-translation parameter,  $c$ , was determined, component by component, in order the translated EoS exactly reproduces the experimental saturated liquid volume at a reduced temperature of 0.8, [ $v_{liq,exp}^{sat}(T_r = 0.8)$ ], that is:

$$c = v_{liq}^{sat,u-CEoS}(T_r = 0.8) - v_{liq,exp}^{sat}(T_r = 0.8) \quad (\text{PIV.18})$$

where  $v_{liq}^{sat,u-CEoS}(T_r = 0.8)$  is the molar volume calculated with the original (*untranslated*) CEoS at  $T_r = 0.8$ .

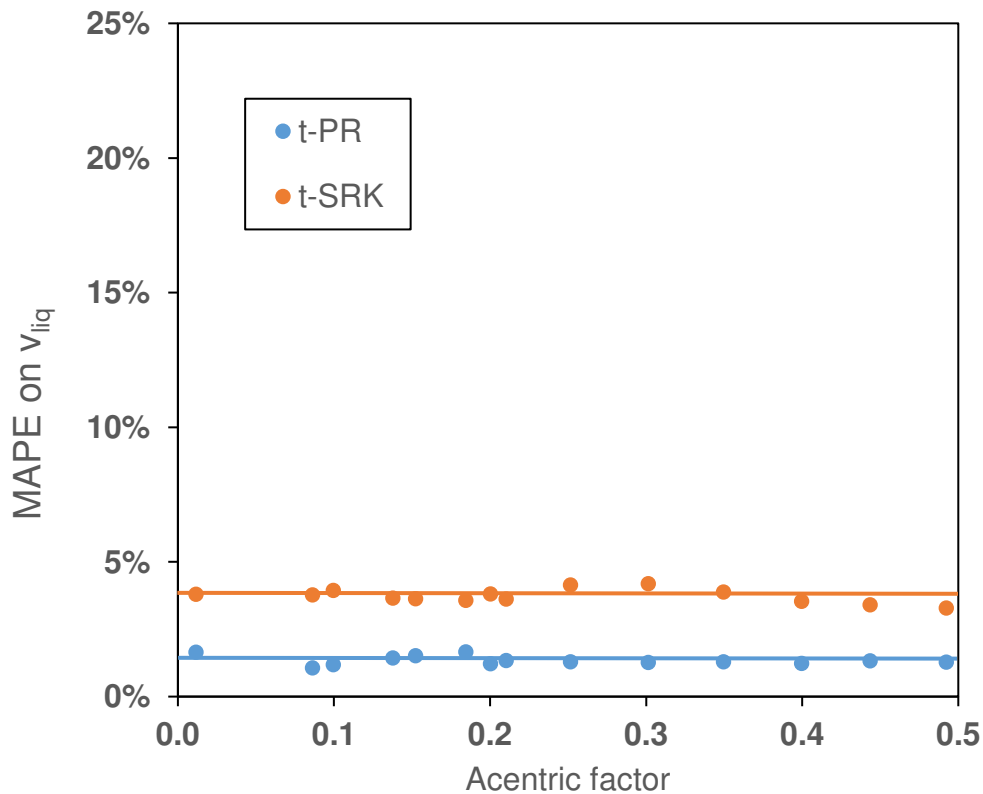


**Figure PIV.2.** Deviation on saturated liquid molar volume ( $v_{liq}^{sat}$ ) up to  $T_r = 0.9$  as a function of the acentric factor  $\omega$ , calculated by the *translated*-SRK and *translated*-PR EoS. The scale has intentionally been kept identical to the one of [Figure PIV.1](#) and the 14 substances are those of [Figure PIV.1](#).

The results are visible in [Figure PIV.2](#) and, in comparison to [Figure PIV.1](#), the change is drastic: for both the translated SRK and PR EoS, the MAPE on  $v_{liq}^{sat}$  is more or less constant regardless of the acentric factor value.

It is no longer possible to assert that the SRK EoS is more suitable for spherical molecules and the PR EoS is more suitable for larger molecules. Independently of the acentric factor value, the *translated*-PR (*t*-PR) EoS leads to smaller deviations on liquid densities than the *translated*-SRK (*t*-SRK). We can thus conclude that  $u$  and  $w$  strongly affect the correlation of liquid densities but have to be selected as universal constants ( $\omega$ -independent) when CEoS are translated. There is thus no benefit to select component-dependent ( $u, w$ ) pairs and to simultaneously translate the EoS. Such a result is extremely important and opens the way to the search for an optimal ( $u, w$ ) set of universal constants that would potentially lead to better results than those obtained with the *t*-PR EoS (about 2% on liquid molar volumes according to [Figure PIV.2](#)).

**Remark:** although not shown, the results depicted in [Figure PIV.2](#) were confirmed by considering an extended database of 1,300 pure compounds – including all families of chemical species – and for which accurate pseudo-experimental liquid densities could be extracted from the DIPPR database.

### PIV.III.III Search for $\omega$ -dependent ( $u, w$ ) parameters to be used with untranslated CEoS that lead to the same performance as ( $u_o, w_o$ ) universal constants used in translated CEoS

What have we learnt?

1) In [Section PIV.III.II](#), it has been shown that the combination of constant universal parameters ( $u_o = 2$ ,  $w_o = -1$ ) of the PR EoS and a component-specific volume-translation parameter leads to quite low deviations over liquid-density data (around 2%).

2) As stated in [Section PIV.II.II](#), by translating an EoS characterized by constant universal parameters ( $u_o, w_o$ ), we obtain component-dependent  $u$  and  $w$  parameters, noted ( $u_t, w_t$ ). The relationship between the ( $u_o, w_o$ ) and ( $u_t, w_t$ ) sets of parameters has been derived (see Eq. [\(PIV.16\)](#)). For the PR EoS ( $u_o = 2$ ,  $w_o = -1$ ), one obtains:

$$\begin{cases} u_t = u_o + (2 + u_o) \left( \frac{c}{b_t} \right) = 2 + 4 \left( \frac{c}{b_t} \right) \\ w_t = w_o + (u_o + 2w_o) \left( \frac{c}{b_t} \right) + (1 + u_o + w_o) \left( \frac{c}{b_t} \right)^2 = -1 + 2 \left( \frac{c}{b_t} \right)^2 \end{cases} \quad (\text{PIV.19})$$

Once again, although ( $u_o, w_o$ ) are constant parameters, ( $u_t, w_t$ ) are component specific, since  $c$  and  $b_t$  are component specific: the substance-dependent volume-translation parameter,  $c$ , is indeed determined by Eq. [\(PIV.18\)](#) and according to Eqs. [\(PIV.5\)](#) and [\(PIV.13\)](#)  $b_t = 0.07780 \frac{RT_{c,\text{exp}}}{P_{c,\text{exp}}} - c$ .

Component-dependent ( $u_t, w_t$ ) parameters stemming from Eq. (PIV.19) lead to an average deviation over liquid-density data of about 2% and can thus be considered as reference values. Consequently, for 14 pure components, they were plotted versus  $\omega$  in Figure PIV.3 in order to highlight the relationship between the component-specific parameters ( $u_t, w_t$ ) on one hand, and  $\omega$  on the other hand. Doing so, it will be possible to evaluate the empirical correlations proposed by Schmidt and Wenzel ( $w = -3\omega$  and  $u = 1 + 3\omega$ ) and see if they moved in the right direction.

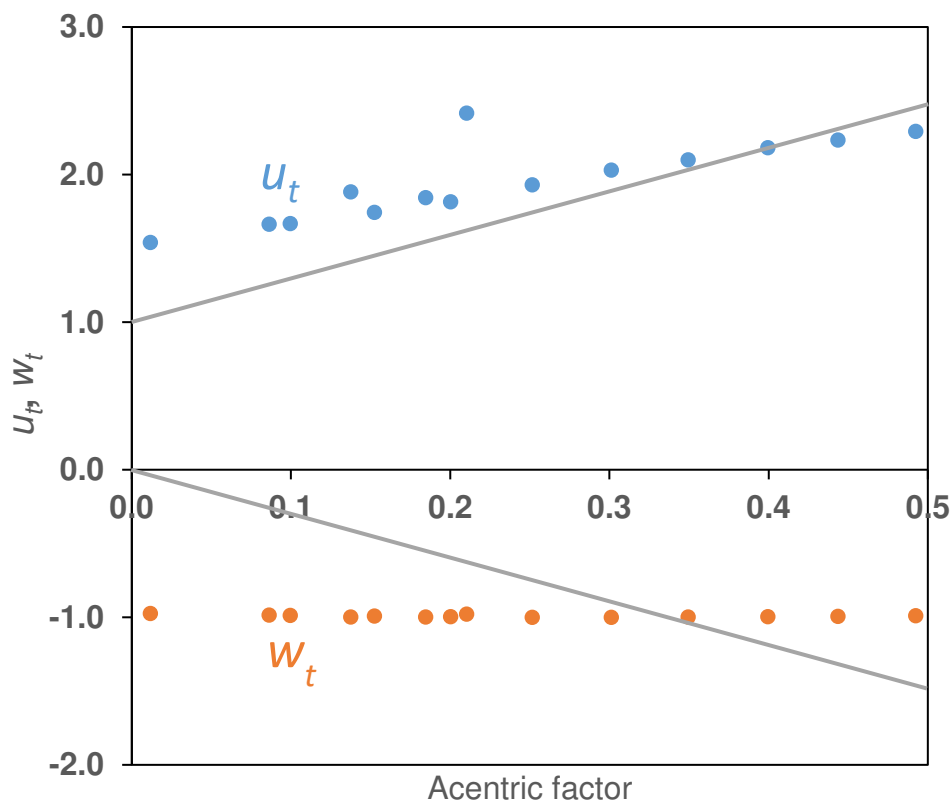


**Figure PIV.3.** Plot of  $u_t$  (●) and  $w_t$  (●) stemming from the  $t$ -PR EoS as a function of the acentric factor  $\omega$ . With such  $u$  and  $w$  parameters, the MAPE on  $v_{liq}^{sat}$  is about 2% (see Figure PIV.2) so that such pairs can be considered as *optimal* values. The 14 substances are those of Figure PIV.1. The two straight lines ( $w = -3\omega$  and  $u = 1 + 3\omega$ ) recall the values recommended by Schmidt and Wenzel.

Figure PIV.3 highlights that to get accurate densities (the same as those obtained with the  $t$ -PR EoS), it is enough to select  $u$  acentric factor-dependent and to keep  $w$  constant ( $w = -1$ ). It is noticeable that  $u$  must be an increasing function of  $\omega$  but the relationship proposed by Schmidt and Wenzel ( $u = 3\omega + 1$ ) has a too steep slope. After considering a database of 1300 components, it was found that a good fit of  $u$  and  $w$  with respect to  $\omega$ , was:

$$\begin{cases} u = 0.7\omega + 1.9 \\ w = -1 \end{cases} \quad (\text{PIV.20})$$

Eq. (PIV.20) clearly establishes that  $(u + w) = 0.9 + 0.7\omega$  is not constant. It takes a value equal to one (as recommended by Schmidt and Wenzel) only for a small molecule like the propane. In 1992, Twu et al. [254] recommended  $(u - w) = 4$  but this relationship deviates significantly from Eq. (PIV.20).

## PIV.IV Search for the optimal $(u,w)$ set from a map reporting deviations between EoS predictions and experimental properties in the $(u,w)$ space

As previously discussed, very few pairs of constant  $(u,w)$  parameters were tested. For untranslated CEoS, we find (0,0) for the VdW EoS, (1,0) for the SRK EoS, (2, -1) for the PR EoS and (3, -2) for the Harmens EoS. Such pairs are however not equivalent at all in terms of correlation of liquid-density data. As an example, we know that the deviations on liquid densities are twice smaller with the PR EoS than with the SRK EoS. It seems thus pertinent to wonder what are the optimal values of  $(u,w)$ , i.e., what are the  $(u,w)$  values that lead to the best correlation of both volumetric and VLE equilibrium data. For clarity, let us recall that  $u$  and  $w$  only have a small influence on the accuracy of VLE predictions.

The previous section also highlighted that the volume translation technique was certainly the best option to make  $u$  and  $w$  component-dependent. Such a technique indeed avoids to develop a correlation between  $(u,w)$  and  $\omega$ . In turn, it necessitates the knowledge of the experimental molar volume at  $T_r = 0.8$ . The strong impact of  $u$  and  $w$  on *translated*-CEoS was also emphasized. As an example, deviations on liquid densities were found to be close to 2% with the *t*-PR EoS and about 4% with the *t*-SRK EoS.

For all these reasons, it was decided to meticulously explore the  $u-w$  space in order to determine the optimal values of these two parameters for both an *untranslated* and a *translated* CEoS.

Note that optimal values of the  $(u,w)$  universal parameters for an untranslated CEoS are searched for comparative purpose only. We know from the previous section that a better strategy exists for improving the reproduction of liquid-density data (i.e., the use of universal  $(u,w)$  constants in a translated CEoS). However, as mentioned previously, the untranslated PR EoS is currently the best CEoS using universal  $(u,w)$  constants in terms of reproduction of liquid-density data and it is interesting to determine if better  $(u,w)$  values could be found for this kind of untranslated EoS.

### PIV.IV.I Exploration of map reporting deviations between EoS predictions and experimental properties in the $u-w$ space

In order to explore the  $u-w$  space, it is necessary to identify the feasible values of  $u$  and  $w$ . According to Segura et al. [256], these parameters must be selected in order to ensure that the volume function of the attractive term ( $v^2 + ubv + wb^2$ ) remains strictly positive in the molar volume range of applicability of the EoS (i.e., for any  $v \geq b$ ) and therefore, that the attractive term of the EoS remains positive and finite, as physically expected. Segura et al. obtained the following set of constraints:

$$\begin{cases} u + w > -1 & \text{if } u > -2 \\ u^2 < 4w & \text{if } u \leq -2 \end{cases} \quad (\text{PIV.21})$$

These constraints are represented in [Figure PIV.4](#) (see the dashed line) and separate the  $u-w$  space in two parts: a first one called “Region III” defines all the unfeasible  $(u,w)$  pairs (i.e., the  $(u,w)$  pairs leading to negative values of  $v^2 + ubv + wb^2$  for  $v \geq b$ ), while the remaining region corresponds to the feasible  $(u,w)$  pairs. This latter can be divided in two sub-regions denoted Region I and Region II in [Figure PIV.4](#). Region I is such that the polynomial  $v^2 + ubv + wb^2$  exhibits complex roots while region

II is associated with real roots. In practice, the representative points of CEoS of the literature all belong to Region II.

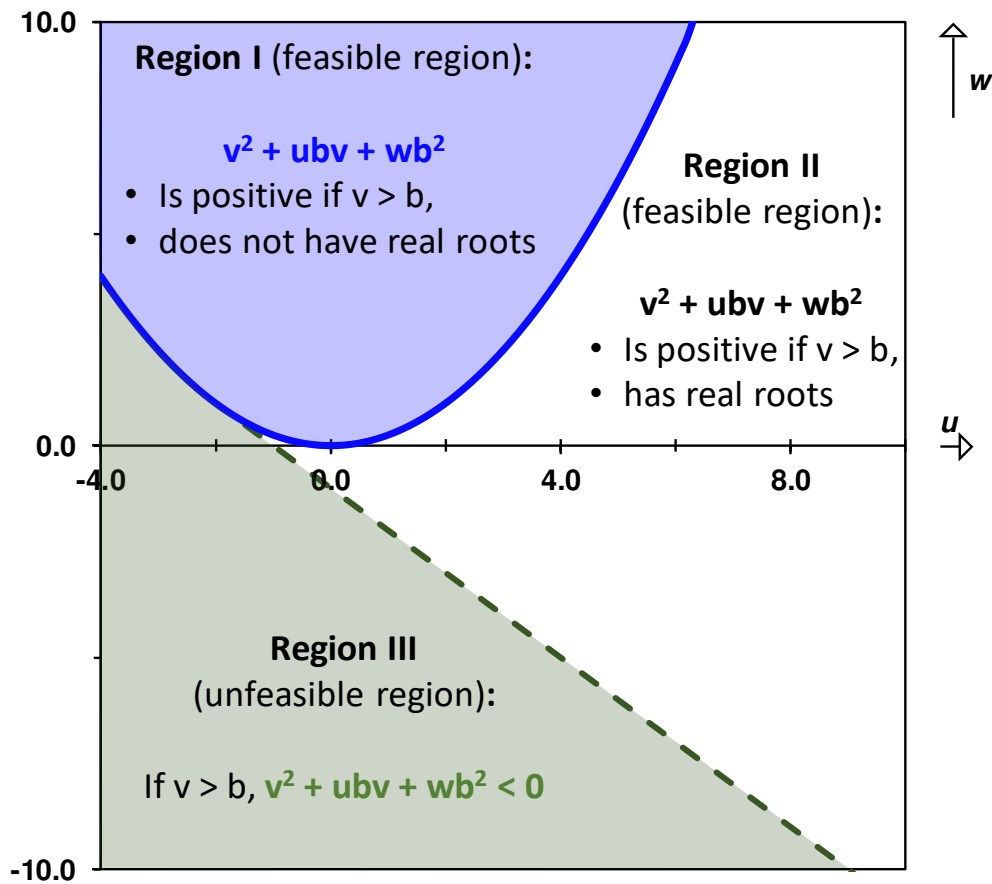


**Figure PIV.4.** Representation of the feasible and unfeasible regions of CEoS in the  $u-w$  space.

In this study, in order to realize a very large screening of  $(u, w)$  pairs, i.e. to explore a very large part of Region II,  $u$  was varied between  $-2$  and  $10$ , while  $w$  was subject to the two above constraints (see Eq. (PIV.21)).

To build the  $u-w$  map, a variation step equal to  $0.05$  was selected for each parameter so that more than  $50,000$   $(u, w)$  combinations were tested.

Clearly, each  $(u, w)$  pair defines a new EoS for which a mathematical expression of the  $\alpha$ -function is required. However, the open literature only defines generalized  $\alpha$ -functions for the RK and PR EoS. In other words,  $\alpha$ -functions are only available for 2 single combinations of the  $(u, w)$  parameters. These well-known expressions are recalled below:

$$\left\{ \begin{array}{l} u=1 \\ w=0 \end{array} \right. ; \text{SRK EoS} ; \left\{ \begin{array}{l} \alpha(T) = [1 + m(1 - \sqrt{T/T_c})]^2 \\ \text{with: } m(\omega_{\text{exp}}) = 0.480 + 1.574\omega_{\text{exp}} - 0.176\omega_{\text{exp}}^2 \end{array} \right. \quad (\text{PIV.22})$$

$$\left\{ \begin{array}{l} u=2 \\ w=-1 \end{array} \right. ; \text{PR EoS} ; \left\{ \begin{array}{l} \alpha(T) = [1 + m(1 - \sqrt{T/T_c})]^2 \\ \text{with: } m(\omega_{\text{exp}}) = 0.37464 + 1.54226\omega_{\text{exp}} - 0.26992\omega_{\text{exp}}^2 \end{array} \right.$$

In order to overcome this lack of information, for each  $(u, w)$  pair, the  $m(\omega_{\text{exp}})$  expression to be used in the Soave  $\alpha$ -function ( $\alpha(T) = [1 + m(1 - \sqrt{T/T_c})]^2$ ) has to be re-determined. For this purpose, a procedure similar to the one used by Soave for the development of the SRK EoS was followed [64]:  $\omega$  values ranging from zero to 1.4 with a step of 0.05 were assumed. For each of these  $\omega$  values, the *experimental* reduced vapor pressures at  $T_r = 0.7$  was determined from the definition of the acentric factor:  $P_r^{\text{sat}}(T_r = 0.7) = 10^{-\omega-1}$ . Once done, the  $m$  value enabling to reproduce exactly this latter quantity is determined. This procedure is possible, i.e., does not require to specify values of  $T_c$  and  $P_c$  because generalized CEoS obey the 3-parameter corresponding states theorem which stipulates that the calculated values of  $P_r^{\text{sat}}$  only depend on  $T_r$  and  $m$ . Finally, the  $m$  values were correlated with respect to  $\omega$  using a third-order polynomial expression:

$$m(\omega) = A + B\omega + C\omega^2 + D\omega^3 \quad (\text{PIV.23})$$

The accuracy of each EoS, i.e. of each  $(u, w)$  combination is assessed by evaluating the deviations between calculated and experimental vapor pressures ( $P^{\text{sat}}$ ), enthalpies of vaporization ( $\Delta_{\text{vap}}H$ ) and saturated molar liquid volumes ( $v_{\text{liq}}^{\text{sat}}$ ) for a huge number of pure components. Indeed, thanks to the DIPPR database, we were able to find 1721 compounds belonging to many different chemical families (hydrocarbons, halogenated, oxygenated, sulfur, nitrogen compounds, etc.) for which at least vapor pressure data could be accurately generated from a temperature-dependent correlation. More information about this database can be found in one of our previous papers [184]. This initial number of 1721 was reduced to 1525 because the behavior of 196 non-classical compounds could not be described properly by the 1-parameter Soave  $\alpha$ -function. They were removed to avoid introducing a bias in the results. We also know that a 1-parameter  $\alpha$ -function cannot catch simultaneously  $P^{\text{sat}}$ ,  $\Delta_{\text{vap}}H$  and liquid heat capacity ( $c_{P,\text{liq}}^{\text{sat}}$ ) data, explaining why this latter property was disregarded here. Table PIV.2 summarizes the available property data for the 1525 components considered in this study.

**Table PIV.2.** Available properties for the 1525 components that are used to determine the optimum values of  $u$  and  $w$ .

Property	Number of compounds
$P^{\text{sat}}$	1525
$\Delta_{\text{vap}}H$	1318
$v_{\text{liq}}^{\text{sat}}$	1300

For each property, the DIPPR correlations are used to generate 50 equidistant data points following the rules explained in [Appendix D2](#). In the end, for each  $(u, w)$  combination, a kind of "global mean percent error (GMPE) per property" expressed through Eqs. (PIV.24) and (PIV.25) for the untranslated and translated EoS, respectively, are calculated:

$$GMPE_{untranslated} = \frac{2 \cdot \overline{MAPE} P^{sat} + \overline{MAPE} \Delta_{vap} H + \overline{MAPE} v_{liq}^{sat}}{4} \quad (PIV.24)$$

$$GMPE_{translated} = \frac{\overline{MAPE} P^{sat} + \overline{MAPE} \Delta_{vap} H + \overline{MAPE} v_{liq}^{sat}}{3} \quad (PIV.25)$$

where:

$$\overline{MAPE} P^{sat} = \frac{\sum_{j=1}^{NC^{P^{sat}}} MAPE_j P^{sat}}{NC^{P^{sat}}} \quad (PIV.26)$$

$$\overline{MAPE} \Delta_{vap} H = \frac{\sum_{j=1}^{NC^{\Delta_{vap} H}} MAPE_j \Delta_{vap} H}{NC^{\Delta_{vap} H}} \quad (PIV.27)$$

$$\overline{MAPE} v_{liq}^{sat} = \frac{\sum_{j=1}^{NC^{v_{liq}^{sat}}} MAPE_j v_{liq}^{sat}}{NC^{v_{liq}^{sat}}} \quad (PIV.28)$$

$NC^{P^{sat}}$ ,  $NC^{\Delta_{vap} H}$  and  $NC^{v_{liq}^{sat}}$  are given in [Table PIV.2](#). These are the number of components for which experimental  $P^{sat}$ ,  $\Delta_{vap} H$  and  $v_{liq}^{sat}$  could be extracted from the DIPPR database. The  $MAPE_j$  on a given property for a component  $j$  is calculated as:

$$MAPE_j prop = \frac{100}{50} \sum_{i=1}^{50} \left| \frac{prop^{DIPPR}(T_i^{prop}) - prop^{CEoS}(T_i^{prop})}{prop^{DIPPR}(T_i^{prop})} \right| \quad (PIV.29)$$

In Eq. (PIV.24), the MAPE on  $P^{sat}$  is counted twice in order to balance the MAPE on  $v_{liq}^{sat}$  which is often high with untranslated CEoS.

#### PIV.IV.II Optimal $(u, w)$ values for untranslated CEoS

The results obtained for all the tested  $(u, w)$  combinations (more than 50,000 with a variation step equal to 0.05) are visible in [Figure PIV.5](#). The  $(u, w)$  pair leading to the smallest value of  $GMPE_{untranslated}$  (Eq. (PIV.24)) is:

$$\begin{cases} u_{opt} = 2.10 \\ w_{opt} = -0.75 \end{cases} \quad (PIV.30)$$

It is however possible to define in [Figure PIV.5](#) a small region of  $(u, w)$  parameters for which the difference between the values of the parameters is not significant in terms of  $GMPE_{untranslated}$  value. In other words, such parameters lead to equivalent minima for the  $GMPE_{untranslated}$  value defined in Eq. [\(PIV.24\)](#). Such a region is characterized by:

$$u \in [1.95, 2.20] \text{ and } w_{opt} = -1.89u + 3.22 \quad (\text{PIV.31})$$

It is noticeable that the PR EoS is quite close to this zone (see [Figure PIV.5](#)). On the other hand, the VdW and RK EoS, as expected, yield to higher values of  $GMPE_{untranslated}$  due to the limitations to reproduce liquid molar volumes. This is particularly true for the VdW EoS and to a lesser extent for the SRK EoS.

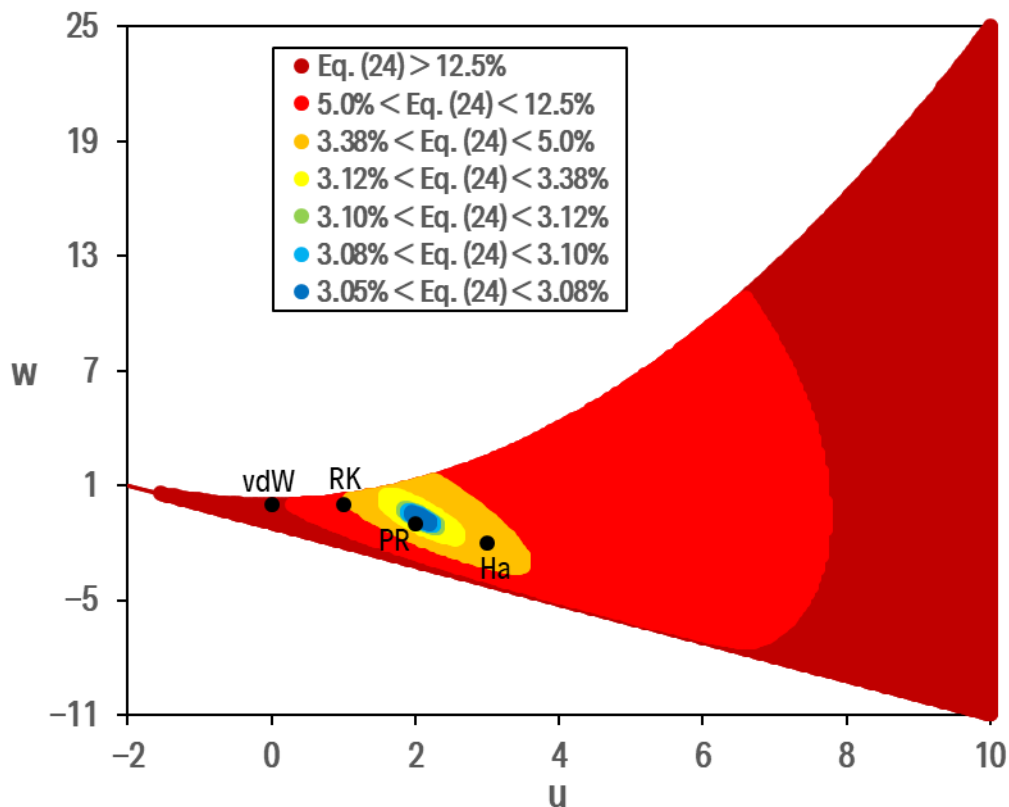


**Figure PIV.5.** Values of the *global mean percentage error per property* (see Eq. [\(PIV.24\)](#)) as a function of the parameters  $u$  and  $w$  for untranslated CEoS.

For a better comparison, [Table PIV.3](#) shows the MAPE on  $P^{sat}$ ,  $\Delta_{vap}H$  and  $v_{liq}^{sat}$  obtained with the VdW, SRK, PR and the optimized untranslated EoS characterized by  $u = 2.10$  and  $w = -0.75$ . All EoS use the Soave  $\alpha$ -function. It is noticeable that the optimized EoS developed in this work makes it possible to gain 1% of accuracy on the prediction of liquid molar volumes in comparison with the PR EoS which was until now the most accurate untranslated CEoS for  $v_{liq}^{sat}$ .

**Table PIV.3.** Comparison of the main untranslated CEoS (VdW, SRK, PR) with the optimized untranslated CEoS developed in this work. Note that all EoS are combined with a Soave-type  $\alpha$ -function.

EoS	$u$	$w$	GMPE <sub>untranslated</sub> (Eq. (PIV.24))	MAPE on $P^{sat}$ (1525 fluids)	MAPE on $\Delta_{vap}H$ (1318 fluids)	MAPE on $v_{liq}^{sat}$ (1300 fluids) ( $T_r < 0.9$ )
VdW	0	0	17%	2.0%	2.7%	60%
SRK	1	0	6.1%	1.8%	2.6%	18%
PR	2	-1	3.3%	1.5%	2.6%	7.6%
<b>This work</b>	<b>2.10</b>	<b>-0.75</b>	<b>3.1%</b>	<b>1.5%</b>	<b>2.5%</b>	<b>6.7%</b>

**Remark:** in this study the CEoS are parameterized classically, i.e. in order to exactly get:  $P^{sat,EoS}(T_{c,exp}) = P_{c,exp}$ . It is however well-known that by constraining a CEoS to pass through the experimental critical coordinates, the compressibility of saturated liquids cannot be represented correctly [69]. The unique solution to get a better accuracy would be to fit the three pure-component parameters (let us say  $b$ ,  $a_c$  and  $m_{Soave}$ ) of a given CEoS to saturated liquid densities and vapor pressures as is conventionally done with SAFT-type EoS. In addition, as explained by Polishuk [257–259], incorrect compressibility values may lead to higher deviations on density data at very high pressures (much higher deviations than those reported in Table PIV.3 for the saturated liquid).

#### PIV.IV.III Optimal $(u, w)$ values for translated CEoS

It is recalled that the volume correction was determined in order to exactly reproduce the liquid molar volume at  $T_r = 0.8$ , for each pure component. The results obtained for all the tested  $(u, w)$  pairs are shown in Figure PIV.6. It is noticeable that they differ notably from those obtained for untranslated CEoS. In the present case, there is not a unique  $(u, w)$  combination leading to a minimum (or a specified) value of Eq. (PIV.25) but instead a valley of  $(u, w)$  combinations all located along a second-order polynomial line. As an example, in Figure PIV.6, the  $(u, w)$  pairs that minimize the  $GMPE_{translated}$  quantity defined by Eq.(PIV.25) are identified by a dark blue line the equation of which is:

$$w_{opt} = 0.14u_{opt}^2 - 0.47u_{opt} - 0.47 \quad (\text{PIV.32})$$

The following couples of parameters:  $\begin{cases} u = 0 \\ w = -0.47 \end{cases}$ ,  $\begin{cases} u = 1 \\ w = -0.80 \end{cases}$ ,  $\begin{cases} u = 2 \\ w = -0.85 \end{cases}$  or  $\begin{cases} u = 3 \\ w = -0.62 \end{cases}$  are thus equivalent and all minimize Eq. (PIV.25).

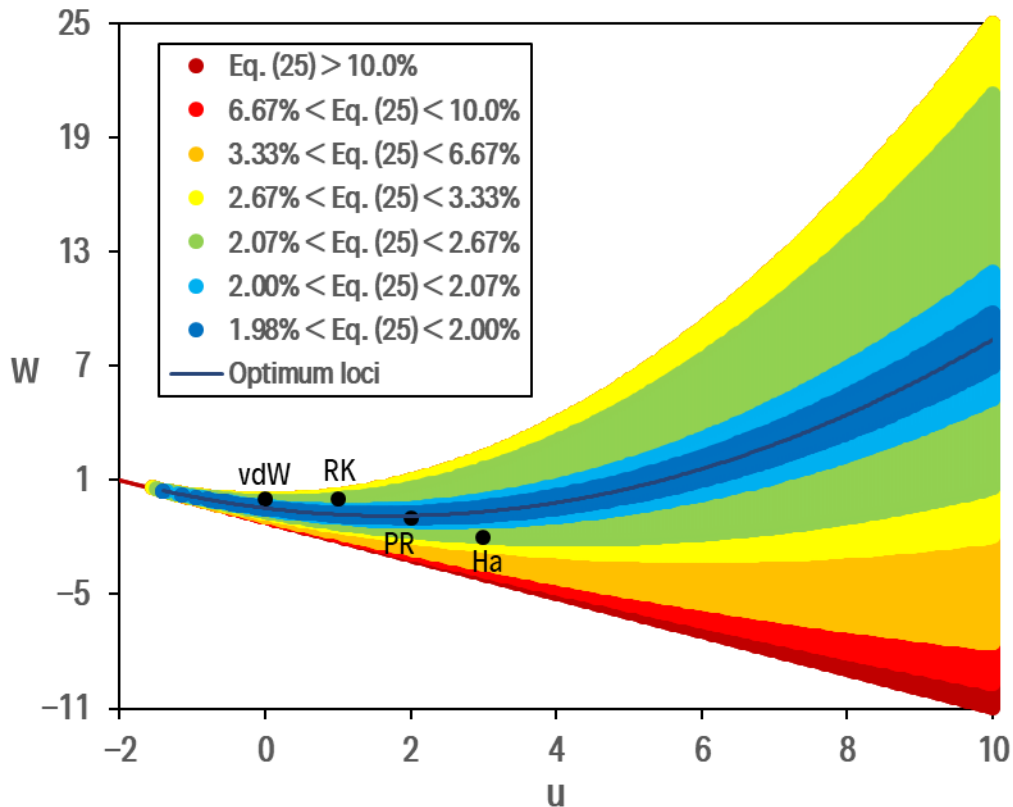


**Figure PIV.6.** Values of the *global mean percentage error per property* (see Eq. (PIV.25)) as a function of the parameters  $u$  and  $w$  for translated CEoS.

By superimposing Figure PIV.5 and Figure PIV.6, it is noticeable that the locus of optimal values drawn in Figure PIV.6 overlaps the small region in Figure PIV.5 that minimizes Eq. (PIV.24). By selecting an  $(u, w)$  pair in this overlapping zone, we get simultaneously the most accurate untranslated and translated CEoS. The  $u$  and  $w$  values satisfying simultaneously Eq. (PIV.31) and Eq. (PIV.32) are:

$$\begin{cases} u_{opt} = 2.16 \\ w_{opt} = -0.86 \end{cases} \quad (\text{PIV.33})$$

In the rest of the paper, the translated CEoS using the  $(u, w)$  values reported in Eq. (PIV.33) is called the  $t$ -OptiM EoS. Table PIV.4 shows the MAPE on  $P^{sat}$ ,  $\Delta_{vap}H$  and  $v_{liq}^{sat}$  obtained with the  $t$ -VdW,  $t$ -SRK,  $t$ -PR and the  $t$ -OptiM EoS. All EoS use the Soave  $\alpha$ -function. Since a volume translation does not change the phase equilibrium conditions [92,132,183], the MAPEs on  $P^{sat}$ , and  $\Delta_{vap}H$  reported in Table PIV.4 are strictly the same as those given in Table PIV.3. Only the deviations on  $v_{liq}^{sat}$  are modified.

The comparison of Table PIV.3 and Table PIV.4 highlights the colossal positive impact of a volume translation. As an example, the MAPE on  $v_{liq}^{sat}$  are reduced from 60% to 4% for the VdW EoS. Similarly, they are reduced from 18 to 3.5% for the SRK EoS. Both the  $t$ -PR and the  $t$ -OptiM EoS show deviations on  $v_{liq}^{sat}$  that are as low as 2%. Such a table makes it also possible to conclude that by selecting  $(u = 2 ; w = -1)$ , Peng and Robinson made a very good choice. This couple of values is indeed extremely

close to the optimal one so that the  $t$ -PR EoS is certainly the most accurate CEoS today available. As a direct consequence, there is only a minor difference between the  $t$ -PR and  $t$ -OptiM EoS in [Table PIV.4](#). The  $t$ -SRK and  $t$ -VdW EoS lie outside but near the region of optimal parameters [see [Figure PIV.6](#) and Eq. ([PIV.32](#))].

**Table PIV.4.** Comparison of the main translated CEoS ( $t$ -VdW,  $t$ -SRK,  $t$ -PR) with the optimized translated CEoS developed in this work and called  $t$ -OptiM. All EoS use a Soave-type  $\alpha$ -function.

EoS	$u$	$w$	GMPE <sub>translated</sub> (Eq. ( <a href="#">PIV.25</a> ))	MAPE on $P^{sat}$ (1525 fluids)	MAPE on $\Delta_{vap}H$ (1318 fluids)	MAPE on $v_{liq}^{sat}$ (1300 fluids) ( $T_r < 0.9$ )
$t$ -VdW	0	0	2.9%	2.0%	2.7%	4.1%
$t$ -SRK	1	0	2.6%	1.8%	2.6%	3.5%
$t$ -PR	2	-1	2.0%	1.5%	2.6%	1.9%
<b><math>t</math>-OptiM</b>	<b>2.16</b>	<b>-0.86</b>	<b>2.0%</b>	<b>1.5%</b>	<b>2.5%</b>	<b>1.9%</b>

#### PIV.IV.IV Optimal translated and consistent CEoS

As stated in the introduction, the second-order polynomial volume function ( $v^2 + ubv + wb^2$ ) has a strong influence on the calculated volumetric properties whereas the  $\alpha$ -function has a strong influence on the calculated VLE properties like  $P^{sat}$ ,  $\Delta_{vap}H$  and  $c_{P,liq}^{sat}$ . It was thus decided to couple the optimized ( $u, w$ ) parameters determined in this study ( $u_{opt} = 2.16$ ,  $w_{opt} = -0.86$ ) with the highly flexible 3-parameter  $\alpha$ -function proposed by Twu in 1991 [[216](#)]:

$$\alpha(T_r) = T_r^{N(M-1)} \exp\left[L(1 - T_r^{MN})\right] \quad (\text{PIV.34})$$

This association should enable to define the most accurate CEoS ever published. In this study, the three  $L, M, N$  parameters were determined for the 1721 pure components recommended by Piña-Martinez et al. [[184](#)] following the fitting procedure these authors advised to implement. In order to guarantee safe property predictions in both subcritical and supercritical domains, the parameters were fit to experimental data in order that the resulting  $\alpha$ -function obeys the following list of constraints:

$$\alpha(T_c) = 1 \text{ and for all } T: \begin{cases} \alpha \geq 0 & \text{and } \alpha(T_r) \text{ continuous} \\ \frac{d\alpha}{dT_r} \leq 0 & \text{and } \frac{d\alpha}{dT_r} \text{ continuous} \\ \frac{d^2\alpha}{dT_r^2} \geq 0 & \text{and } \frac{d^2\alpha}{dT_r^2} \text{ continuous} \\ \frac{d^3\alpha}{dT_r^3} \leq 0 \end{cases} \quad (\text{PIV.35})$$

An  $\alpha$ -function that fulfills all of the conditions reported in Eq. ([PIV.35](#)) can be considered as *consistent* (according to Le Guennec et al. [[185,198,199](#)]). In addition to the  $t$ -OptiM CEoS, and for possible comparison with well-acknowledged CEoS, such a procedure was also applied to the  $t$ -PR,  $t$ -RK and  $t$ -

VdW thus defining the *tc*-OptiM, *tc*-PR, *tc*-RK and *tc*-VdW CEoS. Here *tc* stands for *translated* and *consistent* to state that the CEoS is used both with a volume translation and the consistent version of the Twu 91  $\alpha$ -function. It is worth including the Schmidt and Wenzel (SW) EoS in the comparison, i.e., to set  $u$  and  $w$  as a function of the acentric factor in order to see the potential advantage of such a procedure. The comparison of all these *translated-consistent* models is presented in Table PIV.5 from which it is possible to highlight that all the *tc*-CEoS give similar and very small deviations on  $P^{sat}$ ,  $\Delta_{vap}H$  and  $c_{P,liq}^{sat}$  thus demonstrating the benefit of using the 3-parameter Twu 91  $\alpha$ -function.

**Table PIV.5.** Comparison of the most famous *translated-consistent* CEoS (*tc*-VdW, *tc*-RK, *tc*-PR, *tc*-SW) with the optimized one developed in this work and called *tc*-OptiM. All EoS are combined with the Twu 91  $\alpha$ -function.

EoS	MAPE on $P^{sat}$ (1721 fluids)	MAPE on $\Delta_{vap}H$ (1453 fluids)	MAPE on $c_{P,liq}^{sat}$ (829 fluids)	MAPE on $v_{liq}^{sat}$ (1489 fluids) ( $T_r < 0.9$ )	MAPE on $v_c$ (1489 fluids)	Untranslated	
						MAPE on $v_{liq}^{sat}$ (1489 fluids) ( $T_r < 0.9$ )	MAPE on $v_c$ (1489 fluids)
<i>tc</i> -VdW	1.2%	2.0%	2.2%	4.2%	25%	60%	48%
<i>tc</i> -RK	1.2%	1.9%	2.2%	3.7%	24%	19%	31%
<i>tc</i> -PR	1.0%	1.9%	2.0%	2.2%	20%	8.5%	21%
<i>tc</i> -SW	0.9%	1.9%	1.9%	2.9%	18%	7.6%	19%
<b><i>tc</i>-OptiM</b>	<b>1.0%</b>	<b>1.9%</b>	<b>2.0%</b>	<b>2.2%</b>	20%	7.6%	20%

Without getting into the details, the error on  $P^{sat}$  is 1% whereas the errors on  $\Delta_{vap}H$  and  $c_{P,liq}^{sat}$  are both 2%. For  $v_{liq}^{sat}$  data, it is not surprising to find back in Table PIV.5 the deviations previously obtained with the *t*-CEoS (see Table PIV.4) since the  $\alpha$ -function has a minor impact on the calculation of liquid densities. In Table PIV.5, the deviations on  $v_{liq}^{sat}$  are however slightly higher than those reported in Table PIV.4 because the number of compounds was significantly increased. It is thus not surprising to see that the *tc*-PR and the *tc*-OptiM EoS give similar deviations on  $v_{liq}^{sat}$  that are also the smallest ones (about 2%). It was indeed concluded in the previous section that the values of  $u$  and  $w$  selected by Peng and Robinson were very close to the optimal ( $u_{opt}$ ,  $w_{opt}$ ) values determined in this study.

The *translated-consistent* form of the SW EoS cannot achieve the same results for  $v_{liq}^{sat}$  as *tc*-PR and *tc*-OptiM (but performs better than *tc*-RK or *tc*-VdW). This confirms our previous conclusions that it is not relevant to select component-dependent ( $u$ ,  $w$ ) parameters and to simultaneously translate the EoS.

The VdW EoS, with the introduction of an efficient temperature-dependence of the attractive term, can reproduce vapor pressure data of 1721 pure fluids, both polar and non-polar, with a deviation of 1.2%. At the same time, the enthalpies of vaporization and liquid heat capacities are correlated with a deviation of about 2%. With the introduction of a constant volume correction, the VdW EoS can reproduce liquid densities with a deviation close to 4% (such deviations reach no less than 60% without volume correction!). Contrary to a priori beliefs, the *tc*-VdW EoS is thus accurate enough to be used for process

design and simulation purposes. These conclusions totally agree with the previous findings of Soave [82] and Tassios [260–263] who brilliantly explained how the VdW EoS could be improved.

## PIV.V Conclusion

In this work, we studied how the  $u$  and  $w$  parameters [involved in the volume function of the attractive term in cubic equations of state ( $v^2 + ubv + wb^2$ )] influence the accuracy of the description of saturated-liquid molar volume data. We concluded that:

As already reported [254], the ability for a CEoS to predict vapor pressure and vapor-liquid equilibrium (VLE) data requires the selection of an appropriate  $\alpha$ -function while the accuracy of the predicted volumetric properties is governed by the volume function of the attractive term.

- The unique solution to predict accurate volumetric properties is to make  $u$  and  $w$  component-dependent.
- The volume translation technique is certainly the best option to make  $u$  and  $w$  component-dependent. Such a technique indeed avoids the development of a correlation between ( $u$ ,  $w$ ) and  $\omega$ . Moreover, its application is straightforward.
- When cubic EoS are translated,  $u$  and  $w$  must be independent. There is indeed no benefit to select  $\omega$ -dependent ( $u$ ,  $w$ ) pairs and to simultaneously translate the EoS.
- The empirical relationships between  $u$  and  $w$  proposed in the open literature:  $u + w = 1$  or  $u - w = 4$  were not deemed as optimal to get the smallest deviations over liquid densities.
- Selecting  $u = 2.16$  and  $-0.86$ , the most accurate untranslated and translated CEoS are simultaneously obtained. By coupling such parameters with (i) a temperature-independent volume translation in order to exactly reproduce the liquid molar volume at  $T_r = 0.8$  and (ii) the highly-flexible Twu 91  $\alpha$ -function, we were able to propose the most accurate CEoS ever published. It was named *tc-OptiM* and is able to correlate the vapor pressures with an error of 1% whereas errors on  $\Delta_{vap}H$ ,  $c_{P,liq}^{sat}$  and  $v_{liq}^{sat}$  are close to 2%.

Results obtained with the *tc-OptiM* EoS are however only slightly better than those obtained with the *tc-PR* [185] CEoS. This is because the values of  $u$  and  $w$  associated with the Peng-Robinson EoS are very close to the optimal ( $u_{opt}$ ,  $w_{opt}$ ) values determined in this study.

- The *tc-VdW* EoS (i.e. the *translated-VdW* EoS coupled with the Twu 91  $\alpha$ -function) is accurate enough to be used for process design and simulation purposes.

From now on, our plans are to extend the *tc-PR* (or *tc-OptiM*) to mixtures by using, e.g., advanced mixing rules like those involved in the *E-PPR78* model [175].



# Publication V : Use of 300 000 experimental data over 1800 pure fluids to assess the performance of 4 CEoS: SRK, PR, *tc*-RK, *tc*-PR.

Andrés Piña-Martínez<sup>1</sup>, Romain Privat<sup>1(\*)</sup>, Jean-Noël Jaubert<sup>1(\*)</sup>

<sup>(1)</sup> Université de Lorraine, École Nationale Supérieure des Industries Chimiques, Laboratoire Réactions et Génie des Procédés (UMR CNRS 7274), 1 rue Grandville, 54000, Nancy, France

## Abstract

The guidelines to constitute a database containing, for 1 800 pure fluids, more than 300 000 pseudo-experimental vapor pressure, liquid density, enthalpy of vaporization and liquid heat capacity data are described. Such a database arises as a tool for fair assessment of performances of pure-component equations of state. In this paper, it is used to assess the performance of four cubic equations of state (CEoS): original Soave-Redlich-Kwong (SRK), original Peng-Robinson (PR) and the *translated-consistent* versions of PR (*tc*-PR) and RK (*tc*-RK).

The deviations between calculated and experimental data are compared for the four CEoS and make it possible to discuss the influence of the  $\alpha$ -function on the calculated vapor-liquid equilibrium properties and how the volume translation impacts the calculated volumetric properties. Eventually, the 1 800 pure components are divided into 1 252 non-self-associating and 548 self-associating compounds and the accuracy of the CEoS depending on the associating character of the molecules is discussed.



## PV.I Introduction

Since the appearance of the first process flowsheet simulators, different physical-property databanks as well as many thermodynamic models have been incorporated in their brochures. Developers often claim that their models perform well in this or that region, can be reliably extrapolated, and are suitable for certain systems or applications. However, it is difficult to have a fair overview of the capabilities and limitations of a given thermodynamic model. Thus, it would be pertinent to define a common basis for comparison. At this stage, the following questions appear: which type of data are available for many fluids? Which type of properties are considered as essential? How could a thermodynamic model be evaluated quantitatively?

These questions have been addressed by Jaubert et al. [130] in their work on the development of a high-quality reference database containing binary-system data for the cross-comparison of thermodynamic models and the assessment of their accuracies. With such a database, it is possible to determine how well a thermodynamic model predicts the behavior of binary mixtures according to the associating character of their components. Moreover, it could be used to assess the impact of mixing-rules selection and the number of parameters included within. Models such as the Peng-Robinson (PR) EoS armed with classical mixing rules and temperature-dependent binary interaction parameters (BIPs), as well as the PC-SAFT EoS with classical mixing rules, no induced association scheme and no regressed BIPs have been graded following the proposed procedure, recently [130,131].

Nevertheless, as stated by Agarwal et al. [264,265], no matter how sophisticated the thermodynamic model may be or the number of parameters the mixture model may have, if the model is not even capable to represent accurately the behavior of the pure fluids contained in the mixture, there is no way to think about accurate and reliable mixture calculations. As a convincing illustration, the reader is referred to Fig. 3 in Agarwal et al. [265].

Keeping this in mind, it seems pertinent to assess the accuracy of a thermodynamic model for pure fluids prior to its extension to mixtures. Therefore, a standard basis of comparison is required. This is the reason for which one of the primary motivations of this work is to serve as a reference for the objective assessment of the performances of thermodynamic models for pure fluids. To reach this objective, this work presents the guidelines that were used for constituting a reference database from the one proposed by the Design Institute for Physical Properties (DIPPR). This latter contains experimental vapor pressure, liquid density, enthalpy-of-vaporization, liquid heat-capacity, as well as critical temperature, pressure and volume data for 1 800 pure fluids. It is believed that such a database, that contains more than 300 000 experimental data points, is the perfect tool to identify the strengths and weaknesses of a given thermodynamic model for pure compounds.

Additionally, the deviations between calculated and experimental data are determined for the > 300 000 data points available in the proposed database for the original Soave-Redlich-Kwong (SRK) [266], original Peng-Robinson (PR) [103], *tc*-RK and *tc*-PR EoS [94] in order to assess their accuracies.

This paper is organized into two sections. In the first one, a detailed description of how the database was built is presented. This includes the choice of key properties, molecules and temperature ranges resulting

---

in more than 300 000 data points that will be used to assess the accuracy of any thermodynamic model for pure components. In the following section, the four CEoS benchmarked in this study are briefly introduced. Their capacity to reproduce experimental data is discussed then. Because it is often said that associating molecules cannot be properly modeled from EoS that are not based on a theory accounting specifically on association bonding, the discussion is oriented toward the relation between the associating character of the studied molecules and the capacity of EoS to model their behavior.

## **PV.II Description of the guidelines to constitute a pure-component reference database**

The objective of this section is to explain our scientific approach and answer the following questions:

- 1) How the existing commercial databases could help to reach our objective (i.e., to define a reference database for evaluating the performance of pure-component thermodynamic models)?
- 2) What is the minimum list of available pure-species properties to be included in the reference database?
- 3) How many molecules should (and could) be included in the pure-component reference database?
- 4) How to define the temperature ranges among which deviations should be calculated?

### **PV.II.I Existing pure-fluid databases**

Concerning pure-fluid experimental data, three databases arise as the most used by researchers working in the chemical engineering thermodynamics field. The first of them is the Design Institute for Physical Properties database (hereafter called using the “DIPPR” acronym), which contains recommended values and accuracy estimates for 34 constant properties and 15 temperature-dependent properties spanning 2 230 compounds. Another database is the Dortmund Data Bank (DDB - <http://www.ddbst.com/ddb.html>), which stores the worldwide largest amount of data for thermophysical properties of pure components and their mixtures. The third one is the ThermoDataEngine (TDE) database of the National Institute of Standards and Technology (NIST), which provides experimental data for nearly 24 000 pure fluids and includes several methods for the evaluation of the uncertainty and thermodynamic consistency of such data.

Since trustful data are contained in the aforementioned databases, any of them may be extremely useful for the definition of model comparison guidelines. Nevertheless, it is worth noting that an important feature of the DIPPR is that, apart from the experimental data points of the 15 temperature-dependent (T-dependent) properties, it proposes a fitting equation used for correlating T-dependent property data, reports the corresponding coefficients and provides an evaluation of the mean error between predictions from the fitting equation and raw data. This enables the generation of pseudo-experimental data evenly distributed over wide ranges of temperature what is desirable for the calculation of property deviations. Considering these features, the 12.3.0 version (May 2020) of the DIPPR database is used in this work as the starting point to build a reference database aimed at assessing the accuracy of EoS for pure fluids.

## PV.II.II Key properties

The definition of key properties imposes a first criterion on the selection of the molecules that should be included in the assessment of a given thermodynamic model. The choice of such properties is based on an overview of the industrial needs but must also include the properties required to parameterize the EoS.

First of all, as stated by Agarwal et al. [265], vapor pressure ( $P^{sat}$ ) cannot be overlooked. Indeed, *regardless of the sophistication of your thermodynamic model and the number of parameters in the mixing rule, you are in trouble if the vapor pressures are inaccurate.* Such a property that defines the endpoints of isothermal ( $P,x,y$ ) phase diagrams is thus of vital importance in the industry and, as shown recently, is mandatory for reliable parameterizations of cubic and SAFT-type EoS [267,268].

The prediction of volumetric properties such as liquid density ( $\rho_{liq}^{sat}$ ) is very important for the proper design of pipelines, pumps or even heat exchangers. Additionally, Ramirez-Velez et al. [268] found that parameterization of SAFT-type EoS can be performed reliably only if both liquid density and vapor pressure data are used. In the case of volume-translated CEoS, it is necessary to have at least one experimental density data point at reduced temperature between 0.7 to 0.8 to properly determine the volume-translation parameter.

Properties such as enthalpies of vaporization ( $\Delta_{vap}H$ ) and liquid heat capacities ( $c_{P,liq}^{sat}$ ) are key for the construction of energy balances. Inaccurate values of such properties may lead to unreliable designs of heat exchangers, expanders or compressors, for instance. Finally, the reproduction of pure-component critical properties (especially  $T_c$ ,  $P_c$  and to a lesser extent  $v_c$ ) is essential for an accurate representation of binary critical lines [269] (made up of binary critical points).

The ideal scenario would be to assess model performances considering molecules for which all the properties of interest ( $P^{sat}$ ,  $\rho_{liq}^{sat}$ ,  $\Delta_{vap}H$  and  $c_{P,liq}^{sat}$ ) were available. Nevertheless, due to a lack of experimental data such a choice would drastically limit the number of pure components that could be embedded in the *pure-component* reference database we plan to build. In consequence, it is necessary to define the indispensable properties that should be available for any molecule included in the proposed database. Such properties are vapor pressure and liquid density; the reasons of this choice are:

- 1) Satisfactory accuracy on the reproduction of  $P^{sat}$  and  $\rho_{liq}^{sat}$  is the minimum requirement for industry and Computer-Aided Product Design (CAPD) developers.

In the case of CEoS, to make an  $\alpha$ -function consistent, the corresponding parameters must be fitted to  $P^{sat}$  data, at least [267]. Moreover, if the volume-translation concept is applied, at least one data point of the  $\rho_{liq}^{sat}(T)$  curve is required.

In the case of SAFT-type EoS, Ramirez-Velez et al. [268] concluded that it is necessary and sufficient to fit EoS PC-SAFT parameters to both  $P^{sat}$  and  $\rho_{liq}^{sat}$  data.

In summary, molecules included in the database should have accurate data for  $P^{sat}$  and  $\rho_{liq}^{sat}$ ; when available,  $\Delta_{vap}H$  and  $c_{P,liq}^{sat}$  must be included.

**Note:** It is worth noting that EoS only predict residual properties. Consequently, for estimating liquid heat capacity, it is necessary to add an ideal-gas heat capacity term ( $c_{P,IG}$ ) to the residual heat capacity. Therefore, an accurate correlation for the  $c_{P,IG}(T)$  function is also needed when accurate  $c_{P,liq}^{sat}$  data are available.

### PV.II.III Assessment of correlations' accuracy

At this point, it has been stated which experimental properties should be available in order to incorporate a pure component in the proposed database. However, even if temperature-dependent correlations are available in the DIPPR database, it is necessary to guarantee their reliability. This is a key issue since, as Agarwal et al. [265] wrote: *one of the most heartbreaking experiences for a thermodynamicist is to watch someone spending a large effort refining a model with far more precision than the basic data allows.*

#### **Presentation of the three types of errors**

In order to evaluate if for a given molecule this or that property correlation is accurate, a strategy inspired by the work of Piña-Martinez et al. [267] has been followed. For each correlation three types of error were defined:

- **Type I error:** error reported in the DIPPR. Such an error is set by the DIPPR developers to the maximum uncertainty among the data series used to determine the coefficients of a correlation.
- **Type II error:** actual average uncertainty. Such an average error (not reported in the DIPPR database) is calculated from the knowledge of the uncertainty associated to each data series that was used to determine the coefficients of a correlation. For a given property and a given pure fluid, it is determined as:

$$Type\ II\ error = \frac{\sum_{j=1}^{n_{series}} N_{data,j} \times Error_j}{\sum_{j=1}^{n_{series}} N_{data,j}} \quad (PV.1)$$

where  $N_{data,j}$  is the number of experimental data points available in the series  $j$  and  $Error_j$  the corresponding experimental error (as reported in the DIPPR database).

- **Type III error:** mean absolute percentage error over 50 points between pseudo-experimental data (generated by a DIPPR correlation) and calculated values returned by the *generalized* version of the *tc*-PR model (the acronym of which is *gen-tc*-PR). It is evaluated according to Eq. (PV.2):

$$Type\ III\ error = \frac{100}{N_T} \sum_{i=1}^{N_T} \left| \frac{X_{i,exp} - X_{i,calc}}{X_{i,exp}} \right| \quad (PV.2)$$

$X_{i,\text{exp}}$  and  $X_{i,\text{calc}}$  correspond to the pseudo-experimental and calculated values of the property  $X$ . In the present study,  $N_T = 50$  (the 50 points are evenly distributed between  $T_{\min}$  and  $T_{\max}$  that define the temperature range in which the correlation is valid).

Type III error was introduced because from our experience with the DIPPR database, it is believed that type-I and type-II errors are often overestimated. Consequently, many correlations would be disregarded if only those for which type-I or type-II errors are lower than 5% would be kept. For this reason, but also to detect possibly typing errors in the coefficients of the correlations or in the reported uncertainties, our idea was to use a predictive EoS, whose accuracy has been attested on many components, to define a type-III error. In this study, an updated version of the predictive *gen-tc*-PR EoS (noted *gen-tc*-PR 2020 hereafter) was used. Such a model [94,267], which only requires the knowledge of  $T_{c,\text{exp}}$ ,  $P_{c,\text{exp}}$  and  $\omega_{\text{exp}}$  writes:

$$P(T, v) = \frac{RT}{(v+c)-b} - \frac{a_c \cdot \alpha(T_r)}{(v+c)(v+c+b)+b(v+c-b)} \quad \text{with:} \quad \left\{ \begin{array}{l} \alpha(T_r) = T_r^{2(M-1)} \exp\left[L(1-T_r^{2M})\right] \\ c = v_{\text{liq}}^{\text{sat},u-PR}(T_r = 0.8) - v_{\text{liq},\text{exp}}^{\text{sat}}(T_r = 0.8) \\ \eta_c = \left[1 + \sqrt[3]{4-2\sqrt{2}} + \sqrt[3]{4+2\sqrt{2}}\right]^{-1} \approx 0.25308 \\ a_c = \frac{40\eta_c + 8}{49 - 37\eta_c} \frac{R^2 T_{c,\text{exp}}^2}{P_{c,\text{exp}}} \approx 0.45724 \frac{R^2 T_{c,\text{exp}}^2}{P_{c,\text{exp}}} \\ b = \frac{\eta_c}{\eta_c + 3} \frac{RT_{c,\text{exp}}}{P_{c,\text{exp}}} \approx 0.07780 \frac{RT_{c,\text{exp}}}{P_{c,\text{exp}}} \end{array} \right. \quad (\text{PV.3})$$

The  $\omega$ -dependent correlations, updated in this work are:

$$\left\{ \begin{array}{l} L = 0.0544 + 0.7536\omega_{\text{exp}} + 0.0297\omega_{\text{exp}}^2 \\ M = 0.8678 - 0.1785\omega_{\text{exp}} + 0.1401\omega_{\text{exp}}^2 \end{array} \right. \quad (\text{PV.4})$$

In [Table PV.1](#), the mean absolute percentage error (MAPE) and the standard deviation (SD) obtained with the *gen-tc*-PR 2020 EoS over 1786 molecules are reported. Such values are important for the acceptance test presented hereafter.

**Table PV.1.** MAPE and SD obtained with the *generalized* version of the *tc*-PR model used for this work.

	Property X:			
	$P^{\text{sat}}$	$v_{\text{liq}}^{\text{sat}}$	$\Delta_{\text{vap}}H$	$C_{P,\text{liq}}^{\text{sat}}$
Number of molecules	1786	1786	1503	895
MAPE <sub>X</sub>	1.7%	2.1%	2.6%	4.8%
SD <sub>X</sub>	1.5%	1.3%	1.6%	4.3%

### Correlation acceptance tests

A correlation is declared as acceptable if it checks both tests described in this section.

**Test 1:** The type III error of a given property correlation  $X$  ( $X \in \{P^{sat}, \rho_{liq}^{sat}, \Delta_{vap}H, c_{P,liq}^{sat}\}$ ) is lower than the threshold of acceptance (noted  $TH_X$ ) defined as follows:

$$TH_X^{test1} = MAPE_X + 6SD_X \quad (PV.5)$$

where  $MAPE_X$  (for *Mean Average Percent Error*) and  $SD_X$  (*Standard Deviation*) of property  $X$  are obtained from [Table PV.1](#).

This test aims at detecting possibly typing errors in the coefficients of the correlations or in the values of uncertainties reported in the DIPPR database. It also aims at disregarding correlations that lead to totally non-expected values so that the properties of such a component cannot be correlated by a classical EoS (this usually happens for a few inorganic molecules). In Eq. (PV.5), it was decided to multiply  $SD_X$  by 6 because it is believed that such a value makes it possible to detect typing errors among the data, to exclude undesired molecules (like metals) but not to reject data that are poorly correlated by the *gen-tc-PR 2020* EoS. To be concrete, let us take an example. Table 1 reports that the average deviation on  $P^{sat}$ , calculated by the *gen-tc-PR 2020* EoS, is 1.7% (and  $SD_{P^{sat}} = 1.5\%$ ). If for a given molecule, the deviation between pseudo-experimental data stemming from a DIPPR correlation and such an EoS is higher than 10.7% ( $MAPE_{P^{sat}} + SD_{P^{sat}}$ ), such a correlation is rejected.

**Table PV.2.** Acceptance thresholds for the different property correlations and types of error.

Error type	Acceptance thresholds for each property				
	$P^{sat}$	$v_{liq}^{sat}$	$\Delta_{vap}H$	$c_{P,liq}^{sat}$	$c_{P,PG}$
Type I (error reported in the DIPPR database)	5%	5%	5%	5%	5%
Type II (average exp. Error calculated by Eq. (PV.1))	5%	5%	5%	5%	5%
Type III (deviation calculated with the gen. <i>tc-PR</i> EoS by Eq. (PV.2))	$TH_X^{test2} = MAPE_X + SD_X^{(*)}$				-%

(\*)  $MAPE_X$  and  $SD_X$  are obtained from [Table PV.1](#).

**Test 2:** At least one out of the three types of error is lower than or equal to its respective acceptance threshold. These values are reported in [Table PV.2](#).

Once again, to be concrete, let us take an example. If for a given molecule:

- 1) the error reported by the DIPPR for the correlation on  $P^{sat}$  is 6%, and
- 2) the average DIPPR average for the correlation on  $P^{sat}$  is 5.1%, and
- 3) the *gen-tc-PR 2020* EoS correlates the pseudo  $P^{sat}$  data with an accuracy of 2% (lower than  $MAPE_{P^{sat}} + SD_{P^{sat}}$ )

the correlation is declared acceptable.

#### PV.II.IV Molecules to be incorporated in the database

The DIPPR provides constant properties and a set of T-dependent correlations for **2 230 molecules**. Among these (see filter 2 below), only the ones having both key properties ( $P^{sat}$ ,  $\rho_{liq}^{sat}$ ) available were kept. In addition, all molecules requiring a specific treatment (see filter 1 below) were disregarded. Therefore, a molecule was declared as suitable if it remained after application of both filters described below.

**Filter 1:** A molecule is removed if:

- $T_c$  is greater than 2000 K. It is considered that such a molecule cannot be accurately represented by an EoS routinely used in process simulators and relying on a corresponding-states principle.
- It is banned by the DIPPR due to ambiguous data, self-accelerating decomposition or instability.
- It is a quantum fluid (e.g., hydrogen, helium ...).

After this filter, 47 molecules were removed and **2 183 remained**.

**Filter 2:** A molecule is removed if one correlation for  $P^{sat}(T)$  or  $\rho_{liq}^{sat}(T)$  is missing or does not pass the acceptance tests presented in [Section Correlation acceptance tests](#). After this filter, 383 molecules were removed and **1 800 remained**.

Note: after this last filter, 385 molecules should be removed actually. Among these molecules were n-dotriacontane and n-hexatriacontane that exhibit an inaccurate correlation for  $P^{sat}(T)$ . Since n-dotriacontane and n-hexatriacontane are included in the benchmark database for binary systems published by Jaubert et al. [\[130\]](#), it was decided not to remove them from the database.

#### PV.II.V Associating character

The thermodynamic behavior of molecules showing associating character, i.e., involved in a hydrogen bond, is considered by most of developers (and SAFT EoS authors in particular) as more complicated than that of non-associating molecules. Thus, capturing associating molecule behavior appears as a challenge. As a consequence, how a model performs with non-self-associating (NSA) and self-associating (SA) molecules gives a deeper insight of its performance. In the case of binary systems, a major feature of the database proposed by Jaubert et al. [\[130\]](#) is that it provides a binary system classification according to the associating character of their components, and, thus, it is possible to have a measure of the complexity of modelling the thermodynamic properties of mixtures depending on the nature and strength of the association phenomena involved in the system.

In this work, the associating character of each pure species was quantified following a methodology explained in [Appendix D1](#). In short, the screening charge density distribution (sigma profile) of each compound was generated and analyzed to determine its tendency to associate. For the 1 800 components involved in the proposed database, it results in **1 252** non-self-associating and **548** self-associating molecules.

## PV.II.VI Temperature ranges and deviations

For a given pure component  $j$  and a given property  $X$  ( $X \in \{P^{sat}, \rho_{liq}^{sat}, \Delta_{vap}H, c_{P,liq}^{sat}\}$ ), 50 equidistant pseudo-experimental data points are generated in their valid temperature range,  $[T_{min}, T_{max}]$ . The temperature ranges for each property are mentioned in the supporting information (see [Appendix D2](#)). Concerning deviations, the mean absolute percentage errors (MAPEs) are evaluated according to Eq. (PV.6) as the average of the absolute percentage deviations between experimental and calculated properties over  $N_T$  temperature points.

$$MAPE_X = \frac{100}{N_T} \sum_{i=1}^{N_T} \left| \frac{X_{j,exp}(T_i) - X_{j,calc}(T_i)}{X_{j,exp}(T_i)} \right| \quad (PV.6)$$

$X_{j,exp}(T_i)$  and  $X_{j,calc}(T_i)$  correspond to the calculated and experimental values of component  $j$ 's property  $X$ , at temperature  $T_i$ . In the present study,  $N_T = 50$ . It is worth noting that the first temperature ( $T_1$ ) and the last temperature ( $T_{50}$ ) of the range correspond exactly to  $T_{min}$  and  $T_{max}$ , respectively.

## PV.II.VII Guidelines summary and data points

The guidelines presented in this work lead to a database containing 1 800 molecules which have accurate correlations for  $P^{sat}$  and  $\rho_{liq}^{sat}$ . Among them, 1 536 fluids possess an accurate correlation for  $\Delta_{vap}H$  and 890 for  $c_{P,liq}^{sat}$ , resulting in a database containing 301 300 high-quality pseudo-experimental points. Moreover, critical properties ( $T_c$ ,  $P_c$  and  $v_c$ ) are available for the 1 800 molecules, which results in 5 400 additional data points. In total, the proposed database contains 306 700 pure-component data points for the assessment of thermodynamic models' performances. The name, the associating character (AC) and the critical properties ( $T_c$ ,  $P_c$  and  $v_c$ ) of each molecule along with the temperature range and the identification (ID) number assigned by the DIPPR to each property correlation are reported in [Appendix D3](#). In addition, [Table PV.3](#) gives a short overview of such a database.

**Table PV.3.** Overview of the data available in the proposed database.

Total number of pure-components: <b>1 800</b> (1 252 Non-self-associating + 548 Self-associating)						
Total number of experimental data points: 306 700						
Number of components for which the property is available:						
$P^{sat}$	$\rho_{liq}^{sat}$	$\Delta_{vap}H$	$c_{P,PG}$ and $c_{P,liq}^{sat}$	$T_c$	$P_c$	$v_c$
1 800	1 800	1 536 <sup>(*)</sup>	890 <sup>(**)</sup>	1 800	1 800	1 800
(90 000 data points)	(90 000 data points)	(76 800 data points)	(44 500 data points)	(1800 data points)	(1800 data points)	(1800 data points)

<sup>(\*)</sup> Among the 1 536 components, 1 114 are non-self-associating and 422 are self-associating.

<sup>(\*\*)</sup> Among the 890 components, 695 are non-self-associating and 195 are self-associating.

**Table PV.4.** Expressions of the SRK, PR, *tc*-RK and *tc*-PR EoS.

SRK	PR	<i>tc</i> -RK	<i>tc</i> -PR
$P(T, v) = \frac{RT}{v-b} - \frac{a_c \cdot \alpha(T)}{v(v+b)}$	$P(T, v) = \frac{RT}{v-b} - \frac{a_c \cdot \alpha(T)}{v(v+b) + b(v-b)}$	$P(T, v) = \frac{RT}{(v+c)-b} - \frac{a_c \cdot \alpha(T_r)}{(v+c)(v+c+b)}$	$P(T, v) = \frac{RT}{(v+c)-b} - \frac{a_c \cdot \alpha(T_r)}{(v+c)(v+c+b) + b(v+c-b)}$
<b><math>\alpha</math>-function</b>			
$\alpha(T_r) = \left[ 1 + m(1 - \sqrt{T_r}) \right]^2 \text{ with } T_r = T/T_c$		$\alpha(T_r) = T_r^{N(M-1)} \exp \left[ L(1 - T_r^{MN}) \right]$	
$m = 0.480 + 1.574\omega_{\text{exp}} - 0.176\omega_{\text{exp}}^2$	$m = 0.37464 + 1.54226\omega_{\text{exp}} - 0.26992\omega_{\text{exp}}^2$	(L, M, N are component-dependent and specific to each equation of state)	
<b>Volume-translation parameter</b>			
<i>Non-applicable</i>		$c = v_{\text{liq}}^{\text{sat}, u-EoS}(T_r = 0.8) - v_{\text{liq}, \text{exp}}^{\text{sat}}(T_r = 0.8)$ ( <i>c</i> is component-dependent and specific to each equation of state)	
<b>Attractive parameter at the critical temperature</b>			
$a_c = \Omega_a \frac{R^2 T_{c, \text{exp}}^2}{P_{c, \text{exp}}}$			
<b>Covolume</b>			
$b = \Omega_b \frac{RT_{c, \text{exp}}}{P_{c, \text{exp}}}$		$b = \Omega_b \frac{RT_{c, \text{exp}}}{P_{c, \text{exp}}} - c$	
$\Omega_a = \frac{1}{9(\sqrt[3]{2}-1)} \approx 0.42748$	$\Omega_a = \frac{8(5X+1)}{49-37X} \approx 0.45724$	$\Omega_a = \frac{1}{9(\sqrt[3]{2}-1)} \approx 0.42748$	$\Omega_a = \frac{8(5X+1)}{49-37X} \approx 0.45724$
$\Omega_b = \frac{\sqrt[3]{2}-1}{3} \approx 0.08664$	$\Omega_b = \frac{X}{X+3} \approx 0.07780$	$\Omega_b = \frac{\sqrt[3]{2}-1}{3} \approx 0.08664$	$\Omega_b = \frac{X}{X+3} \approx 0.07780$
	$X = \left[ 1 + \sqrt[3]{4-2\sqrt{2}} + \sqrt[3]{4+2\sqrt{2}} \right]^{-1} \approx 0.25308$		$X = \left[ 1 + \sqrt[3]{4-2\sqrt{2}} + \sqrt[3]{4+2\sqrt{2}} \right]^{-1} \approx 0.25308$



### PV.III Benchmark of the SRK, PR, *tc*-RK and *tc*-PR EoS

In this section, the performances of four CEoS are evaluated by assessing their accuracy over the 306 700 pseudo-experimental data points available in the reference database for pure compounds developed in this work.

#### PV.III.I Models

The first two CEoS are the well-known Soave-Redlich-Kwong (SRK) [266] and Peng-Robinson (PR) [103] EoS. The other two models are the *translated* [95,132] and *consistent* [270,271] versions of the RK (*tc*-RK) and PR (*tc*-PR) EoS [94]. The detailed expressions of the SRK, PR, *tc*-RK and *tc*-PR EoS are summarized in Table PV.4. It is worth recalling that for the *tc*-RK and *tc*-PR models, *translated* stands for the fact that the substance-dependent volume-translation parameter,  $c$ , was determined, component by component, in order the translated EoS exactly reproduces the experimental saturated liquid volume at a reduced temperature of 0.8, [ $v_{liq,exp}^{sat}(T_r = 0.8)$ ], that is:

$$c = v_{liq}^{sat,u-CEoS}(T_r = 0.8) - v_{liq,exp}^{sat}(T_r = 0.8) \quad (PV.7)$$

where  $v_{liq}^{sat,u-CEoS}(T_r = 0.8)$  is the molar volume calculated with the original (*untranslated*) CEoS at  $T_r = 0.8$ . In turn, *consistent* stands for the fact that such EoS are coupled with an  $\alpha$ -function that passes the consistency test developed by Le Guennec et al. [94,270,271] and therefore guarantees safe property predictions in both the subcritical and supercritical domains. Such a consistency test is expressed as a list of constraints recalled in Eq. (PV.8); any  $\alpha$ -function obeying these constraints is considered as consistent. This set of conditions has been called *consistency test for an  $\alpha$ -function* by analogy to the consistency tests developed to certify the quality of experimental binary VLE data.

$$\text{For any reduced temperature } (T_r): \left\{ \begin{array}{l} \alpha(T_r) \geq 0 \text{ and } \alpha \text{ continuous} \\ \frac{d\alpha(T_r)}{dT_r} \leq 0 \quad \text{and} \quad \frac{d\alpha}{dT_r} \text{ continuous} \\ \frac{d^2\alpha(T_r)}{dT_r^2} \geq 0 \quad \text{and} \quad \frac{d^2\alpha}{dT_r^2} \text{ continuous} \\ \frac{d^3\alpha(T_r)}{dT_r^3} \leq 0 \end{array} \right. \quad (PV.8)$$

As shown in Table PV.4, the *tc*-RK and *tc*-PR EoS are armed with the highly flexible 3-parameter  $\alpha$ -function proposed by Twu et al. in 1991 [272]:

$$\alpha(T_r) = T_r^{N(M-1)} \exp\left[L(1 - T_r^{MN})\right] \quad (PV.9)$$

For the 1 800 pure components available in the proposed database, the three  $L$ ,  $M$ ,  $N$  parameters were determined for both the *tc*-RK and *tc*-PR EoS following the fitting procedure that Piña-Martinez et al. [184] advised to implement. In short, the  $L$ ,  $M$ ,  $N$  parameters were determined in order to reproduce the best as possible  $P^{sat}$  (at least), and/or  $\Delta_{vap}H$  and/or  $c_{P,liq}^{sat}$  (if available) experimental data and to guarantee that the  $\alpha$ -function is *consistent*. Resulting parameters are reported in Appendix D4.

## PV.III.II Results and discussion

The MAPEs on  $\{P^{sat}, v_{liq}^{sat}, \Delta_{vap}H, c_{P,liq}^{sat}, v_c\}$ , as defined in Eq. (PV.6), are reported in Table PV.5 for the PR, SRK, *tc*-RK and *tc*-PR EoS. The detail of deviations for each molecule is reported in Appendix D5.

From the  $\alpha$ -function standpoint, it is possible to observe the huge and well-known impact of the choice of a generalized or component-dependent function. In the case of the PR EoS, when it is coupled with the Twu91  $\alpha$ -function (case of the *tc*-PR EoS) rather than with a Soave-type one (original PR EoS), MAPE on  $P^{sat}$  is divided by almost 3, MAPE on  $\Delta_{vap}H$  is 1% lower, and MAPE on  $c_{P,liq}^{sat}$  is almost divided by 3. Although the reductions are smaller, the same trends are observed for the RK EoS when coupled with a Soave-type or a Twu91  $\alpha$ -function. It is noticeable that the original SRK yields to quite better results on  $c_{P,liq}^{sat}$  than the original PR.

**Table PV.5.** MAPE on  $P^{sat}$ ,  $v_{liq}^{sat}$ ,  $\Delta_{vap}H$ ,  $c_{P,liq}^{sat}$ ,  $v_c$ ,  $T_c$  and  $P_c$  as predicted by the SRK, PR, *tc*-RK and *tc*-PR EoS.

EoS	MAPE on $P^{sat}$ (1800 fluids)	MAPE on $v_{liq}^{sat}$ (1800 fluids) ( $T_r < 0.9$ )	MAPE on $\Delta_{vap}H$ (1536 fluids)	MAPE on $c_{P,liq}^{sat}$ (890 fluids)	MAPE on $v_c$ (1800 fluids)	MAPE on $T_c$ & $P_c$ (*) (1800 fluids)	Global average deviation over the 306 700 available data points
SRK	2.3%	19%	3.0%	5.5%	31%	0%	8.0%
PR	2.8%	8.8%	3.1%	7.3%	21%	0%	5.4%
<i>tc</i> -RK	1.2%	3.5%	2.0%	2.7%	24%	0%	2.4%
<i>tc</i> -PR	1.0%	2.1%	1.9%	2.5%	20%	0%	1.9%

(\*) Such MAPEs are exactly zero since the 4 EoS are parameterized in order to exactly reproduce  $T_{c,exp}$  and  $P_{c,exp}$ .

Concerning the impact of the different volumetric functions included in the attractive term of the investigated CEoS, the SRK EoS leads to larger deviations (19%) on  $v_{liq}^{sat}$  than the PR EoS (8%). In turn, the impact of a volume translation is enormous since it is possible to observe a reduction from 19% (SRK) to 3.5% (*tc*-RK), and from 8.8% (PR) to 2.1% (*tc*-PR). It is worth recalling that, as a general trend, the SRK EoS predicts volumes that are much larger than the experimental ones. In turn, the volumes predicted by the PR EoS may be larger or smaller than the experimental ones depending on the studied fluid. In the latter case, negative values of the volume-translation parameter (*c*) are reported.

Table PV.5 makes it possible to conclude that the *tc*-PR EoS with an average overall deviation lower than 2% over the 306 700 available experimental data points is extremely accurate. It is probably not only the safest (the *consistent* character of the  $\alpha$ -function of such an EoS ensures safe property predictions in both subcritical and supercritical domains) but also the most accurate cubic EoS available.

**Associating character**

As previously mentioned, the 1 800 pure fluids are divided into two groups: those that are self-associating (SA) and those that are not (NSA). MAPE on  $\{P^{sat}, v_{liq}^{sat}, \Delta_{vap}H, c_{P,liq}^{sat}, v_c\}$ , for the 1 252 NSA and the 548 SA compounds are reported in [Table PV.6](#). A first point is that, for the original SRK and PR EoS, the difference in performance between NSA and SA compounds is noticeable for all the properties of interest. For the *translated* and *consistent* models, similar deviations are observed for SA and NSA compounds except for the  $c_{P,liq}^{sat}$  property for which deviations double when switching from NSA to SA compounds. It is however believed that this difference is not very significant. A detailed analysis of the results obtained with the *tc*-PR EoS shows that the vast majority of SA compounds (around 70%) have deviations on  $c_{P,liq}^{sat}$  that are lower than 2%. Half of the SA components have even deviations on  $c_{P,liq}^{sat}$  that are lower than 1.5 %. On the other hand, a small number of SA components have deviations higher than 20% that makes inevitably increase the average deviation value for this category of components. [Table PV.6](#) shows that for SA compounds, the average deviation on  $c_{P,liq}^{sat}$  is 4.2% whereas the calculated standard deviation was found to be as high as 3.8%. On the other hand, for NSA components, the standard deviation is close to zero. A simple comparison of average deviations (between SA and NSA components) is thus not very relevant. Another weakness of the comparison of deviations between SA and NSA components is the small number of SA components for which experimental heat capacities are available (less than 200).

**Table PV.6.** MAPE on  $P^{sat}$ ,  $v_{liq}^{sat}$ ,  $\Delta_{vap}H$ ,  $c_{P,liq}^{sat}$  and  $v_c$  depending on the associating character as predicted by the SRK, PR, *tc*-RK and *tc*-PR EoS.

EoS		MAPE on	MAPE on $v_{liq}^{sat}$	MAPE on	MAPE on	MAPE on $v_c$
		$P^{sat}$ (1800 fluids)	(1800 fluids) ( $T_r < 0.9$ )	$\Delta_{vap}H$ (1536 fluids)	$c_{P,liq}^{sat}$ (890 fluids)	(1800 fluids)
SRK	NSA	2.1% (1252 fluids)	18% (1252 fluids)	2.8% (1114 fluids)	4.9% (695 fluids)	30% (1252 fluids)
	SA	2.9% (548 fluids)	21% (548 fluids)	3.5% (422 fluids)	7.6% (195 fluids)	33% (548 fluids)
PR	NSA	2.3%	7.7%	3.0%	6.8%	20%
	SA	4.0%	11%	3.5%	9.0%	23%
<i>tc</i> -RK	NSA	1.1%	3.6%	2.0%	2.3%	23%
	SA	1.4%	3.2%	1.9%	4.4%	25%
<i>tc</i> -PR	NSA	0.9%	2.0%	2.0%	2.1%	19%
	SA	1.2%	2.3%	1.8%	4.2%	21%

To have a deeper insight into the role played by association and to better understand the relationship between the ability of an EoS to accurately reproduce the properties of pure species and their associating character, it is now decided to define a criterion for *quality modelling*. Using the latter, molecules will be labelled as *well*

or *badly* represented and it will be possible to analyze how the SA and NSA fluids distribute between the 2 categories. The proposed criterion of modelling quality compares the deviations obtained on  $P^{sat}$  and  $v_{liq}^{sat}$  for a given fluid to the mean deviations obtained for all the NSA fluids. For a given molecule, if deviations on  $P^{sat}$  and  $v_{liq}^{sat}$  slightly depart from the corresponding mean values for NSA fluids, the molecule is considered as well modeled. Otherwise, it falls in the “badly-modeled” category. Deviations on  $P^{sat}$  and  $v_{liq}^{sat}$  were retained because such properties are available for the 1 800 molecules and, as previously discussed are considered as key properties. The mean reference deviations on  $P^{sat}$  and  $v_{liq}^{sat}$  were calculated over the 1 252 NSA components only simply because the 4 studied CEoS do not contain associating terms and were initially intended to describe NSA components only. By only considering NSA compounds instead of all pure components of the database, a more severe test is proposed to affect a molecule to the “*well-modeled*” category. Quantitatively speaking, a pure component  $j$  will be considered as “*well-modeled*” by a given EoS provided:

$$\left\{ \begin{array}{l} \left( MAPE_{P^{sat}}^{EoS} \right)_j \leq \overline{MAPE}_{P^{sat}}^{EoS,NSA} + SD_{P^{sat}}^{EoS,NSA} \\ \text{and} \\ \left( MAPE_{v_{liq}^{sat}}^{EoS} \right)_j \leq \overline{MAPE}_{v_{liq}^{sat}}^{EoS,NSA} + SD_{v_{liq}^{sat}}^{EoS,NSA} \end{array} \right. \quad (PV.10)$$

where  $SD_X^{EoS,NSA}$  and  $\overline{MAPE}_X^{EoS,NSA}$  denote the mean SD and MAPE for property  $X$  calculated with a given EoS over the 1 252 NSA components of the database. If one or both conditions of Eq. (PV.10) are not satisfied, the pure component is considered as “*badly modeled*”.

Results are presented in Figure PV.1 to Figure PV.4 and deserve discussion. A key point is that regardless of the considered CEoS, about 75% of pure components are well represented, according to the criterion defined in Eq. (PV.10) (see the left panel in each figure). In addition, the database contains 70% (1 252/1 800) of NSA fluids and 30% of SA components. At a first sight, it could be believed that the 75% well-modeled molecules match the NSA fluids plus some SA components. This is however not the case at all.

Another striking fact is that almost 67% of the SA molecules are “well modeled”, while almost 20% of the NSA compounds are “badly modeled”. Once again, we might have been tempted to believe that all the NSA fluids would be “well modeled” by CEoS but this is not the case. On the other hand, one would not have predicted that classical CEoS reproduce satisfactorily more than half of the SA molecules without adding an association term.

In order to further analyze the results, we decided to investigate if there was a correlation between the degree of hydrogen bonding and the accuracy with which the experimental data were correlated. In other words, we wanted to investigate if the performance for short-chain associating molecules (where the weight of association is definitively very important) is less reliable or it follows similar trends than for SA compounds that possess a long organic chain, these long alkyl chains being likely to hide the effect of association. It was thus decided to split the 548 SA components into two categories: the short-chain and the long-chain components. We found that 125 molecules (among the 548) had a molecular weight lower or equal to that of n-pentanol and they were (somewhat arbitrary) classified as short-chain. The remaining 423 molecules were classified as long-chain. Calculations were performed with the *tc*-PR EoS and made it possible to conclude that there is definitively no link between the strength of the hydrogen bond and the accuracy of the calculations. Indeed 62% of the short-

chain molecules and 68% of the long-chain molecules were found to be well-modeled. The difference between these 2 percentages is small and not statistically significant. Water, methanol and ethanol were declared badly-modeled but many other short alcohols (propargyl alcohol, allyl alcohol, 2-methyl-2-propanol, 2-butanol, 1,2-propylene glycol ...) were declared well modeled. In addition, we observed some results for which it is difficult to find an explanation. As an example, considering the 2 isomers: 1-butanol and 2-butanol, it is found that the first one is well modeled but not the second one. Their structures are however highly similar.

Finally, a closer inspection across various chemical groups (defined by the DIPPR) is proposed. [Table PV.7](#) shows the distribution of well-modeled compounds for different chemical groups and for each EoS. It is possible to observe that the four EoS have a ratio of well-modeled molecules greater than 65% and often close to 80% for alkanes, alkenes, alkynes, aromatics, esters, ethers, ketones, aldehydes, epoxides, peroxides, halogen compounds, amines, amides, sulfur and silicon compounds. Alcohols have 61% of well-modeled molecules except with the *tc*-PR model, which yields a ratio of 53%. Nitriles are modeled the worst and this is related mostly to high deviations on  $v_{liq}^{sat}$ . Such large deviations on  $v_{liq}^{sat}$  can however not be ascribed to the strong associating character of these compounds. A detailed analysis of the chemical structure of the 31 nitrile compounds available in the DIPPR database reveals that the majority of these molecules are polyfunctional (in addition to the nitrile group, some contains double bonds, other contain a hydroxyl group, a NH<sub>2</sub> group, a methoxy group ...). It is believed that such a complexity explains the loss of accuracy that is observed. In turn, organic acids are not well-modeled by the original SRK and PR EoS while the *tc*-RK and *tc*-PR models achieve a ratio of 80% of well-modeled molecules.

To conclude this section, it can be highlighted that modern CEoS like the *tc*-PR and *tc*-RK EoS have the capacity to model accurately around 70% of SA compounds and 80% of NSA compounds. It is believed that this result counterbalances most of comments about the inadequacy of EoS that do not include a specific association term in their formulation to model SA compounds.

## PV.IV Conclusion

In this study, guidelines for the constitution of a pure-compound database stemming from the DIPPR for the assessment of the performance of thermodynamic model for pure compounds has been presented. These guidelines provide the number of molecules, the property data to be incorporated, and the temperature ranges between which pseudo-experimental points should be generated.

Application of such guidelines led to a database containing 1 800 molecules for which, in addition to the critical coordinates ( $T_c$ ,  $P_c$  and  $v_c$ ), accurate correlations for  $P^{sat}$  and  $\rho_{liq}^{sat}$  are available. Among them, 1 536 fluids also possess an accurate correlation for  $\Delta_{vap}H$  and 890 for  $c_{P,liq}^{sat}$ , resulting in a database containing 306 700 high-quality pseudo-experimental data points.

In addition, the accuracy of the SRK, PR, *tc*-RK and *tc*-PR EoS has been investigated by calculating the deviations between experimental data points embedded in the developed reference database and calculated values returned by the CEoS. Results obtained over 1 800 compounds and more than 306 000 data points highlight:

- The use of the highly flexible, component-dependent Twu91  $\alpha$ -function drastically improves the reproduction of vapor pressures, enthalpies of vaporization and liquid heat capacities.

- The spectacular improvement in the reproduction of liquid molar volumes when a substance-dependent volume-translation parameter is used.
- The impressive accuracy of the *tc*-PR EoS that got an average overall deviation lower than 2% over the 306 700 available experimental data points. Excellent results are obtained for all the properties, except the molar critical volumes.
- The striking fact that not all the non-self-associating molecules are well modeled by the studied CEoS and that almost 2/3 of the self-associating compounds of the database are represented with high accuracy by CEoS. At this step, one might wonder whether the addition of an association term is the right solution to improve the accuracy of EoS. The answer to this extremely complex question is not yet clear for the authors of this paper but they plan to publish their conclusion soon, in a next paper. At this step, it could be argued that EoS are mostly developed and used in academia and industry to calculate phase equilibria and thermodynamic properties of fluid mixtures. This is obviously true but it is believed that this study over thousands of pure components deserves attention because, as stated by Agarwal and recalled in this paper: *regardless of the sophistication of your thermodynamic model and the number of parameters in the mixing rule, you are in trouble if the vapor pressures are inaccurate. No matter how many parameters your mixture model may have, the end points of isothermal (P,x,y) phase diagrams will always be calculated incorrectly.*

Finally, the authors hope that the proposed guidelines and database will be widely adopted by the scientific community to identify the strengths and weaknesses of a given thermodynamic model. Moreover, this database should help model developers to test new concepts in the formulation of EoS for pure compounds.

**Table PV.7.** Distribution of well-modeled compounds across different chemical groups for the SRK, PR, *tc*-RK and *tc*-PR EoS.

<b>Group</b>	<b>SRK</b>	<b>PR</b>	<b><i>tc</i>-RK</b>	<b><i>tc</i>-PR</b>
Alkanes	88%	90%	85%	94%
Alkenes	92%	90%	84%	87%
Aromatics	80%	85%	87%	83%
Alkynes	83%	83%	78%	83%
Polyfunctional Compounds	71%	63%	82%	74%
Esters/Ethers	69%	73%	84%	79%
Organic Acids	49%	35%	80%	79%
Inorganic Compounds	63%	67%	63%	60%
Ketones/Aldehydes	88%	93%	80%	93%
Nitrogen Compounds	64%	62%	71%	75%
Alcohols	61%	61%	61%	53%
Other Compounds	33%	56%	67%	44%
Organic Salts	69%	62%	54%	46%
Epoxides	94%	100%	61%	83%
Peroxides	100%	73%	100%	73%
Halogen Compounds	81%	86%	72%	80%
Nitriles	13%	13%	23%	35%
Amines/Amides	70%	70%	72%	68%
Sulfur Compounds	88%	91%	79%	90%
Silicon Compounds	75%	77%	80%	72%

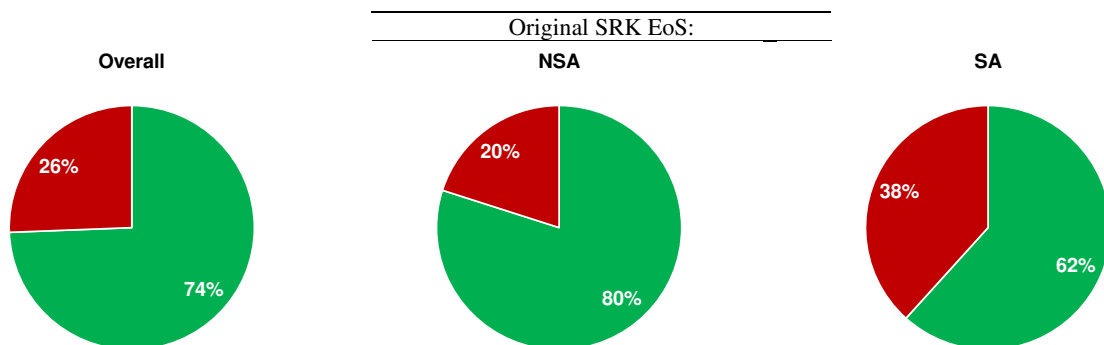


**Figure PV.1.** Ratio of well and badly modeled molecules by the SRK EoS classified into non-self-associating (NSA) and self-associating (SA) fluids. Green: well-modeled molecules. Red: Badly-modeled molecules.

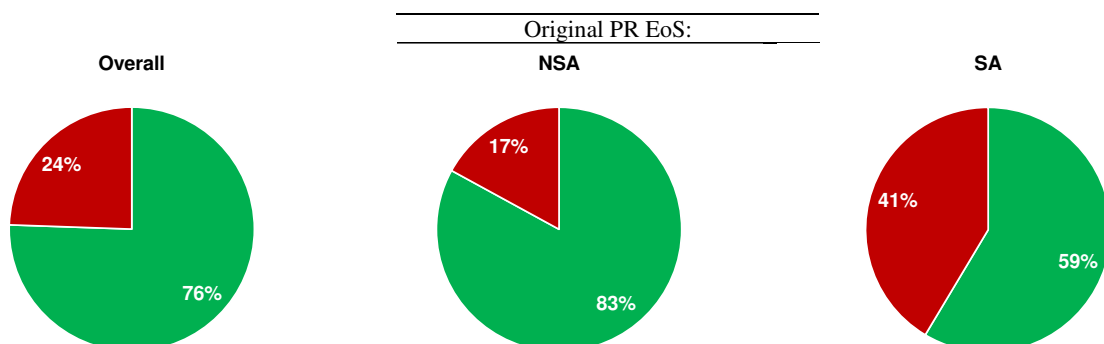


**Figure PV.2.** Ratio of well and badly modeled molecules by the PR EoS classified into non-self-associating (NSA) and self-associating (SA) fluids. Green: well-modeled molecules. Red: Badly-modeled molecules.

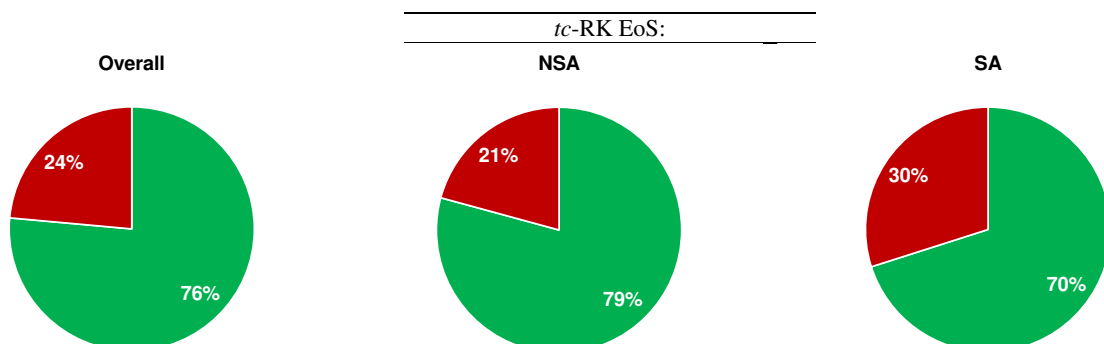


**Figure PV.3.** Ratio of well and badly modeled molecules by the *tc*-RK EoS classified into non-self-associating (NSA) and self-associating (SA) fluids. Green: well-modeled molecules. Red: Badly-modeled molecules.

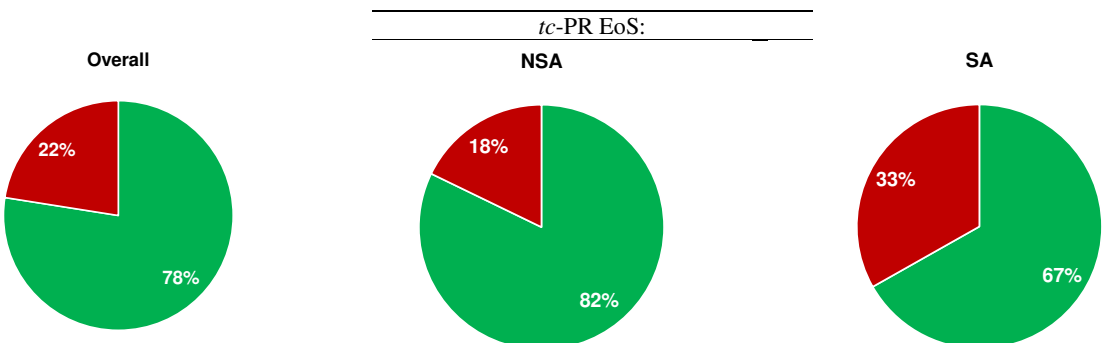


**Figure PV.4.** Ratio of well and badly modeled molecules by the *tc*-PR EoS classified into non-self-associating (NSA) and self-associating (SA) fluids. Green: well-modeled molecules. Red: Badly-modeled molecules.

# Publication VI : A benchmark database containing binary-system-high-quality-certified data for cross-comparing thermodynamic models and assessing their accuracy

Jean-Noël Jaubert<sup>1(\*)</sup>, Yohann Le Guennec<sup>1,2</sup>, Andrés Piña-Martinez<sup>1</sup>, Nicolas Ramirez-Velez<sup>1</sup>, Silvia Lasala<sup>1</sup>, Bastian Schmid<sup>2</sup>, Ilias K. Nikolaidis<sup>3</sup>, Ioannis G. Economou<sup>3(\*)</sup>, Romain Privat<sup>1(\*)</sup>

<sup>(1)</sup> *Université de Lorraine, École Nationale Supérieure des Industries Chimiques, Laboratoire Réactions et Génie des Procédés (UMR CNRS 7274), 1 rue Grandville, 54000, Nancy, France.*

<sup>(2)</sup> *Ypso-Facto, 19 avenue Foch, 54000 Nancy, France.*

<sup>(3)</sup> *DDBST GmbH, Marie-Curie-Straße 10, Oldenburg D-26129, Germany.*

<sup>(4)</sup> *National Center for Scientific Research "Demokritos", Institute of Nanoscience and Nanotechnology, Molecular Thermodynamics and Modelling of Materials Laboratory, GR e 153 10, Aghia Paraskevi Attikis, Greece.*

## Abstract

In the last two centuries, equations of state (EoS) have become a key tool for the correlation and prediction of thermodynamic properties of fluids. They can be applied not only to pure substances as well as to mixtures but they also constitute the heart of commercially available computer-aided-process-design software. In the last twenty years, thousands of publications were devoted to the development of sophisticated models or to the improvement of already existing EoS. Chemical engineering thermodynamics is thus a field under steady development and to assess the accuracy of a thermodynamic model or to cross-compare two models, it is necessary to confront model predictions with experimental data. In this context, the importance of a reliable free-to-access benchmark database is pivotal and becomes absolutely necessary. The goal of this paper is thus to present a database, specifically designed to assess the accuracy of a thermodynamic model or cross-compare models, to explain how it was developed and to enlighten how to use it.

A total of 200 non-electrolytic binary systems have been selected and divided into 9 groups according to the *associating character* of the components, i.e., their ability to be involved in a hydrogen bond (the nature and strength of the association phenomena is indeed considered as a measure of the complexity to model the thermodynamic properties of mixtures). The methodology for assessing the performance of a given model is then described. As an illustration, the Peng-Robinson EoS with classical Van der Waals mixing rules and a temperature-dependent binary interaction parameter ( $k_{ij}$ ) has been used to correlate the numerous data included in the proposed database and its performance has been assessed following the proposed methodology.



## PVI.I Introduction

Commercially available computer-aided-process-design software require thermodynamic models to design, develop, analyze and optimize chemical processes. As a result of their great potential, equations of state represent the cornerstone of thermodynamic models [273]. Indeed, combining an EoS and ideal-gas heat capacities enables to calculate not only phase equilibria, but also all the thermodynamic properties needed for energy and exergy balances (enthalpy, entropy, exergy, heat capacities, etc.). It can be argued that in 2020, chemical engineering thermodynamics is a field under steady growth since new models are continuously under development. In the academic community, it is often assumed that the accuracy of incoming models is increasing over the years, as they become more sophisticated. However, industry sometimes seems skeptical when weighing the value gained by using a more complex model, and rarely updates [274] or replaces its thermodynamic models with newer ones unless a clear advantage is evident. As a rule of thumb, it takes 10 years [275] for a new model to be conceived, developed, validated and accepted by the industry. It is believed that such a time lapse is extensive because, among other reasons, developers usually do not confront model predictions to experimental data that cover a wide range of compositions, temperatures and pressures. Moreover, the comparison between experimental data and model predictions is often limited to phase equilibria, ignoring other properties like enthalpies and heat capacities. For a new model, the absence of serious validation seems to be the major obstacle to its industrialization. Although scientists spend a great deal of time building and revising EoS, and much journal space is dedicated to introducing these valuable tools, the question of their accuracy inevitably arises because these models are, by definition, a simplification of reality.

In this paper, in order to address the relevant issue of model reliability, it was decided to build a high-quality reference database usable for assessing the accuracy of a thermodynamic model or to cross-compare the performances of two different models.

This work was conducted with the full support of the Working Party (WP) on Thermodynamics and Transport Properties (<https://wp-ttp.dk/>) of the European Federation of Chemical Engineering (<https://efce.info/>). In 2010, this WP published [275] a paper entitled: "Industrial requirements for thermodynamics and transport properties" and one of the many conclusions, which fully justifies this work, was : *"new models are published very frequently, but unfortunately most, if not all, of these models are tested against only a few data sets. The issue of having large, standardized set of data against which all models may be tested is a very pertinent one that needs addressing and will be of great benefit, as it will allow models to be compared on equal footing"*.

In the first part of this paper devoted to the building of a benchmark database, a total of 200 non-electrolytic binary systems was selected to cover all categories of mixtures and divided into 9 groups according to the *associating character* of the components, i.e., to their ability to be involved in a hydrogen bond. The nature and strength of the association phenomena is indeed considered as a measure of the complexity to model the thermodynamic properties of mixtures. In the second part of this paper, it is explained how to assess the accuracy of an EoS and to grade it with the proposed database. In particular, the exact procedure that has to be used to unambiguously calculate the deviations between model predictions and experimental data is discussed in detail and emphasis is given to the selection of specified and calculated variables. For illustration purposes, in the last part, the Peng-Robinson EoS with classical Van der Waals mixing rules and a temperature-dependent  $k_{ij}$  is scored after being used to correlate the various data of the proposed database. The grades are then interpreted through a discussion dealing with the accuracy of such a thermodynamic model.

---

## PVI.II Criterion to build a benchmark database

### PVI.II.I Literature review

Two databases that contain a vast number of experimental data points are widely used by researchers in the area of applied thermodynamics. The first one is the Dortmund Data Bank (DDB) (<http://www.ddbst.com/ddb.html>), that provides the largest data bank worldwide for thermophysical properties of pure components and their mixtures. In February 2020, the DDB contained 8.7 million data points for approximately 75,000 components from 88,200 references. The second one, provided by the National Institute of Standards and Technology (NIST), also contains pure-component and mixture data, divided in 90 Nation's Standard Reference Data (SRD) databases (<https://www.nist.gov/srd>). The trustworthiness of the data is assessed by experts, so that they can be used with confidence to make significant decisions.

Although extremely useful, such databases cannot be used as such to assess the accuracy of a thermodynamic model. Firstly, they are so comprehensive that a model evaluation procedure accounting for all the data would require an excessive amount of time. Secondly, the different types of systems (e.g., those that form ideal solutions, that contain size-asymmetric components, etc.) and data (e.g., vapor-liquid equilibrium (VLE) data, liquid-liquid-equilibrium (LLE) data, etc.) are not equitably distributed; an evaluation over these data would lead to biased conclusions about the model efficiency. Our goal is thus to build a sub-database from these very complete databases after a strict selection of the systems and data so that the diversity of molecular interactions and all kinds of fluid-phase behavior are represented.

To the best of our knowledge, the unique benchmark database for non-electrolytic and non-polymeric systems available in the literature is the one proposed by Danner and Gess in 1990 [276]. This database that embeds data for 104 binary systems shows the following characteristics:

- Only subcritical VLE data are available.
- Data quality is ensured by performing consistency tests.
- Pure compounds are classified according to their polarity, from nonpolar to strongly polar, leading to the definition of nine classes of binary systems.
- For a given class, binary systems are categorized with respect to their deviations from ideality and there is an even distribution between ideal and non-ideal systems.

In our opinion, such a database has many desirable features, including the classification scheme of the binary systems. However, several weak points can be pointed out: VLE data are limited to the subcritical domain and other types of phase equilibrium data, e.g., LLE, vapor-liquid-liquid equilibrium (VLLE), or derived properties like enthalpies and heat capacities are not included. Moreover, such a database was made available by their authors "on a 5 1/4 or 3 1/2 inch MS-DOS formatted floppy disk" and we cannot assert that it is still possible to get a copy or to read this support.

This short literature review makes it possible to conclude that the time has come to propose a revised version of the database developed by Danner and Gess [276] which we hope will be widely adopted by others for assessing the accuracy of a thermodynamic model or cross-comparing two models. To guide the reader over the understanding of the choices we made to build this database, the following sections aim to address three questions:

1. Which thermophysical properties should be included?
2. Which binary systems?
3. How many systems and how many data?

## **PVI.II.II Which thermophysical properties should be included?**

To answer this question, we must be aware of the industrial needs. The paper by Hendriks et al. [275] explains that simultaneous description of different thermodynamic properties and phase equilibrium types (VLE, LLE, VLLE) is of great importance. It is also stated that thermodynamic modelers should no longer be satisfied with EoS that are capable of reproducing VLE data with a reasonable accuracy at low pressures but are either untested or fail to reproduce other regions of the phase space and other properties.

As explained below, we followed these recommendations but we have decided to go one step further in the selection of the thermophysical properties.

First, it is indisputable that a good reproduction of phase equilibrium data is mandatory to ensure that processes meet their compositional specifications. However, depending on the temperature and pressure conditions, phase equilibrium data may involve two subcritical compounds, a subcritical and a supercritical compound or possibly two supercritical compounds. In the two latter cases, binary critical points appear on the corresponding phase diagrams. For some systems, azeotropic behavior and three-phase VLLE can occur as well. To consider such a diversity, it was decided to embed all kinds of phase equilibrium data in the developed database, i.e., VLE, LLE, VLLE and azeotropic data points and to cover a very wide range of compositions, temperatures and pressures. Binary critical points were also included because we know by experience that a good representation of the critical lines [277] leads to an accurate restitution of phase diagrams on the entire temperature and pressure ranges. Such lines indeed fix the global topology [278] of the isothermal and isobaric phase diagrams for any fixed temperature or pressure, respectively. Convinced by the importance of critical points, a special emphasis was given to binary systems for which such data were available.

A proper reproduction of energetic mixing properties (enthalpy and heat capacity changes on mixing) contributes to a good quantification of utility needs and energy losses in a chemical engineering process. Such a knowledge is typically required for performing heat integration in chemical plants. Unlike phase equilibrium properties, the calculation of enthalpy and heat capacity changes on mixing (hereafter simply called mixing enthalpy and mixing heat capacity) with an EoS involves the derivative of the EoS expression with respect to the temperature. Consequently,  $h^M$  data help to determine the temperature dependence of the phase equilibrium what supports their value. As a matter of fact, a good reproduction of experimental phase diagrams does not ensure accurate estimations of mixing properties and consequently, of energy-balance terms. The same conclusion was drawn by Agarwal et al. [245] who wrote: “...if you are modeling a system with significant excess enthalpies and you have a good VLE fit, this does not automatically ensure you have a good overall model from an energy balance point of view.” This highlights the necessity of considering mixing enthalpy and mixing heat capacity data for evaluating model performances. In his Ph.D. thesis, Qian [279] reached the same conclusion but also demonstrated that it was possible for the Peng-Robinson (PR) EoS with temperature-dependent binary interaction parameters (BIPs) to accurately correlate both fluid-phase equilibria and mixing properties if both types of data were included in the regression procedure. Eventually, we decided to include both mixing enthalpy and mixing heat capacity data in the proposed benchmark database.

To conclude this section, we want to emphasize that we intentionally did not incorporate excess volume data in the proposed database. This is because we know by experience that volume change on mixing are generally small (and often very small). As a direct consequence, the calculated density of a phase mainly depends on the accuracy with which the density of the pure components is calculated but is only slightly influenced by the used mixing rules. This implies that before grading a thermodynamic model with the proposed database, it is necessary to give information on how the model behaves to correlate/predict the properties of pure compounds and in particular the vapor pressures, the liquid densities, the enthalpies of vaporization and the liquid heat capacities.

It was also decided to exclude electrolytic systems and to only consider fluid-state binary systems meaning that the proposed database does not include liquid-solid, solid-solid or adsorption [280] equilibrium data.

### **PVI.II.III Which binary systems should be included?**

Danner and Gess database retained our attention as it does not only compile experimental data but also provides a classification for binary systems revealing their thermodynamic complexity (here *thermodynamic complexity* means a measure of the non-ideal character of a system inducing difficulties for a model to reproduce thermodynamic macroscopic properties). In the paper by Danner and Gess, pure compounds were categorized with respect to their polarity and were classified as nonpolar, weakly polar, strongly polar or very strongly polar. Such authors define polarity as the ability for a molecule to donate or accept a hydrogen atom and the presence of hydrogen bonding. Starting from these 4 categories of pure compounds, Danner and Gess defined 9 classes of binary systems (nonpolar/nonpolar, nonpolar/weakly polar, etc.) and for each class, their database includes a variety of systems ranging from ideal to highly non-ideal. We were totally convinced by this approach and decided to propose a somehow similar classification of binary systems but giving more emphasis on the *associating character* of the pure compounds, i.e., on their ability to be involved in a hydrogen bond, rather than on their polarity. Indeed, the various publications devoted to the CPA [124,164,281] or SAFT [151,282–292] EoS clearly indicate that an actual scientific challenge for EoS is their ability to properly describe the very complex association phenomena.

#### **Definition of the “associating character” of a pure compound**

In this paper, “association” means association only by hydrogen bonding. In classical physical chemistry [293], hydrogen bonds are defined as an attractive interaction between a hydrogen atom from a molecule or a molecular fragment A–H in which A is more electronegative than H, and a highly electronegative atom (denoted B) in the same or a different molecule that possesses a lone pair of electrons. There is no strict cut-off for an ability to participate in hydrogen bonding but nitrogen (N), oxygen (O) or fluor (F) atoms participate most effectively. From the definition above, the formation of a hydrogen bond can be regarded as the electrostatic interaction between a partial positive charge ( $\delta^+$ ) located on the labile hydrogen atom and a partial negative charge ( $\delta^-$ ) located on B that possesses a lone pair of electrons (see Figure PVI.1). The distance between the atoms H and B is classically taken as indication of the hydrogen bond strength; it typically varies between 160 and 200 pm.



**Figure PVI.1.** (a) Illustration of the definition of a hydrogen bond (red dashed line). The arrows indicate the more electronegative atom, i.e., the direction in which the shared pair of electrons (of the covalent bond) is shifted. (b) case of the pentafluoroethane-dimethyl ether system.

To create an association by hydrogen bonding, it is needed the conjunction of (i) a labile hydrogen atom and (ii) a lone pair of electrons. It thus becomes possible to classify the pure components in 4 categories according to their "*associating character*", i.e., depending on whether they have a labile hydrogen atom and / or a lone pair of electrons or none of them.

- Category 1 (*associating character* denoted NA for “Non-Associating”): the molecule has neither a labile hydrogen atom nor a lone pair of electrons. It is nonpolar. Molecules like alkanes and mono-halogenated compounds are included in this family. In short, this category includes nonpolar/non-associating components.
- Category 2 (*associating character* denoted HA for “Hydrogen-Acceptor”): the molecule possesses a lone pair of electrons (on an electronegative atom) but no labile hydrogen atom. Consequently, the molecule is polar. Ketones, aldehydes, ether, and ternary amines belong to this family. In short, this category includes polar but non-associating components.
- Category 3 (*associating character* denoted HD for “Hydrogen-Donor”): the molecule has a labile hydrogen atom but does not possess a lone pair of electrons and thus, is polar. Di-, tri-halogenated compounds or the ones with a terminal alkyne group belong to this family. The labile hydrogen earns its acidity from the electronegativity of its closest neighbors. In short, this category includes polar but non-associating components.
- Category 4 (*associating character* denoted SA for “Self-Associating”): the molecule possesses both a labile hydrogen atom and a lone pair of electrons. It is strongly polar. Such molecules fulfill the two necessary and sufficient conditions to establish a hydrogen bond. They are thus self-associating. Water, alcohols and carboxylic acids belong to this family. In short, this category includes polar and associating components.

Table S1 of the Supporting Information ([Appendix E](#)) lists the 107 pure compounds included in the proposed database and indicates for each of them the corresponding *associating character* among “Non-Associating” (NA), “Hydrogen-Acceptor” (HA), “Hydrogen-Donor” (HD) or “Self-Associating” (SA).

### **Definition of binary association codes to describe association in solution**

With this *associating character* coding, the binary systems in the database were immediately divided into the following ten families by performing all the possible combinations (see [Table PVI.1](#)) and a *binary association code* (BAC) was assigned to each family. From our experience, much less experimental data are reported for HA/HA and HD/HD binary systems than for any other family. The lack of experimental data for HD/HD binary systems can be explained by noticing that HD molecules are mostly refrigerants that are generally encountered as pure compounds in chemical processes. Therefore, it was decided to merge HA/HA and

HD/HD families that are both non-associating mixtures, into a single family, thus reducing the number of BACs to nine.

**Table PVI.1.** Definition of the ten families of binary systems and their corresponding BAC (*binary association code*).

Component 1	Component 2	Binary association code (BAC)	Type of exhibited association
NA (Non-Associating) <i>nonpolar</i>	NA (Non-Associating) <i>nonpolar</i>	1	Mixtures without association
HA (Hydrogen-Acceptor) <i>polar but non-associating</i>	NA (Non-Associating) <i>nonpolar</i>	2	
HD (Hydrogen-Donor) <i>polar but non-associating</i>	NA (Non-Associating) <i>nonpolar</i>	3	
HA (Hydrogen-Acceptor) <i>polar but non-associating</i>	HA (Hydrogen-Acceptor) <i>polar but non-associating</i>	4	
HD (Hydrogen-Donor) <i>polar but non-associating</i>	HD (Hydrogen-Donor) <i>polar but non-associating</i>		
SA (Self-Associating) <i>polar and associating</i>	NA (Non-Associating) <i>nonpolar</i>	5	Mixtures in which self-association takes place (but tends to be broken)
HD (Hydrogen-Donor) <i>polar but non-associating</i>	HA (Hydrogen-Acceptor) <i>polar but non-associating</i>	6	Mixtures in which cross-association takes place alone
SA (Self-Associating) <i>polar and associating</i>	HD (Hydrogen-Donor) <i>polar but non-associating</i>	7	Mixtures in which both cross-association and self-association take place
SA (Self-Associating) <i>polar and associating</i>	HA (Hydrogen-Acceptor) <i>polar but non-associating</i>	8	
SA (Self-Associating) <i>polar and associating</i>	SA (Self-Associating) <i>polar and associating</i>	9	

From [Table PVI.1](#), it is possible to determine at a glance in which binary systems hydrogen bonds occur. Indeed, the requirement for the existence of a hydrogen bond remains to be the presence of both a labile hydrogen atom and a lone pair of electrons. In the case, the labile hydrogen atom and the lone pair of electrons originate from the two different species, the hydrogen bond is said to be formed by “cross association” between compounds 1 and 2. The last column of [Table PVI.1](#) highlights that all types of binary systems (those in which no-association, self-association, cross-association or both cross-association and self-association are taking place) are included in the proposed database. In other words, four categories of binary systems based on the type of association they exhibit can be distinguished:

- Binary systems having a small BAC value (from 1 to 4) cannot exhibit association and are expected to be easily correlated by any sophisticated enough thermodynamic model. In that sense, the BAC plays the role of thermodynamic-complexity degree (for small BAC value, the thermodynamic complexity is low and this complexity increases with the BAC).
- In binary systems belonging to the BAC 5, a NA (Non-Associating) component faces a SA (Self-Associating) component so that self-association (at least partially) persists in the mixture. The non-associating molecules tend to break the hydrogen bond network while SA molecules tend to resist so that liquid-phase partial immiscibility is often observed in this family (these two compounds do not like being mixed together and often prefer to be each one in a separate liquid phase). In [Table PVI.1](#), such systems are thus considered as: “mixtures in which self-association tends to be broken”. All binary systems of water + alkane or alcohol + alkane types belong to this family.

- BAC 6 results from the mixing of a component that has a labile hydrogen atom with another component that possesses a lone pair of electrons causing a cross-association phenomenon. The two components do not exhibit association when they are pure but their mixture exhibits hydrogen bonding. Consequently, these two molecules are more attracted to each other in mixture than when they are pure; therefore, such mixtures usually exhibit negative deviations from ideality.

For binary association codes 7 to 9, more complex phenomena occur as a self-associating compound is mixed with another molecule likely to generate a hydrogen bonding with it. Therefore, it is not always possible to determine a priori how the mixture is going to behave (thermodynamically) and if the mixing leads to an intensification or a relaxation of hydrogen bonding.

### **Quantification of deviations from ideality**

For each class of binary system, identified by its BAC, our motivation is to include in the proposed database a large variety of binary systems revealing the variety of deviation-from-ideality types. This section aims to explain how such deviations were sorted both from quantitative and qualitative viewpoints. Qualitatively, a system will be named ideal if it is formed by molecules having (i) similar sizes, (ii) similar shapes, and (iii) showing similar energetic interactions (nature & strength), regardless of the temperature, pressure and composition [294]. On the contrary, a system is considered as non-ideal if a noticeable departure from the three aforementioned criteria is observed. If deviations from ideality are the consequence of a difference in molecular sizes and/or shapes only, the excess enthalpy ( $h^E$ ) is negligible and the solution is called *athermal*; consequently, the excess Gibbs energy is proportional to the mixture excess entropy ( $g^E \approx -Ts^E$ ) and it is said that deviations from ideality originate from entropic effects. In the same way, if deviations from ideality are solely caused by a difference in energetic interactions, the excess entropy ( $s^E$ ) is negligible and the solution is called *regular*; consequently,  $g^E \approx h^E$ . In such a case, deviations from ideality are the consequence of enthalpic effects. Naturally, both effects may coexist in a non-ideal solution and in this case, it is said that deviations from ideality are the consequence of combined effects (of enthalpic and entropic natures). Such an overview of the possible causes of deviations from ideality is important as many thermodynamic models are built by summing the contributions of an enthalpic (related to the energetic interactions in the system) and an entropic (related to the size of the molecules) terms. In order to provide a benchmark database for EoS model evaluation, it is necessary to include mixture data spanning the whole range of departure-from-ideality types (from ideal to non-ideal, including enthalpic, entropic and combined effects). Doing so, our database will allow the identification of model failures in their enthalpic and/or entropic modelling patterns.

Quantitative information on how deviations from ideality were quantified and how the origin of such deviations was assessed is now detailed. To start, it is worth recalling that to determine the magnitude of the deviations from ideality, the activity coefficients have to be calculated from experimental VLE data. It can be done easily by using the VLE relationship stemming from the  $\gamma$ - $\phi$  approach:

$$\gamma_i(T, \mathbf{x}) = P_{\text{exp}} \cdot y_{i,\text{exp}} / [P_i^{\text{sat}}(T_{\text{exp}}) \cdot x_{i,\text{exp}}] \quad (\text{PVI.1})$$

Eq. (PVI.1) however requires a correlation to estimate the vapor pressure of component  $i$ , so that only subcritical VLE data ( $T < T_{c,i}$ ) can be used to estimate the deviations from ideality. In the case subcritical VLE data are not available for a system included in our database, the message: *deviations from ideality not assessed* is reported for such a system in [Table PVI.2](#).

For each binary system for which subcritical VLE data were available, a set of 4 parameters ( $p_1, p_2, p_3, p_4$ ) of the Margules excess Gibbs energy model were fit over both VLE data and enthalpy of mixing data (when available).

$$\begin{cases} \frac{g^E(T, \mathbf{x})}{RT} = x_1 \cdot x_2 \cdot A(T) \\ A(T) = p_1 - p_2 T - p_3 \ln T + p_4 \exp\left(\frac{1}{T}\right) \end{cases} \quad (\text{PVI.2})$$

The  $p_i$  parameters were determined in order to minimize the mean average percent error (MAPE) between calculated and experimental VLE and  $h^M$  data. The mathematical expression of  $h^E$  (and thus  $h^M$ ) can be straightforwardly derived from Eq. (PVI.2):

$$h^E = g^E - T \left( \frac{\partial g^E}{\partial T} \right)_X \quad (\text{PVI.3})$$

For VLE calculations, the  $\gamma$ - $\phi$  approach was used assuming that the gas phase is perfect and by neglecting the Poynting factor. In other words, the following classical VLE relation, especially suitable to correlate subcritical data, was used:

$$Py_i = P_i^{sat} x_i \gamma_i \quad (\text{PVI.4})$$

The vapor pressures were calculated by means of correlations extracted from the DIPPR database.

Once the 4 parameters ( $p_1, p_2, p_3, p_4$ ) have been fit, the magnitude of the deviations from ideality can be estimated. For each temperature involved in the regression procedure,  $g^E$ ,  $h^E$  and  $s^E$  were calculated at the unique composition  $x_1 = 0.50$ . Based on our experience, a binary system can be considered as *ideal* (see Table PVI.2) if  $\left| g^E / RT \right|_{x=0.5} < 0.1$  for each of the considered temperatures. If not, the system is declared non-ideal.

For non-ideal systems, the origin of the deviations from ideality (entropic, enthalpic or combined) was only evaluated when  $h^M$  experimental data were available and thus included in the regression procedure. We indeed noticed that the calculation of the excess enthalpy and entropy of a binary system could be very uncertain when the four  $p_i$  parameters were determined over VLE data only. For non-ideal systems, when  $h^M$  data were lacking, the systems were thus declared (see Table PVI.2): *non-ideal with non-assessed causes*. In turn, when  $h^M$  data were available:

1. If  $\left| (h^E / RT) / (s^E / R) \right|_{x=0.5} > 2$  for all temperatures, it was considered that non-ideality stemmed from enthalpic effects. In Table PVI.2, the system is labelled: *non-ideal with enthalpic causes*.
2. If  $\left| (h^E / RT) / (s^E / R) \right|_{x=0.5} < \frac{1}{2}$  for all temperatures, it was considered that non-ideality stemmed from entropic effects. In Table PVI.2, the system is labelled: *non-ideal with entropic causes*.
3. Otherwise, deviations from ideality are the consequence of combined effects, i.e., both enthalpic and entropic effects and none is dominant. In Table PVI.2, the system is labelled: *non-ideal with enthalpic and entropic causes*.

An overview of how the deviations from ideality are distributed among the nine BACs can be found in Table PVI.2 whereas the different steps that were followed to build the proposed database are summarized in Figure PVI.2.

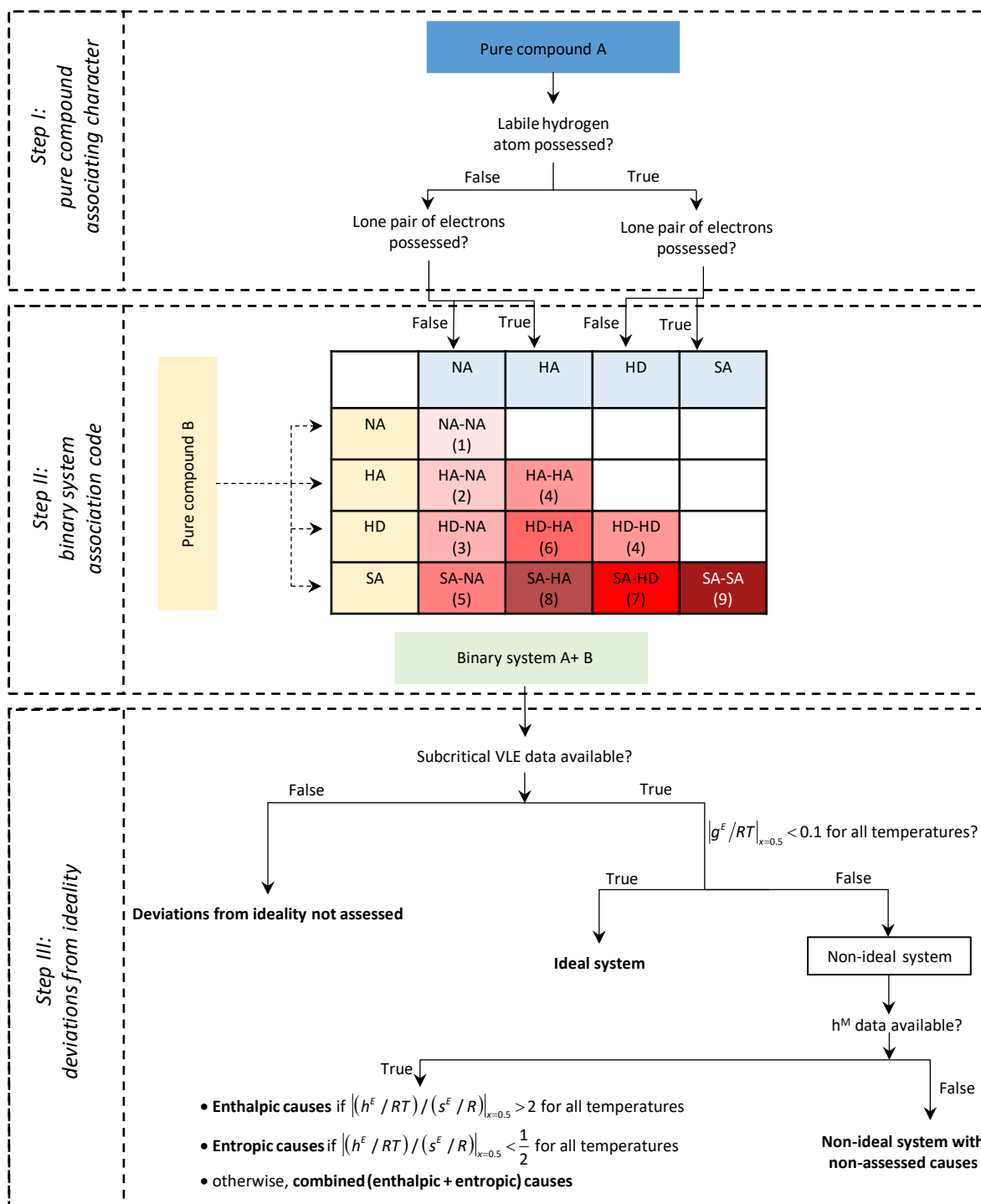


Figure PVI.2. Procedure followed to build the proposed database.

#### PVI.II.IV How many systems and how many data should be included?

Commercial databases, especially the Dortmund Data Bank, report VLE data for tens of thousands of binary systems. It would be impractical to cross-compare EoS on such a huge number of data; therefore, our objective is to work with a much smaller number of wisely chosen binary systems in order to cover all categories of mixtures. For each of the nine families of binary systems – defined each by a distinct BAC – our objective is to consider systems, deemed as well representative of their family. Among these systems, our ambition is to reach a distribution of  $1/4$  of systems containing high-pressure VLE data (for which deviations from ideality cannot be assessed),  $1/4$  of ideal systems and  $1/2$  of non-ideal systems. The non-ideal systems should include similar number of systems for which the origin of the deviations from ideality could not be assessed due to a lack of  $h^M$  data or stem from enthalpic, entropic or (enthalpic + entropic) effects. In order to have a meaningful representation of such a diversity, it was found acceptable to include around 20 binary systems per BAC.

Another key point is to only retain high-quality-certified data explaining why the consistency of the data were checked with the help of four consistency tests: the point test [295], the integral test [296], the differential test and the infinite-dilution test [297], all performed with the Data Preparation Package (DPP) which is a software package for the regression of thermophysical property models commercialized by Dechema. It is however worth noting that the aforementioned tests only apply to VLE data when both compounds are subcritical. As a direct consequence, among the many data included in our benchmark database, only the quality of the subcritical data can be guaranteed. For an ideal binary system, passing the point test was considered as a sufficient consistency condition while for non-ideal systems, the point test and two of the three remaining tests had to be passed in order to keep the experimental data in our database. Indeed, as explained by Wisniak et al. [298] the quality of the equilibrium data should be checked using simultaneously several of the available consistency tests.

In the end, the proposed database comprises 200 binary systems and contains about 30,000 experimental data points (around 18,000 VLE/LLE data points, 8,500  $h^M$  data, 1,500  $c_P^M$  data, and 2,000 data points relative to critical points, azeotropic points or three-phase lines).

#### PVI.II.V The built database

An extensive screening of thousands of binary systems was first realized and a complex strategy was developed in order to only keep the 200 systems that met our criteria in terms of (i) types of association, (ii) deviations from ideality, (iii) quality, quantity and diversity of the experimental data. Indeed, as previously discussed, we made our best in order that the selected systems are such that phase equilibrium data (VLE, LLE, VLLE, azeotrope) and mixing properties ( $h^M$ ,  $c_P^M$ ) are abundant in large temperature, pressure and composition ranges.

As previously stated, an overview of how the deviations from ideality are distributed among the nine BACs can be found in Table PVI.2. Similarly, an overview of how the different types of data are distributed among the 9 BACs can be found in Table PVI.3. For each BAC, Table PVI.4 to Table PVI.12 detail the list of the selected binary systems, specify the origin of the deviations from ideality and list the references in which the experimental data can be found. A scan of the 958 original references from which the data were extracted was realized and the authors are committed to sending a copy of an article to any reader of this paper that would, e.g., necessitate more details on the used experimental setup.

**Remark:** [Table PVI.3](#) shows that the proposed database contains information for 225 azeotropic points. Some of them can however not be found in the original publications from which the data were extracted. We indeed decided for some azeotropic systems to interpolate the experimental VLE data in order to determine the temperature, pressure and composition of the azeotropic point.

Several Excel files are available as Supporting Information ([Appendix E](#)):

- The first one, named *Database.xlsx*, is a *light* Excel file that only contains the experimental data and the corresponding references. This file comprises 201 sheets. The first one named “ReadMe” provides an overview of the database and explains how it is organized. The 200 other sheets contain each the data related to a given binary system.
- The nine others, one for each BAC, and named *BACi with visualization of the data.xlsx* (i=1 to 9) are *large-size* Excel files that provide figures to have a visualization of the experimental data (as a complement to data tables) and the singularities of the binary systems. These files contain several sheets. Here also, the first one, named “ReadMe” provides an overview of the database and explains how it is organized whereas the other sheets contain each, the data related to a given binary system.

The following part of this article ([Section PVI.III](#)) aims at explaining how the proposed database should be used to grade a thermodynamic model in order to assess its accuracy. For illustrative purpose, [Section PVI.IV](#) clarifies the grading of the thermodynamic model: {Peng-Robinson EoS + classical VdW mixing rules + a temperature-dependent BIP} and opens a discussion around its accuracy.



**Table PVI.2.** Overview of how the deviations from ideality are distributed among the nine binary association codes (BACs) for the 200 binary systems of the proposed database (the abbreviations used for the *associating character* of a pure compound are: NA for “Non-Associating”, HA for “Hydrogen-Acceptor”, HD for “Hydrogen-Donor” and SA for “Self-Associating”).

Binary association code (BAC)	Deviations from ideality not assessed <sup>(*)</sup>	Ideal	Non-ideal with enthalpic causes	Non-ideal with entropic causes	Non-ideal with enthalpic and entropic causes	Non-ideal with non-assessed causes <sup>(**)</sup>
<b>1</b> (NA - NA)	38%	15%	15%	4%	19%	8%
<b>2</b> (HA-NA)	29%	29%	13%	4%	17%	8%
<b>3</b> (HD-NA)	10%	30%	15%	0%	10%	35%
<b>4</b> (HA-HA or HD-HD)	32%	32%	14%	5%	9%	9%
<b>5</b> (SA-NA)	33%	11%	22%	0%	22%	11%
<b>6</b> (HD-HA)	28%	16%	4%	0%	28%	24%
<b>7</b> (SA-HD)	44%	0%	6%	25%	25%	0%
<b>8</b> (SA-HA)	23%	15%	27%	4%	23%	8%
<b>9</b> (SA-SA)	9%	30%	22%	9%	17%	13%

(\*) non-availability of subcritical VLE data (refer to [Figure PVI.2](#))

(\*\*) non-availability of  $h^M$  data (refer to [Figure PVI.2](#))

**Table PVI.3.** Overview of the distribution of the different types of experimental data among the nine binary association codes (BACs) for the 200 binary systems of the proposed database (the abbreviations used for the *associating character* of a pure compound are: NA for “Non-Associating”, HA for “Hydrogen-Acceptor”, HD for “Hydrogen-Donor” and SA for “Self-Associating”).

Binary association code (BAC)	Subcritical liquid phase <sup>(*)</sup> composition	Subcritical vapor phase (or 2 <sup>nd</sup> liquid phase <sup>(**)</sup> ) composition	Supercritical liquid phase <sup>(*)</sup> composition	Supercritical vapor phase (or 2 <sup>nd</sup> liquid phase <sup>(**)</sup> ) composition	Azeotropic point	Critical point	Enthalpy of mixing	Heat capacity of mixing	three-phase line	Sum	%
<b>1 (NA - NA)</b>	1323	1336	2293	2203	11	252	1314	231	16	8979	<b>18.8%</b>
<b>2 (HA-NA)</b>	1406	1406	1195	1148	22	319	1532	27	0	7055	<b>14.7%</b>
<b>3 (HD-NA)</b>	1087	1087	306	306	44	49	258	30	0	3167	<b>6.6%</b>
<b>4 (HA-HA or HD-HD)</b>	904	904	561	561	7	60	454	15	0	3466	<b>7.2%</b>
<b>5 (SA-NA)</b>	1237	1219	343	378	35	130	1525	155	25	5047	<b>10.5%</b>
<b>6 (HD-HA)</b>	1112	1112	410	410	18	63	466	99	0	3690	<b>7.7%</b>
<b>7 (SA-HD)</b>	741	711	0	0	13	0	498	26	0	1989	<b>4.2%</b>
<b>8 (SA-HA)</b>	2140	2119	915	881	42	193	1408	144	12	7854	<b>16.4%</b>
<b>9 (SA-SA)</b>	2299	2287	149	149	33	50	1115	507	13	6602	<b>13.8%</b>
<b>Sum</b>	12249	12181	6172	6036	225	1116	8570	1234	66	47849	
<b>%</b>	<b>25,6%</b>	<b>25,5%</b>	<b>12,9%</b>	<b>12,6%</b>	<b>0,47%</b>	<b>2,33%</b>	<b>17,91%</b>	<b>2,58%</b>	<b>0,14%</b>		

(\*) *Liquid phase* refers indifferently to a VLE or a LLE data point. For a LLE, it designates the composition of the  $\alpha$ -liquid phase.

(\*\*) 2<sup>nd</sup> liquid phase designates the composition of the  $\beta$ -liquid phase in the case of a LLE.

**Table PVI.4.** List of the 26 binary systems for which the binary association code is: BAC=1 (NA-NA). Such a BAC corresponds to a binary system involving a “Non-Associating” (NA) molecule + another “Non-Associating” (NA) molecule. Corresponding origin of the deviations from ideality and list of the references in which the experimental data can be found. By convention, *Molecule 1* refers to the more volatile component.

<i>Origin of the deviations from ideality</i>	<i>Molecule 1</i>	<i>Molecule 2</i>	<i>References</i>
Deviations from ideality not assessed	methane	propane	[299–311]
	methane	n-hexane	[309,312–319]
	methane	n-heptane	[309,320–323]
	nitrogen	ethane	[324–331]
	methane	n-decane	[332–337]
	ethane	n-heptane	[338–343]
	nitrogen	n-pentane	[344–346]
	nitrogen	n-decane	[347,348]
	methane	n-tetracosane	[349–352]
	ethane	n-hexatriacontane	[353–355]
Ideal	n-hexane	cyclohexane	[356–368]
	benzene	toluene	[369–378]
	propane	isopentane	[379]
	cyclohexane	methylcyclohexane	[357,378,380–383]
Non-ideal with non-assessed causes	ethane	propane	[384–396]
	methane	n-butane	[309,319,397–401]

<i>Origin of the deviations from ideality</i>	<i>Molecule 1</i>	<i>Molecule 2</i>	<i>References</i>
Non-ideal with enthalpic causes	argon	methane	[402–411]
	n-heptane	monochlorobenzene	[412–418]
	cyclohexane	monochlorobenzene	[381,418–423]
	1,2-dichloroethane	carbon tetrachloride	[424–429]
Non-ideal with entropic causes	1,2-dichloroethane	toluene	[373,430–434]
Non-ideal with enthalpic and entropic causes	Nitrogen	methane	[402,435–440,329,441,442,410,443,411]
	methane	ethane	[307,309,328,329,444–448]
	benzene	n-heptane	[357,378,413,449–465]
	benzene	cyclohexane	[359,368,459,466–483]
	ethylene	xenon	[484–486]

**Table PVI.5.** List of the 24 binary systems for which the binary association code is: BAC=2 (HA-NA). Such a BAC corresponds to a binary system involving a “Hydrogen-Acceptor” (HA) molecule + a “Non-Associating” (NA) molecule. Corresponding origin of the deviations from ideality and list of the references in which the experimental data can be found. By convention, *Molecule 1* refers to the more volatile component.

<i>Origin of the deviations from ideality</i>	<i>Molecule 1</i>	<i>Molecule 2</i>	<i>References</i>
Deviations from ideality not assessed	carbon dioxide	toluene	[487–501]
	carbon dioxide	n-decane	[502–513]
	methane	carbon dioxide	[303,447,514–523]
	carbon dioxide	cyclopentane	[524,525]
	nitrogen	carbon dioxide	[326,515–517,521,526–537]
	methane	hydrogen sulfide	[538–540]
	carbon dioxide	n-dotriacontane	[541–543]
Ideal	methyl tert-butyl ether	n-heptane	[544–548]
	ethyl acetate	toluene	[549–552]
	carbon tetrachloride	1,4-dioxane	[553–558]
	methyl ethyl ketone	benzene	[559–562]
	methyl tert-pentyl ether	n-heptane	[563–566]
	methyl tert-butyl ether	toluene	[567–570]
	1,2,3,4-tetrahydronaphthalene	quinoline	[571,572]
Non-ideal with non-assessed causes	ethylene	carbon dioxide	[573–579]

<i>Origin of the deviations from ideality</i>	<i>Molecule 1</i>	<i>Molecule 2</i>	<i>References</i>
	carbon dioxide	propane	[303,310,395,527,580–588]
	acetone	n-hexane	[589–595]
Non-ideal with enthalpic causes	n-pentane	acetone	[589,593,595–597]
	acetone	cyclohexane	[366,466,598–605]
Non-ideal with entropic causes	benzene	n-methyl-2-pyrrolidone	[606–611]
	carbon dioxide	ethane	[447,585,612–621]
Non-ideal with enthalpic and entropic causes	carbon dioxide	n-butane	[395,529,574,584–587,622–629]
	n-hexane	methyl ethyl ketone	[455,562,630–633]
	acetone	benzene	[466,554,634–642]

**Table PVI.6.** List of the 20 binary systems for which the binary association code is: BAC=3 (HD-NA). Such a BAC corresponds to a binary system involving a “Hydrogen-Donor” (HD) molecule + a “Non-Associating” (NA) molecule. Corresponding origin of the deviations from ideality and list of the references in which the experimental data can be found. By convention, *Molecule 1* refers to the more volatile component.

<i>Origin of the deviations from ideality</i>	<i>Molecule 1</i>	<i>Molecule 2</i>	<i>References</i>
Deviations from ideality not assessed	ethylene	dichloromethane	[643]
	nitrogen	chlorodifluoromethane	[644–647]
Ideal	chloroform	Benzene	[373,639,648–654]
	chloroform	1,2-dichloroethane	[655–657]
	chloroform	carbon tetrachloride	[658–661]
	1,1,1-trifluoroethane	2,3,3,3-tetrafluoropropene	[662]
	ethyl fluoride	1,1,1,2-tetrafluoroethane	[663]
	propylene	chlorodifluoromethane	[664]
	Non-ideal with non-assessed causes	difluoromethane	Propane
trifluoromethane		Ethane	[670,671]
carbon tetrafluoride		chlorodifluoromethane	[672,673]
pentafluoroethane		Propane	[666,668,674–676]
carbon tetrafluoride		trifluoromethane	[677]
hexafluoroethane		1,1,1,2-tetrafluoroethane	[664,678]
decafluorobutane		1,1,1,3,3-pentafluorobutane	[679]
Non-ideal with enthalpic causes	chlorodifluoromethane	dichlorodifluoromethane	[680–685]

---

<i>Origin of the deviations from ideality</i>	<i>Molecule 1</i>	<i>Molecule 2</i>	<i>References</i>
	dichloromethane	carbon tetrachloride	<a href="#">[425,428,659,686]</a>
	chloroform	n-hexane	<a href="#">[687–693]</a>
Non-ideal with enthalpic and entropic causes	chloroform	n-heptane	<a href="#">[687,690,691,693–695]</a>
	dichloromethane	n-pentane	<a href="#">[696–698]</a>

---

**Table PVI.7.** List of the 22 binary systems for which the binary association code is: BAC=4 (HA-HA or HD-HD). Such a BAC corresponds to a binary system involving two “Hydrogen-Acceptor” (HA) molecules or two “Hydrogen-Donor” (HD) molecules. Corresponding origin of the deviations from ideality and list of the references in which the experimental data can be found. By convention, *Molecule 1* refers to the more volatile component.

<i>Origin of the deviations from ideality</i>	<i>Molecule 1</i>	<i>Molecule 2</i>	<i>References</i>
Deviations from ideality not assessed	carbon dioxide	dimethyl ether	[699–701]
	carbon dioxide	hydrogen sulfide	[702–705]
	carbon dioxide	ethyl acetate	[706–710]
	carbon dioxide	carbon disulfide	[711,712]
	carbon dioxide	dimethyl carbonate	[713–718]
	carbon monoxide	carbon dioxide	[719–721]
	oxygen	carbon dioxide	[532,533,722–725]
Ideal	pentafluoroethane	1,1,1,2-tetrafluoroethane	[726–730]
	chlorodifluoromethane	1,1,1,2-tetrafluoroethane	[731,732]
	difluoromethane	1,1,1,2-tetrafluoroethane	[726,727,729,730,733–737]
	1,1,1,2-tetrafluoroethane	1,1-difluoroethane	[664,738,739]
	ethyl acetate	1,4-dioxane	[553,740–742]
	dimethyl carbonate	diethyl carbonate	[743–745]
	1,2-epoxybutane	dimethyl carbonate	[746]
Non-ideal with non-assessed causes	dimethyl ether	sulfur dioxide	[747–749]

---

<i>Origin of the deviations from ideality</i>	<i>Molecule 1</i>	<i>Molecule 2</i>	<i>References</i>
	trifluoromethane	chlorodifluoromethane	<a href="#">[750,751]</a>
	diethyl ether	acetone	<a href="#">[651,752,753]</a>
Non-ideal with enthalpic causes	carbon disulfide	acetone	<a href="#">[754–756]</a>
	triethylamine	1,4-dioxane	<a href="#">[757,758]</a>
Non-ideal with entropic causes	thiophene	sulfolane	<a href="#">[759]</a>
	tetrahydrofuran	N,N-dimethylformamide	<a href="#">[760,761]</a>
Non-ideal with enthalpic and entropic causes	n-butyl acetate	N,N-dimethylformamide	<a href="#">[762,763]</a>

---

**Table PVI.8.** List of the 18 binary systems for which the binary association code is: BAC=5 (SA-NA). Such a BAC corresponds to a binary system involving a “Self-Associating” (SA) molecule + a “Non-Associating” (NA) molecule. Corresponding origin of the deviations from ideality and list of the references in which the experimental data can be found. By convention, *Molecule 1* refers to the more volatile component.

<i>Origin of the deviations from ideality</i>	<i>Molecule 1</i>	<i>Molecule 2</i>	<i>References</i>
Deviations from ideality not assessed	n-butane	water	[764–768]
	water	benzene	[769–773]
	ethane	1-propanol	[774–779]
	nitrogen	ammonia	[780–782]
	ethane	water	[765]
	nitrogen	water	[783–793]
Ideal	diethylamine	benzene	[413,794,795]
	diethylamine	monochlorobenzene	[413,796]
Non-ideal with non-assessed causes	ethane	methanol	[776,797–802]
	propane	methanol	[803–807]
Non-ideal with enthalpic causes	1-propanol	benzene	[468,808–816]
	ethanol	benzene	[458,461,476,648,813,816–826]
	isopropanol	2,2,4-trimethylpentane	[827–834]
	2-butanol	cyclohexane	[835–840]
Non-ideal with enthalpic and entropic causes	1-propanol	n-hexane	[841–847]

---

<i>Origin of the deviations from ideality</i>	<i>Molecule 1</i>	<i>Molecule 2</i>	<i>References</i>
	ethanol	n-heptane	<a href="#">[848–864]</a>
	methanol	n-hexane	<a href="#">[847,856,865–873]</a>
	methanol	benzene	<a href="#">[813,816,823,874–884]</a>

---

**Table PVI.9.** List of the 25 binary systems for which the binary association code is: BAC=6 (HD-HA). Such a BAC corresponds to a binary system involving a “Hydrogen-Donor” (HD) molecule + a “Hydrogen-Acceptor” (HA) molecule. Corresponding origin of the deviations from ideality and list of the references in which the experimental data can be found. By convention, *Molecule 1* refers to the more volatile component.

<i>Origin of the deviations from ideality</i>	<i>Molecule 1</i>	<i>Molecule 2</i>	<i>References</i>
Deviations from ideality not assessed	carbon dioxide	chlorodifluoromethane	[644,645,751,885]
	carbon dioxide	1,1,1,2-tetrafluoroethane	[886–889]
	carbon dioxide	1,1,1,2,3,3,3-heptafluoropropane	[890,891]
	trifluoromethane	carbon disulfide	[751]
	chloroform	diisopropyl ether	[693,758,892,893]
	1,1,1-trifluoroethane	dimethyl ether	[894]
	chloroform	n-butyl ethyl ether	[892,895]
Ideal	carbon dioxide	difluoromethane	[737,896–898]
	difluoromethane	dimethyl ether	[899–901]
	difluoromethane	sulfur dioxide	[902]
	ethyl acetate	trichloroethylene	[903]
Non-ideal with non-assessed causes	sulfur dioxide	1,1,1,2,3,3,3-heptafluoropropane	[904]
	chlorodifluoromethane	dimethyl ether	[905]
	chlorodifluoromethane	carbon disulfide	[751]
	pentafluoroethane	dimethyl ether	[675,906]
	3-pentanone	1,1,2,2-tetrachloroethane	[907]

<i>Origin of the deviations from ideality</i>	<i>Molecule 1</i>	<i>Molecule 2</i>	<i>References</i>
	dimethyl ether	1,1,1,3,3,3-hexafluoropropane	[908,909]
Non-ideal with enthalpic causes	dichloromethane	carbon disulfide	[910,911]
	acetone	chloroform	[640,642,652,688,693,758,912–919]
	chloroform	ethyl acetate	[920–923]
	chloroform	tetrahydrofuran	[655,693,924–927]
Non-ideal with enthalpic and entropic causes	chloroform	di-n-propyl ether	[693,892,893,895,928,929]
	methyl acetate	chloroform	[693,920,930,931]
	cyclopentanone	1,1,2,2-tetrachloroethane	[932–934]
	ethyl acetate	1,1,2,2-tetrachloroethane	[935,936]

**Table PVI.10.** List of the 16 binary systems for which the binary association code is: BAC=7 (SA-HD). Such a BAC corresponds to a binary system involving a “Self-Associating” (SA) molecule + a “Hydrogen-Donor” (HD) molecule. Corresponding origin of the deviations from ideality and list of the references in which the experimental data can be found. By convention, *Molecule 1* refers to the more volatile component.

<i>Origin of the deviations from ideality</i>	<i>Molecule 1</i>	<i>Molecule 2</i>	<i>References</i>
Deviations from ideality not assessed	chloroform	1-butanol	[650,937,938]
	1-propanol	trichloroethylene	[939,940]
	trichloroethylene	1-butanol	[940,941]
	isopropanol	trichloroethylene	[939,942]
	2-butanol	trichloroethylene	[941,942]
	1-hexyne	acetonitrile	[943,944]
	isopropanol	chloroform	[938,945,946]
Non-ideal with enthalpic causes	ethanol	1-heptyne	[947,948]
Non-ideal with entropic causes	ethanol	chloroform	[650,695,938,949–954]
	chloroform	acetic acid	[955–959]
	methanol	halothane	[960–962]
	trichloroethylene	2-methoxyethanol	[963,964]
Non-ideal with enthalpic and entropic causes	chloroform	acetonitrile	[965–970]
	ethyl formate	chloroform	[920,922]
	chloroform	1-propanol	[651,938,971,972]
	n-propyl formate	1,1,2,2-tetrachloroethane	[935,973]

**Table PVI.11.** List of the 26 binary systems for which the binary association code is: BAC=8 (SA-HA). Such a BAC corresponds to a binary system involving a “Self-Associating” (SA) molecule + a “Hydrogen-Acceptor” (HA) molecule. Corresponding origin of the deviations from ideality and list of the references in which the experimental data can be found. By convention, *Molecule 1* refers to the more volatile component.

<i>Origin of the deviations from ideality</i>	<i>Molecule 1</i>	<i>Molecule 2</i>	<i>References</i>
Deviations from ideality not assessed	carbon dioxide	water	[974–992]
	carbon dioxide	ethanol	[487,510,775,847,993–1007]
	ethanol	methyl tert-butyl ether	[548,1008–1012]
	carbon dioxide	2-methyl-1-propanol	[1013–1018]
	carbon monoxide	methanol	[1019–1021]
	carbon dioxide	1-pentanol	[510,1015,1022–1025]
Ideal	diethylamine	ethyl acetate	[741,742]
	diethylamine	triethylamine	[1026–1029]
	2-methyl-2-propanol	methyl tert-butyl ether	[1030–1033]
	acetonitrile	1,4-dioxane	[1034–1036]
Non-ideal with non-assessed causes	dimethyl ether	water	[701,1037–1040]
	carbon dioxide	methanol	[488,489,510,701,847,999,1004,1007,1019,1041–1051]
Non-ideal with enthalpic causes	methanol	ethyl acetate	[1052–1059]
	isopropanol	diisopropyl ether	[829,1010,1060,1061]
	methanol	n-butyl acetate	[1057,1062–1064]

Publications

<i>Origin of the deviations from ideality</i>	<i>Molecule 1</i>	<i>Molecule 2</i>	<i>References</i>
	diethyl ether	ethanol	[1065–1067]
	methanol	1,4-dioxane	[1068–1073]
	methanol	thiophene	[874]
	ethanol	di-n-butyl ether	[1067,1074–1076]
Non-ideal with entropic causes	methanol	diisopropyl ether	[1010,1077–1079]
	methanol	methyl tert-butyl ether	[545,547,548,1009,1078,1080–1084]
	ethanol	ethyl acetate	[1054,1057,1058,1076,1085–1092]
Non-ideal with enthalpic and entropic causes	acetone	water	[603,878,1093–1104]
	ethanol	methyl ethyl ketone	[559,1105–1112]
	ethanol	acetone	[854,1113–1118]
	methanol	acetone	[599,603,1098,1119–1124]

**Table PVI.12.** List of the 23 binary systems for which the binary association code is: BAC=9 (SA-SA). Such a BAC corresponds to a binary system involving a “Self-Associating” (SA) molecule + another “Self-Associating” (SA) molecule. Corresponding origin of the deviations from ideality and list of the references in which the experimental data can be found. By convention, *Molecule 1* refers to the more volatile component.

<i>Origin of the deviations from ideality</i>	<i>Molecule 1</i>	<i>Molecule 2</i>	<i>References</i>
Deviations from ideality not assessed	water	ethylenediamine	[1125–1127]
	water	1-pentanol	[1128–1131]
	methanol	1-butanol	[878,1132–1136]
Ideal	ethanol	acetic acid	[1092,1137–1140]
	methanol	ethanol	[923,1136,1141–1147]
	2-methyl-2-propanol	1-butanol	[1148–1150]
	ethanol	3-methyl-1-butanol	[1151–1153]
	methanol	3-methyl-1-butanol	[1153–1155]
	methanol	1-propanol	[864,1101,1136,1146,1147,1156–1159]
	ammonia	water	[1160–1169]
Non-ideal with non-assessed causes	ammonia	acetonitrile	[1170]
	water	allyl alcohol	[1171,1172]
Non-ideal with enthalpic causes	water	phenol	[1173–1179]
	methyl formate	methanol	[1180–1184]
	ethyl formate	water	[1185,1186]

Publications

<i>Origin of the deviations from ideality</i>	<i>Molecule 1</i>	<i>Molecule 2</i>	<i>References</i>
	ethanol	ethyl formate	[1184,1187–1189]
	1-butanol	nitromethane	[1147,1190–1194]
Non-ideal with entropic causes	water	2-butoxyethanol	[1195–1200]
	water	propylene glycol monomethyl ether	[1196]
Non-ideal with enthalpic and entropic causes	ethanol	water	[1085,1101,1142,1201–1221]
	water	acetonitrile	[1222–1231]
	methanol	water	[1098,1204,1218,1219,1232–1249]
	isopropanol	water	[854,1206,1250–1256]



### **PVI.III Grading of a thermodynamic model by means of the proposed database in order to assess its accuracy**

This section focuses initially on the methodology that has to be followed in order to evaluate the deviations between model predictions and experimental data (in particular, which property of each data set must be specified and which property must be calculated from the thermodynamic model and compared to an experimental value). It is then explained how a thermodynamic model may be graded. The methodology described hereafter to assess the accuracy of a model is specific but we believe this approach is necessary to fairly compare the scores obtained by two thermodynamic models. It is exactly what happens with the grading of students: the professor establishes a very detailed marking scheme before marking the examination papers.

#### **PVI.III.I Evaluation of the deviations between model predictions and experimental data**

In order to fairly cross-compare two thermodynamic models, we are convinced that the deviations between model predictions and experimental data have to be calculated in the same way, i.e., following the same procedure. However, in accordance with the Gibbs's phase rule there is not a unique way to perform a fluid-phase equilibrium (VLE, LLE, VLLE, critical point, azeotropic point) calculation. It is always necessary to first determine the *variance* (also called *the number of degrees of freedom*) of the system, then to specify a number of intensive variables equal to the variance and finally to calculate the other intensive variables (those that will be compared to the experimental data). The variables that are specified and those that are calculated can however be freely chosen. To fix the ideas, let us consider the VLE calculation of a binary system for which the temperature  $T$ , pressure  $P$  and composition of the liquid ( $x_1$ ) and gas ( $y_1$ ) phases were experimentally measured. For such a system the number of degrees of freedom (the variance) is equal to 2 and it is thus necessary to specify two variables among  $(T, P, x_1, y_1)$  and to calculate the two others. The arbitrary choice made in this paper is to specify  $T$  and  $P$  (i.e., to fix  $T$  and  $P$  to their experimental values) and to calculate, in turn,  $x_1$  and  $y_1$ . There are thus no deviations between model predictions and experimental values of  $T$  and  $P$  but instead deviations over  $x_1$  and  $y_1$ . Specifying  $T$  and  $P$  and calculating  $x_1$  and  $y_1$  is somehow similar to a T,P-flash calculation [1257]. For each property available in the proposed database, [Table PVI.13](#) reports the variance, the specified and the calculated variables. In other words, [Table PVI.13](#) dictates the methodology that has to be strictly followed in order to evaluate the deviations between model predictions and experimental data by means of the proposed database.

[Table PVI.13](#) highlights that for systems of variance equal to 2 (two-phase equilibrium binary systems), we arbitrarily decided that temperature and pressure should be specified whereas phase compositions should be calculated. For systems of unitary variance (binary critical point, binary azeotropic point, binary three-phase equilibrium), we decided that the temperature should be specified and that other variables (critical pressure and composition, azeotropic pressure and composition, three-phase pressure and compositions) should be calculated.

**Table PVI.13.** Specified and calculated variables for the different binary-system properties involved in the database.

Property	Variance	Measured variables	Specified variables	Calculated variables (to be compared with experimental data values)
Critical point	1	$T, P, x_1$	$T$	$P, x_1$
Azeotropic point	1	$T, P, x_1$	$T$	$P, x_1$
Two-phase equilibrium data (VLE or LLE)	2	$\begin{cases} T, P, x_1, y_1 \text{ for VLE} \\ T, P, x_1^\alpha, x_1^\beta \text{ for LLE} \end{cases}$	$T, P$	$\begin{cases} x_1, y_1 \text{ for VLE} \\ x_1^\alpha, x_1^\beta \text{ for LLE} \end{cases}$
Three-phase equilibrium data (VLLE)	1	$T, P, x_1^\alpha, x_1^\beta, y_1$	$T$	$P, x_1^\alpha, x_1^\beta, y_1$
Enthalpy of mixing	N.A. <sup>(*)</sup>	$T, P, z_1, h^M$	$T, P, z_1$	$h^M$
Heat capacity of mixing	N.A. <sup>(*)</sup>	$T, P, z_1, c_P^M$	$T, P, z_1$	$c_P^M$

(\*) Not Applicable because global variables (here global mole fractions  $z_1$  and  $z_2 = 1 - z_1$ ) are involved. Let us indeed recall that the phase rule that defines the variance only considers intensive variables specific to one of the phases.

The calculation of the deviations between model predictions and experimental data for mixing properties does not need to make arbitrary choices on the specified and calculated variables; there is indeed a unique way to perform the calculation. For such properties, the temperature, the pressure, the global composition  $z_1$ , and  $h^M$  (or  $c_P^M$ ) are experimentally determined. Depending on  $(T, P, z_1)$ , the binary system can be either in a one-phase or in a two-phase region so that a T,P-flash calculation has first to be performed at specified temperature, pressure and global composition in order to determine the number of phases in equilibrium, their composition and their proportions. Once done,  $h^M$  or  $c_P^M$  can be straightforwardly calculated for the specified  $(T, P, z_1)$  values [1258]. It is worth noting that the experimentalists who performed  $h^M$  or  $c_P^M$  measurements do not mention systematically the pressure at which the measurements were conducted although such a value is required to perform the calculation from an EoS. This usually happens for mixing properties related to a liquid phase on which the pressure has a negligible influence. When this happened, the assumed experimental pressure was determined by trial and errors so that the calculated physical state of the system agrees with the experimentally-observed state. The first guessed pressure is always the atmospheric pressure. In the Excel files *database.xlsx* and *BACi with visualization of the data.xlsx* (i=1 to 9) – available as Supporting Information (Appendix E) – that contain all the experimental data, the experimental pressure appears as **unknown** and the assumed experimental pressure is indicated in parentheses. For clarity, an example is given in Figure PVI.3. In this example, the unknown (not stated) experimental pressure has to be replaced by the atmospheric pressure (1.0132 bar).

---

**Enthalpy of mixing (Methane + Ethane system)**

---

Miller, R. C. - Staveley, L. A. K., *Advances in Cryogenic Engineering*. (1960) 493-500

<b>T / K =</b>	<b>91.50</b>
<b>P / bar =</b>	<b>UNKNOWN (1.0132)</b>
$h^M / \text{J.mol}^{-1}$	$x_1$
67.00	0.2825
80.00	0.4008
82.70	0.5105
84.90	0.6039
77.60	0.7044
65.80	0.7879

**Figure PVI.3.** Notation used in the files *database.xlsx* and *BACi with visualization of the data.xlsx* (i=1 to 9) when the experimental pressure is not mentioned.

Lastly, for any calculated property  $X$ , the MAPE (Mean Absolute Percentage Error) was selected to quantify the deviation between experimental and calculated data:

$$MAPE_X (\%) = \frac{1}{N_{data}} \sum_{i=1}^{N_{data}} 100 \cdot \left| \frac{X_i^{EXP} - X_i^{MODEL}}{X_i^{EXP}} \right| \quad (\text{PVI.5})$$

### PVI.III.II Treatment of “out-of-model” data points

It may happen that the isothermal or isobaric phase diagram – calculated with the thermodynamic model we want to grade – does not have the expected topology. To fix the ideas, it may happen that a model does not predict the existence of a homogeneous azeotrope that is however experimentally observed. In such a case, the MAPE on  $P_{az}$  and  $x_{az}$  cannot be evaluated and the corresponding experimental data point is said to be “*out of model*” (not calculable by the model). When such a situation arises, the experimental data point must be rejected, i.e., not taken into account in Eq. (PVI.5) to evaluate the  $MAPE_X (\%)$ . In other words, we simply apply:  $N_{data} = N_{data} - 1$  in Eq. (PVI.5). Here below, are detailed all the cases in which *out of model* data points could appear.

**Case 1:** at specified T and P ( $T = T_{exp}$  and  $P = P_{exp}$ ), a 2-phase system is experimentally observed whereas the model predicts a 1-phase system. All the experimental data points for which the model predicts a 1-phase system are declared “out of model”. This case is illustrated in [Figure PVI.4](#) (panel a).

**Case 2:** at specified T and P ( $T = T_{exp}$  and  $P = P_{exp}$ ), a 2-phase system is experimentally observed and a 2-phase system is also predicted by the model. However, it was experimentally found that  $y_{1,exp} > x_{1,exp}$  (respectively  $y_{1,exp} < x_{1,exp}$ ) and the model predicts the wrong topology, i.e., predicts  $y_{1,cal} < x_{1,cal}$  (respectively  $y_{1,cal} > x_{1,cal}$ ). All these experimental data points are declared *out of model*. This case – that typically appears when the azeotropic composition is not properly predicted by the model – is illustrated in [Figure PVI.4](#) (panel b).

**Case 3:** a homogeneous azeotrope is experimentally observed at  $T = T_{\text{exp}}$  whereas the model predicts a different topology (a zeotropic behavior or a heterogeneous azeotrope). The experimental homogeneous azeotropic point is declared "out of model". This case is illustrated in Figure PVI.4 (panel b and c).

**Case 4:** a 3-phase line (VLE) is experimentally observed at  $T = T_{\text{exp}}$  whereas the model does not predict such a behavior. The experimental 3-phase line is thus declared "out of model". This case is illustrated in Figure PVI.4 (panel d).

**Case 5:** the number of calculated critical points at  $T = T_{\text{exp}}$  is different to the number of critical points experimentally observed. As an example, the binary system may exhibit 2 experimental critical points whereas 1 or zero are returned by the model (see e.g. Figure PVI.4 – panel e). The opposite may also happen: the binary system exhibits a unique critical point but 2 are returned by the model (see, e.g., Figure PVI.4 – panel f).

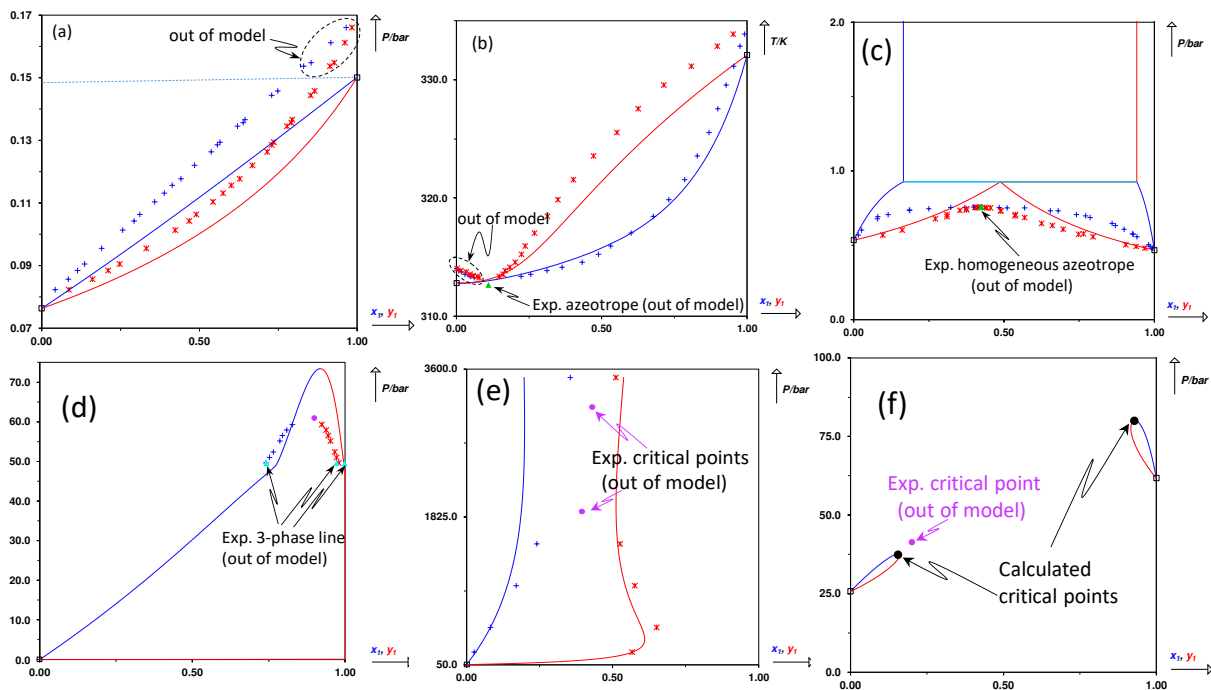


**Figure PVI.4.** Illustration of all the cases in which *out of model* data points can appear. For such exp. data points, the MAPE cannot be evaluated. (a): experimentally 2-phase data points that are found to be 1-phase by the model. (b) An azeotropic system is predicted as a zeotropic system so that the homogeneous azeotrope is declared out of model. In addition, for small mole fractions,  $y_{1,\text{exp}} > x_{1,\text{exp}}$  whereas the model predicts the opposite. (c) A homogeneous azeotrope is predicted as heterogeneous. (d) A 3-phase line is not predicted by the model. (e) 2 critical points that are not predicted by the model are experimentally observed. (f) The model predicts 2 critical points whereas only one is experimentally observed.

### PVI.III.III Grading of a thermodynamic model

Our objective is to give a unique mark over 20 to a given thermodynamic model to immediately be able to benchmark its accuracy against the accuracy of other models. A grade of 20/20 is the highest attainable mark. It is only obtained if the model is able to exactly reproduce (with 0% deviation) all the experimental data available in the proposed database. In all other cases, a score lower than 20 will be assigned to the model. Once the MAPEs are calculated (see Eq. (PVI.5)), the scoring of a thermodynamic model starts by giving a mark over 20 to each of the nine families of binary systems, each identified by its BAC. Such a mark is actually an average over ten marks (one for each of the ten calculated properties defined in the last column of Table PVI.13), that are:

- |   |   |
|---|---|
| 1) critical pressure,                               | (6) gas phase (or 2 <sup>nd</sup> liquid phase) composition |
| (2) critical composition,                           | ( $y_1, x_1^\beta$ ),                                       |
| (3) azeotropic pressure,                            | (7) three-phase pressure,                                   |
| (4) azeotropic composition,                         | (8) three-phase compositions,                               |
| (5) liquid phase composition ( $x_1, x_1^\alpha$ ), | (9) mixing enthalpy,  |
|   | (10) mixing heat capacity.                                  |

Once done, a thermodynamic model is characterized by nine marks (one for each BAC). In a second step, the number of marks is reduced from nine to four by averaging the marks got by some BACs in order to only retain four categories of binary systems based on the type of association they exhibit:

- The marks obtained by  $BAC_1 + BAC_2 + BAC_3 + BAC_4$  are averaged because all these systems do not exhibit association (see Table PVI.1). In Eq. (PVI.6), the resulting average mark is noted  $mark_{NA}$  (where NA stands for "no association").

- The mark obtained by  $BAC_5$  is kept as a single mark because in this type of systems - and only in this one - self-association tends to be broken (see Table PVI.1). In Eq. (PVI.6),  $mark_{BAC_5}$  is noted  $mark_{SA}$  (where SA stands for "self-association")

- The mark obtained by  $BAC_6$  is kept as a single mark because in this type of systems - and only in this one - cross-association without the presence of self-association is observed.  $BAC_6$  refers to binary systems in which cross-association takes place alone (see Table PVI.1). In Eq. (PVI.6),  $mark_{BAC_6}$  is noted  $mark_{CA}$  (where CA stands for "cross-association")

- The marks obtained by  $BAC_7 + BAC_8 + BAC_9$  are averaged because all these systems both exhibit cross-association and self-association (see Table PVI.1). In Eq. (PVI.6), the resulting average mark is noted  $mark_{CA+SA}$  (where CA+SA stands for "cross-association + self-association").

The unique final mark given to a thermodynamic model is obtained by averaging the 4 marks (see Eq. (PVI.6)) relative to (i) systems without association, (ii) systems in which self-association tends to be

broken, (iii) systems in which cross-association takes place alone and (iv) systems in which both cross-association and self-association take place.

$$\left\{ \begin{array}{l} \text{Final mark} \\ \text{of a thermodynamic model} \\ \text{(over 20)} \end{array} \right. = \frac{1}{4} \times \left[ \underbrace{\text{mark}_{NA}}_{\text{no association}} + \underbrace{\text{mark}_{SA}}_{\text{self-association}} + \underbrace{\text{mark}_{CA}}_{\text{cross-association}} + \underbrace{\text{mark}_{CA+SA}}_{\text{cross-association}} \right. \\ \left. \underbrace{\hspace{15em}}_{\text{+ self-association}} \right] \\ \text{average of 4 marks} \\ \text{with: } \left\{ \begin{array}{l} \text{mark}_{NA} = \frac{\text{mark}_{BAC_1} + \text{mark}_{BAC_2} + \text{mark}_{BAC_3} + \text{mark}_{BAC_4}}{4} \\ \text{mark}_{SA} = \text{mark}_{BAC_5} \\ \text{mark}_{CA} = \text{mark}_{BAC_6} \\ \text{mark}_{CA+SA} = \frac{\text{mark}_{BAC_7} + \text{mark}_{BAC_8} + \text{mark}_{BAC_9}}{3} \end{array} \right. \quad \text{(PVI.6)}$$

The procedure aimed at giving a mark over 20 to a given BAC ( $\text{mark}_{BAC_i}$ ) is now detailed. As previously stated, such mark is, in itself, the average value of 10 marks (in liquid phase composition  $x$  (or  $x^\alpha$ ), gas phase (or 2<sup>nd</sup> liquid phase) composition  $y$  (or  $x^\beta$ ), three-phase pressure  $P_{LLV}$ , three-phase compositions  $z_{LLV}$ , critical pressure  $P_c$ , critical composition  $x_c$ , azeotropic pressure  $P_{az}$ , azeotropic composition  $x_{az}$ , mixing enthalpy  $h^M$ , mixing heat capacity  $c_p^M$ ), each defined below.

- (1) Mark in liquid phase composition ( $x$  for VLE and  $x^\alpha$  for LLE):

$$\text{Mark}_{x \text{ or } x^\alpha} = 20 - 0.5 \times \left[ \frac{\text{MAPE on } x_1 \text{ or } x_1^\alpha (\%) + \text{MAPE on } x_2 \text{ or } x_2^\alpha (\%)}{2} \right] \quad \text{(PVI.7)}$$

where  $x_i$  (respectively  $x_i^\alpha$ ) is the mole fraction of component  $i$  in the liquid phase (respectively  $\alpha$ -liquid phase).

- (2) Mark in gas phase ( $y$ ) or 2<sup>nd</sup> liquid phase ( $x^\beta$ ) composition:

$$\text{Mark}_{y \text{ or } x^\beta} = 20 - 0.5 \times \left[ \frac{\text{MAPE on } y_1 \text{ or } x_1^\beta (\%) + \text{MAPE on } y_2 \text{ or } x_2^\beta (\%)}{2} \right] \quad \text{(PVI.8)}$$

where  $y_i$  (respectively  $x_i^\beta$ ) is the mole fraction of component  $i$  in the gas or second liquid phase.

**Remark:** very small (or close to 1) mole fractions may lead to huge percent deviations. As an example, at  $T/K = 377.59$  K and  $P = 1.379$  bar, the solubility of n-butane in water is  $x_{1,\text{exp}} = 0.000002$ . In the case a model calculates  $x_1 = 0.000082$ , the corresponding  $\frac{1}{2} \times (\text{MAPE on } x_1 + \text{MAPE on } x_2)$  relative to this unique data point is about 2000 % even though the absolute deviation is extremely small ( $|x_{1,\text{exp}} - x_{1,\text{cal}}| = 0.00008$ ). Such a datapoint can thus have a huge influence on the calculated  $\text{Mark}_{x \text{ or } x^\alpha}$  (or  $\text{Mark}_{y \text{ or } x^\beta}$ ). To avoid such a bias, if:

$$\begin{cases} z_{1, \text{exp}} < 0.01 \\ \text{or} \\ z_{1, \text{exp}} > 0.99 \end{cases} \text{ and simultaneously } \frac{1}{2} \times (\text{MAPE on } z_1 + \text{MAPE on } z_2) > 45\% \quad (\text{PVI.9})$$

where  $z_1$  stands for the mole fraction of component 1 in the liquid or gas phase of a 2-phase system (VLE or LLE), the corresponding datapoint is rejected (we here mean, it is not taken into account in Eq. (PVI.5) in order to annihilate its influence on the calculated  $Mark_{x \text{ or } x^\alpha}$  (or  $Mark_{y \text{ or } y^\beta}$ )).

- (3) Mark in three-phase pressure,  $P_{LLV}$  :

$$Mark_{P_{LLV}} = 20 - 0.50 \times \text{MAPE on } P_{LLV} (\%) \quad (\text{PVI.10})$$

- (4) Mark in three-phase composition,  $z_{LLV}$  :

$$Mark_{z_{LLV}} = 20 - 0.5 \times \sum_{i=1}^2 \left[ \frac{\text{MAPE on } x_i^\alpha (\%) + \text{MAPE on } x_i^\beta (\%) + \text{MAPE on } y_i (\%)}{6} \right] \quad (\text{PVI.11})$$

where  $x_i^\alpha$ ,  $x_i^\beta$ ,  $y_i$  are the mole fractions of component  $i$  in each of the three equilibrium phases.

- (5) Mark in critical pressure,  $P_c$  :

$$Mark_{P_c} = 20 - 0.75 \times \text{MAPE on } P_c (\%) \quad (\text{PVI.12})$$

- (6) Mark in critical composition,  $x_c$  :

$$Mark_{x_c} = 20 - 0.5 \times \left[ \frac{\text{MAPE on } x_{1,c} (\%) + \text{MAPE on } x_{2,c} (\%)}{2} \right] \quad (\text{PVI.13})$$

where  $x_{i,c}$  is the mole fraction of component  $i$  at the critical point.

- (7) Mark in azeotropic pressure,  $P_{az}$  :

$$Mark_{P_{az}} = 20 - 0.50 \times \text{MAPE on } P_{az} (\%) \quad (\text{PVI.14})$$

- (8) Mark in azeotropic composition,  $x_{az}$  :

$$Mark_{x_{az}} = 20 - 0.5 \times \left[ \frac{\text{MAPE on } x_{1,az} (\%) + \text{MAPE on } x_{2,az} (\%)}{2} \right] \quad (\text{PVI.15})$$

where  $x_{i,az}$  is the mole fraction of component  $i$  at the azeotropic point.

- (9) Mark in mixing enthalpy,  $h^M$  :

$$Mark_{h^M} = 20 - 0.25 \times \frac{1}{N_{data}} \sum_{i=1}^{N_{data}} \frac{1}{2} \left( 100 \cdot \left| \frac{h_i^{M,EXP} - h_i^{M,MODEL}}{h_i^{M,EXP}} \right| + 100 \cdot \left| \frac{h_i^{M,EXP} - h_i^{M,MODEL}}{h_i^{M,MODEL}} \right| \right) \quad (\text{PVI.16})$$

Remarks:

1.  $h^M$  goes to zero when the mole fraction of the studied phase ( $z_1$ ) goes to zero or one. In such cases, huge percent deviations and consequently very bad marks on  $h^M$  can be obtained. To avoid such a bias, if in Eq. (PVI.16):

$$\frac{1}{2} \left( 100 \cdot \left| \frac{h_i^{M,EXP} - h_i^{M,MODEL}}{h_i^{M,EXP}} \right| + 100 \cdot \left| \frac{h_i^{M,EXP} - h_i^{M,MODEL}}{h_i^{M,MODEL}} \right| \right) > 80\% , \text{ this quantity is set to } 80\% .$$

2. Eq. (PVI.16) highlights that we here decided to make the average between 2 MAPEs: one calculated with the classical definition (see Eq. (PVI.5)) and one obtained by introducing  $h_i^{M,MODEL}$  (i.e., the calculated value) at the denominator. This procedure is selected in order to obtain the same mark when calculated values of  $h^M$  are  $n$  times (e.g. twice) smaller or  $n$  times larger than the experimental values. To fix the ideas, let us assume that  $h^{M,EXP} = 100 \text{ J} \cdot \text{mol}^{-1}$ . If the calculated value is 50 times too small, let us say:  $h^{M,MODEL} = 2 \text{ J} \cdot \text{mol}^{-1}$  then Eq. (PVI.5) returns a  $MAPE_{h^M} (\%) = 98\%$ . In contrast, if the calculated value is 50 times too large, that is:  $h^{M,MODEL} = 5000 \text{ J} \cdot \text{mol}^{-1}$  then Eq. (PVI.5) returns a  $MAPE_{h^M} (\%) = 4900\%$ . As a direct consequence, the classical MAPE definition favors the case where  $h^{M,MODEL}$  is 50 times below  $h^{M,EXP}$ . However, for both cases ( $h^{M,MODEL} = 2 \text{ J} \cdot \text{mol}^{-1}$  or  $h^{M,MODEL} = 5000 \text{ J} \cdot \text{mol}^{-1}$ ), the average of the 2 MAPEs embedded in Eq. (PVI.16) is exactly the same. For the selected example:

$$\frac{1}{2} \left( 100 \cdot \left| \frac{h_i^{M,EXP} - h_i^{M,MODEL}}{h_i^{M,EXP}} \right| + 100 \cdot \left| \frac{h_i^{M,EXP} - h_i^{M,MODEL}}{h_i^{M,MODEL}} \right| \right) = 2499\% .$$

In practice,  $h^M$  is used to evaluate molar enthalpies of the streams ( $h_{stream} = z_1 h_1 + z_2 h_2 + h^M$ ) that are involved in the energy balance of a given process. The mark determined by Eq. (PVI.16) thus needs to capture the influence of  $h^M$  on such a balance. One possibility to reach this target is to convert the difference  $|h_i^{M,EXP} - h_i^{M,MODEL}|$  into terms of temperature effect [1258]  $\Delta T_h$  through:

$$\Delta T_h = \frac{|h_i^{M,EXP} - h_i^{M,MODEL}|}{c_P} \quad (\text{PVI.17})$$

where  $c_P$  is the molar isobaric heat capacity of the mixture.  $\Delta T_h$  quantifies the error made in the estimation of the final temperature of a mixture obtained by mixing two pure compounds at isobaric and adiabatic conditions. From our experience in process simulation, we decided to consider that  $\Delta T_h = 1.4 \text{ K}$  was a good reference. In many cases, such a deviation is reached when  $h^M$  is estimated with a deviation of around 20% and Eq. (PVI.16) is conceived so that with this deviation the mark is equal to 15/20.

- (10) Mark in mixing heat capacity,  $c_P^M$  :

$$Mark_{c_P^M} = 20 - 0.10 \times \frac{1}{N_{data}} \sum_{i=1}^{N_{data}} \frac{1}{2} \left( 100 \cdot \left| \frac{c_{P,i}^{M,EXP} - c_{P,i}^{M,MODEL}}{c_{P,i}^{M,EXP}} \right| + 100 \cdot \left| \frac{c_{P,i}^{M,EXP} - c_{P,i}^{M,MODEL}}{c_{P,i}^{M,MODEL}} \right| \right) \quad (\text{PVI.18})$$

This mark was built in a similar manner to  $Mark_{h^M}$  so that the following remarks apply.

**Remarks:**

1. Analogously to  $h^M$ ,  $c_P^M$  goes to zero when the mole fraction of the studied phase ( $z_i$ ) goes to zero or one. In such cases, huge percent deviations and consequently very bad marks on  $c_P^M$  can be obtained. To avoid such a bias, if in Eq. (PVI.18):

$$\frac{1}{2} \left( 100 \cdot \left| \frac{c_{P,i}^{M,EXP} - c_{P,i}^{M,MODEL}}{c_{P,i}^{M,EXP}} \right| + 100 \cdot \left| \frac{c_{P,i}^{M,EXP} - c_{P,i}^{M,MODEL}}{c_{P,i}^{M,MODEL}} \right| \right) > 200\% \text{ this quantity is set to } 200\%.$$

The choice of Eq. (PVI.18) is based on the fact that for the data points embedded in the proposed database, we noticed that a deviation of 50% on  $c_P^M$  lead to an average deviation of only 2% on the molar isobaric heat capacity of the corresponding stream calculated as:  $c_{P,stream} = z_1 c_{P,1} + z_2 c_{P,2} + c_P^M$ . In consequence, Eq. (PVI.18) is built so that a deviation of 50% on  $c_P^M$  leads to a good mark of 15/20.

**Important remark:** any mark below zero is raised to zero.

And, in the end:

$$Mark_{BAC_i} = \text{average} \left( \begin{array}{l} Mark_{x \text{ or } x^\alpha}; Mark_{y \text{ or } x^\beta}; Mark_{P_{LLV}}; Mark_{z_{LLV}}; Mark_{P_c}; \\ Mark_{x_c}; Mark_{P_{az}}; Mark_{x_{az}}; Mark_{h^M}; Mark_{c_P^M} \end{array} \right) \quad (\text{PVI.19})$$

To conclude, ten marks (at the most) are attributed to a given BAC. Obviously, when experimental data are missing for one or several properties, the corresponding mark(s) cannot be calculated and is(are) removed from Eq. (PVI.19). As an example, none of the binary systems embedded in BAC<sub>2</sub> contain 3-phase equilibrium data so that  $Mark_{P_{LLV}}$  and  $Mark_{z_{LLV}}$  cannot be evaluated. For BAC<sub>2</sub>, the given mark (Eq. (PVI.19)) is the average of only 8 marks (instead of 10).

It is worth noting that the previous equations (from Eq. (PVI.7) to Eq. (PVI.18)) give the greatest weight to the critical pressures that fix the topology of a binary system and are thus, in our view, extremely important while less attention is given to mixing enthalpies and even less to mixing heat capacities. In practical terms, according to Eq. (PVI.12), a MAPE of 13 % on the critical pressures leads to a  $Mark_{P_c}$  of 10/20 and a MAPE of 26 % leads to a  $Mark_{P_c}$  of 0/20. By contrast, from Eq. (PVI.18), a similar MAPE of 13 % on the mixing heat capacities leads to a  $Mark_{c_P^M}$  of 18.7/20 and a MAPE of 26 % leads to a  $Mark_{c_P^M}$  of 17.4/20.

## PVI.IV Illustration: grading and discussion around the accuracy of the Peng-Robinson EoS with classical mixing rules and a temperature-dependent BIP

### PVI.IV.I The model

In this section, it was decided to use the benchmark database developed in this study to assess the accuracy and to grade the Peng-Robinson [65,66] (PR) EoS with classical mixing rules and a temperature-dependent BIP (denoted  $k_{ij}$ ). We found no reason to introduce a volume shift because all the experimental properties contained in the database are unaffected by a temperature-independent volume translation [132,183].

For a pure component, the PR EoS is:

$$P = \frac{RT}{v - b_i} - \frac{a_i(T)}{v(v + b_i) + b_i(v - b_i)} \quad (\text{PVI.20})$$

Although non-consistent [185,198,199] at very high temperatures, it was decided to classically use the Soave-type [64]  $\alpha$ -function proposed by Peng and Robinson [66] in 1978. An updated version has however recently been developed by Piña-Martinez [67] and coworkers (including Peng). We thus used:

$$\text{and } \left\{ \begin{array}{l} R = 8.314472 \text{ J} \cdot \text{mol}^{-1} \cdot \text{K}^{-1} \\ X = \left[ 1 + \sqrt[3]{4 - 2\sqrt{2}} + \sqrt[3]{4 + 2\sqrt{2}} \right]^{-1} \approx 0.253076587 \\ b_i = \Omega_b \frac{RT_{c,i}}{P_{c,i}} \text{ with: } \Omega_b = \frac{X}{X + 3} \approx 0.0777960739 \\ a_i(T) = a_{c,i} \alpha_i(T) \text{ with } \left\{ \begin{array}{l} a_{c,i} = \Omega_a \frac{R^2 T_{c,i}^2}{P_{c,i}} \text{ and } \Omega_a = \frac{8(5X + 1)}{49 - 37X} \approx 0.457235529 \\ \alpha_i(T) = \left[ 1 + m_i \left( 1 - \sqrt{\frac{T}{T_{c,i}}} \right) \right]^2 \end{array} \right. \\ \text{if } \omega_i \leq 0.491 \text{ then } m_i = 0.37464 + 1.54226\omega_i - 0.26992\omega_i^2 \\ \text{if } \omega_i > 0.491 \text{ then } m_i = 0.379642 + 1.48503\omega_i - 0.164423\omega_i^2 + 0.016666\omega_i^3 \end{array} \right. \quad (\text{PVI.21})$$

where  $P$  is the pressure,  $R$  is the gas constant,  $T$  is the temperature,  $a_i$  and  $b_i$  are the cohesive parameter and molar co-volume of pure component  $i$  respectively,  $v$  is the molar volume,  $T_{c,i}$  is the experimental critical temperature,  $P_{c,i}$  is the experimental critical pressure and  $\omega_i$  is the experimental acentric factor of pure  $i$ . Such experimental properties were extracted from the DIPPR database, thus avoiding their estimation by group contribution methods [1259].

To apply this EoS to a mixture, mixing rules are necessary to calculate the values of  $a$  and  $b$  of the mixture. Classical Van der Waals one-fluid mixing rules [246] are used in this study:

$$\begin{cases} a(T, \mathbf{z}) = \sum_{i=1}^N \sum_{j=1}^N z_i z_j \sqrt{a_i(T) \cdot a_j(T)} [1 - k_{ij}(T)] \\ b(\mathbf{z}) = \sum_{i=1}^N z_i b_i \end{cases} \quad (\text{PVI.22})$$

where  $z_i$  represents the mole fraction of component  $i$  and  $N$  is the number of components in the mixture (in this work,  $N = 2$ ). The  $k_{ij}(T)$  parameter is the BIP characterizing the molecular interactions between molecules  $i$  and  $j$ . In this study, the equation that gives the changes of  $k_{ij}$  with respect to temperature (see Eq. (PVI.23)) is the one used in the well-established PPR78 [114,175,1260–1263] and PR<sub>2</sub>SRK [1264] models and contains 2 parameters ( $A_{ij}$  and  $B_{ij}$ ) for the binary system  $i + j$ .

$$k_{ij}(T) = \frac{A_{ij} \left( \frac{298.15}{T} \right)^{\frac{B_{ij}-1}{A_{ij}}} - \left( \frac{\sqrt{a_i}}{b_i} - \frac{\sqrt{a_j}}{b_j} \right)^2}{2 \times \frac{\sqrt{a_i}}{b_i} \times \frac{\sqrt{a_j}}{b_j}} \quad (\text{PVI.23})$$

## PVI.IV.II The fitting procedure

The selected model is a correlative (i.e., non-predictive) model and for a given binary system, the two parameters involved in Eq. (PVI.23) have to be fitted against experimental data. In this work, it was decided that the two parameters would be determined, system by system, in order to ensure the best reproduction of the experimental data available in the proposed database by minimizing an objective function accounting for the deviations between experimental data (VLE data, LLE data, VLLE data, critical data, azeotropic data, heat capacity of mixing data and enthalpy of mixing data) and model predictions. The selected objective function expression is:

$$F_{\text{obj}} = \frac{\left( F_{\text{obj}, x \text{ or } x^\alpha} + F_{\text{obj}, y \text{ or } x^\beta} + F_{\text{obj}, P_{LLV}} + F_{\text{obj}, z_{LLV}} + F_{\text{obj}, P_c} \right) + F_{\text{obj}, x_c} + F_{\text{obj}, P_{az}} + F_{\text{obj}, x_{az}} + F_{\text{obj}, h^M} + F_{\text{obj}, c_p^M}}{n_{x \text{ or } x^\alpha} + n_{y \text{ or } x^\beta} + 2n_{\text{triph}} + 2n_{\text{crit}} + 2n_{\text{az}} + n_{h^M} + n_{c_p^M}} \quad (\text{PVI.24})$$

- $F_{\text{obj}, x \text{ or } x^\alpha}$  quantifies the deviations on the liquid phase composition for VLE data and on the  $\alpha$ -liquid phase for LLE data:

$$\begin{cases} F_{\text{obj}, x \text{ or } x^\alpha} = 100 \sum_{i=1}^{n_{x \text{ or } x^\alpha}} 0.5 \left( \frac{|\Delta x|}{x_{1, \text{exp}} \text{ (or } x_{1, \text{exp}}^\alpha)} + \frac{|\Delta x|}{x_{2, \text{exp}} \text{ (or } x_{2, \text{exp}}^\alpha)} \right)_i \\ \text{with: } |\Delta x| = \left| x_{1, \text{exp}} \text{ (or } x_{1, \text{exp}}^\alpha) - x_{1, \text{cal}} \text{ (or } x_{1, \text{cal}}^\alpha) \right| \end{cases} \quad (\text{PVI.25})$$

$$F_{\text{obj}, x \text{ or } x^\alpha} / n_{x \text{ or } x^\alpha}$$

$n_{x \text{ or } x^\alpha}$  is the number of data points for which the liquid phase composition  $x_1$  (VLE data) or the  $\alpha$ -liquid phase composition  $x_1^\alpha$  (LLE data) is known.

*Remark:* as previously explained, very small mole fractions may lead to huge percent deviations. When this happens, the fitting algorithm is going to change the parameters in order to reduce this huge deviation to the detriment of other compositions. To avoid such a bias, if  $x_{1, \text{exp}} < 0.01$  (or  $x_{1, \text{exp}} > 0.99$ )

and simultaneously  $50 \left( \frac{|\Delta x|}{x_{1, \text{exp}} \text{ (or } x_{1, \text{exp}}^\alpha)} + \frac{|\Delta x|}{x_{2, \text{exp}} \text{ (or } x_{2, \text{exp}}^\alpha)} \right) > 45\%$ , the corresponding deviation was not included in the calculation of  $F_{\text{obj}, x \text{ or } x^\alpha}$ .

- $F_{\text{obj}, y \text{ or } x^\beta}$  quantifies the deviations on the gas phase composition for VLE data and on the  $\beta$ -liquid phase for LLE data:

$$\left\{ \begin{array}{l} F_{\text{obj}, y \text{ or } x^\beta} = 100 \sum_{i=1}^{n_{y \text{ or } x^\beta}} 0.5 \left( \frac{|\Delta y|}{y_{1, \text{exp}} \text{ (or } x_{1, \text{exp}}^\beta)} + \frac{|\Delta y|}{x_{2, \text{exp}} \text{ (or } x_{2, \text{exp}}^\beta)} \right)_i \\ \text{with: } |\Delta y| = |y_{1, \text{exp}} \text{ (or } x_{1, \text{exp}}^\beta) - y_{1, \text{cal}} \text{ (or } x_{1, \text{cal}}^\beta)| \end{array} \right. \quad (\text{PVI.26})$$

$n_{y \text{ or } x^\beta}$  is the number of data points for which the gas phase composition  $y_1$  (VLE data) or the  $\beta$ -liquid phase composition  $x_1^\beta$  (LLE data) is known.

*Remark:* here also, in order to avoid a bias, if  $y_{1, \text{exp}} > 0.99$  (or  $y_{1, \text{exp}} < 0.01$ ) and simultaneously  $50 \left( \frac{|\Delta y|}{y_{1, \text{exp}} \text{ (or } x_{1, \text{exp}}^\beta)} + \frac{|\Delta y|}{x_{2, \text{exp}} \text{ (or } x_{2, \text{exp}}^\beta)} \right) > 45\%$ , the corresponding deviation was not included in the calculation of  $F_{\text{obj}, y \text{ or } x^\beta}$ .

- $F_{\text{obj}, P_{LLV}}$  quantifies the deviations on the three-phase pressure (VLLE data):

$$F_{\text{obj}, P_{LLV}} = 100 \sum_{i=1}^{n_{\text{triph}}} \left( \frac{|P_{LLV, \text{exp}} - P_{LLV, \text{cal}}|}{P_{LLV, \text{exp}}} \right)_i \quad (\text{PVI.27})$$

$n_{\text{triph}}$  is the number of three-phase pressure data.

- $F_{\text{obj}, z_{LLV}}$  quantifies the deviations on the three-phase composition (VLLE data):

$$F_{\text{obj}, z_{LLV}} = 100 \sum_{i=1}^{n_{\text{triph}}} \frac{1}{6} \left( \frac{|\Delta x^\alpha|}{x_{1, \text{exp}}^\alpha} + \frac{|\Delta x^\alpha|}{x_{2, \text{exp}}^\alpha} + \frac{|\Delta x^\beta|}{x_{1, \text{exp}}^\beta} + \frac{|\Delta x^\beta|}{x_{2, \text{exp}}^\beta} + \frac{|\Delta y|}{y_{1, \text{exp}}} + \frac{|\Delta y|}{y_{2, \text{exp}}} \right)_i \quad (\text{PVI.28})$$

with:

$$\left\{ \begin{array}{l} |\Delta x^\alpha| = |x_{1, \text{exp}}^\alpha - x_{1, \text{cal}}^\alpha| = |x_{2, \text{exp}}^\alpha - x_{2, \text{cal}}^\alpha| \\ |\Delta x^\beta| = |x_{1, \text{exp}}^\beta - x_{1, \text{cal}}^\beta| = |x_{2, \text{exp}}^\beta - x_{2, \text{cal}}^\beta| \\ |\Delta y| = |y_{1, \text{exp}} - y_{1, \text{cal}}| = |y_{2, \text{exp}} - y_{2, \text{cal}}| \end{array} \right.$$

$n_{triph}$  being the number of three-phase composition data (VLLE data).

- $F_{obj, P_c}$  quantifies the deviations on the critical pressure:

$$F_{obj, P_c} = 100 \sum_{i=1}^{n_{crit}} \left( \frac{|P_{c, exp} - P_{c, cal}|}{P_{c, exp}} \right)_i \quad (PVI.29)$$

$n_{crit}$  is the number of critical pressure data.

- $F_{obj, x_c}$  quantifies the deviations on the critical composition:

$$F_{obj, x_c} = 100 \sum_{i=1}^{n_{crit}} 0.5 \left( \frac{|\Delta x_c|}{x_{c1, exp}} + \frac{|\Delta x_c|}{x_{c2, exp}} \right) |\Delta x_c| = |x_{c1, exp} - x_{c1, cal}| = |x_{c2, exp} - x_{c2, cal}| \quad (PVI.30)$$

$n_{crit}$  is the number of critical composition data.

- $F_{obj, P_{az}}$  quantifies the deviations on the azeotropic pressure:

$$F_{obj, P_{az}} = 100 \sum_{i=1}^{n_{az}} \left( \frac{|P_{az, exp} - P_{az, cal}|}{P_{az, exp}} \right)_i \quad (PVI.31)$$

$n_{az}$  is the number of azeotropic pressure data.

- $F_{obj, x_{az}}$  quantifies the deviations on the azeotropic composition:

$$F_{obj, x_{az}} = 100 \sum_{i=1}^{n_{az}} 0.5 \left( \frac{|\Delta x_{az}|}{x_{az1, exp}} + \frac{|\Delta x_{az}|}{x_{az2, exp}} \right) |\Delta x_{az}| = |x_{az1, exp} - x_{az1, cal}| = |x_{az2, exp} - x_{az2, cal}| \quad (PVI.32)$$

$n_{az}$  is the number of azeotropic composition data.

- $F_{obj, h^M}$  quantifies the deviations on the mixing enthalpies:

$$F_{obj, h^M} = 100 \sum_{i=1}^{n_{h^M}} 0.5 \left( \left| \frac{h_{exp}^M - h_{cal}^M}{h_{exp}^M} \right| + \left| \frac{h_{exp}^M - h_{cal}^M}{h_{cal}^M} \right| \right)_i \quad (PVI.33)$$

$n_{h^M}$  is the number of mixing enthalpy data points.

- $F_{obj, c_p^M}$  quantifies the deviations on the mixing heat capacities:

$$F_{obj, c_p^M} = 100 \sum_{i=1}^{n_{c_p^M}} 0.5 \left( \left| \frac{c_{p, exp}^M - c_{p, cal}^M}{c_{p, exp}^M} \right| + \left| \frac{c_{p, exp}^M - c_{p, cal}^M}{c_{p, cal}^M} \right| \right)_i \quad (PVI.34)$$

$n_{c_p^M}$  is the number of mixing heat capacity data points.

***Important remark:*** Section PVI.III of this paper, devoted to the grading of a thermodynamic model, dictates the methodology that has to be strictly followed in order to evaluate the deviations between model predictions and experimental data by means of the proposed database. If not, it becomes impossible to fairly compare two thermodynamic models.

In turn, the parameterization of the tested EoS (in the present case, the fitting procedure described above in Section PVI.IV.II) is not imposed and can be freely chosen. We are of the opinion that a researcher who wants to score a thermodynamic model (defined as the association of an EoS and a parameterization procedure) should be free to choose the number of adjustable parameters in the model, the experimental data to which such parameters are fitted and the weighting given for each considered property during the fitting stage of the model parameters. In the previous section, a correlative model (the PR EoS with classical mixing rules and a T-dependent  $k_{ij}$ ) was selected so that the experimental data of the proposed database were used to fit the parameters of Eq. (PVI.23). In the case our goal would have been to assess the accuracy of a predictive thermodynamic model in which the binary interaction parameters are determined by group-contribution (e.g., PSRK [1265,1266], VTPR [1267,1268], UMR-PRU [125,1269], PPR78 [114], MHV1-UNIFAC [1270], etc.), the experimental data of the proposed database would not have been used for parameterization purpose.

From the above, an EoS may thus get different grades depending on its parameterization. For example, it would be possible in this paper to grade the PR EoS by setting all  $k_{ij}$  to zero. By doing so, a lower score than with temperature-dependent  $k_{ij}$  would be obtained. In short, a grade is in fact always given to a model, i.e., to the association of both {an equation of state + a selected parameterization}. The proposed database can thus be used to test the influence of the parameterization on EoS performance and we know by experience [69] that such an influence may be huge.

### **PVI.IV.III System-by-system results of the fitting procedure**

A system-by-system analysis of the {PR EoS + classical mixing rules with a T-dependent  $k_{ij}$ } performances to correlate the data included in the proposed database can be found in Table S2 of the Supporting Information (Appendix E). This very detailed analysis (over 1000 pages) includes:

1. information on how the system deviates from ideality,
2. the values of the  $A$  and  $B$  optimal parameters (see Eq.(PVI.23)),
3. the values of the ten objective functions (from Eq. (PVI.25) to Eq.(PVI.34)). In the Supporting Information,
  - *MAPE on  $x$*  refers to Eq. (PVI.25)
  - *MAPE on  $y$*  refers to Eq. (PVI.26)
  - *MAPE on  $P_{LLV}$*  refers to Eq. (PVI.27)
  - *MAPE on  $z_{LLV}$*  refers to Eq. (PVI.28)
  - *MAPE on  $P_c$*  refers to Eq. (PVI.29)
  - *MAPE on  $x_c$*  refers to Eq. (PVI.30)

- *MAPE on  $P_{az}$*  refers to Eq. (PVI.31)
- *MAPE on  $x_{az}$*  refers to Eq. (PVI.32)
- *MAPE on  $h^M$*  refers to Eq. (PVI.33)
- *MAPE on  $c_p^M$*  refers to Eq. (PVI.34)

the so-called GPED (global phase equilibrium diagram) – calculated by the PR EoS – enabling to immediately identify the binary system class according to the scheme proposed by Van Konynenburg and Scott [278],

4. all the experimental data with the corresponding references,
5. all the deviations between experimental data and model correlation graphically illustrated by hundreds of figures. Explanations on “*how* to read the charts” are available at the beginning of the Supporting Information ([Appendix E](#)).

#### **PVI.IV.IV Grading of the model: PR EoS + classical mixing rules with a T-dependent $k_{ij}$**

For each binary association code, the MAPEs on liquid phase composition  $x$ , gas phase composition  $y$ , three-phase pressure  $P_{LLV}$ , three-phase composition  $z_{LLV}$ , critical pressure  $P_c$ , critical composition  $x_c$ , azeotropic pressure  $P_{az}$ , azeotropic composition  $x_{az}$ , mixing enthalpy  $h^M$  and mixing heat capacity  $c_p^M$  are resumed in [Table PVI.14](#).

Such MAPEs make it possible to give a score over 20 to each of the 9 BACs by averaging the 10 marks in  $x$ ,  $y$ ,  $P_{LLV}$ ,  $z_{LLV}$ ,  $P_c$ ,  $x_c$ ,  $P_{az}$ ,  $x_{az}$ ,  $h^M$  and  $c_p^M$  (see Eq. (PVI.19)). Such marks can be found in [Table PVI.15](#). At the end, as previously explained, the marks obtained by BACs 1 to 4 and BACs 7 to 9 are averaged in order to only retain 4 categories (BAC<sub>1</sub>-BAC<sub>4</sub>; BAC<sub>5</sub>; BAC<sub>6</sub>; BAC<sub>7</sub>-BAC<sub>9</sub>) of binary systems based on the type of association they exhibit. By averaging the marks of these 4 categories of binary systems (see Eq.(PVI.6)), the model: {PR EoS + classical mixing rules with a T-dependent  $k_{ij}$ } receives the final mark of **12.3/20**.



**Table PVI.14.** Overview of the MAPE between experimental data and values calculated with the model:  $\{PR\ EoS + \text{classical mixing rules with a } T\text{-dependent } k_{ij}\}$  for the 200 binary systems included in the proposed database that are classified in 9 binary association codes (BACs). The abbreviations used for the *associating character* of a pure compound are: NA for “Non-Associating”, HA for “Hydrogen-Acceptor”, HD for “Hydrogen-Donor” and SA for “Self-Associating”.

Binary association code	Type of association	MAPE on:									
		$x$	$y$	$P_{LLV}$	$z_{LLV}$	$P_c$	$x_c$	$P_{az}$	$x_{az}$	$h^M$	$C_p^M$
		Eq. (PVI.25)	Eq. (PVI.26)	Eq. (PVI.27)	Eq. (PVI.28)	Eq. (PVI.29)	Eq. (PVI.30)	Eq. (PVI.31)	Eq. (PVI.32)	Eq. (PVI.33)	Eq. (PVI.34)
1 (NA - NA)		7.9%	7.9%	1.3%	42.7%	3.6%	12.9%	1.0%	5.0%	21.7%	34.7%
2 (HA-NA)	Mixtures without association	8.8%	6.8%	-	-	2.4%	9.0%	1.0%	6.1%	16.3%	160.3%
3 (HD-NA)		6.9%	5.7%	-	-	5.2%	15.8%	0.6%	3.7%	12.5%	70.5%
4 (HA-HA or HD-HD)		7.5%	7.2%	-	-	4.0%	11.1%	5.6%	9.6%	13.5%	104.5%
5 (SA-NA)	Mixtures in which self-association tends to be broken	40.0%	14.9%	5.2%	69.9%	10.9%	46.0%	4.9%	13.8%	32.4%	200%
6 (HD-HA)	Mixtures in which cross-association takes place alone	6.0%	6.1%	-	-	3.5%	21.5%	2.0%	9.6%	23.6%	43.1%
7 (SA-HD)	Mixtures in which	15.2%	12.3%	-	-	-	-	2.5%	9.6%	84.4%	188.0%
8 (SA-HA)	both cross-association and self-association take place	24.9%	15.7%	24.5%	39.1%	13.0%	28.4%	3.9%	11.0%	37.2%	164.4%
9 (SA-SA)		33.9%	22.6%	6.4%	32.7%	5.5%	13.2%	1.1%	24.4%	39.7%	182.4%

**Table PVI.15.** Rating of the 9 binary association codes in order to finally grade the model:  $\{PR\ EoS + \text{classical mixing rules with a } T\text{-dependent } k_{ij}\}$ . The abbreviations used for the *associating character* of a pure compound are: NA for “Non-Associating”, HA for “Hydrogen-Acceptor”, HD for “Hydrogen-Donor” and SA for “Self-Associating”.

Binary association code (BAC)	Type of association	Mark on:										Binary association code mark Eq. (PVI.19)	Mark (over 20) by type of association Eq. (PVI.6)	Final mark of the PR EoS with classical MR and T-dependent BIPS Eq. (PVI.6)
		$x$ Eq. (PVI.7)	$y$ Eq. (PVI.8)	$P_{LLV}$ Eq. (PVI.10)	$z_{LLV}$ Eq. (PVI.11)	$P_c$ Eq. (PVI.12)	$x_c$ Eq. (PVI.13)	$P_{az}$ Eq. (PVI.14)	$x_{az}$ Eq. (PVI.15)	$h^M$ Eq. (PVI.16)	$C_P^M$ Eq. (PVI.18)			
<b>1</b> (NA - NA)		16.0	16.1	19.3	<b>0.0</b>	17.3	13.6	19.5	17.5	14.6	16.5	15.0		
<b>2</b> (HA-NA)	Mixtures without association	15.6	16.6	-	-	18.2	15.5	19.5	16.9	15.9	4.0	15.3	$\underbrace{mark_{NA}}_{\text{no association}} = 15.5$	
<b>3</b> (HD-NA)		16.5	17.2	-	-	16.1	12.1	19.7	18.2	16.9	13.0	16.2		
<b>4</b> (HA-HA or HD-HD)		16.2	16.4	-	-	17.0	14.4	17.2	15.2	16.6	9.6	15.3		
<b>5</b> (SA-NA)	Mixtures in which self-association tends to be broken	<b>0.0</b>	12.6	17.4	<b>0.0</b>	11.8	<b>0.0</b>	17.5	13.1	11.9	<b>0.0</b>	8.4	$\underbrace{mark_{SA}}_{\text{self-association}} = 8.4$	
<b>6</b> (HD-HA)	Mixtures in which cross-association takes place alone	17.0	16.9	-	-	17.4	9.2	19.0	15.2	14.1	15.7	15.6	$\underbrace{mark_{CA}}_{\text{cross-association}} = 15.6$	
<b>7</b> (SA-HD)	Mixtures in which both cross-association and self-association take place	12.4	13.9	-	-	-	-	18.8	15.2	<b>0.0</b>	1.2	10.2	$\underbrace{mark_{CA+SA}}_{\text{cross-association + self-association}} = 9.8$	
<b>8</b> (SA-HA)		7.5	12.2	7.7	0.45	10.3	5.8	18.0	14.5	10.7	3.6	9.1		
<b>9</b> (SA-SA)		3.1	8.7	16.8	3.6	15.8	13.4	19.5	7.8	10.1	1.8	10.0		

**12.3/20**

### PVI.IV.V Discussion around the accuracy of the model: PR EoS + classical mixing rules with a T-dependent $k_{ij}$

At this step, it is possible to analyze the results obtained with the PR EoS coupled to classical mixing rules and a T-dependent  $k_{ij}$ . The marks reported in Table PVI.15 are plotted in Figure PVI.5 for each category of binary systems based on the type of association they exhibit.

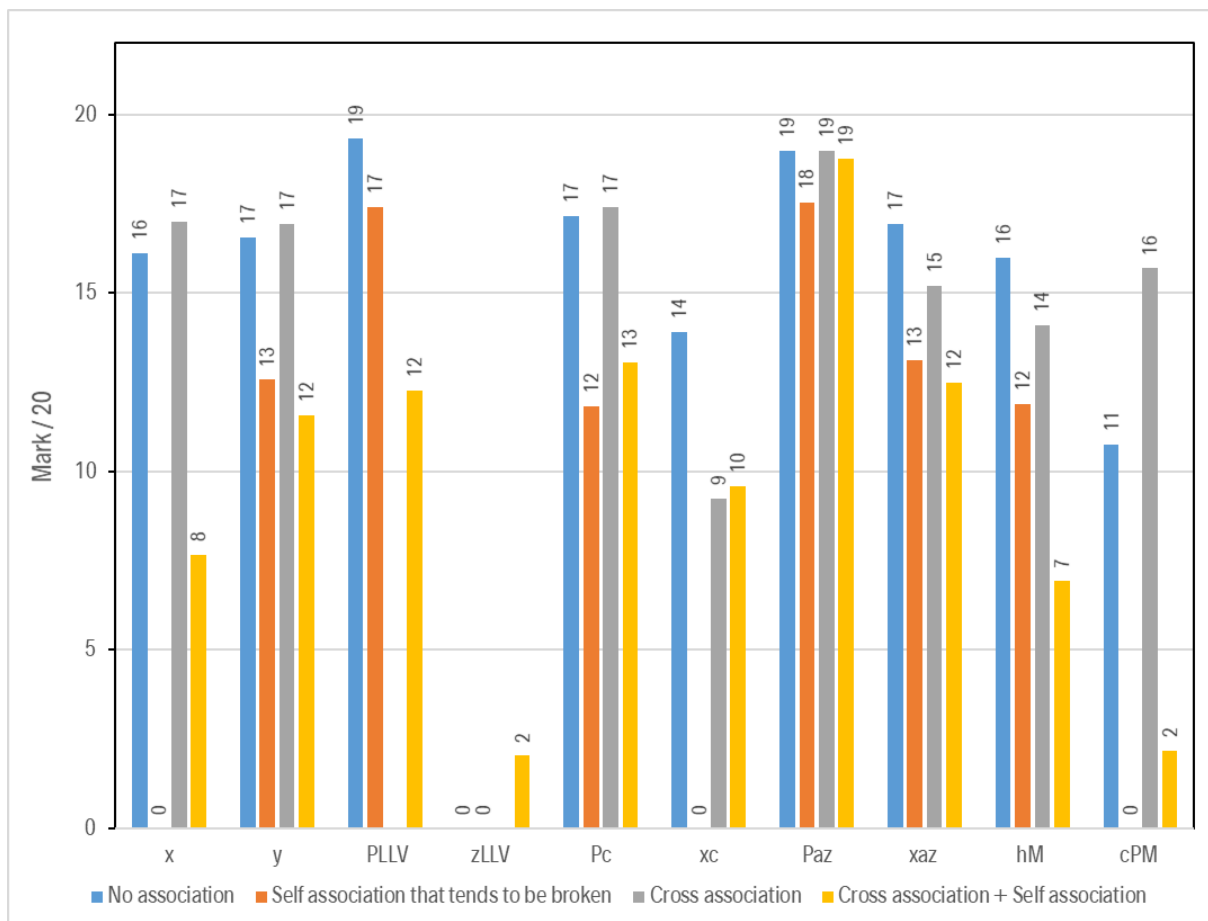


**Figure PVI.5.** Overview of the accuracy of the model: {PR EoS + classical mixing rules with a T-dependent  $k_{ij}$ } by plotting the marks in ten properties for the four categories of binary systems based on the type of association they exhibit.

Figure PVI.5 and Table PVI.15 highlight that with an excellent mark of 15.6/20, the binary systems that exhibit cross-association alone are those which are correlated with the highest accuracy by the model: {PR EoS + classical mixing rules with a T-dependent  $k_{ij}$ }. For such binary systems, the two molecules form hydrogen bonds after mixing thus stabilizing the liquid phase and preventing from phase splitting. As a general rule, mixtures of this family exhibit negative deviations from ideality and belong to type I in the classification scheme of Van Konynenburg and Scott.

With the poorest rating of 8.4/20, binary systems belonging to BAC 5 cannot be accurately correlated with the PR EoS even when temperature-dependent BIPs are used. Three marks are equal to zero. In such systems, a non-associating component is mixed with a self-associating compound so that self-association (partially) persists in the mixture. The non-associating molecules tend to break the hydrogen bond network but the self-associating compounds withstand so that liquid-phase splitting is often

observed in this family. As previously stated, such systems were thus classified as: “mixtures in which self-association tends to be broken”. As a general rule, they exhibit positive deviations from ideality and three-phase equilibrium at low temperature. Many of them belong to type-III systems in the classification scheme of Van Konynenburg and Scott. All binary systems water + alkane or alcohol + alkane belong to this family. They are generally considered by model developers as the most difficult systems to correlate. It can be reasonably thought that either the addition of an association term or the use of more-sophisticated mixing rules could help the PR EoS to quantitatively reproduce the behavior of such systems.

Mixtures in which both cross-association and self-association take place fall into the middle scoring range by receiving a mark of 9.8/20. This is the result of two antagonistic effects: on the one hand, hydrogen bonds between two identical self-associating molecules are broken by dilution effect and this behavior is highly difficult to describe with the model: {PR EoS + classical mixing rules with a T-dependent  $k_{ij}$ } while on the other hand, new hydrogen bonds are formed by cross-association; this latter behavior can be modeled accurately with the selected model, as explained above. Many of these systems belong to type-I systems in the classification scheme of Van Konynenburg and Scott (although some may fall into type III).

As expected, systems that do not exhibit association received the very good mark of 15.5/20. The identified weakness is the inaccurate correlation of the composition of the phases in equilibrium when the system exhibits a three-phase line. This weakness highlights the difficulty to simultaneously correlate VLE and LLE data with a unique set of adjustable parameters. Non-associating systems often belong to type-I systems but some fall into type-III, especially when the 2 compounds show a high size-asymmetry.

This analysis allows to conclude that, with an overall score of 12.3/20, the PR EoS with classical mixing rules and a temperature-dependent  $k_{ij}$  can be safely used in process and product design applications as long as systems in which hydrogen bonds are broken without the possibility to form new ones are not involved.

A similar analysis is possible from the viewpoint of system ideality:

Figure PVI.6 shows that except for the liquid phase composition (including the critical composition), all the other properties are correlated with a similar accuracy both for ideal and non-ideal systems. It is observed that deviations on mixing enthalpies can become huge when the deviations from ideality originate from entropic effects but this result is not significant because in such a case experimental and calculated  $h^M$  values are both low.

It is thus possible to conclude that deviations from ideality are not the key parameters to be accounted for when highlighting the strengths and the weaknesses of a model. A classification of the binary systems based on the type of association they exhibit, as the one proposed in this paper is much more pertinent.

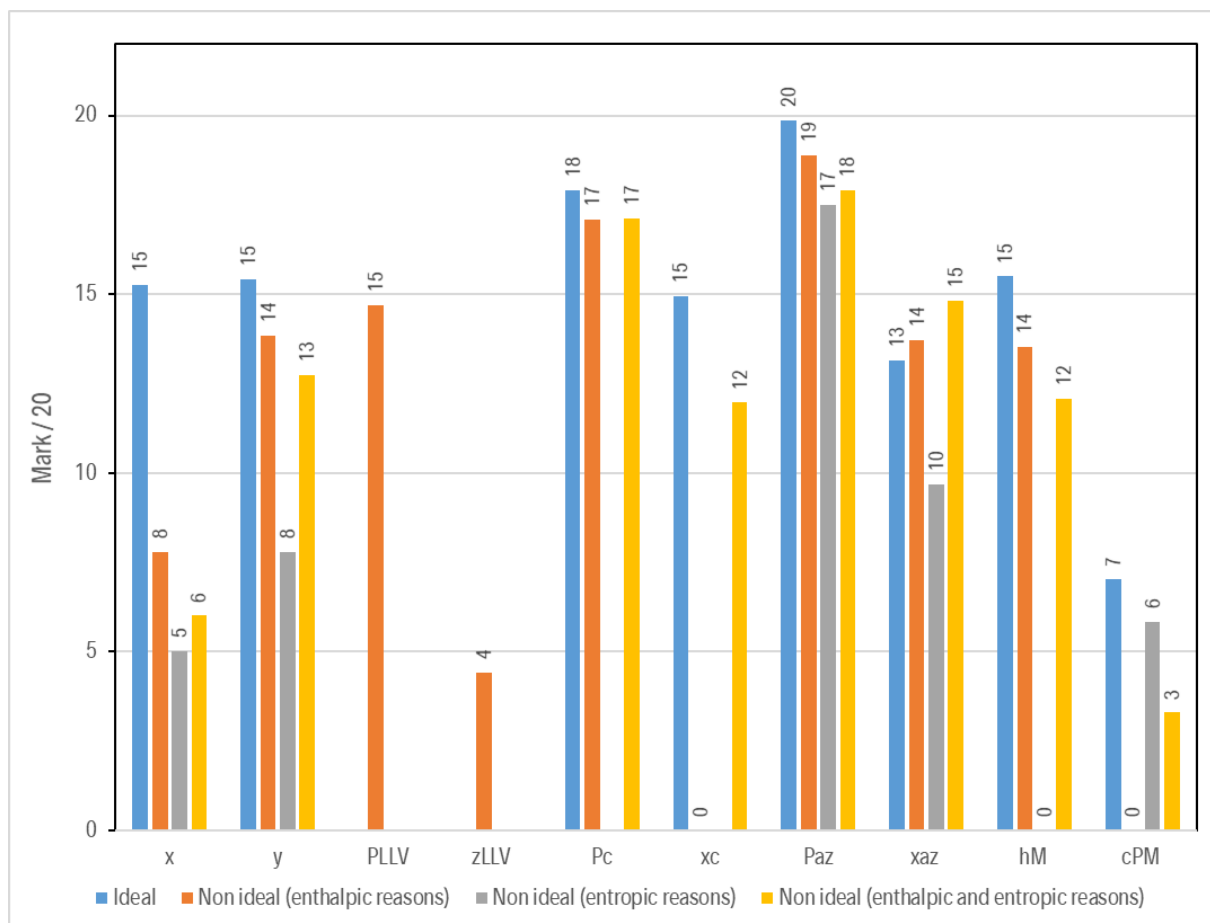


**Figure PVI.6.** Marks in 10 properties calculated for five categories of binary systems based on how they deviate from ideality (marks on VLLE data are not shown due to a lack of information for some categories of binary systems).

## PVI.V Conclusions

A benchmark database is presented in this paper to enable a proposed-standardized assessment of the performance of a given thermodynamic model or to compare two models. To classify database's systems on the base of their thermodynamic complexity, 107 pure components were first divided into four categories according to their “*associating character*” and nine classes of binary systems were defined combining these four pure component categories. Each of these classes is identified by a *binary association code* (BAC). We are indeed convinced that binary systems must be classified according to the type of association they exhibit. For each class of systems, the proposed database includes a variety of binary systems ranging from ideal to highly non-ideal. In the end, the proposed database embeds 200 binary mixtures uniformly distributed among the nine BACs and includes for each system both phase equilibrium data (VLE, LLE, VLLE, azeotropic data, critical data) and energetic data ( $h^M$  and  $c_p^M$  data). For each property, a detailed procedure explaining how deviations between model predictions and experimental data have to be estimated is provided.

Finally, the performances of the Peng-Robinson EoS with classical Van der Waals mixing rules and a temperature-dependent binary interaction parameter were evaluated over the full database. In the light of the obtained results, a discussion about the strengths and weaknesses of the model was conducted.

Such a thermodynamic model got an overall respectable score of 12.3/20. Its main weak point is the poor correlation of systems in which hydrogen bonds are broken without the possibility to form new ones. For such complex systems, the addition of an association term to the EoS and the selection of more sophisticated mixing rules could help to improve the model efficiency.

Last but not least, we hope that the proposed database will be widely adopted by the scientific community to identify the strengths and weaknesses of the many published thermodynamic models and to identify the remaining scientific obstacles that need to be overcome. We also hope that such a database will be used by model developers to test a new concept. As an example, experimental data of binary systems, the BAC of which is 7,8 or 9 could be very useful to test the influence of various association schemes.

# Publication VII : What is the optimal activity coefficient model to be combined with the translated-consistent Peng-Robinson (tc-PR) equation of state through advanced mixing rules? Cross-comparison and grading of the Wilson, UNIQUAC and NRTL a<sup>E</sup> models against a benchmark database involving 200 binary systems.

Andrés Piña-Martinez<sup>1</sup>, Romain Privat<sup>1(\*)</sup>, Ilias K. Nikolaidis<sup>2</sup>, Ioannis G. Economou<sup>2,3(\*)</sup>, Jean-Noël Jaubert<sup>1(\*)</sup>

<sup>(1)</sup> Université de Lorraine, École Nationale Supérieure des Industries Chimiques, Laboratoire Réactions et Génie des Procédés (UMR CNRS 7274), 1 rue Grandville, 54000, Nancy, France

<sup>(2)</sup> National Center for Scientific Research “Demokritos”, Institute of Nanoscience and Nanotechnology, Molecular Thermodynamics and Modelling of Materials Laboratory, GR – 153 10 Aghia Paraskevi Attikis, Greece

<sup>(3)</sup> Texas A&M University at Qatar, Chemical Engineering Program, PO Box 23874, Doha, Qatar

## Abstract

The extension of the *translated-consistent* Peng-Robinson (tc-PR) equation of state (EoS) to mixtures has been investigated. For this purpose, advanced EoS/ $a_{res}^{E,\gamma}$  mixing rules are used to combine the tc-PR EoS with the residual part of an activity coefficient model chosen among Wilson, NRTL and UNIQUAC. The performances of the three resulting EoS versions are compared against a high-quality reference database containing binary-system data for the cross-comparison of thermodynamic models and the assessment of their accuracy. It is shown that the best choice to extend the tc-PR EoS to mixtures along with EoS/ $a_{res}^{E,\gamma}$  mixing rules is to use the residual part of the Wilson activity coefficient model ( $a_{res}^{E,Wilson}$ ). After grading, the resulting model, named “tc-PR-Wilson”, received a mark of 12.4 / 20. It has a clear advantage over the other investigated models in this study which are all below 12 / 20. Observing that some experimental data could not be compared to a calculated value (typically, when the model does not predict the right topology of a phase diagram like, e.g., predicting a heterogeneous azeotrope instead of a homogeneous one), a new performance indicator (“success ratio”) was introduced as the ratio of the number of datapoints for which the model can reproduce qualitatively the experimental data behavior over the total number of experimental data. The success ratio of the tc-PR-Wilson model reaches 96%; this model distinguishes especially in the correlation of liquid and gas phase compositions, azeotropic points and three-phase pressures.



## PVII.1 Introduction

Phase-equilibrium thermodynamics is one of the cornerstones of computer-aided process design (CAPD). The availability of accurate thermodynamic models, capable of estimating saturation and caloric properties, is crucial and necessary to understand and obtain reliable designs of unit operations such as distillation, absorption, extraction, adsorption and leaching, which are essential unit operations in chemical industry.

Equations of state (EoS) are developed with the aim to increase their range of applicability (in terms of mixture type, composition, temperature and pressure conditions) and to improve the accuracy of mass and energy balances that are necessary for the design of chemical processes. The development of EoS can be divided into two stages: 1) the formulation of a model for pure components and 2) its extension to mixtures. In both stages a key point is the parameterization, i.e., the allocation of numerical values to component-dependent parameters.

With the aim of developing a reliable and accurate EoS for process design, Le Guennec et al. [94] introduced the pure-component *translated-consistent* Peng-Robinson (*tc-PR*) cubic equation of state (CEoS):

$$P(T, v) = \frac{RT}{v + c_i - b_i} - \frac{a_i(T)}{(v + c_i)(v + c_i + b_i) + b_i(v + c_i - b_i)}$$

$$\text{with: } \begin{cases} a_i(T) = a_{c,i} \cdot \alpha_i(T_r) ; T_r = \frac{T}{T_{c,i,\text{exp}}} \\ \alpha_i(T_r) = T_r^{N_i(M_i-1)} \exp\left[L_i(1 - T_r^{M_i N_i})\right] \\ c_i = v_{i,\text{liq}}^{\text{sat},u-PR}(T_r = 0.8) - v_{i,\text{liq},\text{exp}}^{\text{sat}}(T_r = 0.8) \\ \eta_c = \left[1 + \sqrt[3]{4 - 2\sqrt{2}} + \sqrt[3]{4 + 2\sqrt{2}}\right]^{-1} \approx 0.25308 \\ a_{c,i} = \frac{40\eta_c + 8}{49 - 37\eta_c} \frac{R^2 T_{c,i,\text{exp}}^2}{P_{c,i,\text{exp}}} \approx 0.45724 \frac{R^2 T_{c,i,\text{exp}}^2}{P_{c,i,\text{exp}}} \\ b_i = \frac{\eta_c}{\eta_c + 3} \frac{RT_{c,i,\text{exp}}}{P_{c,i,\text{exp}}} \approx 0.07780 \frac{RT_{c,i,\text{exp}}}{P_{c,i,\text{exp}}} \end{cases} \quad (\text{PVII.1})$$

In Eq. (PVII.1), the attractive term  $a(T)$  is classically expressed as the product of its value at the critical temperature ( $a_c$ ) and the so-called  $\alpha$ -function. The covolume, i.e., the molar volume when the pressure tends to infinity (here noted  $v_i^\infty$ ) is related to the parameter  $b_i$  through:  $v_i^\infty = b_i - c_i$ . Such a model is called *translated* [1271,1272] because the substance-dependent volume-translation parameter,  $c_i$ , is determined, component by component, in order the translated EoS exactly reproduces the experimental saturated liquid volume at a reduced temperature of 0.8,  $[v_{i,\text{liq},\text{exp}}^{\text{sat}}(T_r = 0.8)]$ , that is:

$$c_i = v_{i,\text{liq}}^{\text{sat},u-CEoS}(T_r = 0.8) - v_{i,\text{liq},\text{exp}}^{\text{sat}}(T_r = 0.8) \quad (\text{PVII.2})$$

where  $v_{i,liq}^{sat,u-CEoS}(T_r = 0.8)$  is the molar volume calculated with the original (*untranslated*) CEoS at  $T_r = 0.8$ . In turn, *consistent* stands for the fact that the *tc*-PR EoS relies on an  $\alpha$ -function that passed the *consistency test* proposed by Le Guennec et al. [270,271]. Such a test is made up of a list of constraints that an  $\alpha$ -function should absolutely fulfill to guarantee safe property predictions in both subcritical and supercritical domains. These constraints are given in Eq. (PVII.3).

$$\text{For any reduced temperature } (T_r): \begin{cases} \alpha(T_r) \geq 0 & \text{and} & \alpha \text{ continuous} \\ \frac{d\alpha}{dT_r}(T_r) \leq 0 & \text{and} & \frac{d\alpha}{dT_r} \text{ continuous} \\ \frac{d^2\alpha}{dT_r^2}(T_r) \geq 0 & \text{and} & \frac{d^2\alpha}{dT_r^2} \text{ continuous} \\ \frac{d^3\alpha}{dT_r^3}(T_r) \leq 0 \end{cases} \quad (\text{PVII.3})$$

As shown in Eq. (PVII.1), the *tc*-PR EoS is coupled with the highly flexible 3-parameter  $\alpha$ -function proposed by Twu et al. in 1991 [272]. Indeed, such an  $\alpha$ -function becomes consistent (satisfies Eq. (PVII.3)) if the three  $L, M, N$  component parameters are determined under constraints following the procedure proposed by Piña-Martinez et al. [184]. The triplets of  $(L_i, M_i, N_i)$  consistent parameters with the corresponding volume-translation parameter  $c_i$  were recently determined and published for 1800 pure compounds  $i$  [1273].

In addition to the two well defined physical properties  $(T_{c,i,exp}, P_{c,i,exp})$ , the *tc*-PR model requires four parameters  $(L_i, M_i, N_i, c_i)$  for a given pure compound  $i$ . It is an extremely accurate CEoS for pure components since it yields an average overall deviation lower than 2% over the 306 700 pseudo-experimental data points available in the pure-compound database that Piña-Martinez et al. [1273] proposed to use in order to cross-compare the ability of EoS in property estimation of pure species. In view of such a low deviation, it is possible to conclude that the 1<sup>st</sup> stage of development of the *tc*-PR EoS, that concerns pure components only, is completed. Therefore, the next step should be to extend the EoS to mixtures.

Extension to mixtures requires mixing rules (MR), and a classical choice is the use of the so-called Van der Waals one-fluid (VdW1f) mixing rules. Other options are related to the use of the advanced EoS/ $g^{E,\gamma}$  or Wong-Sandler (EoS/ $a^{E,\gamma}$ ) MR. In this work, advanced MR (EoS/ $a_{res}^{E,\gamma}$ ) derived by equaling the residual part of the excess Helmholtz energy from an EoS and from an explicit activity coefficient model (ACM) are retained. The research objective is to determine which ACM among the Wilson, UNIQUAC and NRTL models is the most suitable to extend the *tc*-PR EoS to mixtures using EoS/ $a_{res}^{E,\gamma}$  mixing rules. For this purpose, it is decided to use the high-quality reference database developed by the authors [130]. Such a database contains binary-system data specifically selected for the cross-comparison of thermodynamic models and the assessment of their accuracy. Models such as the Peng-Robinson (PR) EoS incorporating classical mixing rules and temperature-dependent binary interaction parameters (BIPs), as well as the PC-SAFT EoS without association term and no regressed BIPs have already been graded against the reference database [130,131].

This paper is organized into two sections. In [Section PVII.II](#), the implementation of the *tc*-PR model coupled with EoS/ $a_{res}^{E,\gamma}$  mixing rules is introduced. This includes a detailed description of the EoS/ $a_{res}^{E,\gamma}$  mixing rules investigated in this work along with the corresponding activity coefficient models. In [Section PVII.III](#), the performances of the three *tc*-PR- $a_{res}^{E,\gamma}$  models are studied. In a first stage, a slight modification of the grading procedure presented by Jaubert et al. [130] and applied to various EoS previously is briefly summarized. Finally, the results of the grading procedure for the models examined here are discussed.

## PVII.II Implementation of the *tc*-PR model coupled with EoS/ $a_{res}^{E,\gamma}$ mixing rules

As stated before, this work aims to extend the *tc*-PR model to mixtures using EoS/ $a_{res}^{E,\gamma}$  mixing rules, derived by equaling the residual part of the excess Helmholtz energy from an EoS ( $a_{res}^{E,EoS}$ ) on one side, to the same quantity stemming from an explicit activity coefficient model (this quantity is denoted  $a_{res}^{E,\gamma}$ ). Three activity coefficient models were tested: the residual part of the Wilson and UNIQUAC models and the purely residual NRTL model. The following part of the present section deals with the introduction of these mixing rules.

Cubic EoS can be expressed through the following generic formulation:

$$P(T, v, \mathbf{z}) = \frac{RT}{v - b_m} - \frac{a_m}{(v - r_1 b_m)(v - r_2 b_m)} \quad (\text{PVII.4})$$

where  $r_1$  and  $r_2$  are two universal constants depending on the selected EoS (see [Table PVII.1](#) for some of the most common cubic EoS), and  $a_m$  and  $b_m$  are the energy (or dispersive, or attractive) and co-volume parameters of the mixture, related to the composition of the mixture  $\mathbf{z}$ , and to the energy ( $a_i(T)$ ) and co-volume ( $b_i$ ) parameters of a given number of pure components by means of properly-defined functions, the so-called mixing rules.

**Table PVII.1.** Parameters  $r_1$  and  $r_2$  for some classical cubic equations of state.

Equation	$r_1$	$r_2$
Van der Waals [63]	0	0
Redlich-Kwong [1274]	-1	0
Peng-Robinson [103]	$-1 - \sqrt{2}$	$-1 + \sqrt{2}$

### PVII.II.I Quadratic Van der Waals mixing rules

A popular choice is the so-called Van der Waals one-fluid (vdW1f) mixing rules, which consider parameters  $a_m$  and  $b_m$  as quadratic functions of the composition:

$$\left\{ \begin{array}{l} a_m = \sum_i \sum_j z_i z_j a_{ij} \\ b_m = \sum_i \sum_j z_i z_j b_{ij} \end{array} \right. \quad \text{(PVII.5)}$$

$$\left\{ \begin{array}{l} a_m = \sum_i \sum_j z_i z_j a_{ij} \\ b_m = \sum_i \sum_j z_i z_j b_{ij} \end{array} \right. \quad \text{(PVII.6)}$$

where  $a_{ij}$  and  $b_{ij}$  are determined from pure-component parameters,  $a_i$  and  $b_i$ , through the application of combining rules. The classically-applied combining rules are the geometric-mean rule for the cross-energy and the arithmetic-mean rule for the cross-co-volume parameter:

$$\left\{ \begin{array}{l} a_{ij} = \sqrt{a_i a_j} (1 - k_{ij}) \\ b_{ij} = \frac{b_i + b_j}{2} (1 - l_{ij}) \end{array} \right. \quad \text{(PVII.7)}$$

$$\left\{ \begin{array}{l} a_{ij} = \sqrt{a_i a_j} (1 - k_{ij}) \\ b_{ij} = \frac{b_i + b_j}{2} (1 - l_{ij}) \end{array} \right. \quad \text{(PVII.8)}$$

where  $k_{ij}$  and  $l_{ij}$  are binary interaction parameters, adjustable over experimental data or obtained from suitable correlations.

### PVII.II.II EoS/ $a_{res}^{E,\gamma}$ mixing rules

Cubic EoS with VdW1f mixing rules lead to very accurate results at low and high pressures for simple mixtures (containing components showing little or no polarity, e.g., hydrocarbons, gases etc.). However, such mixing rules cannot be applied with success to polar mixtures. In return, excess Gibbs energy ( $g^E$ ) models (activity coefficient models) are applicable at low pressures and are able to correlate phase equilibrium data for polar mixtures. From this observation arises the idea to combine cubic EoS and activity coefficient models in order to obtain a single model suitable for describing the phase equilibria of polar and non-polar mixtures from low to high pressures. This combination of EoS and  $g^E$  models is possible via the so-called EoS/ $g^E$  approach, which is essentially a set of mixing rules for the energy parameter of cubic EoS [1275]. The starting point for deriving EoS/ $g^E$  models is to equal the expressions of the excess Gibbs energy obtained from an EoS [ $g^{E,EoS}(T, P, \mathbf{z})$ ] with that from an explicit activity coefficient model [ $g^{E,\gamma}(T, \mathbf{z})$ ]. By construction, this latter is temperature- and composition-dependent but pressure-independent; however, the  $g^{E,EoS}$  quantity depends on pressure, temperature and composition explaining why a reference pressure, noted  $P_{ref}$ , needs to be selected before equaling the two quantities. The starting equation to derive EoS/ $g^E$  models is thus:

$$g^{E,EoS}(T, P_{ref}, \mathbf{z}) = g^{E,\gamma}(T, \mathbf{z}) \quad \text{(PVII.9)}$$

The activity coefficient model may be chosen among the classical forms of molar excess Gibbs energy functions (such as Redlich-Kister, Margules, Wilson, Van Laar, NRTL, UNIQUAC, UNIFAC and

others). Eq. (PVII.9) is the cornerstone of the approach pioneered by Huron and Vidal (HV) [1276], who assumes infinite reference pressure; and by Michelsen [1277–1279] who employed the zero-pressure reference and deduced the MHV-1 and MHV-2 mixing rules.

However the consistency of Eq. (PVII.9) can be questioned for the following two main observations:

1. In accordance with the way they were derived, low-pressure  $g^{E,\gamma}$  models classically used to calculate activity coefficients should be better regarded as  $a^E$  models (they will be noted  $a^{E,\gamma}$  hereafter to avoid confusion with the same quantity stemming from the EoS);
2. In Eq. (PVII.9), the combinatorial part and the residual part of  $g^E$  stemming from the EoS and from the activity coefficient model do not match. Although  $g^{E,EoS} = g^{E,\gamma}$ , we do not get:  $g_{combinatorial}^{E,EoS} = g_{combinatorial}^{E,\gamma}$  and  $g_{residual}^{E,EoS} = g_{residual}^{E,\gamma}$ . We can thus expect poor results when athermal or regular solutions that only require a combinatorial or a residual contribution are modeled. To derive mixing rules, and contrary to Eq. (PVII.9), it is believed that a particular attention has to be given separately to the combinatorial and residual contributions. It is advised to equal separately the combinatorial and residual contributions stemming from the EoS and from the  $a^{E,\gamma}$  model in order to ascertain to equal quantities that contain the same information.

These 2 observations led to modify the way classically used to derive mixing rules and resulted in the formulation of EoS/ $a_{res}^{E,\gamma}$  mixing rules that are used in this work. Let us come back to the consequences of the 2 aforementioned observations for a better understanding of the derivation of EoS/ $a_{res}^{E,\gamma}$  mixing rules.

→ As pointed out by Wong and Sandler [126] but also by Jaubert and Privat [127], observation (1) is supported by the fact that the pressure dependency of activity coefficient models ( $g^{E,\gamma}$ ) is always ignored. Indeed, all excess Gibbs energy models should theoretically depend on pressure but our current knowledge on liquid theory still lacks of accuracy and relies on the incompressible liquid assumption. In consequence, all activity coefficient models predict:  $v^{E,\gamma} = -\left(\partial g^{E,\gamma} / \partial P\right)_{T,z} = 0$ . Although the experimental values of  $v^E$  are often small, such a result is thermodynamically inconsistent ( $g^E$  should indeed be a function of composition, temperature and pressure) and must be seen as a theoretical weakness. Since  $g^{E,\gamma} = a^{E,\gamma} + P \cdot v^{E,\gamma}$ , the developers of  $g^{E,\gamma}$  models (UNIQUAC, Wilson, etc.) decided to construct expressions for  $a^{E,\gamma}$  and to use them to determine activity coefficients. As an illustration, in their paper relative to the derivation of their mixing rules, Wong and Sandler [126] write: “if one examines the derivation of  $g^E$  models, it is evident that it is really a model for  $a^E$  which has been derived”. In conclusion, all  $g^{E,\gamma}$  are in fact  $a^{E,\gamma}$  models and some of them, like NRTL or Van Laar, that do not contain combinatorial contribution are even only residual contributions of  $a^{E,\gamma}$  models (denoted  $a_{res}^{E,\gamma}$ ). At low pressures, it is reasonable to assume that  $g^E \approx a^E$ . However, to define mixing rules for EoS that are used under high pressures, we see no reason to keep such an approximation and consequently, we propose to derive mixing rules by equaling the expression of the excess Helmholtz energy from an EoS with the one of a low-pressure  $a^{E,\gamma}$  model (rather than equaling excess Gibbs energies). It is exactly what Wong and Sandler [126] made 30 years ago during the development of their mixing rules under infinite pressure.

→ The second observation is a consequence of the natural division of the excess Gibbs energy ( $g^E = h^E - Ts^E$ ) in enthalpic (or energetic or residual or regular-solution) and entropic (or combinatorial or athermal-solution) contributions. A proper modeling of athermal solutions thus requires an appropriate combinatorial term whereas appropriate residual term is required for regular solutions. Each of the combinatorial and residual terms need to be accurately known for solutions in which deviations from ideality are the consequence of both enthalpic and entropic effects. It is thus necessary to analyze in detail the features of the combinatorial contributions and residual contributions stemming from an  $a^{E,\gamma}$  model and from a CEoS.

Let us start our analysis with the combinatorial contribution and let us see if equaling the combinatorial contributions from the EoS and from an  $a^{E,\gamma}$  model makes sense. To do so, the following equation is considered:

$$a_{comb}^{E,EoS}(T, P, \mathbf{z}) = a_{comb}^{E,\gamma}(T, \mathbf{z}) \quad (\text{PVII.10})$$

First, let us recall that the combinatorial contribution to  $a^E$  stemming from a CEoS is similar to a Flory-Huggins expression in form of free volume [1280]:

$$a_{comb}^{E,EoS}(T, P, \mathbf{z}) = RT \sum_i x_i \ln \left( \frac{v_i - b_i}{v - b_m} \right) \quad (\text{PVII.11})$$

On the other hand, the same quantity from an activity coefficient model is either zero (Van Laar, NRTL) or a Flory-Huggins expression (Wilson) or a Flory-Huggins expression corrected by a Staverman-Guggenheim (SG) term (UNIQUAC):

$$\left\{ \begin{array}{l} a_{comb}^{E,NRTL} = a_{comb}^{E, Van Laar} = 0 \\ a_{comb}^{E,Wilson} = RT \sum_i x_i \ln \left( \frac{v_i}{v} \right) \\ a_{comb}^{E,UNIQUAC} = RT \sum_i x_i \ln \left( \frac{v_i}{v} \right) + SG \text{ term} \end{array} \right. \quad (\text{PVII.12})$$

By comparing Eq. (PVII.11) and Eq. (PVII.12), it is clearly impossible to find a mixing rule on  $b_m$  so that both equations become identical. We must thus conclude that CEoS will never be able to reproduce the combinatorial  $a_{comb}^{E,\gamma}(T, \mathbf{z})$  expression stemming from an activity coefficient model. In other words, we could state that the knowledge of  $a_{comb}^{E,\gamma}(T, \mathbf{z})$  is not helpful to derive mixing rules explaining why it is believed that Eq. (PVII.9) is not a suitable starting point. A key point is the acknowledgment of Eq. (PVII.11) to be particularly suitable to describe deviations from ideality attributed to size and shape differences of the components [1281]. There is thus no need of an external  $a_{comb}^{E,\gamma}(T, \mathbf{z})$  expression. This conclusion is supported also by the observation of the low performance of mixing rules obtained by equaling (under zero pressure) excess Gibbs energy quantities ( $g^{E,EoS}$  and  $g^{E,\gamma}$ ) containing non-identical combinatorial contributions which, in consequence, do not vanish when equaling the two excess quantities. The resulting consequence is the appearance of the well-documented “double-

combinatorial term” issue. The reader is here referred to the book by Kontogeorgis and Folas [124] and especially to section 6.6 for more details.

Let us continue our analysis with the residual contribution and let us see the consequence of writing:

$$a_{res}^{E,EoS}(T, P, \mathbf{z}) = a_{res}^{E,\gamma}(T, \mathbf{z}) \quad (\text{PVII.13})$$

The residual contribution to  $a^E$  stemming from a CEoS is:

$$a_{res}^{E,EoS}(T, P, \mathbf{z}) = \sum_i z_i \frac{a_i}{b_i(r_1 - r_2)} \ln\left(\frac{v_i - b_i r_2}{v_i - b_i r_1}\right) - \frac{a_m}{b_m(r_1 - r_2)} \ln\left(\frac{v - b r_2}{v - b r_1}\right) \quad (\text{PVII.14})$$

Before equaling such a mathematical relation to  $a_{res}^{E,\gamma}(T, \mathbf{z})$ , a reference pressure has to be specified.

Following the pioneering works of Huron, Vidal and Michelsen, it is here proposed to successively select  $P_{ref} = +\infty$  and  $P_{ref} = 0$ . The derivations of the corresponding mixing rules for  $a_m/b_m$  at the two considered reference pressures are presented in [Appendix F1](#).

- Case 1:  $P_{ref} = +\infty$

By combining Eq. (PVII.13) with Eq. (PVII.14) under infinite pressure, we get (the reader is referred to Appendix A1 of the Supporting Information for all the details):

$$\frac{a_m}{b_m} = \sum_i z_i \frac{a_i}{b_i} + \frac{a_{res}^{E,\gamma}(T, \mathbf{z})}{\Lambda_{EoS}} \quad \text{with: } \Lambda_{EoS} = \frac{1}{r_2 - r_1} \ln\left(\frac{1 - r_2}{1 - r_1}\right) \quad (\text{PVII.15})$$

We can thus state that after selecting freely a MR for the covolume  $b_m$ , Eq. (PVII.15) makes it possible to univocally determine  $a_m$ .

- Case 2:  $P_{ref} = 0$

As detailed in Appendix A1 of the Supporting Information, by combining Eq. (PVII.13) with Eq. (PVII.14) under zero pressure, we get:

$$\frac{a_m}{b_m} = \sum_i z_i \frac{a_i}{b_i} + \frac{a_{res}^{E,\gamma}(T, \mathbf{z})}{\Lambda_{EoS}} \quad \text{with: } \Lambda_{EoS} = \frac{1}{r_2 - r_1} \ln\left(\frac{1 - r_2}{1 - r_1}\right) \quad (\text{PVII.16})$$

Remarkably, the expressions of the mixing rule for  $a_m/b_m$  obtained from the case at  $P_{ref} = +\infty$  (Eq. (PVII.15)) and  $P_{ref} = 0$  (Eq. (PVII.16)) are strictly identical. In consequence, the use of Eq. (PVII.13) to develop a mixing rule for  $a_m/b_m$  seems particularly appropriate since the result is independent of the reference pressure (zero or infinite).

The proposed MR is summarized in Eq. (PVII.17):

$$\left\{ \begin{array}{l} b_m : \text{any mixing rule} \\ \frac{a_m}{b_m} = \sum_i z_i \frac{a_i}{b_i} + \frac{a_{res}^{E,\gamma}}{\Lambda_{EoS}} \\ \text{with } \Lambda_{EoS} = \frac{1}{r_2 - r_1} \ln\left(\frac{1 - r_2}{1 - r_1}\right) \end{array} \right. \quad (\text{PVII.17})$$

It is worth noting that existing NRTL, WILSON, UNIQUAC or UNIFAC parameters (e.g. compiled in the DECHEMA Chemistry Data Series) were determined at low pressure and low temperature ( $P \leq \min(P_{c,i}), T \leq \min(T_{c,i})$ ) and are supposed to be used with the  $\gamma$ - $\phi$  approach, assuming that the gas phase is perfect. On the contrary, the parameters to be used with the proposed MR were determined in larger domains of temperature and pressure that include the supercritical region in which the gas phase is far from being perfect. In addition, when the proposed MR are used, the combinatorial part of  $g^E$  stems from the EoS and it is thus different from the one embedded in the NRTL, UNIQUAC or WILSON activity coefficient models. For all these reasons, existing parameters cannot be used with the proposed EoS/ $a_{res}^{E,\gamma}$  mixing rules.

### PVII.II.III Implementation of the $tc$ -PR- $a_{res}^{E,\gamma}$ models

In this section, the  $tc$ -PR EoS (Eq. (PVII.1)) coupled with EoS/ $a_{res}^{E,\gamma}$  mixing rules (Eq. (PVII.17)) embedding the residual part of the Wilson and UNIQUAC models and the  $a_{res}^{E,\gamma}$  NRTL model is presented.

First of all, for the covolume of the mixture ( $b_m$ ), it has been applied the classical quadratic mixing rule with the generalized formulation of the combining rule proposed by Lorentz for  $b_{ij}$  [124]:

$$\left\{ \begin{array}{l} b_m = \sum_i \sum_j z_i z_j b_{ij} \\ b_{ij} = \left( \frac{b_i^{1/s} + b_j^{1/s}}{2} \right)^s \end{array} \right. \quad (\text{PVII.18})$$

where the parameter  $s$  has been set to 3/2. This specific value arises from optimization procedures aimed at selecting the  $s$  value making it possible to reproduce the phase equilibria of athermal mixtures (typically mixtures containing 2 alkanes of different sizes) in an optimal way; for the sake of brevity, the detailed results – which are part of Yohann Le Guennec's thesis [1282] – are detailed in Appendix F2. Following Privat et al.'s advices [1272], a linear MR has been chosen for the volume translation

parameter:  $c_m(\mathbf{z}) = \sum_i z_i \cdot c_i$ . To sum up, when applied to a mixture, the  $tc$ -PR EoS takes the following expression:

$$P(T, v, \mathbf{z}) = \frac{RT}{v + c_m - b_m} - \frac{a_m(T, \mathbf{z})}{(v + c_m)(v + c_m + b_m) + b_m(v + c_m - b_m)}$$

$$\text{with: } \begin{cases} b_m = \sum_i \sum_j z_i z_j \left( \frac{b_i^{2/3} + b_j^{2/3}}{2} \right)^{3/2} \\ a_m = b_m \left[ \sum_i z_i \frac{a_i}{b_i} + \frac{a_{res}^{E,\gamma}}{\Lambda_{PR}} \right] \text{ with } \Lambda_{PR} = -\sqrt{2}/2 \cdot \ln(1 + \sqrt{2}) \\ c_m = \sum_i z_i \cdot c_i \end{cases} \quad (\text{PVII.19})$$

### tc-PR-Wilson

EoS/ $a_{res}^{E,\gamma}$  mixing rules that combine the residual part of the Wilson [1283] activity coefficient model (obtained by subtracting the combinatorial term to the complete model expression:  $a_{res}^{E,Wilson} = a^{E,Wilson} - a_{comb}^{E,Wilson}$ ) and the tc-PR EoS is called tc-PR-Wilson hereafter.

For a binary system, the residual part of the  $a^{E,Wilson}$  model is:

$$\left\{ \begin{aligned} \frac{a_{res}^{E,Wilson}(T, \mathbf{z})}{RT} &= \underbrace{\left\{ -z_1 \ln \left[ z_1 + z_2 \frac{v_2^*}{v_1^*} \exp\left(-\frac{A_{12}}{T}\right) \right] - z_2 \ln \left[ z_2 + z_1 \frac{v_1^*}{v_2^*} \exp\left(-\frac{A_{21}}{T}\right) \right] \right\}}_{a^{E,Wilson}/RT} \\ &\quad - \underbrace{\left[ z_1 \ln \left( \frac{v_1^*}{z_1 v_1^* + z_2 v_2^*} \right) + z_2 \ln \left( \frac{v_2^*}{z_1 v_1^* + z_2 v_2^*} \right) \right]}_{a_{comb}^{E,Wilson}/RT} \end{aligned} \right\} \quad (\text{PVII.20})$$

$v_i^*$  was arbitrarily merged with the covolume (molar volume under infinite pressure) so that:

$$v_i^* = b_i - c_i$$

The 2 temperature-independent parameters  $A_{12}$  and  $A_{21}$  have to be fitted to experimental data.

It is worth recalling that the Wilson  $g^E/RT$  expression (first part of Eq. (PVII.20)) is incapable of representing liquid-liquid equilibria (LLE). This is because the instability criterion  $\partial(x_i \cdot \gamma_i)/\partial x_i < 0$  is never violated [1284]. In other words, whatever the values of the 2 parameters, the activity ( $(x_i \cdot \gamma_i)$ ) is always an increasing function of the composition ( $x_i$ ). Tsuboka and Katayama [1285] (TK) however demonstrated that the residual part of the Wilson model [Eq. (PVII.20)], named the TK-Wilson model was able to reproduce LLE. In short, such a deficiency of the Wilson model comes from the combinatorial part. The results obtained in this paper (see the following sections) highlight that the combination of the residual part of the Wilson model to a cubic EoS in which the combinatorial part of is given by Eq. (PVII.11) totally fixes this deficiency. The tc-PR-Wilson model was indeed able to accurately correlate the LLE and VLLE data that are included in the reference database developed by Jaubert et al. [130].

### **tc-PR-UNIQUAC**

EoS/ $a_{res}^{E,\gamma}$  mixing rules that combine the residual part of the UNIQUAC [128] activity coefficient model ( $a_{res}^{E,UNIQUAC}$ ) and the *tc*-PR EoS is called *tc*-PR-UNIQUAC hereafter. For a binary system, the residual part of the  $a_{res}^{E,UNIQUAC}$  model is:

$$\begin{aligned} \frac{a_{res}^{E,UNIQUAC}(T, \mathbf{z})}{RT} = & -q_1 z_1 \ln \left[ \frac{z_1 q_1}{z_1 q_1 + z_2 q_2} + \frac{z_2 q_2}{z_1 q_1 + z_2 q_2} \exp\left(-\frac{A_{12}}{T}\right) \right] \\ & - q_2 z_2 \ln \left[ \frac{z_2 q_2}{z_1 q_1 + z_2 q_2} + \frac{z_1 q_1}{z_1 q_1 + z_2 q_2} \exp\left(-\frac{A_{21}}{T}\right) \right] \end{aligned} \quad (\text{PVII.21})$$

$q_1$  and  $q_2$  are the Van der Waals surface areas of molecules 1 and 2 divided by a reference surface of  $2.5 \cdot 10^9 \text{ cm}^2 \cdot \text{mol}^{-1}$  in order to get dimensionless parameters. In this paper, they were extracted from the DIPPR database. Temperature-independent parameters  $A_{12}$  and  $A_{21}$  have to be fitted to experimental data.

### **tc-PR-NRTL**

EoS/ $a_{res}^{E,\gamma}$  mixing rules that combine the purely residual NRTL [57] activity coefficient model ( $a_{res}^{E,NRTL} = a^{E,NRTL}$ ) and the *tc*-PR EoS is called *tc*-PR-NRTL hereafter. For a binary system, the NRTL model is:

$$\frac{a_{res}^{E,NRTL}(T, \mathbf{z})}{RT} = z_1 z_2 \left[ \frac{\frac{A_{21}}{T} \exp\left(-\alpha \frac{A_{21}}{T}\right)}{z_1 + z_2 \exp\left(-\alpha \frac{A_{21}}{T}\right)} + \frac{\frac{A_{12}}{T} \exp\left(-\alpha \frac{A_{12}}{T}\right)}{z_2 + z_1 \exp\left(-\alpha \frac{A_{12}}{T}\right)} \right] \quad (\text{PVII.22})$$

The parameter  $\alpha$  has been set to 0.3 and the 2 temperature-independent ones ( $A_{12}$  and  $A_{21}$ ) were fitted to experimental data.

### **PVII.II.IV Implementation of the PR-Van Laar model**

It is worth recalling that the first benchmarked model against the binary-system database proposed by Jaubert et al. [130] was the PR EoS armed with classical Van der Waals mixing and combining rules (Eqs. (PVII.5)-(PVII.8)) with  $l_{12} = l_{21} = 0$  and temperature-dependent binary interaction parameters ( $k_{12}(T) = k_{21}(T)$ ):

$$k_{12}(T) = \frac{A_{12} \cdot \left(\frac{298.15}{T}\right)^{\left(\frac{B_{12}-1}{A_{12}}\right)} - \left(\frac{\sqrt{a_1(T)}}{b_1} - \frac{\sqrt{a_2(T)}}{b_2}\right)^2}{2 \frac{\sqrt{a_1(T) \cdot a_2(T)}}{b_1 \cdot b_2}} \quad (\text{PVII.23})$$

Temperature-independent parameters:  $A_{12} = A_{21}$  and  $B_{12} = B_{21}$  were fitted over available experimental data.

Such a model can also be seen [1261,1264] as the PR EoS coupled with EoS/ $a_{res}^{E,\gamma}$  mixing rules involving the purely residual Van Laar  $a_{res}^{E,\gamma}$  model. For a binary system, the Van Laar model reads:

$$\left\{ \begin{array}{l} \frac{a_{res}^{E, Van Laar}(T, \mathbf{z})}{RT} = -\frac{\Lambda_{PR}}{RT} \cdot \frac{z_1 z_2 b_1 b_2 E_{12}(T)}{z_1 b_1 + z_2 b_2} \\ \text{with: } E_{12}(T) = A_{12} \cdot \left( \frac{298.15}{T} \right)^{\left( \frac{B_{12}}{A_{12}} - 1 \right)} \end{array} \right. \quad (\text{PVII.24})$$

Eq. (PVII.24) shows that the Van Laar model is in fact a 1-parameter  $a_{res}^{E,\gamma}$  model ( $E_{12}$ ). Such a unique parameter is however temperature-dependent so that, at the end, 2 parameters per binary system ( $A_{12}$  and  $B_{12}$ ) have to be fitted on experimental data.

Like the *tc*-PR-Wilson, *tc*-PR-UNIQUAC and *tc*-PR-NRTL, the PR-Van Laar model is an extension of the Peng-Robinson EoS to mixtures with the help of advanced EoS/ $a_{res}^{E,\gamma}$  mixing rules. However, contrary to the *tc*-PR-Wilson, *tc*-PR-UNIQUAC and *tc*-PR-NRTL, the PR-Van Laar model is not translated, includes in its formulation a linear mixing rule for the covolume and a non-consistent Soave-type  $\alpha$ -function. It thus cannot be named *tc*-PR-Van Laar. In other words, it cannot be considered as an extension of the *tc*-PR EoS to mixtures. Although advanced EoS/ $a_{res}^{E,\gamma}$  mixing rules were used, such differences exclude the PR-Van Laar model from *tc*-PR EoS extensions to mixtures (it should be seen as a PR EoS extension to mixtures). On the other hand, similarly to the *tc*-PR- $a_{res}^{E,\gamma}$  models, the PR-Van Laar model contains two adjustable parameters. Since it was the first model to be graded against the database proposed by Jaubert et al. [130], we found pertinent to include the PR-Van Laar model in the comparison and grading of the three *tc*-PR- $a_{res}^{E,\gamma}$  models selected in this study. Our plan is to use the PR-Van Laar model as a reference model during the discussion devoted to the capabilities and weaknesses of the studied *tc*-PR- $a_{res}^{E,\gamma}$  models.

*Note:* as mentioned before, two temperature-independent adjustable parameters per model were fitted to experimental data. For this purpose, it was decided to select the same objective function as Jaubert et al. [130]. The regressed binary interaction parameters for the three *tc*-PR- $a_{res}^{E,\gamma}$  and the PR-Van Laar models are reported in Appendix F3.

It also should be noted that using temperature-independent parameters for the three *tc*-PR- $a_{res}^{E,\gamma}$  models is a first step before moving to more complex and more accurate approaches. Indeed, from our experience, ignoring the temperature dependency of the 2 parameters embedded in activity-coefficient models typically leads to less accurate results.

### PVII.III Grading of the *tc*-PR-Wilson, *tc*-PR-UNIQUAC and *tc*-PR-NRTL models

In this section, the performances of three *tc*-PR- $a_{res}^{E,\gamma}$  and PR-Van Laar models are presented. First, the grading procedure presented by Jaubert et al. [130] is briefly summarized. Then, some modifications on the grading are presented in order to better consider the impact of the *out-of-model* points in the final

mark. This is indeed an issue that emerged as important during the grading of the PC-SAFT EoS with zero  $k_{ij}$  [1286]. Finally, the results of the grading procedure are discussed.

### PVII.III.I Grading procedure

A methodology was developed recently by Jaubert and co-workers towards addressing the issue of model reliability and grading [130]. A high-quality reference database was built that can be used for assessing the accuracy of a thermodynamic model or to cross-compare the performances of different models [130]. A specific procedure for the calculation of the deviations between model calculations and experimental data was discussed in detail, as well as a methodology for grading a thermodynamic model was proposed. In total, 200 non-electrolytic binary mixtures were selected to cover all categories of mixtures. They were divided into 9 groups (each characterized by a so-called *binary association code*, BAC) according to the associating character of the two components, i.e., to their ability to be involved in a hydrogen bond (see Table S1 in Appendix F3). During the grading of a thermodynamic model, only four categories of binary systems are retained based on the type of association they exhibit (see the last column of Table S1 in Appendix F3).

In general, for each binary system of the database, ten properties were experimentally determined: liquid phase composition  $x$ , gas phase composition (or second liquid phase composition)  $y$ , three-phase pressure  $P_{LLV}$ , three-phase composition  $z_{LLV}$ , critical pressure  $P_c$ , critical composition  $x_c$ , azeotropic pressure  $P_{azeo}$ , azeotropic composition  $x_{azeo}$ , mixing enthalpy  $h^M$  and mixing heat capacity  $c_P^M$ .

The grading procedure proposed by Jaubert et al. [130] consists of the following main steps:

1. For each of the nine BACs, the Mean Average Percentage Error (MAPE) between model calculations and experimental data for each type of available experimental properties (10 at the most) is calculated as follows:

$$MAPE_{prop}^{BAC_i} (\%) = \frac{1}{N_{data}} \sum_{j=1}^{N_{data}} 100 \cdot \left| \frac{P_j^{EXP} - P_j^{MODEL}}{P_j^{EXP}} \right| \quad (PVII.25)$$

2. For a given BAC, a mark (max score is 20) is then calculated for each type of available experimental properties. At the end, a BAC receives 10 marks at the most depending on the availability of the experimental data. For an available experimental property (noted  $prop$ ),  $prop \in \{x, y, P_{LLV}, z_{LLV}, P_c, x_c, P_{azeo}, x_{azeo}, h^M, c_P^M\}$ , the general mark expression is given by:

$$Mark_{prop}^{BAC_i} = 20 - \alpha_{prop} \cdot MAPE_{prop}^{BAC_i} \quad (PVII.26)$$

where  $\alpha_{prop} = 0.5$  with the exception of  $\alpha_{P_c} = 0.75$ ,  $\alpha_{h^M} = 0.25$  and  $\alpha_{c_P^M} = 0.10$  and any mark below zero is raised to zero. For important details and the exact methodology, the reader is referred to the original publication [130].

3. The mark attributed to a given BAC is calculated by averaging the marks received by the available experimental properties of such a BAC (given at step 2):

$$Mark^{BAC_i} = average \left( \begin{array}{l} Mark_{x \text{ or } x^\alpha}^{BAC_i}; Mark_{y \text{ or } x^\beta}^{BAC_i}; Mark_{P_{LLV}}^{BAC_i}; Mark_{z_{LLV}}^{BAC_i}; Mark_{P_c}^{BAC_i}; \\ Mark_{x_c}^{BAC_i}; Mark_{P_{az}}^{BAC_i}; Mark_{x_{az}}^{BAC_i}; Mark_{h^M}^{BAC_i}; Mark_{c_P^M}^{BAC_i} \end{array} \right) \quad (PVII.27)$$

4. Calculation of the marks for the four categories of binary systems retained according to the type of association they exhibit (see the last column of Table S1 in Appendix A3 of the Supporting Information) by averaging the marks of the BACs belonging to each of them.

$$\left\{ \begin{array}{l} mark_{\text{Mixtures without association}} = \frac{mark^{BAC_1} + mark^{BAC_2} + mark^{BAC_3} + mark^{BAC_4}}{4} \\ mark_{\text{Mixtures with self-association}} = mark^{BAC_5} \\ mark_{\text{Mixtures with cross-association}} = mark^{BAC_6} \\ mark_{\text{Mixtures with cross-association and self-association}} = \frac{mark^{BAC_7} + mark^{BAC_8} + mark^{BAC_9}}{3} \end{array} \right. \quad (PVII.28)$$

Calculation of the final mark of the thermodynamic model by averaging the mark of the four considered categories of binary systems (determined at step 4).

$$\underbrace{\left[ \begin{array}{l} \textit{Final mark} \\ \textit{of a thermodynamic} \\ \textit{model (over 20)} \end{array} \right]} = \frac{1}{4} \times \left[ \underbrace{mark_{\text{Mixtures without association}} + mark_{\text{Mixtures with self-association}} + mark_{\text{Mixtures with cross-association}} + mark_{\text{Mixtures with cross-association and self-association}}}_{\text{average of 4 marks}} \right] \quad (PVII.29)$$

In this work, two modifications to the original grading procedure are introduced. The first one tends to correct a difference of treatment in the calculation of the deviation on the fluid phase compositions depending on whether they belong or not to a 3-phase line. Indeed, as pointed out by Jaubert et al. [130], very small mole fractions (or close to 1) may lead to huge percent deviations and introduce a bias in the  $Mark_{z_{LLV}}^{BAC_i}$  attributed to a given BAC. To avoid this issue, it is necessary to determine for each 3-phase line of a given BAC (one after the other), the Absolute Relative Deviation ( $ARD_{z_{LLV}}^{3-\varphi \text{ line}}$ ) between calculated and experimental compositions by:

$$\left\{ \begin{array}{l} ARD_{z_{LLV}}^{3-\varphi \text{ line}} = \sum_{j=1}^2 \left[ \frac{ARD \text{ on } x_j^\alpha (\%) + ARD \text{ on } x_j^\beta (\%) + ARD \text{ on } y_j (\%)}{6} \right] \end{array} \right. \quad (PVII.30)$$

$$\left\{ \begin{array}{l} \text{with: } ARD \text{ on } z_j (\%) = 100 \cdot \left| \frac{z_j^{EXP} - z_j^{MODEL}}{z_j^{EXP}} \right| \end{array} \right. \quad (PVII.31)$$

where  $x_j^\alpha$ ,  $x_j^\beta$  and  $y_j$  are the mole fractions of component  $j$  in each of the three equilibrium phases.

In this work, it was decided to apply to Eq. (PVII.30) the same procedure as the one used to calculate the deviations on liquid or gas phase composition of a classical VLE data point. Consequently, if  $z_1$  stands for the mole fraction of component 1 in one of the three phases ( $z_1 = x_1^\alpha$  and/or  $x_1^\beta$  and/or  $y_1$ ), an experimental phase composition is *rejected* (and thus, is not taken into account in Eq. (PVII.30) in order to annihilate its influence on the calculated  $ARD_{z_{LLV}}^{3-\varphi \text{ line}}$ ) provided:

$$\left\{ \begin{array}{l} z_{1, \text{exp}} < 0.01 \\ \text{or} \\ z_{1, \text{exp}} > 0.99 \end{array} \right. \text{ and simultaneously } \frac{1}{2} \times (\text{ARD on } z_1 + \text{ARD on } z_2) > 45\% \quad (\text{PVII.32})$$

This modification makes it compulsory in Eq. (PVII.30) to keep only the deviations on 3-phase line compositions passing the test introduced in Eq. (PVII.32). Indeed, for a given 3-phase line the calculation of  $ARD_{z_{LLV}}^{3-\varphi \text{ line}}$  depends on how many phases, and their respective mole fractions, are rejected. As an example, in the case where only 1 phase composition out of 3 is rejected, 4 deviations (instead of 6) are calculated and the denominator of Eq. (PVII.30) must be adapted accordingly. Similarly if 2 phase compositions among 3 are rejected, only 2 deviations will be calculated and included in Eq. (PVII.30). Finally, if the compositions of the 3 phases are rejected, no  $ARD_{z_{LLV}}^{3-\varphi \text{ line}}$  is calculated for such a 3-phase line. In this latter case, we apply:  $N_{3-\varphi \text{ lines}}^{BAC_i} = N_{3-\varphi \text{ lines}}^{BAC_i} - 1$ , where  $N_{3-\varphi \text{ lines}}^{BAC_i}$  designates the number of 3-phase lines for which an ARD could be calculated.

Once done, for a given BAC, the calculation of the mark on  $z_{LLV}$  is straightforward:

$$\text{Mark}_{z_{LLV}}^{BAC_i} = 20 - 0.5 \times \frac{1}{N_{3-\varphi \text{ lines}}^{BAC_i}} \sum_{j=1}^{N_{3-\varphi \text{ lines}}^{BAC_i}} ARD_{z_{LLV}}^{3-\varphi \text{ line}} \quad (\text{PVII.33})$$

The second modification is related to the inclusion of *out-of-model* (OM) points in the grading procedure. Before discussing the details of such a modification, it would be pertinent to recall the definition of an *out-of-model* point. An experimental point is considered *out-of-model* if the thermodynamic model does not predict its existence, and, in consequence, the experimental value cannot be compared to a calculated one and thus, cannot be considered in a MAPE calculation. For instance, it may happen that a model does not predict the existence of a homogeneous azeotrope that is experimentally observed, however. For a more detailed explanation, the reader is referred to Jaubert et al. [130].

For the purpose of this section, i.e., to better understand the influence of OM data points, consider the case presented in Figure PVII.1.. Recalling that deviations over bubble and dew-point compositions are calculated at the temperature and pressure of the experimental data, one observes that there are more *out-of-model* points in Figure PVII.1.b than in Figure PVII.1.a. In consequence, the number of data points considered in the MAPE calculation is greater in case A than in case B. It may happen that the consideration of more points in the MAPE calculation (case A) results in a higher MAPE value than in the case where less data points are taken into account (case B). In the illustration example considered here, the MAPE for case B appears lower while the calculated phase-diagram does not have the right magnitude. To illustrate this and for the sake of simplicity, consider only MAPE on  $x$ . For case A in Figure PVII.1., it is obtained  $MAPE_x^A = 10.6\%$  over 9 points, while for case B, 4 points are declared *out-of-model*, which results in  $MAPE_x^B = 7.7\%$  over 5 points. The marks for case A and B are 14/20 and 16/20, respectively. It does not seem fair at all since, graphically, model associated with case A has a better predictive capacity than model associated with case B since it can predict the existence of more data points.

In order to avoid this type of issue, a slight modification in the second step of the grading procedure is introduced. For a given  $BAC_i$ , the calculation of the mark for property  $prop$  becomes:

$$\left\{ \begin{array}{l} Mark_{prop}^{BAC_i} = \left( 20 - \alpha_{prop} \cdot MAPE_{prop}^{BAC_i} \right) \cdot \underbrace{SR_{prop}^{BAC_i}}_{\text{success ratio}} \\ SR_{prop}^{BAC_i} = 1 - \frac{N_{OM,prop}^{BAC_i}}{N_{exp,prop}^{BAC_i}} \\ prop \in \left\{ x, y, P_{LLV}, z_{LLV}, P_c, x_c, P_{azeo}, x_{azeo}, h^M, c_P^M \right\} \end{array} \right. \quad (PVII.34)$$

$SR_{prop}^{BAC_i}$  corresponds to the “success ratio” of the model to reproduce the property  $prop$  for binary systems involved in  $BAC_i$ .  $N_{OM,prop}^{BAC_i}$  and  $N_{exp,prop}^{BAC_i}$  are the number of *out-of-model* points and the number of experimental data points for the property  $prop$  for binary systems available in  $BAC_i$ . Therefore,  $SR_{prop}^{BAC_i}$  represents the actual fraction of the number of points not declared *out-of-model*, (i.e., the number of points for which a deviation between calculated and experimental data can be evaluated divided by the number of experimental points). For clarity, let us here recall that *out-of-model* data points do not occur for enthalpy and heat capacity of mixing data because it is always possible to calculate these properties at specified T, P,  $z_1$ . It follows that the success ratio is always equal to 1 for  $h^M$  and  $c_P^M$ .

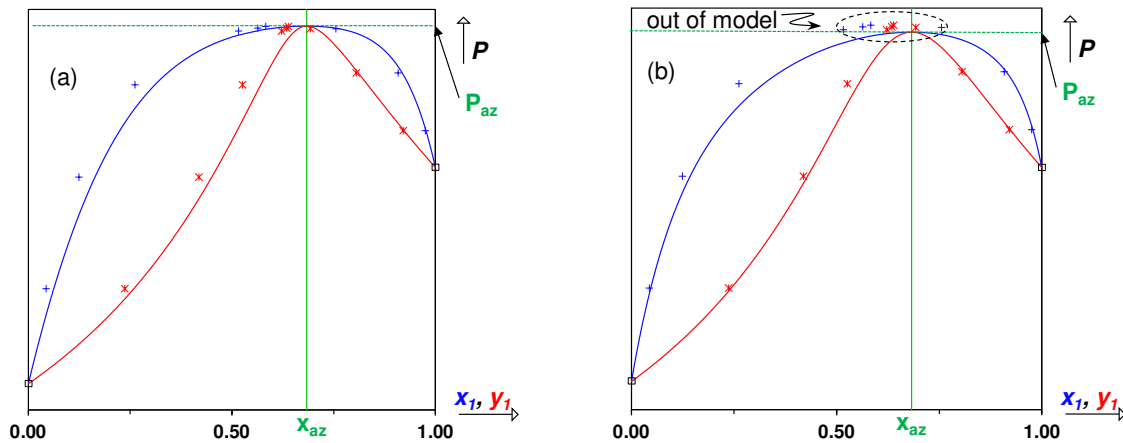


**Figure PVII.1.** a) Calculated and experimental isothermal pressure - composition VLE phase diagram that does not exhibit *out-of-model* points. b) Phase diagrams exhibiting *out-of-model* points due to an underestimation of the experimental azeotropic pressure by the model. (\*): experimental dew points. (+): experimental bubble points. (–): calculated dew curve. (–): calculated bubble curve.  $P_{az}$ : calculated azeotropic pressure.  $x_{az}$ : calculated azeotropic composition.

Coming back to the example of Figure PVII.1., for case A:  $MAPE_x^A = 10.6\%$  and  $SR_x^A = 1$  (100% of the experimental data were predicted by the model), and for case B  $MAPE_x^B = 7.7\%$  and  $SR_x^B = 5/9 = 0.56$  (only 56% of the experimental data were predicted by the model). It results in marks

(over 20) of 14 and 9 for cases A and B, respectively. Such a result agrees with what is expected from a model evaluation procedure.

We can here assert that this second modification of the grading procedure makes inevitably decrease the mark obtained by a thermodynamic model. This is simply because the success ratios are equal to 1 at the most.

### PVII.III.II Grading results

Following the procedure described above, the final marks over 20 and the associated success ratios (see Eq. (PVII.34)) for the *tc*-PR-Wilson, *tc*-PR-UNIQUAC, *tc*-PR-NRTL and PR-Van Laar models are summarized in Table PVII.2.

#### Remarks:

At this step, it is worth recalling that in the paper by Jaubert et al. [130], the PR-Van Laar model received a mark of 12.3/20. In this study, the mark reported in Table PVII.2 is lower and only reaches 11.5/20. This is a simple consequence of the new grading procedure which makes inevitably decrease the final mark by penalizing the presence of out-of-model data points.

Similarly in the paper by Nikolaidis et al. [1286], the PC-SAFT EoS with zero  $k_{ij}$  received a mark of 5.1/20. Once recalculated by considering success ratios lower than 1 as explained in this study, the mark should be slightly lower.

The detail of the calculated MAPEs, success ratios and corresponding marks are reported in Table PVII.3 and Table PVII.4 for *tc*-PR-Wilson, Table PVII.5 and Table PVII.6 for *tc*-PR-UNIQUAC, Table PVII.7 and Table PVII.8 for *tc*-PR-NRTL, and Table PVII.9 and Table PVII.10 for PR-Van Laar.

**Table PVII.2.** Final marks and corresponding success ratios of the *tc*-PR-Wilson, *tc*-PR-UNIQUAC, *tc*-PR-NRTL and PR-Van Laar models using the grading procedure described by Jaubert et al. [130] and slightly updated in Section PVII.III.I. x: liquid phase composition data ( $x_1$  or  $x_1^\alpha$ ). y: gas phase (or 2<sup>nd</sup> liquid phase) composition data ( $y_1$  or  $x_1^\beta$ ). LLV: three-phase lines data. Crit: critical point data. Az: azeotropic data.

Model	Final mark (over 20)	Success ratios <sup>(*)</sup>					
		Overall <sup>(**)</sup>	x	y	LLV	Crit	Az
<i>tc</i> -PR-Wilson	12.4	96%	95%	94%	83%	96%	97%
<i>tc</i> -PR-UNIQUAC	11.8	97%	96%	95%	79%	94%	87%
<i>tc</i> -PR-NRTL	11.4	96%	94%	94%	77%	96%	86%
PR-Van Laar	11.5	95%	93%	93%	82%	93%	72%

<sup>(\*)</sup> "Out of model" data points do not occur for enthalpy and heat capacity of mixing data, because it is always possible to calculate these properties at specified  $T$ ,  $P$ ,  $z_1$

<sup>(\*\*)</sup> The calculation of the overall success ratio includes the  $h^M$  and  $C_P^M$  data for which such ratios are 1.

The *tc*-PR-Wilson model takes the lead over the other models with a mark of 12.4 / 20. In terms of success ratio, the four models yield excellent overall success ratios since they are higher than 95%. Differences between the studied models are observed for the success ratios of three-phase line and azeotropic point calculations. For both of them, it is observed that the *tc*-PR-Wilson model reaches the highest ratios. This is important from a qualitative standpoint because it means that this model is capable of predicting the right phase behavior topology for most of the binary systems present in the benchmark database.

From a quantitative standpoint, the overall marks per property, are plotted in Figure PVII.2. Such marks are calculated following Eq. (PVII.35) that is:

$$\text{Overall mark}_{prop} = \frac{1}{4} \times \left[ \frac{\text{mark}^{BAC_1} + \text{mark}^{BAC_2} + \text{mark}^{BAC_3} + \text{mark}^{BAC_4}}{4} + \text{mark}^{BAC_5} + \frac{\text{mark}^{BAC_6} + \text{mark}^{BAC_7} + \text{mark}^{BAC_8} + \text{mark}^{BAC_9}}{3} \right] \quad (\text{PVII.35})$$

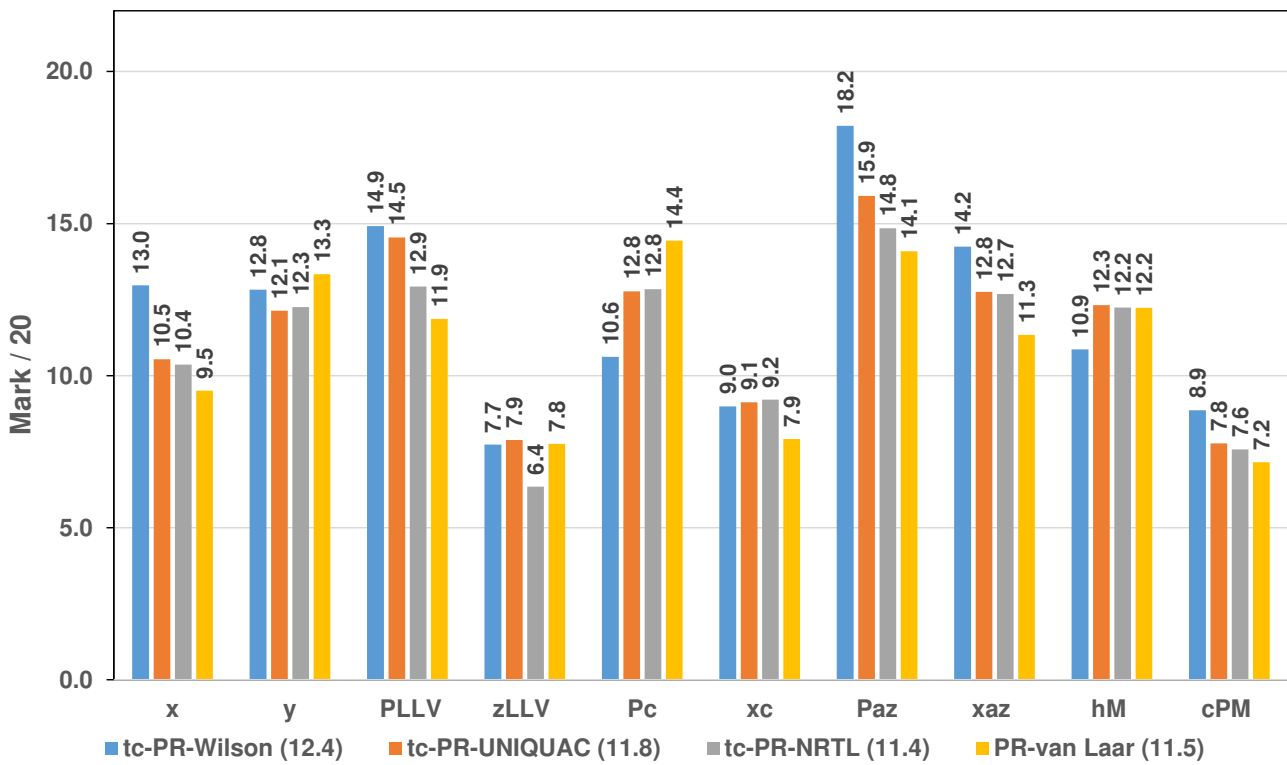


**Figure PVII.2.** Overview of the accuracy of the *tc*-PR-Wilson, *tc*-PR-UNIQUAC, *tc*-PR-NRTL and PR-van Laar by plotting the overall marks per property ( $prop \in \{x, y, P_{LLV}, z_{LLV}, P_c, x_c, P_{azeo}, x_{azeo}, h^M, c_P^M\}$ ) as returned by Eq. (PVII.35). The complete database, i.e., the 200 binary systems are considered here.

It is possible to observe that the *tc*-PR-Wilson reaches the highest overall marks for liquid compositions, azeotropic pressures and compositions, three-phase pressures and mixing heat capacities, which results in 5 out of 10 properties.

The PR-Van Laar model gives the best results for gas phase compositions and critical pressures. In turn, three-phase compositions are similarly reproduced by the *tc*-PR-UNIQUAC, *tc*-PR-Wilson and PR-Van Laar models. These properties are not reproduced accurately regardless of the investigated models. A similar trend is observed for critical compositions since all the *tc*-PR- $a_{res}^{E,\gamma}$  model versions perform similarly by showing marks below 10 / 20.

In the next section, the discussion is focused on the performance of the investigated models in relation with the type of association exhibited by the binary systems.

**Table PVII.3.** Overview of the MAPEs between experimental data and model predictions along with the corresponding success ratios (*tc*-PR-Wilson) for the 200 binary systems included in the benchmark database proposed by Jaubert et al. [130]. The mixtures are classified in 9 BACs as proposed by Jaubert et al. [130]. The abbreviations used for the associating character of a pure compound are: NA for “Non-Associating”, HA for “Hydrogen-Acceptor”, HD for “Hydrogen-Donor” and SA for “Self-Associating”. Dots (-) indicate that no experimental data are available in the database for the respective properties.

Binary association code	Type of association	MAPE and corresponding success ratio (SR) on:														
		$x$	$SR_x$	$y$	$SR_y$	$P_{LLV}$	$z_{LLV}$	$SR_{LLV}$	$P_c$	$x_c$	$SR_c$	$P_{az}$	$x_{az}$	$SR_{az}$	$h^M$	$C_P^M$
1 (NA - NA)		8.0%	0.98	7.6%	0.97	3.2%	24.6%	0.56	7.7%	19.0%	0.98	0.8%	8.1%	1.00	34.6%	185.3%
2 (HA-NA)	Mixtures without association	10.0%	0.95	7.3%	0.95	-	-	-	6.0%	10.5%	0.99	1.7%	6.0%	1.00	31.4%	150.9%
3 (HD-NA)		8.6%	0.88	6.9%	0.88	-	-	-	5.9%	17.3%	0.98	2.6%	6.4%	1.00	18.6%	155.2%
4 (HA-HA or HD-HD)		8.9%	0.97	7.6%	0.97	-	-	-	5.6%	13.7%	1.00	15.8%	9.9%	1.00	24.2%	176.3%
5 (SA-NA)	Mixtures in which self-association tends to be broken	16.2%	0.90	25.6%	0.91	3.3%	29.6%	0.84	41.8%	57.8%	0.98	1.4%	8.3%	0.97	31.4%	104.5%
6 (HD-HA)	Mixtures in which cross-association takes place alone	8.2%	0.96	7.5%	0.96	-	-	-	3.1%	14.8%	1.00	1.5%	11.4%	1.00	40.3%	85.3%
7 (SA-HD)	Mixtures in which both cross-association and self-association take place	12.6%	0.98	10.0%	0.98	-	-	-	-	-	-	1.4%	7.6%	1.00	50.3%	64.4%
8 (SA-HA)		16.6%	0.94	10.7%	0.94	1.4%	13.1%	1.00	19.6%	23.9%	0.85	1.9%	15.1%	0.98	42.4%	84.1%
9 (SA-SA)		21.3%	0.94	12.6%	0.94	2.7%	8.9%	1.00	6.3%	8.7%	0.98	5.5%	28.7%	0.85	49.4%	117.6%
<b>Overall</b>		<b>12.5%</b>	<b>0.95</b>	<b>10.3%</b>	<b>0.94</b>	<b>2.7%</b>	<b>20.3%</b>	<b>0.83</b>	<b>12.6%</b>	<b>20.8%</b>	<b>0.96</b>	<b>2.7%</b>	<b>11.8%</b>	<b>0.97</b>	<b>36.9%</b>	<b>123.4%</b>

**Table PVII.4.** Rating of the 9 binary association codes in order to obtain the final grade of the *tc*-PR-Wilson model.

Binary association code (BAC)	Type of association	Mark on:										Binary association code mark	Mark (over 20) by type of association	Final mark of the <i>tc</i> -PR-Wilson model
		$x$	$y$	$P_{LLV}$	$z_{LLV}$	$P_c$	$x_c$	$P_{az}$	$x_{az}$	$h^M$	$c_p^M$			
<b>1</b> (NA - NA)	Mixtures without association	15.7	15.7	10.3	4.3	14.0	10.3	19.6	15.9	11.4	1.5	11.9	$\underbrace{mark_{NA}}_{\text{no association}} = 13.2$	<b>12.4/20</b>
<b>2</b> (HA-NA)		14.2	15.4	-	-	15.3	14.6	19.2	17.0	12.1	4.9	14.1		
<b>3</b> (HD-NA)		13.8	14.6	-	-	15.3	11.1	18.7	16.8	15.3	4.5	13.8		
<b>4</b> (HA-HA or HD-HD)		15.1	15.7	-	-	15.8	13.1	12.1	15.1	13.9	2.4	12.9		
<b>5</b> (SA-NA)	Mixtures in which self-association tends to be broken	10.8	6.5	15.4	4.4	<b>0.0</b>	<b>0.0</b>	18.7	15.4	12.1	9.6	9.3	$\underbrace{mark_{SA}}_{\text{self-association}} = 9.3$	
<b>6</b> (HD-HA)	Mixtures in which cross-association takes place alone	15.3	15.6	-	-	17.6	12.6	19.2	14.3	9.9	11.5	14.5	$\underbrace{mark_{CA}}_{\text{cross-association}} = 14.5$	
<b>7</b> (SA-HD)	Mixtures in which both cross-association and self-association take place	13.4	14.7	-	-	-	-	19.3	16.2	7.4	13.6	14.1	$\underbrace{mark_{CA+SA}}_{\text{cross-association + self-association}} = 12.8$	
<b>8</b> (SA-HA)		11.0	13.7	19.3	13.4	4.5	6.8	18.6	12.1	9.4	11.6	12.1		
<b>9</b> (SA-SA)		8.8	12.9	18.7	15.6	15.0	15.4	14.6	4.8	7.6	8.2	12.2		
<b>Overall mark (Eq. (PVII.35))</b>		<b>13.0</b>	<b>12.8</b>	<b>14.9</b>	<b>7.7</b>	<b>10.6</b>	<b>9.0</b>	<b>18.2</b>	<b>14.2</b>	<b>10.9</b>	<b>8.9</b>	<b>12.4</b>		

**Table PVII.5.** Overview of the MAPEs between experimental data and model predictions along with the corresponding success ratios (*tc*-PR-UNIQUEAC) for the 200 binary systems included in the benchmark database proposed by Jaubert et al. [130]. The mixtures are classified in 9 BACs as proposed by Jaubert et al. [130]. The abbreviations used for the associating character of a pure compound are: NA for “Non-Associating”, HA for “Hydrogen-Acceptor”, HD for “Hydrogen-Donor” and SA for “Self-Associating”. Dots (-) indicate that no experimental data are available in the database for the respective properties.

Binary association code	MAPE and corresponding success ratio (SR) on:														
	$x$	$SR_x$	$y$	$SR_y$	$P_{LLV}$	$z_{LLV}$	$SR_{LLV}$	$P_c$	$x_c$	$SR_c$	$P_{az}$	$x_{az}$	$SR_{az}$	$h^M$	$C_P^M$
1 (NA - NA)	10.0%	0.99	9.1%	0.97	4.1%	21.0%	0.81	5.7%	20.1%	0.98	5.7%	12.4%	1.00	29.7%	185.0%
2 (HA-NA)	9.9%	0.96	7.7%	0.96	-	-	-	5.4%	11.9%	0.98	1.4%	5.4%	1.00	26.2%	160.1%
3 (HD-NA)	8.9%	0.90	7.1%	0.90	-	-	-	5.9%	16.3%	0.98	2.1%	7.9%	1.00	16.6%	161.3%
4 (HA-HA or HD-HD)	10.6%	0.96	8.1%	0.96	-	-	-	5.5%	13.8%	1.00	15.0%	10.1%	1.00	23.1%	158.7%
5 (SA-NA)	27.6%	0.93	28.7%	0.94	4.1%	30.3%	0.56	10.7%	58.2%	0.89	3.2%	7.8%	0.71	32.1%	168.0%
6 (HD-HA)	6.5%	0.96	6.3%	0.96	-	-	-	2.9%	11.5%	0.97	1.4%	6.5%	1.00	22.8%	57.3%
7 (SA-HD)	32.4%	0.97	17.9%	0.98	-	-	-	-	-	-	0.7%	8.1%	0.77	50.9%	47.0%
8 (SA-HA)	23.2%	0.94	12.3%	0.94	1.3%	14.0%	1.00	29.3%	24.9%	0.77	2.8%	20.9%	0.76	39.3%	120.5%
9 (SA-SA)	27.4%	0.96	15.5%	0.95	2.7%	13.1%	1.00	6.0%	8.7%	0.98	6.1%	34.3%	0.79	42.2%	124.7%
<b>Overall</b>	<b>16.5%</b>	<b>0.96</b>	<b>11.9%</b>	<b>0.95</b>	<b>3.1%</b>	<b>19.9%</b>	<b>0.79</b>	<b>9.4%</b>	<b>21.0%</b>	<b>0.94</b>	<b>3.3%</b>	<b>13.5%</b>	<b>0.87</b>	<b>32.8%</b>	<b>136.0%</b>

**Table PVII.6.** Rating of the 9 binary association codes in order to obtain the final grade of the *tc*-PR-UNIQUAC model.

Binary association code (BAC)	Mark on:										Binary association code mark	Mark (over 20) by type of association	Final mark of the <i>tc</i> -PR-UNIQUAC model
	$x$	$y$	$P_{LLV}$	$z_{LLV}$	$P_c$	$x_c$	$P_{az}$	$x_{az}$	$h^M$	$C_P^M$			
1 (NA - NA)	14.8	15.0	14.6	7.7	15.4	9.8	17.2	13.8	12.6	1.5	12.2		
2 (HA-NA)	14.5	15.5	-	-	15.7	13.8	19.3	17.3	13.5	4.0	14.2	$\underbrace{mark_{NA}}_{\text{no association}} = 13.3$	
3 (HD-NA)	14.0	14.8	-	-	15.2	11.6	19.0	16.1	15.9	3.9	13.8		
4 (HA-HA or HD-HD)	14.2	15.4	-	-	15.8	13.1	12.5	14.9	14.2	4.1	13.0		
5 (SA-NA)	5.8	5.3	10.1	2.7	10.7	<b>0.0</b>	13.2	11.5	12.0	3.2	7.4	$\underbrace{mark_{SA}}_{\text{self-association}} = 7.4$	<b>11.8/20</b>
6 (HD-HA)	16.1	16.2	-	-	17.3	13.8	19.3	16.7	14.3	14.3	16.0	$\underbrace{mark_{CA}}_{\text{cross-association}} = 16.0$	
7 (SA-HD)	3.7	10.8	-	-	-	-	15.1	12.3	7.3	15.3	10.7	$\underbrace{mark_{CA+SA}}_{\text{cross-association} + \text{self-association}} = 10.6$	
8 (SA-HA)	7.9	13.0	19.3	13.0	<b>0.0</b>	5.8	14.2	7.3	10.2	8.0	9.9		
9 (SA-SA)	6.0	11.7	18.7	13.4	15.2	15.3	13.4	2.2	9.5	7.5	11.3		
<b>Overall mark (Eq. (PVII.35))</b>	<b>10.5</b>	<b>12.1</b>	<b>14.5</b>	<b>7.9</b>	<b>12.8</b>	<b>9.1</b>	<b>15.9</b>	<b>12.8</b>	<b>12.3</b>	<b>7.8</b>	<b>11.8</b>		

**Table PVII.7.** Overview of the MAPEs between experimental data and model predictions along with the corresponding success ratios (*tc*-PR-NRTL) for the 200 binary systems included in the benchmark database proposed by Jaubert et al. [130]. The mixtures are classified in 9 BACs as proposed by Jaubert et al. [130]. The abbreviations used for the associating character of a pure compound are: NA for “Non-Associating”, HA for “Hydrogen-Acceptor”, HD for “Hydrogen-Donor” and SA for “Self-Associating”. Dots (-) indicate that no experimental data are available in the database for the respective properties.

Binary association code	MAPE and corresponding success ratio (SR) on:														
	$x$	$SR_x$	$y$	$SR_y$	$P_{LLV}$	$z_{LLV}$	$SR_{LLV}$	$P_c$	$x_c$	$SR_c$	$P_{az}$	$x_{az}$	$SR_{az}$	$h^M$	$C_p^M$
1 (NA - NA)	9.9%	0.97	8.8%	0.96	3.2%	14.7%	0.75	6.7%	20.5%	0.97	5.4%	8.0%	1.00	30.0%	184.7%
2 (HA-NA)	11.0%	0.96	7.9%	0.95	-	-	-	3.8%	9.3%	0.99	1.2%	4.3%	1.00	28.6%	160.0%
3 (HD-NA)	8.4%	0.90	7.1%	0.90	-	-	-	5.8%	16.5%	0.98	1.9%	6.7%	1.00	17.5%	160.8%
4 (HA-HA or HD-HD)	9.9%	0.95	7.8%	0.95	-	-	-	5.7%	12.0%	1.00	40.2%	20.2%	1.00	22.7%	158.7%
5 (SA-NA)	27.7%	0.87	27.3%	0.94	12.1%	35.8%	0.96	13.5%	58.5%	0.93	3.6%	12.9%	0.71	31.2%	142.3%
6 (HD-HA)	6.7%	0.96	6.2%	0.96	-	-	-	3.2%	14.7%	1.00	1.2%	4.6%	0.94	22.6%	75.9%
7 (SA-HD)	39.6%	0.93	20.8%	0.94	-	-	-	-	-	-	1.3%	10.4%	0.69	48.9%	95.8%
8 (SA-HA)	20.5%	0.95	11.8%	0.95	2.0%	17.3%	0.92	22.4%	23.1%	0.86	1.1%	18.4%	0.88	39.4%	139.8%
9 (SA-SA)	22.4%	0.91	11.9%	0.90	2.4%	9.4%	0.31	6.2%	7.3%	0.98	2.7%	15.1%	0.64	48.7%	102.5%
<b>Overall</b>	<b>15.6%</b>	<b>0.94</b>	<b>11.2%</b>	<b>0.94</b>	<b>7.1%</b>	<b>24.8%</b>	<b>0.77</b>	<b>8.7%</b>	<b>20.3%</b>	<b>0.96</b>	<b>3.5%</b>	<b>10.9%</b>	<b>0.86</b>	<b>33.9%</b>	<b>128.3%</b>

**Table PVII.8.** Rating of the 9 binary association codes in order to obtain the final grade of the *tc*-PR-NRTL model.

Binary association code (BAC)	Mark on:										Binary association code mark	Mark (over 20) by type of association	Final mark of the <i>tc</i> -PR-NRTL model
	$x$	$y$	$P_{LLV}$	$z_{LLV}$	$P_c$	$x_c$	$P_{az}$	$x_{az}$	$h^M$	$C_P^M$			
1 (NA - NA)	14.7	15.0	13.8	9.5	14.6	9.5	17.3	16.0	12.5	1.5	12.4		
2 (HA-NA)	13.9	15.3	-	-	16.9	15.1	19.4	17.9	12.8	4.0	14.4	$\underbrace{mark_{NA}}_{\text{no association}} = 12.9$	
3 (HD-NA)	14.2	14.8	-	-	15.3	11.5	19.0	16.7	15.6	3.9	13.9		
4 (HA-HA or HD-HD)	14.3	15.3	-	-	15.7	14.0	<b>0.0</b>	9.9	14.3	4.1	11.0		
5 (SA-NA)	5.4	6.0	13.4	2.0	9.2	<b>0.0</b>	13.0	9.7	12.2	5.8	7.7	$\underbrace{mark_{SA}}_{\text{self-association}} = 7.7$	<b>11.4/20</b>
6 (HD-HA)	16.0	16.3	-	-	17.6	12.6	18.3	16.7	14.3	12.4	15.5	$\underbrace{mark_{CA}}_{\text{cross-association}} = 15.5$	
7 (SA-HD)	0.2	9.0	-	-	-	-	13.4	10.3	7.8	10.4	8.5	$\underbrace{mark_{CA+SA}}_{\text{cross-association} + \text{self-association}} = 9.6$	
8 (SA-HA)	9.2	13.4	17.4	10.4	2.8	7.3	17.2	9.5	10.2	6.0	10.3		
9 (SA-SA)	8.0	12.7	5.8	4.7	15.1	16.0	11.9	7.9	7.8	9.7	10.0		
<b>Overall mark (Eq. (PVII.35))</b>	<b>10.4</b>	<b>12.3</b>	<b>12.9</b>	<b>6.4</b>	<b>12.8</b>	<b>9.2</b>	<b>14.8</b>	<b>12.7</b>	<b>12.2</b>	<b>7.6</b>	<b>11.4</b>		

**Table PVII.9.** Overview of the MAPEs between experimental data and model predictions along with the corresponding success ratios (PR-Van Laar) for the 200 binary systems included in the benchmark database proposed by Jaubert et al. [130]. The mixtures are classified in 9 BACs as proposed by Jaubert et al. [130]. The abbreviations used for the associating character of a pure compound are: NA for “Non-Associating”, HA for “Hydrogen-Acceptor”, HD for “Hydrogen-Donor” and SA for “Self-Associating”. Dots (-) indicate that no experimental data are available in the database for the respective properties.

Binary association	MAPE and corresponding success ratio (SR) on:														
	Code	$x$	$SR_x$	$y$	$SR_y$	$P_{LLV}$	$z_{LLV}$	$SR_{LLV}$	$P_c$	$x_c$	$SR_c$	$P_{az}$	$x_{az}$	$SR_{az}$	$h^M$
1 (NA - NA)	7.9%	0.97	7.9%	0.96	1.3%	19.3%	0.31	3.6%	12.9%	0.95	1.0%	5.1%	1.00	21.7%	34.7%
2 (HA-NA)	8.8%	0.96	6.8%	0.95	-	-	-	2.4%	9.0%	0.97	0.9%	6.2%	1.00	16.3%	160.3%
3 (HD-NA)	6.9%	0.94	5.7%	0.94	-	-	-	5.2%	15.7%	0.98	0.6%	3.7%	0.95	12.5%	70.5%
4 (HA-HA or HD-HD)	7.5%	0.97	7.2%	0.97	-	-	-	4.0%	11.1%	1.00	5.6%	9.6%	1.00	13.5%	104.4%
5 (SA-NA)	40.0%	0.83	14.9%	0.93	5.2%	24.0%	0.96	9.0%	44.1%	0.88	4.9%	13.8%	0.37	32.4%	200.0%
6 (HD-HA)	6.0%	0.93	6.1%	0.93	-	-	-	3.5%	21.5%	1.00	2.0%	9.6%	1.00	23.6%	43.1%
7 (SA-HD)	15.2%	0.85	12.3%	0.85	-	-	-	-	-	-	2.4%	9.6%	0.85	84.4%	188.0%
8 (SA-HA)	24.9%	0.92	15.7%	0.90	24.5%	17.4%	1.00	12.9%	28.4%	0.84	3.9%	11.0%	0.64	37.2%	164.4%
9 (SA-SA)	33.9%	0.89	22.6%	0.89	4.2%	13.3%	1.00	5.6%	13.2%	0.96	6.6%	24.4%	0.45	39.6%	182.4%
<b>Overall</b>	<b>16.6%</b>	<b>0.93</b>	<b>11.3%</b>	<b>0.93</b>	<b>8.9%</b>	<b>19.5%</b>	<b>0.82</b>	<b>5.5%</b>	<b>18.1%</b>	<b>0.94</b>	<b>6.6%</b>	<b>9.2%</b>	<b>0.74</b>	<b>30.5%</b>	<b>139.6%</b>

**Table PVII.10.** Rating of the 9 binary association codes in order to obtain the final grade of the PR-Van Laar model.

Binary association code (BAC)	Mark on:										Binary association code mark	Mark (over 20) by type of association	Final mark of the PR-Van Laar model
	$x$	$y$	$P_{LLV}$	$z_{LLV}$	$P_c$	$x_c$	$P_{az}$	$x_{az}$	$h^M$	$C_P^M$			
1 (NA - NA)	15.6	15.4	6.0	3.2	16.5	12.9	19.5	17.5	14.6	16.5	13.8		
2 (HA-NA)	15.0	15.8	-	-	17.7	15.1	19.5	16.9	15.9	4.0	15.0	$\underbrace{mark_{NA}}_{\text{no association}} = 14.9$	
3 (HD-NA)	15.6	16.2	-	-	15.8	11.9	18.8	17.3	16.9	13.0	15.7		
4 (HA-HA or HD-HD)	15.7	15.9	-	-	17.0	14.4	17.2	15.2	16.6	9.6	15.2		
5 (SA-NA)	<b>0.0</b>	11.6	16.7	7.7	11.7	<b>0.0</b>	6.5	4.9	11.9	<b>0.0</b>	7.1	$\underbrace{mark_{SA}}_{\text{self-association}} = 7.1$	<b>11.5/20</b>
6 (HD-HA)	15.8	15.7	-	-	17.4	9.2	19.0	15.2	14.1	15.7	15.3	$\underbrace{mark_{CA}}_{\text{cross-association}} = 15.3$	
7 (SA-HD)	10.5	11.7	-	-	-	-	15.9	12.9	<b>0.0</b>	1.2	8.7	$\underbrace{mark_{CA+SA}}_{\text{cross-association + self-association}} = 8.9$	
8 (SA-HA)	6.9	11.0	7.8	11.3	8.6	4.9	11.6	9.3	10.7	3.6	8.6		
9 (SA-SA)	2.7	7.7	17.9	13.3	15.2	12.9	8.8	3.5	10.1	1.8	9.4		
<b>Overall mark (Eq. (PVII.35))</b>	<b>9.5</b>	<b>13.3</b>	<b>11.9</b>	<b>7.8</b>	<b>14.4</b>	<b>7.9</b>	<b>14.1</b>	<b>11.3</b>	<b>12.2</b>	<b>7.2</b>	<b>11.5</b>		

### PVII.III.III Discussion

Among the 9 BACs, the properties of mixtures from BAC<sub>6</sub> (HD + HA molecules that exhibit cross association) is the most accurately predicted by the *tc*-PR-Wilson, *tc*-PR-UNIQUAC and *tc*-PR-NRTL models with a mark of 14.5 / 20, 16.0 / 20 and 15.5 / 20, respectively; while the PR-Van Laar model yields the highest performance for BAC<sub>3</sub> (HD + NA molecules) scoring a mark of 15.7 / 20. On the other hand, mixtures belonging to BAC<sub>5</sub>, in which self-association takes place but tends to be broken, are represented unsatisfactorily by all the studied models.

In terms of association degree (see Figure PVII.3), the *tc*-PR-Wilson performs better than the rest of the models for families where self-association is taking place (BAC 5 and BACs 7 to 9). In the case of systems that do not exhibit association (BACs 1 to 4), the PR-Van Laar model has the advantage. Finally, the *tc*-PR-UNIQUAC model correlates the best binary systems that exhibit cross-association (BAC 6).

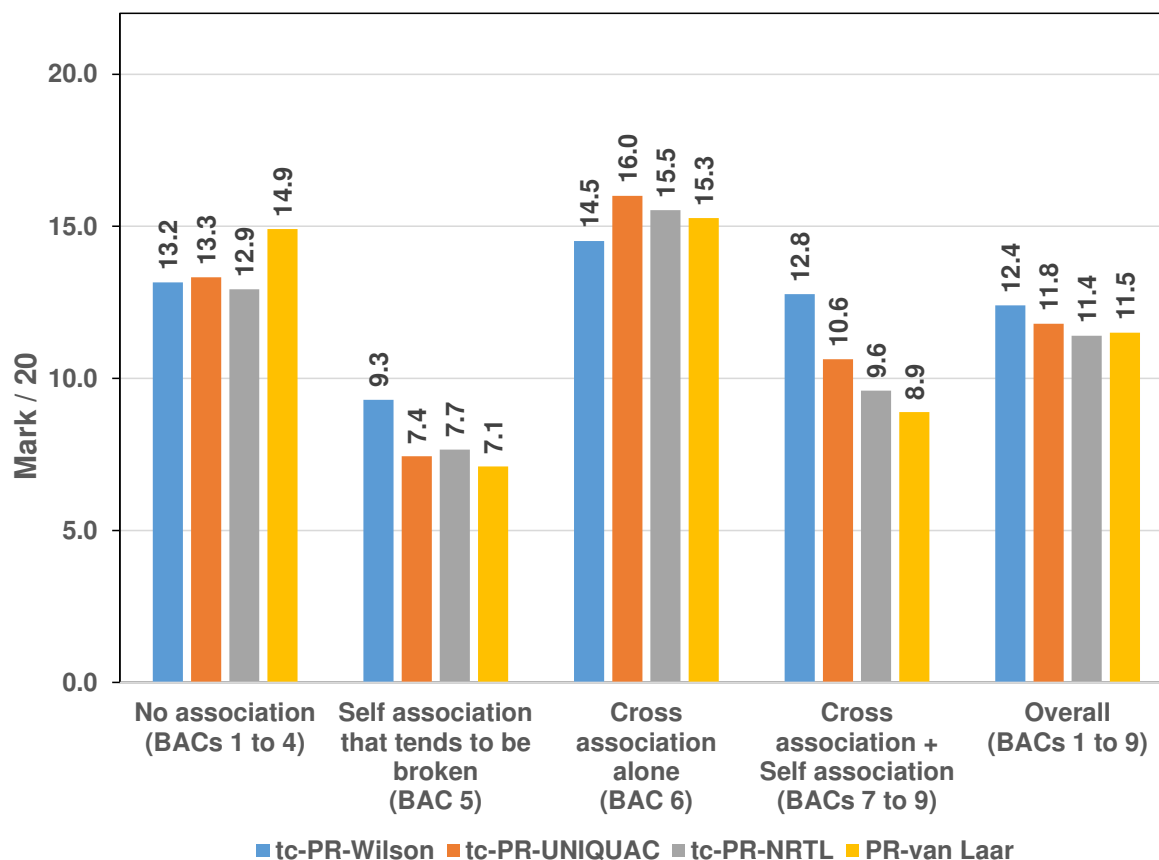


**Figure PVII.3.** Overview of the accuracy of the *tc*-PR-Wilson, *tc*-PR-UNIQUAC, *tc*-PR-NRTL and PR-Van Laar by plotting the average marks for the four categories of binary systems based on the type of association they exhibit.

In order to have a deeper insight, the marks over the ten properties of interest are plotted for the four considered models. First, in Figure PVII.4, for the category grouping BACs 1 to 4 it is possible to observe that the PR-Van Laar model yields to higher marks for all the properties except for  $P_{LLV}$  and  $z_{LLV}$ . An important fact to be highlighted is the clear advantage for the PR-Van Laar model in the

prediction of  $c_P^M$  data. This is illustrated in [Figure PVII.5](#) for the binary system Cyclohexane + Monochlorobenzene for which there is a huge difference between the calculated  $c_P^M$  with PR-Van Laar and the other three  $tc$ -PR- $a_{res}^{E,\gamma}$  models. This led us to think that the difference in the temperature dependence of the Van Laar parameter with respect to those of the  $tc$ -PR- $a_{res}^{E,\gamma}$  models, which are temperature-independent, could be the responsible for such results.

In addition, in [Figure PVII.6](#), it is possible to observe that the four models overestimate critical pressures for the binary system Nitrogen + n-pentane but PR-Van Laar yields to better results than  $tc$ -PR- $a_{res}^{E,\gamma}$  models. Once again, the question of the temperature dependence of the parameters involved in the  $a_{res}^{E,\gamma}$  models arises. Indeed, as illustrated in [Figure PVII.6](#), the PR-Van Laar and  $tc$ -PR-NRTL models predict almost the same critical pressure at  $T = 398.3K$  but at  $T = 447.9K$  the  $tc$ -PR-NRTL model presents some limitations to catch the right phase behavior.

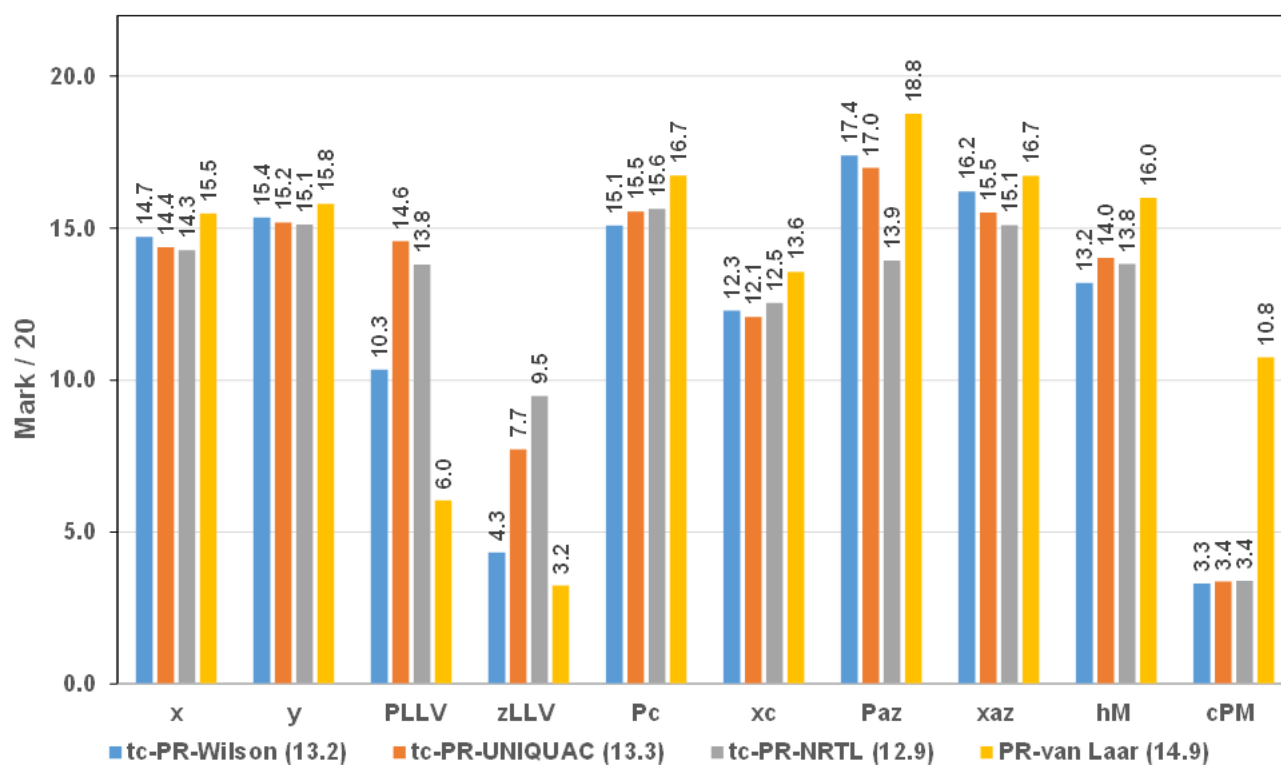


**Figure PVII.4.** Overview of the accuracy of the  $tc$ -PR-Wilson,  $tc$ -PR-UNIQUAC,  $tc$ -PR-NRTL and PR-Van Laar by plotting the marks on ten properties for the category including mixtures without association (BACs 1 to 4).

Despite the limitations observed for some systems and illustrated in [Figure PVII.5](#) and [Figure PVII.6](#), the  $tc$ -PR- $a_{res}^{E,\gamma}$  models are able to correlate with high accuracy the non-associating binary systems. The binary system  $CH_4 + N_2$  shown in [Figure PVII.7](#) perfectly demonstrates the strength of such models for such systems.

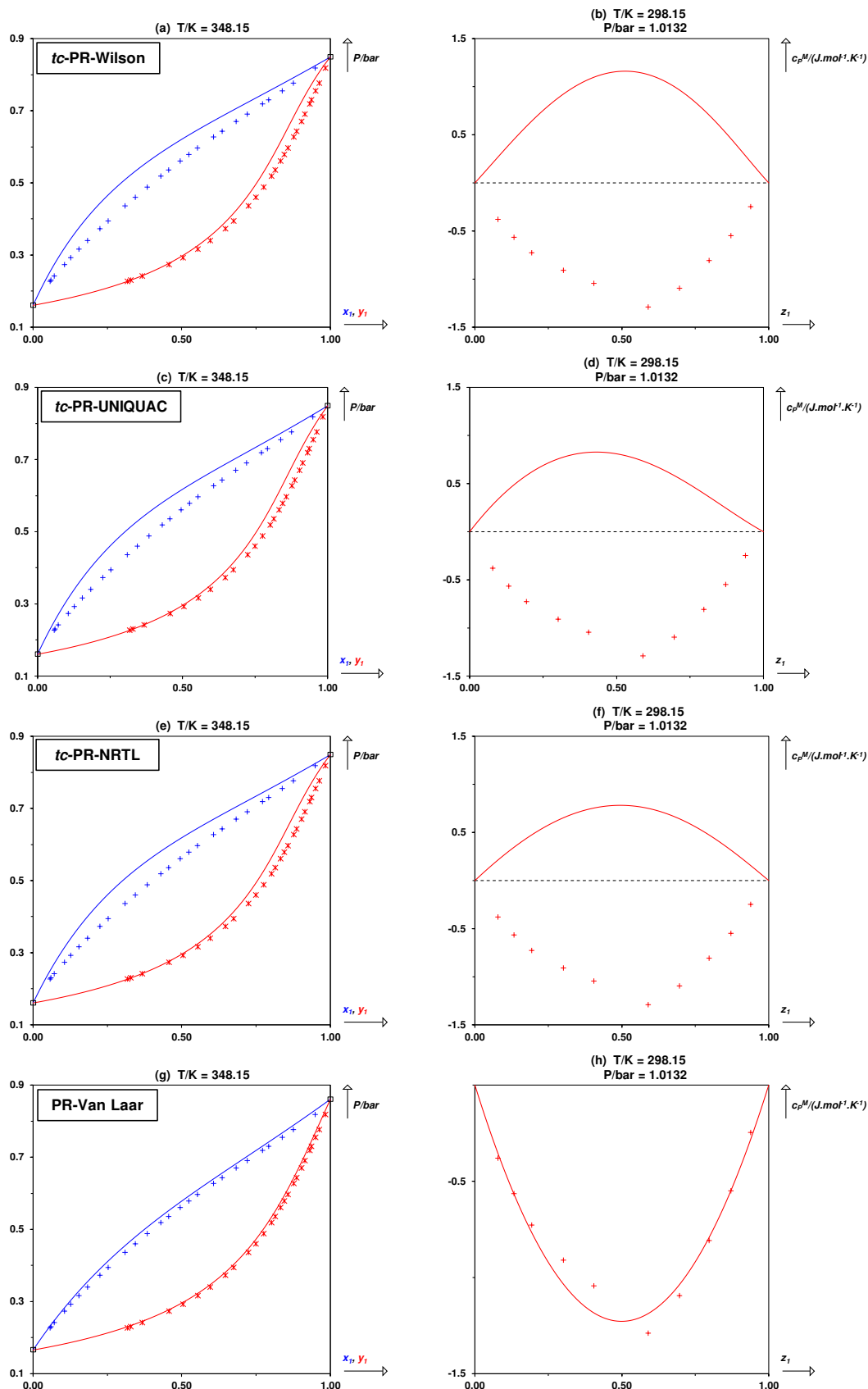


**Figure PVII.5.** Pressure – composition VLE phase diagrams (left) and mixing heat capacity – composition diagrams (right) for the binary system Cyclohexane (1) + Monochlorobenzene calculated with the *tc*-PR-Wilson (a, b), *tc*-PR-UNIQUAC (c, d), *tc*-PR-NRTL (e, f) and PR-Van Laar (g, h) models. Phase equilibrium diagrams convention: (\*): experimental dew points. (+): experimental bubble points. (–): calculated dew curve. (–): calculated bubble curve. Caloric properties diagrams convention: (+): experimental data. (–): calculated curve.

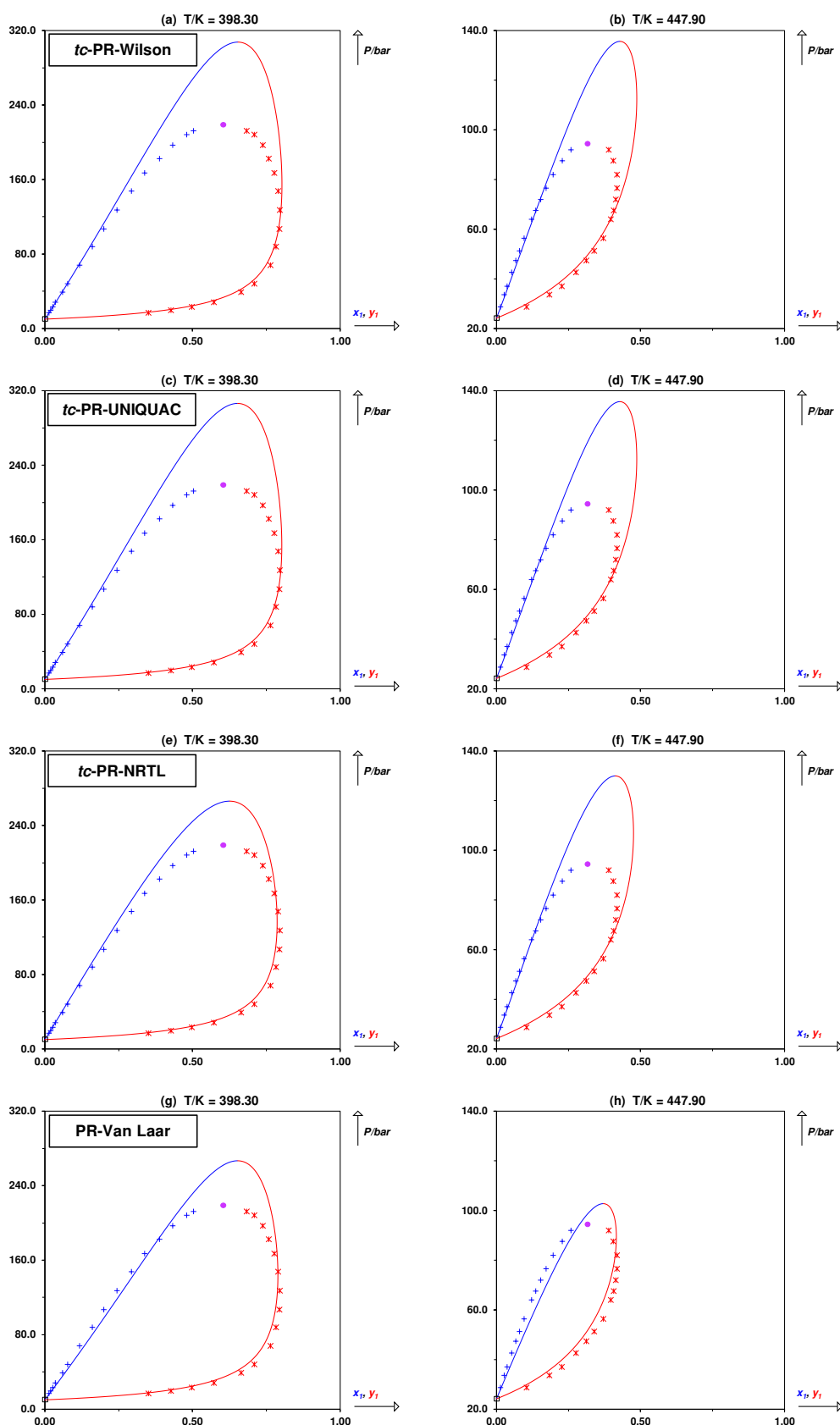


**Figure PVII.6.** Pressure – composition VLE phase diagrams for the binary system  $N_2$  (1) + n-pentane calculated with the *tc*-PR-Wilson (a, b), *tc*-PR-UNIQUAC (c, d), *tc*-PR-NRTL (e, f) and PR-Van Laar (g, h) models. Phase equilibrium diagrams convention: (\*): experimental dew points. (+): experimental bubble points. (•): experimental critical point. (–): calculated dew curve. (–): calculated bubble curve.

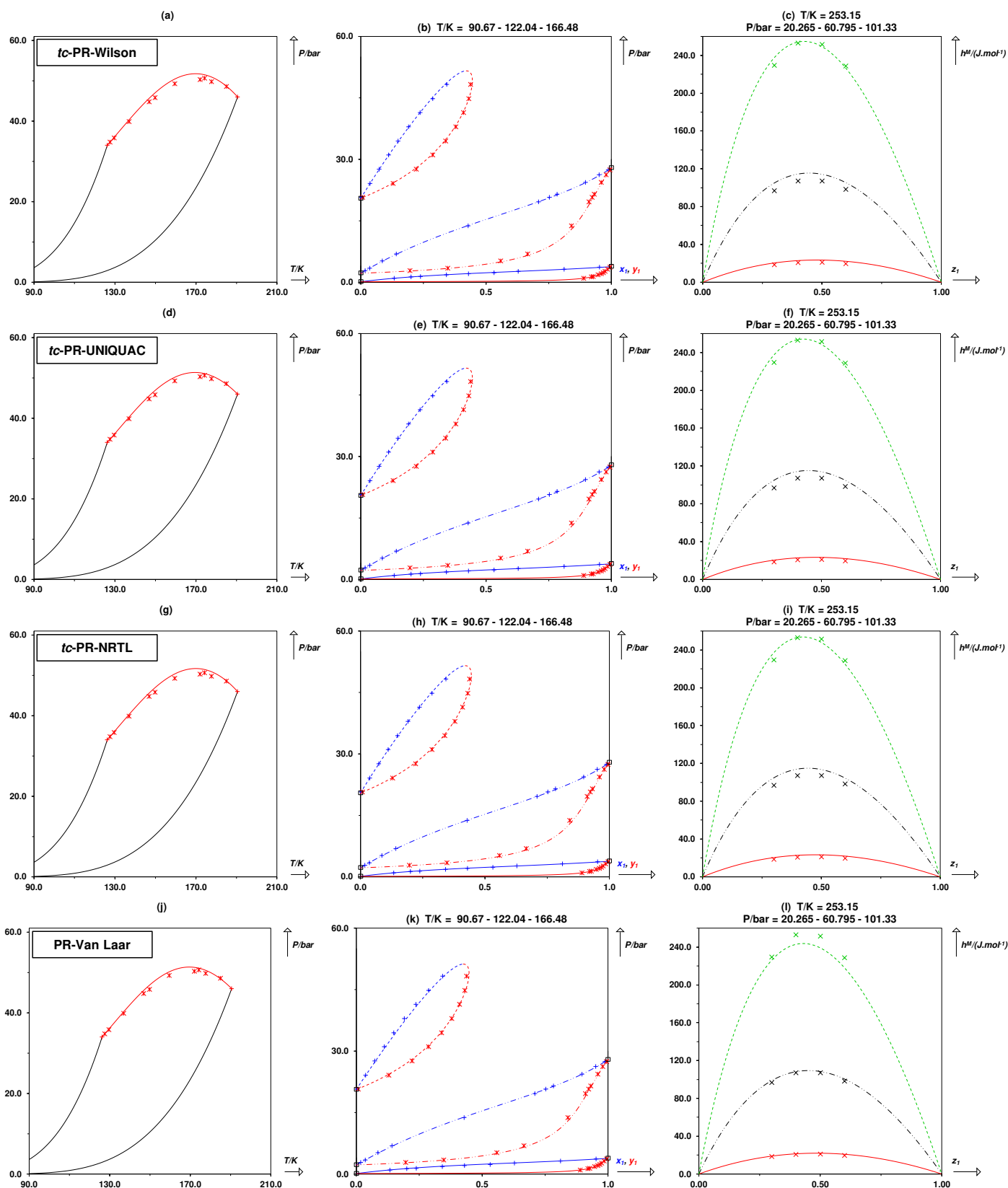


**Figure PVII.7.** Global Phase-Equilibrium Diagrams (GPEDs) (left), pressure – composition VLE phase diagrams (center) and mixing heat capacity – composition diagrams (right) for the binary system N<sub>2</sub> (1) + Methane calculated the *tc*-PR-Wilson (a, b, c), *tc*-PR-UNIQUAC (d, e, f), *tc*-PR-NRTL (g, h, i) and PR-Van Laar (j, k, l) models. GPED convention: (\*) experimental critical points. (–) calculated critical line. (–) calculated vapor-pressure curves of pure components. Phase equilibrium diagrams convention: (\*): experimental dew points. (+): experimental bubble points. (–): calculated dew curve. (–): calculated bubble curve.

Considering now the other category in which the systems do not exhibit self-association (BAC6), it should be noted that the four models perform very well, as shown in Figure PVII.8. Most of the systems exhibit negative deviations from ideality so that the liquid phase does not tend to split. As a direct consequence, no 3-phase VLE data are available in this category. In particular, all the models correlate equivalently bubble and dew point compositions, as well as critical pressures. In terms of azeotropic pressures, they are correlated with high accuracy (see Figure PVII.8) by all the models with a slight disadvantage for the *tc*-PR-NRTL model. In turn, the *tc*-PR-UNIQUAC model reproduces critical compositions accurately, while the PR-Van Laar model seems to show some limitations compared to *tc*-PR- $a_{res}^{E,\gamma}$  models. Concerning  $h^M$  predictions, *tc*-PR-Wilson presents a clear disadvantage compared to the other models, which perform almost equivalently. Finally, once again the PR-Van Laar model takes the lead on the correlation of  $c_P^M$  data, as observed with the binary system Methyl acetate + Chloroform presented in Figure PVII.9.

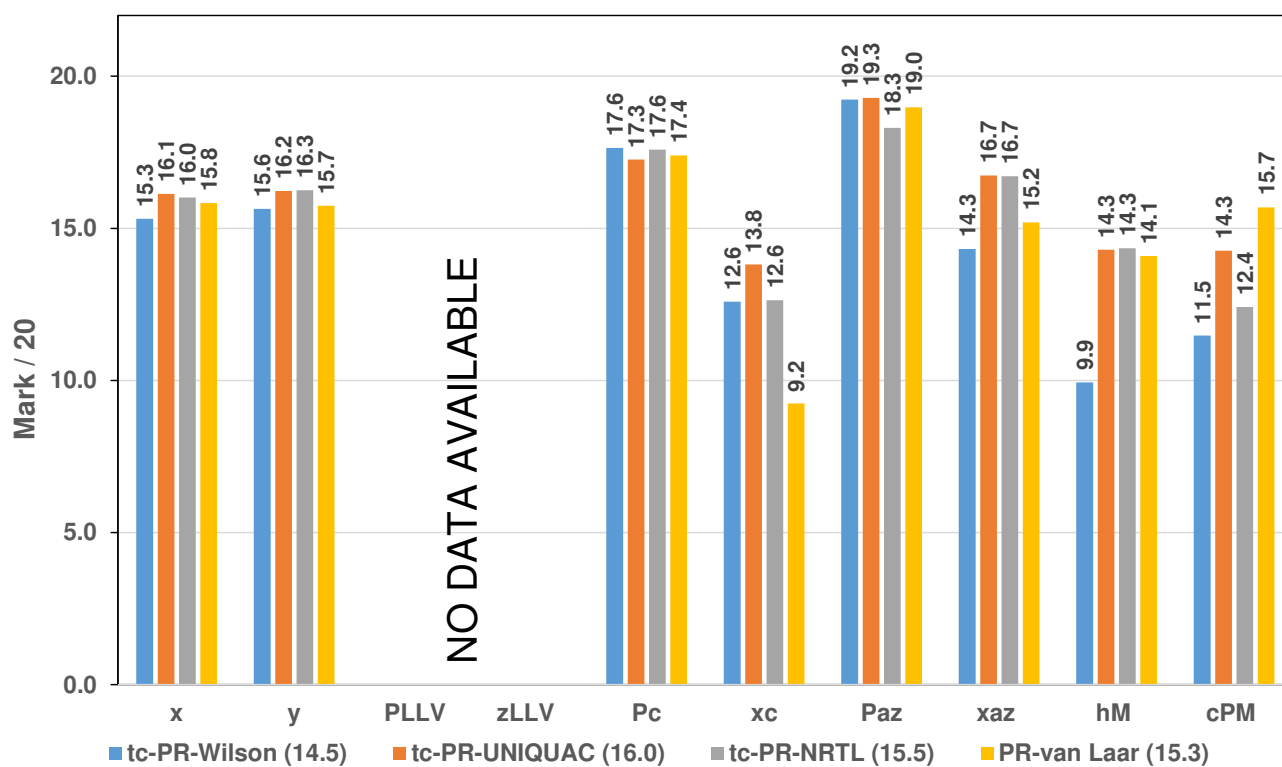


**Figure PVII.8.** Overview of the accuracy of the *tc*-PR-Wilson, *tc*-PR-UNIQUAC, *tc*-PR-NRTL and PR-Van Laar by plotting the marks on ten properties for the category including mixtures in which cross-association takes place alone.

As previously stated, binary systems belonging to BAC 6 are the most accurately correlated by CEoS. Another representative example, exhibiting negative deviations from ideality and for which very negative  $h^M$  data are available is shown in Figure PVII.10.

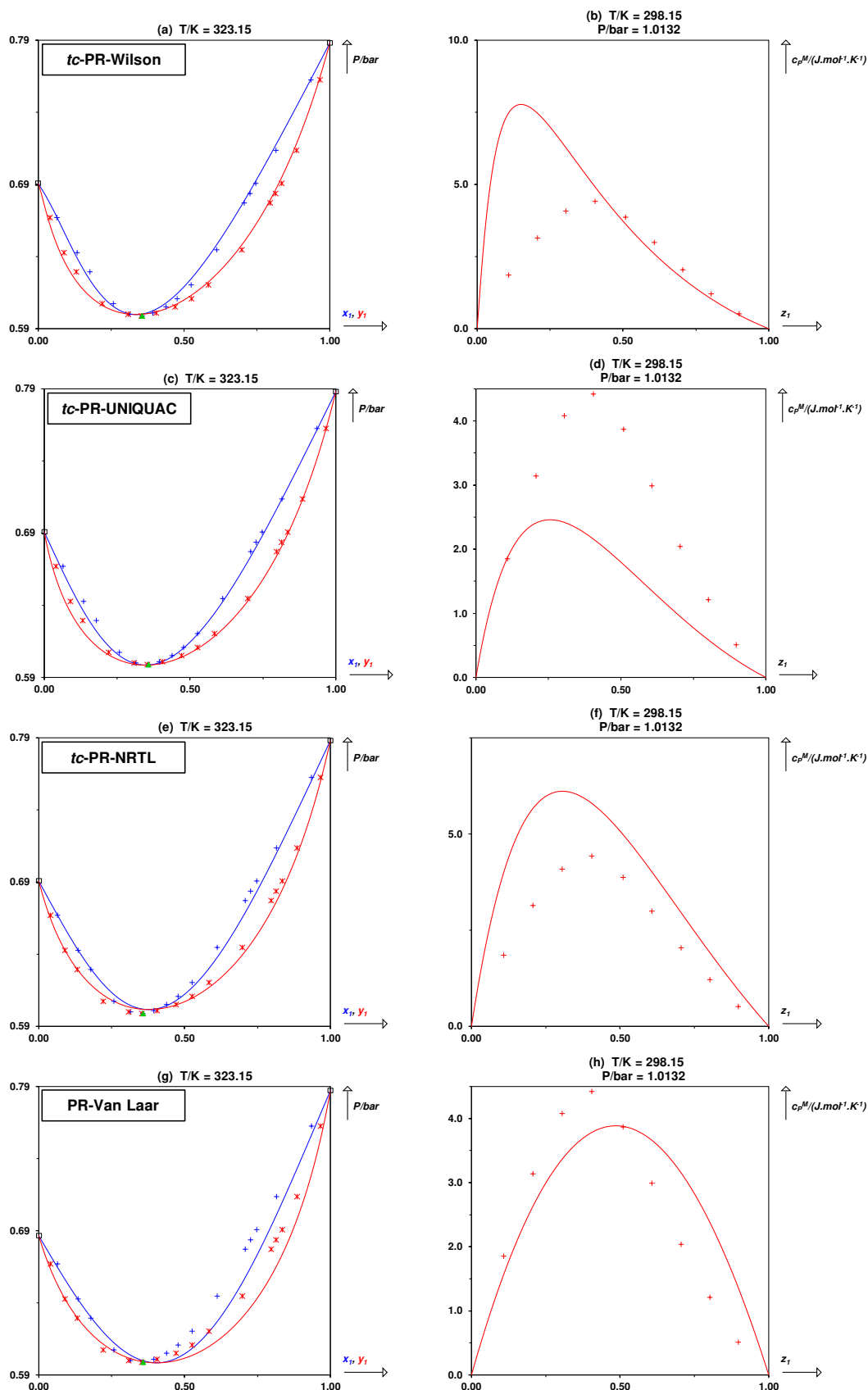


**Figure PVII.9.** Pressure – composition VLE phase diagrams (left) and mixing heat capacity – composition diagrams (right) for the binary system Methyl acetate (1) + Chloroform calculated with the *tc*-PR-Wilson (a, b), *tc*-PR-UNIQUAC (c, d), *tc*-PR-NRTL (e, f) and PR-Van Laar (g, h) models. Phase equilibrium diagrams convention: (\*): experimental dew points. (+): experimental bubble points. (▲): experimental azeotropic point. (–): calculated dew curve. (–): calculated bubble curve. Caloric properties diagrams convention: (+): experimental data. (–): calculated curve.

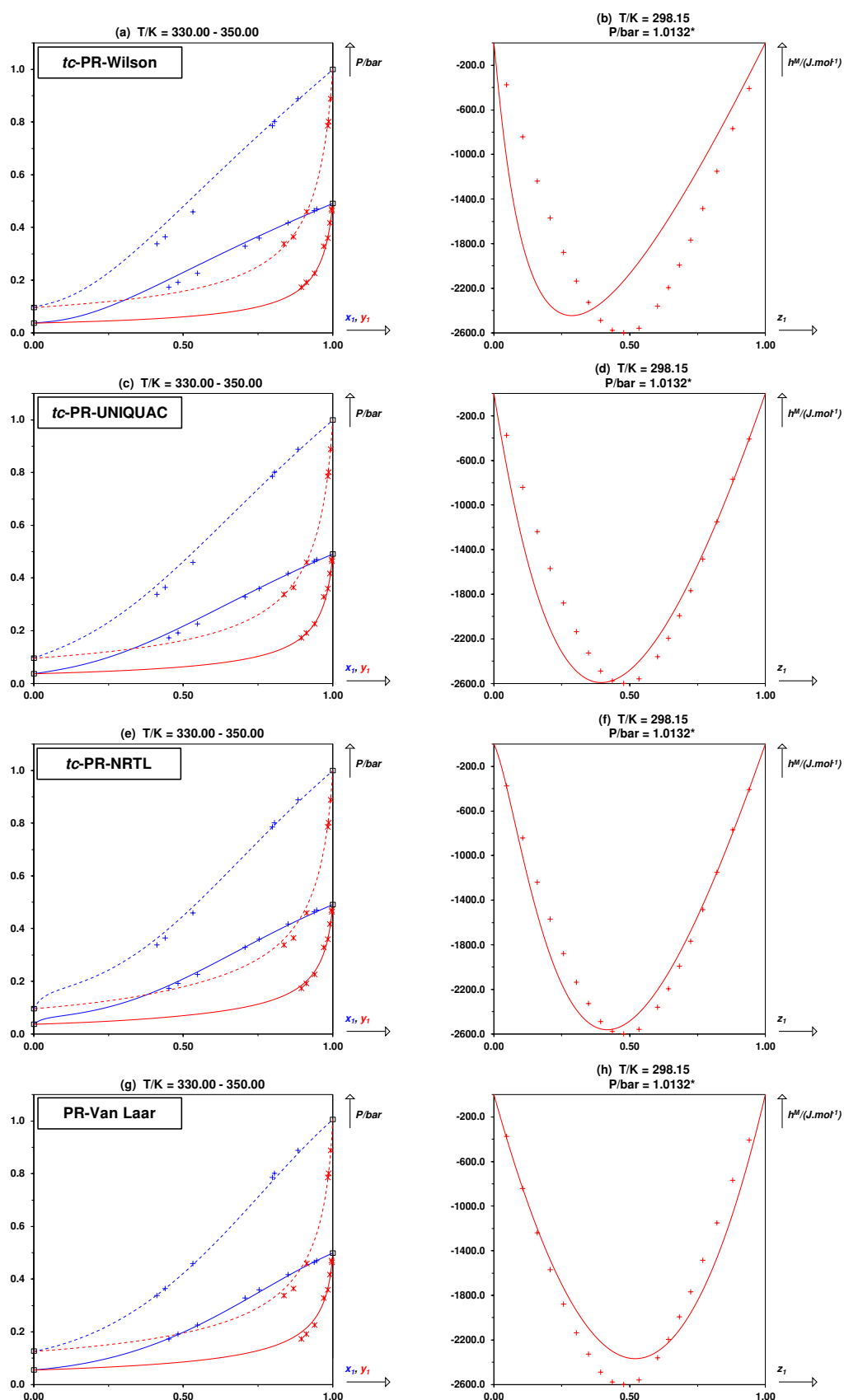


**Figure PVII.10.** Pressure – composition VLE phase diagrams (left) and mixing heat capacity – composition diagrams (right) for the binary system Ethyl acetate (1) + 1, 1, 2, 2-tetrachloroethane calculated with the *tc*-PR-Wilson (a, b), *tc*-PR-UNIQUAC (c, d), *tc*-PR-NRTL (e, f) and PR-Van Laar (g, h) models. Phase equilibrium diagrams convention: (\*): experimental dew points. (+): experimental bubble points. (–): calculated dew curve. (–): calculated bubble curve. Caloric properties diagrams convention: (+): experimental data. (–): calculated curve.

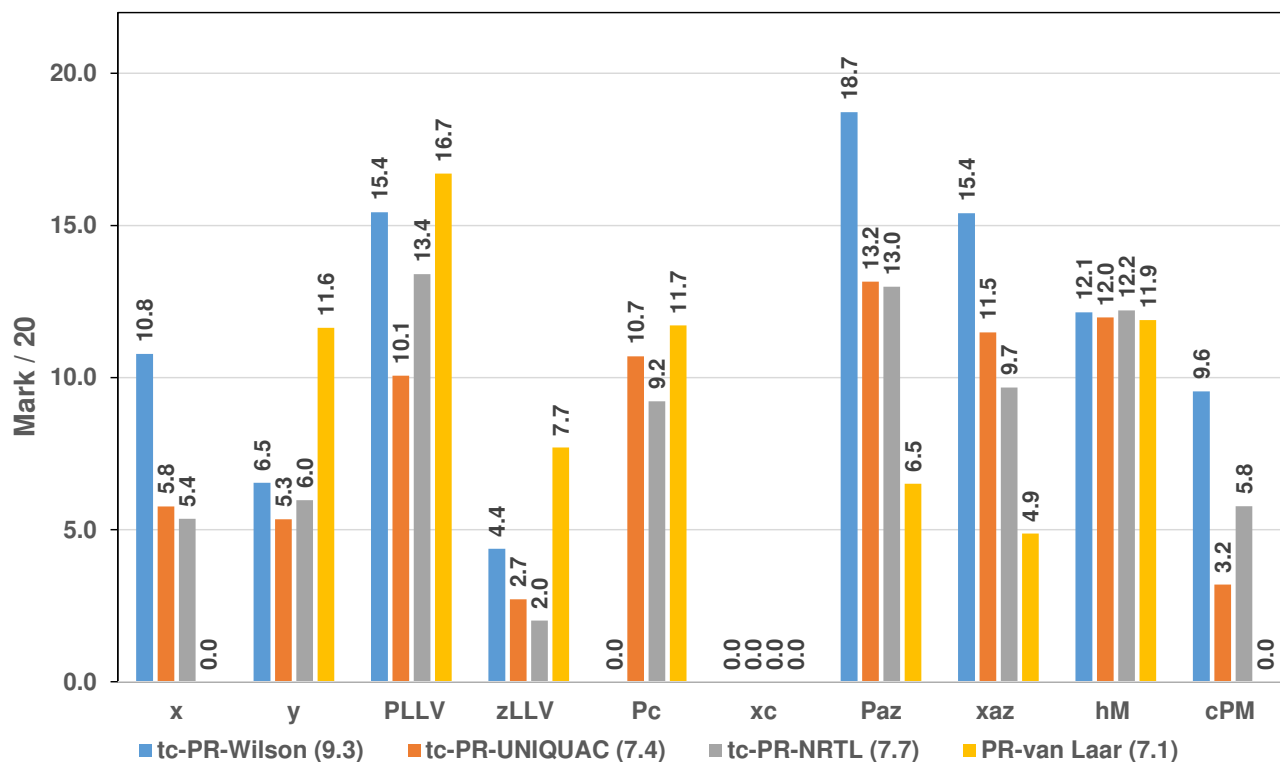


**Figure PVII.11.** Overview of the accuracy of the *tc*-PR-Wilson, *tc*-PR-UNIQUAC, *tc*-PR-NRTL and PR-Van Laar by plotting the marks on ten properties for the category including mixtures in which self-association tends to be broken

The two remaining categories (BAC5 and BACs 7 to 9) are those where at least self-association takes place. The first one, in which self-association tends to be broken, gathers systems from BAC<sub>5</sub> only. The marks on the ten properties of interest are plotted in [Figure PVII.11](#). They are the lowest in comparison to the other 3 categories highlighting the difficulty of CEoS to correlate systems that contain a self-associating compound like water and a non-associating component (e.g., a hydrocarbon). It is important to highlight that the *tc*-PR-Wilson model catches the right topology for almost all the systems of the considered BAC. For instance, in [Figure PVII.12](#), pressure – composition VLE phase diagrams correlated by the four considered models for the binary system Methanol + Benzene are presented. It is possible to notice the clear difference between the diagram predicted by the *tc*-PR-Wilson model and the remaining ones. On this example, such an improvement on the diagram topology prediction entails a higher accuracy on azeotropic compositions and pressures, and, in a lesser extent, on bubble compositions. The most visible effect of having the correct topology can be seen in [Figure PVII.12](#), on the h<sup>M</sup>-composition diagrams. Indeed, all the models except the *tc*-PR-Wilson predict a false LLE at 288.15 K and 1.0132 bar. As a direct consequence, the calculated h<sup>M</sup>-composition diagrams exhibit a straight line between the compositions of the 2 liquid phases (from  $x_1 \approx 0.25$  to  $x_1 \approx 0.95$ ). The h<sup>M</sup>-composition diagram calculated with the *tc*-PR-Wilson has however the expected shape since such a model predicts a homogeneous liquid phase at 288.15 K and 1.0132 bar. A discussion around the shape of the h<sup>M</sup>-composition diagram can be found in recently published papers [[1287,1288](#)]. For a system such as Ethane + Water (see [Figure PVII.13](#)) that exhibits gas-gas equilibria and is thus a complex type III system in the classification scheme of van Konynenburg and Scott [[1289,1290](#)], the *tc*-PR-Wilson

yields a 100% success ratio of calculated over experimental critical points. However, it overestimates critical pressures and yields to a very poor score. The critical pressure overestimation is a consequence of the extreme steepness of the critical line that starts at the water critical point, in a (P,T) projection. A temperature change of 2 K induces a change in the critical pressure around 1000 bar.

Finally, the details of the behavior predictions of the binary systems belonging to BACs 7 to 9, i.e., in which cross- and self-association take place, are discussed (see [Figure PVII.14](#)). Firstly, it should be highlighted the outstanding performances of the *tc*-PR-UNIQUAC and *tc*-PR-Wilson models regarding the prediction of 3-phase line pressures. They obtain a mark of 19/20 for such a property with a success ratio of 100%. This is illustrated in [Figure PVII.15](#) with the binary system Dimethyl ether + Water. Another point to underline is the better accuracy on the bubble and dew compositions as well as on the azeotropic pressures obtained with the *tc*-PR-Wilson model with respect to the other models.

The analysis presented in this section makes it possible to conclude that the best choice to extend the *tc*-PR EoS to mixtures along with EoS/ $a_{res}^{E,\gamma}$  mixing rules is to use the residual part of the Wilson  $a_{res}^{E,\gamma}$  model. Such a model, with a mark of 12.4 / 20, has the advantage over the other investigated models in this study. Moreover, it reaches a satisfactory overall success ratio of 96%, i.e., this model is able to predict the existence of nearly all data points observed experimentally. The *tc*-PR-Wilson model distinguishes especially in the prediction of liquid and gas phase compositions, azeotropic points and three-phase line pressures.

The weaknesses of the *tc*-PR-Wilson model are related to the reproduction of critical points, particularly for the systems in which self-association takes place (BAC<sub>5</sub> and BACs 7 to 9). In addition, the prediction of three-phase compositions needs to be improved for those systems that do not exhibit association or such that self-association tends to be broken. Finally, efforts are also required for improving the reproduction of caloric properties.

## PVII.IV Conclusions

In the present work, the extension of the translated-consistent Peng-Robinson (*tc*-PR) EoS to mixtures has been investigated. For this purpose, the *tc*-PR EoS incorporated EoS/ $a_{res}^{E,\gamma}$  mixing rules derived by equaling the residual parts of the excess Helmholtz energy obtained from an EoS and from an explicit activity coefficient model such as Wilson, NRTL and UNIQUAC. The performance of the three resulting models was compared against the experimental data of the benchmark database, published by Jaubert et al. [\[130\]](#).

In the light of the obtained results, it is possible to conclude that the best choice to extend the *tc*-PR EoS to mixtures along with EoS/ $a_{res}^{E,\gamma}$  mixing rules is to use the residual part of the Wilson  $a_{res}^{E,\gamma}$  model, named *tc*-PR-Wilson. This conclusion is supported by the fact that the *tc*-PR-Wilson reaches the best results from the quantitative and qualitative standpoints. Nevertheless, improvements have to be made to better predict the behavior of systems in which hydrogen bonds are broken without the possibility to form new ones, as well as in the prediction of caloric properties for systems in which self-association does not take place.

Although beyond the scope of the present article, the very good performances of the PR-Van Laar model (which is a non-predictive version of the *E*-PPR78 model [114,1262] relying on classical mixing rules with temperature-dependent binary interaction parameters  $k_{ij}(T)$ ) should be acknowledged for its capacity to estimate caloric properties ( $h^M$  and  $c_p^M$ ) more accurately than most of other (more advanced) EoS and to reproduce phase diagrams of mixtures containing non-polar and non-associating compounds with a very reasonable accuracy.

The next step is to study the influence of the temperature dependence of the binary interaction parameters of the *tc*-PR-Wilson model on the reproduction of VLE, LLE, VLLE and caloric properties data. Next, the development of a group-contribution-based predictive *tc*-PR-Wilson model could start.

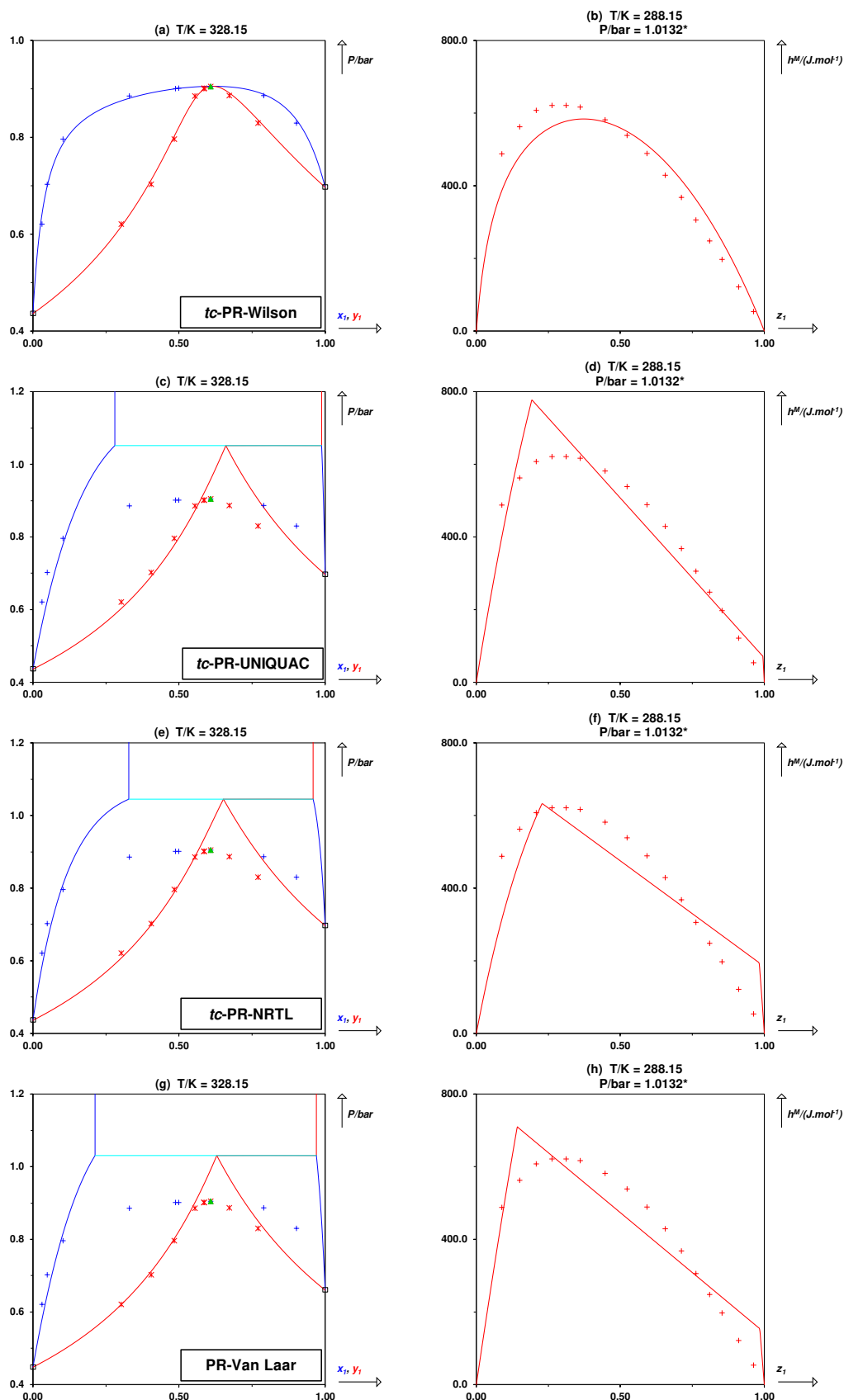


**Figure PVII.12.** Pressure – composition VLE phase diagrams (left) and mixing enthalpy – composition diagrams (right) for the binary system Methanol (1) + Benzene calculated with the *tc*-PR-Wilson (a, b), *tc*-PR-UNIQUAC (c, d), *tc*-PR-NRTL (e, f) and PR-Van Laar (g, h) models. Phase equilibrium diagrams convention: (\*): experimental dew points. (+): experimental bubble points. (▲): experimental azeotropic point. (–): calculated dew curve. (–): calculated bubble curve. (–): calculated three-phase line. Caloric properties diagrams convention: (+): experimental data. (–): calculated curve.

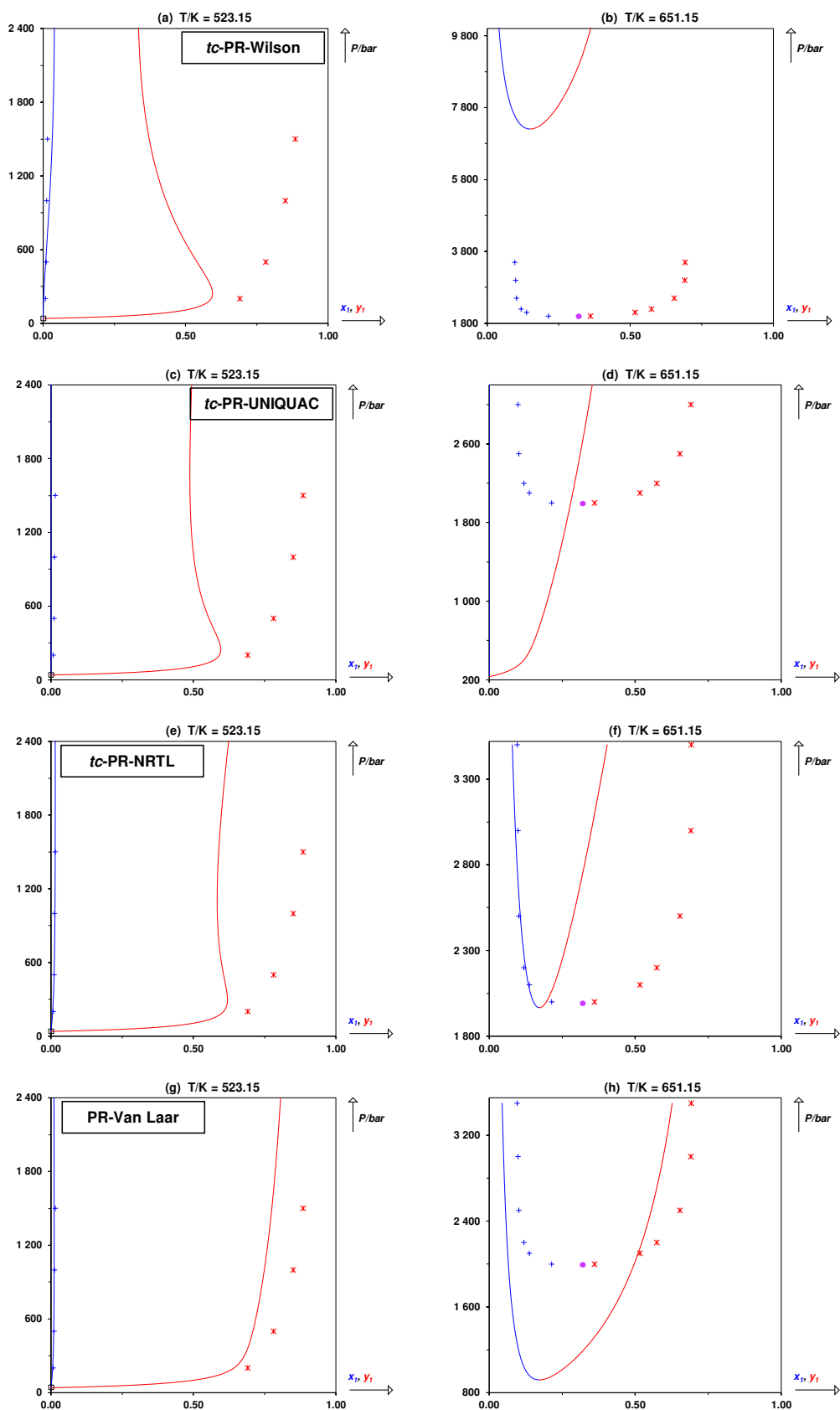


**Figure PVII.13.** Pressure – composition VLE phase diagrams for the binary system Ethane (1) + Water calculated with the *tc*-PR-Wilson (a, b), *tc*-PR-UNIQUAC (c, d), *tc*-PR-NRTL (e, f) and PR-Van Laar model (g, h) models. Phase equilibrium diagrams convention: (\*): experimental dew points. (+): experimental bubble points. (o): experimental critical point. (—): calculated dew curve. (—): calculated bubble curve.

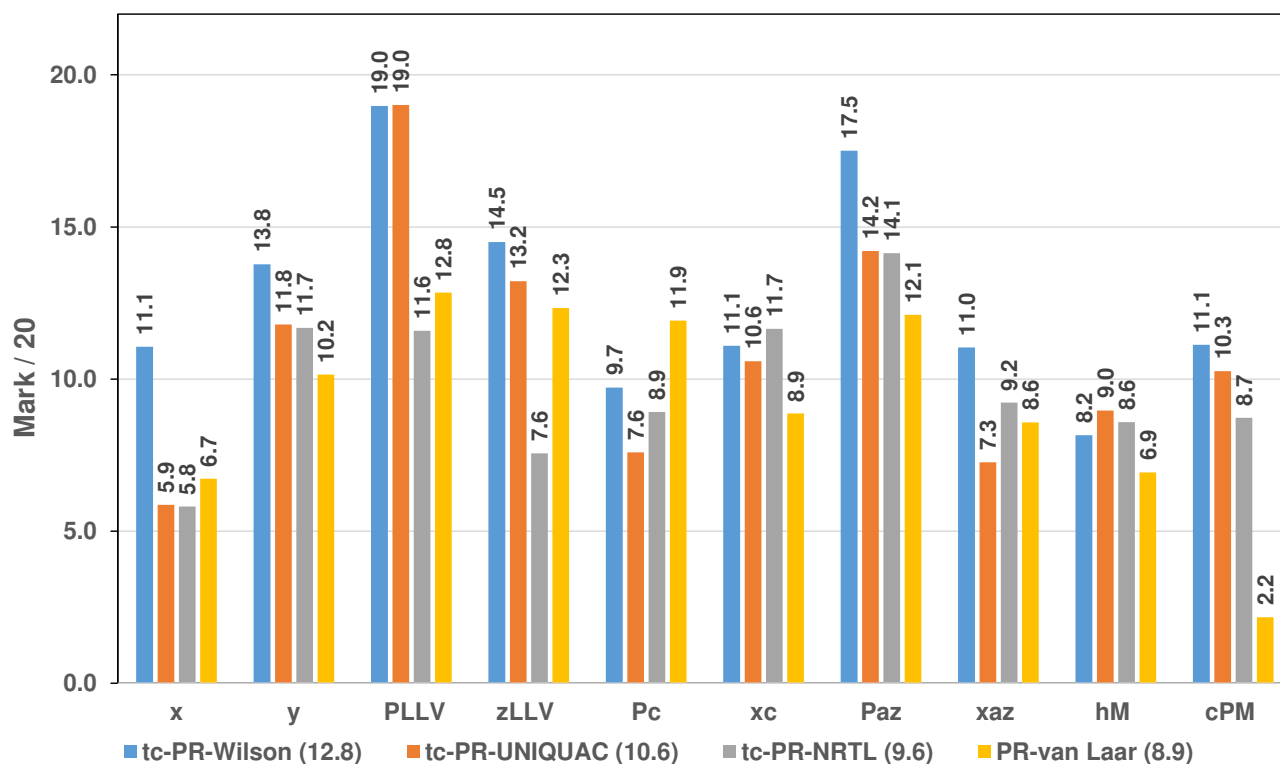


**Figure PVII.14.** Overview of the accuracy of the *tc*-PR-Wilson, *tc*-PR-UNIQUAC, *tc*-PR-NRTL and PR-Van Laar by plotting the marks on ten properties for the category including mixtures in which both cross- and self-association take place (BACS 7 to 9).

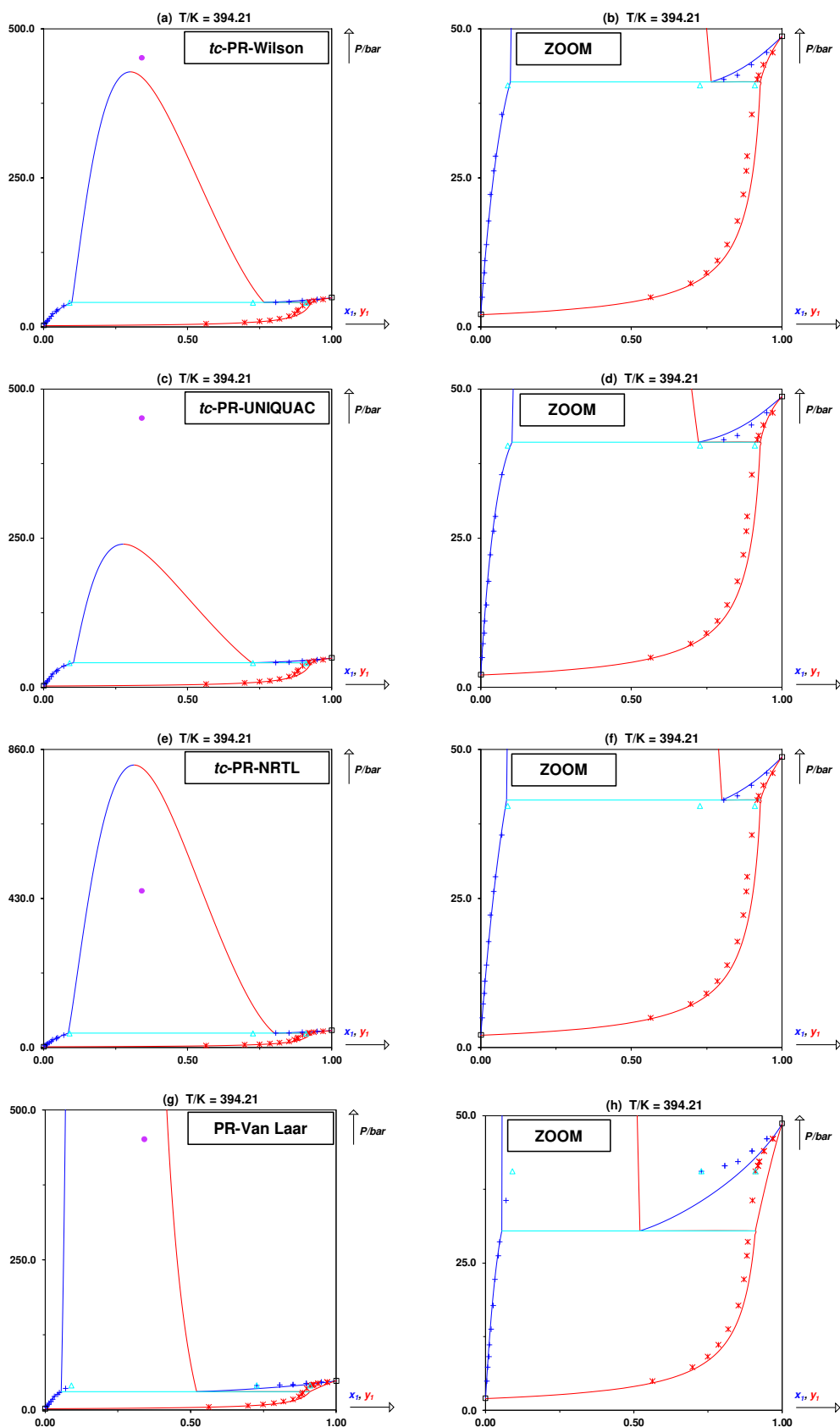


**Figure PVII.15.** Pressure – composition VLE phase diagrams for the binary system Dimethyl ether (1) + Water calculated with the *tc*-PR-Wilson (a, b), *tc*-PR-UNIQUAC (c, d), *tc*-PR-NRTL (e, f) and PR-Van Laar model (g, h) models. Phase equilibrium diagrams convention: (\*): experimental dew points. (+): experimental bubble points. (•): experimental critical point. (▲): experimental three-phase line compositions. (–): calculated dew curve. (–): calculated bubble curve. (–): calculated three-phase line.



## **Publication VIII : Design of promising working fluids for emergent combined cooling, heating and power (CCHP) systems.**

Andrés Pina-Martinez<sup>1</sup>, Silvia Lasala<sup>1(\*)</sup>, Romain Privat<sup>1</sup>, Véronique Falk, Jean-Noël Jaubert<sup>1(\*)</sup>

*<sup>(1)</sup>Université de Lorraine, École Nationale Supérieure des Industries Chimiques, Laboratoire Réactions et Génie des Procédés (UMR CNRS 7274), 1 rue Grandville, 54000, Nancy, France*

### **Abstract**

Combined Cooling, Heating and Power (CCHP) systems enable the simultaneous supply of electricity, heating and cooling thus meeting the major energy needs of humans in a single device. Conventional CCHP systems consist in the combination of a prime mover, a heating and a cooling system, each of them operating with a thermodynamically suitable working fluid. Recently, novel CCHP cycles, based on the use of a single working fluid for the whole operation, have been proposed. Since the choice of the working fluid represents a design challenge in the development of such technologies, in this work a product-design approach for the selection of suitable working fluids for emergent CCHP applications is presented. A database search is implemented to screen about 60 000 structures included in the DDB, the DIPPR and the NIST TDE databases. The screening considers thermodynamic, process-related, constructional, safety and environmental constraints. Moreover, the *tc*-PR equation of state is used in order to ensure the quality of the calculation of thermo-physical properties and the performance assessment of promising working fluids. This study shows that flammable fluids such as vinylacetylene or HFC-152 have a good potential for CCHP applications. In the case of reinforced safety restrictions, HCFO-1233zd(E) seems to be an interesting candidate since it is non-flammable and non-toxic.



## PVIII.I Introduction

According to the International Energy Agency (IEA), “modern economies depend on the reliable and affordable delivery of electricity” [1]. Furthermore, heating arises as the largest energy end-use, since it accounts for the half of the total energy consumption in the world. Refrigeration and especially cooling demand have been growing steadily since the half of the last century. Therefore, it is undeniable that society on these days depends deeply on electricity, heating and cooling supply, to such an extent that the way to make it more efficient, environmentally friendly and sustainable constitutes one of the major challenges of this century. It is evident that from the scale of residential to industrial uses, there might be simultaneous needs of electricity, heat and cold. This opened the way to different technologies such as combined heat and power (CHP) or combined cooling, heating and power (CCHP) systems.

Conventional CHP/CCHP systems consist of different subsystems (prime mover, heat recovery system, cooling system) for each objective, which, in turn, contain different working fluids and do not operate on the same thermodynamic cycle. Moreover, CHP/CCHP systems operate with single-phase expanders and/or compressors. Recently, Briola [6] and Briola et al. [7] presented a novel CCHP cycle, inspired by the patents of Mokadam [8] and Fabris [9], operating with two-phase expanders and compressors. Such a cycle enables the development of an all-in-one device capable of producing electric, heating and cooling power with a single working fluid. Among the design challenges of this novel CCHP system, the working fluid selection appears as a key stage of its development.

In the open literature, research on working-fluid design for classical CCHP systems is built on the findings of previous studies conducted on Organic Rankine Cycle (ORC). Maraver et al. [1291] worked on the optimization of biomass-fueled ORCs used as prime movers coupled with absorption or adsorption cooling units. They considered promising working fluids used in commercially available ORC units [10] such as n-pentane, octamethyltrisiloxane (MDM) and toluene; as well as non-used in commercial ORC devices molecules like n-heptane and dodecamethylcyclohexasiloxane (D6). The thermodynamic properties of the fluids were obtained from CoolProp 3.0 [1292], while working fluid performances were assessed using a process model of the CCHP system. Hong and Shi [11] studied solar-driven ORC coupled with absorption chillers. They evaluated HFC-123, HFC-141b and HCFO-1233zd(E) as working fluids. Performances were obtained from a CCHP model, which called RefProp [1293] in order to calculate thermodynamic properties. Based on previous studies, Al-Sulaiman et al. [12] selected n-octane as working fluid for solar-driven CCHP systems. Analogously, Huang et al. [13] decided to evaluate HFC-245fa in biomass-fueled CCHP systems.

By considering working fluid selection for all-in-one CCHP configurations, it is possible to highlight the work of Briola and co-workers [14]. They considered the wet pure fluids available in the Aspen Plus 9.0 database and defined technical and environmental constraints. They identified four working fluids (chloroform, methyl iodide, phosphorous trichloride and thiacyclopropane) and performed a sensitivity analysis of the trigeneration cycle they designed [7]. Nevertheless, it is possible to point out that since no (or relaxed) toxicological constraints were included in the selection, the four investigated fluids are highly toxic. Moreover, relaxed environmental constraints were used since chloroform and methyl iodide are severely high-ozone-depleting substances (ODS).

---

According to the available studies, it is thus possible to identify the following shortcomings in the reviewed CCHP working fluid design:

- the number of investigated working fluids is rather small and/or influenced by previous studies on ORC configurations;
- a systematic evaluation of thermodynamic and constructional along with toxicological, flammability and environmental criteria has not been conducted for CCHP systems (by constructional criteria, it is here referred to technical limitations due to the prosaic construction of operation units; in the present, this is essentially the maximum allowed pressure before material failure and the management of air entry in low-pressure systems).

In order to address these issues, this study aims at implementing a product design approach by screening more than 60 000 structures available in the Dortmund Data Bank (DDB), the Design Institute for Physical Properties (DIPPR) database and the NIST ThermoData Engine 103b (NIST TDE 103b) with the aim of finding suitable candidates for CCHP applications. Furthermore, this work considers thermodynamic, process-related, environmental, flammability and toxicity aspects in the selection process as well as performance assessment by means of cycle simulations. In order to ensure that the performance of CCHP fluids is computed reliably, the *translated* [95,132]-*consistent* [198,199] Peng-Robinson (*tc*-PR) model [184,185] is used to estimate saturation and caloric properties.

This paper is organized in five sections. In [Section PVIII.II](#), a brief overview of the product design framework is presented. Additionally, the methodologies with large-space exploration of working fluids for ORC and vapor-compression (VC) refrigeration configurations are introduced. This section is closed with the strengths and weaknesses of the reviewed methodologies, and arguments supporting the choice of a database search are discussed. In [Section PVIII.III](#), a detailed description of the CCHP cycle studied in this work is provided. Then, the solution methodology for the exploration of different candidates including thermodynamic, process-related, environmental, flammability and toxicity constraints is presented in [Section PVIII.IV](#). The 2 case studies we decided to analyze are described in [Section PVIII.V](#), and the screening results are discussed in [Section PVIII.VI](#).

## **PVIII.II Product design framework applied to the selection of working fluids**

According to Moggridge and Cussler [140], product design is the process of identifying the best set of candidates that fit desired product functional criteria. This process can be represented by four principal steps as follows:

5. Needs. What needs should the product fill?
6. Ideas. What different solutions/formulations could fill this need?
7. Selection. Which products are the most promising?
8. Manufacture. How can the product be made and critically tested?

In turn, Gani [141] proposes a modified version of Moggridge and Cussler's main stages of product design, well adapted to molecular products:

6. Needs and goals. What needs/target properties should the product fill?
7. Generation. What different feasible molecules can be tested?
8. Selection. Which candidates are the most promising?
9. Manufacture. How can the product be made?
10. Performance. Does the product actually satisfy the desired performances?

In the first step, the requirements and the functionalities of the product must be defined. Moreover, it is necessary, and sometimes a hard task, to convert these requirements into quantitative specifications. After this stage, a list of candidates, usually referred to as “design space”, that could satisfy these needs is generated. Then the best candidates are selected in stage 3, and finally, in ‘manufacture’, a process design stage is implemented to determine how the product will be made. Performances can be studied using experimental trials or mathematical models. The most common chemical product design methods consist of:

- Experiment-based trial and error: this approach is used when mathematical models for the estimation of the target (desired) properties are not available. It is often required past knowledge and experience to define the design space. Experimental design approach is frequently used then. This procedure is limited frequently by a fixed amount of chemical, time, and financial resources.
- Model-based search techniques: this approach is used when reliable and validated mathematical models for the estimation of all the target properties are available. Such models have contributed to the development of the computer-aided molecular design (CAMD) framework. The design space can be quite wide; however, to reduce this space (i.e., the number of candidate molecules), past knowledge and experience may be invoked.
- Hybrid experiment-model based techniques: this approach is used when only certain properties can be estimated by mathematical models. The most common option is to use models to reduce the list of candidates to a small number of molecules, which may be further evaluated by means of the experiment-based trial and error approach. In such a way, by reducing the design space, the time and resources spent on the experimental effort are reduced.

Databases: Database search is suitable for designing simple molecular products and ingredients selection for some formulated products. Using databases often ensures property reliability and allow a fast generation of the feasible candidates list [142]. Usually, databases are used for preselection of candidates and, in a further stage, their performances are assessed with model-based techniques or experiments.

- Heuristics: this approach is supported by heuristic rules (i.e., empirical rules easing the convergence process but are not necessarily optimal) that help to make design decisions, as well as reliable selections. Such rules result from a combination of experience and available knowledge.

Different methods of product design have been used in ORC and VC refrigeration cycles. The literature review presented in the following sections is focused on methodologies with large space exploration of working fluids for these types of cycles. For detailed information about experimental or heuristic

approaches used in working fluid selection for ORC or VC refrigeration applications, the reader can refer to the work of Quoilin et al. [1294], Bao and Zhao [1295] or Motta-Babiloni et al. [1296].

### **PVIII.II.I Working-fluid design for vapor-compression refrigeration applications**

Early efforts focused on refrigerant design have been addressed by Joback [1297], Joback and Stephanopoulos [1298], followed by Gani et al. [1299]. They described a structured methodology based on a group-contribution (GC) approach for the formation of feasible chemical compounds, prediction of target properties and screening of candidates. Only constructional and thermodynamic properties were considered. Moreover, the performances of working fluids were not assessed through cycle simulations. Duvedi and Achenie [1300] proposed a mathematical programming-based approach for CAMD and included for the first time environmental constraints represented by the Ozone Depletion Potential (ODP) for chlorofluorocarbons (CFC). Ourique and Silva-Telles [1301], Marcoulaki and Kokossis [1302], Sahinidis et al. [1303] and Samudra and Sahinidis [138] studied the problem of refrigerant design but they were more focused on new optimization approaches for CAMD. Particularly, Sahinidis et al. [1303] pointed out that current approaches (until 2003) used mostly thermodynamic objectives in order to retrofit refrigeration systems, i.e., to design molecules with similar properties to those of existing compounds. Moreover, they recognized that properties such as flammability, toxicity, ozone depletion and chemical stability were difficult to predict, which precluded them from being included in CAMD approaches. In 2012, Kazakov et al. [1304] presented computational tools to screen potential candidates for VC refrigeration cycles. They were able to compute the Global Warming Potential (GWP) and the lower flammability limit for more than 56 000 compounds from the PubChem database. Additional filters such as critical temperature, toxicity and stability were included and they came up with a list of about 1200 fluids, which were further studied by McLinden et al. [144].

### **PVIII.II.II Working-fluid design for ORC applications**

Extensive research has been focused on working fluid design for ORCs. In 2010, Papadopoulos et al. [1305] proposed by the first time an approach based on CAMD (model-based) for the systematic design and selection of optimal working fluids for low-temperature ORC systems operating between 90 °C and 20-25 °C. They included 15 target properties related to thermodynamic, environment, safety and process aspects. They came up with 44 potential working fluids, which they classified into conventional and unconventional molecules. Palma-Flores et al. [1306] used the CAMD approach (model-based) to find new compounds with the potential of being suitable working fluids in ORC processes for waste energy recovery from low-temperature heat sources. The design space consisted of  $8.2178 \cdot 10^9$  possible combinations of functional groups to form a molecule. They identified 32 potential working fluids, whose performances were further studied using ASPEN PLUS for ORC simulations. Another CAMD-based approach for the design of optimal working fluids for ORC applications was developed by Lampe et al. [1307]. They used the perturbed-chain statistical associating fluid theory (PC-SAFT) equation of state as thermodynamic model. They used a GC method to calculate, from the molecular structure, the PC-SAFT pure-component parameters: segment number ( $m$ ), segment diameter ( $\sigma$ ) and segment energy parameter ( $\epsilon/k$ ). Preißinger et al. [145] conducted a database search and screened about 72 million chemical structures contained in the PubChem database by applying the COSMO-RS methodology.

They evaluated ORC configurations for waste heat recovery from passenger cars and trucks. The authors implemented a scoring system for each working fluid considering criteria related to thermodynamic, constructional, safety and environmental aspects. In 2020, Bowskill et al. [147] proposed a computer-based method for the integrated process and working-fluid design for organic Rankine cycles. The approach is combined with the use of the predictive SAFT- $\gamma$  Mie group-contribution methodology for thermo-physical property calculations. This enabled them to study 58 960 prospective fluids and their capabilities for three case studies.

### **PVIII.II.III Strengths and weaknesses**

Whether CAMD or database search approaches were used for ORC or VC refrigeration applications, the strengths and weaknesses of both methodologies do not depend on the studied system. For instance, the CAMD framework offers the largest design space and the possibility to find global optimal solutions. Nevertheless, the lack of reliable property models implemented in CAMD tools, for all the considered chemical families, may lead to the exclusion of environmental or safety targets, which are extremely important for the working-fluid design. On the other hand, database search does not provide the largest possible design spaces and, thus, may miss potential candidates but enables the fast generation of feasible candidate lists. Moreover, by combining different databases, it is possible to include more target properties in the design approach.

Recognizing the forces and limitations of CAMD and database search methodologies, it is considered nevertheless that, for the purpose of this work, the latter offers the best trade-off between design space and considered target properties.

### **PVIII.III CCHP cycle description**

In this work, a simplified version of the CCHP cycle proposed by Briola [6] in his patent is considered. This cycle operates with a single working fluid and allows expansions and compressions to take place in the single-phase regions as well as in the two-phase domain. This section describes the interest of going from power to (heating + power) and (heating + power + cooling) systems. This transition is depicted with an ideal Rankine cycle and the required modifications that enable such a cycle to become a CCHP cycle operating with a single working fluid.

*Note to the reader:* The way of analyzing the different cycle configurations in this section is mainly graphical, and is supported with temperature-entropy (T-s) diagrams. Furthermore, all the considered cycles are ideal, i.e., they do not involve any internal irreversibilities. In consequence, the specific entropy changes of the working fluid during a process are only due to heat transfer. Considering this, the amount of specific heat exchanged is given by:

$$\delta q_{rev} = Tds \quad (\text{PVIII.1})$$

In consequence, in a (T-s) diagram, a given amount of heat can be represented as the area below the curve of the corresponding process. Keeping this in mind, a heat-addition process follows the direction of increasing specific entropy, a heat-rejection process follows the direction of decreasing specific entropy, and an adiabatic process takes place at constant specific entropy. In order to illustrate the

usefulness of (T-s) diagrams, the derivation of the expression for the net work and the thermal efficiency of a Carnot cycle is presented in [Appendix G1](#).

### PVIII.III.I From power to combined heating and power

Consider an internally reversible Rankine cycle, as shown in [Figure PVIII.1](#). The fluid in a liquid state is compressed isentropically by a pump (1-2), heated at constant pressure in an evaporator (2-3) until partial or total vaporization is reached, expanded isentropically in a turbine (3-4), and condensed at constant pressure (4-1) to the initial state.

Now, consider a performance indicator (PI) that accounts for the useful effect generated in the surroundings. Generally speaking, useful effects can be the net work done, and/or the cooling and heating effects provided to the surroundings. This indicator can be defined as the ratio between the useful effects generated by the machine and the energy supplied to the engine for its operation.

$$PI \equiv \frac{\text{useful effects}}{\text{supply}} \quad (\text{PVIII.2})$$

For the machine considered in [Figure PVIII.1](#), two cases can be analyzed. In the first case,  $T_A$  is the ambient temperature, and no useful heating effect is provided to the surroundings. In consequence, the machine only produces useful work and the performance indicator is much lower than 100%. For the second case, let  $T_A$  be higher than the ambient temperature, and consider that heat is provided to an end-user at  $T_A$ . Now, the machine provides two useful effects: power and heat. It is thus a CHP (combined heat and power) system, and the performance indicator becomes:

$$PI = \frac{|w_{net}| + |q_A|}{q_{HS}} = 100\% \quad (\text{PVIII.3})$$

For this type of engines, the performance indicator is also called energy utilization factor (EUF).

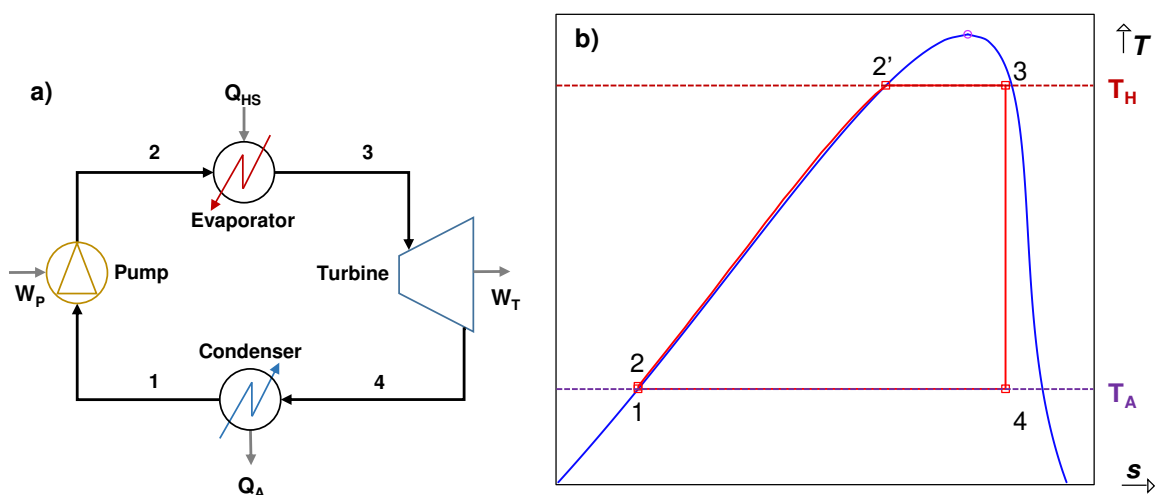


**Figure PVIII.1.** a) Schematic view of an ideal Rankine cycle. b) Sketch to the corresponding temperature-entropy diagram.

The CHP system just described before is not practical because it cannot adjust to the variations in power and heat loads. A more practical CHP configuration is shown in [Figure PVIII.2](#). Now, the expansion (3-4) of the original cycle ([Figure PVIII.1](#)) is split into two stages (3-4) and (5-6), while the process (4-5) is intended to provide the required specific heating power ( $q_M$ ) at  $T_M$ .

In order to have a look of the impact of the variations of specific heat loads and the temperature at which it is required, consider the two superposed cycles shown in [Figure PVIII.3](#). Let the cycle formed by the states (1-2-2'-3-4-5-6-1) be the cycle A, and that formed by states (1-2-2'-3-4-5'-6'-1) be the cycle B. The specific net work output of cycles A and B is given by the area of polygons 1-2-2'-3-4-5-6-1 and 1-2-2'-3-4-5'-6'-1, respectively. In turn, as shown in [Figure PVIII.4](#), the heating power ( $|q_M|$ ) for cycle A is given by the area of the polygon 4-5-B-D, while that of cycle B corresponds to the area of the polygon 4-5'-C-D. It is thus possible to observe that the specific net work output of cycle A is lower than that of cycle B, while the heating power of the former is greater than that of the latter. In terms of EUF ( $|w_{net} + q_M|/q_{HS}$ ), it is found that  $EUF_A > EUF_B$ , since the gain of specific net work output of cycle B (5-5'-6-6') is lower than the increase of specific heating power provided by cycle A (5-5'-B-C). It is thus demonstrated graphically that CHP machines are characterized by a higher thermal efficiency when they operate in a regime in which the demand of heating power is greater than that of electric power.

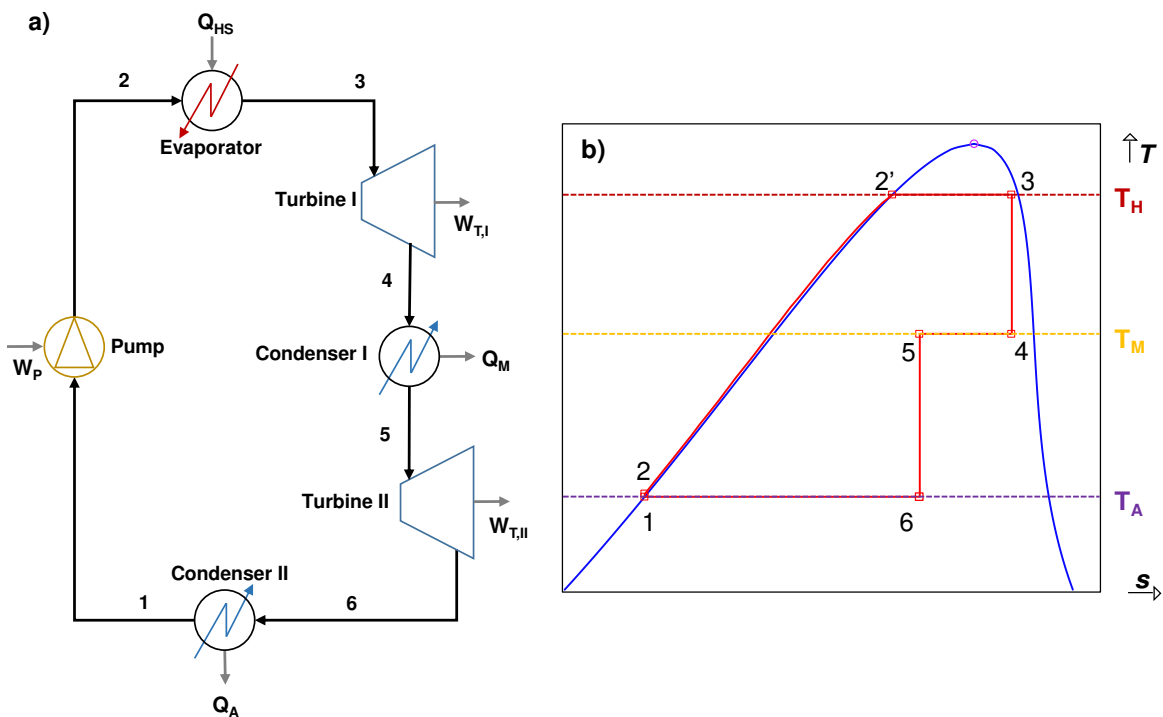


**Figure PVIII.2.** a) Schematic view of an ideal CHP cycle. b) Sketch of the corresponding temperature-entropy diagram.

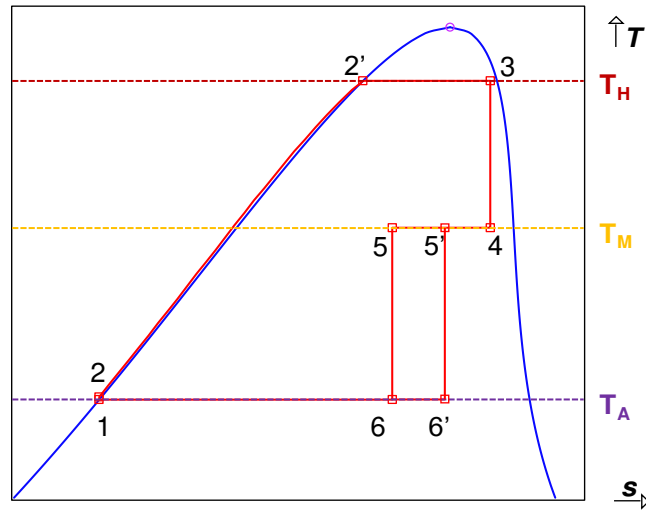


**Figure PVIII.3.** Sketch of the temperature-entropy diagram of two CHP cycles: cycle A (1-2-2'-3-4-5-6-1), cycle B (1-2-2'-3-4-5'-6'-1).

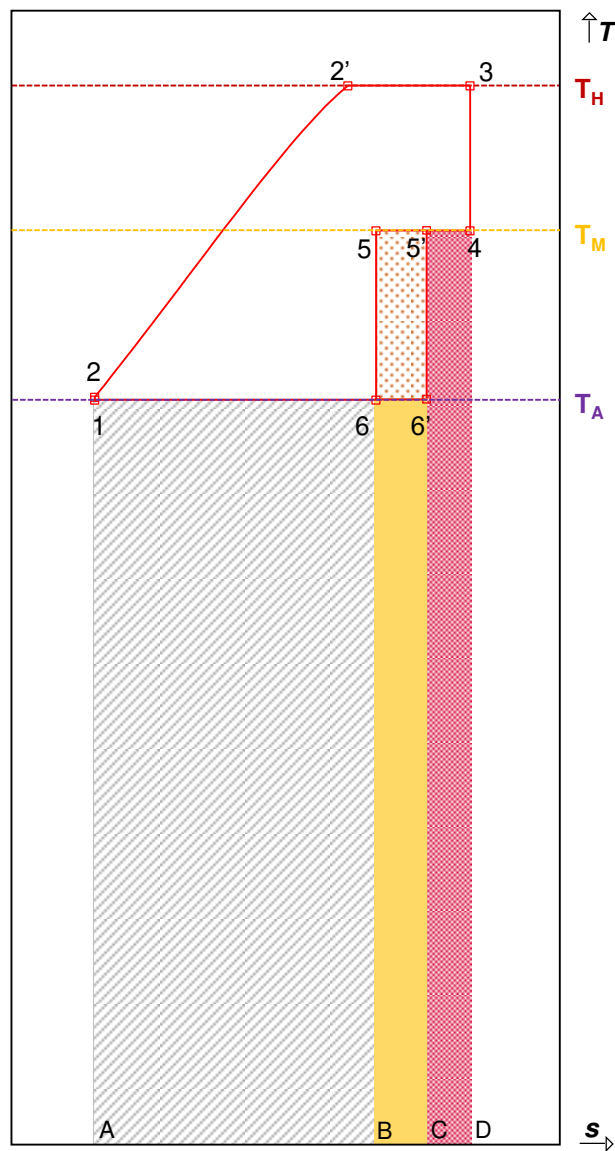


**Figure PVIII.4.** Enlarged temperature-entropy diagram for the CHP cycles considered in [Figure PVIII.3](#).

Now, the case shown in [Figure PVIII.5](#) is examined. Let the cycle formed by the states (1-2-2'-3-4-5-6-1) be the cycle A, and that formed by states (1-2-2'-3-4'-5'-6-1) be the cycle B. The only difference is that  $T_{M,A} > T_{M,B}$ . In this case, it is observed that, as for the previous scenario:  $|w_{net}|_A < |w_{net}|_B$  and  $|q_M|_A > |q_M|_B$ . Nevertheless, the EUF of both cycles is the same. Indeed,  $|q_A|$  and  $q_{HS}$  are the same in the two cycles so that the useful specific energy  $|w_{net} + q_M|$  is not modified in order not to break the first law that simply writes:  $q_{HS} = |w_{net} + q_M + q_A|$ . Such a useful specific energy, defined by the area of the polygon 1-2-2'-3-C-B-6-1 in [Figure PVIII.5](#), remains thus constant in spite of the relative changes in  $|w_{net}|$  and  $|q_M|$ . In other words, the loss (or gain) in  $|w_{net}|$  for one cycle is compensated by the gain (or loss) in  $|q_M|$  by the other.

The operation of an ideal CHP system has thus been presented. It is observed that the EUF depends on the relation between the mechanical and thermal power required by the end-user. In the next section, the addition of a refrigeration subcycle is described. For this purpose, the working fluid should be able to absorb heat at a temperature lower than the ambient temperature  $T_A$ . In addition, the cooling effect generated by the refrigeration subcycle and its impact on the EUF are discussed.

### **PVIII.III.II CCHP configuration**

To move from a CHP to a CCHP cycle, a part of the cycle must be dedicated to refrigeration (i.e., absorption of a specific heat at a temperature  $T_C$  lower than  $T_A$ , the temperature of the environment). To do so, consider that fluid exiting from the condenser of the CHP cycle (see point 1 in [Figure PVIII.2](#)) is directed toward a refrigeration subcycle. In the CCHP cycle, this point is called "7". Therefore, instead of pumping the working fluid back to the evaporator as done in the CHP configuration, the fluid is expanded isentropically (7-8), heated at constant pressure in an evaporator (8-9), compressed isentropically (9-10), and, finally condensed at constant pressure (10-1). The amount of specific heat absorbed isothermally by the working fluid from the low-temperature source at  $T_C$  represents a cooling effect in the surroundings. The CCHP configuration is shown in [Figure 4-2](#).

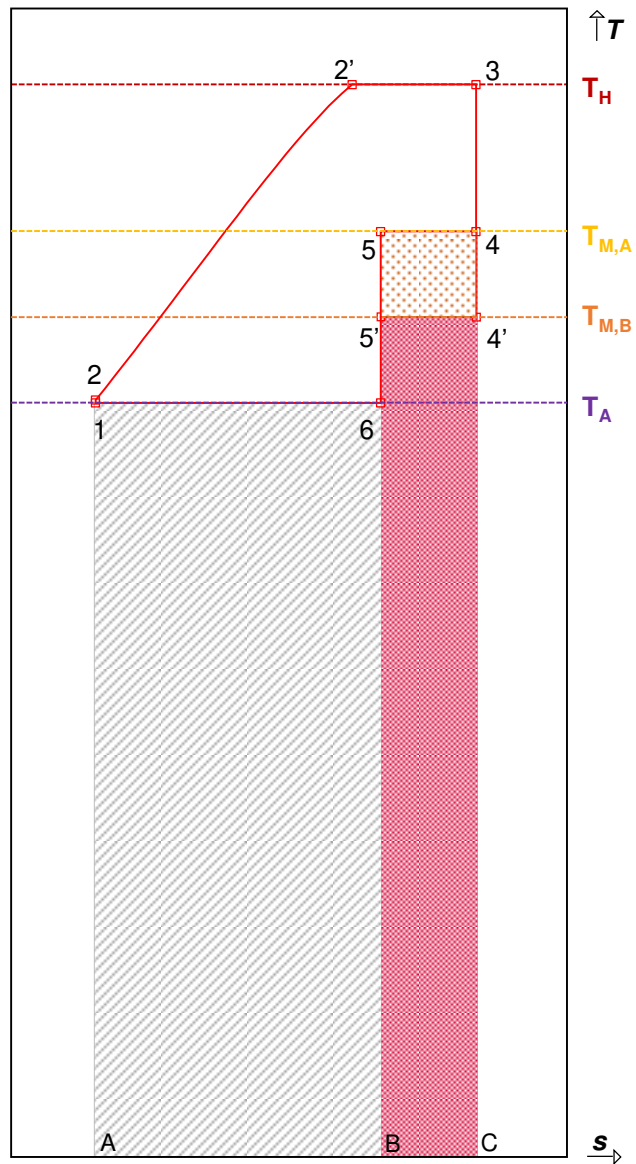


**Figure PVIII.5.** Enlarged temperature-entropy diagram for two CHP cycles providing heat at different temperatures.

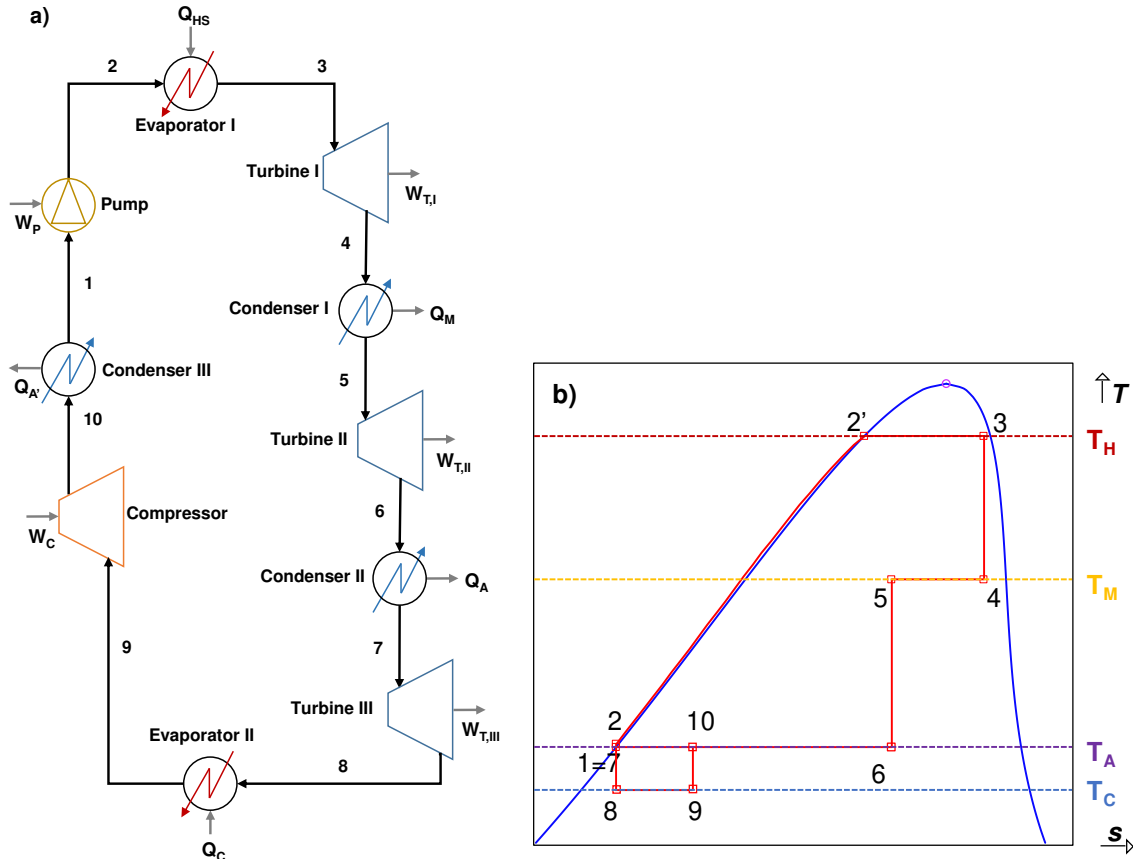


**Figure PVIII.6.** a) Schematic view of an ideal CCHP cycle. b) Sketch of the corresponding temperature-entropy diagram.

Even if there is only one fluid flowing in the cycle, it is possible to distinguish a CHP subcycle (1-2-2'-3-4-5-6-1), responsible for the supply of electric and heating power, and a cooling subsystem (7-8-9-10), thus defining a CCHP cycle. Part of the power output of the CHP is used to supply the required power input of the cooling system. Therefore, the net output power of the CCHP systems becomes:

$$|w_{net}|_{CCHP} = |w_{net}|_{CHP} - w_{net,cooling} = [|w_{T,I} + w_{T,II} - w_P] - (w_C - |w_{T,III}|) \quad (PVIII.4)$$

It is clear that the specific net work supplied by the CCHP system is lower than that of the CHP one. Graphically,  $|w_{net}|_{CHP}$  is the area of polygon (1-2-2'-3-4-5-6-1) whereas  $w_{net,cooling}$  is the area of the rectangle (7-8-9-10) so that the difference of both these areas is the net work supplied by the CCHP system. Similarly, the useful effects generated by the CCHP cycle are not the same as for a CHP machine. The EUF of the CCHP cycle defined as:

$$EUF_{CCHP} = \frac{|w_{net}|_{CCHP} + |q_M| + q_C}{q_{HS}} \quad (PVIII.5)$$

results to be higher than that of the CHP configuration due to the fact that the specific cooling power is added to the useful effects and that the reduction of the CCHP net output specific power is lower than the cooling effect ( $q_C > w_{net,cooling}$ ).

### PVIII.III.III Actual CCHP configuration and degrees of freedom

After the description of the ideal CCHP configuration, it is necessary to analyze which variables are specified in the problem, and if, at least, it is solvable. For instance, in an actual scenario of trigeneration, the most of the time, the required electric, heating and cooling powers are fixed by the end-users.

In order to have a simple indication of how many variables need to be specified to make a system of equations solvable, it is possible to perform a degree-of-freedom analysis. It is a simple way to make sure that the number of variables and equations is in balance prior to attempting solution. In general, the degrees of freedom can be expressed as:

$$DF = n_{\text{var}} - n_{\text{eq}} - n_{\text{spec}} \quad (\text{PVIII.6})$$

where  $n_{\text{var}}$ ,  $n_{\text{eq}}$  and  $n_{\text{spec}}$  are the number of variables, independent equations and specified variables, respectively.

The assumptions used for the modelling of the CCHP cycle are:

1. The system operates in steady-state conditions.
2. The pressure drop across the heat exchangers is negligible.
3. The minimum temperature difference between the hot and cold streams (i.e., the pinch point) in heat exchangers is equal to 10 K.
4. The isentropic efficiencies of the turbines, compressor and pump are known.

With such information, it is possible to perform the degree-of-freedom analysis. There are 37 variables involved in the CCHP model, most of them being introduced in [Figure 4-2](#):

- Mass flowrate ( $\dot{m}$ ) (1 variable).
- Two independent intensive state variables per stream in order to define the physical state of the working fluid and all the other state variables. The present case includes 10 streams and thus, 20 variables. Independent state variables mean that the couple of variables can be freely chosen but has to be different from  $(T, P)$  when the working fluid is at vapor-liquid equilibrium.
- Duties of compressor ( $\dot{w}_c$ ) (1), pump ( $\dot{w}_p$ ) (1), expanders ( $\dot{w}_{T,I}$ ,  $\dot{w}_{T,II}$ ,  $\dot{w}_{T,III}$ ) (3) and heat exchangers ( $\dot{Q}_{HS}$ ,  $\dot{Q}_M$ ,  $\dot{Q}_A$ ,  $\dot{Q}_C$ ,  $\dot{Q}_{A'}$ ) (5): 10 variables.
- The net output power ( $\dot{w}_{net}$ ) (1)
- Specific enthalpies at the exit of the compressor, pump, expanders when they are considered as reversible and adiabatic, i.e., isentropic (5 variables). These variables (noted  $h_i^s$ ) are involved in the isentropic-efficiency definitions of these operation units and used accordingly to estimate the corresponding actual duties.

The number of independent equations results from:

- 10 independent energy balances (1 per operation unit).
- 5 additional relations between isentropic efficiencies and actual duties of compressor, pump and turbines.
- 1 additional relation stemming from the equation of definition of the net output power.

Concerning the specified variables, they are defined as explained hereafter and are summarized in [Table PVIII.1](#).

**Table PVIII.1.** Summary of the specified variables and specifications equations for the CCHP system studied in this work.

Specified variables	Specification equations
$T_1 = T_6 = T_7$	Equal to ambient temperature
$P_{10}$	$P_{10} = P^{sat}(T_7)$
$T_3$	Temperature of the heat source decreased by 10 K (pinch point condition)
$T_5$	Fixed by end-user heating needs
$P_4$	$P_4 = P^{sat}(T_5)$
$T_8 = T_9$	Fixed at $T_C$ by end-user cooling needs
$P_2$	$P_2 = P^{sat}(T_3)$
Qualities $x_1$ and $x_7$	Points 1 and 7 that are located on the bubble curve, thus: $x_1 = x_7 = 0$
$\dot{Q}_M, \dot{Q}_C, \dot{W}_{net}$	Fixed by end-user needs
Isentropic efficiencies of the 3 expanders	See notes
Isentropic efficiencies of the compressor	See notes
Isentropic efficiencies of the pump	See notes

#### Notes:

- In this work, it is assumed that the input specific heat comes from renewable thermal sources such as biomass, geothermal or solar. It is considered that the heat source temperature is at least 160 °C.
- It might have been tempting to specify  $T_{10}$ , which according to [Figure 4-2](#), is equal to the temperature at points 1, 6 and 7; however, a variant of this flow diagram would correspond to the case where point 10 is in the gaseous region. If this happened, we would have  $T_{10} > T_{ambient}$ . It is thus more relevant to introduce a specification on  $P_{10}$  rather than on  $T_{10}$ .
- Similarly, temperature  $T_4$  could be specified by imposing  $T_4 = T_5$  (see [Figure 4-2](#)). However, a variant of this flowsheet would correspond to the case where point 4 is in the gaseous region. If this happened, we would obtain  $T_4 > T_5$ . It is thus more relevant to introduce a specification on  $P_4$  rather than on  $T_4$ .

Expander: Briola et al. [\[7,14\]](#) in their proposal suggest the use of two-phase expanders such as those commercialized by Energent Corp., Electrathem of BEP Europe. The reported isentropic efficiencies range between 0.45 and 0.85.

Compressor: Briola et al. [\[7,14\]](#) found that some prototypes of two-phase compressors may be used. The reported isentropic efficiencies range between 0.35 and 0.75.

Pump: The isentropic efficiency of the pump is the same as that used by Briola et al. [\[7,14\]](#), which ranges between 0.7 to 0.9 [\[147\]](#).

In summary, there are 37 unknown variables, 16 independent equations and 20 specified variables, yielding (from eq. (PVIII.6)) to one degree of freedom, i.e., one variable needs to be fixed prior to attempting solution.

An interesting point to analyze is the outlet of the vapor generator at  $T_3$ . Since in the considered architecture the fluid should be in the two-phase region at  $T_3$ , the maximum vapor quality at the outlet of the vapor generator ( $x_3$ ) is equal to 1 (saturated-vapor state). To properly parametrize the studied cycle, one needs to answer the questions:

- how does the choice of  $x_3$  impact the cycle performances?
- Is  $x_3 = 1$  a condition that leads to higher thermal efficiency?

These questions are addressed in [Appendix G2](#), in which it is demonstrated that the vapor quality of point 3 should be fixed at the maximum allowed value  $x_3 = 1$  in order to operate at the highest thermal efficiency. In consequence, in order to fulfill the degree of freedom, it is decided to set the specification for the vapor quality of point 3 at  $x_3 = 1$ .

Once the problem is set for attempting solution, the 16 calculated variables are:

- the mass flowrate ( $\dot{m}$ );
- the specific enthalpies of points 2, 4, 5, 6, 8, 9 and 10 ( $h_2, h_4, h_5, h_6, h_8, h_9, h_{10}$ );
- the duties of the pump ( $\dot{W}_P$ ), 3 turbines ( $\dot{W}_{T,I}, \dot{W}_{T,II}, \dot{W}_{T,III}$ ) and the compressor ( $\dot{W}_C$ );
- the duties of evaporator I ( $\dot{Q}_{HS}$ ) and condensers II and III ( $\dot{Q}_A, \dot{Q}_{A'}$ ).

Assuming that the starting point is point 1, a possible sequence of the calculations is:

- Calculation of  $h_2$ :  $h_2 = h_1 + \underbrace{(h_2^s - h_1)}_{>0} / \eta_p$ .
- Calculation of  $h_4$ :  $h_4 = h_3 + \eta_{T,I} \underbrace{(h_4^s - h_3)}_{<0}$ .
- Calculation of  $h_8$ :  $h_8 = h_7 + \eta_{T,III} \underbrace{(h_8^s - h_7)}_{<0}$ .

At this step, the five following variables:  $h_5, \dot{m}, h_6, h_9$  and  $h_{10}$  must be simultaneously determined by solving the following system of 5 equations:

$$\left\{ \begin{array}{l} \dot{Q}_M = \dot{m} \cdot (h_5 - h_4) \quad (a) \\ h_6 = h_5 + \eta_{T,II} \underbrace{(h_6^s - h_5)}_{<0} \quad (b) \\ \dot{Q}_C = \dot{m} \cdot (h_9 - h_8) \quad (c) \quad (PVIII.7) \\ h_{10} = h_9 + \underbrace{(h_{10}^s - h_9)}_{>0} / \eta_c \quad (d) \\ \dot{W}_{net} = \dot{m} \cdot [(h_2 - h_1) + (h_4 - h_3) + (h_6 - h_5) + (h_8 - h_7) + (h_{10} - h_9)] \quad (e) \end{array} \right.$$

The system can be solved by trial-and-error, for example. The calculation sequence is the following:

1. Define an initial guess of  $h_5$  between the specific enthalpy of the saturated liquid at  $T_5$  and  $h_4$ .
2. Calculate  $\dot{m}$  from Eq. (PVIII.7)-a.
3. Calculate  $h_6$  from Eq. (PVIII.7)-b.
4. Calculate  $h_9$  from Eq. (PVIII.7)-c.
5. Calculate  $h_{10}$  from Eq. (PVIII.7)-d.
6. Calculate  $|\dot{W}_{net}|$  from Eq. (PVIII.7)-e and compare it with the specification  $|\dot{W}_{net}^{spec}|$ . If the calculated and specified values of  $|\dot{W}_{net}|$  do not agree, try another guess for  $h_5$  and go back to step 2. If  $|\dot{W}_{net}^{calc}| < |\dot{W}_{net}^{spec}|$ , increase the value of  $h_5$ . Otherwise, decrease the value of  $h_5$ .

Once the system is solved, calculation of the eight remaining variables is straightforward:

- Calculation of  $\dot{W}_p$ :  $\dot{W}_p = \dot{m} \cdot (h_2 - h_1)$ .
- Calculation of  $\dot{W}_{T,I}$ :  $\dot{W}_{T,I} = \dot{m} \cdot (h_4 - h_3)$ .
- Calculation of  $\dot{W}_{T,II}$ :  $\dot{W}_{T,II} = \dot{m} \cdot (h_6 - h_5)$ .
- Calculation of  $\dot{W}_{T,III}$ :  $\dot{W}_{T,III} = \dot{m} \cdot (h_8 - h_7)$ .
- Calculation of  $\dot{W}_c$ :  $\dot{W}_c = \dot{m} \cdot (h_{10} - h_9)$ .
- Calculation of  $\dot{Q}_{HS}$ :  $\dot{Q}_{HS} = \dot{m} \cdot (h_3 - h_2)$ .
- Calculation of  $\dot{Q}_A$ :  $\dot{Q}_A = \dot{m} \cdot (h_7 - h_6)$ .
- Calculation of  $\dot{Q}_{A'}$ :  $\dot{Q}_{A'} = \dot{m} \cdot (h_1 - h_{10})$ .

For the two case studies considered in this work, the numerical values of the specified variables are presented in [Section PVIII.V](#).

## PVIII.IV Working-fluid selection methodology

In [Section PVIII.II](#), a general overview of the product design framework has been presented. Such framework can be applied to different types of products from coatings and process fluids to solvents and functional devices. In this section, a working-fluid selection methodology for the novel CCHP cycle presented in [Section PVIII.III](#) is detailed. The proposed methodology follows the main stages defined by Gani [141]: 1) Needs and goals; 2) Generation; 3) Selection; 4) Manufacture; 5) Performance.

A scheme of the product-design approach adopted in this work for the selection of suitable working fluids for CCHP applications is presented in [Figure PVIII.7](#). The needs and goals are defined in the target properties section. Moreover, the requirements of suitable fluids are described, as well as the estimation methods and bibliographic survey employed to obtain the values of such properties for each candidate. Then, the initial set of candidates is defined by means of database search. Next, the screening order is presented followed by the performance evaluation, which is supported by the  $tc$ -PR equation of state. It is worth noting that Gani et al. [143] explained that in the case of basic chemicals, such as refrigerants or solvents, for which the end-use properties are often directly related to their molecular

structure, the manufacturing process does not affect product properties, and, therefore, stage 4 (manufacture) can be excluded from the design procedure.

### PVIII.IV.I Target properties

#### Critical temperature

Pure compounds do not condense above the critical temperature. Since one of the main features of the novel CCHP cycle is that the whole operation may take place in the two-phase region, it seems highly intuitive to define critical temperature as the initial criterion of the screening. Considering that the temperature of the hot source is not lower than 160 °C and a minimum temperature approach of 10 K in the evaporator, the maximum temperature reached by the working fluid during the operation is set to 150 °C. Consequently, for acceptable performance, the critical temperature should be high enough to allow a sufficient enthalpy of vaporization of the working fluid in evaporator I. In typical applications such as steam power plants or vapor compression cycles, the critical temperature is not approached within 40-50 C, which implies to set the minimum value of the critical temperature to 200 °C. Nevertheless, in order to avoid making this criterion very stringent, it was decided to force the critical temperature of the fluid to be higher than 155 °C.

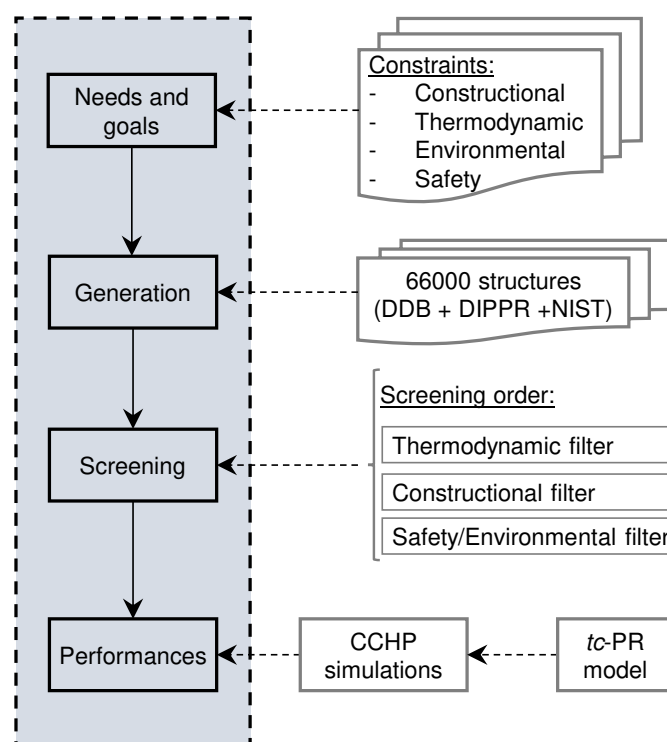


**Figure PVIII.7.** Scheme of the product-design approach adopted in this work for the selection of suitable working fluids for CCHP applications.

#### Triple-point temperature

At low temperature, freezing within the system should be avoided. For this reason, the triple-point temperature should be lower than the minimum temperature of the cycle ( $T_C = T_9$ ). The triple-point temperature should not be approached closer than 5 K.

**Operating pressures ( $P^{\text{sat}}$  @  $T_C$  and  $P^{\text{sat}}$  @  $T_H$ )**

First, in the evaporator I, the saturation pressure at temperature  $T_3$  cannot be too high because it may result in mechanical failure. Quoilin et al. [1294] suggest that for ORCs, the maximum pressure of the cycle should be 30 bar. However, this limit was set to 35 bar with the aim of avoiding the exclusion of promising candidates at this stage of the screening procedure.

On the other hand, caution should be taken for fluids with an excessively low saturation pressure at  $T_C$  since operating at sub-ambient pressures would lead to air entry into the system, resulting in reduced performances of the cycle. The minimum operating pressure (vapor pressure at  $T_C$ ) should be higher than 750 mbar. This choice is based on the work of Preißinger et al. [145], who focused on ORC for mobile applications.

**Density ( $\rho_{\text{dv}}$  @  $T_C$ )**

In evaporator II, the density of the dry saturated vapor at temperature  $T_C$  affects the surface area of the cross-section of the evaporator pipes. In particular, as stated by Lemort et al. [1294], the lower this density, the greater this surface area. It is considered that suitable working fluids should have a saturated vapor density higher than  $0.01 \text{ kg/m}^3$  at  $T_C$ .

**Safety (Toxicity, AIT = autoignition temperature)**

- Since n-pentane, which is a flammable and a potential toxic fluid, is already used in some commercial applications, it is decided that suitable fluids for the novel CCHP cycle should not be more flammable or toxic than n-pentane.

Toxicity and flammability information of substances is available from the Globally Harmonized System (GHS) of Classification and Labelling of Chemicals. The GHS provides harmonized criteria for classifying substances and mixtures according to their health, environmental and physical hazards. In addition, it includes hazard communication elements, as well as requirements for labelling and safety data sheets. Hazard identification mainly consists of three elements: hazard pictograms, hazard codes (H-codes) and hazard statements.

Physical hazards are related with explosion, flammability, oxidation, gases under pressure, self-reactivity and corrosion. They cover codes from H200 to H290. Health hazards include acute toxicity, skin/eye damage, respiratory/skin sensitization, germ cell mutagenicity, carcinogenicity and reproductive toxicology. They are identified by codes from H300 to H373. Finally, environmental hazards are focused on aquatic organisms and are represented by codes from H400 to H420.

As an illustration, the GHS classification of n-pentane is presented in [Figure PVIII.8](#). It is possible to observe the hazard pictograms, codes and statements. Such information has been gathered in the public-domain PubChem database of the National Institutes of Health [1308]. The database contains more than 100 million compounds but the GHS classification is available for about 150 thousands of them.

Considering the toxicity classification of n-pentane as a reference, fluids are not suitable for CCHP applications if they exhibit one or more of the following criteria:

- Carcinogenic (all categories)

- Mutagenic (all categories)
- Reproductive effects (all categories)
- Acute toxic to humans (categories 1, 2, 3)
- Toxicity to specific human organs (categories SE1, RE1, SE2, RE2)
- Acute and chronic aquatic toxic (category 1)

From the flammability standpoint, since n-pentane is classified as an extremely flammable fluid, it is decided not to consider a specific filter for this property. Instead, a filter on autoignition temperature (AIT) is considered. According to the ATEX directive [1309], the maximum surface temperature of the system may not exceed 80 % of the autoignition temperature of the substance. If this threshold is exceeded, it is still possible to use the fluid but the required equipment to satisfy safety constraints will be more expensive. Considering that the maximum temperature of the cycle (heat source temperature) is 160 °C, the working fluid should have an autoignition temperature greater than 200 °C. Nevertheless, in order to provide flexibility concerning the heat source temperature, it is decided to set the threshold at 240 °C.

## Pentane

### GHS Classification

Pictogram(s)	 Flammable    Irritant    Health Hazard    Environmental Hazard
Signal	<b>Danger</b>
GHS Hazard Statements	H224 (10.56%): Extremely flammable liquid and vapor [ <b>Danger</b> Flammable liquids] H225 (89.44%): Highly Flammable liquid and vapor [ <b>Danger</b> Flammable liquids] H304 (100%): May be fatal if swallowed and enters airways [ <b>Danger</b> Aspiration hazard] H336 (99.85%): May cause drowsiness or dizziness [ <b>Warning</b> Specific target organ toxicity, single exposure; Narcotic effects] H411 (100%): Toxic to aquatic life with long lasting effects [Hazardous to the aquatic environment, long-term hazard]
Precautionary Statement Codes	P210, P233, P240, P241, P242, P243, P261, P271, P273, P280, P301+P310, P303+P361+P353, P304+P340, P312, P331, P370+P378, P391, P403+P233, P403+P235, P405, and P501 (The corresponding statement to each P-code can be found at the <a href="#">GHS Classification</a> page.)
ECHA C&L Notifications Summary	<i>Aggregated GHS information provided by 1354 companies from 36 notifications to the ECHA C&amp;L Inventory. Each notification may be associated with multiple companies.            Information may vary between notifications depending on impurities, additives, and other factors. The percentage value in parenthesis indicates the notified classification ratio from companies that provide hazard codes. Only hazard codes with percentage values above 10% are shown.</i>

**Figure PVIII.8.** GHS classification of n-pentane. Obtained from the public-domain PubChem database of the National Institutes of Health [1308].

### Compatibility

The working fluid should be compatible with the polymers used in seals and not have a corrosive effect on metals in the system. Information about the latter condition is present in the GHS classification available in the PubChem database. For the screening procedure, it has been imposed the compatibility of the fluid with steel.

### **Global Warming Potential (GWP)**

With the aim of quantifying and communicating the relative contributions to climate change of emissions of different substances, emission metrics such as Global Warming Potential (GWP) can be used. It has arisen as the default metric for transferring emissions of different non-CO<sub>2</sub> gases to a common scale, often called “CO<sub>2</sub> equivalent emissions”. The GWP is defined as the time-integration radiative forcing (RF) due to a pulse emission of a given component  $i$  ( $RF_i$ ), relative to a pulse emission of an equal mass of CO<sub>2</sub> ( $RF_{CO_2}$ ):

$$GWP_i(TH) = \frac{\int_0^{TH} RF_i(t) dt}{\int_0^{TH} RF_{CO_2}(t) dt} \quad (\text{PVIII.8})$$

where  $TH$  represents the time horizon, usually set as 20, 50 or 100 years. The GWP for a time horizon of 100 years has been adopted for policy-makers to implement the multi-gas approach as done in the 1997 Kyoto Protocol.

For RF calculation two input parameters are required: the *radiative efficiency* and the atmospheric lifetime of the gas. Hodnebrog et al. [1310] provide a comprehensive and consistent analysis of such input parameters required to calculate values of the GWP. The GWP values used for the screening process were obtained from the Appendix A of the Scientific Assessment of Ozone Depletion: 2018 [1311]. This report includes the GWP values estimated by Hodnebrog et al. as well as those published in the previous Assessment Reports by the Intergovernmental Panel on Climate Change (IPCC). Suitable working fluids for the novel CCHP cycle should have a GWP lower than 150, as established by the EU F-gas regulation [1312].

### **Ozone Depletion Potential (ODP)**

The metric used for quantifying the effect of various ozone-depleting substances (ODS) on the ozone layer is called ozone depletion potential (ODP). The ODP is defined as the integrated change in total ozone per unit mass emission of a specific ozone-depleting substance relative to the integrated change in total ozone per unit mass emissions of CFC-11 (trichlorofluoromethane). As well as for GWP values, ODP was reported from the Scientific Assessment of Ozone Depletion: 2018.

EU regulation No 1005/2009 on substances that deplete the ozone layer [1313] is the implementation of the Montreal Protocol in European law. It is worth noting that some non-zero ODP molecules are not regulated by that framework. Indeed, as suggested by Eyerer et al. [1314] in 2019, the substance with the smallest ODP, which is classified as an ODS in the EU regulation No 1005/2009 [1313], has an ODP of 0.01. Considering this information, it is decided to set the cutoff for ODP at  $10^{-3}$ .

## **PVIII.IV.II Chemical design space. Data curation and preparation**

In this work, the experimental data contained in the Dortmund Data Bank (DDB – version 2020 <http://www.ddbst.com/ddb.html>), the Design Institute for Physical Properties (DIPPR – version 2020) and the NIST ThermoData Engine 103b (NIST TDE 103b) databases are used.

The first step (“pre-screening”) of the screening process is performed by selecting all the pure fluids:

- for which the critical temperature ( $T_{crit}$ ) data is available (we indeed search fluids so that  $T_{crit} > 155$  °C).
- for which melting temperature ( $T_{mel}$ ) or triple-point temperature ( $T_{tp}$ ) data is available (one of our target properties is that  $T_{mel}$  (or  $T_{tp}$ )  $< T_9$ ).
- for which the critical pressure ( $P_{crit}$ ) and the acentric factor ( $\omega$ ) are either available or estimable in order to enable the application of the  $tc$ -PR equation of state that requires the knowledge of  $T_{crit}$ ,  $P_{crit}$  and  $\omega$ .

The DDB-2020 database contains experimental data for 66 425 molecules. If we apply the pre-screening described above, 1 415 pure fluids remain, as shown in [Figure PVIII.9](#).

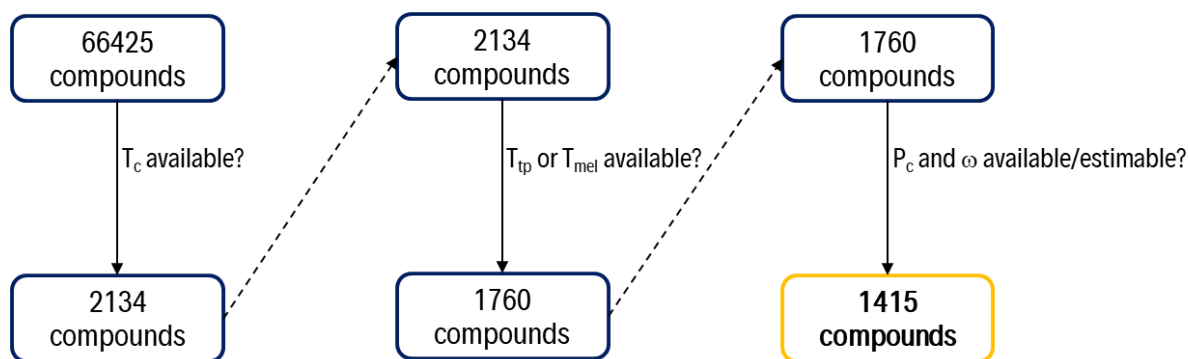


**Figure PVIII.9.** Pre-screening on DDB-2020 database.

Next, the DIPPR-2020 database provides data for nearly 2 200 pure fluids and, as shown in [Figure PVIII.10](#), 2 119 molecules remain if the pre-screening described above is applied.

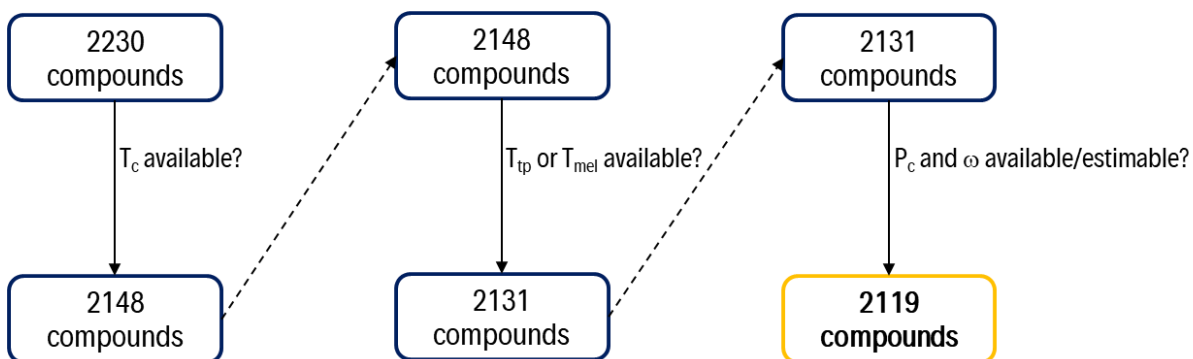


**Figure PVIII.10.** Pre-screening on DIPPR-2020 database.

Finally, the NIST TDE 103b database contains nearly 30 220 pure fluids and, as shown in [Figure PVIII.11](#), 745 molecules remain if the pre-screening described above is applied.

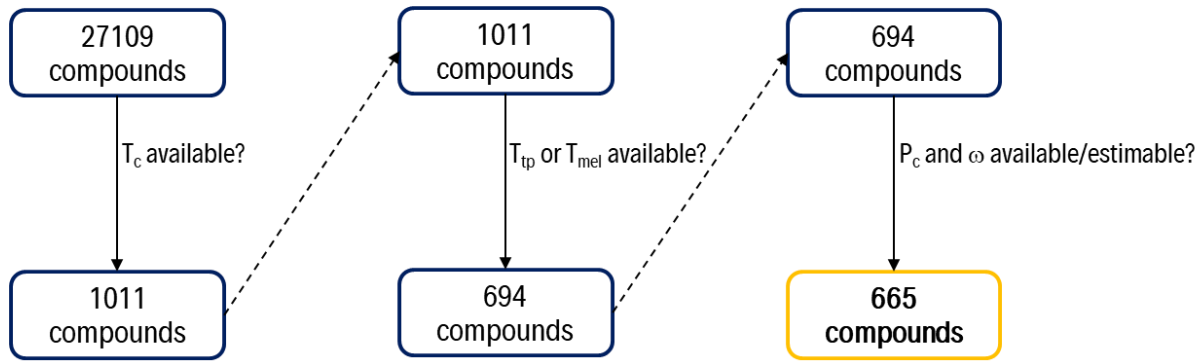


**Figure PVIII.11.** Pre-screening on the NIST TDE 103b database.

As a conclusion of this pre-screening step, the initial count for further screening is **2 540 pure fluids**: 1 129 molecules are only contained in the DIPPR database, 421 molecules are only contained in the DDB database and 990 molecules are contained in both of them. The 625 compounds coming from the NIST TDE are already contained either in the DDB or the DIPPR databases.

The fact that only 990 pure fluids are present in both DDB and DIPPR databases reflects the complementarity of these databases and, thus, the importance of maximizing the number of different considered databases.

### PVIII.IV.III Thermodynamic model

As stated before, in order to ensure the accuracy of thermodynamic property calculations and CCHP simulations, the *translated* and *consistent tc-PR* equation of state has been retained. Such a model is acknowledged as an accurate cubic equation of state; it requires 6 component-dependent parameters ( $T_{crit,exp}$ ,  $P_{crit,exp}$ ,  $v_{liq,exp}^{sat}(T_r = 0.8)$ ,  $L$ ,  $M$ ,  $N$ ) and writes:

$$P(T, v) = \frac{RT}{v-b} - \frac{a_c \cdot \alpha(T_r)}{(v+c)(v+b+2c) + (b+c)(v-b)}$$

$$with: \begin{cases} \alpha(T_r) = T_r^{N(M-1)} \exp[L(1-T_r^{MN})] \\ c = v_{liq}^{sat,u-PR}(T_r = 0.8) - v_{liq,exp}^{sat}(T_r = 0.8) \\ \eta_c = \left[1 + \sqrt[3]{4-2\sqrt{2}} + \sqrt[3]{4+2\sqrt{2}}\right]^{-1} \approx 0.25308 \\ a_c = \frac{40\eta_c + 8}{49 - 37\eta_c} \frac{R^2 T_{crit,exp}^2}{P_{crit,exp}} \approx 0.45724 \frac{R^2 T_{crit,exp}^2}{P_{crit,exp}} \\ b = \frac{\eta_c}{\eta_c + 3} \frac{RT_{crit,exp}}{P_{crit,exp}} - c \approx 0.07780 \frac{RT_{crit,exp}}{P_{crit,exp}} - c \end{cases} \quad (PVIII.9)$$

It is noticeable that the substance-dependent volume-translation parameter,  $c$ , is determined, component by component, in order that the *translated* EoS exactly reproduces the experimental saturated-liquid molar volume at a reduced temperature of 0.8, [ $v_{liq,exp}^{sat}(T_r = 0.8)$ ], that is:

$$c = v_{liq}^{sat,u-CEoS}(T_r = 0.8) - v_{liq,exp}^{sat}(T_r = 0.8) \quad (PVIII.10)$$

where  $v_{liq}^{sat,u-CEoS}(T_r = 0.8)$  is the molar volume calculated with the original (*untranslated*) CEoS at  $T_r = 0.8$ .

Another key feature is the use of the highly flexible Twu 91  $\alpha$ -function [216]:

$$\alpha(T) = (T/T_c)^{N(M-1)} \exp\left[L\left(1 - (T/T_c)^{MN}\right)\right] \quad (\text{PVIII.11})$$

By determining the 3 parameters  $L$ ,  $M$  and  $N$  from a constrained fitting procedure to well-chosen vapor-liquid equilibrium data, the Twu 91  $\alpha$ -function can pass the consistency test of Le Guennec et al. [198] thus guaranteeing safe property predictions in both subcritical and supercritical domains. Consistent  $L$ ,  $M$ ,  $N$  parameters were published by Pina-Martinez et al. [184] for around 2000 fluids. For other components, they can be determined from second order polynomial correlations with respect to the acentric factor [184].

The key properties that should be properly predicted in this work by the CEoS are: vapor pressure, density, enthalpy and entropy. In order to ensure the accuracy capabilities of any model, it is necessary to compare its predictions against experimental data. In the case of vapor pressure, density and enthalpy plenty of data are available in pure-compound databases. It is worth recalling that in the case of enthalpy and entropy, data of enthalpy and entropy of vaporization are retained. The  $tc$ -PR model is able to correlate the vapor pressures with an error of 1 % whereas errors on enthalpy/entropy of vaporization and density are close to 2 % [184,1315] for more than 1700 molecules.

#### PVIII.IV.IV Screening procedure

It is worth recalling that among the target properties, critical temperatures, triple-point temperatures, vapor pressures and densities are available for 2 540 pure fluids. The first two properties were directly collected from the DDB and DIPPR databases, and the last two ones were estimated with the  $tc$ -PR model. On the other hand, safety, compatibility and environmental properties are not all available for all the 2 540 fluids. Consequently, it seems necessary to establish a proper order of screening which guarantees that, at each filter stage, the considered target property is available for the remaining list of fluids.

The first five filters dealt with (1) critical temperature, (2) triple-point temperature, (3) vapor pressure at  $T_c$ , (4) density at  $T_c$  and (5) vapor pressure at  $T_H = T_3$  because, as mentioned before, they are available for the 2 540 molecules of the design space. Next, since toxicity information is reported for 150 thousand molecules in the PubChem database, it was decided then to apply this sixth filter. The next two filters concerned GWP and ODP; they were applied at this stage because even if the measured/calculated GWP and ODP values are not available, it is possible to estimate approximately the GWP or ODP of most of molecules from their chemical structure. Eventually, compatibility and autoignition temperature (AIT) filters were applied.

The resulting screening order is presented in [Table PVIII.2](#).

**Table PVIII.2.** Screening order retained for this work.

Step	Criterion
1	$T_{crit}$
2	$T_{tp}$
3	$p^{sat} @ T_C$
4	$\rho_{dv} @ T_C$
5	$p^{sat} @ T_H$
6	Toxicity
7	GWP
9	ODP
10	AIT
11	Material compatibility

### PVIII.IV.V Performance evaluation

After the fluid screening procedure, the performance of the CCHP configuration operating with the list of selected fluids was investigated. For this purpose, two primary indicators were used: the energy utilization factor (EUF) and the volumetric capacity ( $Q_v$ ). The EUF, as discussed in [Section PVIII.III](#), is defined as the ratio between the useful effects generated by the machine and the specific energy supplied to the engine for its operation. It provides a measure of the energy efficiency (operating cost) of the system. It yields to:

$$EUF_{CCHP} = \frac{|w_{net}| + |q_M| + q_C}{q_{HS}} \quad (\text{PVIII.12})$$

The volumetric capacity is defined as the refrigeration capacity per unit of volume of working fluid flowing into the compressor (point 9) and it gives a measure of the equipment size (capital cost).  $Q_v$  can be expressed as:

$$Q_v = \frac{\dot{Q}_C}{(\dot{m} / \rho_9)} \quad (\text{PVIII.13})$$

Another important indicator is the primary energy savings ratio (PESR). This parameter provides information on how much primary energy is saved by using a multigeneration system instead of separated ones to supply heating ( $|\dot{Q}_M|$ ), cooling ( $\dot{Q}_C$ ) and electric ( $|\dot{W}_{net}|$ ) power. Note that since different systems are compared and they may operate with different mass flowrates, it is necessary to define PESR using powers rather than specific energy as done for EUF. PESR is thus defined as:

$$PESR = \frac{\dot{Q}_{HS,SS} - \dot{Q}_{HS,CCHP}}{\dot{Q}_{HS,SS}} = 1 - \frac{\dot{Q}_{HS,CCHP}}{\dot{Q}_{HS,SS}} \quad (\text{PVIII.14})$$

where  $\dot{Q}_{HS,CCHP}$  and  $\dot{Q}_{HS,SS}$  are the amount of energy per unit of time from the heat source required by the CCHP system and separated systems (SS) to provide electric, heating and cooling powers

respectively. To determine  $\dot{Q}_{HS,CCHP}$  and  $\dot{Q}_{HS,SS}$ , it is necessary to know the efficiency of: 1) a reference power plant, 2) a reference heating system, and 3) a reference cooling system. Considering the reference efficiencies for the electric, heating and cooling systems, the PESR can be expressed as:

$$PESR = 1 - \frac{\dot{Q}_{HS,CCHP}}{\frac{|\dot{W}_{net}|}{\eta_{ref,e}} + \frac{|\dot{Q}_M|}{\eta_{ref,h}} + \frac{\dot{Q}_C}{\eta_{ref,e} \cdot \eta_{ref,c}}} \quad (PVIII.15)$$

This is illustrated in [Figure PVIII.12](#).

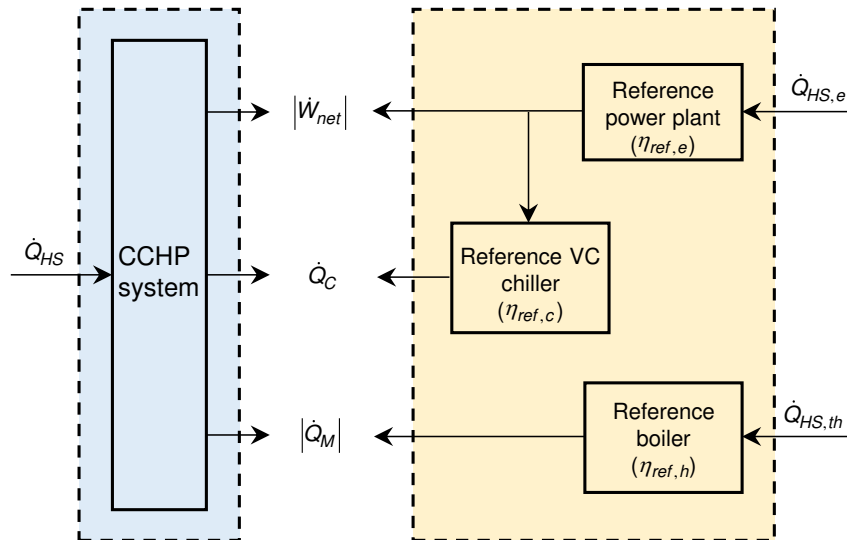


**Figure PVIII.12.** Illustration of the comparison between a conventional generation and trigeneration systems.

Regarding the reference power plant and its efficiency, the EU regulation No 2015/2402 [1316] establishes that the harmonized efficiency reference for the production of electricity using solid biomass is  $\eta_{th,e} = 0.30$ , assuming 15 °C as ambient temperature and a heat source temperature of 300 °C. However, the temperature levels considered in this work are 20 °C and 150 °C. It would be thus unfair to consider the same efficiency. To overcome this problem, it is proposed to calculate the ratio between the reference plant considered by the EU regulation and a Carnot engine operating at the considered temperature levels. Then, this ratio can be used to obtain the efficiency of a reference power plant whose temperature levels are 15 °C and 150 °C.

The thermal efficiency of a Carnot engine operating between 15 °C and 300 °C is 0.50, i.e., the ORC plant considered by the EU regulation No 2015/2402 [1316] runs at a 60 % of the efficiency of the corresponding Carnot engine. For the temperature levels considered in this work (20 °C-150 °C), the Carnot efficiency is equal to 0.31. In consequence, the thermal efficiency of the reference power plant for PESR calculations is  $\eta_{ref,e} = 0.31 \cdot 0.6 = 0.19$ .

In turn, the reference heating system is a biomass-fueled boiler, in which the heat generated by biomass combustion is utilized to produce hot water or steam to satisfy heat needs. For the sake of simplicity, it

is assumed that the harmonized efficiency reference for production of heat is the same for hot water or steam generation. The EU regulation No 2015/2402 [1316] sets this value at  $\eta_{ref,h} = 0.86$ .

Finally, for the reference cooling system, the EU regulation No 2016/2281 [1317] introduces an indicator named seasonal space cooling energy efficiency ( $\eta_{s,c}$ ) as a benchmark parameter for cooling systems. It is defined as the reference annual cooling demand pertaining to the cooling season covered by a cooling system, and the annual energy consumption for cooling. This parameter considers the varying weather conditions during the year. Therefore, it could be assumed as an average coefficient of performance (COP). For electric, air-to-air air conditioners, this value is set to  $\eta_{ref,c} = \eta_{s,c} = 2.57$ .

## **PVIII.V Case studies and operating specifications**

Two case studies related to different CCHP end-users are investigated to assess the impact of operating conditions on the list of promising working fluids. The underlying equations described in Section PVIII.III are the same for both case studies. The only differences among them are specifications.

For both case studies, the heat source temperature is 160 °C. For the sake of simplicity, it is assumed that the overall required duty by the end-users is equal to 100 kW ( $|\dot{W}_{net}| + |\dot{Q}_M| + \dot{Q}_C = \dot{m}(|w_{net}| + |q_M| + q_C)$ ). In addition, the cooling, heating and electric needs are quantified as a percentage of the total duty requirements. It is worth noting that the overall required duty of 100 kW is a calculation basis.

### **PVIII.V.I Case study 1: Residential/Commercial user**

For case study 1, it is assumed that for the residential/commercial users:

- The cooling needs include air-conditioning, and they represent 30 % of the total duty. Comfort temperatures in summer range between 20 and 25 °C. To reach such temperatures, the working fluid should enter the evaporator II at 10 °C, i.e., at 20 °C decreased by the pinch point temperature.
- The heating needs account for the 40 % of the total duty and are related to space heating or hot water requirements. Heating power is commonly required at 90 °C.
- The electric power required to drive machines, devices and essential equipment reaches the remaining 30 % of the total duty.

The distribution of cooling, heating and power needs are based on Reference [1318].

## PVIII.V.II Case study 2: Food industry

For case study 2, it is assumed that for the food industry:

- The cooling needs include food storage and preservation, and they represent 20 % of the total duty. The set-point temperature within fridges is usually maintained between 2 and 5 °C. To reach such temperatures, the working fluid should enter the evaporator II at -10 °C.
- The heating needs, in turn, represent 60 % of the total duty and are related to the production of low-pressure steam or to specific processes such as pasteurization. Heating power is commonly required at 130 °C.
- The electric power required to drive machines, devices and essential equipment reaches the remaining 20 % of the total duty.

The distribution of cooling, heating and power needs are based on the work of Compton et al. [1319].

The resulting screening criteria and the relevant process conditions for both case studies are summarized in Table PVIII.3 and Table PVIII.4 respectively.

**Table PVIII.3.** Summary of filtering criteria.

Step	Criterion	Case study 1		Case study 2	
		Residential/Commercial		Food industry	
1	$T_{crit}$	> 155 °C			
2	$T_{tp}$	< 5 °C		< -15 °C	
3	$P^{sat} @ T_C$	> 750 mbar @ 10 °C		> 750 mbar @ -10 °C	
4	$\rho_{dv} @ T_C$	> 0.01 kg/m <sup>3</sup> @ 10 °C		> 0.01 kg/m <sup>3</sup> @ -10 °C	
5	$P^{sat} @ T_H$	< 35 bar @ 150 °C			
6	Toxicity	Exclude categories 1, 2 and 3 of acute toxicity			
7	GWP	< 150			
8	ODP	< 10 <sup>-3</sup>			
9	AIT	> 240 °C			
10	Material compatibility	Compatible at least with steel			

**Table PVIII.4.** Summary of operating specifications.

Parameter	Symbol	Units	Case study 1 Residential/ commercial	Case study 2 Food industry
Overall duty	-	kW	100	
Heating power share	$ \dot{Q}_M $	kW	40	60
Cooling power share	$\dot{Q}_C$	kW	30	20
Electric power share	$ \dot{W}_{net} $	kW	30	20
State 1: temperature	$T_1$	°C	20 °C	
State 1: vapor quality	$x_1$	-	0.0	
State 2: pressure	$P_2$	bar	$P^{sat}(150\text{ °C})$	
State 3: temperature	$T_3$	°C	150	
<b>State 3: vapor quality</b>	$x_3$	-	<b>1.0</b>	
State 4: pressure	$P_4$	bar	$P^{sat}(90\text{ °C})$	$P^{sat}(130\text{ °C})$
State 5: temperature	$T_5$	°C	90 °C	130 °C
State 6: temperature	$T_6$	°C	20 °C	
State 7: temperature	$T_7$	°C	20 °C	
State 7: vapor quality	$x_7$	-	0.0	
State 8: temperature	$T_8$	°C	10 °C	-10 °C
State 9: temperature	$T_9$	°C	10 °C	-10 °C
State 10: pressure	$P_{10}$	bar	$P^{sat}(20\text{ °C})$	
Isentropic efficiency of turbine I and II	$\eta_{T,I}$	-	0.75	
	$\eta_{T,II}$	-		
Isentropic efficiency of turbine III	$\eta_{T,III}$	-	0.65	
Isentropic efficiency of compressor	$\eta_C$	-	0.65	
Isentropic efficiency of pump	$\eta_P$	-	0.85	

(\*) The specification in bold was selected to fulfill the degree of freedom.

## PVIII.VI Results

### PVIII.VI.I Screening results

The progress of compound elimination from the initial pool of 2540 candidates for the considered case studies is given in [Table PVIII.5](#).

**Table PVIII.5.** Progress of the number of compounds passing the successive filters from the initial pool of 2540 candidates for the two considered case studies.

Step	Criterion	Case study 1 Residential/commercial	Case study 2 Food industry	Case study 2: relaxed constraint (filter 3)
0	Initial count		2540 (fluids)	
1	$T_{crit}$	2394		2394
2	$T_{tp}$	1568		1465
3	$P^{sat} @ T_C$	40	5	39
4	$\rho_{dv} @ T_C$	40	5	39
5	$P^{sat} @ T_H$	24	0	23
6	Toxicity	10	0	10
7	GWP	10	0	10
8	ODP	10	0	10
9	AIT	9	0	9
10	Material compatibility	9	0	9

The critical temperature filter eliminates almost 150 molecules for both case studies. This filter screened out very light molecules such as oxygen, nitrogen or hydrogen, as well as alkanes, alkenes and alkynes with less than 4 carbon atoms. Well-known high-GWP refrigerants such as HCFC-22, HFC-32, HFC-134a and HFC-143a were eliminated. Furthermore, low-GWP molecules including HFO-1234ze(E), HFO-1234ze(Z), HCFO-1336mzz(E), HFO-1234yf or HFO-1234zf were excluded.

The triple-point temperature constraint eliminated almost 830 (case study 1) and 930 (case study 2) additional compounds from different chemical families. Among the excluded molecules, very heavy molecules were found in both cases (e.g., alkanes and alkenes with more than 14 carbons). Moreover, a wide range of aromatic compounds, from benzene ( $C_6H_6$ ) to naphthalene ( $C_{10}H_8$ ), were also eliminated. In a general trend, oxygenated compounds (acids, ketones, aldehydes) with more than 2 carbon and 2 oxygen atoms, nitrogenated compounds with more than 6 carbon atoms, sulfur molecules with more than 4 carbon atoms, as well as halogenated compounds with more than 2 bromine, chlorine and/or iodine atoms were excluded.

It was observed that the minimum operating pressure ( $P^{sat}(T_C)$ ) was a very constraining criterion. In [Figure PVIII.13](#), the vapor pressure at  $T_C = 10$  °C is plotted against critical temperature for the 1 568 molecules remaining after filter 2 for case study 1. It is possible to observe that working fluids with higher values of  $T_{crit}$  operate at lower pressures (implying a higher risk of air infiltration into the

system). Only 40 of the 1 568 fluids have  $P^{sat}(T_C)$  higher than the typical lower bound pressure limit of 750 mbar (also selected in this work, see [Table PVIII.3](#)). It is interesting to remark that refrigerants (i.e., used in purely refrigeration/cooling applications) do not have critical temperatures larger than 105 °C [1296] in order to avoid too low operating pressures at evaporating temperatures ranging from -20 °C to 5 °C. Nevertheless, the filter on  $T_{crit}$  for CCHP applications was set to 155 °C with the aim of absorbing heat from a source at 160 °C. This shows that the objective of supplying work, heat and cold with a single working fluid represents, *per se*, a highly selective condition.

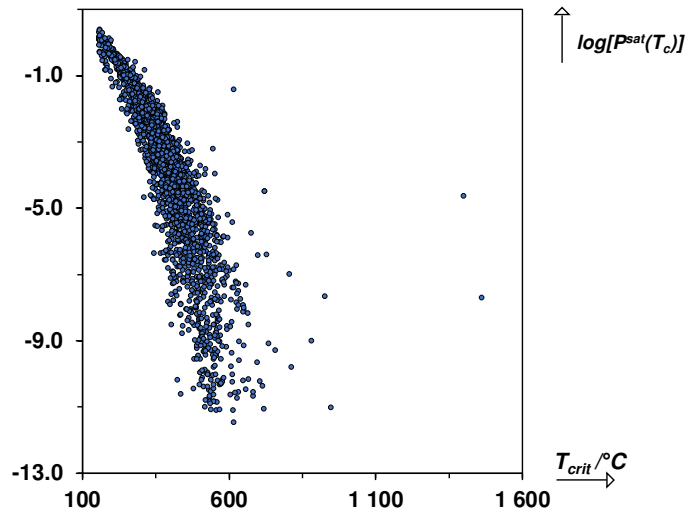


**Figure PVIII.13.** Saturation pressure at  $T_C = 10$  °C versus critical temperature for the 1568 molecules remaining after filter 2 for case study 1.

In addition, screening for case study 2 showed that no molecule of the design space can meet the specified requirements. It was decided to relax the filter on  $P_{min}$  in order to obtain exactly the same number of molecules as in case 1, at the end of the screening procedure. It was found necessary to impose  $P_{min} = P^{sat}(T_C)$  higher than 325 mbar in order to obtain a final list of 9 molecules. It is worth recalling that the initial constraint for  $P_{min}$  ( $P_{min} \geq 750$  mbar) was already “relaxed”. The new condition may be critical since the investment needed for the construction of well-sealed devices to avoid air infiltration into the cycle could seriously impact the machine cost. This should be considered very carefully because one of the requirements of decentralized energy systems is that their components must be simple and easy to manufacture and design [1294].

At this point, it is interesting to have a look at common reference fluids used in ORC systems that were excluded during the screening process for the two cases studies. For instance, n-pentane, isopentane, HFC-365mfc and toluene are excluded due to their low minimum pressure (see [Table PVIII.6](#)). It should be noted that these fluids are rarely condensed at temperatures lower than 30-40 °C, while in this work conditions required for the supply of cooling power can reach -10 °C. It is worth noting that beyond the minimal pressure criterion, HFC-365mfc would still have been eliminated due to its high GWP.

**Table PVIII.6.** Minimum operating pressures ( $P^{sat}(T_C)$ ) of four reference fluids for the two considered case studies.

Molecules	$P_{\min} = P^{sat}(10^{\circ}\text{C}) / \text{mbar}$	$P_{\min} = P^{sat}(-10^{\circ}\text{C}) / \text{mbar}$
n-pentane	382	152
Isopentane	523	220
HFC-365mfc	296	105
Toluene	17	5

The maximum pressure filter excluded 16 additional fluids. The maximum value in pressure is reached by SO<sub>2</sub> with around 70 bar. A promising molecule (non-flammable, non-toxic) is HFC-143 but it exceeds the constraint by almost 11 bar. Next, the toxicity filter rejected several chlorinated compounds due to their carcinogenic or acutely toxic character. Examples of such molecules are ethyl chloride, HCFC-11, phosgene (CCl<sub>2</sub>O), dichlorosilane (Cl<sub>2</sub>H<sub>2</sub>Si) and boron trichloride (BCl<sub>3</sub>).

Finally, filters on ODP and GWP did not exclude any molecule among the remaining ones after filter 6, while the constraint on AIT only eliminated methyl ethyl ether. The final list of 9 promising candidates is presented in Table PVIII.7. The well-known tradeoff between flammability and environmental impact is observed [144,145]. In order to reduce the GWP and ODP, molecules should be less halogenated, which implies that flammability increases. It is observed that to satisfy constraints on GWP and ODP, 7 over 9 fluids are extremely flammable while the 2 remaining ones are non-flammable. In addition, among these fluids, none of them belongs to categories 1, 2 or 3 of acute toxicity.

## PVIII.VI.II Performance results

In this section, the performances in terms of EUF and  $Q_v$  for the final nine working fluids are evaluated. Results are summarized in Figure PVIII.14, Table PVIII.7 and Table PVIII.8. The accuracy of the *tc*-PR model on the properties of interest such as vapor pressure, density and enthalpy of vaporization is presented in Table PVIII.9. Since “optimal” molecules are those which exhibit high EUF and high  $Q_v$ , the inverses of such indicators are plotted, so that candidates satisfying both objectives lie at the lower left corner of the figure.

1. Cyclobutane gives the best EUF for both case studies. No special toxicological issues are associated with it according to the GHS classification. It has no ODP and a negligible GWP. However, cyclobutane is an extremely flammable fluid and may be the less stable molecule of the list as a consequence of angle strain related to its bonds. Furthermore, a CCHP system operating with cyclobutane could experience air infiltration because the minimal pressure of the cycle is lower than atmospheric pressure.
2. 1-Butene-3-yne (vinylacetylene) exhibits the greatest volumetric capacity and its EUF is only 2 % lower compared to cyclobutane. It does not have issues concerning ODP and GWP. As well as cyclobutane, it is an extremely flammable molecule. From the constructional standpoint, it has a minimum pressure around 1.18 bar, which guarantees that air does not enter into the

system during operation. Nevertheless, it has the lowest AIT among the whole list of fluids and it could have stability problems since it contains double and triple bonds.

The refrigerant HFC-152 has similar capabilities as 1-Butene-3-yne in terms of EUF. It is non-toxic, has a low GWP (53) and zero ODP. HFC-152 should not present problems concerning stability due to the presence of fluorine atoms and the absence of unsaturated bonds. As well as for 1-Butene-3-yne, CCHP systems containing HFC-152 do not have issues related to air infiltration. It is worth noting that Preißinger et al. [145] found that this fluid was a promising candidate for ORC for mobile applications.

3. 1,2-butadiene performs similarly as 1-Butene-3-yne and HFC-152 in terms of EUF, and exhibits a 20 % loss in  $Q_v$  compared with 1-Butene-3-yne. It fulfills environmental and toxicological criteria. Furthermore, CCHP cycles operating with 1,2-butadiene have a slight sub-atmospheric minimum pressure. However, this fluid is a cumulated diene, characterized by adjacent carbon-carbon double bonds, and tends to be unstable.
4. Cis-2-butene yields a 7 % loss in EUF compared to cyclobutane and only a 2.5 % loss in  $Q_v$  compared to 1-Butene-3-yne. It has negligible GWP, no ODP and does not provoke serious adverse health effects. It displays an excellent minimum pressure (1.23 bar) and guarantees the tightness of the device.

HCFO-1233zd(E) also achieves a 7 % loss in EUF with respect to cyclobutane but has the worst volumetric capacity among the list of fluids. Nevertheless, it has the advantage of being non-flammable, non-toxic and having low GWP (4) and ODP (equal to 0.0004). Furthermore, it has been well-investigated and some authors (e.g., Eyerer et al. [1314]) studied the possibility of using it as a drop-in replacement of HFC-245fa in ORC systems. Moreover, they showed that HCFO-1233zd(E) is compatible with common polymers, namely ethylene-propylene-diene rubber (EPDM), fluororubber (FKM), nitrile-butadiene rubber (NBR) and chlorobutadiene rubber (CR), used in ORC systems. Concerning constructional constraints, it is worth noting that it has the lowest minimum operating pressure (785 mbar), which could result in important costs to avoid air infiltration.

5. Neopentane (2,2-dimethylpropane) presents a reduction of about 11 % in EUF compared to cyclobutane and 25 % in  $Q_v$  with respect to 1-Butene-3-yne. It is extremely flammable, and has negligible GWP and no ODP. Furthermore, CCHP systems containing neopentane should not have issues related with sealing tightness since its minimum operating pressure is around 1.03 bar.

HCFO-1224yd(Z) has a loss of 11.5 % and 32 % in EUF and  $Q_v$ , respectively. As HCFO-1233zd(E), it has low GWP (1) and ODP (0.0002). Moreover, it is non-flammable and non-toxic. It has also been studied by Eyerer and co-workers [1314] as a drop-in candidate for the replacement of HFC-245fa in ORC systems.

6. Trimethyl silane has the worst performance in terms of EUF and achieves a 20 % loss in volumetric capacity. It is extremely flammable, and has negligible GWP and no ODP. It fulfills toxicological constraints as well as constructional requirements.

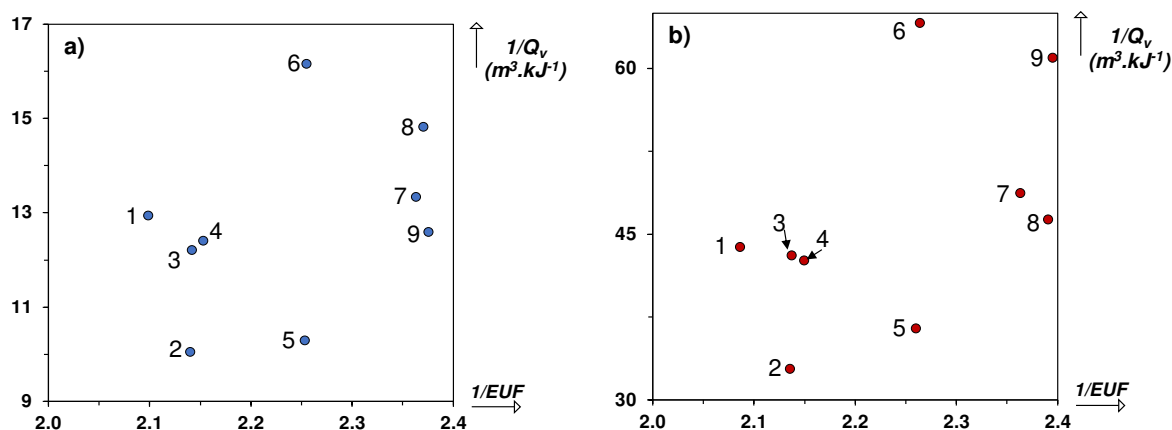


**Figure PVIII.14.** Inverse of volumetric capacity versus inverse of energy utilization factor for the 9 molecules remaining after the screening procedure: a) Case study 1. b) Case study 2. The numbers correspond to the ranking of each molecule as shown in [Table PVIII.8](#).

Concerning the PESR for case study 1, the nine fluids reach positive values for this indicator, i.e., all of them lead to savings of primary energy compared to the use of separated systems for each objective. On the other hand, for case study 2, only the top 4 molecules of the list enable to reduce the consumption of primary energy.

## PVIII.VII Conclusions

In the present work, a product-design approach for the selection of suitable working fluids for novel Combined Heating, Cooling and Power applications has been presented. In addition, the CCHP cycle has been described as a transition from a power to a (power + heating) to a (power + heating + cooling) cycle. This is accompanied by a degree-of-freedom analysis.

The main conclusions of this work are:

- Concerning the working-fluid selection, a database search has been implemented to screen about 60 000 species included in the DDB, the DIPPR and the NIST TDE 103b databases. The screening approach considered thermodynamic, process-related, constructional, safety and environmental constraints. Moreover, the  $tc$ -PR model has been used for the first time in order to ensure the quality of the calculation of thermo-physical properties, while providing a high level of accuracy for the target properties and the performance assessment of promising working fluids.
- The screening coupled with the performance evaluation have demonstrated that flammable fluids such as vinylacetylene or HFC-152 have a good potential for CCHP applications. In the case where highly constraining safety restrictions are imposed, HCFO-1233zd(E) could be an interesting candidate since it is non-flammable and non-toxic.
- Furthermore, the results revealed an antagonism between the objectives of single-fluid CCHP systems. This is reflected by the fact that fluids with higher critical temperatures, and, thus, potentially better in terms of energy utilization, will lead to constructional problems since they operate at too low pressures in the evaporator at which cooling power is supplied.

Finally, it is worth recalling that the study has intended to give an overview about promising working fluids which should be considered for further theoretical and experimental investigations. This work opens the way to implement database search methodologies to find suitable working fluids for more sophisticated CCHP applications.

This work provides an original and comprehensive working-fluid design approach enabling the selection of the most appropriate working fluid for CCHP systems, over a large number of fluids, and a wide number of design conditions and constraints. Additionally, further research should address the development of two-phase expanders and compressors in order to guarantee the scale-up of this architecture of CCHP systems.



**Table PVIII.7.** List of 9 candidates passing the screening filters for the two considered case studies. Note: Filter on  $P_{\min}$  for case study 2 is relaxed.

CAS	Name	Formula	SMILES	ASHRAE designation	GWP	ODP	Flammability category	$T_{\text{crit}}$ (°C)	$P_{\text{crit}}$ (bar)
<b>Alkanes, alkenes, alkynes</b>									
463-82-1	Neopentane	C <sub>5</sub> H <sub>12</sub>	CC(C)(C)C		<1	0	1	160.65	31.96
590-19-2	1,2-butadiene	C <sub>4</sub> H <sub>6</sub>	C=C=CC		<1	0	1	178.85	43.60
590-18-1	Cis-2-butene	C <sub>4</sub> H <sub>8</sub>	C/C=C\C		<1	0	1	162.35	42.10
689-97-4	Vinylacetylene	C <sub>4</sub> H <sub>4</sub>	C=CC#C		<1	0	1	180.85	48.60
<b>Cycloalkanes, cycloalkenes, cycloalkynes</b>									
287-23-0	Cyclobutane	C <sub>4</sub> H <sub>8</sub>	C1CCC1		<1	0	1	186.78	49.80
<b>Fluorinated alkanes</b>									
624-72-6	1,2-difluoroethane	C <sub>2</sub> H <sub>4</sub> F <sub>2</sub>	FCCF	HFC-152	53	0	1	171.85	43.40
<b>Halogenated alkenes (fluorine plus chlorine)</b>									
102687-65-0	(E)-1-chloro-3,3,3-trifluoro-1-propene	C <sub>3</sub> H <sub>2</sub> ClF <sub>3</sub>	C(/C=C/Cl)(F)(F)F	HCFO-1233zd(E)	4	0.0004	4	166.45	36.24
111512-60-8	(Z)-1-chloro-2,3,3,3-tetrafluoropropene	C <sub>3</sub> HClF <sub>4</sub>	C(=C(\C(F)(F)F)/F)/Cl	HCFO-1224yd(Z)	1	0.0002	4	155.54	33.37
<b>Silanes</b>									
993-07-7	Trimethyl silane	C <sub>3</sub> H <sub>10</sub> Si	C[SiH](C)(C)		<1	0	1	158.85	31.90

**Table PVIII.8.** CCHP cycle performances for the nine candidates passing the screening filters. Ranking is based on EUF.

Case study 1					Case study 2				
Name/ASHRAE designation	Rank	EUF	Q <sub>v</sub> (kJ.m <sup>-3</sup> )	PESR (%)	Name/ASHRAE designation	Rank	EUF	Q <sub>v</sub> (kJ.m <sup>-3</sup> )	PESR (%)
Cyclobutane	1	0.4766	772.9	23.0	Cyclobutane	1	0.4794	228.1	5.4
Vinylacetylene	2	0.4673	995.5	21.5	Vinylacetylene	2	0.4683	304.6	3.1
HFC-152	3	0.4669	819.1	21.4	HFC-152	3	0.4679	232.1	3.1
1,2-butadiene	4	0.4645	805.8	21.0	1,2-butadiene	4	0.4653	234.7	2.5
Cis-2-butene	5	0.4438	971.1	17.4	Cis-2-butene	5	0.4425	274.2	-2.5
HCFO-1233zd(E)	6	0.4435	618.6	17.3	HCFO-1233zd(E)	6	0.4418	156.0	-2.7
Neopentane	7	0.4232	749.9	13.3	Neopentane	7	0.4232	205.3	-7.2
HCFO-1224yd(Z)	8	0.4219	674.6	13.1	Trimethyl silane	8	0.4183	215.8	-8.4
Trimethyl silane	9	0.421	794.0	12.9	HCFO-1224yd(Z)	9	0.4176	164.0	-8.6

**Table PVIII.9.** Parameters corresponding to the tc-PR model and the mean absolute percentage average (MAPE) on the properties of interest for the nine candidates passing the screening filters. The calculation of MAPEs is described in reference [184].

Name	L	M	N	c (cm <sup>3</sup> .mol <sup>-1</sup> )	MAPE on $P^{sat}$	$T_{min}$ (K)	$T_{max}$ (K)	MAPE on $\Delta_{vap}H$	$T_{min}$ (K)	$T_{max}$ (K)	MAPE on $\rho_{liq}^{sat}$	$T_{min}$ (K)	$T_{max}$ (K)
Neopentane	0.1268	0.8494	2.5591	-5.9633	0.21%	256.60	433.80	1.66%	256.60	425.12	1.37%	256.60	390.42
1,2-butadiene	1.1829	0.9640	0.5059	4.4542	1.61%	234.20	452.00	2.45%	136.95	442.96	1.48%	136.95	406.80
Cis-2-butene	0.4528	0.8193	1.1794	-1.3958	0.40%	228.32	435.50	1.32%	134.26	426.79	1.40%	134.26	391.95
Vinylacetylene	1.6720	0.8480	0.3360	3.1708	4.18%	231.48	454.00	1.39%	173.15	444.92	2.00%	173.15	408.60
Cyclobutane	0.2137	0.8638	2.0678	-2.3922	0.11%	235.06	459.93	1.80%	182.48	450.73	3.12%	182.48	413.94
1,2-difluoroethane	0.8080	0.8640	0.7967	22.5137	1.63%	234.28	445.00	4.02%	215.00	436.10	5.13%	179.60	400.50
HCFO-1233zd(E)	0.5136	0.9352	1.5679	-1.3501	0.86%	237.15	439.60				1.23%	300.00	395.64
HCFO-1224yd(Z)	0.4724	0.9129	1.7702	0.2541	1.32%	300.00	428.69				1.14%	300.00	385.82
Trimethyl silane	1.0052	1.0000	0.6166	-3.3422	0.54%	229.02	432.00	1.35%	137.26	423.36	1.24%	137.26	388.80



## Bibliography

- [1] Electricity – Global Energy Review 2020 – Analysis, IEA. (n.d.). <https://www.iea.org/reports/global-energy-review-2020/electricity> (accessed April 13, 2021).
- [2] Renewable energy | Fact Sheets on the European Union | European Parliament, (n.d.). <https://www.europarl.europa.eu/factsheets/en/sheet/70/renewable-energy> (accessed July 14, 2021).
- [3] Directive (EU) 2018/2001 of the European Parliament and of the Council of 11 December 2018 on the promotion of the use of energy from renewable sources (Text with EEA relevance.), 2018. <http://data.europa.eu/eli/dir/2018/2001/oj/eng> (accessed June 23, 2021).
- [4] O. US EPA, Distributed Generation of Electricity and its Environmental Impacts, US EPA. (2015). <https://www.epa.gov/energy/distributed-generation-electricity-and-its-environmental-impacts> (accessed July 14, 2021).
- [5] Share of energy consumption from renewable sources in Europe — European Environment Agency, (n.d.). <https://www.eea.europa.eu/data-and-maps/indicators/renewable-gross-final-energy-consumption-5/assessment> (accessed July 16, 2021).
- [6] S. Briola, Plant and method for the supply of electric power and/or mechanical power, heating power and/or cooling power, WO2017158511A1, 2017. <https://patents.google.com/patent/WO2017158511A1/en> (accessed April 13, 2021).
- [7] S. Briola, P. Di Marco, R. Gabbrielli, Thermodynamic sensitivity analysis of a novel trigeneration thermodynamic cycle with two-phase expanders and two-phase compressors, *Energy*. 127 (2017) 335–350. <https://doi.org/10.1016/j.energy.2017.03.135>.
- [8] R.G. Mokadam, Cooling apparatus and process, US3621667A, 1971. <https://patents.google.com/patent/US3621667A/en> (accessed April 13, 2021).
- [9] G. Fabris, Rotating single cycle two-phase thermally activated heat pump, (1993). <https://www.osti.gov/biblio/6408044> (accessed April 13, 2021).
- [10] D. Maraver, J. Royo, V. Lemort, S. Quoilin, Systematic optimization of subcritical and transcritical organic Rankine cycles (ORCs) constrained by technical parameters in multiple applications, *Appl. Energy*. 117 (2014) 11–29. <https://doi.org/10.1016/j.apenergy.2013.11.076>.
- [11] X. Hong, F. Shi, Comparative Analysis of Small-Scale Integrated Solar ORC-Absorption Based Cogeneration Systems, *Energies*. 13 (2020) 946. <https://doi.org/10.3390/en13040946>.
- [12] F.A. Al-Sulaiman, I. Dincer, F. Hamdullahpur, Exergy modeling of a new solar driven trigeneration system, *Sol. Energy*. 85 (2011) 2228–2243. <https://doi.org/10.1016/j.solener.2011.06.009>.
- [13] Y. Huang, Y.D. Wang, S. Rezvani, D.R. McIlveen-Wright, M. Anderson, J. Mondol, A. Zacharopoulos, N.J. Hewitt, A techno-economic assessment of biomass fuelled trigeneration system integrated with organic Rankine cycle, *Appl. Therm. Eng.* 53 (2013) 325–331. <https://doi.org/10.1016/j.applthermaleng.2012.03.041>.
- [14] S. Briola, R. Gabbrielli, A. Fino, A. Bischi, P. Di Marco, Working fluid selection and extensive sensitivity analysis for the thermodynamic optimization of a novel trigeneration cycle with two-phase expanders and compressors, *Energy*. 179 (2019) 709–726. <https://doi.org/10.1016/j.energy.2019.05.051>.
- [15] J.M. Prausnitz, R.N. Lichtenthaler, E.G. de Azevedo, *Molecular Thermodynamics of Fluid-Phase Equilibria*, Pearson Education, 1998.
- [16] B.E. Poling, J.M. Prausnitz, J.P. O’Connell, *The Properties of Gases and Liquids*, 5th ed., McGraw-Hill, New York, 2001.
- [17] M.L. Michelsen, J.M. Mollerup, *Thermodynamic models: fundamentals & computational aspects*, 2. ed, Tie-Line Publications, Holte, 2007.
- [18] J.-N. Jaubert, R. Privat, *Thermodynamic Models for Chemical Processes.*, ISTE Press LTD - ELSEVIER, London, 2021. <https://doi.org/10.1016/C2016-0-01224-X>.
- [19] J.W. Gibbs, On the Equilibrium of Heterogeneous Substances, *Transactions of the Connecticut Academy of Sciences*. 3 (1876) 108–248.
- [20] P.D. Ting, P.C. Joyce, P.K. Jog, W.G. Chapman, M.C. Thies, Phase equilibrium modeling of mixtures of long-chain and short-chain alkanes using Peng–Robinson and SAFT, *Fluid Phase Equilibria*. 206 (2003) 267–286. [https://doi.org/10.1016/S0378-3812\(03\)00003-7](https://doi.org/10.1016/S0378-3812(03)00003-7).
- [21] P.D. Ting, P.C. Joyce, P.K. Jog, W.G. Chapman, M.C. Thies, Corrigendum to “Phase equilibrium modeling of mixtures of long-chain and short-chain alkanes using Peng–Robinson and SAFT” [*Fluid Phase Equilibria* 206 (2003) 267–286], *Fluid Phase Equilibria*. 209 (2003) 309. [https://doi.org/10.1016/S0378-3812\(03\)00242-5](https://doi.org/10.1016/S0378-3812(03)00242-5).
- [22] L. Sun, H. Zhao, C. McCabe, Predicting the phase equilibria of petroleum fluids with the SAFT-VR approach, *AIChE J.* 53 (2007) 720–731. <https://doi.org/10.1002/aic.11110>.

- [23] F.M. Vargas, D.L. Gonzalez, G.J. Hirasaki, W.G. Chapman, Modeling asphaltene phase behavior in crude oil systems using the perturbed chain form of the statistical associating fluid theory (PC-SAFT) equation of state, *Energy Fuels*. 23 (2009) 1140–1146. <https://doi.org/10.1021/ef8006678>.
- [24] S.R. Panuganti, M. Tavakkoli, F.M. Vargas, D.L. Gonzalez, W.G. Chapman, SAFT model for upstream asphaltene applications, *Fluid Phase Equilibria*. 359 (2013) 2–16. <https://doi.org/10.1016/j.fluid.2013.05.010>.
- [25] X. Liang, W. Yan, K. Thomsen, G.M. Kontogeorgis, On petroleum fluid characterization with the PC-SAFT equation of state, *Fluid Phase Equilibria*. 375 (2014) 254–268. <https://doi.org/10.1016/j.fluid.2014.05.005>.
- [26] W. Yan, F. Varzandeh, E.H. Stenby, PVT modeling of reservoir fluids using PC-SAFT EoS and Soave-BWR EoS, *Fluid Phase Equilibria*. 386 (2015) 96–124. <https://doi.org/10.1016/j.fluid.2014.11.022>.
- [27] X. Liang, W. Yan, K. Thomsen, G.M. Kontogeorgis, Modeling the liquid–liquid equilibrium of petroleum fluid and polar compounds containing systems with the PC-SAFT equation of state, *Fluid Phase Equilibria*. 406 (2015) 147–155. <https://doi.org/10.1016/j.fluid.2015.07.042>.
- [28] F. Varzandeh, E.H. Stenby, W. Yan, General approach to characterizing reservoir fluids for EoS models using a large PVT database, *Fluid Phase Equilibria*. 433 (2017) 97–111. <https://doi.org/10.1016/j.fluid.2016.10.018>.
- [29] M.S. Wertheim, Fluids with highly directional attractive forces. I. Statistical thermodynamics, *J. Stat. Phys.* 35 (1984) 19–34. <https://doi.org/10.1007/BF01017362>.
- [30] M.S. Wertheim, Fluids with highly directional attractive forces. II. Thermodynamic perturbation theory and integral equations, *J. Stat. Phys.* 35 (1984) 35–47. <https://doi.org/10.1007/BF01017363>.
- [31] M.S. Wertheim, Fluids with highly directional attractive forces. III. Multiple attraction sites, *J. Stat. Phys.* 42 (1986) 459–476. <https://doi.org/10.1007/BF01127721>.
- [32] M.S. Wertheim, Fluids with highly directional attractive forces. IV. Equilibrium polymerization, *J. Stat. Phys.* 42 (1986) 477–492. <https://doi.org/10.1007/BF01127722>.
- [33] M.S. Wertheim, Fluids of dimerizing hard spheres, and fluid mixtures of hard spheres and dispheres, *J. Chem. Phys.* 85 (1986) 2929–2936. <https://doi.org/10.1063/1.451002>.
- [34] W.G. Chapman, G. Jackson, K.E. Gubbins, Phase equilibria of associating fluids: chain molecules with multiple bonding sites, *Mol. Phys.* 65 (1988) 1057–1079. <https://doi.org/10.1080/00268978800101601>.
- [35] W.G. Chapman, K.E. Gubbins, G. Jackson, M. Radosz, New reference equation of state for associating liquids, *Ind. Eng. Chem. Res.* 29 (1990) 1709–1721. <https://doi.org/10.1021/ie00104a021>.
- [36] S.H. Huang, M. Radosz, Equation of state for small, large, polydisperse, and associating molecules, *Ind. Eng. Chem. Res.* 29 (1990) 2284–2294. <https://doi.org/10.1021/ie00107a014>.
- [37] S.H. Huang, M. Radosz, Equation of state for small, large, polydisperse, and associating molecules: extension to fluid mixtures, *Ind. Eng. Chem. Res.* 30 (1991) 1994–2005. <https://doi.org/10.1021/ie00056a050>.
- [38] J.-N. Jaubert, R. Privat, E. Voutsas, Phase Behavior of Natural Gas Systems, in: *Handb. Nat. Gas Transm. Process.*, Elsevier, 2019: pp. 37–101. <https://linkinghub.elsevier.com/retrieve/pii/B9780128158173000022> (accessed November 24, 2018).
- [39] N.F. Carnahan, K.E. Starling, Equation of state for nonattracting rigid spheres, *J. Chem. Phys.* 51 (1969) 635–636. <https://doi.org/10.1063/1.1672048>.
- [40] G.A. Mansoori, N.F. Carnahan, K.E. Starling, T.W. Leland, Equilibrium thermodynamic properties of the mixture of hard spheres, *J. Chem. Phys.* 54 (1971) 1523–1525. <https://doi.org/10.1063/1.1675048>.
- [41] I.G. Economou, Statistical associating fluid theory: a successful model for the calculation of thermodynamic and phase equilibrium properties of complex fluid mixtures, *Ind. Eng. Chem. Res.* 41 (2002) 953–962. <https://doi.org/10.1021/ie0102201>.
- [42] G.M. Kontogeorgis, G.K. Folas, *Thermodynamic models for industrial applications*, John Wiley & Sons, Ltd, Chichester, UK, 2010. <https://doi.org/10.1002/9780470747537>.
- [43] Y.-H. Fu, S.I. Sandler, A simplified SAFT equation of state for associating compounds and mixtures, *Ind. Eng. Chem. Res.* 34 (1995) 1897–1909. <https://doi.org/10.1021/ie00044a042>.
- [44] T. Kraska, K.E. Gubbins, Phase equilibria calculations with a modified SAFT equation of state. 1. Pure alkanes, alkanols, and water, *Ind. Eng. Chem. Res.* 35 (1996) 4727–4737. <https://doi.org/10.1021/ie9602320>.
- [45] T. Kraska, K.E. Gubbins, Phase equilibria calculations with a modified SAFT equation of state. 2. Binary mixtures of *n*-alkanes, 1-alkanols, and water, *Ind. Eng. Chem. Res.* 35 (1996) 4738–4746. <https://doi.org/10.1021/ie960233s>.
- [46] F.J. Blas, L.F. Vega, Prediction of binary and ternary diagrams using the statistical associating fluid theory (SAFT) equation of state, *Ind. Eng. Chem. Res.* 37 (1998) 660–674. <https://doi.org/10.1021/ie970449+>.

- [47] A. Gil-Villegas, A. Galindo, P.J. Whitehead, S.J. Mills, G. Jackson, A.N. Burgess, Statistical associating fluid theory for chain molecules with attractive potentials of variable range, *J. Chem. Phys.* 106 (1997) 4168–4186. <https://doi.org/10.1063/1.473101>.
- [48] T. Lafitte, D. Bessieres, M.M. Piñeiro, J.-L. Daridon, Simultaneous estimation of phase behavior and second-derivative properties using the statistical associating fluid theory with variable range approach, *J. Chem. Phys.* 124 (2006) 024509. <https://doi.org/10.1063/1.2140276>.
- [49] T. Lafitte, M.M. Piñeiro, J.-L. Daridon, D. Bessières, A Comprehensive Description of Chemical Association Effects on Second Derivative Properties of Alcohols through a SAFT-VR Approach, *J. Phys. Chem. B.* 111 (2007) 3447–3461. <https://doi.org/10.1021/jp0682208>.
- [50] J. Gross, G. Sadowski, Perturbed-chain SAFT: an equation of state based on a perturbation theory for chain molecules, *Ind. Eng. Chem. Res.* 40 (2001) 1244–1260. <https://doi.org/10.1021/ie0003887>.
- [51] J. Gross, G. Sadowski, Application of the perturbed-chain SAFT equation of state to associating systems, *Ind. Eng. Chem. Res.* 41 (2002) 5510–5515. <https://doi.org/10.1021/ie010954d>.
- [52] M. Margules, Über die Zusammensetzung der gesättigten Dämpfe von Mischungen, 104 (1895) 1243–1278.
- [53] O. Redlich, A.T. Kister, Algebraic representation of thermodynamic properties and the classification of solutions, *Ind. Eng. Chem.* 40 (1948) 345–348. <https://doi.org/10.1021/ie50458a036>.
- [54] J.J. van Laar, Zur Theorie der Dampfspannungen von binären Gemischen, *Z. Für Phys. Chem.* 83U (1913) 599–608. <https://doi.org/10.1515/zpch-1913-8342>.
- [55] G. Scatchard, Equilibria in non-electrolyte solutions in relation to the vapor pressures and densities of the components., *Chem. Rev.* 8 (1931) 321–333. <https://doi.org/10.1021/cr60030a010>.
- [56] J.H. Hildebrand, S.E. Wood, The derivation of equations for regular solutions, *J. Chem. Phys.* 1 (1933) 817–822. <https://doi.org/10.1063/1.1749250>.
- [57] H. Renon, J.M. Prausnitz, Local compositions in thermodynamic excess functions for liquid mixtures, *AIChE J.* 14 (1968) 135–144. <https://doi.org/10.1002/aic.690140124>.
- [58] P.J. Flory, Thermodynamics of high polymer solutions, *J. Chem. Phys.* 10 (1942) 51–61. <https://doi.org/10.1063/1.1723621>.
- [59] M.L. Huggins, Some properties of solutions of long-chain compounds., *J. Phys. Chem.* 46 (1942) 151–158. <https://doi.org/10.1021/j150415a018>.
- [60] G.M. Wilson, Vapor-Liquid Equilibrium. XI. A New Expression for the Excess Free Energy of Mixing, *J. Am. Chem. Soc.* 86 (1964) 127–130. <https://doi.org/10.1021/ja01056a002>.
- [61] D.S. Abrams, J.M. Prausnitz, Statistical thermodynamics of liquid mixtures: A new expression for the excess Gibbs energy of partly or completely miscible systems, *AIChE J.* 21 (1975) 116–128. <https://doi.org/10.1002/aic.690210115>.
- [62] A. Fredenslund, R.L. Jones, J.M. Prausnitz, Group-contribution estimation of activity coefficients in nonideal liquid mixtures, *AIChE J.* 21 (1975) 1086–1099. <https://doi.org/10.1002/aic.690210607>.
- [63] J.D. Van der Waals, On the continuity of the gaseous and liquid states, Leiden, 1873.
- [64] G. Soave, Equilibrium constants from a modified Redlich-Kwong equation of state, *Chem. Eng. Sci.* 27 (1972) 1197–1203. [https://doi.org/10.1016/0009-2509\(72\)80096-4](https://doi.org/10.1016/0009-2509(72)80096-4).
- [65] D.-Y. Peng, D.B. Robinson, A new two-constant equation of state, *Ind. Eng. Chem. Fundam.* 15 (1976) 59–64. <https://doi.org/10.1021/i160057a011>.
- [66] D.B. Robinson, D.-Y. Peng, The characterization of the heptanes and heavier fractions for the GPA Peng–Robinson programs (RR-28), *Res. Rep. GPA.* (1978) 1–36.
- [67] A. Pina-Martinez, R. Privat, J.-N. Jaubert, D.-Y. Peng, Updated versions of the generalized Soave  $\alpha$ -function suitable for the Redlich-Kwong and Peng-Robinson equations of state, *Fluid Phase Equilibria.* 485 (2019) 264–269. <https://doi.org/10.1016/j.fluid.2018.12.007>.
- [68] R. Privat, E. Moine, B. Sirjean, R. Gani, J.-N. Jaubert, Application of the corresponding-state law to the parametrization of statistical associating fluid theory (SAFT)-type models: generation and use of “generalized charts,” *Ind. Eng. Chem. Res.* 58 (2019) 9127–9139. <https://doi.org/10.1021/acs.iecr.8b06083>.
- [69] E. Moine, A. Piña-Martinez, J.-N. Jaubert, B. Sirjean, R. Privat, *I*-PC-SAFT: an Industrialized version of the volume-translated PC-SAFT equation of state for pure components, resulting from experience acquired all through the years on the parameterization of SAFT-type and cubic models, *Ind. Eng. Chem. Res.* 58 (2019) 20815–20827. <https://doi.org/10.1021/acs.iecr.9b04660>.
- [70] J.O. Valderrama, The state of the cubic equations of state, *Ind. Eng. Chem. Res.* 42 (2003) 1603–1618. <https://doi.org/10.1021/ie020447b>.
- [71] E.C. Voutsas, G.D. Pappa, K. Magoulas, D.P. Tassios, Vapor liquid equilibrium modeling of alkane systems with Equations of State: “Simplicity versus complexity,” *Fluid Phase Equilibria.* 240 (2006) 127–139. <https://doi.org/10.1016/j.fluid.2005.12.010>.

- [72] M.F. Alfradique, M. Castier, Critical points of hydrocarbon mixtures with the Peng–Robinson, SAFT, and PC-SAFT equations of state, *Fluid Phase Equilibria*. 257 (2007) 78–101. <https://doi.org/10.1016/j.fluid.2007.05.012>.
- [73] H. Segura, D. Seiltgens, A. Mejía, F. Llovell, L.F. Vega, An accurate direct technique for parameterizing cubic equations of state: Part I. Determining the cohesion temperature function in the low-temperature range, *Fluid Phase Equilibria*. 265 (2008) 66–83. <https://doi.org/10.1016/j.fluid.2008.01.003>.
- [74] F. Llovell, L.F. Vega, D. Seiltgens, A. Mejía, H. Segura, An accurate direct technique for parametrizing cubic equations of state: Part III. Application of a crossover treatment, *Fluid Phase Equilibria*. 264 (2008) 201–210. <https://doi.org/10.1016/j.fluid.2007.11.006>.
- [75] S.B. Kiselev, J.F. Ely, Crossover saft equation of state: application for normal alkanes, *Ind. Eng. Chem. Res.* 38 (1999) 4993–5004. <https://doi.org/10.1021/ie990387i>.
- [76] S.B. Kiselev, J.F. Ely, H. Adidharma, M. Radosz, A crossover equation of state for associating fluids, *Fluid Phase Equilibria*. 183–184 (2001) 53–64. [https://doi.org/10.1016/S0378-3812\(01\)00420-4](https://doi.org/10.1016/S0378-3812(01)00420-4).
- [77] Z.-Q. Hu, J.-C. Yang, Y.-G. Li, Crossover SAFT equation of state for pure supercritical fluids, *Fluid Phase Equilibria*. 205 (2003) 1–15. [https://doi.org/10.1016/S0378-3812\(02\)00091-2](https://doi.org/10.1016/S0378-3812(02)00091-2).
- [78] C. Coquelet, A. Chapoy, D. Richon, Development of a new alpha function for the Peng–Robinson equation of state: comparative study of alpha function models for pure gases (natural gas components) and water-gas systems, *Int. J. Thermophys.* 25 (2004) 133–158. <https://doi.org/10.1023/B:IJOT.0000022331.46865.2f>.
- [79] M.A. Trebble, P.R. Bishnoi, Development of a new four-parameter cubic equation of state, *Fluid Phase Equilib.* 35 (1987) 1–18.
- [80] C.H. Twu, J.E. Coon, J.R. Cunningham, A new generalized alpha function for a cubic equation of state. Part 1: Peng-Robinson equation, *Fluid Phase Equilibria*. 105 (1995) 49–59. [https://doi.org/10.1016/0378-3812\(94\)02601-V](https://doi.org/10.1016/0378-3812(94)02601-V).
- [81] C.H. Twu, J.E. Coon, J.R. Cunningham, A new generalized alpha function for a cubic equation of state. Part 2: Redlich-Kwong equation, *Fluid Phase Equilibria*. 105 (1995) 61–69. [https://doi.org/10.1016/0378-3812\(94\)02602-W](https://doi.org/10.1016/0378-3812(94)02602-W).
- [82] G. Soave, Improvement of the Van Der Waals equation of state, *Chem. Eng. Sci.* 39 (1984) 357–369. [https://doi.org/10.1016/0009-2509\(84\)80034-2](https://doi.org/10.1016/0009-2509(84)80034-2).
- [83] C.H. Twu, A Modified Redlich-Kwong Equation of State for Highly Polar, supercritical Systems, in: *Proc. Int. Symp. Thermodyn. Chem. Eng. Ind.*, 1988: p. 148.
- [84] G.A. Melhem, R. Saini, B.M. Goodwin, A modified Peng-Robinson equation of state, *Fluid Phase Equilibria*. 47 (1989) 189–237. [https://doi.org/10.1016/0378-3812\(89\)80176-1](https://doi.org/10.1016/0378-3812(89)80176-1).
- [85] R.M. Gibbons, A.P. Laughton, An equation of state for polar and non-polar substances and mixtures, *J. Chem. Soc. Faraday Trans. 2.* 80 (1984) 1019. <https://doi.org/10.1039/f29848001019>.
- [86] C.H. Twu, D. Bluck, J.R. Cunningham, J.E. Coon, A cubic equation of state with a new alpha function and a new mixing rule, *Fluid Phase Equilibria*. 69 (1991) 33–50. [https://doi.org/10.1016/0378-3812\(91\)90024-2](https://doi.org/10.1016/0378-3812(91)90024-2).
- [87] J.L. Daridon, B. Lagourette, H. Saint-Guirons, P. Xans, A cubic equation of state model for phase equilibrium calculation of alkane + carbon dioxide + water using a group contribution kij, *Fluid Phase Equilibria*. 91 (1993) 31–54. [https://doi.org/10.1016/0378-3812\(93\)85077-Y](https://doi.org/10.1016/0378-3812(93)85077-Y).
- [88] R. Stryjek, J.H. Vera, PRSV: an improved Peng-Robinson equation of state for pure compounds and mixtures, *Can. J. Chem. Eng.* 64 (1986) 323–333. <https://doi.org/10.1002/cjce.5450640224>.
- [89] J.F. Boston, P.M. Mathias, Phase equilibria in a third-generation process simulator, in: *Proc. 2nd Int. Conf. Phase Equilibria Fluid Prop. Chem. Process Ind.*, West Berlin, 1980: pp. 17–21.
- [90] P.M. Mathias, T.W. Copeman, Extension of the Peng-Robinson equation of state to complex mixtures: evaluation of the various forms of the local composition concept, *Fluid Phase Equilibria*. 13 (1983) 91–108. [https://doi.org/10.1016/0378-3812\(83\)80084-3](https://doi.org/10.1016/0378-3812(83)80084-3).
- [91] P.M. Mathias, A versatile phase equilibrium equation of state, *Ind. Eng. Chem. Process Des. Dev.* 22 (1983) 385–391. <https://doi.org/10.1021/i200022a008>.
- [92] A. Pénélox, E. Rauzy, R. Freze, A consistent correction for Redlich-Kwong-Soave volumes, *Fluid Phase Equilibria*. 8 (1982) 7–23. [https://doi.org/10.1016/0378-3812\(82\)80002-2](https://doi.org/10.1016/0378-3812(82)80002-2).
- [93] Y. Le Guennec, S. Lasala, R. Privat, J.-N. Jaubert, A consistency test for  $\alpha$ -functions of cubic equations of state, *Fluid Phase Equilibria*. 427 (2016) 513–538. <https://doi.org/10.1016/j.fluid.2016.07.026>.
- [94] Y. Le Guennec, R. Privat, J.-N. Jaubert, Development of the translated-consistent  $tc$ -PR and  $tc$ -RK cubic equations of state for a safe and accurate prediction of volumetric, energetic and saturation properties of pure compounds in the sub- and super-critical domains, *Fluid Phase Equilibria*. 429 (2016) 301–312. <https://doi.org/10.1016/j.fluid.2016.09.003>.

- [95] J.-N. Jaubert, R. Privat, Y. Le Guennec, L. Coniglio, Note on the properties altered by application of a Pénélox-type volume translation to an equation of state, *Fluid Phase Equilibria*. 419 (2016) 88–95. <https://doi.org/10.1016/j.fluid.2016.03.012>.
- [96] Y. Le Guennec, R. Privat, J.-N. Jaubert, Development of the translated-consistent tc-PR and tc-RK cubic equations of state for a safe and accurate prediction of volumetric, energetic and saturation properties of pure compounds in the sub- and super-critical domains, *Fluid Phase Equilibria*. 429 (2016) 301–312. <https://doi.org/10.1016/j.fluid.2016.09.003>.
- [97] P.L. Chueh, J.M. Prausnitz, Vapor-liquid equilibria at high pressures: Calculation of partial molar volumes in nonpolar liquid mixtures, *AIChE J.* 13 (1967) 1099–1107. <https://doi.org/10.1002/aic.690130612>.
- [98] G. Gao, J.-L. Daridon, H. Saint-Guirons, P. Xans, F. Montel, A simple correlation to evaluate binary interaction parameters of the Peng-Robinson equation of state: binary light hydrocarbon systems, *Fluid Phase Equilibria*. 74 (1992) 85–93. [https://doi.org/10.1016/0378-3812\(92\)85054-C](https://doi.org/10.1016/0378-3812(92)85054-C).
- [99] R. Stryjek, Correlation and prediction of VLE data for n-alkane mixtures, *Fluid Phase Equilibria*. 56 (1990) 141–152. [https://doi.org/10.1016/0378-3812\(90\)85099-V](https://doi.org/10.1016/0378-3812(90)85099-V).
- [100] A. Kordas, K. Magoulas, S. Stamataki, D. Tassios, Methane hydrocarbon interaction parameters correlation for the Peng-Robinson and the t-mPR equation of state, *Fluid Phase Equilibria*. 112 (1995) 33–44. [https://doi.org/10.1016/0378-3812\(95\)02787-F](https://doi.org/10.1016/0378-3812(95)02787-F).
- [101] J.O. Valderrama, A.A. Ibrahim, L.A. Cisternas, Temperature-dependent interaction parameters in cubic equations of state for nitrogen-containing mixtures, *Fluid Phase Equilibria*. 59 (1990) 195–205. [https://doi.org/10.1016/0378-3812\(90\)85034-8](https://doi.org/10.1016/0378-3812(90)85034-8).
- [102] J.O. Valderrama, P.F. Arce, A.A. Ibrahim, Vapour-liquid equilibrium of H<sub>2</sub>S-hydrocarbon mixtures using a generalized cubic equation of state, *Can. J. Chem. Eng.* 77 (1999) 1239–1243. <https://doi.org/10.1002/cjce.5450770622>.
- [103] D. Peng, D. Robinson, A New Two-Constant Equation of State, *Ind. Eng. Chem. Fundam.* 15 (1976) 59–64. <https://doi.org/10.1021/i160057a011>.
- [104] S.J. Han, H.M. Lin, K.C. Chao, Vapor-liquid equilibrium of molecular fluid mixtures by equation of state, *Chem. Eng. Sci.* 43 (1988) 2327–2367. [https://doi.org/10.1016/0009-2509\(88\)85170-4](https://doi.org/10.1016/0009-2509(88)85170-4).
- [105] G. Soave, Improvement of the van der Waals Equation of State, *Chem. Eng. Sci.* 39 (1984) 357–369.
- [106] N.G. Voros, D.P. Tassios, Vapor-liquid equilibria in nonpolar/weakly polar systems with different types of mixing rules, *Fluid Phase Equilibria*. 91 (1993) 1–29. [https://doi.org/10.1016/0378-3812\(93\)85076-X](https://doi.org/10.1016/0378-3812(93)85076-X).
- [107] A. Anderko, Equation-of-state methods for the modelling of phase equilibria, *Fluid Phase Equilibria*. 61 (1990) 145–225. [https://doi.org/10.1016/0378-3812\(90\)90011-B](https://doi.org/10.1016/0378-3812(90)90011-B).
- [108] A.Z. Panagiotopoulos, R.C. Reid, New Mixing Rule for Cubic Equations of State for Highly Polar, Asymmetric Systems, in: *Equ. State*, American Chemical Society, 1986: pp. 571–582. <https://doi.org/10.1021/bk-1986-0300.ch028>.
- [109] Y. Adachi, H. Sugie, A new mixing rule—modified conventional mixing rule, *Fluid Phase Equilibria*. 28 (1986) 103–118. [https://doi.org/10.1016/0378-3812\(86\)85072-5](https://doi.org/10.1016/0378-3812(86)85072-5).
- [110] R. Stryjek, J.H. Vera, PRSV: an improved Peng-Robinson equation of state for pure compounds and mixtures, *Can. J. Chem. Eng.* 64 (1986) 323–333. <https://doi.org/10.1002/cjce.5450640224>.
- [111] R. Sandoval, G. Wilczek-Vera, J.H. Vera, Prediction of ternary vapor-liquid equilibria with the PRSV equation of state, *Fluid Phase Equilibria*. 52 (1989) 119–126. [https://doi.org/10.1016/0378-3812\(89\)80318-8](https://doi.org/10.1016/0378-3812(89)80318-8).
- [112] J. Schwartztruber, F. Galivel-Solastiouk, H. Renon, Representation of the vapor-liquid equilibrium of the ternary system carbon dioxide - propane - methanol and its binaries with a cubic equation of state : a new mixing rule, *Fluid Phase Equilibria*. 38 (1987) 217–226. [https://doi.org/10.1016/0378-3812\(87\)85002-1](https://doi.org/10.1016/0378-3812(87)85002-1).
- [113] M.-J. Huron, J. Vidal, New mixing rules in simple equations of state for representing vapour-liquid equilibria of strongly non-ideal mixtures, *Fluid Phase Equilibria*. 3 (1979) 255–271. [https://doi.org/10.1016/0378-3812\(79\)80001-1](https://doi.org/10.1016/0378-3812(79)80001-1).
- [114] J.-N. Jaubert, F. Mutelet, VLE predictions with the Peng-Robinson equation of state and temperature-dependent  $k_{ij}$  calculated through a group contribution method, *Fluid Phase Equilibria*. 224 (2004) 285–304. <https://doi.org/10.1016/j.fluid.2004.06.059>.
- [115] D.S.H. Wong, S.I. Sandler, A theoretically correct mixing rule for cubic equations of state, *AIChE J.* 38 (1992) 671–680. <https://doi.org/10.1002/aic.690380505>.
- [116] M.L. Michelsen, A modified Huron-Vidal mixing rule for cubic equations of state, *Fluid Phase Equilibria*. 60 (1990) 213–219. [https://doi.org/10.1016/0378-3812\(90\)85053-D](https://doi.org/10.1016/0378-3812(90)85053-D).
- [117] T. Holderbaum, J. Gmehling, PSRK: a group contribution equation of state based on UNIFAC, *Fluid Phase Equilibria*. 70 (1991) 251–265. [https://doi.org/10.1016/0378-3812\(91\)85038-V](https://doi.org/10.1016/0378-3812(91)85038-V).

- [118] E. Voutsas, K. Magoulas, D. Tassios, Universal mixing rule for cubic equations of state applicable to symmetric and asymmetric systems: results with the Peng–Robinson equation of state, *Ind. Eng. Chem. Res.* 43 (2004) 6238–6246. <https://doi.org/10.1021/ie049580p>.
- [119] J. Ahlers, J. Gmehling, Development of an universal group contribution equation of state, *Fluid Phase Equilibria*. 191 (2001) 177–188. [https://doi.org/10.1016/S0378-3812\(01\)00626-4](https://doi.org/10.1016/S0378-3812(01)00626-4).
- [120] J. Ahlers, J. Gmehling, Development of a universal group contribution equation of state. 2. Prediction of vapor–liquid equilibria for asymmetric systems, *Ind. Eng. Chem. Res.* 41 (2002) 3489–3498. <https://doi.org/10.1021/ie020047o>.
- [121] J. Chen, K. Fischer, J. Gmehling, Modification of PSRK mixing rules and results for vapor–liquid equilibria, enthalpy of mixing and activity coefficients at infinite dilution, *Fluid Phase Equilibria*. 200 (2002) 411–429. [https://doi.org/10.1016/S0378-3812\(02\)00048-1](https://doi.org/10.1016/S0378-3812(02)00048-1).
- [122] C. Boukouvalas, N. Spiliotis, P. Coutsikos, N. Tzouvaras, D. Tassios, Prediction of vapor-liquid equilibrium with the LCVM model: a linear combination of the Vidal and Michelsen mixing rules coupled with the original UNIFAC and the *t*-mPR equation of state, *Fluid Phase Equilibria*. 92 (1994) 75–106. [https://doi.org/10.1016/0378-3812\(94\)80043-X](https://doi.org/10.1016/0378-3812(94)80043-X).
- [123] S. Dahl, M.L. Michelsen, High-pressure vapor-liquid equilibrium with a UNIFAC-based equation of state, *AIChE J.* 36 (1990) 1829–1836. <https://doi.org/10.1002/aic.690361207>.
- [124] G.M. Kontogeorgis, G.K. Folas, *Thermodynamic models for industrial applications*, John Wiley & Sons, Ltd, Chichester, UK, 2010. <https://doi.org/10.1002/9780470747537>.
- [125] E. Voutsas, K. Magoulas, D. Tassios, Universal mixing rule for cubic equations of state applicable to symmetric and asymmetric systems: results with the Peng–Robinson equation of state, *Ind. Eng. Chem. Res.* 43 (2004) 6238–6246. <https://doi.org/10.1021/ie049580p>.
- [126] D.S.H. Wong, S.I. Sandler, A theoretically correct mixing rule for cubic equations of state, *AIChE J.* 38 (1992) 671–680. <https://doi.org/10.1002/aic.690380505>.
- [127] J.-N. Jaubert, R. Privat, Cubic equations of state: what’s new since Van der Waals? Which future?, in: *ESAT 2012 Plenary Lect.*, Postdam, 2012.
- [128] D.S. Abrams, J.M. Prausnitz, Statistical thermodynamics of liquid mixtures: A new expression for the excess Gibbs energy of partly or completely miscible systems, *AIChE J.* 21 (1975) 116–128. <https://doi.org/10.1002/aic.690210115>.
- [129] J.O. Valderrama, The state of the cubic equations of state, *Ind. Eng. Chem. Res.* 42 (2003) 1603–1618. <https://doi.org/10.1021/ie020447b>.
- [130] J.-N. Jaubert, Y. Le Guennec, A. Piña-Martinez, N. Ramirez-Velez, S. Lasala, B. Schmid, I.K. Nikolaidis, I.G. Economou, R. Privat, Benchmark database containing binary-system-high-quality-certified data for cross-comparing thermodynamic models and assessing their accuracy, *Ind. Eng. Chem. Res.* 59 (2020) 14981–15027. <https://doi.org/10.1021/acs.iecr.0c01734>.
- [131] I.K. Nikolaidis, R. Privat, J.-N. Jaubert, I.G. Economou, Assessment of the PC-SAFT equation of state against a benchmark database of high-quality binary-system data, *Ind. Eng. Chem. Res.* (2021).
- [132] R. Privat, J.-N. Jaubert, Y. Le Guennec, Incorporation of a volume translation in an equation of state for fluid mixtures: which combining rule? Which effect on properties of mixing?, *Fluid Phase Equilibria*. 427 (2016) 414–420. <https://doi.org/10.1016/j.fluid.2016.07.035>.
- [133] I.P. on C. Change, *Safeguarding the Ozone Layer and the Global Climate System: Special Report of the Intergovernmental Panel on Climate Change*, Cambridge University Press, 2005.
- [134] Cogen - COGEN Europe - The European Association for the Promotion of Cogeneration, (n.d.). <https://www.cogeneurope.eu/> (accessed April 13, 2021).
- [135] P. Breeze, Chapter 2 - Electricity Generation and the Environment, in: P. Breeze (Ed.), *Power Gener. Technol.* Third Ed., Newnes, 2019: pp. 15–31. <https://doi.org/10.1016/B978-0-08-102631-1.00002-X>.
- [136] J. Xu, J. Sui, B. Li, M. Yang, Research, development and the prospect of combined cooling, heating, and power systems, *Energy*. 35 (2010) 4361–4367. <https://doi.org/10.1016/j.energy.2009.03.019>.
- [137] D.W. Wu, R.Z. Wang, Combined cooling, heating and power: A review, *Prog. Energy Combust. Sci.* 32 (2006) 459–495. <https://doi.org/10.1016/j.peccs.2006.02.001>.
- [138] A.P. Samudra, N.V. Sahinidis, Optimization-based framework for computer-aided molecular design, *AIChE J.* 59 (2013) 3686–3701. <https://doi.org/https://doi.org/10.1002/aic.14112>.
- [139] Seider Warren, Seader J.D., Lewin Daniel, Widagdo Soemantri, *PRODUCT AND PROCESS DESIGN PRINCIPLES: Synthesis, Analysis, and Evaluation*, 3rd ed., Wiley, 2009.
- [140] G.D. Moggridge, E.L. Cussler, An Introduction to Chemical Product Design, *Chem. Eng. Res. Des.* 78 (2000) 5–11. <https://doi.org/10.1205/026387600527022>.
- [141] R. Gani, Chemical product design: challenges and opportunities, *Comput. Chem. Eng.* 28 (2004) 2441–2457. <https://doi.org/10.1016/j.compchemeng.2004.08.010>.
- [142] L. Zhang, H. Mao, Q. Liu, R. Gani, Chemical product design – recent advances and perspectives, *Curr. Opin. Chem. Eng.* 27 (2020) 22–34. <https://doi.org/10.1016/j.coche.2019.10.005>.

- [143] R. Gani, K. Dam-Johansen, K.M. Ng, Chapter 1 - Chemical Product Design – A Brief Overview, in: K.M. Ng, R. Gani, K. Dam-Johansen (Eds.), *Comput. Aided Chem. Eng.*, Elsevier, 2007: pp. 1–20. [https://doi.org/10.1016/S1570-7946\(07\)80004-6](https://doi.org/10.1016/S1570-7946(07)80004-6).
- [144] M.O. McLinden, A.F. Kazakov, J.S. Brown, P.A. Domanski, A thermodynamic analysis of refrigerants: Possibilities and tradeoffs for Low-GWP refrigerants, *Int. J. Refrig.-Rev. Int. Froid.* 38 (2014) 80–92. <https://doi.org/10.1016/j.ijrefrig.2013.09.032>.
- [145] M. Preißinger, J.A.H. Schwöbel, A. Klamt, D. Brüggemann, Multi-criteria evaluation of several million working fluids for waste heat recovery by means of Organic Rankine Cycle in passenger cars and heavy-duty trucks, *Appl. Energy.* 206 (2017) 887–899. <https://doi.org/10.1016/j.apenergy.2017.08.212>.
- [146] Y. Le Guennec, R. Privat, J.-N. Jaubert, Development of the translated-consistent *tc*-PR and *tc*-RK cubic equations of state for a safe and accurate prediction of volumetric, energetic and saturation properties of pure compounds in the sub- and super-critical domains, *Fluid Phase Equilibria.* 429 (2016) 301–312. <https://doi.org/10.1016/j.fluid.2016.09.003>.
- [147] D.H. Bowskill, U.E. Tropp, S. Gopinath, G. Jackson, A. Galindo, C.S. Adjiman, Beyond a heuristic analysis: integration of process and working-fluid design for organic Rankine cycles, *Mol. Syst. Des. Eng.* 5 (2020) 493–510. <https://doi.org/10.1039/C9ME00089E>.
- [148] S.H. Huang, M. Radosz, Equation of state for small, large, polydisperse, and associating molecules, *Ind. Eng. Chem. Res.* 29 (1990) 2284–2294. <https://doi.org/10.1021/ie00107a014>.
- [149] F.J. Blas, L.F. Vega, Thermodynamic behaviour of homonuclear and heteronuclear Lennard-Jones chains with association sites from simulation and theory, *Mol. Phys.* 92 (1997) 135–150. <https://doi.org/10.1080/002689797170707>.
- [150] F.J. Blas, L.F. Vega, Prediction of binary and ternary diagrams using the statistical associating fluid theory (SAFT) equation of state, *Ind. Eng. Chem. Res.* 37 (1998) 660–674. <https://doi.org/10.1021/ie970449+>.
- [151] A. Gil-Villegas, A. Galindo, P.J. Whitehead, S.J. Mills, G. Jackson, A.N. Burgess, Statistical associating fluid theory for chain molecules with attractive potentials of variable range, *J. Chem. Phys.* 106 (1997) 4168–4186. <https://doi.org/10.1063/1.473101>.
- [152] J. Gross, G. Sadowski, Perturbed-Chain SAFT: An Equation of State Based on a Perturbation Theory for Chain Molecules, *Ind. Eng. Chem. Res.* 40 (2001) 1244–1260. <https://doi.org/10.1021/ie0003887>.
- [153] T. Lafitte, A. Apostolakou, C. Avenaño, A. Galindo, C.S. Adjiman, E.A. Müller, G. Jackson, Accurate statistical associating fluid theory for chain molecules formed from Mie segments, *J. Chem. Phys.* 139 (2013) 154504. <https://doi.org/10.1063/1.4819786>.
- [154] I.K. Nikolaidis, L.F.M. Franco, L.N. Vechot, I.G. Economou, Modeling of physical properties and vapor–liquid equilibrium of ethylene and ethylene mixtures with equations of state, *Fluid Phase Equilibria.* 470 (2018) 149–163. <https://doi.org/10.1016/j.fluid.2018.01.021>.
- [155] O. Pfohl, T. Giese, R. Dohrn, G. Brunner, 1. Comparison of 12 equations of state with respect to gas-extraction processes: reproduction of pure-component properties when enforcing the correct critical temperature and pressure, *Ind. Eng. Chem. Res.* 37 (1998) 2957–2965. <https://doi.org/10.1021/ie970524g>.
- [156] C. McCabe, A. Gil-Villegas, G. Jackson, Predicting the high-pressure phase equilibria of methane + *n*-hexane using the SAFT-VR approach, *J. Phys. Chem. B.* 102 (1998) 4183–4188. <https://doi.org/10.1021/jp980335r>.
- [157] A. Galindo, F.J. Blas, Theoretical examination of the global fluid phase behavior and critical phenomena in carbon dioxide + *n*-alkane binary mixtures, *J. Phys. Chem. B.* 106 (2002) 4503–4515. <https://doi.org/10.1021/jp013402h>.
- [158] F.J. Blas, A. Galindo, Study of the high pressure phase behaviour of CO<sub>2</sub> + *n*-alkane mixtures using the SAFT-VR approach with transferable parameters, *Fluid Phase Equilibria.* 194–197 (2002) 501–509. [https://doi.org/10.1016/S0378-3812\(01\)00651-3](https://doi.org/10.1016/S0378-3812(01)00651-3).
- [159] F.J. Blas, L.F. Vega, Critical behavior and partial miscibility phenomena in binary mixtures of hydrocarbons by the statistical associating fluid theory, *J. Chem. Phys.* 109 (1998) 7405–7413. <https://doi.org/10.1063/1.477363>.
- [160] J.C. Pàmies, L.F. Vega, Vapor–liquid equilibria and critical behavior of heavy *n*-alkanes using transferable parameters from the soft-saft equation of state, *Ind. Eng. Chem. Res.* 40 (2001) 2532–2543. <https://doi.org/10.1021/ie000944x>.
- [161] M. Cismondi, E.A. Brignole, J. Mollerup, Rescaling of three-parameter equations of state: PC-SAFT and SPHCT, *Fluid Phase Equilibria.* 234 (2005) 108–121. <https://doi.org/10.1016/j.fluid.2005.06.002>.
- [162] A. Bouza, C.M. Colina, C.G. Olivera-Fuentes, Parameterization of molecular-based equations of state, *Fluid Phase Equilibria.* 228–229 (2005) 561–575. <https://doi.org/10.1016/j.fluid.2004.08.043>.

- [163] A.P.C.M. Vinhal, W. Yan, G.M. Kontogeorgis, Evaluation of equations of state for simultaneous representation of phase equilibrium and critical phenomena, *Fluid Phase Equilibria*. 437 (2017) 140–154. <https://doi.org/10.1016/j.fluid.2017.01.011>.
- [164] G.M. Kontogeorgis, E.C. Voutsas, I.V. Yakoumis, D.P. Tassios, An equation of state for associating fluids, *Ind. Eng. Chem. Res.* 35 (1996) 4310–4318. <https://doi.org/10.1021/ie9600203>.
- [165] I.V. Yakoumis, G.M. Kontogeorgis, E.C. Voutsas, D.P. Tassios, Vapor-liquid equilibria for systems using the CPA Equation of state, *Fluid Phase Equilibria*. 130 (1997) 31–47. [https://doi.org/10.1016/S0378-3812\(96\)03200-1](https://doi.org/10.1016/S0378-3812(96)03200-1).
- [166] I.V. Yakoumis, G.M. Kontogeorgis, E.C. Voutsas, E.M. Hendriks, D.P. Tassios, Prediction of phase equilibria in binary aqueous systems containing alkanes, cycloalkanes, and alkenes with the cubic-plus-association equation of state, *Ind. Eng. Chem. Res.* 37 (1998) 4175–4182. <https://doi.org/10.1021/ie970947i>.
- [167] I. Polishuk, Standardized Critical Point-Based Numerical Solution of Statistical Association Fluid Theory Parameters: The Perturbed Chain-Statistical Association Fluid Theory Equation of State Revisited, *Ind. Eng. Chem. Res.* 53 (2014) 14127–14141. <https://doi.org/10.1021/ie502633e>.
- [168] E.B. Postnikov, A.L. Goncharov, N. Cohen, I. Polishuk, Estimating the liquid properties of 1-alkanols from C<sub>5</sub> to C<sub>12</sub> by FT-EoS and CP-PC-SAFT: Simplicity versus complexity, *J. Supercrit. Fluids*. 104 (2015) 193–203. <https://doi.org/10.1016/j.supflu.2015.06.007>.
- [169] H. Lubarsky, I. Polishuk, Implementation of the critical point-based revised PC-SAFT for modelling thermodynamic properties of aromatic and haloaromatic compounds, *J. Supercrit. Fluids*. 97 (2015) 133–144. <https://doi.org/10.1016/j.supflu.2014.10.016>.
- [170] I. Polishuk, Y. Sidik, D. NguyenHuynh, Predicting phase behavior in aqueous systems without fitting binary parameters I: CP-PC-SAFT EOS, aromatic compounds, *AIChE J.* 63 (2017) 4124–4135. <https://doi.org/10.1002/aic.15715>.
- [171] I. Polishuk, Implementation of CP-PC-SAFT for predicting thermodynamic properties and gas solubility in 1-alkyl-3-methylimidazolium bis(trifluoromethylsulfonyl)imide ionic liquids without fitting binary parameters, *Ind. Eng. Chem. Res.* 56 (2017) 7845–7857. <https://doi.org/10.1021/acs.iecr.7b01846>.
- [172] X. Liang, G.M. Kontogeorgis, New Variant of the Universal Constants in the Perturbed Chain-Statistical Associating Fluid Theory Equation of State, *Ind. Eng. Chem. Res.* 54 (2015) 1373–1384. <https://doi.org/10.1021/ie503925h>.
- [173] X. Liang, B. Maribo-Mogensen, K. Thomsen, W. Yan, G.M. Kontogeorgis, Approach to improve speed of sound calculation within PC-SAFT framework, *Ind. Eng. Chem. Res.* 51 (2012) 14903–14914. <https://doi.org/10.1021/ie3018127>.
- [174] X. Liang, K. Thomsen, W. Yan, G.M. Kontogeorgis, Prediction of the vapor–liquid equilibria and speed of sound in binary systems of 1-alkanols and n-alkanes with the simplified PC-SAFT equation of state, *Fluid Phase Equilibria*. 360 (2013) 222–232. <https://doi.org/10.1016/j.fluid.2013.09.037>.
- [175] J.-W. Qian, J.-N. Jaubert, R. Privat, Phase equilibria in hydrogen-containing binary systems modeled with the Peng-Robinson equation of state and temperature-dependent binary interaction parameters calculated through a group-contribution method, *J. Supercrit. Fluids*. 75 (2013) 58–71. <https://doi.org/10.1016/j.supflu.2012.12.014>.
- [176] G. Soave, Equilibrium Constants from a Modified Redlich-Kwong Equation of State, *Chem. Eng. Sci.* 27 (1972) 1197–. [https://doi.org/10.1016/0009-2509\(72\)80096-4](https://doi.org/10.1016/0009-2509(72)80096-4).
- [177] H.G. Rackett, Equation of state for saturated liquids, *J. Chem. Eng. Data*. 15 (1970) 514–517. <https://doi.org/10.1021/je60047a012>.
- [178] R.W. Hankinson, G.H. Thomson, A new correlation for saturated densities of liquids and their mixtures, *AIChE J.* 25 (1979) 653–663. <https://doi.org/10.1002/aic.690250412>.
- [179] E. Hendriks, G.M. Kontogeorgis, R. Dohrn, J.-C. de Hemptinne, I.G. Economou, L.F. Žilnik, V. Vesovic, Industrial Requirements for Thermodynamics and Transport Properties, *Ind. Eng. Chem. Res.* 49 (2010) 11131–11141. <https://doi.org/10.1021/ie101231b>.
- [180] D. Nguyen-Huynh, J.-C. de Hemptinne, R. Lugo, J.-P. Passarello, P. Tobaly, Simultaneous liquid–liquid and vapour–liquid equilibria predictions of selected oxygenated aromatic molecules in mixtures with alkanes, alcohols, water, using the polar GC-PC-SAFT, *Chem. Eng. Res. Des.* 92 (2014) 2912–2935. <https://doi.org/10.1016/j.cherd.2014.05.018>.
- [181] H. Lubarsky, I. Polishuk, D. NguyenHuynh, Implementation of GC-PPC-SAFT and CP-PC-SAFT for predicting thermodynamic properties of mixtures of weakly- and non-associated oxygenated compounds, *J. Supercrit. Fluids*. 115 (2016) 65–78. <https://doi.org/10.1016/j.supflu.2016.04.013>.
- [182] H. Lubarsky, I. Polishuk, D. NguyenHuynh, The group contribution method (GC) versus the critical point-based approach (CP): predicting thermodynamic properties of weakly- and non-associated oxygenated compounds by GC-PPC-SAFT and CP-PC-SAFT, *J. Supercrit. Fluids*. 110 (2016) 11–21. <https://doi.org/10.1016/j.supflu.2015.12.007>.

- [183] J.-N. Jaubert, R. Privat, Y. Le Guennec, L. Coniglio, Note on the properties altered by application of a Pénélox-type volume translation to an equation of state, *Fluid Phase Equilibria*. 419 (2016) 88–95. <https://doi.org/10.1016/j.fluid.2016.03.012>.
- [184] A. Pina-Martinez, Y. Le Guennec, R. Privat, J.-N. Jaubert, P.M. Mathias, Analysis of the combinations of property data that are suitable for a safe estimation of consistent Two  $\alpha$ -function parameters: updated parameter values for the translated-consistent  $tc$ -PR and  $tc$ -RK cubic equations of state, *J. Chem. Eng. Data*. 63 (2018) 3980–3988. <https://doi.org/10.1021/acs.jced.8b00640>.
- [185] Y. Le Guennec, R. Privat, J.-N. Jaubert, Development of the translated-consistent  $tc$ -PR and  $tc$ -RK cubic equations of state for a safe and accurate prediction of volumetric, energetic and saturation properties of pure compounds in the sub- and super-critical domains, *Fluid Phase Equilibria*. 429 (2016) 301–312. <https://doi.org/10.1016/j.fluid.2016.09.003>.
- [186] S.S. Chen, A. Kreglewski, Applications of the augmented Van der Waals theory of fluids.: I. Pure fluids, *Berichte Bunsenges. Für Phys. Chem.* 81 (1977) 1048–1052. <https://doi.org/10.1002/bbpc.19770811037>.
- [187] N.C. Patel, A.S. Teja, A new cubic equation of state for fluids and fluid mixtures, *Chem. Eng. Sci.* 37 (1982) 463–473. [https://doi.org/10.1016/0009-2509\(82\)80099-7](https://doi.org/10.1016/0009-2509(82)80099-7).
- [188] M. Cismondi, J. Mollerup, Development and application of a three-parameter RK–PR equation of state, *Fluid Phase Equilibria*. 232 (2005) 74–89. <https://doi.org/10.1016/j.fluid.2005.03.020>.
- [189] H.W. Xiang, Vapor pressures from a corresponding-states principle for a wide range of polar molecular substances, *Int. J. Thermophys.* 22 (2001) 919–932. <https://doi.org/10.1023/A:1010787302081>.
- [190] H.W. Xiang, The new simple extended corresponding-states principle: vapor pressure and second virial coefficient, *Chem. Eng. Sci.* 57 (2002) 1439–1449. [https://doi.org/10.1016/S0009-2509\(02\)00017-9](https://doi.org/10.1016/S0009-2509(02)00017-9).
- [191] T.W. Leland, P.S. Chapplear, The corresponding states principle - A review of current theory and practice, *Ind. Eng. Chem.* 60 (1968) 15–43. <https://doi.org/10.1021/ie50703a005>.
- [192] W.V. Wilding, R.L. Rowley, A four-parameter corresponding-states method for the prediction of thermodynamic properties of polar and nonpolar fluids, *Int. J. Thermophys.* 7 (1986) 525–539. <https://doi.org/10.1007/BF00502387>.
- [193] W.V. Wilding, J.K. Johnson, R.L. Rowley, Thermodynamic properties and vapor pressures of polar fluids from a four-parameter corresponding-states method, *Int. J. Thermophys.* 8 (1987) 717–735. <https://doi.org/10.1007/BF00500790>.
- [194] C.A. Passut, R.P. Danner, Development of a four-parameter corresponding states method: vapor pressure prediction, *AIChE Symp. Ser.* 70 (1974) 30–36.
- [195] J.O. Valderrama, L.A. Cisternas, On the choice of a third (and fourth) generalizing parameter for equations of state, *Chem. Eng. Sci.* 42 (1987) 2957–2961. [https://doi.org/10.1016/0009-2509\(87\)87061-6](https://doi.org/10.1016/0009-2509(87)87061-6).
- [196] G.Z.A. Wu, L.I. Stiel, A generalized equation of state for the thermodynamic properties of polar fluids, *AIChE J.* 31 (1985) 1632–1644. <https://doi.org/10.1002/aic.690311007>.
- [197] J.O. Hirschfelder, R.J. Buehler, H.A. McGee, J.R. Sutton, Generalized equation of state for gases and liquids, *Ind. Eng. Chem.* 50 (1958) 375–385. <https://doi.org/10.1021/ie50579a039>.
- [198] Y. Le Guennec, S. Lasala, R. Privat, J.-N. Jaubert, A consistency test for  $\alpha$ -functions of cubic equations of state, *Fluid Phase Equilibria*. 427 (2016) 513–538. <https://doi.org/10.1016/j.fluid.2016.07.026>.
- [199] Y. Le Guennec, R. Privat, S. Lasala, J.-N. Jaubert, On the imperative need to use a consistent  $\alpha$ -function for the prediction of pure-compound supercritical properties with a cubic equation of state, *Fluid Phase Equilibria*. 445 (2017) 45–53. <https://doi.org/10.1016/j.fluid.2017.04.015>.
- [200] A.M. Palma, A.J. Queimada, J.A.P. Coutinho, Using a volume shift in perturbed-chain statistical associating fluid theory to improve the description of speed of sound and other derivative properties, *Ind. Eng. Chem. Res.* 57 (2018) 11804–11814. <https://doi.org/10.1021/acs.iecr.8b02646>.
- [201] C. McCabe, S.B. Kiselev, Application of crossover theory to the SAFT-VR equation of state: SAFT-VRX for pure fluids, *Ind. Eng. Chem. Res.* 43 (2004) 2839–2851. <https://doi.org/10.1021/ie034288n>.
- [202] M. Ewing, A.R. Goodwin, J.P. Trusler, Thermophysical properties of alkanes from speeds of sound determined using a spherical resonator 3. n-Pentane, *J. Chem. Thermodyn.* 21 (1989) 867–877. [https://doi.org/10.1016/0021-9614\(89\)90035-9](https://doi.org/10.1016/0021-9614(89)90035-9).
- [203] B.A. Belinskii, S.K. Ikramov, Comprehensive investigation of the acoustical parameters, viscosity, and density of n-pentane over a wide pressure interval, *Sov. Phys.-Acoust.* 18 (1973) 300–303.
- [204] Z.S. Ding, J. Alliez, C. Boned, P. Xans, Automation of an ultrasound velocity measurement system in high-pressure liquids, *Meas. Sci. Technol.* 8 (1997) 154–161. <https://doi.org/10.1088/0957-0233/8/2/007>.
- [205] R.G. Ismagilov, G.V. Ermakov, Speed of sound in superheated organic liquids, *Teplofiz. Vysok. Temp.* 20 (1982) 677–682.
- [206] B.S. Kir'yakov, N.F. Otpushchennikov, Dependence of speed of sound on pressure in liquid, *Ultrazvuk Fiz.-Him. Svoisva Veshecha*. (1971) 104–112.

- [207] A. Lainez, J.A. Zollweg, W.B. Streett, Speed-of-sound measurements for liquid n-pentane and 2,2-dimethylpropane under pressure, *J. Chem. Thermodyn.* 22 (1990) 937–948. [https://doi.org/10.1016/0021-9614\(90\)90183-Q](https://doi.org/10.1016/0021-9614(90)90183-Q).
- [208] B. Orge, M. Iglesias, A. Rodríguez, J.M. Canosa, J. Tojo, Mixing properties of (methanol, ethanol, or 1-propanol) with (n-pentane, n-hexane, n-heptane and n-octane) at 298.15 K, *Fluid Phase Equilibria.* 133 (1997) 213–227. [https://doi.org/10.1016/S0378-3812\(97\)00031-9](https://doi.org/10.1016/S0378-3812(97)00031-9).
- [209] N.F. Otpushchennikov, B.S. Kir'yakov, P.P. Panin, Velocity of sound and some thermodynamic properties of liquid n-pentane in a wide range of temperatures and pressures, *Izv Vyssh Uchebn Zaved Neft Gaz.* 17 (1974) 73–77.
- [210] E.G. Richardson, The rheology of transitions, *Rheol. Acta.* 1 (1958) 251–257.
- [211] E.G. Richardson, R.I. Tait, Ratios of specific heat and high-frequency viscosities in organic liquids under pressure, derived from ultrasonic propagation, *Philos. Mag.* 2 (1957) 441–454. <https://doi.org/10.1080/14786435708243834>.
- [212] J.C. Swanson, Pressure coefficients of acoustic velocity for nine organic liquids, *J. Chem. Phys.* 2 (1934) 689–693. <https://doi.org/10.1063/1.1749375>.
- [213] H. Tahani, Determination of the velocity of sound in reservoir fluids using an equation of state, Heriot-Watt University, 2011.
- [214] V.V. Zotov, Y.F. Melikhov, G.A. Mel'nikov, Y.A. Neruchev, Sound velocity in liquid hydrocarbons, *Skorost Zvuka V Zhidkikh Uglevodorodakh.* (1995).
- [215] V.N. Verveiko, G.A. Mel'nikov, N.F. Otpushchennikov, Experimental installation for measurements of speed and absorption of ultrasonic waves in liquids in a wide interval of temperatures and pressure to 8000 atmospheres, *Ultrazvuk Termodin Svoistva Veshchestva.* (1986) 59–74.
- [216] C.H. Twu, D. Bluck, J.R. Cunningham, J.E. Coon, A cubic equation of state with a new alpha function and a new mixing rule, *Fluid Phase Equilibria.* 69 (1991) 33–50. [https://doi.org/10.1016/0378-3812\(91\)90024-2](https://doi.org/10.1016/0378-3812(91)90024-2).
- [217] B.E. Poling, J.M. Prausnitz, J.P. O'Connell, *The properties of gases and liquids*, 5th ed, McGraw-Hill, New York, 2001.
- [218] Y. Le Guennec, S. Lasala, R. Privat, J.-N. Jaubert, A consistency test for  $\alpha$ -functions of cubic equations of state, *Fluid Phase Equilibria.* 427 (2016) 513–538. <https://doi.org/10.1016/j.fluid.2016.07.026>.
- [219] Y. Le Guennec, R. Privat, S. Lasala, J.-N. Jaubert, On the imperative need to use a consistent  $\alpha$ -function for the prediction of pure-compound supercritical properties with a cubic equation of state, *Fluid Phase Equilibria.* 445 (2017) 45–53. <https://doi.org/10.1016/j.fluid.2017.04.015>.
- [220] C.H. Twu, D. Bluck, J.R. Cunningham, J.E. Coon, A cubic equation of state with a new alpha function and a new mixing rule, *Fluid Phase Equilibria.* 69 (1991) 33–50. [https://doi.org/10.1016/0378-3812\(91\)90024-2](https://doi.org/10.1016/0378-3812(91)90024-2).
- [221] J.-N. Jaubert, R. Privat, Y. Le Guennec, L. Coniglio, Note on the properties altered by application of a Pénélox-type volume translation to an equation of state, *Fluid Phase Equilibria.* 419 (2016) 88–95. <https://doi.org/10.1016/j.fluid.2016.03.012>.
- [222] R. Privat, J.-N. Jaubert, Y. Le Guennec, Incorporation of a volume translation in an equation of state for fluid mixtures: which combining rule? which effect on properties of mixing?, *Fluid Phase Equilibria.* 427 (2016) 414–420. <https://doi.org/10.1016/j.fluid.2016.07.035>.
- [223] A. Pénélox, E. Rauzy, R. Freze, A consistent correction for Redlich-Kwong-Soave volumes, *Fluid Phase Equilibria.* 8 (1982) 7–23. [https://doi.org/10.1016/0378-3812\(82\)80002-2](https://doi.org/10.1016/0378-3812(82)80002-2).
- [224] D.-Y. Peng, D.B. Robinson, A new two-constant equation of state, *Ind. Eng. Chem. Fundam.* 15 (1976) 59–64. <https://doi.org/10.1021/i160057a011>.
- [225] O. Redlich, J.N.S. Kwong, On the thermodynamics of solutions. V. An equation of state. Fugacities of gaseous solutions, *Chem. Rev.* 44 (1949) 233–244.
- [226] I.H. Bell, M. Satyro, E.W. Lemmon, Consistent Two Parameters for More than 2500 Pure Fluids from Critically Evaluated Experimental Data, *J. Chem. Eng. Data.* (2018). <https://doi.org/10.1021/acs.jced.7b00967>.
- [227] R. Privat, J.-N. Jaubert, Classification of global fluid-phase equilibrium behaviors in binary systems, *Chem. Eng. Res. Des.* 91 (2013) 1807–1839. <https://doi.org/10.1016/j.cherd.2013.06.026>.
- [228] J.-W. Qian, R. Privat, J.-N. Jaubert, Predicting the phase equilibria, critical phenomena, and mixing enthalpies of binary aqueous systems containing alkanes, cycloalkanes, aromatics, alkenes, and gases (N<sub>2</sub>, CO<sub>2</sub>, H<sub>2</sub>S, H<sub>2</sub>) with the PPR78 equation of state, *Ind. Eng. Chem. Res.* 52 (2013) 16457–16490. <https://doi.org/10.1021/ie402541h>.
- [229] C.H. Twu, A modified Redlich-Kwong equation of state for highly polar, supercritical systems, in: *Int. Symp. Thermodyn. Chem. Eng. Ind.*, 1988: pp. 148–169.
- [230] H.G. Rackett, Equation of state for saturated liquids, *J. Chem. Eng. Data.* 15 (1970) 514–517. <https://doi.org/10.1021/je60047a012>.

- [231] C.F. Spencer, R.P. Danner, Improved equation for prediction of saturated liquid density, *J. Chem. Eng. Data.* 17 (1972) 236–241. <https://doi.org/10.1021/je60053a012>.
- [232] J.O. Valderrama, The State of the Cubic Equations of State, *Ind. Eng. Chem. Res.* 42 (2003) 1603–1618. <https://doi.org/10.1021/ie020447b>.
- [233] G. Soave, Equilibrium constants from a modified Redlich-Kwong equation of state, *Chem. Eng. Sci.* 27 (1972) 1197–1203. [https://doi.org/10.1016/0009-2509\(72\)80096-4](https://doi.org/10.1016/0009-2509(72)80096-4).
- [234] D. Peng, D. Robinson, A New Two-Constant Equation of State, *Ind. Eng. Chem. Fundam.* 15 (1976) 59–64. <https://doi.org/10.1021/i160057a011>.
- [235] J.S. Lopez-Echeverry, S. Reif-Acherman, E. Araujo-Lopez, Peng-Robinson equation of state: 40 years through cubics, *Fluid Phase Equilibria.* 447 (2017) 39–71. <https://doi.org/10.1016/j.fluid.2017.05.007>.
- [236] F. Yang, Q. Liu, Y. Duan, Z. Yang, On the temperature dependence of the  $\alpha$  function in the cubic equation of state, *Chem. Eng. Sci.* 192 (2018) 565–575. <https://doi.org/10.1016/j.ces.2018.08.014>.
- [237] M.S. Graboski, T.E. Daubert, A Modified Soave Equation of State for Phase Equilibrium Calculations. 1. Hydrocarbon Systems, *Ind. Eng. Chem. Process Des. Dev.* 17 (1978) 443–448. <https://doi.org/10.1021/i260068a009>.
- [238] G. Soave, Improving the treatment of heavy hydrocarbons by the SRK EOS, *Fluid Phase Equilibria.* 84 (1993) 339–342. [https://doi.org/10.1016/0378-3812\(93\)85131-5](https://doi.org/10.1016/0378-3812(93)85131-5).
- [239] G. Soave, M. Barolo, A. Bertucco, Estimation of high-pressure fugacity coefficients of pure gaseous fluids by a modified SRK equation of state, *Fluid Phase Equilibria.* 91 (1993) 87–100. [https://doi.org/10.1016/0378-3812\(93\)85081-V](https://doi.org/10.1016/0378-3812(93)85081-V).
- [240] D.B. Robinson, D.-Y. Peng, The characterization of the heptanes and heavier fractions for the GPA Peng–Robinson programs (RR-28), *Res. Rep. GPA.* (1978) 1–36.
- [241] J.-N. Jaubert, F. Mutelet, VLE predictions with the Peng-Robinson equation of state and temperature-dependent  $k_{ij}$  calculated through a group contribution method, *Fluid Phase Equilibria.* 224 (2004) 285–304. <https://doi.org/10.1016/j.fluid.2004.06.059>.
- [242] J.-N. Jaubert, R. Privat, F. Mutelet, Predicting the phase equilibria of synthetic petroleum fluids with the PPR78 approach, *AIChE J.* 56 (2010) 3225–3235. <https://doi.org/10.1002/aic.12232>.
- [243] A. Pina-Martinez, Y. Le Guennec, R. Privat, J.-N. Jaubert, P.M. Mathias, Analysis of the combinations of property data that are suitable for a safe estimation of consistent Two  $\alpha$ -function parameters. Updated parameter values for the translated-consistent  $tc$ -PR and  $tc$ -RK cubic equations of state., *J. Chem. Eng. Data.* (2018) (under review).
- [244] J.-N. Jaubert, R. Privat, Relationship between the binary interaction parameters ( $k_{ij}$ ) of the Peng-Robinson and those of the Soave-Redlich-Kwong equations of state: application to the definition of the PR2SRK model, *Fluid Phase Equilibria.* 295 (2010) 26–37. <https://doi.org/10.1016/j.fluid.2010.03.037>.
- [245] R. Agarwal, Y.-K. Li, O. Santollani, M.A. Satyro, A. Vieler, Uncovering the realities of simulation. Part II., *Chem. Eng. Prog.* 97 (2001) 64–72.
- [246] G.M. Kontogeorgis, R. Privat, J.-N. Jaubert, Taking another look at the van der waals equation of state—almost 150 years later, *J. Chem. Eng. Data.* (2019). <https://doi.org/10.1021/acs.jced.9b00264>.
- [247] A. Harmens, A cubic equation of state for the prediction of  $N_2$ -Ar- $O_2$  phase equilibrium, *Cryogenics.* 17 (1977) 519–522. [https://doi.org/10.1016/0011-2275\(77\)90146-1](https://doi.org/10.1016/0011-2275(77)90146-1).
- [248] G. Schmidt, H. Wenzel, A modified van der Waals type equation of state, *Chem. Eng. Sci.* 35 (1980) 1503–1512. [https://doi.org/10.1016/0009-2509\(80\)80044-3](https://doi.org/10.1016/0009-2509(80)80044-3).
- [249] A. Harmens, H. Knapp, Three-parameter cubic equation of state for normal substances, *Ind. Eng. Chem. Fundam.* 19 (1980) 291–294. <https://doi.org/10.1021/i160075a010>.
- [250] G.G. Fuller, A modified Redlich-Kwong-Soave equation of state capable of representing the liquid state, *Ind. Eng. Chem. Fundam.* 15 (1976) 254–257. <https://doi.org/10.1021/i160060a005>.
- [251] O. Pfohl, Evaluation of an improved volume translation for the prediction of hydrocarbon volumetric properties, *Fluid Phase Equilibria.* 163 (1999) 157–159. [https://doi.org/10.1016/S0378-3812\(99\)00199-5](https://doi.org/10.1016/S0378-3812(99)00199-5).
- [252] P. Ungerer, H.B. De Sant’Ana, Reply to the letter to the editor by O. Pfohl about the paper “Evaluation of an improved volume translation for the prediction of hydrocarbon volumetric properties” [FPE 154, 193–204 (1999)], *Fluid Phase Equilibria.* 163 (1999) 161–162. [https://doi.org/10.1016/S0378-3812\(99\)00198-3](https://doi.org/10.1016/S0378-3812(99)00198-3).
- [253] V. Kalikhman, D. Kost, I. Polishuk, About the physical validity of attaching the repulsive terms of analytical EOS models by temperature dependencies, *Fluid Phase Equilibria.* 293 (2010) 164–167. <https://doi.org/10.1016/j.fluid.2010.03.003>.
- [254] C.H. Twu, J.E. Coon, J.R. Cunningham, A new cubic equation of state, *Fluid Phase Equilibria.* 75 (1992) 65–79. [https://doi.org/10.1016/0378-3812\(92\)87007-A](https://doi.org/10.1016/0378-3812(92)87007-A).
- [255] R. Clausius, Ueber das verhalten der kohlendäure in bezug auf druck, volumen und temperatur, *Ann. Phys.* 245 (1880) 337–357. <https://doi.org/10.1002/andp.18802450302>.

- [256] H. Segura, D. Seiltgens, A. Mejía, F. Llovel, L.F. Vega, An accurate direct technique for parameterizing cubic equations of state: Part II. Specializing models for predicting vapor pressures and phase densities, *Fluid Phase Equilibria*. 265 (2008) 155–172. <https://doi.org/10.1016/j.fluid.2008.01.013>.
- [257] I. Polishuk, Till which pressures the fluid phase EOS models might stay reliable?, *J. Supercrit. Fluids*. 58 (2011) 204–215. <https://doi.org/10.1016/j.supflu.2011.05.014>.
- [258] I. Polishuk, Addressing the issue of numerical pitfalls characteristic for SAFT EOS models, *Fluid Phase Equilibria*. 301 (2011) 123–129. <https://doi.org/10.1016/j.fluid.2010.11.021>.
- [259] I. Polishuk, Hybridizing SAFT and cubic eos: what can be achieved?, *Ind. Eng. Chem. Res.* 50 (2011) 4183–4198. <https://doi.org/10.1021/ie102420n>.
- [260] P. Watson, M. Cascella, D. May, S. Salerno, D. Tassios, Prediction of vapor pressures and saturated molar volumes with a simple cubic equation of state: Part II: The Van der Waals - 711 EOS, *Fluid Phase Equilibria*. 27 (1986) 35–52. [https://doi.org/10.1016/0378-3812\(86\)87039-X](https://doi.org/10.1016/0378-3812(86)87039-X).
- [261] G.J. Czerwiński, P. Tomasula, D. Tassios, Vapor - liquid equilibria with the vdW - 711 equation of state, *Fluid Phase Equilibria*. 42 (1988) 63–83. [https://doi.org/10.1016/0378-3812\(88\)80050-5](https://doi.org/10.1016/0378-3812(88)80050-5).
- [262] I.P. Androulakis, N.S. Kalospiros, D.P. Tassios, Thermophysical properties of pure polar and nonpolar compounds with a modified VdW-711 equation of state, *Fluid Phase Equilibria*. 45 (1989) 135–163. [https://doi.org/10.1016/0378-3812\(89\)80254-7](https://doi.org/10.1016/0378-3812(89)80254-7).
- [263] D.P. Tassios, *Applied Chemical Engineering Thermodynamics*, Springer Berlin Heidelberg, Berlin, Heidelberg, 1993. <https://doi.org/10.1007/978-3-662-01645-9>.
- [264] R. Agarwal, Y.-K. Li, M.A. Satyro, A. Vieler, Uncovering the realities of simulation. Part I, *Chem. Eng. Prog.* 97 (2001) 42–52.
- [265] R. Agarwal, Y.-K. Li, M.A. Satyro, A. Vieler, Uncovering the realities of simulation. Part II, *Chem. Eng. Prog.* 97 (2001) 64–72.
- [266] G. Soave, Equilibrium constants from a modified Redlich-Kwong equation of state, *Chem. Eng. Sci.* 27 (1972) 1197–1203. [https://doi.org/10.1016/0009-2509\(72\)80096-4](https://doi.org/10.1016/0009-2509(72)80096-4).
- [267] A. Pina-Martinez, Y. Le Guennec, R. Privat, J.-N. Jaubert, P. Mathias, Analysis of the combinations of property data that are suitable for a safe estimation of consistent Two  $\alpha$ -function parameters. Updated parameter values for the translated-consistent tc-PR and tc-RK cubic equations of state., *J Chem Eng Data*. (2018).
- [268] N. Ramírez-Vélez, A. Piña-Martinez, J.-N. Jaubert, R. Privat, Parameterization of SAFT Models: Analysis of Different Parameter Estimation Strategies and Application to the Development of a Comprehensive Database of PC-SAFT Molecular Parameters, *J. Chem. Eng. Data*. 65 (2020) 5920–5932. <https://doi.org/10.1021/acs.jced.0c00792>.
- [269] R. Privat, J.-N. Jaubert, Classification of global fluid-phase equilibrium behaviors in binary systems, *Chem. Eng. Res. Des.* 91 (2013) 1807–1839. <https://doi.org/10.1016/j.cherd.2013.06.026>.
- [270] Y. Le Guennec, S. Lasala, R. Privat, J.-N. Jaubert, A consistency test for alpha-functions of cubic equations of state, *Fluid Phase Equilibria*. 427 (2016) 513–538. <https://doi.org/10.1016/j.fluid.2016.07.026>.
- [271] Y. Le Guennec, R. Privat, S. Lasala, J.-N. Jaubert, On the imperative need to use a consistent  $\alpha$ -function for the prediction of pure-compound supercritical properties with a cubic equation of state, *Fluid Phase Equilibria*. 445 (2017) 45–53. <https://doi.org/10.1016/j.fluid.2017.04.015>.
- [272] C. Twu, D. Bluck, J. Cunningham, J. Coon, A Cubic Equation of State with a New Alpha Function and a New Mixing Rule, *Fluid Phase Equilibria*. 69 (1991) 33–50. [https://doi.org/10.1016/0378-3812\(91\)90024-2](https://doi.org/10.1016/0378-3812(91)90024-2).
- [273] G.M. Kontogeorgis, X. Liang, A. Arya, I. Tsvintzelis, Equations of state in three centuries. Are we closer to arriving to a single model for all applications?, *Chem. Eng. Sci.* X. 7 (2020) 100060. <https://doi.org/10.1016/j.cesx.2020.100060>.
- [274] C.-C. Chen, P.M. Mathias, Applied thermodynamics for process modeling, *AIChE J.* 48 (2002) 194–200. <https://doi.org/10.1002/aic.690480202>.
- [275] E. Hendriks, G.M. Kontogeorgis, R. Dohrn, J.-C. de Hemptinne, I.G. Economou, L.F. Žilnik, V. Vesovic, Industrial Requirements for Thermodynamics and Transport Properties, *Ind. Eng. Chem. Res.* 49 (2010) 11131–11141. <https://doi.org/10.1021/ie101231b>.
- [276] R.P. Danner, M.A. Gess, A data base standard for the evaluation of vapor-liquid-equilibrium models, *Fluid Phase Equilibria*. 56 (1990) 285–301. [https://doi.org/10.1016/0378-3812\(90\)85109-N](https://doi.org/10.1016/0378-3812(90)85109-N).
- [277] R. Privat, J.-N. Jaubert, Classification of global fluid-phase equilibrium behaviors in binary systems, *Chem. Eng. Res. Des.* 91 (2013) 1807–1839. <https://doi.org/10.1016/j.cherd.2013.06.026>.
- [278] P.H.V. Konynenburg, R.L. Scott, Critical Lines and Phase Equilibria in Binary Van Der Waals Mixtures, *Philos. Trans. R. Soc. Math. Phys. Eng. Sci.* 298 (1980) 495–540. <https://doi.org/10.1098/rsta.1980.0266>.

- [279] J. Qian, Développement du modèle *E*-PPR78 pour prédire les équilibres de phases et les grandeurs de mélange de systèmes complexes d'intérêt pétrolier sur de larges gammes de températures et de pressions, Institut National Polytechnique de Lorraine, 2011.
- [280] J. Benkhedda, J.-N. Jaubert, D. Barth, L. Perrin, M. Bailly, Adsorption isotherms of *m*-xylene on activated carbon: measurements and correlation with different models, *J. Chem. Thermodyn.* 32 (2000) 401–411. <https://doi.org/10.1006/jcht.1999.0613>.
- [281] G.M. Kontogeorgis, M.L. Michelsen, G.K. Folas, S. Derawi, N. von Solms, E.H. Stenby, Ten Years with the CPA (Cubic-Plus-Association) Equation of State. Part 1. Pure Compounds and Self-Associating Systems, *Ind. Eng. Chem. Res.* 45 (2006) 4855–4868. <https://doi.org/10.1021/ie051305v>.
- [282] J. Gross, G. Sadowski, Perturbed-Chain SAFT: An Equation of State Based on a Perturbation Theory for Chain Molecules, *Ind. Eng. Chem. Res.* 40 (2001) 1244–1260. <https://doi.org/10.1021/ie0003887>.
- [283] F. Llovel, L.F. Vega, Global fluid phase equilibria and critical phenomena of selected mixtures using the crossover soft-saft equation, *J. Phys. Chem. B.* 110 (2006) 1350–1362. <https://doi.org/10.1021/jp0551465>.
- [284] F. Llovel, L.F. Vega, Prediction of thermodynamic derivative properties of pure fluids through the soft-saft equation of state, *J. Phys. Chem. B.* 110 (2006) 11427–11437. <https://doi.org/10.1021/jp0608022>.
- [285] F. Llovel, C.J. Peters, L.F. Vega, Second-order thermodynamic derivative properties of selected mixtures by the soft-SAFT equation of state, *Fluid Phase Equilibria.* 248 (2006) 115–122. <https://doi.org/10.1016/j.fluid.2006.07.018>.
- [286] F. Llovel, L.F. Vega, Phase equilibria, critical behavior and derivative properties of selected *n*-alkane/*n*-alkane and *n*-alkane/1-alkanol mixtures by the crossover soft-SAFT equation of state, *J. Supercrit. Fluids.* 41 (2007) 204–216. <https://doi.org/10.1016/j.supflu.2006.10.001>.
- [287] G.M.C. Silva, J. Justino, P. Morgado, M. Teixeira, L.M.C. Pereira, L.F. Vega, E.J.M. Filipe, Detailed surface characterization of highly fluorinated liquid alcohols: Experimental surface tensions, molecular simulations and soft-SAFT theory, *J. Mol. Liq.* 300 (2020) 112294. <https://doi.org/10.1016/j.molliq.2019.112294>.
- [288] I. Polishuk, J.M. Garrido, Comparison of SAFT-VR-Mie and CP-PC-SAFT in predicting phase behavior of associating systems IV. Methanol–aliphatic hydrocarbons, *J. Mol. Liq.* 291 (2019) 111321. <https://doi.org/10.1016/j.molliq.2019.111321>.
- [289] I. Polishuk, R. Privat, J.-N. Jaubert, Novel methodology for analysis and evaluation of SAFT-type equations of state, *Ind. Eng. Chem. Res.* 52 (2013) 13875–13885. <https://doi.org/10.1021/ie4020155>.
- [290] I. Polishuk, J.M. Garrido, Comparison of SAFT-VR-Mie and CP-PC-SAFT in predicting phase behavior of associating systems III. Aliphatic hydrocarbons - 1-propanol, 1-butanol and 1-pentanol, *J. Mol. Liq.* 279 (2019) 492–502. <https://doi.org/10.1016/j.molliq.2019.01.151>.
- [291] I. Polishuk, J.M. Garrido, Comparison of SAFT-VR-Mie and CP-PC-SAFT in predicting phase behavior of associating systems II. Ammonia – Hydrocarbons, *J. Mol. Liq.* 269 (2018) 657–665. <https://doi.org/10.1016/j.molliq.2018.08.098>.
- [292] I. Polishuk, J.M. Garrido, Comparison of SAFT-VR-Mie and CP-PC-SAFT in predicting phase behavior of associating systems I. Ammonia–water, methanol, ethanol and hydrazine, *J. Mol. Liq.* 265 (2018) 639–653. <https://doi.org/10.1016/j.molliq.2018.05.112>.
- [293] P.W. Atkins, J. De Paula, *Atkins' physical chemistry*, Oxford University Press, Oxford, 2011.
- [294] R. Privat, J.-N. Jaubert, Discussion around the paradigm of ideal mixtures with emphasis on the definition of the property changes on mixing, *Chem. Eng. Sci.* 82 (2012) 319–333. <https://doi.org/10.1016/j.ces.2012.07.030>.
- [295] H.C. Van Ness, S.M. Byer, R.E. Gibbs, Vapor-Liquid equilibrium: Part I. An appraisal of data reduction methods, *AIChE J.* 19 (1973) 238–244. <https://doi.org/10.1002/aic.690190206>.
- [296] O. Redlich, A.T. Kister, Algebraic Representation of Thermodynamic Properties and the Classification of Solutions, *Ind. Eng. Chem.* 40 (1948) 345–348. <https://doi.org/10.1021/ie50458a036>.
- [297] K. Kojima, H. Man Moon, K. Ochi, Thermodynamic consistency test of vapor-liquid equilibrium data, *Fluid Phase Equilibria.* 56 (1990) 269–284. [https://doi.org/10.1016/0378-3812\(90\)85108-M](https://doi.org/10.1016/0378-3812(90)85108-M).
- [298] J. Wisniak, J. Ortega, L. Fernández, A fresh look at the thermodynamic consistency of vapour-liquid equilibria data, *J. Chem. Thermodyn.* 105 (2017) 385–395. <https://doi.org/10.1016/j.jct.2016.10.038>.
- [299] D.P.L. Poon, B.C.-Y. Lu, Phase Equilibria for Systems Containing Nitrogen, Methane, and Propane, in: *Adv. Cryog. Eng.*, 1995: pp. 292–299.
- [300] I. Wichterle, R. Kobayashi, Vapor-liquid equilibrium of methane-propane system at low temperatures and high pressures, *J. Chem. Eng. Data.* 17 (1972) 4–9. <https://doi.org/10.1021/je60052a019>.
- [301] A.R. Price, R. Kobayashi, Low Temperature Vapor-Liquid Equilibrium in Light Hydrocarbon Mixtures: Methane-Ethane-Propane System., *J. Chem. Eng. Data.* 4 (1959) 40–52. <https://doi.org/10.1021/je60001a007>.

- [302] I. Wichterle, R. Kobayashi, Vapor-liquid equilibrium of methane-ethane-propane system at low temperatures and high pressures, *J. Chem. Eng. Data.* 17 (1972) 13–18. <https://doi.org/10.1021/je60052a017>.
- [303] L.A. Webster, A.J. Kidnay, Vapor-Liquid Equilibria for the Methane-Propane-Carbon Dioxide Systems at 230 K and 270 K, *J. Chem. Eng. Data.* 46 (2001) 759–764. <https://doi.org/10.1021/je000307d>.
- [304] W.W. Akers, J.F. Burns, W.R. Fairchild, Low-Temperature Phase Equilibria: Methane-Propane System, *Ind. Eng. Chem.* 46 (1954) 2531–2534. <https://doi.org/10.1021/ie50540a038>.
- [305] H.H. Reamer, B.H. Sage, W.N. Lacey, Phase Equilibria in Hydrocarbon Systems. Volumetric and Phase Behavior of the Methane-Propane System., *Ind. Eng. Chem.* 42 (1950) 534–539. <https://doi.org/10.1021/ie50483a037>.
- [306] K. Watanabe, M. Kuroki, M. Ogura, I. Saito, Vapour-Liquid-Equilibrium of LNG, *TEION KOGAKU J. Cryog. Supercond. Soc. Jpn.* 4 (1969) 292–301. <https://doi.org/10.2221/jcsj.4.292>.
- [307] R.C. Miller, L.A.K. Staveley, Excess Enthalpies for Some Binary Liquid Mixtures of Low-Molecular-Weight Alkanes, in: *Adv. Cryog. Eng.*, 1960: pp. 493–500.
- [308] A.J.B. Cutler, J.A. Morrison, Excess thermodynamic functions for liquid mixtures of methane + propane, *Trans. Faraday Soc.* 61 (1965) 429. <https://doi.org/10.1039/tf9656100429>.
- [309] D.J. Hutchings, E.J. Lewis, C.J. Wormald, Excess enthalpies of mixtures of methane + each of the n-alkanes from ethane to n-octane, *J. Chem. Thermodyn.* 10 (1978) 559–566. [https://doi.org/10.1016/0021-9614\(78\)90044-7](https://doi.org/10.1016/0021-9614(78)90044-7).
- [310] J.G. Roof, J.D. Baron, Critical loci of binary mixtures of propane with methane, carbon dioxide, and nitrogen, *J. Chem. Eng. Data.* 12 (1967) 292–293. <https://doi.org/10.1021/je60034a003>.
- [311] B.H. Sage, W.N. Lacey, J.G. Schaafsma, Phase Equilibria in Hydrocarbon Systems II. Methane-Propane System, *Ind. Eng. Chem.* 26 (1934) 214–217. <https://doi.org/10.1021/ie50290a020>.
- [312] Y.-N. Lin, R.J.J. Chen, P.S. Chapplelear, R. Kobayashi, Vapor-liquid equilibrium of the methane-n-hexane system at low temperature, *J. Chem. Eng. Data.* 22 (1977) 402–408. <https://doi.org/10.1021/je60075a007>.
- [313] M.E. Kandil, M.J. Thoma, T. Syed, J. Guo, B.F. Graham, K.N. Marsh, S.H. Huang, E.F. May, Vapor-Liquid Equilibria Measurements of the Methane + Pentane and Methane + Hexane Systems at Temperatures from (173 to 330) K and Pressures to 14 MPa, *J. Chem. Eng. Data.* 56 (2011) 4301–4309. <https://doi.org/10.1021/je200101x>.
- [314] G.S. Stepanova, Y.I. Vybornova, Phase equilibriums of methane-hexane system, *Tr Vses Nauchno Issled Inst Prir Gazov.* (1962) 203–208.
- [315] J. Shim, J.P. Kohn, Multiphase and Volumetric Equilibria of Methane-n-Hexane Binary System at Temperatures Between -110° and 150° C., *J. Chem. Eng. Data.* 7 (1962) 3–8. <https://doi.org/10.1021/je60012a002>.
- [316] R.S. Poston, J.J. McKetta, Vapor-Liquid Equilibrium in the Methane-n-Hexane System., *J. Chem. Eng. Data.* 11 (1966) 362–363. <https://doi.org/10.1021/je60030a021>.
- [317] R.D. Gunn, J.J. McKetta, N. Ata, Measurement and prediction of high-pressure phase equilibria with a dilute component in the gas phase: The methane-n-hexane system, *AIChE J.* 20 (1974) 347–353. <https://doi.org/10.1002/aic.690200221>.
- [318] P. Marteau, J. Obriot, A. Barreau, V. Ruffier-Meray, E. Behar, Experimental determination of the phase behavior of binary mixtures: methane-hexane and methane-benzene, *Fluid Phase Equilibria.* 129 (1997) 285–305. [https://doi.org/10.1016/S0378-3812\(96\)03125-1](https://doi.org/10.1016/S0378-3812(96)03125-1).
- [319] D.G. Elliott, Y.N. Lin, T.C. Chu, P.S. Chapplelear, R. Kobayashi, K-values for the methane - n-butane, methane - n-pentane, and methane - n-hexane systems, *GPA Res. Rep.* (1976) 1–19.
- [320] H.L. Chang, L.J. Hurt, R. Kobayashi, Vapor-liquid equilibria of light hydrocarbons at low temperatures and high pressures: The methane-n-heptane system, *AIChE J.* 12 (1966) 1212–1216. <https://doi.org/10.1002/aic.690120629>.
- [321] H.H. Reamer, B.H. Sage, W.N. Lacey, Phase Equilibria in Hydrocarbon Systems. Volumetric and Phase Behavior of the Methane- n-Heptane System, *Ind. Eng. Chem. Chem. Eng. Data Ser.* 1 (1956) 29–42. <https://doi.org/10.1021/i460001a007>.
- [322] J.L. Oscarson, J.Y. Coxam, S.E. Gillespie, R.M. Izatt, Excess enthalpies of mixing methane with methanol, n-heptane, toluene and methylcyclohexane at 255.4 and 310.9 K and 13.8 MPa, *Fluid Phase Equilibria.* 114 (1996) 161–174. [https://doi.org/10.1016/0378-3812\(95\)02813-7](https://doi.org/10.1016/0378-3812(95)02813-7).
- [323] R.J.J. Chen, P.S. Chapplelear, R. Kobayashi, Vapor Phase Data for the Binary Systems of Methane with n-Butane, n-Pentane, n-Hexane, and n-Heptane, *GPA Res. Rep.* (1976) 1–14.
- [324] R. Stryjek, P.S. Chapplelear, R. Kobayashi, Low-temperature vapor-liquid equilibriums of nitrogen-ethane system, *J. Chem. Eng. Data.* 19 (1974) 340–343. <https://doi.org/10.1021/je60063a024>.

- [325] L. Grausø, A. Fredenslund, J. Møllerup, Vapour-liquid equilibrium data for the systems C<sub>2</sub>H<sub>6</sub> + N<sub>2</sub>, C<sub>2</sub>H<sub>4</sub> + N<sub>2</sub>, C<sub>3</sub>H<sub>8</sub> + N<sub>2</sub>, and C<sub>3</sub>H<sub>6</sub> + N<sub>2</sub>, *Fluid Phase Equilibria*. 1 (1977) 13–26. [https://doi.org/10.1016/0378-3812\(77\)80022-8](https://doi.org/10.1016/0378-3812(77)80022-8).
- [326] T.S. Brown, E.D. Sloan, A.J. Kidnay, Vapor-liquid equilibria in the nitrogen + carbon dioxide + ethane system, *Fluid Phase Equilibria*. 51 (1989) 299–313. [https://doi.org/10.1016/0378-3812\(89\)80372-3](https://doi.org/10.1016/0378-3812(89)80372-3).
- [327] S. Zeck, H. Knapp, Vapor—liquid and vapor—liquid—liquid phase equilibria for binary and ternary systems for nitrogen, ethane and methanol: Experiment and data reduction, *Fluid Phase Equilibria*. 25 (1986) 303–322. [https://doi.org/10.1016/0378-3812\(86\)80006-1](https://doi.org/10.1016/0378-3812(86)80006-1).
- [328] M.K. Gupta, G.C. Gardner, M.J. Hegarty, A.J. Kidnay, Liquid-vapor equilibria for the N<sub>2</sub> + CH<sub>4</sub> + C<sub>2</sub>H<sub>6</sub> system from 260 to 280 K, *J. Chem. Eng. Data*. 25 (1980) 313–318. <https://doi.org/10.1021/je60087a016>.
- [329] R.T. Ellington, B.E. Eakin, J.D. Parent, D.C. Gami, O.T. Bloomer, Vapor-liquid phase equilibria in the binary systems of CH<sub>4</sub>, C<sub>2</sub>H<sub>6</sub>, and N<sub>2</sub>, *Thermodyn. Transp. Prop. Gases Liq. Solids Pap. Present. Symp. Therm. Prop.* 1 (1959) 180–194.
- [330] H.J. Guedes, J.A. Zollweg, E.J. Filipe, L.F. Martins, J.C. Calado, Thermodynamics of liquid (nitrogen + ethane), *J. Chem. Thermodyn.* 34 (2002) 669–678. <https://doi.org/10.1006/jcht.2001.0936>.
- [331] P. Yu, I.M. Elshayal, B.C.-Y. Lu, Liquid-liquid-vapor equilibria in the nitrogen-methane-ethane system, *Can. J. Chem. Eng.* 47 (1969) 495–498. <https://doi.org/10.1002/cjce.5450470516>.
- [332] K.T. Koonce, R. Kobayashi, A Method for Determining the Solubility of Gases in Relatively Nonvolatile Liquids: Solubility of Methane in n-Decane., *J. Chem. Eng. Data*. 9 (1964) 490–494. <https://doi.org/10.1021/je60023a004>.
- [333] H. Lentz, P. Nuernerich, Die Bestimmung der Zusammensetzung koexistierender Phasen binärer Mischungen aus Nodenlinien und Volumen, *Chem Ing Tech.* 73 (2001) 1162–1164. [https://doi.org/10.1002/1522-2640\(200109\)73:9<1162::AID-CITE1162>3.0.CO;2-4](https://doi.org/10.1002/1522-2640(200109)73:9<1162::AID-CITE1162>3.0.CO;2-4).
- [334] H.H. Reamer, R.H. Olds, B.H. Sage, W.N. Lacey, Phase Equilibria in Hydrocarbon Systems, *Ind. Eng. Chem.* 34 (1942) 1526–1531. <https://doi.org/10.1021/ie50396a025>.
- [335] H.M. Lavender, B.H. Sage, W.N. Lacey, Gas-liquid equilibrium constants, methane-decane system, *Oil Gas J.* 39 (1940) 48–49.
- [336] H.-M. Lin, H.M. Sebastian, J.J. Simnick, K.-C. Chao, Gas-liquid equilibrium in binary mixtures of methane with N-decane, benzene, and toluene, *J. Chem. Eng. Data*. 24 (1979) 146–149. <https://doi.org/10.1021/je60081a004>.
- [337] H.C. Wiese, H.H. Reamer, B.H. Sage, Phase equilibria in hydrocarbon systems. Phase behavior in the methane-propane-n-decane system, *J. Chem. Eng. Data*. 15 (1970) 75–82. <https://doi.org/10.1021/je60044a018>.
- [338] W.B. Kay, Liquid-Vapor Phase Equilibrium Relations in the Ethane-n-Heptane System, *Ind. Eng. Chem.* 30 (1938) 459–465. <https://doi.org/10.1021/ie50340a023>.
- [339] H.M. Cota, G. Thodos, Critical Temperatures and Critical Pressures of Hydrocarbon Mixtures. Methane Ethane-n-Butane System., *J. Chem. Eng. Data*. 7 (1962) 62–65. <https://doi.org/10.1021/je60012a018>.
- [340] V.S. Mehra, G. Thodos, Vapor-Liquid Equilibrium in the Ethane-n-Heptane System., *J. Chem. Eng. Data*. 10 (1965) 211–214. <https://doi.org/10.1021/je60026a001>.
- [341] O. Ekiner, G. Thodos, Critical temperatures and pressures of the ethane-n-heptane system, *Can. J. Chem. Eng.* 43 (1965) 205–208. <https://doi.org/10.1002/cjce.5450430411>.
- [342] V.S. Mehra, G. Thodos, Vapor-liquid equilibrium constants for the ethane-butane-n-heptane system at 300° and 350°F, *J. Chem. Eng. Data*. 13 (1968) 155–160. <https://doi.org/10.1021/je60037a004>.
- [343] H. Singh, F.P. Lucien, N.R. Foster, Critical Properties for Binary Mixtures of Ethane Containing Low Concentrations of n-Alkane, *J. Chem. Eng. Data*. 45 (2000) 131–135. <https://doi.org/10.1021/je990220w>.
- [344] F. Kurata, G.W. Swift, Experimental Measurements of Vapor-Liquid Equilibrium Data for the Ethane - Carbon Dioxide and Nitrogen - n-Pentane Binary Systems, *GPA Res. Rep.* (1971) 1–10.
- [345] H. Kalra, D.B. Robinson, G.J. Besserer, The equilibrium phase properties of the nitrogen-n-pentane system, *J. Chem. Eng. Data*. 22 (1977) 215–218. <https://doi.org/10.1021/je60073a023>.
- [346] G. Silva-Oliver, G. Eliosa-Jiménez, F. García-Sánchez, J.R. Avendaño-Gómez, High-pressure vapor-liquid equilibria in the nitrogen-n-pentane system, *Fluid Phase Equilibria*. 250 (2006) 37–48. <https://doi.org/10.1016/j.fluid.2006.09.018>.
- [347] A. Azarnoosh, J.J. McKetta, Nitrogen-n-Decane System in the Two-Phase Region., *J. Chem. Eng. Data*. 8 (1963) 494–496. <https://doi.org/10.1021/je60019a005>.
- [348] F. García-Sánchez, G. Eliosa-Jiménez, G. Silva-Oliver, B.E. García-Flores, Vapor-Liquid Equilibrium Data for the Nitrogen + n-Decane System from (344 to 563) K and at Pressures up to 50 MPa, *J. Chem. Eng. Data*. 54 (2009) 1560–1568. <https://doi.org/10.1021/je800881t>.

- [349] E. Flöter, T.W. de Loos, J. de Swaan Arons, High pressure solid-fluid and vapour-liquid equilibria in the system (methane + tetracosane), *Fluid Phase Equilibria*. 127 (1997) 129–146. [https://doi.org/10.1016/S0378-3812\(96\)03157-3](https://doi.org/10.1016/S0378-3812(96)03157-3).
- [350] C.-P. Huang, D.-S. Jan, F.-N. Tsai, Modeling of Methane Solubility in Heavy n-Paraffins., *J. Chem. Eng. Jpn.* 25 (1992) 182–186. <https://doi.org/10.1252/jcej.25.182>.
- [351] J.. Arnaud, P. Ungerer, E. Behar, G. Moracchini, J. Sanchez, Excess volumes and saturation pressures for the system methane + n-tetracosane at 374 K. Representation by improved EOS mixing rules, *Fluid Phase Equilibria*. 124 (1996) 177–207. [https://doi.org/10.1016/S0378-3812\(96\)03101-9](https://doi.org/10.1016/S0378-3812(96)03101-9).
- [352] D. Suleiman, C.A. Eckert, Phase Equilibria of Alkanes in Natural Gas Systems. 1. Alkanes in Methane, *J. Chem. Eng. Data*. 40 (1995) 2–11. <https://doi.org/10.1021/je00017a001>.
- [353] C.E. Schwarz, I. Nieuwoudt, J.H. Knoetze, Phase equilibria of long chain n-alkanes in supercritical ethane: Review, measurements and prediction, *J. Supercrit. Fluids*. 46 (2008) 226–232. <https://doi.org/10.1016/j.supflu.2008.05.007>.
- [354] F.N. Tsai, S.H. Huang, H.M. Lin, K.C. Chao, Solubility of methane, ethane, and carbon dioxide in n-hexatriacontane, *J. Chem. Eng. Data*. 32 (1987) 467–469. <https://doi.org/10.1021/je00050a025>.
- [355] K.A.M. Gasem, B.A. Bufkin, A.M. Raff, R.L. Robinson, Solubilities of ethane in heavy normal paraffins at pressures to 7.8 MPa and temperatures from 348 to 423 K, *J. Chem. Eng. Data*. 34 (1989) 187–191. <https://doi.org/10.1021/je00056a012>.
- [356] M. Martin, J. Youings, Vapour pressures and excess Gibbs free energies of cyclohexane + n-hexane, + n-heptane and + n-octane at 298. 15 K, *Aust. J. Chem.* 33 (1980) 2133. <https://doi.org/10.1071/CH9802133>.
- [357] G.C. Benson, G.C. Benson, S.C. Anand, O. Kiyohara, Thermodynamic properties of some cycloalkane-cycloalkanol systems at 298. 15.deg.K. II, *J. Chem. Eng. Data*. 19 (1974) 258–261. <https://doi.org/10.1021/je60062a027>.
- [358] M.P. Susarev, S.T. Chen, Calculation of vapor-liquid equilibrium in ternary systems from the data on binary systems. The system benzene-n-hexane-cyclohexane, *Russ J Phys Chem*. 37 (1963) 938–943.
- [359] K. Ridgway, P.A. Butler, Physical properties of the ternary system benzene-cyclohexane-hexane, *J. Chem. Eng. Data*. 12 (1967) 509–515. <https://doi.org/10.1021/je60035a012>.
- [360] H.S. Myers, [Vapor-liquid] equilibrium for naphthenes and paraffins, *Pet Refin.* 36 (1957) 175–178.
- [361] M.A. Siddiqi, K. Lucas, An isothermal high-pressure flow calorimeter the excess enthalpy of (cyclohexane + n-hexane) at different pressures at 288.15, 298.15, and 313.15 K, *J. Chem. Thermodyn.* 14 (1982) 1183–1190. [https://doi.org/10.1016/0021-9614\(82\)90042-8](https://doi.org/10.1016/0021-9614(82)90042-8).
- [362] M.. Ewing, K.. Marsh, The enthalpy of mixing of n-hexane + cyclohexane at 288.15 and 318.15 K, *J. Chem. Thermodyn.* 2 (1970) 295–296. [https://doi.org/10.1016/0021-9614\(70\)90094-7](https://doi.org/10.1016/0021-9614(70)90094-7).
- [363] J.J. Christensen, R.M. Izatt, D.J. Eatough, L.D. Hansen, The effect of pressure on the excess enthalpies of cyclohexane + n-hexane at 298.15 K, *J. Chem. Thermodyn.* 10 (1978) 25–34. [https://doi.org/10.1016/0021-9614\(78\)90145-3](https://doi.org/10.1016/0021-9614(78)90145-3).
- [364] A. Heintz, R.N. Lichtenthaler, An Isothermal Flow Calorimeter for Pressures to 600 bar, *Berichte Bunsenges. Für Phys. Chem.* 83 (1979) 853–856. <https://doi.org/10.1002/bbpc.19790830816>.
- [365] J. Gmehling, B. Meents, Excess enthalpy. Cyclohexane-hexane system, *Int Data Ser Sel Data Mix. Ser A*. (1992) 144.
- [366] J. Gmehling, B. Krentscher, Excess enthalpies of 12 binary liquid mixtures containing cyclohexane at elevated temperatures and pressures (up to 416 K and 1.9 MPa), *ELDATA Int Electron J Phys-Chem Data*. 1 (1995) 181–190.
- [367] A. Saito, R. Tanaka, Excess volumes and heat capacities of binary mixtures formed from cyclohexane, hexane, and heptane at 298.15 K, *J. Chem. Thermodyn.* 20 (1988) 859–865. [https://doi.org/10.1016/0021-9614\(88\)90075-4](https://doi.org/10.1016/0021-9614(88)90075-4).
- [368] D.W. Hissong, W.B. Kay, Critical properties of hydrocarbons. II. Correlational studies, *Proc Am Pet Inst Refin Dep.* 48 (1968) 397–463.
- [369] K.-D. Kassmann, H. Knapp, Vapor-Liquid Equilibria for Binary and Ternary Mixtures of Benzene, Toluene and n-Butyraldehyde, *Berichte Bunsenges. Für Phys. Chem.* 90 (1986) 452–458. <https://doi.org/10.1002/bbpc.19860900514>.
- [370] S. Saito, Separation of hydrocarbons. 2. Vapor-liquid equilibria of normal paraffin-aromatic systems, *Asahi Garasu Kogyo Gijutsu Shoreikai Kenkyu Hokoku.* 15 (1969) 397–407.
- [371] Z. Jin, A. Hu, K. Liu, VLE of Binary and Ternary Systems for BTX Mixtures, *Chem. Eng. China*. 19 (1991) 56–60.
- [372] H. Schuberth, Phasengleichgewichtsmessungen. II. Vorausberechnung von Gleichgewichtsdaten dampfförmig-flüssig idealer binärer Systeme und Prüfung derselben mittels einer neuen Gleichgewichtsapparatur, *J. Für Prakt. Chem.* 6 (1958) 129–138. <https://doi.org/10.1002/prac.19580060209>.

- [373] E. Baud, Thermal analysis of binary mixtures, *Bull Soc Chim Fr.* 17 (1915) 329–345.
- [374] K.-Y. Hsu, H. Lawrence Clever, The excess enthalpies of the 15 binary mixtures formed from cyclohexane, benzene, toluene, 1,4-dimethylbenzene, 1,2,4-trimethylbenzene, and 1,3,5-trimethylbenzene at 298.15 K, *J. Chem. Thermodyn.* 7 (1975) 435–442. [https://doi.org/10.1016/0021-9614\(75\)90273-6](https://doi.org/10.1016/0021-9614(75)90273-6).
- [375] S. Murakami, V.T. Lam, G.C. Benson, The thermodynamic properties of binary aromatic systems II. Excess enthalpies and volumes of benzene + toluene and toluene + isomeric xylene mixtures at 25 °C, *J. Chem. Thermodyn.* 1 (1969) 397–407. [https://doi.org/10.1016/0021-9614\(69\)90070-6](https://doi.org/10.1016/0021-9614(69)90070-6).
- [376] M. Diaz Pena, C. Menduina, Semicontinuous calorimeter for measuring heats of mixing, *Quim.* 69 (1973) 857–868.
- [377] J.L. Fortier, G.C. Benson, Heat capacities of some binary aromatic hydrocarbon mixtures containing benzene or toluene, *J. Chem. Eng. Data.* 24 (1979) 34–37. <https://doi.org/10.1021/je60080a015>.
- [378] W.B. Kay, D. Hissong, The critical properties of hydrocarbons. I. Simple mixtures, *Proc Am Pet Inst Refin Dep.* 47 (1967) 653–722.
- [379] W.E. Vaughan, F.C. Collins, P-V-T-x Relations of the System Propane-Isopentane, *Ind. Eng. Chem.* 34 (1942) 885–890. <https://doi.org/10.1021/ie50391a027>.
- [380] X. Zhang, Y. Zheng, W. Zhao, Measurement and correlation of vapor liquid equilibrium data for benzene cyclohexane methyl cyclohexane DMF systems, *Nat. Gas Chem. Ind.* 22 (1997) 52–55.
- [381] B.S. Harsted, E.S. Thomsen, Excess enthalpies from flow microcalorimetry 3. Excess enthalpies for binary liquid mixtures of aliphatic and aromatic hydrocarbons, carbon tetrachloride, chlorobenzene, and carbon disulphide, *J. Chem. Thermodyn.* 7 (1975) 369–376. [https://doi.org/10.1016/0021-9614\(75\)90175-5](https://doi.org/10.1016/0021-9614(75)90175-5).
- [382] J.B. Ott, K.N. Marsh, R.H. Stokes, Excess enthalpies, excess Gibbs free energies, and excess volumes for (cyclohexane + n-hexane), and excess Gibbs free energies and excess volumes for (cyclohexane + methylcyclohexane) at 298.15 and 308.15 K, *J. Chem. Thermodyn.* 12 (1980) 1139–1148. [https://doi.org/10.1016/S0021-9614\(80\)80006-1](https://doi.org/10.1016/S0021-9614(80)80006-1).
- [383] K. Tamura, Excess heat capacities of the mixtures containing methylcyclohexane at 298.15 K, *Fluid Phase Equilibria.* 182 (2001) 303–312. [https://doi.org/10.1016/S0378-3812\(01\)00407-1](https://doi.org/10.1016/S0378-3812(01)00407-1).
- [384] L. Djordjevich, R.A. Budenholzer, Vapor-liquid equilibrium data for ethane-propane system at low temperatures, *J. Chem. Eng. Data.* 15 (1970) 10–12. <https://doi.org/10.1021/je60044a020>.
- [385] M. Hirata, S. Suda, T. Hakuta, K. Nagahama, Light hydrocarbon vapor-liquid equilibria, *Mem Fac Technol Tokyo Metropol Univ.* 19 (1969) 103–122.
- [386] V.G. Skripka, I.E. Nikitina, L.A. Zhdanovich, A.G. Sirotin, O.A. Ben'yaminovich, Liquid-vapor phase equilibria at low temperatures in binary systems formed by components of natural gas, *Gazov Promst.* 15 (1970) 35–36.
- [387] C.J. Blanc, J.C.B. Setier, Vapor-liquid equilibria for the ethane-propane system at low temperature, *J. Chem. Eng. Data.* 33 (1988) 111–115. <https://doi.org/10.1021/je00052a015>.
- [388] A.Q. Clark, K. Stead, (Vapour + liquid) phase equilibria of binary, ternary, and quaternary mixtures of CH<sub>4</sub>, C<sub>2</sub>H<sub>6</sub>, C<sub>3</sub>H<sub>8</sub>, C<sub>4</sub>H<sub>10</sub>, and CO<sub>2</sub>, *J. Chem. Thermodyn.* 20 (1988) 413–427. [https://doi.org/10.1016/0021-9614\(88\)90178-4](https://doi.org/10.1016/0021-9614(88)90178-4).
- [389] L.C. Kahre, Liquid density of light hydrocarbon mixtures, *J. Chem. Eng. Data.* 18 (1973) 267–270. <https://doi.org/10.1021/je60058a030>.
- [390] H. Pöll, H. Huemer, F. Moser, Eine Apparatur zur Bestimmung von Dampf-Flüssigkeits-Gleichgewichten unter erhöhtem Druck, *Monatshefte Für Chem.* 111 (1980) 1159–1164. <https://doi.org/10.1007/BF00909673>.
- [391] J. Miksovsky, I. Wichterle, Liquid-vapor equilibrium. LXX. Vapor-liquid equilibria in the ethane-propane system at high pressures, *Collect Czech Chem Commun.* 40 (1975) 365–370. <https://doi.org/10.1135/cccc19750365>.
- [392] D.E. Matschke, G. Thodos, Vapor-liquid equilibria for the ethane-propane system, *J Chem Eng Data.* 7 (1962) 232–234. <https://doi.org/10.1021/je60013a022>.
- [393] J.B. Ott, P.R. Brown, J.D. Moore, A.C. Lewellen, Excess molar enthalpies and excess molar volumes for (propane + ethane) over the temperature range from 273.15 K to 373.15 K and the pressure range from 5 MPa to 15 MPa, *J. Chem. Thermodyn.* 29 (1997) 149–178. <https://doi.org/10.1006/jcht.1996.0144>.
- [394] S. Horstmann, K. Fischer, J. Gmehling, Experimental determination of critical data of mixtures and their relevance for the development of thermodynamic models, *Chem. Eng. Sci.* 56 (2001) 6905–6913. [https://doi.org/10.1016/S0009-2509\(01\)00332-3](https://doi.org/10.1016/S0009-2509(01)00332-3).
- [395] L.J. Van Poolen, C.D. Holcomb, Critical temperatures, pressures, and densities for the mixtures CO<sub>2</sub>-C<sub>3</sub>H<sub>8</sub>, CO<sub>2</sub>-nC<sub>4</sub>H<sub>10</sub>, C<sub>2</sub>H<sub>6</sub>-C<sub>3</sub>H<sub>8</sub>, and C<sub>3</sub>H<sub>8</sub>-nC<sub>4</sub>H<sub>10</sub>, *Fluid Phase Equilibria.* 165 (1999) 157–168. [https://doi.org/10.1016/S0378-3812\(99\)00275-7](https://doi.org/10.1016/S0378-3812(99)00275-7).

- [396] P. Uchytíl, I. Wichterle, Liquid-vapour critical region of the most volatile component of a ternary system. I. Vapour-liquid equilibria in the ethane - propane - n-butane system, *Fluid Phase Equilibria*. 15 (1983) 209–217. [https://doi.org/10.1016/0378-3812\(83\)80153-8](https://doi.org/10.1016/0378-3812(83)80153-8).
- [397] L.C. Kahre, Low-temperature K data for methane-butane, *J. Chem. Eng. Data*. 19 (1974) 67–71. <https://doi.org/10.1021/je60060a014>.
- [398] D.G. Elliot, R.J.J. Chen, P.S. Chappellear, R. Kobayashi, Vapor-liquid equilibrium of methane-butane system at low temperatures and high pressures, *J. Chem. Eng. Data*. 19 (1974) 71–77. <https://doi.org/10.1021/je60060a015>.
- [399] H.C. Wiese, J. Jacobs, B.H. Sage, Phase equilibria in the hydrocarbon systems. Phase behavior in the methane-propane-n-butane system, *J. Chem. Eng. Data*. 15 (1970) 82–91. <https://doi.org/10.1021/je60044a021>.
- [400] R.H. Sage, B.L. Hicks, W.N. Lacey, Phase Equilibria in Hydrocarbon Systems, *Ind. Eng. Chem.* 32 (1940) 1085–1092. <https://doi.org/10.1021/ie50368a014>.
- [401] T.J. Rigas, D.F. Mason, G. Thodos, Vapor-Liquid Equilibria. Microsampling Technique Applied to a New Variable-Volume Cell, *Ind. Eng. Chem.* 50 (1958) 1297–1300. <https://doi.org/10.1021/ie50585a039>.
- [402] F.B. Sprow, J.M. Prausnitz, Vapor-Liquid equilibria for five cryogenic mixtures, *AIChE J.* 12 (1966) 780–784. <https://doi.org/10.1002/aic.690120427>.
- [403] J.C.G. Calado, L.A.K. Staveley, Excess Gibbs Energy of Argon-Methane Liquid Mixtures at 115.77°K, *J. Chem. Phys.* 56 (1972) 4718–4719. <https://doi.org/10.1063/1.1677927>.
- [404] L.V. Shatskaya, N.A. Zhirmova, Liquid-vapor phase equilibria in two-component systems at low temperatures. I. Argon-methane system, *Russ J Phys Chem.* 50 (1976) 298–298.
- [405] H. Kehlen, F.-U. Schneider, S. Haufe, W. Barnitzke, Auswertung von Taudruckmessungen binärer Systeme im Mitteldruckbereich, *Z. Für Phys. Chem.* 264O (1983). <https://doi.org/10.1515/zpch-1983-26497>.
- [406] L.J. Christiansen, A. Fredenslund, Vapour-liquid equilibria of the CH<sub>4</sub>-Ar-CO system, *Cryogenics*. 14 (1974) 10–14. [https://doi.org/10.1016/0011-2275\(74\)90037-X](https://doi.org/10.1016/0011-2275(74)90037-X).
- [407] L.J. Christiansen, A. Fredenslund, J. Møllerup, Vapour-liquid equilibrium of the CH<sub>4</sub>-Ar, CH<sub>4</sub>-CO, and Ar-CO systems at elevated pressures, *Cryogenics*. 13 (1973) 405–413. [https://doi.org/10.1016/0011-2275\(73\)90076-3](https://doi.org/10.1016/0011-2275(73)90076-3).
- [408] K.L. Lewis, G. Saville, L.A.K. Staveley, Excess enthalpies of liquid oxygen + argon, oxygen + nitrogen, and argon + methane, *J. Chem. Thermodyn.* 7 (1975) 389–400. [https://doi.org/10.1016/0021-9614\(75\)90178-0](https://doi.org/10.1016/0021-9614(75)90178-0).
- [409] S.E. Mosedale, C.J. Wormald, The enthalpy of mixing of argon + methane at 123, 130, 140, and 145 K, at pressures up to 9.12 MPa, *J. Chem. Thermodyn.* 9 (1977) 483–490. [https://doi.org/10.1016/0021-9614\(77\)90149-5](https://doi.org/10.1016/0021-9614(77)90149-5).
- [410] K.L. Lewis, S.E. Mosedale, C.J. Wormald, The enthalpies of mixing of methane + argon, methane + nitrogen, and methane + hydrogen in the gaseous and two-phase regions, *J. Chem. Thermodyn.* 9 (1977) 121–131. [https://doi.org/10.1016/0021-9614\(77\)90077-5](https://doi.org/10.1016/0021-9614(77)90077-5).
- [411] C.J. Wormald, K.L. Lewis, S. Mosedale, The excess enthalpies of hydrogen + methane, hydrogen + nitrogen, methane + nitrogen, methane + argon, and nitrogen + argon at 298 and 201 K at pressures up to 10.2 MPa, *J. Chem. Thermodyn.* 9 (1977) 27–42. [https://doi.org/10.1016/0021-9614\(77\)90194-X](https://doi.org/10.1016/0021-9614(77)90194-X).
- [412] H.I. Paul, J. Krug, H. Knapp, Measurements of VLE,  $vE$  and  $hE$  for binary mixtures of n-alkanes with chloro-alkylbenzenes, *Fluid Phase Equilibria*. 39 (1988) 307–324. [https://doi.org/10.1016/0378-3812\(88\)85010-6](https://doi.org/10.1016/0378-3812(88)85010-6).
- [413] J.W. Bayles, T.M. Letcher, Thermodynamics of some binary liquid mixtures containing aliphatic amines, *J. Chem. Eng. Data*. 16 (1971) 266–271. <https://doi.org/10.1021/je60050a026>.
- [414] M.N.M. Al-Hayan, J.A.M. Al-Kandary, Isobaric vapour-liquid equilibria for binary mixtures of n-heptane with bromobenzene, chlorobenzene and fluorobenzene at atmospheric pressure, *Fluid Phase Equilibria*. 240 (2006) 109–113. <https://doi.org/10.1016/j.fluid.2005.11.020>.
- [415] A. Raviprasad, K. Venkateswara Rao, C. Chiranjivi, Isobaric vapor-liquid equilibrium data for the systems n-heptane-chlorobenzene and trichloroethylene-methyl isobutyl ketone (MIBK), *Indian Chem Eng.* 18 (1976) 47–49.
- [416] E. Wilhelm, A. Inglese, J.-P.E. Grolier, H.V. Kehiaian, Enthalpy of Mixing of Chlorobenzene, 1,2-Dichlorobenzene, and 1,3-Dichlorobenzene with Some n-Alkanes, *Ber Bunsen-Ges Phys Chem.* 82 (1978) 384–388.
- [417] J.P.E. Grolier, K. Sosnkowska-Kehiaian, H.V. Kehiaian, Enthalpies de mélange des chlorures organiques avec des hydrocarbures, *J Chim Phys Phys Chim Biol.* 70 (1973) 367–373. <https://doi.org/10.1051/jcp/1973700367>.

- [418] H. Bendiab, G. Roux-Desgranges, A.H. Roux, J.-P.E. Grolier, D. Patterson, Excess heat capacities of ternary systems containing chlorobenzene or chloronaphthalene, *J. Solut. Chem.* 23 (1994) 307–323. <https://doi.org/10.1007/BF00973552>.
- [419] M. Díaz Peña, A. Compostizo, A. Crespo Colín, I. Escudero, Activity coefficients and excess Gibbs free energies at 348.15 K in cyclohexane+chlorobenzene, +fluorobenzene, and +thiophene, *J. Chem. Thermodyn.* 12 (1980) 1051–1055. [https://doi.org/10.1016/0021-9614\(80\)90160-3](https://doi.org/10.1016/0021-9614(80)90160-3).
- [420] M.P. Rolemberg, M.A. Krähenbühl, Vapor–Liquid Equilibria of Binary and Ternary Mixtures of Benzene, Cyclohexane, and Chlorobenzene at 40.0 kPa and 101.3 kPa, *J. Chem. Eng. Data.* 46 (2001) 256–260. <https://doi.org/10.1021/je000059l>.
- [421] R. Tanaka, S. Murakami, R. Fujishiro, Excess enthalpies of mixing of a polar liquid + a non-polar liquid at 298.15 K, *J. Chem. Thermodyn.* 6 (1974) 209–218. [https://doi.org/10.1016/0021-9614\(74\)90172-4](https://doi.org/10.1016/0021-9614(74)90172-4).
- [422] K. Amaya, Thermodynamical Studies on Binary Systems Consisting of Polar and Non-polar Liquids. II. The Measurement of the Heats of Mixing for Binary Systems of Polar and Non-polar Liquids, *Bull. Chem. Soc. Jpn.* 34 (1961) 1278–1285. <https://doi.org/10.1246/bcsj.34.1278>.
- [423] A.V. Anantaraman, S.N. Bhattacharyya, S.R. Palit, Weak dipolar interaction in solutions. Systems: cyclohexane+chlorobenzene and carbon tetrachloride+chlorobenzene, *Trans. Faraday Soc.* 57 (1961) 40. <https://doi.org/10.1039/tf9615700040>.
- [424] J. Munoz Embid, C. Berro, S. Otin, H.V. Kehiaian, Isothermal vapor-liquid equilibria, excess enthalpies, and excess volumes of 1-chlorobutane + tetrachloromethane, 1,2-dichloroethane + tetrachloromethane, and 1,2-dichloroethane + 1-chlorobutane mixtures, *J. Chem. Eng. Data.* 35 (1990) 266–271. <https://doi.org/10.1021/je00061a012>.
- [425] Y. Azpiazu, F. Royo, C. Gutiérrez-Losa, Vapour pressures of (tetrachloromethane +  $\alpha,\omega$ -dichloroalkane), *J. Chem. Thermodyn.* 16 (1984) 561–565. [https://doi.org/10.1016/0021-9614\(84\)90007-7](https://doi.org/10.1016/0021-9614(84)90007-7).
- [426] M. Sagnes, V. Sanchez, Vapor-liquid equilibria for fourteen systems consisting of chlorinated hydrocarbons and alcohols, *J. Chem. Eng. Data.* 16 (1971) 351–354. <https://doi.org/10.1021/je60050a038>.
- [427] I. Baños, J. Valero, M. Gracia, C.G. Losa, Conformational Equilibrium and Calorimetric Behaviour of Systems Containing 1,2-Dichloroethane, *Berichte Bunsenges. Für Phys. Chem.* 87 (1983) 866–871. <https://doi.org/10.1002/bbpc.19830871007>.
- [428] B. Marongiu, Excess Enthalpies of  $\alpha,\omega$ -Dichloroalkane (C1 - C6) + Tetrachloromethane, *Int Data Ser Sel Data Mix. Ser A.* (1988) 1–6.
- [429] E. Wilhelm, A. Faradjzadeh, J.-P.E. Grolier, Molar excess heat capacities and excess volumes of 1,2-dichloroethane + cyclooctane, + mesitylene, and + tetrachloromethane, *J. Chem. Thermodyn.* 11 (1979) 979–984. [https://doi.org/10.1016/0021-9614\(79\)90047-8](https://doi.org/10.1016/0021-9614(79)90047-8).
- [430] S.R.M. Ellis, R.M. Contractor, Vapor-liquid equilibria at reduced pressure, *Chem Eng Lond.* 15 (1964) 10–13.
- [431] A.P. Rollet, P. Toledano, G. Elkaim, M. Sonez, Ebulliometry of volatile solutes. II, *Publ Sci Univ Alger Ser B.* 2 (1956) 403–425.
- [432] H. Tschamler, Über binäre flüssige Mischungen VI: Mischungswärmen, Molwärmern, Volumeeffekte und Zustands-diagramme von 1,2-Dichloräthan mit Benzol und n-Alkylbenzolen, *Monatshefte Für Chem.* 79 (1948) 499–507. <https://doi.org/10.1007/BF00898687>.
- [433] J. Ortega, J. Placido, Excess enthalpies of 12 binary liquid mixtures of  $\alpha,\omega$ -dichloroalkanes (C2, C4, C6) + benzene, toluene, ethylbenzene, or butylbenzene at 298.15 K, *ELDATA Int Electron J Phys Chem Data.* 2 (1996) 111–120.
- [434] E. Wilhelm, J.-P.E. Grolier, M.H.K. Ghassemi, Molar Heat Capacities of Binary Liquid Mixtures: 1,2-Dichloroethane + Benzene, + Toluene, and + p-Xylene, *Berichte Bunsenges. Für Phys. Chem.* 81 (1977) 925–930. <https://doi.org/10.1002/bbpc.19770811009>.
- [435] W.R. Parrish, M.J. Hiza, Liquid-Vapor Equilibria in the Nitrogen-Methane System between 95 and 120 K, in: *Adv. Cryog. Eng.*, 1995: pp. 300–308.
- [436] X.H. Han, Y.J. Zhang, Z.J. Gao, Y.J. Xu, Q. Wang, G.M. Chen, Vapor–Liquid Equilibrium for the Mixture Nitrogen (N<sub>2</sub>) + Methane (CH<sub>4</sub>) in the Temperature Range of (110 to 125) K, *J. Chem. Eng. Data.* 57 (2012) 1621–1626. <https://doi.org/10.1021/je201299u>.
- [437] R. Stryjek, P.S. Chapplear, R. Kobayashi, Low-temperature vapor-liquid equilibria of nitrogen-methane system, *J. Chem. Eng. Data.* 19 (1974) 334–339. <https://doi.org/10.1021/je60063a023>.
- [438] M.R. Cines, J.T. Roach, R.J. Hogan, C.H. Roland, Nitrogen-methane vapor-liquid equilibria, *Chem Eng Progr Symp Ser.* 49 (1953) 1–10.
- [439] O.T. Bloomer, J.D. Parent, Liquid-vapor phase behavior of the methane-nitrogen system, *Chem Eng Progr Symp Ser.* 49 (1953) 11–24.
- [440] A.J. Kidnay, R.C. Miller, W.R. Parrish, M.J. Hiza, Liquid-vapour phase equilibria in the N<sub>2</sub>-CH<sub>4</sub> system from 130 to 180 K, *Cryogenics.* 15 (1975) 531–540. [https://doi.org/10.1016/0011-2275\(75\)90149-6](https://doi.org/10.1016/0011-2275(75)90149-6).

- [441] L.W. Brandt, L. Stroud, Phase Equilibria in Natural Gas Systems. Apparatus with Windowed Cell for 800 P.S.I.G. and Temperatures to  $-320^{\circ}$  F., *Ind. Eng. Chem.* 50 (1958) 849–852. <https://doi.org/10.1021/ie50581a046>.
- [442] D.. McClure, K.. Lewis, R.. Miller, L.A.. Staveley, Excess enthalpies and Gibbs free energies for nitrogen + methane at temperatures below the critical point of nitrogen, *J. Chem. Thermodyn.* 8 (1976) 785–792. [https://doi.org/10.1016/0021-9614\(76\)90057-4](https://doi.org/10.1016/0021-9614(76)90057-4).
- [443] R.R. Klein, C.O. Bennett, B.F. Dodge, Experimental heats of mixing for gaseous nitrogen and methane, *AIChE J.* 17 (1971) 958–965. <https://doi.org/10.1002/aic.690170432>.
- [444] E.J.S. Gomes de Azevedo, J.C.G. Calado, Thermodynamics of liquid methane+ethane, *Fluid Phase Equilibria.* 49 (1989) 21–34. [https://doi.org/10.1016/0378-3812\(89\)80003-2](https://doi.org/10.1016/0378-3812(89)80003-2).
- [445] R.C. Miller, A.J. Kidnay, M.J. Hiza, Liquid + vapor equilibria in methane + ethene and in methane + ethane from 150.00 to 190.00 K, *J. Chem. Thermodyn.* 9 (1977) 167–178. [https://doi.org/10.1016/0021-9614\(77\)90082-9](https://doi.org/10.1016/0021-9614(77)90082-9).
- [446] I. Wichterle, R. Kobayashi, Vapor-liquid equilibrium of methane-ethane system at low temperatures and high pressures, *J. Chem. Eng. Data.* 17 (1972) 9–12. <https://doi.org/10.1021/je60052a022>.
- [447] M.S.-W. Wei, T.S. Brown, A.J. Kidnay, E.D. Sloan, Vapor + Liquid Equilibria for the Ternary System Methane + Ethane + Carbon Dioxide at 230 K and Its Constituent Binaries at Temperatures from 207 to 270 K, *J. Chem. Eng. Data.* 40 (1995) 726–731. <https://doi.org/10.1021/je00020a002>.
- [448] J. Davalos, W.R. Anderson, R.E. Phelps, A.J. Kidnay, Liquid-Vapor Equilibria at 250.00K for Systems Containing Methane, Ethane, and Carbon Dioxide, *J. Chem. Eng. Data.* 21 (1976) 81–84. <https://doi.org/10.1021/je60068a030>.
- [449] G. Werner, H. Schuberth, Das Phasengleichgewicht flüssig-flüssig des Systems Benzol/n-Heptan/Acetonitril sowie die Phasengleichgewichte dampfförmig-flüssig der entsprechenden binären Systeme bei  $20,0^{\circ}$  C, *J. Für Prakt. Chem.* 31 (1966) 225–239. <https://doi.org/10.1002/prac.19660310501>.
- [450] K.R. Harris, P.J. Dunlop, Vapour pressures and excess Gibbs energies of mixtures of benzene with chlorobenzene, n-hexane, and n-heptane at  $25^{\circ}$ C, *J. Chem. Thermodyn.* 2 (1970) 805–811. [https://doi.org/10.1016/0021-9614\(70\)90023-6](https://doi.org/10.1016/0021-9614(70)90023-6).
- [451] Y. Sun, W.H. Yen, Vapor Pressures and Excess Gibbs Free Energies of Benzene-Cyclohexane, Benzene-n-Heptane and Cyclohexane-n-Heptane, *Gaodeng Xuexiao Huaxue Xuebao.* 7 (1986) 54–58.
- [452] U. Messow, D. Schuetze, R. Pfestorf, D. Kuchenbecker, K. Suehnel, Thermodynamische Untersuchungen an Lösungsmittel/n-Paraffin-Systemen, *Z Phys Chem Leipz.* 258 (1977) 24–32.
- [453] D.A. Palmer, B.D. Smith, Thermodynamic excess property measurements for acetonitrile-benzene-n-heptane system at  $45^{\circ}$ C, *J. Chem. Eng. Data.* 17 (1972) 71–76. <https://doi.org/10.1021/je60052a037>.
- [454] L.S. Kudryavtseva, H. Viit, O.G. Eisen, Vapor-liquid equilibrium in 1-heptene-heptane, 1-heptene-octane, heptane-octane, benzene-thiophene, benzene-heptane, and thiophene-heptane binary systems at  $55.\text{deg.}$ , *Eesti NSV Tead Akad Toim Keem Geol.* 20 (1971) 292–296.
- [455] D.O. Hanson, M. Van Winkle, Alteration of the relative volatility of hexane-1-hexene by oxygenated and chlorinated solvents, *J. Chem. Eng. Data.* 12 (1967) 319–325. <https://doi.org/10.1021/je60034a009>.
- [456] I. Brown, Liquid-Vapour Equilibria. III. The Systems Benzene- n-heptane, n-Hexane-chlorobenzene, and cyclohexane-nitrobenzene, *Aust. J. Chem.* 5 (1952) 530. <https://doi.org/10.1071/CH9520530>.
- [457] I. Brown, A. Ewald, Liquid-Vapour Equilibria II. The System Benzene-Heptane, *Aust. J. Chem.* 4 (1951) 198. <https://doi.org/10.1071/CH9510198>.
- [458] R.L. Nielsen, J.H. Weber, Vapor-Liquid Equilibria at Subatmospheric Pressures. Binary and Ternary Systems Containing Ethyl Alcohol, Benzene, and n-Heptane., *J. Chem. Eng. Data.* 4 (1959) 145–151. <https://doi.org/10.1021/je60002a011>.
- [459] L. Sieg, Flüssigkeit-Dampf-Gleichgewichte in binären Systemen von Kohlenwasserstoffen verschiedenen Typs: Flüssigkeit-Dampf-Gleichgewichte in binären Systemen von Kohlenwasserstoffen verschiedenen Typs, *Chem. Ing. Tech.* 22 (1950) 322–326. <https://doi.org/10.1002/cite.330221503>.
- [460] T. Michishita, Y. Arai, S. Saito, Vapor-liquid equilibria of hydrocarbons at atmospheric pressure, *Kagaku Kogaku.* 35 (1971) 111–0. <https://doi.org/10.1252/kakoronbunshu1953.35.111>.
- [461] Q. Wang, G. Chen, S. Han, Study on the Vapor-Liquid Equilibria under Pressure for Binary Systems, *Ranliao Huaxue Xuebao.* 18 (1990) 185–192.
- [462] R. Vilcu, F. Stanciu, Excess thermodynamic functions from calorimetric data, *Rev Roum Chim.* 11 (1966) 175–182.
- [463] I. Hammerl, M.T. Raetzsch, Enthalpies of mixing of normal paraffins with aromatics, *Wiss Z Tech Hochsch Chem Leuna-Mersebg.* 15 (1973) 175–178.
- [464] R. Tanaka, Excess heat capacities for mixture of benzene with n-heptane at 293.15, 298.15, and 303.15 K, *J. Chem. Eng. Data.* 32 (1987) 176–177. <https://doi.org/10.1021/je00048a014>.
- [465] M.H. Karbalai Ghassemi, J.P.E. Grolier, Excess heat capacity. Cyclohexane-n-hexane system, *Int Data Ser Sel Data Mix. Ser A.* 1976 (1976) 95–96.

- [466] A. Tasić, B. Djordjević, D. Grozdanić, N. Afgan, D. Malić, Vapour—liquid equilibria of the systems acetone—benzene, benzene—cyclohexane and acetone—cyclohexane at 25°C, *Chem. Eng. Sci.* 33 (1978) 189–197. [https://doi.org/10.1016/0009-2509\(78\)85053-2](https://doi.org/10.1016/0009-2509(78)85053-2).
- [467] R.A. Mentzer, R.A. Greenkorn, K.C. Chao, Bubble pressures and vapor-liquid equilibria for four binary hydrocarbon mixtures, *J. Chem. Thermodyn.* 14 (1982) 817–830. [https://doi.org/10.1016/0021-9614\(82\)90155-0](https://doi.org/10.1016/0021-9614(82)90155-0).
- [468] K. Kurihara, M. Uchiyama, K. Kojima, Isothermal Vapor–Liquid Equilibria for Benzene + Cyclohexane + 1-Propanol and for Three Constituent Binary Systems, *J. Chem. Eng. Data.* 42 (1997) 149–154. <https://doi.org/10.1021/je9602475>.
- [469] T. Boublík, An estimate of limiting values of relative volatility with help of the theorem of corresponding states. II. Binary systems of tetrachloromethane, benzene, and cyclohexane, *Collect. Czechoslov. Chem. Commun.* 28 (1963) 1771–1779. <https://doi.org/10.1135/cccc19631771>.
- [470] G. Scatchard, S.E. Wood, J.M. Mochel, Vapor–Liquid Equilibrium. III. Benzene–Cyclohexane Mixtures., *J. Phys. Chem.* 43 (1939) 119–130. <https://doi.org/10.1021/j150388a009>.
- [471] J. Dong, C. Feng, Y. Li, Isothermal Vapor–Liquid Equilibrium for Methanol and 2,3-Dimethyl-1-butene at 343.06 K, 353.27 K, 363.19 K, and 372.90 K, *J. Chem. Eng. Data.* 56 (2011) 2386–2392. <https://doi.org/10.1021/je101304x>.
- [472] B. Wiśniewska, J. Gregorowicz, S. Malanowski, Development of a vapour-liquid equilibrium apparatus to work at pressures up to 3 MPa, *Fluid Phase Equilibria.* 86 (1993) 173–186. [https://doi.org/10.1016/0378-3812\(93\)87174-Y](https://doi.org/10.1016/0378-3812(93)87174-Y).
- [473] C. Lafuente, J. Pardo, J. Santate, F. Royo, J. Urieta, Use of a Fischer-Labodest apparatus to study the liquid-vapor equilibrium of the benzene-cyclohexane system at different pressures, *Rev Acad Cienc Exact Fis Quim Nat Zaragoza.* 47 (1992) 183–190.
- [474] V.N.K. Rao, D.R. Swami, M.N. Rao, Vapor-liquid equilibria of Benzene–n-hexane and benzene-cyclohexane systems, *AIChE J.* 3 (1957) 191–197. <https://doi.org/10.1002/aic.690030213>.
- [475] K. Elliott, C.J. Wormald, A precision differential flow calorimeter the excess enthalpy of benzene + cyclohexane between 280.15 K and 393.15 K, *J. Chem. Thermodyn.* 8 (1976) 881–893. [https://doi.org/10.1016/0021-9614\(76\)90166-X](https://doi.org/10.1016/0021-9614(76)90166-X).
- [476] W.-D. Yan, R.-S. Lin, W.-H. Yen, Excess enthalpies of seven binary liquid systems, *Thermochim. Acta.* 169 (1990) 171–184. [https://doi.org/10.1016/0040-6031\(90\)80143-M](https://doi.org/10.1016/0040-6031(90)80143-M).
- [477] S. Didaoui-Nemouchi, A. Ait-Kaci, M. Rogalski, Enthalpies of mixing of binary and ternary mixtures containing diisopropylether, benzene and cyclohexane at 303.15 K, *J. Therm. Anal. Calorim.* 79 (2005) 85–88. <https://doi.org/10.1007/s10973-004-0566-5>.
- [478] H.C. van Ness, M.M. Abbott, Excess enthalpy. Benzene-cyclohexane system, *Int Data Ser Sel Data Mix. Ser A.* 1974 (1974) 160–161.
- [479] J. Lohmann, R. Bölts, J. Gmehling, Excess Enthalpy Data for Seven Binary Systems at Temperatures between 50 and 140 °C, *J. Chem. Eng. Data.* 46 (2001) 208–211. <https://doi.org/10.1021/je000297g>.
- [480] R. Tanaka, Determination of excess heat capacities of (benzene + tetrachloromethane and + cyclohexane) between 293.15 and 303.15 K by use of a Picker flow calorimeter, *J. Chem. Thermodyn.* 14 (1982) 259–268. [https://doi.org/10.1016/0021-9614\(82\)90016-7](https://doi.org/10.1016/0021-9614(82)90016-7).
- [481] R. Páramo, M. Zouine, C. Casanova, New Batch Cells Adapted To Measure Saturated Heat Capacities of Liquids, *J. Chem. Eng. Data.* 47 (2002) 441–448. <https://doi.org/10.1021/je0155103>.
- [482] P.J. D'arcy, J.D. Hazlett, O. Kiyohara, G.C. Benson, Excess heat capacities of mixtures of benzene with cyclohexane at 298.15 K, *Thermochim. Acta.* 21 (1977) 297–300. [https://doi.org/10.1016/0040-6031\(77\)85030-2](https://doi.org/10.1016/0040-6031(77)85030-2).
- [483] J.-P.E. Grolier, E. Wilhelm, M.H. Hamed, Molar Heat Capacity and Isothermal Compressibility of Binary Liquid Mixtures: Carbon Tetrachloride + Benzene, Carbon Tetrachloride + Cyclohexane and Benzene + Cyclohexane, *Berichte Bunsenges. Für Phys. Chem.* 82 (1978) 1282–1290. <https://doi.org/10.1002/bbpc.19780821204>.
- [484] J.C.G. Calado, V.A.M. Soares, Thermodynamics of liquid ethylene + xenon at 161.38 K, *J. Chem. Thermodyn.* 9 (1977) 911–913. [https://doi.org/10.1016/0021-9614\(77\)90176-8](https://doi.org/10.1016/0021-9614(77)90176-8).
- [485] M. Nunes da Ponte, D. Chokappa, J.C.G. Calado, J. Zollweg, W.B. Streett, Vapor-liquid equilibrium in the xenon + ethene system, *J Phys Chem.* 90 (1986) 1147–1152. <https://doi.org/10.1021/j100278a037>.
- [486] A. Lainez, L.P. Rebelo, J.C. Calado, W. Streett, J. Zollweg, Excess enthalpies of liquid (ethene + xenon) at 162.9 K, *J. Chem. Thermodyn.* 19 (1987) 35–38. [https://doi.org/10.1016/0021-9614\(87\)90159-5](https://doi.org/10.1016/0021-9614(87)90159-5).
- [487] W. Wu, J. Ke, M. Poliakoff, Phase Boundaries of CO<sub>2</sub> + Toluene, CO<sub>2</sub> + Acetone, and CO<sub>2</sub> + Ethanol at High Temperatures and High Pressures, *J. Chem. Eng. Data.* 51 (2006) 1398–1403. <https://doi.org/10.1021/je060099a>.

- [488] P. Naidoo, D. Ramjugernath, J.D. Raal, A new high-pressure vapour–liquid equilibrium apparatus, *Fluid Phase Equilibria*. 269 (2008) 104–112. <https://doi.org/10.1016/j.fluid.2008.05.002>.
- [489] J.C. Zhang, X.Y. Wu, W.L. Cao, Phase Equilibrium Properties of Supercritical Carbon Dioxide in Binary System, *Gaodeng Xuexiao Huaxue Xuebao*. 23 (2002) 10–13.
- [490] J.H. Hong, R. Kobayashi, Multicomponent vapor-liquid equilibria measurements for the development of an extractive distillation process for the processing of gas issuing from a carbon dioxide/EOR project, *Ind Eng Chem Process Des. Dev.* 25 (1986) 584–589. <https://doi.org/10.1021/i200033a041>.
- [491] S.D. Fink, H.C. Hershey, Modeling the vapor-liquid equilibria of 1,1,1-trichloroethane + carbon dioxide and toluene + carbon dioxide at 308, 323, and 353 K, *Ind. Eng. Chem. Res.* 29 (1990) 295–306. <https://doi.org/10.1021/ie00098a022>.
- [492] S.D. Park, C.H. Kim, C.S. Choi, Phase equilibria and mixture densities measurements of carbon dioxide-toluene system under high pressure, *Hwahak Konghak*. 28 (1990) 438–443.
- [493] C.-H. Kim, P. Vimalchand, M.D. Donohue, Vapor-liquid equilibria for binary mixtures of carbon dioxide with benzene, toluene and p-xylene, *Fluid Phase Equilibria*. 31 (1986) 299–311. [https://doi.org/10.1016/0378-3812\(86\)87014-5](https://doi.org/10.1016/0378-3812(86)87014-5).
- [494] W.O. Morris, M.D. Donohue, Vapor-liquid equilibria in mixtures containing carbon dioxide, toluene, and 1-methylnaphthalene, *J. Chem. Eng. Data*. 30 (1985) 259–263. <https://doi.org/10.1021/je00041a007>.
- [495] H.-J. Ng, D.B. Robinson, Equilibrium-phase properties of the toluene-carbon dioxide system, *J. Chem. Eng. Data*. 23 (1978) 325–327. <https://doi.org/10.1021/je60079a020>.
- [496] C. Wormald, J. Eyears, Excess molar enthalpies and excess molar volumes of  $\{x\text{CO}_2 + (1-x)\text{C}_6\text{H}_5\text{CH}_3\}$  at 298.15, 304.10, and 308.15 K from 7.5 to 12.6 MPa, *J. Chem. Thermodyn.* 19 (1987) 845–856. [https://doi.org/10.1016/0021-9614\(87\)90031-0](https://doi.org/10.1016/0021-9614(87)90031-0).
- [497] D. Cordray, J. Christensen, R. Izatt, The excess enthalpies of (carbon dioxide + toluene) at 308.15, 358.15, and 573.15 K from 6.98 to 16.63 MPa, *J. Chem. Thermodyn.* 18 (1986) 647–656. [https://doi.org/10.1016/0021-9614\(86\)90066-2](https://doi.org/10.1016/0021-9614(86)90066-2).
- [498] C. Pando, J.A. Renuncio, R. Schofield, R. Izatt, J. Christensen, The excess enthalpies of (carbon dioxide + toluene) at 308.15, 385.15, and 413.15 K from 7.60 to 12.67 MPa, *J. Chem. Thermodyn.* 15 (1983) 747–755. [https://doi.org/10.1016/0021-9614\(83\)90141-6](https://doi.org/10.1016/0021-9614(83)90141-6).
- [499] J. Christensen, D. Zebolsky, R. Izatt, The excess enthalpies of (carbon dioxide + toluene) at 470.15 and 573.15 K from 7.60 to 12.67 MPa, *J. Chem. Thermodyn.* 17 (1985) 1–10. [https://doi.org/10.1016/0021-9614\(85\)90025-4](https://doi.org/10.1016/0021-9614(85)90025-4).
- [500] J.T. Reaves, A.T. Griffith, C.B. Roberts, Critical Properties of Dilute Carbon Dioxide + Entrainer and Ethane + Entrainer Mixtures, *J. Chem. Eng. Data*. 43 (1998) 683–686. <https://doi.org/10.1021/je9702753>.
- [501] H. Zhang, Z. Liu, B. Han, Critical points and phase behavior of toluene-CO<sub>2</sub> and toluene-H<sub>2</sub>-CO<sub>2</sub> mixture in CO<sub>2</sub>-rich region, *J. Supercrit. Fluids*. 18 (2000) 185–192. [https://doi.org/10.1016/S0896-8446\(00\)00081-4](https://doi.org/10.1016/S0896-8446(00)00081-4).
- [502] R. Jiménez-Gallegos, L.A. Galicia-Luna, O. Elizalde-Solis, Experimental Vapor–Liquid Equilibria for the Carbon Dioxide + Octane and Carbon Dioxide + Decane Systems, *J. Chem. Eng. Data*. 51 (2006) 1624–1628. <https://doi.org/10.1021/je060111z>.
- [503] Y. Iwai, N. Hosotani, T. Morotomi, Y. Koga, Y. Arai, High-Pressure Vapor-Liquid Equilibria for Carbon Dioxide + Linalool, *J. Chem. Eng. Data*. 39 (1994) 900–902. <https://doi.org/10.1021/je00016a059>.
- [504] N. Nagarajan, R.L. Robinson, Equilibrium phase compositions, phase densities, and interfacial tensions for carbon dioxide + hydrocarbon systems. 2. Carbon dioxide + n-decane, *J. Chem. Eng. Data*. 31 (1986) 168–171. <https://doi.org/10.1021/je00044a012>.
- [505] H.H. Reamer, B.H. Sage, Phase Equilibria in Hydrocarbon Systems. Volumetric and Phase Behavior of the n-Decane-CO<sub>2</sub> System., *J. Chem. Eng. Data*. 8 (1963) 508–513. <https://doi.org/10.1021/je60019a010>.
- [506] H. Inomata, K. Tuchiya, K. Arai, S. Saito, Measurement of vapor-liquid equilibria at elevated temperatures and pressures using a flow type apparatus., *J. Chem. Eng. Jpn.* 19 (1986) 386–391. <https://doi.org/10.1252/jcej.19.386>.
- [507] H.M. Sebastian, J.J. Simnick, H.-M. Lin, K.-C. Chao, Vapor-liquid equilibrium in binary mixtures of carbon dioxide + n-decane and carbon dioxide + n-hexadecane, *J. Chem. Eng. Data*. 25 (1980) 138–140. <https://doi.org/10.1021/je60085a012>.
- [508] C. Pando, J.A.R. Renuncio, T.A. McFall, R.M. Izatt, J.J. Christensen, The excess enthalpies of (carbon dioxide + decane) from 283.15 to 323.15 K at 7.58 MPa, *J. Chem. Thermodyn.* 15 (1983) 173–180. [https://doi.org/10.1016/0021-9614\(83\)90157-X](https://doi.org/10.1016/0021-9614(83)90157-X).
- [509] J.J. Christensen, D. Cordray, R.M. Izatt, The excess enthalpies of (carbon dioxide + decane) from 293.15 to 573.15 K at 12.50 MPa, *J. Chem. Thermodyn.* 18 (1986) 53–61. [https://doi.org/10.1016/0021-9614\(86\)90043-1](https://doi.org/10.1016/0021-9614(86)90043-1).

- [510] G.S. Gurdial, N.R. Foster, S.L.J. Yun, K.D. Tilly, Phase Behavior of Supercritical Fluid—Entrainer Systems, in: *Supercrit. Fluid Eng. Sci.*, 1992: pp. 34–45.
- [511] E. Gulari, H. Saad, Y.C. Bae, Effect of Critical Phenomena on Transport Properties in the Supercritical Region, in: *Supercrit. Fluids*, 1987: pp. 2–14.
- [512] N. Juntarachat, S. Bello, R. Privat, J.-N. Jaubert, Validation of a new apparatus using the dynamic method for determining the critical properties of binary mixtures containing CO<sub>2</sub> and a n-alkane, *Fluid Phase Equilibria*. 325 (2012) 66–70. <https://doi.org/10.1016/j.fluid.2012.04.010>.
- [513] N.G. Polikhronidi, R.G. Batyrova, I.M. Abdulgatov, G.V. Stepanov, Isochoric Heat Capacity of CO<sub>2</sub> + n-Decane Mixtures in the Critical Region, *Int. J. Thermophys.* 27 (2006) 729–759. <https://doi.org/10.1007/s10765-006-0056-z>.
- [514] S.C. Mraw, S.-C. Hwang, R. Kobayashi, Vapor-liquid equilibrium of the methane-carbon dioxide system at low temperatures, *J. Chem. Eng. Data*. 23 (1978) 135–139. <https://doi.org/10.1021/je60077a014>.
- [515] T.A. Al-Sahhaf, A.J. Kidnay, E.D. Sloan, Liquid + vapor equilibria in the nitrogen + carbon dioxide + methane system, *Ind. Eng. Chem. Fundam.* 22 (1983) 372–380. <https://doi.org/10.1021/i100012a004>.
- [516] F.A. Somait, A.J. Kidnay, Liquid-vapor equilibria at 270.00 K for systems containing nitrogen, methane, and carbon dioxide, *J. Chem. Eng. Data*. 23 (1978) 301–305. <https://doi.org/10.1021/je60079a019>.
- [517] N. Xu, J. Dong, Y. Wang, J. Shi, High pressure vapor liquid equilibria at 293 K for systems containing nitrogen, methane and carbon dioxide, *Fluid Phase Equilibria*. 81 (1992) 175–186. [https://doi.org/10.1016/0378-3812\(92\)85150-7](https://doi.org/10.1016/0378-3812(92)85150-7).
- [518] N. Xu, J. Dong, Y. Wang, J. Shi, Vapor Liquid Equilibria For N<sub>2</sub>-CH<sub>4</sub>-CO<sub>2</sub> System Near Critical Region, *Huagong Xuebao*. 43 (1992) 640–644.
- [519] J.I. Lee, A.E. Mather, The excess enthalpy of gaseous mixtures of carbon dioxide with methane, *Can. J. Chem. Eng.* 50 (1972) 95–100. <https://doi.org/10.1002/cjce.5450500117>.
- [520] A.O. Barry, S.C. Kaliaguine, R.S. Ramalho, Direct determination of enthalpy of mixing for the binary gaseous system methane-carbon dioxide by an isothermal flow calorimeter, *J. Chem. Eng. Data*. 27 (1982) 258–264. <https://doi.org/10.1021/je00029a010>.
- [521] Y. Arai, G.-I. Kaminishi, S. Saito, The Experimental Determination Of The P-V-T-X Relations For The Carbon Dioxide-Nitrogen And The Carbon Dioxide-Methane Systems, *J. Chem. Eng. Jpn.* 4 (1971) 113–122. <https://doi.org/10.1252/jcej.4.113>.
- [522] S.C. Mraw, S.C. Hwang, R. Kobayashi, The Vapor-Liquid Equilibrium of the CH<sub>4</sub> - CO<sub>2</sub> System at Low Temperatures, *GPA Res. Rep.* (1977) 1–18.
- [523] S.C. Hwang, H.M. Lin, P.S. Chappellear, R. Kobayashi, Dew-Point Values for the Methane - Carbon Dioxide System, *GPA Res. Rep.* (1976) 1–14.
- [524] N.N. Shah, J.A. Zollweg, W.B. Streett, Vapor-liquid equilibrium in the system carbon dioxide + cyclopentane from 275 to 493 K at pressures to 12.2 MPa, *J. Chem. Eng. Data*. 36 (1991) 188–192. <https://doi.org/10.1021/je00002a014>.
- [525] C.J. Eckert, S.I. Sandler, Vapor-liquid equilibria for the carbon dioxide-cyclopentane system at 37.7, 45.0, and 60.0.degree.C, *J. Chem. Eng. Data*. 31 (1986) 26–28. <https://doi.org/10.1021/je00043a008>.
- [526] Zhang Zhanzhu, Guo Liping, Yang Xiadong, H. Knapp, Vapor And Liquid Equilibrium For Nitrogen - Ethane - Carbon Dioxide Ternary System, *Huagong Xuebao*. 50 (1999) 392–398.
- [527] B. Yucelen, A.J. Kidnay, Vapor–Liquid Equilibria in the Nitrogen + Carbon Dioxide + Propane System from 240 to 330 K at Pressures to 15 MPa, *J. Chem. Eng. Data*. 44 (1999) 926–931. <https://doi.org/10.1021/je980321e>.
- [528] T.S. Brown, E.D. Sloan, A.J. Kidnay, Vapor-liquid equilibria for the ternary system N<sub>2</sub> + CO<sub>2</sub> + n-C<sub>4</sub>H<sub>10</sub> at 250 and 270 K, *Int. J. Thermophys.* 15 (1994) 1211–1219. <https://doi.org/10.1007/BF01458829>.
- [529] T.S. Brown, V.G. Niesen, E.D. Sloan, A.J. Kidnay, Vapor-liquid equilibria for the binary systems of nitrogen, carbon dioxide, and n-butane at temperatures from 220 to 344 K., *Fluid Phase Equilibria*. 53 (1989) 7–14. [https://doi.org/10.1016/0378-3812\(89\)80067-6](https://doi.org/10.1016/0378-3812(89)80067-6).
- [530] T.A. Al-Sahhaf, Vapor—liquid equilibria for the ternary system N<sub>2</sub> + CO<sub>2</sub> + CH<sub>4</sub> at 230 and 250 K, *Fluid Phase Equilibria*. 55 (1990) 159–172. [https://doi.org/10.1016/0378-3812\(90\)85010-8](https://doi.org/10.1016/0378-3812(90)85010-8).
- [531] M. Yorizane, S. Yoshimura, H. Masuoka, Vapor liquid equilibrium at high pressures. N<sub>2</sub>-CO<sub>2</sub>, H<sub>2</sub>-CO<sub>2</sub> systems, *Kagaku Kogaku*. 34 (1970) 953–957. <https://doi.org/10.1252/kakoronbunshu1953.34.953>.
- [532] G.H. Zenner, L.I. Dana, Liquid-vapor equilibrium compositions of carbon dioxide-oxygen-nitrogen mixtures, *Chem Eng Progr Symp Ser.* 59 (1963) 36–41.
- [533] G.I. Kaminishi, T. Toriumi, Gas-liquid equilibrium under high pressures. VI. Vapor-liquid phase equilibrium in the CO<sub>2</sub>-H<sub>2</sub>, CO<sub>2</sub>-N<sub>2</sub>, and CO<sub>2</sub>-O<sub>2</sub> systems, *Kogyo Kagaku Zasshi*. 69 (1966) 175–178.
- [534] I.R. Krichevskii, N.E. Khazanova, L.S. Lesnevskaya, L.Y. Sandalova, Liquid-gas equilibrium in the nitrogen-carbon dioxide system under elevated pressures, *Khim Promst Mosc.* (1962) 169–171.

- [535] B. Bian, Y. Wang, J. Shi, E. Zhao, B.C.-Y. Lu, Simultaneous determination of vapor-liquid equilibrium and molar volumes for coexisting phases up to the critical temperature with a static method, *Fluid Phase Equilibria*. 90 (1993) 177–187. [https://doi.org/10.1016/0378-3812\(93\)85012-B](https://doi.org/10.1016/0378-3812(93)85012-B).
- [536] J.I. Lee, A.E. Mather, Excess enthalpy of gaseous mixtures of nitrogen and carbon dioxide, *J. Chem. Eng. Data*. 17 (1972) 189–192. <https://doi.org/10.1021/je60053a042>.
- [537] A.V. Hejmadi, D.L. Katz, J.E. Powers, Experimental determination of the enthalpy of mixing of N + CO<sub>2</sub> under pressure, *J. Chem. Thermodyn.* 3 (1971) 483–496. [https://doi.org/10.1016/S0021-9614\(71\)80030-7](https://doi.org/10.1016/S0021-9614(71)80030-7).
- [538] H.H. Reamer, B.H. Sage, W.N. Lacey, Phase Equilibria in Hydrocarbon Systems - Volumetric and Phase Behavior of the Methane-Hydrogen Sulfide System, *Ind. Eng. Chem.* 43 (1951) 976–981. <https://doi.org/10.1021/ie50496a052>.
- [539] J.P. Kohn, F. Kurata, Heterogeneous phase equilibria of the methane—hydrogen sulfide system, *AIChE J.* 4 (1958) 211–217. <https://doi.org/10.1002/aic.690040217>.
- [540] A.O. Barry, S.C. Kaliaguine, R.S. Ramalho, Excess enthalpies of the binary system methane-hydrogen sulfide by flow calorimetry, *J. Chem. Eng. Data*. 27 (1982) 436–439. <https://doi.org/10.1021/je00030a020>.
- [541] D.J. Fall, K.D. Luks, Phase equilibria behavior of the systems carbon dioxide + n-dotriacontane and carbon dioxide + n-docosane, *J. Chem. Eng. Data*. 29 (1984) 413–417. <https://doi.org/10.1021/je00038a013>.
- [542] F.N. Tsai, J.S. Yau, Solubility of carbon dioxide in n-tetracosane and in n-dotriacontane, *J. Chem. Eng. Data*. 35 (1990) 43–45. <https://doi.org/10.1021/je00059a014>.
- [543] M. Spee, G.M. Schneider, Fluid phase equilibrium studies on binary and ternary mixtures of carbon dioxide with hexadecane, 1-dodecanol, 1,8-octanediol and dotriacontane at 393.2 K and at pressures up to 100 MPa, *Fluid Phase Equilibria*. 65 (1991) 263–274. [https://doi.org/10.1016/0378-3812\(91\)87029-9](https://doi.org/10.1016/0378-3812(91)87029-9).
- [544] J.J. Segovia, M.C. Martín, C. R. Chamorro, E.A. Montero, M.A. Villamañán, Excess thermodynamic functions for ternary systems containing fuel oxygenates and substitution hydrocarbons: 2. Total-pressure data and GE for methyl tert-butyl ether/n-heptane/1-hexene at 313.15 K This paper is part of the doctoral thesis of J.J. Segovia.1, *Fluid Phase Equilibria*. 152 (1998) 265–276. [https://doi.org/10.1016/S0378-3812\(98\)00384-7](https://doi.org/10.1016/S0378-3812(98)00384-7).
- [545] J.D. Lee, T.J. Lee, S.J. Park, Infinite dilution activity coefficients and vapor-liquid equilibria for the binary systems containing MTBE, *Hwahak Konghak*. 33 (1995) 527–534.
- [546] J. Wisniak, E. Magen, M. Shachar, I. Zeroni, R. Reich, H. Segura, Isobaric Vapor–Liquid Equilibria in the Systems Methyl 1,1-Dimethylethyl Ether + Hexane and + Heptane, *J. Chem. Eng. Data*. 42 (1997) 243–247. <https://doi.org/10.1021/je960301h>.
- [547] E. Tusel-Langer, J.M. Garcia Alonso, M.A. Villamañán Olfos, R.N. Lichtenthaler, Excess enthalpies of mixtures containing n-heptane, methanol and methyl tert-butyl ether (MTBE), *J. Solut. Chem.* 20 (1991) 153–163. <https://doi.org/10.1007/BF00651647>.
- [548] K. Han, S. Xia, P. Ma, F. Yan, T. Liu, Measurement of critical temperatures and critical pressures for binary mixtures of methyl tert-butyl ether (MTBE)+alcohol and MTBE+alkane, *J. Chem. Thermodyn.* 62 (2013) 111–117. <https://doi.org/10.1016/j.jct.2013.03.002>.
- [549] A.D. Carr, H.W. Kropholler, Vapor Liquid Equilibria at Atmospheric Pressure. Binary Systems of Ethyl Acetate-Benzene, Ethyl Acetate-Toluene, and Ethyl Acetate-p-Xylene, *J. Chem. Eng. Data*. 7 (1962) 26–28. <https://doi.org/10.1021/je60012a007>.
- [550] S. Delcros, E. Jiménez, L. Romani, A.H. Roux, J.-P.E. Grolier, H.V. Kehiaian, Linear alkanolates + aromatic hydrocarbon binary mixtures: new excess enthalpy measurements and DISQUAC analysis of thermodynamic properties, *Fluid Phase Equilibria*. 111 (1995) 71–88. [https://doi.org/10.1016/0378-3812\(95\)02838-6](https://doi.org/10.1016/0378-3812(95)02838-6).
- [551] J. Gmehling, B. Meents, Excess enthalpy. Ethyl ethanoate-toluene system, *Int Data Ser Sel Data Mix. Ser A*. (1992) 177.
- [552] E. Jiménez, Excess heat capacities and excess volumes of (an n-alkylalkanoate + heptane or decane or toluene), *J. Chem. Thermodyn.* 26 (1994) 817–827. <https://doi.org/10.1006/jcht.1994.1098>.
- [553] M. Steinbrecher, H.-J. Bittrich, Das isotherme Flüssigkeits-Dampf-Gleichgewicht der binären Systeme zwischen den Komponenten Tetrachlormethan, Äthylacetat und Dioxan, *Z. Für Phys. Chem.* 2320 (1966). <https://doi.org/10.1515/zpch-1966-23228>.
- [554] J. Drobige, E. Lindenau, A new apparatus to determine the isothermal liquid-vapor equilibrium, *Wiss Z Tech Hochsch Chem Leuna-Mersebg.* 8 (1966) 144–147.
- [555] M.D. Guillen, C. Gutierrez Losa, Excess enthalpies and excess volumes of n-hexane + and of tetrachloromethane + furan, + 1,4-dioxane, + tetrahydrofuran, and + tetrahydropyran, *J. Chem. Thermodyn.* 10 (1978) 567–576. [https://doi.org/10.1016/0021-9614\(78\)90045-9](https://doi.org/10.1016/0021-9614(78)90045-9).

- [556] S. Murakami, G.C. Benson, An isothermal dilution calorimeter for measuring enthalpies of mixing, *J. Chem. Thermodyn.* 1 (1969) 559–572. [https://doi.org/10.1016/0021-9614\(69\)90016-0](https://doi.org/10.1016/0021-9614(69)90016-0).
- [557] F. Becker, M. Kiefer, H. Koukol, Kontinuierliche Bestimmung von Mischungswärmen durch quasi-isotherme Wärmeflußkalorimetrie, *Z Phys Chem NF.* 80 (1972) 29–43.
- [558] I. McKinnon, A. Williamson, Heats of mixing of CCl<sub>4</sub> with dioxane, *Aust. J. Chem.* 17 (1964) 1374. <https://doi.org/10.1071/CH9641374>.
- [559] T. Ohta, J. Koyabu, I. Nagata, Vapor–liquid equilibria for the ternary Ethanol–2-butanone–benzene system at 298.15 K, *Fluid Phase Equilibria.* 7 (1981) 65–73. [https://doi.org/10.1016/0378-3812\(81\)87006-9](https://doi.org/10.1016/0378-3812(81)87006-9).
- [560] M. Diaz Peña, A. Crespo Colin, A. Compostizo, Isothermal liquid-vapour equilibria 2. The binary systems formed by benzene + acetone, + methyl ethyl ketone, + methyl propyl ketone, and + methyl isobutyl ketone, *J. Chem. Thermodyn.* 10 (1978) 1101–1106. [https://doi.org/10.1016/0021-9614\(78\)90084-8](https://doi.org/10.1016/0021-9614(78)90084-8).
- [561] V.N. Kumarkrishna Rao, D.R. Swami, M. Narasinga Rao, High-pressure vapor-liquid equilibria of nonideal solutions. II. Benzene-methyl ethyl ketone system, *J Sci Ind Res Sect B.* 16 (1957) 195–201.
- [562] O. Kiyohara, G.C. Benson, J.-P.E. Grolier, Thermodynamic properties of binary mixtures containing ketones I. Excess enthalpies of some aliphatic ketones + n-hexane, + benzene, and + tetrachloromethane, *J. Chem. Thermodyn.* 9 (1977) 315–323. [https://doi.org/10.1016/0021-9614\(77\)90052-0](https://doi.org/10.1016/0021-9614(77)90052-0).
- [563] C.R. Chamorro, J.J. Segovia, M.C. Martín, E.A. Montero, M.A. Villamañán, Phase equilibrium properties of binary and ternary systems containing tert-amylmethyl ether (TAME) as oxygenate additive and gasoline substitution hydrocarbons at 313.15 K, *Fluid Phase Equilibria.* 156 (1999) 73–87. [https://doi.org/10.1016/S0378-3812\(99\)00033-3](https://doi.org/10.1016/S0378-3812(99)00033-3).
- [564] A. Mejía, H. Segura, M. Cartes, Vapor–Liquid Equilibrium in the Binary Systems 2-Butanol + tert-Amyl Methyl Ether, 2-Butanol + Heptane, and Heptane + tert-Amyl Methyl Ether, *J. Chem. Eng. Data.* 56 (2011) 2256–2265. <https://doi.org/10.1021/je101250d>.
- [565] K. Kammerer, R.N. Lichtenthaler, Excess enthalpy HE of binary mixtures containing alkanes, methanol and tert-amyl-methyl ether (TAME), *Thermochim. Acta.* 271 (1996) 49–58. [https://doi.org/10.1016/0040-6031\(95\)02588-X](https://doi.org/10.1016/0040-6031(95)02588-X).
- [566] Z. Tong, G.C. Benson, L.L. Wang, B.C.-Y. Lu, Excess Enthalpies of Ternary Mixtures Consisting of a Normal Alkane, Methyl tert-Butyl Ether, and tert-Amyl Methyl Ether, *J. Chem. Eng. Data.* 41 (1996) 865–869. <https://doi.org/10.1021/je960078o>.
- [567] D.G. Vorenberg, J.D. Raal, D. Ramjugernath, Vapor–Liquid Equilibrium Measurements of MTBE and TAME with Toluene, *J. Chem. Eng. Data.* 50 (2005) 56–59. <https://doi.org/10.1021/je049867t>.
- [568] J. Plura, J. Matouš, J.P. Novák, J. Šobr, Vapour-liquid equilibrium in the methyl tert-butyl ether-n-hexane and methyl tert-butyl ether-toluene systems, *Collect. Czechoslov. Chem. Commun.* 44 (1979) 3627–3631. <https://doi.org/10.1135/cccc19793627>.
- [569] R. Reich, M. Cartes, J. Wisniak, H. Segura, Phase Equilibria in the Systems Methyl 1,1-Dimethylethyl Ether + Benzene and + Toluene, *J. Chem. Eng. Data.* 43 (1998) 299–303. <https://doi.org/10.1021/je970248c>.
- [570] T.M. Letcher, U. Domańska, Excess molar enthalpies of (2,2,4-trimethylpentane, or 1-heptene, or 1-hexene, or toluene+methyl 1,1-dimethylethyl ether) and of (1-heptene, or 1-hexene, or toluene+1,1-dimethylpropyl ether) at the temperatures 298.15 K and 308.15 K, *J. Chem. Thermodyn.* 29 (1997) 721–730. <https://doi.org/10.1006/jcht.1997.0198>.
- [571] V.G. Niesen, V.F. Yesavage, Vapor-liquid equilibria for m-cresol/tetralin and tetralin/quinoline at temperatures between 523 and 598 K, *J. Chem. Eng. Data.* 33 (1988) 253–258. <https://doi.org/10.1021/je00053a009>.
- [572] S. Mahmood, Q. Zhao, V.N. Kabadi, High-Temperature VLE for the Tetralin–Quinoline System, *J. Chem. Eng. Data.* 46 (2001) 994–999. <https://doi.org/10.1021/je000069m>.
- [573] J. Mollerup, Vapour/liquid equilibrium in ethylene + carbon dioxide and ethane + carbon dioxide, *J. Chem. Soc. Faraday Trans. 1 Phys. Chem. Condens. Phases.* 71 (1975) 2351. <https://doi.org/10.1039/f19757102351>.
- [574] K. Nagahama, H. Konishi, D. Hoshino, M. Hirata, Binary Vapor-Liquid Equilibria Of Carbon Dioxide-Light Hydrocarbons At Low Temperature, *J. Chem. Eng. Jpn.* 7 (1974) 323–328. <https://doi.org/10.1252/jcej.7.323>.
- [575] H.K. Bae, K. Nagahama, M. Hirata, Isothermal vapor-liquid equilibria for the ethylene-carbon dioxide system at high pressure, *J. Chem. Eng. Data.* 27 (1982) 25–27. <https://doi.org/10.1021/je00027a007>.
- [576] G.G. Haselden, D.M. Newitt, S.M. Shah, Two-Phase Equilibrium in Binary and Ternary Systems. V. Carbon Dioxide-Ethylene. VI. Carbon Dioxide-Propylene, *Proc. R. Soc. Math. Phys. Eng. Sci.* 209 (1951) 1–14. <https://doi.org/10.1098/rspa.1951.0183>.

- [577] C.J. Wormald, J.M. Eyears, Excess molar enthalpies of (carbon dioxide + ethene) in the liquid and near-critical regions, *J. Chem. Thermodyn.* 33 (2001) 775–786. <https://doi.org/10.1006/jcht.2000.0778>.
- [578] J.S. Rowlinson, J.R. Sutton, J.F. Weston, Liquid-vapor equilibrium in the ternary system carbon dioxide-nitrous oxide-ethylene, *Proceedings.* (1958) 10–14.
- [579] N.E. Khazanova, E.E. Sominskaya, A.V. Zakharova, M.B. Rozovskii, N.L. Nechimailo, Systems with azeotropism at high pressures. X. Phase and volume relations in the ethylene-carbon dioxide system, *Zh Fiz Khim.* 53 (1979) 1594–1597.
- [580] J.H. Kim, M.S. Kim, Vapor–liquid equilibria for the carbon dioxide+propane system over a temperature range from 253.15 to 323.15K, *Fluid Phase Equilibria.* 238 (2005) 13–19. <https://doi.org/10.1016/j.fluid.2005.09.006>.
- [581] H.H. Reamer, B.H. Sage, W.N. Lacey, Phase Equilibria in Hydrocarbon Systems. Volumetric and Phase Behavior of the Propane-Carbon Dioxide System, *Ind. Eng. Chem.* 43 (1951) 2515–2520. <https://doi.org/10.1021/ie50503a035>.
- [582] K. Tanaka, Y. Higashi, R. Akasaka, Y. Kayukawa, K. Fujii, Measurements of the Vapor–Liquid Equilibrium for the CO<sub>2</sub> + R290 Mixture, *J. Chem. Eng. Data.* 54 (2009) 1029–1033. <https://doi.org/10.1021/je800938s>.
- [583] V.G. Niesen, J.C. Rainwater, Critical locus, (vapor + liquid) equilibria, and coexisting densities of (carbon dioxide + propane) at temperatures from 311 K to 361 K, *J. Chem. Thermodyn.* 22 (1990) 777–795. [https://doi.org/10.1016/0021-9614\(90\)90070-7](https://doi.org/10.1016/0021-9614(90)90070-7).
- [584] F.H. Poettmann, D.L. Katz, Phase Behavior of Binary Carbon Dioxide-Paraffin Systems, *Ind. Eng. Chem.* 37 (1945) 847–853. <https://doi.org/10.1021/ie50429a017>.
- [585] G. Morrison, J.M. Kincaid, Critical point measurements on nearly polydisperse fluids, *AIChE J.* 30 (1984) 257–262. <https://doi.org/10.1002/aic.690300213>.
- [586] N. Juntarachat, S. Bello, R. Privat, J.-N. Jaubert, Validation of a New Apparatus Using the Dynamic Method for Determining the Critical Properties of Binary Gas/Gas Mixtures, *J. Chem. Eng. Data.* 58 (2013) 671–676. <https://doi.org/10.1021/je301209u>.
- [587] S. Horstmann, K. Fischer, J. Gmehling, Experimental Determination of Critical Points of Pure Components and Binary Mixtures Using a Flow Apparatus, *Chem. Eng. Technol.* 22 (1999) 839–842. [https://doi.org/10.1002/\(SICI\)1521-4125\(199910\)22:10<839::AID-CEAT839>3.0.CO;2-L](https://doi.org/10.1002/(SICI)1521-4125(199910)22:10<839::AID-CEAT839>3.0.CO;2-L).
- [588] J. Ke, M.W. George, M. Poliakoff, B. Han, H. Yan, How Does the Critical Point Change during the Hydrogenation of Propene in Supercritical Carbon Dioxide?, *J. Phys. Chem. B.* 106 (2002) 4496–4502. <https://doi.org/10.1021/jp0129333>.
- [589] W. Rall, K. Schäfer, Thermodynamische Untersuchungen an flüssigen Mischsystemen von Aceton und n-Pentan sowie von Aceton und n-Hexan, *Z Elektrochem.* 63 (1959) 1019–1024.
- [590] L.S. Kudryavtseva, M.P. Susarev, Liquid-vapor equilibria in the systems acetone-hexane and hexane-ethyl alcohol at 35, 45, and 55 and 760mmHg, *Zh Prikl Khim.* 36 (1963) 1419–1424.
- [591] G. Kolasińska, M. Góral, J. Giza, Vapour-Liquid Equilibria and Excess Gibbs Free Energy in Binary Systems of Acetone with Aliphatic and Aromatic Hydrocarbons at 313 15 K, *Z. Für Phys. Chem.* 2630 (1982). <https://doi.org/10.1515/zpch-1982-26317>.
- [592] J. Acosta, A. Arce, J. Martínez-Ageitos, E. Rodil, A. Soto, Vapor–Liquid Equilibrium of the Ternary System Ethyl Acetate + Hexane + Acetone at 101.32 kPa, *J. Chem. Eng. Data.* 47 (2002) 849–854. <https://doi.org/10.1021/je0102917>.
- [593] K. Schaefer, Excess enthalpies of acetone + n-alkane (C3–C6) binary mixtures, *Int Data Ser Sel Data Mix. Ser A.* (1978) 74–77.
- [594] P.P. Singh, R. Malik, S. Maken, W.E. Acree, S.A. Tucker, Thermochemical investigations of associated solutions. 10. Excess enthalpies and excess volumes of ternary acetone + bromoform + n-hexane mixtures, *Thermochim. Acta.* 162 (1990) 291–309. [https://doi.org/10.1016/0040-6031\(90\)80350-8](https://doi.org/10.1016/0040-6031(90)80350-8).
- [595] W.B. Kay, P-T-x Diagrams in the Critical Region. Acetone-n-Alkane Systems, *J. Phys. Chem.* 68 (1964) 827–831. <https://doi.org/10.1021/j100786a021>.
- [596] S.W. Campbell, R.A. Wilsak, G. Thodos, Isothermal vapor-liquid equilibrium measurements for the n-pentane-acetone system at 372.7, 397.7, and 422.6 K, *J. Chem. Eng. Data.* 31 (1986) 424–430. <https://doi.org/10.1021/je00046a016>.
- [597] R.F. Hajjar, R.H. Cherry, W.B. Kay, Critical properties of the vapor—liquid equilibria of the binary system acetone—n-pentane, *Fluid Phase Equilibria.* 25 (1986) 137–146. [https://doi.org/10.1016/0378-3812\(86\)80011-5](https://doi.org/10.1016/0378-3812(86)80011-5).
- [598] P.S. Puri, J. Polak, J.A. Ruether, Vapor-liquid equilibria of acetone-cyclohexane and acetone-isopropanol systems at 25°C, *J. Chem. Eng. Data.* 19 (1974) 87–89. <https://doi.org/10.1021/je60060a007>.
- [599] A.N. Marinichev, M.P. Susarev, Liquid-vapor equilibria in the systems acetone-methanol and acetone-cyclohexane at 35, 45, and 55° and a pressure of 760 mm, *J Appl Chem USSR.* 38 (1965) 371–375.

- [600] A. Crespo Colin, A. Compostizo, M. Díaz Peña, Excess Gibbs energy and excess volume of (cyclohexane + 2-propanone) and of (cyclohexane+2-butanone), *J. Chem. Thermodyn.* 16 (1984) 497–502. [https://doi.org/10.1016/0021-9614\(84\)90208-8](https://doi.org/10.1016/0021-9614(84)90208-8).
- [601] A. Mejía, H. Segura, M. Cartes, C. Calvo, Vapor–liquid equilibria and interfacial tensions for the ternary system acetone+2,2'-oxybis[propane]+cyclohexane and its constituent binary systems, *Fluid Phase Equilibria.* 270 (2008) 75–86. <https://doi.org/10.1016/j.fluid.2008.06.006>.
- [602] T. Pfeffer, B. Löwen, S. Schulz, Calorimetric measurement of the partial molar excess enthalpy at infinite dilution  $iE_{\infty}$  and its meaning for the calculation of the concentration and temperature dependence of the molar excess enthalpy  $hE$ , *Fluid Phase Equilibria.* 106 (1995) 139–167. [https://doi.org/10.1016/0378-3812\(94\)02630-J](https://doi.org/10.1016/0378-3812(94)02630-J).
- [603] B. Löwen, S. Schulz, Excess molar enthalpies of acetone + water, cyclohexane, methanol, 1-propanol, 2-propanol, 1-butanol and 1-pentanol at 283.15, 298.15, 323.15, 343.15 and 363.15 K, *Thermochim. Acta.* 262 (1995) 69–82. [https://doi.org/10.1016/0040-6031\(95\)02278-A](https://doi.org/10.1016/0040-6031(95)02278-A).
- [604] B. Marongiu, Excess enthalpy. 2-Propanone-cyclohexane system, *Int DATA Ser Sel Data Mix. Ser A.* 1987 (1987) 1–6.
- [605] P.P. Singh, R. Malik, S. Maken, W.E. Acree, A.I. Zvaigzni, Thermochemical investigations of associated solutions, *Thermochim. Acta.* 165 (1990) 113–127. [https://doi.org/10.1016/0040-6031\(90\)80211-G](https://doi.org/10.1016/0040-6031(90)80211-G).
- [606] J. Linek, I. Wichterle, K.N. Marsh, Vapor-Liquid Equilibria for N-Methyl-2-pyrrolidone + Benzene, +Toluene, +Heptane, and +Methylcyclohexane, *J. Chem. Eng. Data.* 41 (1996) 1212–1218. <https://doi.org/10.1021/je9601826>.
- [607] B. Blanco, S. Beltrán, J.L. Cabezas, J. Coca, Phase Equilibria of Binary Systems Formed by Hydrocarbons from Petroleum Fractions and the Solvents N-Methylpyrrolidone and N,N-Dimethylformamide. 1. Isobaric Vapor - Liquid Equilibria, *J. Chem. Eng. Data.* 42 (1997) 938–942. <https://doi.org/10.1021/je970059u>.
- [608] S.K. Gupta, B.S. Rawat, A.N. Goswami, S.M. Nanoti, R. Krishna, Isobaric vapour—liquid equilibria of the systems: Benzene—triethylene glycol, toluene—triethylene glycol and benzene—N-methylpyrrolidone, *Fluid Phase Equilibria.* 46 (1989) 95–102. [https://doi.org/10.1016/0378-3812\(89\)80278-X](https://doi.org/10.1016/0378-3812(89)80278-X).
- [609] T.M. Letcher, P.K. Naicker, Excess molar enthalpies and excess molar volumes of mixtures containing N-methyl-2-pyrrolidinone and an aromatic hydrocarbon at  $T = 298.15$  K and  $p = 0.101325$  MPa, *J. Chem. Thermodyn.* 31 (1999) 1585–1595. <https://doi.org/10.1006/jcht.1999.0555>.
- [610] Y. Chhikara, J.S. Yadav, D. Sharma, V.K. Sharma, Thermodynamic and topological investigations of molecular interactions in binary and ternary mixtures containing 1-methyl pyrrolidin-2-one at  $T = 308.15$  K, *J. Chem. Thermodyn.* 43 (2011) 737–749. <https://doi.org/10.1016/j.jct.2010.12.016>.
- [611] J. Gmehling, B. Meents, Excess enthalpy. 1-Methyl-2-pyrrolidinone - benzene system, *Int Data Ser Sel Data Mix. Ser A.* (1992) 211.
- [612] T.S. Brown, A.J. Kidnay, E.D. Sloan, Vapor—liquid equilibria in the carbon dioxide-ethane system, *Fluid Phase Equilibria.* 40 (1988) 169–184. [https://doi.org/10.1016/0378-3812\(88\)80028-1](https://doi.org/10.1016/0378-3812(88)80028-1).
- [613] K.P. Wallis, P. Clancy, J.A. Zollweg, W.B. Streett, Excess thermodynamic properties for  $\{x\text{CO}_2 + (1 - x)\text{C}_2\text{H}_6\}$  (I): experiment and theory, *J. Chem. Thermodyn.* 16 (1984) 811–823. [https://doi.org/10.1016/0021-9614\(84\)90028-4](https://doi.org/10.1016/0021-9614(84)90028-4).
- [614] K. Ohgaki, T. Katayama, Isothermal vapor-liquid equilibrium data for the ethane—carbon dioxide system at high pressures, *Fluid Phase Equilibria.* 1 (1977) 27–32. [https://doi.org/10.1016/0378-3812\(77\)80023-X](https://doi.org/10.1016/0378-3812(77)80023-X).
- [615] C. Wormald, J. Eyers, Excess molar enthalpies and excess molar volumes of  $\{x\text{CO}_2 + (1 - x)\text{C}_2\text{H}_6\}$  up to 308.4 K and 11.0 MPa, *J. Chem. Thermodyn.* 20 (1988) 323–331. [https://doi.org/10.1016/0021-9614\(88\)90129-2](https://doi.org/10.1016/0021-9614(88)90129-2).
- [616] C.J. Wormald, R.W. Hodgetts, Excess enthalpies and volumes for (carbon dioxide + ethane) at  $T = 291.6$  K, close to the minimum in the critical locus, *J. Chem. Thermodyn.* 29 (1997) 75–85. <https://doi.org/10.1006/jcht.1996.0141>.
- [617] N.E. Khazanova, L.S. Lesnevskaya, A.V. Zakharova, Liquid-vapor equilibrium in the ethane-CO<sub>2</sub> system, *Khim Promst Mosc.* 44 (1966) 364–365.
- [618] L. Gil, S.F. Otín, J.M. Embid, M.A. Gallardo, S. Blanco, M. Artal, I. Velasco, Experimental setup to measure critical properties of pure and binary mixtures and their densities at different pressures and temperatures, *J. Supercrit. Fluids.* 44 (2008) 123–138. <https://doi.org/10.1016/j.supflu.2007.11.003>.
- [619] N.E. Khazanova, E.E. Sominskaya, A.V. Zakharova, M.B. Rozovski, Thermodynamic properties of the ethane-carbon dioxide system and the pressure-volume-temperature-normality data, *Teplofiz Svoistva Veshchestv Mater.* 10 (1976) 213–219.

- [620] A.R.H. Goodwin, M.R. Moldover, Phase border and density determinations in the critical region of (carbon dioxide+ethane) determined from dielectric permittivity measurements, *J. Chem. Thermodyn.* 29 (1997) 1481–1494. <https://doi.org/10.1006/jcht.1997.0257>.
- [621] S. Horstmann, K. Fischer, J. Gmehling, P. Kolář, Experimental determination of the critical line for (carbon dioxide + ethane) and calculation of various thermodynamic properties for (carbon dioxide + n-alkane) using the PSRK model, *J. Chem. Thermodyn.* 32 (2000) 451–464. <https://doi.org/10.1006/jcht.2000.0611>.
- [622] H. Kalra, T.R. Krishnana, D.B. Robinson, Equilibrium-phase properties of carbon dioxide-butane and nitrogen-hydrogen sulfide systems at subambient temperatures, *J. Chem. Eng. Data.* 21 (1976) 222–225. <https://doi.org/10.1021/je60069a027>.
- [623] L.A. Weber, Vapour-liquid equilibria measurements for carbon dioxide with normal and isobutane from 250 to 280 K, *Cryogenics.* 25 (1985) 338–342. [https://doi.org/10.1016/0011-2275\(85\)90019-0](https://doi.org/10.1016/0011-2275(85)90019-0).
- [624] V.G. Niesen, (Vapor + liquid) equilibria and coexisting densities of (carbon dioxide + n-butane) at 311 to 395 K, *J. Chem. Thermodyn.* 21 (1989) 915–923. [https://doi.org/10.1016/0021-9614\(89\)90150-X](https://doi.org/10.1016/0021-9614(89)90150-X).
- [625] J.J.C. Hsu, N. Nagarajan, R.L. Robinson, Equilibrium phase compositions, phase densities, and interfacial tensions for carbon dioxide + hydrocarbon systems. 1. Carbon dioxide + n-butane, *J. Chem. Eng. Data.* 30 (1985) 485–491. <https://doi.org/10.1021/je00042a036>.
- [626] M.E. Pozo de Fernandez, J.A. Zollweg, W.B. Streett, Vapor-liquid equilibrium in the binary system carbon dioxide + n-butane, *J. Chem. Eng. Data.* 34 (1989) 324–328. <https://doi.org/10.1021/je00057a019>.
- [627] L.A. Weber, Simple apparatus for vapor-liquid equilibrium measurements with data for the binary systems of carbon dioxide with n-butane and isobutane, *J. Chem. Eng. Data.* 34 (1989) 171–175. <https://doi.org/10.1021/je00056a007>.
- [628] R.H. Olds, H.H. Reamer, B.H. Sage, W.N. Lacey, The n-Butane–Carbon Dioxide System, *Ind. Eng. Chem.* 41 (1949) 475–482. <https://doi.org/10.1021/ie50471a011>.
- [629] A.D. Leu, D.B. Robinson, Equilibrium phase properties of the n-butane-carbon dioxide and isobutane-carbon dioxide binary systems, *J. Chem. Eng. Data.* 32 (1987) 444–447. <https://doi.org/10.1021/je00050a017>.
- [630] E. Lladosa, N.F. Martínez, J.B. Montón, J. de la Torre, Measurements and correlation of vapour–liquid equilibria of 2-butanone and hydrocarbons binary systems at two different pressures, *Fluid Phase Equilibria.* 307 (2011) 24–29. <https://doi.org/10.1016/j.fluid.2011.05.004>.
- [631] S. Murakami, K. Amaya, R. Fujishiro, Heats of Mixing for Binary Mixtures. The Energy of Hydrogen Bonding between Alcohol and Ketone Molecules, *Bull. Chem. Soc. Jpn.* 37 (1964) 1776–1780. <https://doi.org/10.1246/bcsj.37.1776>.
- [632] A. Kreglewski, W.B. Kay, Critical constants of conformed mixtures, *J. Phys. Chem.* 73 (1969) 3359–3366. <https://doi.org/10.1021/j100844a035>.
- [633] W.B. Kay, C.L. Young, Gas-liquid critical properties. 2-Butanone (methyl ethyl ketone)-n-hexane system, *Int Data Ser Sel Data Mix. Ser A.* 1975 (1975) 139–156.
- [634] J. Kraus, J. Linek, Liquid-vapor equilibrium. XLVIII. Systems acetone-benzene, acetone-toluene, benzene-methyl ethyl ketone, methyl ethyl ketone-toluene, and methyl ethyl ketone-ethylbenzene, *Collect. Czechoslov. Chem. Commun.* 36 (1971) 2547–2567. <https://doi.org/10.1135/cccc19712547>.
- [635] E. Müller, H. Stage, Experimentelle Vermessung von Dampf-Flüssigkeits-Phasengleichgewichten dargestellt am Beispiel des Siedeverhaltens von Fettsäuren, 1961.
- [636] K.W. Free, H.P. Hutchinson, Isobaric Vapor-Liquid Equilibria for the Ternary System Acetone-Benzene-Chlorobenzene., *J. Chem. Eng. Data.* 4 (1959) 193–197. <https://doi.org/10.1021/je60003a001>.
- [637] T. Ishikawa, R. Watari, K. Kosakai, M. Hirata, Vapor-liquid equilibriums of binary systems containing acetone at 760 mm of mercury. Acetone with aromatic hydrocarbons, *Mem Fac Technol Tokyo Metropol Univ.* 21 (1971) 1883–1896.
- [638] J.A. Monick, H.D. Allen, C.J. Marlies, Vapor-liquid equilibrium data for fatty acids and fatty methyl esters at low pressures, *Oil Soap.* 23 (1946) 177–182. <https://doi.org/10.1007/BF02545630>.
- [639] K. Kojima, K. Tochigi, K. Kurihara, M. Nakamichi, Isobaric vapor-liquid equilibria for acetone + chloroform + benzene and the three constituent binary systems, *J. Chem. Eng. Data.* 36 (1991) 343–345. <https://doi.org/10.1021/je00003a024>.
- [640] Y. Akamatsu, H. Ogawa, S. Murakami, Molar excess enthalpies, molar excess volumes and molar isentropic compressions of mixtures of 2-propanone with heptane, benzene and trichloromethane at 298.15 K, *Thermochim. Acta.* 113 (1987) 141–150. [https://doi.org/10.1016/0040-6031\(87\)88317-X](https://doi.org/10.1016/0040-6031(87)88317-X).
- [641] H.-H. Möbius, Mischungsenthalpien und Mischbarkeit von Aceton, Benzol und Wasser, *J. Für Prakt. Chem.* 2 (1955) 95–104. <https://doi.org/10.1002/prac.19550020108>.

- [642] K. Yamanaka, H. Ogawa, S. Murakami, Excess molar isobaric heat capacities of mixtures of 2-propanone with heptane, benzene, and trichloromethane at 298.15 K, *Thermochim. Acta.* 169 (1990) 193–201. [https://doi.org/10.1016/0040-6031\(90\)80145-O](https://doi.org/10.1016/0040-6031(90)80145-O).
- [643] E.S. Lebedeva, S.M. Khodeeva, Phase equilibrium and volume relations in the system methylene chloride-ethylene, *Tr Gos Nauchno Issled Proektn Inst Azotn Promst Prod Org Sin.* 13 (1963) 79–90.
- [644] X. Wang, Y. Wang, J. Shi, B.C.Y. Lu, Isothermal vapor-liquid equilibria at elevated pressures for the systems containing nitrogen, carbon dioxide, and chlorodifluoromethane, *J. Chem. Eng. Data.* 36 (1991) 436–439. <https://doi.org/10.1021/je00004a027>.
- [645] J. Nohka, E. Sarashina, Y. Arai, S. Saito, Correlation Of Vapor-Liquid Equilibria For Systems Containing A Polar Component By The Bwr Equation, *J. Chem. Eng. Jpn.* 6 (1973) 10–17. <https://doi.org/10.1252/jcej.6.10>.
- [646] X. Wang, Y.S. Wang, Vapor-liquid equilibria for nitrogen-carbon dioxide-chlorodifluoromethane at moderate pressure, *Nanjing Huagong Xueyuan Xuebao.* 13 (1991) 35–44.
- [647] V.Y. Maslennikova, N.P. Goryunova, D.S. Tsiklis, Phase equilibria in the nitrogen-Freon 12 and nitrogen-Freon 22 systems, *Russ J Phys Chem.* 41 (1967) 383–385.
- [648] H. Fu, X. Mo, S. Han, H. Li, Study on Isothermal Vapor-Liquid Equilibrium for Ethanol - Benzene, Chloroform - Benzene and Ethanol - Chloroform Binary Systems, *Shiyou Xuebao Shiyou Jiagong.* 11 (1995) 87–92.
- [649] I. Nagata, Vapor-Liquid Equilibrium at Atmospheric Pressure for the Ternary System, Methyl Acetate-Chloroform-Benzene., *J. Chem. Eng. Data.* 7 (1962) 360–366. <https://doi.org/10.1021/je60014a012>.
- [650] G.-H. Chen, Q. Wang, Z.-M. Ma, X.-H. Yan, S.-J. Han, Phase equilibria at superatmospheric pressures for systems containing halohydrocarbon, aromatic hydrocarbon, and alcohol, *J. Chem. Eng. Data.* 40 (1995) 361–366. <https://doi.org/10.1021/je00018a003>.
- [651] H. Hirobe, Thermochemical studies, *J Fac Sci Univ Tokyo Sect 1.* 1 (1926) 155–222.
- [652] I. Nagata, K. Tamura, S. Tokuriki, Excess enthalpies and complex formation of acetonitrile with acetone, chloroform, and benzene, *Thermochim. Acta.* 47 (1981) 315–331. [https://doi.org/10.1016/0040-6031\(81\)80110-4](https://doi.org/10.1016/0040-6031(81)80110-4).
- [653] R.P. Rastogi, J. Nath, R.R. Misra, Thermodynamics of weak interactions in liquid mixtures of chloroform and aromatic hydrocarbons, *J. Chem. Thermodyn.* 3 (1971) 307–317. [https://doi.org/10.1016/S0021-9614\(71\)80047-2](https://doi.org/10.1016/S0021-9614(71)80047-2).
- [654] J.-P.E. Grolier, G. Roux-Desgranges, Z.S. Kooner, J.F. Smith, L.G. Hepler, Thermal and volumetric properties of chloroform+benzene mixtures and the ideal associated solution model of complex formation, *J. Solut. Chem.* 16 (1987) 745–752. <https://doi.org/10.1007/BF00652577>.
- [655] H.I. Paul, Experimentelle untersuchung der flüssigkeits -dampf-phasengleichgewichte und volumetrischen eigenschaften binärer und ternärer mischungen, VDI-Verlag, Düsseldorf, 1987.
- [656] M.N.. Al-Hayan, D.M.. Newsham, Isobaric vapour-liquid equilibria for mixtures containing halogenated hydrocarbons at atmospheric pressure: I. Binary mixtures of trichloromethane+ 1, 2-dichloroethane, 1, 2-dichloroethane+ 1, 1, 2, 2-tetrachloroethane, trichloromethane+ 1, 1, 2, 2-tetrachloroethane and n-heptane+ 1, 1, 2, 2-tetrachloroethane, *Fluid Phase Equilibria.* 166 (1999) 91–100. [https://doi.org/10.1016/S0378-3812\(99\)00297-6](https://doi.org/10.1016/S0378-3812(99)00297-6).
- [657] J. Munoz Embid, A.H. Roux, J.P.E. Grolier, Excess enthalpy. Trichloromethane - 1,2-dichloroethane system, *Int Data Ser Sel Data Mix. Ser A.* 1990 (1990) 59–78.
- [658] M. Góral, P. Oracz, S. Warycha, Vapour-liquid equilibria. IV. The ternary system carbon tetrachloride-methanol-chloroform at 293.15 K, *Fluid Phase Equilibria.* 44 (1988) 77–93. [https://doi.org/10.1016/0378-3812\(88\)80104-3](https://doi.org/10.1016/0378-3812(88)80104-3).
- [659] G. Rulewicz, H. Schuberth, E. Leibnitz, Untersuchungen über das Dampf-Flüssigkeits-Phasengleichgewicht des Systems Methylenchlorid/Chloroform/Tetrachlorkohlenstoff bei 45°C unter Verwendung einer gaschromatographischen Analysenmethode, *J. Für Prakt. Chem.* 37 (1968) 122–136. <https://doi.org/10.1002/prac.19680370303>.
- [660] R. Krauze, M. Serwinski, Liquid-vapor equilibrium in the system chloroform-carbon tetrachloride, *Zesz Nauk Politech Lodz Chem.* 24 (1973) 53–63.
- [661] M.A. Siddiqi, K. Lucas, Excess enthalpy of the system chloroform + carbon tetrachloride and a thermodynamic evaluation of its state dependence, *Fluid Phase Equilibria.* 16 (1984) 87–98. [https://doi.org/10.1016/0378-3812\(84\)85023-2](https://doi.org/10.1016/0378-3812(84)85023-2).
- [662] P. Hu, L.-X. Chen, Z.-S. Chen, Vapor-liquid equilibria for the 1,1,1,2-tetrafluoroethane (HFC-134a)+1,1,1,2,3,3,3-heptafluoropropane (HFC-227ea) and 1,1,1-trifluoroethane (HFC-143a)+2,3,3,3-tetrafluoroprop-1-ene (HFO-1234yf) systems, *Fluid Phase Equilibria.* 360 (2013) 293–297. <https://doi.org/10.1016/j.fluid.2013.09.056>.

- [663] X. Dong, M. Gong, Y. Zhang, J. Wu, Vapor–Liquid Equilibria of the Fluoroethane (R161) + 1,1,1,2-Tetrafluoroethane (R134a) System at Various Temperatures from (253.15 to 292.92) K, *J. Chem. Eng. Data.* 53 (2008) 2193–2196. <https://doi.org/10.1021/je800505y>.
- [664] M. Kleiber, Vapor-liquid equilibria of binary refrigerant mixtures containing propylene or R134a, *Fluid Phase Equilibria.* 92 (1994) 149–194. [https://doi.org/10.1016/0378-3812\(94\)80046-4](https://doi.org/10.1016/0378-3812(94)80046-4).
- [665] S. Bobbo, L. Fedele, R. Camporese, R. Stryjek, VLE measurements and modeling for the strongly positive azeotropic R32+propane system, *Fluid Phase Equilibria.* 199 (2002) 175–183. [https://doi.org/10.1016/S0378-3812\(01\)00798-1](https://doi.org/10.1016/S0378-3812(01)00798-1).
- [666] J.H. Kim, M.S. Kim, Y. Kim, Vapor–liquid equilibria for pentafluoroethane + propane and difluoromethane + propane systems over a temperature range from 253.15 to 323.15 K, *Fluid Phase Equilibria.* 211 (2003) 273–287. [https://doi.org/10.1016/S0378-3812\(03\)00237-1](https://doi.org/10.1016/S0378-3812(03)00237-1).
- [667] C. Coquelet, A. Chareton, A. Valtz, A. Baba-Ahmed, D. Richon, Vapor–Liquid Equilibrium Data for the Azeotropic Difluoromethane + Propane System at Temperatures from 294.83 to 343.26 K and Pressures up to 5.4 MPa, *J. Chem. Eng. Data.* 48 (2003) 317–323. <https://doi.org/10.1021/je020115d>.
- [668] L.J. Van Poolen, C.D. Holcomb, J.C. Rainwater, Isoplethic Method to Estimate Critical Lines for Binary Fluid Mixtures from Subcritical Vapor–Liquid Equilibrium: Application to the Azeotropic Mixtures R32 + C3H8 and R125 + C3H8, *Ind. Eng. Chem. Res.* 40 (2001) 4610–4614. <https://doi.org/10.1021/ie010215x>.
- [669] Y. Higashi, Experimental determination of the critical locus for the difluoromethane (R32) and propane (R290) system, *Fluid Phase Equilibria.* 219 (2004) 99–103. <https://doi.org/10.1016/j.fluid.2004.02.004>.
- [670] Y. Zhang, M. Gong, H. Zhu, J. Wu, Vapor–Liquid Equilibrium Data for the Ethane + Trifluoromethane System at Temperatures from (188.31 to 243.76) K, *J. Chem. Eng. Data.* 51 (2006) 1411–1414. <https://doi.org/10.1021/je0601107>.
- [671] A. Kordikowski, M. Poliakoff, Acoustic probing of phase equilibria in near-critical fluids, *Fluid Phase Equilibria.* 150–151 (1998) 493–499. [https://doi.org/10.1016/S0378-3812\(98\)00296-9](https://doi.org/10.1016/S0378-3812(98)00296-9).
- [672] V.A. Baginskii, N.D. Zakharov, N.I. Lapardin, Study and calculation of the liquid-vapor phase equilibrium of mixtures of refrigerants, *Issled Teplofiz Svoistv Rab Veshchestv Protseessov Teploobm. V Kholod Tekhn L.* 9 (1989) 9–15.
- [673] G.K. Lavrenchenko, V.N. Valyakin, Liquid-liquid, liquid-liquid-vapor, and liquid-vapor equilibria in binary Freon and Freon-hydrocarbon mixtures based on tetrafluoromethane (R14), *Teplofiz Svoistva Veshchestv Mater.* 22 (1985) 10–18.
- [674] S.-X. Hou, Y.-Y. Duan, Isothermal vapor–liquid equilibria for the pentafluoroethane+propane and pentafluoroethane+1,1,1,2,3,3,3-heptafluoropropane systems, *Fluid Phase Equilibria.* 290 (2010) 121–126. <https://doi.org/10.1016/j.fluid.2009.09.008>.
- [675] S. Bobbo, L. Fedele, R. Camporese, R. Stryjek, Hydrogen-bonding of HFCs with dimethyl ether: evaluation by isothermal VLE measurements, *Fluid Phase Equilibria.* 199 (2002) 153–160. [https://doi.org/10.1016/S0378-3812\(01\)00813-5](https://doi.org/10.1016/S0378-3812(01)00813-5).
- [676] J.S. Lim, J.Y. Park, K.-S. Lee, J.-D. Kim, B.G. Lee, Measurement of Vapor–Liquid Equilibria for the Binary Mixture of Pentafluoroethane (HFC-125) + Propane (R-290), *J. Chem. Eng. Data.* 49 (2004) 750–755. <https://doi.org/10.1021/je030156p>.
- [677] W.L. Kubic, F.P. Stein, An experimental and correlative study of the vapor-liquid equilibria of the tetrafluoromethane-chlorotrifluoromethane system, *Fluid Phase Equilibria.* 5 (1981) 289–304. [https://doi.org/10.1016/0378-3812\(80\)80062-8](https://doi.org/10.1016/0378-3812(80)80062-8).
- [678] H. Madani, A. Valtz, C. Coquelet, A.H. Meniai, D. Richon, Vapor–liquid equilibrium data for the (hexafluoroethane +1,1,1,2-tetrafluoroethane) system at temperatures from 263 to 353K and pressures up to 4.16MPa, *Fluid Phase Equilibria.* 268 (2008) 68–73. <https://doi.org/10.1016/j.fluid.2008.04.002>.
- [679] H. Madani, A. Valtz, C. Coquelet, Isothermal vapor–liquid equilibrium data for the decafluorobutane (R3110)+1,1,1,3,3-pentafluorobutane (R365mfc) system at temperatures from 333K to 441K, *Fluid Phase Equilibria.* 354 (2013) 109–113. <https://doi.org/10.1016/j.fluid.2013.06.031>.
- [680] M. Kriebel, Liquid-vapor phase equilibriums of the binary system difluoromonochloromethane (R 22)-difluorodichloromethane (R 12), *Kaeltetechnik.* 19 (1967) 8–14.
- [681] Y. Feng, C. Li, Z. Shou, Vapor-Liquid Equilibrium for Freon-22 and Freon-12 Vapor Phase Fugacity from a Generalized Virial Equation, *Zhejiang Daxue Xuebao.* 19 (1985) 58–67.
- [682] H. Nishiumi, S. Kohmatsu, T. Yokoyama, A. Konda, Phase Behavior of the Binary Refrigerant Mixtures HCF22 - CFC12 and HCF22 - HCFC123, *Fluid Phase Equilib.* 104 (1995) 131–143. [https://doi.org/10.1016/0378-3812\(94\)02644-G](https://doi.org/10.1016/0378-3812(94)02644-G).
- [683] Z.I. Geller, V.F. Chaikovskii, A.V. Egorov, Heats of mixing of Freons, *Teplofiz Svoist Zhidk.* (1973) 148–152.
- [684] Z.I. Geller, V.F. Chaikovskii, A.V. Egorov, Heats of mixing of Freons 112 and 115 with Freon 22, *Kholod Tekh.* 48 (1971) 29–30.

- [685] Y. Higashi, S. Okazaki, Y. Takaishi, M. Uematsu, K. Watanabe, Measurements of the vapor-liquid coexistence curve for the binary R12 + R22 system in the critical region, *J Chem Eng Data*. 29 (1984) 31–36. <https://doi.org/10.1021/je00035a012>.
- [686] M.A. Siddiqi, K. Lucas, The excess enthalpy of (tetrachloromethane + carbon disulphide) and (tetrachloromethane + dichloromethane) over a range of temperatures and pressures, *J. Chem. Thermodyn.* 15 (1983) 1181–1187. [https://doi.org/10.1016/0021-9614\(83\)90009-5](https://doi.org/10.1016/0021-9614(83)90009-5).
- [687] T.. Bissell, A.. Williamson, Vapour pressures and excess Gibbs energies of n-hexane and of n-heptane + carbon tetrachloride and + chloroform at 298.15 K, *J. Chem. Thermodyn.* 7 (1975) 131–136. [https://doi.org/10.1016/0021-9614\(75\)90260-8](https://doi.org/10.1016/0021-9614(75)90260-8).
- [688] L.S. Kudryavtseva, M.P. Susarev, Liquid-vapor equilibrium in systems chloroform-hexane and acetone-chloroform, *J Appl Chem USSR*. 36 (1963) 1231–1237.
- [689] W. Brzostowski, L. Verhoeye, Thermodynamic properties of mixtures of hexane and chloroform, *Rocz Chem.* 42 (1968) 507–515.
- [690] J. Ortega, J. Placido, Excess enthalpies of trichloromethane + n-alkanes. Measurement and comparison with the DISQUAC model, *Int Electron J Phys Chem Data*. 1 (1995) 59–68.
- [691] T.G. Bissell, G.E. Okafor, A.G. Williamson, Enthalpies and volumes of mixing of alkanes with carbon tetrachloride, chloroform, and methylene chloride at 25 °C, *J. Chem. Thermodyn.* 3 (1971) 393–399. [https://doi.org/10.1016/S0021-9614\(71\)80056-3](https://doi.org/10.1016/S0021-9614(71)80056-3).
- [692] B.R. Sharma, G.S. Pundeer, P.P. Singh, Thermodynamics of weak interactions: excess enthalpies and excess Gibbs free energies of mixing, *Thermochim. Acta.* 11 (1975) 105–114. [https://doi.org/10.1016/0040-6031\(75\)80013-X](https://doi.org/10.1016/0040-6031(75)80013-X).
- [693] D. Fenclova, V. Dohnal, S. Perez-Casas, C. Frigolet, M. Costas, Excess heat capacities, excess enthalpies, and excess volumes of trichloromethane + some oxygenated solvents or + the corresponding homomorphic hydrocarbons at 298.15 K, *ELDATA Int Electron J Phys Chem Data*. 1 (1995) 217–237.
- [694] L. Abello, Enthalpies d'excès des systèmes binaires constitués d'hydrocarbures benzéniques et du chloroforme ou du méthylchloroforme - I. — Résultats expérimentaux, *J Chim Phys Phys Chim Biol.* 70 (1973) 1355–1359. <https://doi.org/10.1051/jcp/1973701355>.
- [695] J.P. Shatas, M.M. Abbott, H.C. Van Ness, Excess thermodynamic functions for ternary systems. II. Chloroform-ethanol-n-heptane at 50°C, *J. Chem. Eng. Data.* 20 (1975) 406–409. <https://doi.org/10.1021/je60067a020>.
- [696] J.L. Zurita, M.L.G. De Soria, M.A. Postigo, M. Katz, Vapor-liquid equilibrium for the n-pentane-dichloromethane system at 298.15 K, *J. Chem. Eng. Data.* 31 (1986) 389–390. <https://doi.org/10.1021/je00046a005>.
- [697] F.G. Tenn, R.W. Missen, A study of the condensation of binary vapors of miscible liquids: Part I: The equilibrium relations, *Can. J. Chem. Eng.* 41 (1963) 12–14. <https://doi.org/10.1002/cjce.5450410105>.
- [698] M.A. Postigo, J.L. Zurita, M.L.G.D. Soria, M. Katz, Excess thermodynamic properties of n-pentane + dichloromethane system at 298.15 K, *Can. J. Chem.* 64 (1986) 1966–1968. <https://doi.org/10.1139/v86-325>.
- [699] C.Y. Tsang, W.B. Streett, Vapor-liquid equilibrium in the system carbon dioxide/dimethyl ether, *J. Chem. Eng. Data.* 26 (1981) 155–159. <https://doi.org/10.1021/je00024a018>.
- [700] A. Jonasson, O. Persson, A. Fredenslund, High Pressure Solubility of Carbon Dioxide and Carbon Monoxide in Dimethyl Ether, *J. Chem. Eng. Data.* 40 (1995) 296–300. <https://doi.org/10.1021/je00017a066>.
- [701] T. Laursen, P. Rasmussen, S.I. Andersen, VLE and VLLE Measurements of Dimethyl Ether Containing Systems, *J Chem Eng Data*. 47 (2002) 198–202. <https://doi.org/10.1021/je010154+>.
- [702] J.K. Ferrell, R.W. Rousseau, D.G. Bass, The solubility of acid gases in methanol, 1979.
- [703] A. Chapoy, C. Coquelet, H. Liu, A. Valtz, B. Tohidi, Vapour-liquid equilibrium data for the hydrogen sulphide (H<sub>2</sub>S)+carbon dioxide (CO<sub>2</sub>) system at temperatures from 258 to 313K, *Fluid Phase Equilibria*. 356 (2013) 223–228. <https://doi.org/10.1016/j.fluid.2013.07.050>.
- [704] D.P. Sobocinski, F. Kurata, Heterogeneous phase equilibria of the hydrogen sulfide-carbon dioxide system, *AIChE J.* 5 (1959) 545–551. <https://doi.org/10.1002/aic.690050425>.
- [705] J.A. Bierlein, W.B. Kay, Phase-Equilibrium Properties of System Carbon Dioxide-Hydrogen Sulfide, *Ind. Eng. Chem.* 45 (1953) 618–624. <https://doi.org/10.1021/ie50519a043>.
- [706] Z. Wagner, J. Pavlíček, Vapour-liquid equilibrium in the carbon dioxide—ethyl acetate system at high pressure, *Fluid Phase Equilibria*. 97 (1994) 119–126. [https://doi.org/10.1016/0378-3812\(94\)85010-0](https://doi.org/10.1016/0378-3812(94)85010-0).
- [707] A. Chrisochou, K. Schaber, U. Bolz, Phase equilibria for enzyme-catalyzed reactions in supercritical carbon dioxide, *Fluid Phase Equilibria*. 108 (1995) 1–14. [https://doi.org/10.1016/0378-3812\(95\)02696-C](https://doi.org/10.1016/0378-3812(95)02696-C).

- [708] F. Zahran, C. Pando, J.A.R. Renuncio, A. Cabañas, Excess molar enthalpies for mixtures of supercritical CO<sub>2</sub> and ethyl acetate and their role in supercritical fluid applications, *J. Chem. Thermodyn.* 51 (2012) 59–64. <https://doi.org/10.1016/j.jct.2012.02.034>.
- [709] H.-S. Byun, M.-Y. Choi, J.-S. Lim, High-pressure phase behavior and modeling of binary mixtures for alkyl acetate in supercritical carbon dioxide, *J. Supercrit. Fluids.* 37 (2006) 323–332. <https://doi.org/10.1016/j.supflu.2005.10.007>.
- [710] N. Juntarachat, R. Privat, L. Coniglio, J.-N. Jaubert, Development of a Predictive Equation of State for CO<sub>2</sub> + Ethyl Ester Mixtures Based on Critical Points Measurements, *J. Chem. Eng. Data.* 59 (2014) 3205–3219. <https://doi.org/10.1021/je5002494>.
- [711] W.-E. Reiff, H. Roth, K. Lucas, Phase equilibria in the binary system carbon disulfide-carbon dioxide, *Fluid Phase Equilibria.* 73 (1992) 323–338. [https://doi.org/10.1016/0378-3812\(92\)80016-3](https://doi.org/10.1016/0378-3812(92)80016-3).
- [712] C.J. Wormald, R.W. Hodgetts, Measurements of HmE for {xCO<sub>2</sub>+(1-x)CS<sub>2</sub>} in the liquid region up to T=300.15 K and p=7.5 MPa, *Fluid Phase Equilibria.* 204 (2003) 303–308. [https://doi.org/10.1016/S0378-3812\(02\)00266-2](https://doi.org/10.1016/S0378-3812(02)00266-2).
- [713] M.H. Lee, J.-H. Yim, J.W. Kang, J.S. Lim, Measurement of VLE data of carbon dioxide+dimethyl carbonate system for the direct synthesis of dimethyl carbonate using supercritical CO<sub>2</sub> and methanol, *Fluid Phase Equilibria.* 318 (2012) 77–82. <https://doi.org/10.1016/j.fluid.2012.01.020>.
- [714] J. Im, M. Kim, J. Lee, H. Kim, Vapor–Liquid Equilibria of Binary Carbon Dioxide + Alkyl Carbonate Mixture Systems, *J. Chem. Eng. Data.* 49 (2004) 243–245. <https://doi.org/10.1021/je034089a>.
- [715] L. Chen, R.J. Zhu, Y. Fang, P.F. Yuan, L.Q. Cao, Y.L. Tian, Vapor-Liquid Equilibrium Data for Carbon Dioxide+Dimethyl Carbonate Binary System, *Wuli Huaxue Xuebao.* 29 (2013) 11–16.
- [716] H. Matsuda, S. Yoshii, A. Nagashima, K. Kurihara, K. Ochi, Excess Molar Enthalpies of the Binary Carbon Dioxide + Dimethyl Carbonate System at Temperatures of (298.15 to 308.15) K and Pressures of (5.0 to 7.5) MPa, *J. Chem. Eng. Data.* 50 (2005) 1419–1424. <https://doi.org/10.1021/je050089u>.
- [717] Y. Sun, Y. Li, J. Zhou, R. Zhu, Y. Tian, Experimental determination and calculation of the critical curves for the binary systems of CO<sub>2</sub> containing ketone, alkane, ester and alcohol, respectively, *Fluid Phase Equilibria.* 307 (2011) 72–77. <https://doi.org/10.1016/j.fluid.2011.05.005>.
- [718] Y. Hou, X. Chen, S. Ren, Z. Song, W. Wu, Phase Behavior, Densities, and Isothermal Compressibility of (Carbon Dioxide + Dimethyl Carbonate), *J. Chem. Eng. Data.* 55 (2010) 1580–1587. <https://doi.org/10.1021/je900691n>.
- [719] S. Huamin, Solubility Of Carbon Monoxide In Methanol And Carbon Dioxide Under High Pressure, *Huaxue Gongcheng.* 19 (1991) 61–69.
- [720] G.-I. Kaminishi, Y. Arai, S. Saito, S. Maeda, Vapor-Liquid Equilibria For Binary And Ternary Systems Containing Carbon Dioxide, *J. Chem. Eng. Jpn.* 1 (1968) 109–116. <https://doi.org/10.1252/jcej.1.109>.
- [721] L.J. Christiansen, A. Fredenslund, N. Gardner, Gas-Liquid Equilibria of the CO<sub>2</sub>-CO and CO<sub>2</sub>-CH<sub>4</sub>-CO Systems, in: *Adv. Cryog. Eng.*, 1995: pp. 309–319.
- [722] A. Fredenslund, G.A. Sather, Gas-liquid equilibrium of the oxygen-carbon dioxide system, *J. Chem. Eng. Data.* 15 (1970) 17–22. <https://doi.org/10.1021/je60044a024>.
- [723] P.L. Chueh, N.K. Muirbrook, J.M. Prausnitz, Multicomponent vapor-liquid equilibria at high pressures: Part II. Thermodynamic analysis, *AIChE J.* 11 (1965) 1097–1102. <https://doi.org/10.1002/aic.690110625>.
- [724] N.K. Muirbrook, J.M. Prausnitz, Multicomponent vapor-liquid equilibria at high pressures: Part I. Experimental study of the nitrogen—oxygen—carbon dioxide system at 0°C, *AIChE J.* 11 (1965) 1092–1096. <https://doi.org/10.1002/aic.690110624>.
- [725] H.S. Booth, J.M. Carter, The Critical Constants of Carbon Dioxide-Oxygen Mixtures, *J. Phys. Chem.* 34 (1930) 2801–2825. <https://doi.org/10.1021/j150318a013>.
- [726] C.N. Kim, Y.M. Park, Vapor–Liquid Equilibrium of HFC-32/134a And HFC-125/134a Systems, *Int J Thermophys.* 20 (1999) 519–530. <https://doi.org/10.1023/A:1022605104490>.
- [727] M. Kobayashi, H. Nishiumi, Vapor–liquid equilibria for the pure, binary and ternary systems containing HFC32, HFC125 and HFC134a, *Fluid Phase Equilibria.* 144 (1998) 191–202. [https://doi.org/10.1016/S0378-3812\(97\)00257-4](https://doi.org/10.1016/S0378-3812(97)00257-4).
- [728] H. Nishiumi, T. Ohno, High pressure vapor-liquid equilibria and critical loci for the HFC125-HFC134a system, *Korean J. Chem. Eng.* 17 (2000) 668–671. <https://doi.org/10.1007/BF02699115>.
- [729] R. Kato, H. Nishiumi, Vapor–liquid equilibria and critical loci of binary and ternary systems composed of CH<sub>2</sub>F<sub>2</sub>, C<sub>2</sub>H<sub>2</sub>F<sub>4</sub> and C<sub>2</sub>H<sub>2</sub>F<sub>6</sub>, *Fluid Phase Equilibria.* 249 (2006) 140–146. <https://doi.org/10.1016/j.fluid.2006.07.017>.
- [730] M. Nagel, K. Bier, Vapor-liquid equilibriums of new refrigerant mixtures as alternatives to R 22 and R 502, *DKV-Tagungsberichte.* 20/2.1 (1993) 39–59.

- [731] K. Arita, T. Tomizawa, Y. Nagakawa, Y. Yoshida, Vapour—liquid equilibrium of the non-azeotropic refrigerant mixture formed by chlorofluoromethane and 1,1,1,2-tetrafluoroethane, *Fluid Phase Equilibria*. 63 (1991) 151–156. [https://doi.org/10.1016/0378-3812\(91\)80027-S](https://doi.org/10.1016/0378-3812(91)80027-S).
- [732] H. Nishiumi, M. Komatsu, T. Yokoyama, S. Kohmatsu, Two- and three-phase equilibria and critical locus for the system of HCFC22-HFC134a, *Fluid Phase Equilibria*. 83 (1993) 109–117. [https://doi.org/10.1016/0378-3812\(93\)87013-Q](https://doi.org/10.1016/0378-3812(93)87013-Q).
- [733] E.-Y. Chung, M.S. Kim, Vapor–Liquid Equilibria for the Difluoromethane (HFC-32) + 1,1,1,2-Tetrafluoroethane (HFC-134a) System, *J. Chem. Eng. Data*. 42 (1997) 1126–1128. <https://doi.org/10.1021/je970071m>.
- [734] X. Cui, G. Chen, C. Li, X. Han, Vapor–liquid equilibrium of difluoromethane +1,1,1,2-tetrafluoroethane systems over a temperature range from 258.15 to 343.15K, *Fluid Phase Equilibria*. 249 (2006) 97–103. <https://doi.org/10.1016/j.fluid.2006.09.017>.
- [735] S. Shimawaki, K. Fijii, Y. Higashi, Precise Measurements of the Vapor-Liquid Equilibria (VLE) of HFC-32/134a Mixtures Using a New Apparatus, *Int J Thermophys*. 23 (2002) 801–808. <https://doi.org/10.1023/A:1015407205188>.
- [736] L.A. Weber, A.M. Silva, Design of a high-pressure ebulliometer, with vapor-liquid equilibrium results for the systems CHF<sub>2</sub> Cl + CF<sub>3</sub> CH<sub>3</sub> and CF<sub>3</sub> CH<sub>2</sub> F + CH<sub>2</sub>F<sub>2</sub>, *Int. J. Thermophys*. 17 (1996) 873–888. <https://doi.org/10.1007/BF01439194>.
- [737] A. Kordikowski, D.G. Robertson, M. Poliakoff, T.D. DiNoia, M. McHugh, A. Aguiar-Ricardo, Acoustic Determination of the Critical Surfaces in the Ternary Systems CO<sub>2</sub> + CH<sub>2</sub>F<sub>2</sub> + CF<sub>3</sub>CH<sub>2</sub>F and CO + C<sub>2</sub>H<sub>4</sub> + CH<sub>3</sub>CH<sub>2</sub> and in Their Binary Subsystems, *J. Phys. Chem. B*. 101 (1997) 5853–5862. <https://doi.org/10.1021/jp9630611>.
- [738] Y. Shi, K. Wang, H. Liu, Y. Hu, Measurement of vapor-liquid equilibria for 1, 1, 1, 2-tetrafluoroethane-1, 1-difluoroethane binary system, *Huadong Ligong Daxue Xuebao*. 21 (1995) 613–618.
- [739] R. Tillner-Roth, An experimental study of the thermodynamic properties of the refrigerant mixture: {1,1,1,2-tetrafluoroethane (R 134a) + 1,1-difluoroethane (R 152a)}, *J. Chem. Thermodyn*. 25 (1993) 1419–1441. <https://doi.org/10.1006/jcht.1993.1144>.
- [740] K. Engelmann, H.J. Bittrich, Estimation of isothermal mixing functions from isobaric liquid-vapor equilibriums, *Wiss Z Tech Hochsch Chem Leuna-Mersebg*. 11 (1969) 213–218.
- [741] K. Engelmann, H.J. Bittrich, Isobaric liquid-vapor equilibriums of the system diethylamine-ethyl acetate, diethylamine-1,4-dioxane and ethyl acetate-1,4-dioxane at reduced pressures, *Wiss Z Tech Hochsch Chem Leuna-Mersebg*. 8 (1966) 289–291.
- [742] K. Engelmann, H.J. Bittrich, Isobaric liquid-vapor equilibriums of the systems diethylamine/ethyl acetate, diethylamine/1,4-dioxane, and ethyl acetate/1,4-dioxane at 760 mm, *Wiss Z Tech Hochsch Chem Leuna-Mersebg*. 8 (1966) 148–153.
- [743] F. Comelli, R. Francesconi, S. Ottani, Isothermal Vapor–Liquid Equilibria of Dimethyl Carbonate + Diethyl Carbonate in the Range (313.15 to 353.15) K, *J. Chem. Eng. Data*. 41 (1996) 534–536. <https://doi.org/10.1021/je950287t>.
- [744] H.-P. Luo, W.-D. Xiao, K.-H. Zhu, Isobaric vapor–liquid equilibria of alkyl carbonates with alcohols, *Fluid Phase Equilibria*. 175 (2000) 91–105. [https://doi.org/10.1016/S0378-3812\(00\)00444-1](https://doi.org/10.1016/S0378-3812(00)00444-1).
- [745] R. Francesconi, F. Comelli, Excess Molar Enthalpies, Densities, and Excess Molar Volumes of Binary Mixtures Containing Esters of Carbonic Acid at 298.15 and 313.15 K, *J. Chem. Eng. Data*. 40 (1995) 811–814. <https://doi.org/10.1021/je00020a016>.
- [746] R. Francesconi, F. Comelli, Vapor–Liquid Equilibria, Excess Molar Enthalpies, and Excess Molar Volumes of Dimethyl Carbonate + 1,2-Epoxybutane at 288.15, 298.15, or 313.15 K, *J. Chem. Eng. Data*. 41 (1996) 736–740. <https://doi.org/10.1021/je950298m>.
- [747] J. Pupezin, S. Ribnikar, Z. Knezevic, V. Dokic, Liquid-vapor equilibrium and thermodynamic properties of the system sulfur dioxide + dimethyl ether, *Bull Boris Kidric Inst Nucl Sci*. 17 (1966) 297–309.
- [748] J.R. Noles, J.A. Zollweg, Isothermal vapor-liquid equilibrium for dimethyl ether + sulfur dioxide, *Fluid Phase Equilibria*. 66 (1991) 275–289. [https://doi.org/10.1016/0378-3812\(91\)85061-X](https://doi.org/10.1016/0378-3812(91)85061-X).
- [749] S. Glowka, A.C. Zawisza, Liquid-vapor equilibriums and thermodynamic functions of methyl ethyl ether-sulfur dioxide system up to 300.deg. and 77.81 atm, *Bull. Acad. Pol. Sci. Ser. Sci. Chim*. 18 (1970) 555–560.
- [750] Feng Yaosheng, C. Li, Z. Shou, Vapor–Liquid Equilibrium for Trifluoromethane and Chlorodifluoromethane, *Huaxue Gongcheng*. 12 (1984) 41–47.
- [751] H. Roth, P. Peters-Gerth, K. Lucas, Experimental vapor-liquid equilibria in the systems R 22-R 23, R 22-Co<sub>2</sub>, Cs<sub>2</sub>-R 22, R 23-Co<sub>2</sub>, Cs<sub>2</sub>-R 23 and their correlation by equations of state, *Fluid Phase Equilibria*. 73 (1992) 147–166. [https://doi.org/10.1016/0378-3812\(92\)85045-A](https://doi.org/10.1016/0378-3812(92)85045-A).
- [752] G.C. Gerrits, On P<sub>x</sub>-Curves of Mixtures of Acetone and Ethyl Ether and of Carbon Tetrachloride and Acetone at 0 °C, *Proc K Ned Akad Wet Nat Sci*. 7 (1905) 162–173.

- [753] J. Sameshima, On The System Acetone—Ethyl Ether., *J. Am. Chem. Soc.* 40 (1918) 1482–1503. <https://doi.org/10.1021/ja02243a002>.
- [754] N.D. Litvinov, Isothermal equilibrium of vapor and liquid in systems of three fully miscible liquids, *Zh Fiz Khim.* 26 (1952) 1405–1412.
- [755] J. von Zawidzki, Über die Dampfdrücke binärer Flüssigkeitsgemische, *Z. Für Phys. Chem.* 35U (1900). <https://doi.org/10.1515/zpch-1900-3514>.
- [756] H. Loiseleur, J.-C. Merlin, R.A. Paris, Diagrammes d'ébullition-rosée (sous 740 mm) des systèmes acétone-sulfure de carbone, acétone-tétrachloréthylène et cyclopentanone-sulfure de carbone, *J. Chim. Phys.* 61 (1964) 1231–1233. <https://doi.org/10.1051/jcp/1964611231>.
- [757] H.J. Bittrich, L.F.T.G. Rodrigues, Dampf-Flüssigkeit-Gleichgewichte der Mischungen von Triethylamin mit Tetrahydrofuran und 1,4-Dioxan, *Z. Für Phys. Chem.* 269O (1988). <https://doi.org/10.1515/zpch-1988-26997>.
- [758] J.-P.E. Grolier, G. Roux-Desgranges, M. Berkane, E. Wilhelm, Heat capacities and densities of mixtures of very polar substances. 3. Mixtures containing either trichloromethane or 1,4-dioxane or diisopropylether, *J. Solut. Chem.* 23 (1994) 153–166. <https://doi.org/10.1007/BF00973543>.
- [759] S. Ahlers, Systematische Messung thermodynamischer Daten für das System Thiophen - Sulfolan zur Erweiterung der Gruppenbeitragsmethode Modified UNIFAC (Dortmund), Universität Oldenburg, 2009.
- [760] K. Geier, H.-J. Bittrich, Zur Thermodynamik der Flüssig-Dampf-Gleichgewichte der binären Systeme n-Hexan/Benzol, Cyclohexan/Benzol und Tetrahydrofuran mit n-hexan, cyclohexan, benzol und dimethylformamid, *Z. Für Phys. Chem.* 260O (1979). <https://doi.org/10.1515/zpch-1979-26094>.
- [761] G. Conti, P. Gianni, E. Matteoli, Excess enthalpies and excess heat capacities of (N,N-dimethylformamide + tetrahydrofuran + cyclohexane) at the temperature 298.15 K, *J. Chem. Thermodyn.* 26 (1994) 1249–1257. <https://doi.org/10.1006/jcht.1994.1142>.
- [762] G.S. Shealy, S.I. Sandler, Vapor-liquid equilibrium for four mixtures containing N,N-dimethylformamide, *J. Chem. Eng. Data.* 30 (1985) 455–459. <https://doi.org/10.1021/je00042a026>.
- [763] P. Venkatesu, R.S. Ramadevi, M.V. Prabhakara Rao, D.H.L. Prasad, Excess Molar Enthalpies of N,N-Dimethylformamide with Chloroethanes and Acetates at 298.15 K, *J. Chem. Eng. Data.* 45 (2000) 515–517. <https://doi.org/10.1021/je990286r>.
- [764] H.H. Reamer, B.H. Sage, W.N. Lacey, Phase Equilibria in Hydrocarbon Systems. n-Butane-Water System in the Two-Phase Region., *Ind. Eng. Chem.* 44 (1952) 609–615. <https://doi.org/10.1021/ie50507a049>.
- [765] A. Danneil, K. Tödheide, E.U. Franck, Verdampfungsgleichgewichte und kritische Kurven in den Systemen Äthan/Wasser und n-Butan/Wasser bei hohen Drücken, *Chem. Ing. Tech. - CIT.* 39 (1967) 816–822. <https://doi.org/10.1002/cite.330391309>.
- [766] N. Lancaster, C. Wormald, Excess molar enthalpies for  $\{x\text{H}_2\text{O} + (1 - x)\text{C}_3\text{H}_6\}$ (g),  $\{x\text{H}_2\text{O} + (1 - x)\text{C}_3\text{H}_8\}$ (g), and  $\{x\text{H}_2\text{O} + (1 - x)\text{C}_4\text{H}_{10}\}$ (g), *J. Chem. Thermodyn.* 18 (1986) 545–550. [https://doi.org/10.1016/0021-9614\(86\)90137-0](https://doi.org/10.1016/0021-9614(86)90137-0).
- [767] Y. Tian, X. Zhao, L. Chen, H. Zhu, H. Fu, High pressure phase equilibria and critical phenomena of water + iso-butane and water + n-butane systems to 695 K and 306 MPa, *J. Supercrit. Fluids.* 30 (2004) 145–153. <https://doi.org/10.1016/j.supflu.2003.09.002>.
- [768] H.H. Reamer, R.H. Olds, B.H. Sage, W.N. Lacey, Phase Equilibria in Hydrocarbon Systems. n-Butane–Water System in Three-Phase Region, *Ind. Eng. Chem.* 36 (1944) 381–383. <https://doi.org/10.1021/ie50412a024>.
- [769] M.S.H. Bader, K.A.M. Gasem, DETERMINATION OF INFINITE DILUTION ACTIVITY COEFFICIENTS FOR ORGANIC-AQUEOUS SYSTEMS USING A DILUTE VAPOR-LIQUID EQUILIBRIUM METHOD, *Chem. Eng. Commun.* 140 (1995) 41–72. <https://doi.org/10.1080/00986449608936454>.
- [770] M. Tu, G. Lai, D. Fei, Phase equilibrium for the system of phosphoric acid-water-benzene, *J Chengdu Univ Sci Technol.* 3 (1982) 65–70.
- [771] W.H. Thompson, J.R. Snyder, Mutual Solubilities of Benzene and Water. Equilibria in the Two Phase Liquid - Liquid Region., *J. Chem. Eng. Data.* 9 (1964) 516–520. <https://doi.org/10.1021/je60023a013>.
- [772] C.J. Wormald, N.M. Lancaster, C.J. Sowden, Benzene–water association Excess molar enthalpy and second virial cross-coefficients for (benzene–water)(g) and (cyclohexane–water)(g), *J. Chem. Soc. Faraday Trans.* 93 (1997) 1921–1926. <https://doi.org/10.1039/a608259i>.
- [773] C.J. Wormald, J. Slater, Excess enthalpies for (water + benzene) in the liquid and supercritical regions at T= 503 K to T= 592 K and p= 16.4 MPa, *J. Chem. Thermodyn.* 28 (1996) 627–636. <https://doi.org/10.1006/jcht.1996.0059>.
- [774] R. Jiménez-Gallegos, L.A. Galicia-Luna, C. Bouchot, L.E. Camacho-Camacho, O. Elizalde-Solis, Experimental Determination and Correlation of Phase Equilibria for the Ethane + 1-Propanol and

- Propane + 1-Propanol Systems, *J. Chem. Eng. Data.* 51 (2006) 1629–1633. <https://doi.org/10.1021/je060112r>.
- [775] K. Suzuki, H. Sue, M. Itou, R.L. Smith, H. Inomata, K. Arai, S. Saito, Isothermal vapor-liquid equilibrium data for binary systems at high pressures: carbon dioxide-methanol, carbon dioxide-ethanol, carbon dioxide-1-propanol, methane-ethanol, methane-1-propanol, ethane-ethanol, and ethane-1-propanol systems, *J. Chem. Eng. Data.* 35 (1990) 63–66. <https://doi.org/10.1021/je00059a020>.
- [776] T.A. McFall, M.E. Post, J.J. Christensen, R.M. Izatt, The excess enthalpies of eight (ethane + alcohol) mixtures at 298.15 K, *J. Chem. Thermodyn.* 13 (1981) 441–446. [https://doi.org/10.1016/0021-9614\(81\)90051-3](https://doi.org/10.1016/0021-9614(81)90051-3).
- [777] J.B. Ott, L.R. Lemon, J.T. Sipowska, P.R. Brown, Excess enthalpies and excess volumes for (ethane + propan-1-ol) at the temperatures (298.15, 323.15, and 348.15) K and at the pressures (5, 10, 12.5, and 15) MPa, *J. Chem. Thermodyn.* 27 (1995) 1033–1045. <https://doi.org/10.1006/jcht.1995.0108>.
- [778] D. Kodama, H. Tanaka, M. Kato, High Pressure Phase Equilibrium for Ethane + 1-Propanol at 314.15 K, *J. Chem. Eng. Data.* 46 (2001) 1280–1282. <https://doi.org/10.1021/je010077i>.
- [779] D.H. Lam, A. Jangkamolkulchai, K.D. Luks, Liquid-liquid-vapor phase equilibrium behavior of certain binary ethane + n-alkanol mixtures, *Fluid Phase Equilibria.* 59 (1990) 263–277. [https://doi.org/10.1016/0378-3812\(90\)80003-T](https://doi.org/10.1016/0378-3812(90)80003-T).
- [780] H.H. Reamer, B.H. Sage, Phase Behavior in the Nitrogen-Ammonia System., *J. Chem. Eng. Data.* 4 (1959) 303–305. <https://doi.org/10.1021/je60004a005>.
- [781] A.E. Lindroos, B.F. Dodge, Phase-equilibria at high pressures; the system nitrogen-ammonia at pressures above 1000 atmospheres, *Chem Eng Progr Symp Ser.* 48 (1952) 10–17.
- [782] E. Naumowicz-Węglińska, W. Wóycicki, Excess enthalpies of gaseous mixtures containing ammonia 2. (Ammonia + nitrogen) and (ammonia + methane), *J. Chem. Thermodyn.* 18 (1986) 1047–1052. [https://doi.org/10.1016/0021-9614\(86\)90019-4](https://doi.org/10.1016/0021-9614(86)90019-4).
- [783] G.K. Folas, E.W. Froyna, J. Lovland, G.M. Kontogeorgis, E. Solbraa, Data and prediction of water content of high pressure nitrogen, methane and natural gas, *Fluid Phase Equilibria.* 252 (2007) 162–174. <https://doi.org/10.1016/j.fluid.2006.12.018>.
- [784] J.B. Goodman, N.W. Kruse, Solubility of Nitrogen in Water at High Pressures and Temperatures, *Ind. Eng. Chem.* 23 (1931) 401–404. <https://doi.org/10.1021/ie50256a015>.
- [785] M. Rigby, J.M. Prausnitz, Solubility of water in compressed nitrogen, argon, and methane, *J. Phys. Chem.* 72 (1968) 330–334. <https://doi.org/10.1021/j100847a064>.
- [786] V.Y. Maslennikova, N.A. Vdovina, D.S. Tsiklis, Solubility of water in compressed nitrogen, *Russ J Phys Chem.* 45 (1971) 1354–1354.
- [787] R. Wiebe, V.L. Gaddy, C. Heinss, Solubility of Nitrogen in Water at 25°C from 25 to 1000 Atmospheres, *Ind. Eng. Chem.* 24 (1932) 927–927. <https://doi.org/10.1021/ie50272a023>.
- [788] P.C. Gillespie, G.M. Wilson, Vapor-liquid equilibrium data on water-substitute gas components: N<sub>2</sub>-H<sub>2</sub>O, H<sub>2</sub>-H<sub>2</sub>O, CO-H<sub>2</sub>O, H<sub>2</sub>-CO-H<sub>2</sub>O, and H<sub>2</sub>S-H<sub>2</sub>O, *GPA Res. Rep.* (1980) 1–34.
- [789] R. Wiebe, V.L. Gaddy, C. Heins, The Solubility of Nitrogen in Water at 50, 75 and 100° from 25 to 1000 Atmospheres, *J. Am. Chem. Soc.* 55 (1933) 947–953. <https://doi.org/10.1021/ja01330a011>.
- [790] V.Y. Maslennikova, Solubility of nitrogen in water, *Tr Gos Nauchno Issled Proektn Inst Azotn Promst Prod Org Sin.* 12 (1971) 82–87.
- [791] P. Richards, C.J. Wormald, T.K. Yerlett, The excess enthalpy of (water + nitrogen) vapour and (water + n-heptane) vapour, *J. Chem. Thermodyn.* 13 (1981) 623–628. [https://doi.org/10.1016/0021-9614\(81\)90032-X](https://doi.org/10.1016/0021-9614(81)90032-X).
- [792] C.. Wormald, C.. Colling, Excess enthalpies for (water + nitrogen)(g) up to 698.2 K and 12.6 MPa, *J. Chem. Thermodyn.* 15 (1983) 725–737. [https://doi.org/10.1016/0021-9614\(83\)90139-8](https://doi.org/10.1016/0021-9614(83)90139-8).
- [793] V.M. Prokhorova, D.S. Tsiklis, Vapor–vapor equilibrium in the system nitrogen–water, *Zh Fiz Khim.* 44 (1970) 2069–2070.
- [794] R. Siedler, L. Grote, E. Kauert, U. Werner, H.J. Bittrich, Zur Thermodynamik der binären Systeme von Benzol mit Diäthylamin und Triäthylamin, *Z. Für Phys. Chem.* 241O (1969). <https://doi.org/10.1515/zpch-1969-24127>.
- [795] I. Velasco, S. Otin, C. Gutierrez Losa, Excess Enthalpies of Some Aliphatic Amine (C<sub>3</sub> - C<sub>8</sub>) + Benzene Mixtures, *Int Data Ser Sel Data Mix. Ser A.* (1981) 60–64.
- [796] C. Dehmelt, M. Finke, H.J. Bittrich, Untersuchungen zur zwischenmolekularen Wechselwirkung in Systemen von Diäthylamin mit aromatischen Komponenten, *Z. Für Phys. Chem.* 255O (1974). <https://doi.org/10.1515/zpch-1974-25533>.
- [797] L. Ruffine, Équilibres de phases à basse température de systèmes complexes CO<sub>2</sub> - hydrocarbures légers - méthanol - eau : mesures et modélisation, 2005.
- [798] L. Ruffine, A. Barreau, I. Brunella, P. Mougín, J. Jose, New Apparatus for Low-Temperature Investigations: Measurements of the Multiphase Equilibrium of Mixtures Containing Methane, Ethane,

- Propane, Butane, Methanol, and Carbon Dioxide, *Ind. Eng. Chem. Res.* 44 (2005) 8387–8392. <https://doi.org/10.1021/ie0506365>.
- [799] K. Ohgaki, F. Sano, T. Katayama, Isothermal vapor-liquid equilibrium data for binary systems containing ethane at high pressures, *J. Chem. Eng. Data.* 21 (1976) 55–58. <https://doi.org/10.1021/je60068a016>.
- [800] K. Ishihara, H. Tanaka, M. Kato, Phase equilibrium properties of ethane+methanol system at 298.15 K, *Fluid Phase Equilibria.* 144 (1998) 131–136. [https://doi.org/10.1016/S0378-3812\(97\)00251-3](https://doi.org/10.1016/S0378-3812(97)00251-3).
- [801] Y.H. Ma, J.P. Kohn, Multiphase and Volumetric Equilibria of the Ethane-Methanol System at Temperatures between  $-40^{\circ}$  and  $100^{\circ}\text{C}$ ., *J. Chem. Eng. Data.* 9 (1964) 3–5. <https://doi.org/10.1021/je60020a002>.
- [802] J. Sipowska, R. Graham, B. Neely, J. Ott, R. Izatt, Excess enthalpies for (ethane + methanol) at 298.15 and 348.15 K and 7.5 and 15 MPa, and at 323.15 K at 7.5, 10, and 15 MPa, *J. Chem. Thermodyn.* 21 (1989) 1085–1093. [https://doi.org/10.1016/0021-9614\(89\)90095-5](https://doi.org/10.1016/0021-9614(89)90095-5).
- [803] A.-D. Lev, D.B. Robinson, S.Y.-K. Chung, C.-J. Chen, The equilibrium phase properties of the propane-methanol and n-Butane-methanol binary systems, *Can. J. Chem. Eng.* 70 (1992) 330–334. <https://doi.org/10.1002/cjce.5450700217>.
- [804] F. Galivel-Solastiouk, S. Laugier, D. Richon, Vapor-liquid equilibrium data for the propane-methanol and propane-methanol-carbon dioxide system, *Fluid Phase Equilibria.* 28 (1986) 73–85. [https://doi.org/10.1016/0378-3812\(86\)85069-5](https://doi.org/10.1016/0378-3812(86)85069-5).
- [805] S.N. Joung, H.Y. Shin, H.S. Kim, K.-P. Yoo, High-Pressure Vapor–Liquid Equilibrium Data and Modeling of Propane + Methanol and Propane + Ethanol Systems, *J. Chem. Eng. Data.* 49 (2004) 426–429. <https://doi.org/10.1021/je0340506>.
- [806] J.T. Sipowska, J.B. Ott, A.T. Woolley, B.G. Marchant, M.S. Gruszkiewicz, Excess enthalpies for (propane + methanol) at the pressure 5 MPa and the temperatures (253.15, 258.15, 263.15, and 273.15) K. The effect of water as an impurity on the (liquid + liquid) equilibria in (propane + methanol), *J. Chem. Thermodyn.* 25 (1993) 999–1004. <https://doi.org/10.1006/jcht.1993.1095>.
- [807] J.T. Sipowska, J.B. Ott, B.J. Neely, R.M. Izatt, Excess enthalpies for (propane + methanol) at the temperatures (298.15, 323.15, 348.15, and 373.15) K and pressures (5, 10, and 15) MPa, and at 363.15K and (5 and 15) MPa, *J. Chem. Thermodyn.* 23 (1991) 551–559. [https://doi.org/10.1016/S0021-9614\(05\)80098-9](https://doi.org/10.1016/S0021-9614(05)80098-9).
- [808] V.V. Udovenko, T.F. Mazanko, Liquid-vapor equilibrium in propyl alcohol-water and propyl alcohol-benzene systems, *Izv Vyssh Uchebn Zaved Khim Khim Tekhnol.* 15 (1972) 1654–1658.
- [809] I. Brown, F. Smith, Liquid-Vapour Equilibria. IX. The Systems n-Propanol + Benzene and n-Butanol + Benzene at  $45^{\circ}\text{C}$ , *Aust. J. Chem.* 12 (1959) 407. <https://doi.org/10.1071/CH9590407>.
- [810] K. Strubl, V. Svoboda, R. Holub, J. Pick, Liquid-vapour equilibrium in the benzene-n-propanol system, *Collect. Czechoslov. Chem. Commun.* 40 (1975) 1647–1656. <https://doi.org/10.1135/cccc19751647>.
- [811] T. Hiaki, K. Tochigi, K. Kojima, Measurement of vapor-liquid equilibria and determination of azeotropic point, *Fluid Phase Equilibria.* 26 (1986) 83–102. [https://doi.org/10.1016/0378-3812\(86\)85006-3](https://doi.org/10.1016/0378-3812(86)85006-3).
- [812] Shouyu Wang, Chenpu Zao, VLE data for benzene-n-propanol-lithium chloride system, *Huaxue Gongcheng.* 19 (1991) 72–76.
- [813] P. Cen, Z. Zhu, The Measurement of Mixing Heat and the Prediction of Vapor-Liquid Equilibrium Data for Hydrocarbon - Alcohol Systems, *Huagong Xuebao.* 35 (1984) 51–65.
- [814] J.P. Chao, M. Dai, Studies on thermodynamic properties of binary systems containing alcohols. VII. Temperature dependence of excess enthalpies for n-propanol + benzene an, *Thermochim. Acta.* 123 (1988) 285–291. [https://doi.org/10.1016/0040-6031\(88\)80032-7](https://doi.org/10.1016/0040-6031(88)80032-7).
- [815] W.M. Recko, Excess heat capacity of the binary systems formed by n-propyl alcohol with benzene, mesitylene, and cyclohexane, *Bull Acad Pol Sci Ser Sci Chim.* 16 (1968) 549–552.
- [816] J.M. Skaates, W.B. Kay, The phase relations of binary systems that form azeotropes, *Chem. Eng. Sci.* 19 (1964) 431–444. [https://doi.org/10.1016/0009-2509\(64\)85070-3](https://doi.org/10.1016/0009-2509(64)85070-3).
- [817] A. Iguchi, Vapor-liquid equilibria at  $25^{\circ}\text{C}$  for binary systems between alcohols and hydrocarbons, *Kagaku Sochi.* 20 (1978) 66–68.
- [818] V.C. Smith, R.L. Robinson, Vapor-Liquid Equilibria at  $25^{\circ}\text{C}$  in the Binary Mixtures Formed by Hexane, Benzene, and Ethanol, *J. Chem. Eng. Data.* 15 (1970) 391–395. <https://doi.org/10.1021/je60046a005>.
- [819] A. Tamir, A. Apelblat, M. Wagner, A new device for measuring isothermal vapor - liquid equilibria, *Fluid Phase Equilibria.* 6 (1981) 237–259. [https://doi.org/10.1016/0378-3812\(81\)85007-8](https://doi.org/10.1016/0378-3812(81)85007-8).
- [820] V.T. Zharov, A.G. Morachevskii, Liquid-vapor equilibrium in the ethyl alcohol-benzene system and the verification of the thermodynamic data, *Zh Prikl Khim.* 36 (1963) 2397–2402.
- [821] V.V. Udovenko, L.G. Fatkulina, Vapor pressure of three-component systems. I. The system ethyl alcohol-1,2-dichloroethane-benzene, *Zh Fiz Khim.* 26 (1952) 719–730.
- [822] R.H. Stokes, C. Burfitt, Enthalpies of dilution and transfer of ethanol in non-polar solvents, *J. Chem. Thermodyn.* 5 (1973) 623–631. [https://doi.org/10.1016/S0021-9614\(73\)80003-5](https://doi.org/10.1016/S0021-9614(73)80003-5).

- [823] J. Zhao, M. Dai, Studies on Thermodynamic Properties of Binary Systems containing Alcohols. I. Excess Enthalpies of C1 to C5 Normal Alcohols + Benzene, *Wuli Huaxue Xuebao*. 2 (1986) 141–145.
- [824] D. Missopolinou, I. Tsivintzelis, C. Panayiotou, Excess enthalpies of binary mixtures of 2-ethoxyethanol with four hydrocarbons at 298.15, 308.15, and 318.15K, *Fluid Phase Equilibria*. 245 (2006) 89–101. <https://doi.org/10.1016/j.fluid.2006.04.016>.
- [825] N. Perrakis, The physical properties of liquid double mixtures in the neighborhood of the critical state of miscibility, *J Chim Phys*. 22 (1925) 280–305.
- [826] R. Tanaka, S. Toyama, Excess Molar Volumes and Excess Molar Heat Capacities for Binary Mixtures of (Ethanol + Benzene, or Toluene, or o-Xylene, or Chlorobenzene) at a Temperature of 298.15 K, *J. Chem. Eng. Data*. 42 (1997) 871–874. <https://doi.org/10.1021/je9700479>.
- [827] E. Neau, C. Blanc, D. Bares, Les fonctions thermodynamiques d'excès du binaire 2 propanol-isooctane, *J. Chim. Phys*. 70 (1973) 843–849. <https://doi.org/10.1051/jcp/1973700843>.
- [828] J. Pavlíček, I. Wichterle, Isothermal (vapour+liquid) equilibria in the binary and ternary systems composed of 2-propanol, 2,2,4-trimethylpentane, and 2,4-dimethyl-3-pentanone, *J. Chem. Thermodyn*. 45 (2012) 83–89. <https://doi.org/10.1016/j.jct.2011.09.007>.
- [829] I. Wichterle, Isothermal vapor-liquid equilibria in the ternary system propan-2-ol + diisopropyl ether + 2,2,4-trimethylpentane and the three binary subsystems at 330 K and 340 K, *ELDATA Int Electron J Phys Chem Data*. 5 (1999) 179–189.
- [830] D.-Y. Lin, C.-H. Tu, (Vapour+liquid) equilibria for binary and ternary mixtures of 2-propanol, tetrahydropyran, and 2,2,4-trimethylpentane at P=101.3kPa, *J. Chem. Thermodyn*. 47 (2012) 260–266. <https://doi.org/10.1016/j.jct.2011.10.025>.
- [831] T. Hiaki, K. Takahashi, T. Tsuji, M. Hongo, K. Kojima, Vapor-Liquid Equilibria of 1-Propanol or 2-Propanol with 2,2,4-Trimethylpentane at 101.3 kPa, *J. Chem. Eng. Data*. 39 (1994) 602–604. <https://doi.org/10.1021/je00015a047>.
- [832] T.-T. Huang, C.-H. Tu, Vapor-Liquid Equilibria for Binary and Ternary Mixtures of 1,3-Dioxolane, 2-Propanol, and 2,2,4-Trimethylpentane at 101.3 kPa, *J. Chem. Eng. Data*. 55 (2010) 513–518. <https://doi.org/10.1021/je900327x>.
- [833] A. Heintz, The Pressure Dependence of the Excess Enthalpy of Mixtures of Isopropanol with Heptane and Isooctane up to 553 bar, *Berichte Bunsenges. Für Phys. Chem*. 85 (1981) 632–635. <https://doi.org/10.1002/bbpc.19810850905>.
- [834] L. Zhang, J. Han, R. Wang, X. Qiu, J. Ji, Isobaric Vapor-Liquid Equilibria for Three Ternary Systems: Water + 2-Propanol + 1-Ethyl-3-methylimidazolium Tetrafluoroborate, Water + 1-Propanol + 1-Ethyl-3-methylimidazolium Tetrafluoroborate, and Water + 1-Propanol + 1-Butyl-3-methylimidazolium Tetrafluoroborate, *J. Chem. Eng. Data*. 52 (2007) 1401–1407. <https://doi.org/10.1021/je700092d>.
- [835] A. Belabbaci, R.M. Villamañán, L. Negadi, M.C. Martín, Vapor-Liquid Equilibria of Binary Mixtures Containing 2-Butanol and Hydrocarbons at 313.15 K, *J. Chem. Eng. Data*. 57 (2012) 982–987. <https://doi.org/10.1021/je201284y>.
- [836] M.E. Araujo, M.R.W. Maciel, A.Z. Francesconi, Excess Gibbs free energies of (hexane + butan-2-ol) and of (cyclohexane + butan-2-ol) at the temperatures (323.15, 338.15, and 348.15) K, *J. Chem. Thermodyn*. 25 (1993) 1295–1299. <https://doi.org/10.1006/jcht.1993.1129>.
- [837] I. Gascón, H. Artigas, P. Cea, M. Domínguez, F.M. Royo, Isobaric Vapour-Liquid Equilibrium of Ternary Mixtures Cyclohexane (or n -Hexane) Plus 1,3-Dioxolane Plus 2-Butanol at 40.0 and 101.3 kPa, *Phys. Chem. Liq*. 41 (2003) 1–13. <https://doi.org/10.1080/00319100290032703>.
- [838] L.-C. Feng, C.-H. Chou, M. Tang, Y.-P. Chen, Vapor-Liquid Equilibria of Binary Mixtures 2-Butanol + Butyl Acetate, Hexane + Butyl Acetate, and Cyclohexane + 2-Butanol at 101.3 kPa, *J. Chem. Eng. Data*. 43 (1998) 658–661. <https://doi.org/10.1021/je9800205>.
- [839] H.T. French, Thermodynamic functions for the systems 1-butanol, 2-butanol, and 2-butanol + cyclohexane, *J. Solut. Chem*. 12 (1983) 869–887. <https://doi.org/10.1007/BF00643927>.
- [840] F. Veselý, V. Dohnal, M. Valentová, J. Pick, Concentration and temperature dependence of heats of mixing of 1-butanol, 2-butanol, and 2-methyl-2-propanol with cyclohexane, *Collect. Czechoslov. Chem. Commun*. 48 (1983) 3482–3494. <https://doi.org/10.1135/cccc19833482>.
- [841] M. Diaz Pena, D.R. Rodriguez Cheda, Liquid-vapor equilibrium. III. Systems of n-propanol-n-hexane at 50. deg. and n-propanol-n-heptane at 60. deg, *Quim*. 66 (1970) 747–755.
- [842] M.R.W. Maciel, A. Francesconi, Excess Gibbs free energies of (n-hexane + propan-1-ol) at 338.15 and 348.15 K and of (n-hexane + propan-2-ol) at 323.15, 338.15, and 348.15 K, *J. Chem. Thermodyn*. 20 (1988) 539–544. [https://doi.org/10.1016/0021-9614\(88\)90081-X](https://doi.org/10.1016/0021-9614(88)90081-X).
- [843] B.C. Oh, Y. Kim, H.Y. Shin, H. Kim, Vapor-liquid equilibria for the system 1-propanol+n-hexane near the critical region, *Fluid Phase Equilibria*. 220 (2004) 41–46. <https://doi.org/10.1016/j.fluid.2003.12.004>.
- [844] J. Gmehling, B. Meents, Excess enthalpy. 1-Propanol - hexane system, *Int Data Ser Sel Data Mix. Ser A*. (1992) 158.

- [845] M.M. Mato, S.M. Cebreiro, P.V. Verdes, J.L. Legido, M.I. Paz Andrade, Thermodynamic properties of the ternary system MTBE+1-propanol+hexane: Application of different group contribution models and empirical methods, *J. Therm. Anal. Calorim.* 80 (2005) 303–309. <https://doi.org/10.1007/s10973-005-0651-4>.
- [846] I. Brown, W. Fock, F. Smith, Heats of mixing. V. Systems of n-alcohols with n-hexane, *Aust. J. Chem.* 17 (1964) 1106. <https://doi.org/10.1071/CH9641106>.
- [847] L. Gil, S.T. Blanco, C. Rivas, E. Laga, J. Fernández, M. Artal, I. Velasco, Experimental determination of the critical loci for {n-C<sub>6</sub>H<sub>14</sub> or CO<sub>2</sub>+alkan-1-ol} mixtures. Evaluation of their critical and subcritical behavior using PC-SAFT EoS, *J. Supercrit. Fluids.* 71 (2012) 26–44. <https://doi.org/10.1016/j.supflu.2012.07.008>.
- [848] C. Berro, M. Rogalski, A. Pénélox, A new ebulliometric technique. Vapour-liquid equilibria in the binary systems ethanol-n-heptane and ethanol-n-nonane, *Fluid Phase Equilibria.* 8 (1982) 55–73. [https://doi.org/10.1016/0378-3812\(82\)80005-8](https://doi.org/10.1016/0378-3812(82)80005-8).
- [849] G.A. Ratcliff, K.C. Chao, Prediction of thermodynamic properties of polar mixtures by a group solution model, *Can. J. Chem. Eng.* 47 (1969) 148–153. <https://doi.org/10.1002/cjce.5450470208>.
- [850] M. Diaz Pena, D.R. Rodriguez Cheda, Liquid-vapor equilibrium. II. Ethanol-n-heptane system at 40 and 60.deg., *Quim.* 66 (1970) 737–745.
- [851] J. Seo, J. Lee, H. Kim, Measurement and Correlation of Vapor–Liquid Equilibria for the 2-Propanol + n-Hexane System near the Critical Region, *J. Chem. Eng. Data.* 48 (2003) 856–859. <https://doi.org/10.1021/je025604s>.
- [852] H.C. Van Ness, C.A. Soczek, N.K. Kochar, Thermodynamic excess properties for ethanol-n-heptane, *J. Chem. Eng. Data.* 12 (1967) 346–351. <https://doi.org/10.1021/je60034a015>.
- [853] C.-P.C. Kao, R.N. Miller, J.F. Sturgis, Double Azeotropy in Binary Mixtures 1,1,1,2,3,4,4,5,5,5-Decafluoropentane + Tetrahydrofuran, *J. Chem. Eng. Data.* 46 (2001) 229–233. <https://doi.org/10.1021/je000212b>.
- [854] A. Lietzmann, B. Loewen, S. Schulz, Excess Molar Enthalpies of Propanone + Heptane, Propanone + Ethanol, Ethanol + Heptane, and 2-Propanol + Water at 283.15, 298.15, 323.15, 343.15, and 363.15 K, *J. Chem. Eng. Data.* 39 (1994) 785–788. <https://doi.org/10.1021/je00016a033>.
- [855] H. Grosse-Wortmann, W. Jost, H.G. Wagner, Kalorimetrische Messungen am System Äthanol - Cyclohexan - n-Heptan, *Z. Für Phys. Chem.* 49 (1966) 74–93. [https://doi.org/10.1524/zpch.1966.49.1\\_2.074](https://doi.org/10.1524/zpch.1966.49.1_2.074).
- [856] H.C. van Ness, M.M. Abbott, Excess enthalpy. Ethanol (ethyl alcohol)-n-hexane system, *Int Data Ser Sel Data Mix. Ser A.* 1976 (1976) 11.
- [857] W. Mier, G. Oswald, E. Tusel-Langer, R.N. Lichtenthaler, Excess Enthalpy HE of Binary Mixtures Containing Alkanes, Ethanol and Ethyl-Tert. Butyl Ether (ETBE), *Berichte Bunsenges. Für Phys. Chem.* 99 (1995) 1123–1130. <https://doi.org/10.1002/bbpc.199500043>.
- [858] R. Tanaka, S. Toyama, S. Murakami, Heat capacities of {x<sub>n</sub>C<sub>n</sub>H<sub>2n</sub>+1OH + (1 - x)<sub>n</sub>C<sub>7</sub>H<sub>16</sub>} for n = 1 to 6 at 298.15 K, *J. Chem. Thermodyn.* 18 (1986) 63–73. [https://doi.org/10.1016/0021-9614\(86\)90044-3](https://doi.org/10.1016/0021-9614(86)90044-3).
- [859] A. Iguchi, Excess molal specific heat of nonelectrolyte solutions, *Kagaku Sochi.* 19 (1977) 64–65.
- [860] W. Mier, R.N. Lichtenthaler, A.H. Roux, J.-P.E. Grolier, Excess molar heat capacities C<sub>Ep,m</sub> and excess molar volumes V<sub>Em</sub> of {x<sub>1</sub>CH<sub>3</sub>(CH<sub>2</sub>)<sub>5</sub>CH<sub>3</sub> + x<sub>2</sub>CH<sub>3</sub>C(CH<sub>3</sub>)<sub>2</sub>CH<sub>2</sub>CH(CH<sub>3</sub>)CH<sub>3</sub> + x<sub>3</sub>CH<sub>3</sub>C(CH<sub>3</sub>)<sub>2</sub>OC<sub>2</sub>H<sub>5</sub> + (1 - x<sub>1</sub> - x<sub>2</sub> - x<sub>3</sub>)C<sub>2</sub>H<sub>5</sub>OH}(l) I. Binary and quaternary mixtures, *J. Chem. Thermodyn.* 26 (1994) 1323–1334. <https://doi.org/10.1006/jcht.1994.1151>.
- [861] J.-L. Fortier, G.C. Benson, Excess heat capacities of binary liquid mixtures determined with a Picker flow calorimeter, *J. Chem. Thermodyn.* 8 (1976) 411–423. [https://doi.org/10.1016/0021-9614\(76\)90061-6](https://doi.org/10.1016/0021-9614(76)90061-6).
- [862] I. Klesper, Messung der spezifischen Wärmen binärer Flüssigkeitsgemische, *Z. Für Phys. Chem.* 51 (1966) 1–12. [https://doi.org/10.1524/zpch.1966.51.1\\_2.001](https://doi.org/10.1524/zpch.1966.51.1_2.001).
- [863] C.-B. Soo, P. Théveneau, C. Coquelet, D. Ramjugernath, D. Richon, Determination of critical properties of pure and multi-component mixtures using a “dynamic–synthetic” apparatus, *J. Supercrit. Fluids.* 55 (2010) 545–553. <https://doi.org/10.1016/j.supflu.2010.10.022>.
- [864] L. Wang, K. Han, S. Xia, P. Ma, F. Yan, Measurement and correlation of critical properties for binary mixtures and ternary mixtures containing gasoline additives, *J. Chem. Thermodyn.* 74 (2014) 161–168. <https://doi.org/10.1016/j.jct.2014.01.025>.
- [865] M. Scheller, H. Schuberth, H.G. Könnecke, Ergebnisse von Dampf-Flüssigkeits-Phasengleichgewichtsuntersuchungen am System n-Hexan/Methylcyclohexan/Methanol bei 60°C, *J. Für Prakt. Chem.* 311 (1969) 974–982. <https://doi.org/10.1002/prac.19693110616>.
- [866] A.M. Blanco, J. Ortega, Experimental study of miscibility, density and isobaric vapor-liquid equilibrium values for mixtures of methanol in hydrocarbons (C<sub>5</sub>, C<sub>6</sub>), *Fluid Phase Equilibria.* 122 (1996) 207–222. [https://doi.org/10.1016/0378-3812\(96\)03037-3](https://doi.org/10.1016/0378-3812(96)03037-3).

- [867] K. Kurihara, T. Iguchi, T. Banaka, K. Ochi, K. Kojima, Measurement and correlation of excess molar enthalpies for the partially miscible systems 2-butanone+water and methanol+hexane, *Fluid Phase Equilibria*. 180 (2001) 59–69. [https://doi.org/10.1016/S0378-3812\(00\)00510-0](https://doi.org/10.1016/S0378-3812(00)00510-0).
- [868] L. Andreoli-Ball, D. Patterson, M. Costas, M. Cáceres-Alonso, Heat capacity and corresponding states in alkan-1-ol–n-alkane systems, *J. Chem. Soc. Faraday Trans. 1 Phys. Chem. Condens. Phases*. 84 (1988) 3991. <https://doi.org/10.1039/f19888403991>.
- [869] M. Costas, D. Patterson, Self-association of alcohols in inert solvents. Apparent heat capacities and volumes of linear alcohols in hydrocarbons, *J. Chem. Soc. Faraday Trans. 1 Phys. Chem. Condens. Phases*. 81 (1985) 635. <https://doi.org/10.1039/f19858100635>.
- [870] L. Gao, Z. Hou, H. Zhang, J. He, Z. Liu, X. Zhang, B. Han, Critical Parameters of Hexane + Carbon Monoxide + Hydrogen and Hexane + Methanol + Carbon Monoxide + Hydrogen Mixtures in the Hexane-Rich Region, *J. Chem. Eng. Data*. 46 (2001) 1635–1637. <https://doi.org/10.1021/je010146t>.
- [871] T.W. de Loos, W. Poot, J. de Swaan Arons, Vapour-liquid equilibria and critical phenomena in methanol + n-alkane systems, *Fluid Phase Equilibria*. 42 (1988) 209–227. [https://doi.org/10.1016/0378-3812\(88\)80060-8](https://doi.org/10.1016/0378-3812(88)80060-8).
- [872] J. Liu, Z. Qin, G. Wang, X. Hou, J. Wang, Critical Properties of Binary and Ternary Mixtures of Hexane + Methanol, Hexane + Carbon Dioxide, Methanol + Carbon Dioxide, and Hexane + Carbon Dioxide + Methanol, *J. Chem. Eng. Data*. 48 (2003) 1610–1613. <https://doi.org/10.1021/je034127q>.
- [873] A. Zawisza, High-pressure liquid-vapour equilibria, critical state, and  $p(V_m, T, x)$  to 448.15 K and 4.053 MPa for  $\{xC_6H_{14} + (1-x)CH_3OH\}$ , *J. Chem. Thermodyn.* 17 (1985) 941–947. [https://doi.org/10.1016/0021-9614\(85\)90007-2](https://doi.org/10.1016/0021-9614(85)90007-2).
- [874] H. Toghiani, R.K. Toghiani, D.S. Viswanath, Vapor-liquid equilibria for the methanol-benzene and methanol-thiophene systems, *J. Chem. Eng. Data*. 39 (1994) 63–67. <https://doi.org/10.1021/je00013a018>.
- [875] K. Strubl, V. Svoboda, R. Holub, Liquid-vapour equilibrium. LV. The system methanol-benzene, *Collect. Czechoslov. Chem. Commun.* 37 (1972) 3522–3531. <https://doi.org/10.1135/cccc19723522>.
- [876] G. Scatchard, S.E. Wood, J.M. Mochel, Vapor-Liquid Equilibrium. VI. Benzene-Methanol Mixtures, *J. Am. Chem. Soc.* 68 (1946) 1957–1960. <https://doi.org/10.1021/ja01214a024>.
- [877] K.L. Butcher, M.S. Medani, Thermodynamic properties of methanol-benzene mixtures at elevated temperatures, *J. Appl. Chem.* 18 (2007) 100–107. <https://doi.org/10.1002/jctb.5010180402>.
- [878] J.R. Battler, R.L. Rowley, Excess enthalpies between 293 and 323 K for constituent binaries of ternary mixtures exhibiting partial miscibility, *J. Chem. Thermodyn.* 17 (1985) 719–732. [https://doi.org/10.1016/0021-9614\(85\)90101-6](https://doi.org/10.1016/0021-9614(85)90101-6).
- [879] F. Vesely, V. Hynek, V. Svoboda, R. Holub, Isothermal calorimeter for measuring endothermic heats of mixing, *Collect. Czech Chem Commun.* 39 (1974) 355–365. <https://doi.org/10.1135/cccc19740355>.
- [880] A.G. Williamson, R.L. Scott, Heats of Mixing of Non-Electrolyte Solutions. I. Ethanol + Benzene and Methanol + Benzene, *J Phys Chem.* 64 (1960) 440–442. <https://doi.org/10.1021/j100833a015>.
- [881] J.W. Hudson, M. Van Winkle, Multicomponent vapor-liquid equilibria in systems of mixed positive and negative deviations, *J. Chem. Eng. Data*. 14 (1969) 310–318. <https://doi.org/10.1021/je60042a025>.
- [882] J. Triday, A. Andrade, F. Aguirre Ode, Isobaric study of the binary systems formed by thiophene or benzene with light alcohols, *Sci. Valpso*. 43 (1978) 1–24.
- [883] K. Strubl, P. Voňka, V. Svoboda, R. Holub, Liquid-vapour equilibrium LVI. Correlation of the benzene-methanol systems, *Collect. Czechoslov. Chem. Commun.* 38 (1973) 468–476. <https://doi.org/10.1135/cccc19730468>.
- [884] I.R. Krichevskii, N.E. Khazanova, L.R. Linshits, The liquid-vapor equilibrium in the benzene-methanol system at high pressures, *Zh Fiz Khim.* 31 (1957) 2711–2716.
- [885] J.M. Lee, B.-C. Lee, C.-H. Cho, Measurement of bubble point pressures and critical points of carbon dioxide and chlorodifluoromethane mixtures using the variable-volume view cell apparatus, *Korean J. Chem. Eng.* 17 (2000) 510–515. <https://doi.org/10.1007/BF02707158>.
- [886] C. Duran-Valencia, G. Pointurier, A. Valtz, P. Guilbot, D. Richon, Vapor-Liquid Equilibrium (VLE) Data for the Carbon Dioxide (CO<sub>2</sub>) + 1,1,1,2-Tetrafluoroethane (R134a) System at Temperatures from 252.95 K to 292.95 K and Pressures up to 2 MPa, *J. Chem. Eng. Data*. 47 (2002) 59–61. <https://doi.org/10.1021/je010075y>.
- [887] G. Silva-Oliver, L.A. Galicia-Luna, Vapor-liquid equilibria for carbon dioxide + 1,1,1,2-tetrafluoroethane (R-134a) systems at temperatures from 329 to 354 K and pressures upto 7.37 MPa, *Fluid Phase Equilibria*. 199 (2002) 213–222. [https://doi.org/10.1016/S0378-3812\(01\)00816-0](https://doi.org/10.1016/S0378-3812(01)00816-0).
- [888] J.S. Lim, J.M. Jin, K.-P. Yoo, VLE measurement for binary systems of CO<sub>2</sub>+1,1,1,2-tetrafluoroethane (HFC-134a) at high pressures, *J. Supercrit. Fluids*. 44 (2008) 279–283. <https://doi.org/10.1016/j.supflu.2007.09.025>.

- [889] Y. Uchida, M. Yasumoto, Y. Yamada, K. Ochi, T. Furuya, K. Otake, Critical Properties of Four HFE + HFC Binary Systems: Trifluoromethoxymethane (HFE-143m) + Pentafluoroethane (HFC-125), + 1,1,1,2-Tetrafluoroethane (HFC-134a), + 1,1,1,2,3,3,3-Heptafluoropropane (HFC-227ea), and + 1,1,1,2,3,3-Hexafluoropropane (HFC-236ea), *J. Chem. Eng. Data.* 49 (2004) 1615–1621. <https://doi.org/10.1021/je0499723>.
- [890] A. Valtz, C. Coquelet, A. Baba-Ahmed, D. Richon, Vapor–liquid equilibrium data for the CO<sub>2</sub> + 1,1,1,2,3,3,3-heptafluoropropane (R227ea) system at temperatures from 276.01 to 367.30 K and pressures up to 7.4 MPa, *Fluid Phase Equilibria.* 207 (2003) 53–67. [https://doi.org/10.1016/S0378-3812\(02\)00326-6](https://doi.org/10.1016/S0378-3812(02)00326-6).
- [891] S.A. Kim, J.S. Lim, J.W. Kang, Isothermal Vapor–Liquid Equilibria for the Binary System of Carbon Dioxide (CO<sub>2</sub>) + 1,1,1,2,3,3,3-Heptafluoropropane (R-227ea), *J. Chem. Eng. Data.* 55 (2010) 4999–5003. <https://doi.org/10.1021/je100583z>.
- [892] J.L. Chevalier, Systèmes binaires chloroforme-éthers aliphatiques - III. — Équilibres liquide-vapeur, *J. Chim. Phys. Phys.-Chim. Biol.* 66 (1969) 1457–1466.
- [893] F. Becker, M. Kiefer, Heat of mixing and formation of compounds in binary liquid systems. III. Ether-chloroform systems, *Z Naturforsch Sec A.* 26 (1971) 1040–1046.
- [894] J. Im, G. Lee, J. Lee, H. Kim, Vapor–liquid equilibria of the 1,1,1-trifluoroethane (HFC-143a)+dimethyl ether (DME) system, *Fluid Phase Equilibria.* 251 (2007) 59–62. <https://doi.org/10.1016/j.fluid.2006.10.017>.
- [895] J.-L. Chevalier, D. Bares, Systèmes binaires chloroforme-éthers aliphatiques - I. — Chaleurs de mélange à 25 °C, *J. Chim. Phys.* 66 (1969) 1448–1452. <https://doi.org/10.1051/jcp/196966s21448>.
- [896] F.P. Stein, R.A. Adams, Vapor-liquid equilibriums for carbon dioxide-difluoromethane system, *J. Chem. Eng. Data.* 16 (1971) 146–149. <https://doi.org/10.1021/je60049a015>.
- [897] F. Rivollet, A. Chapoy, C. Coquelet, D. Richon, Vapor–liquid equilibrium data for the carbon dioxide (CO<sub>2</sub>) + difluoromethane (R32) system at temperatures from 283.12 to 343.25 K and pressures up to 7.46 MPa, *Fluid Phase Equilibria.* 218 (2004) 95–101. <https://doi.org/10.1016/j.fluid.2003.12.002>.
- [898] A. Diefenbacher, M. Türk, (Vapour+liquid) Equilibria of binary mixtures of CO<sub>2</sub>, CH<sub>2</sub>F<sub>2</sub>, CHF<sub>3</sub>, and SF<sub>6</sub>, *J. Chem. Thermodyn.* 34 (2002) 1361–1375. [https://doi.org/10.1016/S0021-9614\(02\)00123-4](https://doi.org/10.1016/S0021-9614(02)00123-4).
- [899] L. Fedele, S. Bobbo, V. De Stefani, R. Camporese, R. Stryjek, Isothermal VLE Measurements for Difluoromethane + Dimethyl Ether and an Evaluation of Hydrogen Bonding, *J Chem Eng Data.* 50 (2005) 128–132. <https://doi.org/10.1021/je049789+>.
- [900] C. Coquelet, A. Valtz, D. Richon, Vapor–liquid equilibrium data for the difluoromethane (R32)–dimethyl ether (RE170) system at temperatures from 283.03 to 363.21K and pressures up to 5.5MPa, *Fluid Phase Equilibria.* 232 (2005) 44–49. <https://doi.org/10.1016/j.fluid.2005.02.013>.
- [901] J. Im, G. Lee, H. Kim, Vapor–Liquid Equilibria of the Difluoromethane + Dimethyl Ether and 1,1,1,2-Tetrafluoroethane + Dimethyl Ether Systems, *J. Chem. Eng. Data.* 51 (2006) 1126–1129. <https://doi.org/10.1021/je060028b>.
- [902] A. Valtz, C. Coquelet, D. Richon, Vapor–Liquid Equilibrium Data for the Sulfur Dioxide (SO<sub>2</sub>) + Difluoromethane (R32) System at Temperatures from 288.07 to 403.16 K and at Pressures up to 7.31 MPa, *Int. J. Thermophys.* 25 (2004) 1695–1711. <https://doi.org/10.1007/s10765-004-7730-9>.
- [903] M.R. Rao, K.V.K. Rao, C.V. Rao, Vapour-liquid equilibria of ethyl acetate-trichloroethylene system, *J. Appl. Chem.* 7 (1957) 666–671. <https://doi.org/10.1002/jctb.5010071205>.
- [904] A. Valtz, C. Coquelet, D. Richon, Vapor–liquid equilibrium data for the sulfur dioxide (SO<sub>2</sub>) + 1,1,1,2,3,3,3-heptafluoropropane (R227ea) system at temperatures from 288.07 to 403.19 K and pressures up to 5.38 MPa, *Fluid Phase Equilibria.* 220 (2004) 75–82. <https://doi.org/10.1016/j.fluid.2004.02.016>.
- [905] J.R. Noles, J.A. Zollweg, Vapor-liquid equilibrium for chlorodifluoromethane + dimethyl ether from 283 to 395 K at pressures to 5.0 MPa, *J. Chem. Eng. Data.* 37 (1992) 306–310. <https://doi.org/10.1021/je00007a008>.
- [906] J. Im, G. Lee, J. Lee, H. Kim, (Vapour+liquid) equilibria of the {pentafluoroethane (HFC-125)+dimethyl ether (DME)} system, *J. Chem. Thermodyn.* 38 (2006) 1510–1514. <https://doi.org/10.1016/j.jct.2006.04.009>.
- [907] M. Teodorescu, K. Aim, I. Wichterle, Isothermal vapour–liquid equilibria for pentan-3-one+1,4-dichlorobutane, +trichloromethane, +1,1,1-trichloroethane, +1,1,2,2-tetrachloroethane binary mixtures, *Fluid Phase Equilibria.* 147 (1998) 215–228. [https://doi.org/10.1016/S0378-3812\(98\)00235-0](https://doi.org/10.1016/S0378-3812(98)00235-0).
- [908] S. Bobbo, L. Fedele, R. Camporese, R. Stryjek, Isothermal vapor–liquid equilibrium for the three binary systems 1,1,1,2,3,3-hexafluoropropane with dimethyl ether or propane, and 1,1,1,3,3,3-hexafluoropropane with dimethyl ether, *Fluid Phase Equilibria.* 174 (2000) 3–12. [https://doi.org/10.1016/S0378-3812\(00\)00413-1](https://doi.org/10.1016/S0378-3812(00)00413-1).

- [909] S. Bobbo, R. Camporese, R. Stryjek, (Vapour + liquid) equilibrium measurements and correlations of the refrigerant mixture {dimethyl ether (RE170) + 1,1,1,3,3,3-hexafluoropropane (R236fa)} at the temperatures (303.68 and 323.75) K, *J. Chem. Thermodyn.* 30 (1998) 1041–1046. <https://doi.org/10.1006/jcht.1998.0369>.
- [910] A.S. Mozzhukhin, I.A. Serafimov, V.I. Zetkin, A.D. Raskina, V.A. Mitropol'skaya, Liquid-vapor equilibrium in a sulfur monochloride-perchloromethyl mercaptan system at low pressures, *J Appl Chem USSR.* 41 (1968) 2764–2766.
- [911] M.A. Siddiqi, K. Lucas, The excess enthalpy of methyl iodide + carbon disulphide, methyl iodide + dichloromethane and dichloromethane + carbon disulphide over a range of temperatures and pressures, *Fluid Phase Equilibria.* 20 (1985) 297–304. [https://doi.org/10.1016/0378-3812\(85\)90048-2](https://doi.org/10.1016/0378-3812(85)90048-2).
- [912] H. Röck, W. Schröder, Dampf-Flüssigkeits-Gleichgewichtsmessungen im System Azeton-Chloroform, *Z Phys Chem NF.* 11 (1957) 41–55. [https://doi.org/10.1524/zpch.1957.11.1\\_2.041](https://doi.org/10.1524/zpch.1957.11.1_2.041).
- [913] O. Vilim, E. Hala, V. Fried, J. Pick, Liquid-vapor equilibria. XII. Fractional steam distillation of the system o-nitroethylbenzene-p-nitroethylbenzene, *Chem Listy.* 48 (1954) 1109–1113.
- [914] E. Beckmann, O. Faust, Die Dampfspannung der Aceton-Chloroformgemische in Abhängigkeit von der Temperatur, *Z. Für Phys. Chem.* 89U (1914). <https://doi.org/10.1515/zpch-1914-8917>.
- [915] H. Segura, A. Mejía, R. Reich, J. Wisniak, S. Loras, Isobaric Vapor-Liquid Equilibria and Densities for the Binary Systems Oxolane + Ethyl 1,1-Dimethylethyl Ether, Oxolane + 2-Propanol and Propan-2-One + Trichloromethane, *Phys. Chem. Liq.* 41 (2003) 283–301. <https://doi.org/10.1080/0031910021000044456>.
- [916] V.E. Sabinin, V.P. Belousov, A.G. Morachevskii, Heats of mixing and evaporation in the acetonechloroform system, *Izv Vyssh Uchebn Zaved Khim Khim Tekhnol.* 10 (1967) 34–38.
- [917] M. Kulaneck, H.J. Bittrich, Heat of solution of the system acetone-chloroform, *Wiss Z Tech Hochsch Chem Leuna-Mersebg.* 4 (1962) 139–141.
- [918] J.W. Morris, P.J. Mulvey, M.M. Abbott, H.C. Van Ness, Excess thermodynamic functions for ternary systems. I. Acetone-chloroform-methanol at 50.deg., *J. Chem. Eng. Data.* 20 (1975) 403–405. <https://doi.org/10.1021/je60067a019>.
- [919] J.-N. Jaubert, R. Privat, N. Juntarachat, General reflection on critical negative azeotropy and upgrade of the Bancroft's rule with application to the acetone+chloroform binary system, *J. Supercrit. Fluids.* 94 (2014) 17–29. <https://doi.org/10.1016/j.supflu.2014.06.014>.
- [920] T. Ohta, H. Asano, I. Nagata, Thermodynamic study of complex formation in four binary liquid mixtures containing chloroform, *Fluid Phase Equilibria.* 4 (1980) 105–114. [https://doi.org/10.1016/0378-3812\(80\)80008-2](https://doi.org/10.1016/0378-3812(80)80008-2).
- [921] I. Nagata, Isobaric Vapor-Liquid Equilibria for the Ternary System Chloroform-Methanol-Ethyl Acetate., *J. Chem. Eng. Data.* 7 (1962) 367–373. <https://doi.org/10.1021/je60014a013>.
- [922] J. Ortega, Excess enthalpy. Trichloromethane-ethyl methanoate system, *Int Data Ser Sel Data Mix. Ser A.* 21 (1993) 40.
- [923] W. Fang, Q. Yu, R. Lin, H. Zong, Vapor heat capacities of some polar-polar binary systems, *Thermochim. Acta.* 352–353 (2000) 19–23. [https://doi.org/10.1016/S0040-6031\(99\)00431-1](https://doi.org/10.1016/S0040-6031(99)00431-1).
- [924] R. Haase, W. Tillmann, Negative values of the entropy of mixing, *Z Phys Chem Munich.* 175 (1992) 209–216.
- [925] S.K. Suri, R.C. Maheshwari, Molar excess enthalpies of arsenic tribromide + benzene, +cyclohexane, and +tetrachloromethane at 313.15 K, *J. Chem. Thermodyn.* 12 (1980) 1191–1192. [https://doi.org/10.1016/S0021-9614\(80\)80013-9](https://doi.org/10.1016/S0021-9614(80)80013-9).
- [926] H.C. van Ness, M.M. Abbott, Excess enthalpy. Trichloromethane (chloroform)-oxolane (tetrahydrofuran) system, *Int Data Ser Sel Data Mix. Ser A.* 1974 (1974) 67.
- [927] A. Inglese, M. Castagnolo, A. Dell'atti, A. de Giglio, Excess heat capacities and excess volumes of binary liquid mixtures of chloroform with cyclic ethers at 298.15 K, *Thermochim. Acta.* 44 (1981) 77–87. [https://doi.org/10.1016/0040-6031\(81\)80273-0](https://doi.org/10.1016/0040-6031(81)80273-0).
- [928] L.A. Beath, A.G. Williamson, Thermodynamics of ether solutions I. Enthalpies of mixing of ethers with carbon tetrachloride and with chloroform, *J. Chem. Thermodyn.* 1 (1969) 51–57. [https://doi.org/10.1016/0021-9614\(69\)90036-6](https://doi.org/10.1016/0021-9614(69)90036-6).
- [929] F. Becker, M. Kiefer, Kontinuierliche Bestimmung von Mischungswärmen durch isotherme Enthalpimetritation, *Z. Für Naturforschung A.* 24 (1969). <https://doi.org/10.1515/zna-1969-0103>.
- [930] I. Nagata, H. Hayashida, Vapor-Liquid Equilibrium Data For The Ternary Systems: Methyl Acetate-2-Propanol-Benzene And Methyl Acetate-Chloroform-Benzene, *J. Chem. Eng. Jpn.* 3 (1970) 161–166. <https://doi.org/10.1252/jcej.3.161>.
- [931] J. Ortega, J. Placido, Excess enthalpies of 14 binary liquid mixtures of trichloromethane + methyl n-alkanoates (C3-C16) at 298.15 K, *ELDATA Int Electron J Phys Chem Data.* 2 (1996) 85–96.

- [932] M. Teodorescu, A. Barhala, D. Dragoescu, Isothermal (vapour+liquid) equilibria for the binary (cyclopentanone or cyclohexanone with 1,1,2,2-tetrachloroethane) systems at temperatures of (343.15, 353.15, and 363.15)K, *J. Chem. Thermodyn.* 38 (2006) 1432–1437. <https://doi.org/10.1016/j.jct.2006.01.010>.
- [933] G. Pathak, A.D. Tripathi, U.D. Phalgune, S.D. Pradhan, Enthalpies of mixing of tetrachloroethane with furan, methylfuran, tetrahydrofuran, cyclopentanone and 1,4-dioxane, *Thermochim. Acta.* 258 (1995) 109–115. [https://doi.org/10.1016/0040-6031\(94\)02236-H](https://doi.org/10.1016/0040-6031(94)02236-H).
- [934] R. Chadha, A.D. Tripathi, Excess Molar Enthalpies of 1,1,2,2-Tetrachloroethane + 2-Methylfuran, + Tetrahydrofuran, + 1,4-Dioxane, and + Cyclopentanone at 308.15 and 318.15 K, *J. Chem. Eng. Data.* 40 (1995) 645–646. <https://doi.org/10.1021/je00019a024>.
- [935] J. Farkova, I. Wichterle, Vapor-liquid equilibria of 1, 1, 2, 2-tetrachloroethane + some n-alkyl n-alkanoates, *ELDATA Int Electron J Phys-Chem Data.* 1 (1995) 13–22.
- [936] J. Ortega, Excess enthalpy. 1,1,2,2-Tetrachloroethane - ethyl ethanoate system, *Int. DATA Ser. Sel. Data Mix. Ser. Thermodyn. Prop. Non-React. Bin. Syst. Org. Subst.* 4 (1991) 249.
- [937] J.-P. Chao, F.-Q. Zhang, M. Dai, Studies of thermodynamic properties of binary mixtures containing an alcohol XVIII. Excess molar enthalpies of each of (one of the four butanols + trichloromethane or 1,2-dichloroethane), *J. Chem. Thermodyn.* 24 (1992) 823–827. [https://doi.org/10.1016/S0021-9614\(05\)80227-7](https://doi.org/10.1016/S0021-9614(05)80227-7).
- [938] I. Nagata, Y. Kawamura, H. Asano, K. Fujiwara, Y. Ogasawara, Excess Enthalpies for Binary Mixtures of Chloroform with Alcohols, *Z Phys Chem Leipz.* 259 (1978) 1109–1116.
- [939] A. Aucejo, V. Gonzalez-Alfaro, J.B. Monton, M.I. Vazquez, Isobaric Vapor-Liquid Equilibria of Trichloroethylene with 1-Propanol and 2-Propanol at 20 and 100 kPa, *J. Chem. Eng. Data.* 40 (1995) 332–335. <https://doi.org/10.1021/je00017a073>.
- [940] H. Iloukhani, Excess Molar Enthalpies for Binary Mixtures with Trichloroethylene + Alkan-1-ols (C3–C8) at 298.15 K, *J. Chem. Eng. Data.* 42 (1997) 802–804. <https://doi.org/10.1021/je970024u>.
- [941] A. Dejoz, V. González-Alfaro, P.J. Miguel, M.I. Vázquez, Isobaric Vapor–Liquid Equilibria of Trichloroethylene with 1-Butanol and 2-Butanol at 20 and 100 kPa, *J. Chem. Eng. Data.* 41 (1996) 89–92. <https://doi.org/10.1021/je950163g>.
- [942] H. Iloukhani, J.B. Parsa, Excess Molar Enthalpies of Binary Mixtures of Trichloroethylene with Six 2-Alkanols at 25°C, *J Solut. Chem.* 30 (2001) 425–433. <https://doi.org/10.1023/A:1010396430848>.
- [943] H.G. Harris, Vapor-liquid equilibria in binary hydrocarbon - polar solvent systems, University of California, 1968.
- [944] H. Desplanches, J.-L. Chevalier, R. Llinas, Étude thermodynamique de solutions d'acétonitrile et d'hydrocarbures acétyléniques, *J. Chim. Phys.* 74 (1977) 259–265. <https://doi.org/10.1051/jcp/1977740259>.
- [945] I. Nagata, Vapor-liquid equilibria for the ternary system 2-propanol-chloroform-benzene at 50°C, *J. Chem. Eng. Data.* 30 (1985) 80–82. <https://doi.org/10.1021/je00039a027>.
- [946] G. Hanumantharao, B.V. Subbarao, ISOBARIC VAPOR-LIQUID-EQUILIBRIA-CHLOROFORM-ISOPROPANOL, TERTIARY BUTANOL-TOLUENE AND TERTIARY BUTANOL-TRICHLOROETHYLENE SYSTEMS, *INDIAN J. Technol.* 12 (1974) 292–295.
- [947] D. Zudkevitch, M. Lindrud, Y.-Z. Chu, Vapor–Liquid Equilibria for Ethanol + Hept-1-yne and Butyric Acid + Butyric Anhydride, *J. Chem. Eng. Data.* 44 (1999) 393–397. <https://doi.org/10.1021/je980210f>.
- [948] T.M. Letcher, F.E.Z. Schoonbaert, B. Bean, The molar excess enthalpies and volumes of 1-alkyne + methanol and + ethanol mixtures at 298.15 K, *Fluid Phase Equilibria.* 61 (1990) 111–119. [https://doi.org/10.1016/0378-3812\(90\)90008-B](https://doi.org/10.1016/0378-3812(90)90008-B).
- [949] G. Scatchard, C.L. Raymond, Vapor—Liquid Equilibrium. II. Chloroform—Ethanol Mixtures at 35, 45 and 55°, *J. Am. Chem. Soc.* 60 (1938) 1278–1287. <https://doi.org/10.1021/ja01273a002>.
- [950] H. Roeck, W. Schroeder, Beitrag zur Kenntnis des Konzentrationsverlaufs thermodynamischer Mischungsfunctionen, *Z Phys Chem NF.* 9 (1956) 277–284.
- [951] V. Bourrelly, J.-L. Chevalier, Appareil pour la détermination rapide des équilibres isothermes liquide-vapeur, *J. Chim. Phys.* 65 (1968) 1561–1564. <https://doi.org/10.1051/jcp/1968651561>.
- [952] E. Hala, V. Fried, J. Pick, O. Vilim, Liquid-vapor equilibria. VII. Calculation of liquid-vapor equilibria in two-component systems from isothermal p-x curves, *Chem Listy.* 47 (1953) 1423–1427.
- [953] A.V. Orchillés, P.J. Miguel, E. Vercher, A. Martínez-Andreu, Isobaric Vapor–Liquid and Liquid–Liquid Equilibria for Chloroform + Ethanol + 1-Ethyl-3-methylimidazolium Trifluoromethanesulfonate at 100 kPa, *J. Chem. Eng. Data.* 53 (2008) 2642–2648. <https://doi.org/10.1021/je800548t>.
- [954] M. Roach, H.C. Van Ness, Excess thermodynamic functions for ternary systems. 10. HE and SE for ethanol/chloroform/1,4-dioxane at 50°C, *J. Chem. Eng. Data.* 29 (1984) 181–183. <https://doi.org/10.1021/je00036a026>.

- [955] A.N. Campbell, E.M. Kartzmark, J.M.T.M. Gieskes, Vapor-Liquid Equilibria, Densities, And Refractivities In The System Acetic Acid – Chloroform – Water At 25 °C, *Can. J. Chem.* 41 (1963) 407–429. <https://doi.org/10.1139/v63-059>.
- [956] J.J. Conti, D.F. Othmer, R. Gilmont, Composition of Vapors from Boiling Binary Solutions. Systems Containing Formic Acid, Acetic Acid, Water, and Chloroform., *J. Chem. Eng. Data.* 5 (1960) 301–307. <https://doi.org/10.1021/je60007a019>.
- [957] A.N. Campbell, J.M.T.M. Gieskes, The Isobaric Boiling Points Of The System: Acetic Acid – Chloroform – Water At A Pressure Of 760 Mm Hg, *Can. J. Chem.* 42 (1964) 186–189. <https://doi.org/10.1139/v64-032>.
- [958] E.V. Abramov, A.S. Mirzayan, V.I. Fedorova, Heats of formation of ternary systems. 1. Acetic acid-pyridine-chloroform system, *Izv Akad Nauk Kaz SSR Ser Khim.* 22 (1972) 26–32.
- [959] F. Ratkovics, Adiabatic calorimeter for determining heats of mixing, *Magy Kem Foly.* 77 (1971) 499–502.
- [960] J. Gmehling, U. Onken, H.W. Schulte, Vapor-liquid equilibriums for the binary systems diethyl ether-halothane (1,1,1-trifluoro-2-bromo-2-chloroethane), halothane-methanol, and diethyl ether-methanol, *J. Chem. Eng. Data.* 25 (1980) 29–32. <https://doi.org/10.1021/je60084a016>.
- [961] D. Fenclova, V. Dohnal, Excess Gibbs energy. Bromochloro-1,1,1-trifluoroethane - methanol system, *Int Data Ser Sel Data Mix. Ser A.* 21 (1993) 100.
- [962] M. Costas, Excess heat capacity. Bromochloro-1,1,1-trifluoroethane - methanol system, *Int Data Ser Sel Data Mix. Ser A.* 21 (1993) 158.
- [963] A. Jonasson, M. Savoia, O. Persson, A. Fredenslund, Isothermal vapor-liquid equilibrium data for ether + glycol, chloroalkene + glycol, epoxy ether + alkane, epoxy ether + alkene, and epoxy ether + chloroalkane systems, *J. Chem. Eng. Data.* 39 (1994) 134–139. <https://doi.org/10.1021/je00013a038>.
- [964] D. Venkatesulu, M.V.P. Rao, D. Veeranna, Excess enthalpies of 2-alkoxyethanols with trichloroethylene and tetrachloroethylene at 298.15 K, *Thermochim. Acta.* 242 (1994) 33–39. [https://doi.org/10.1016/0040-6031\(94\)85006-2](https://doi.org/10.1016/0040-6031(94)85006-2).
- [965] M. Lazarte, A.C. Gómez Marigliano, H.N. Sólamo, Excess Molar Volume, Viscosity, and Molar Refraction Deviations, and Liquid?Vapor Equilibrium at 303.15 K for Chloroform + Acetonitrile Binary Mixture. An Infrared Study, *J. Solut. Chem.* 33 (2004) 1549–1563. <https://doi.org/10.1007/s10953-004-1393-9>.
- [966] I. Nagata, Y. Kawamura, Excess thermodynamic functions and complex formation in binary liquid mixtures containing acetonitrile, *Fluid Phase Equilibria.* 3 (1979) 1–11. [https://doi.org/10.1016/0378-3812\(79\)80023-0](https://doi.org/10.1016/0378-3812(79)80023-0).
- [967] F. Mato, M. Sanchez, Liquid-vapor equilibriums of binary mixtures of acetonitrile, *An. Real Soc. Espanola Fis. Quimica Ser. B Quimica.* 63 (1967) 1–11.
- [968] Y.P. Handa, D.E. Jones, Molar excess enthalpies of acetonitrile + chloroform and of acetonitrile + chloroform-d1 at 298 K, *Can. J. Chem.* 55 (1977) 2977–2979. <https://doi.org/10.1139/v77-414>.
- [969] I. Nagata, K. Tamura, Excess enthalpies of acetonitrile + trichloromethane, + ethyl acetate, and + methyl acetate, and of (acetonitrile + trichloromethane) + ethyl acetate and + methyl acetate at 308.15 K, *J. Chem. Thermodyn.* 15 (1983) 721–724. [https://doi.org/10.1016/0021-9614\(83\)90138-6](https://doi.org/10.1016/0021-9614(83)90138-6).
- [970] H.C. Zegers, G. Somsen, Volumes and heat capacities of mixtures of dimethylformamide with several dialkylacetamides, *Fluid Phase Equilibria.* 18 (1984) 299–311. [https://doi.org/10.1016/0378-3812\(84\)85013-X](https://doi.org/10.1016/0378-3812(84)85013-X).
- [971] I. Nagata, Isothermal (vapour + liquid) equilibria of propan-1-ol + acetonitrile and + trichloromethane and of (propan-1-ol + acetonitrile + trichloromethane), *J. Chem. Thermodyn.* 17 (1985) 1017–1022. [https://doi.org/10.1016/0021-9614\(85\)90086-2](https://doi.org/10.1016/0021-9614(85)90086-2).
- [972] Wang Shouyu, Cai Shuxing, VLE Data for Chloroform - n-Propanol and its System Containing Salt, *Huaxue Gongcheng.* 22 (1994) 36–40.
- [973] J. Ortega, Excess enthalpy. 1,1,2,2-Tetrachloroethane - propyl methanoate system, *Int. DATA Ser. Sel. Data Mix. Ser. Thermodyn. Prop. Non-React. Bin. Syst. Org. Subst.* 4 (1991) 248.
- [974] Y.D. Zel'venskii, The solubility of carbon dioxide in water under pressure, *Zh Khim Prom.* 14 (1937) 1250–1257.
- [975] S.-X. Hou, G.C. Maitland, J.P.M. Trusler, Measurement and modeling of the phase behavior of the (carbon dioxide+water) mixture at temperatures from 298.15K to 448.15K, *J. Supercrit. Fluids.* 73 (2013) 87–96. <https://doi.org/10.1016/j.supflu.2012.11.011>.
- [976] P.C. Gillespie, G.M. Wilson, Vapor-Liquid and Liquid-Liquid Equilibria: Water - Methane, Water - Carbon Dioxide, Water - Hydrogen Sulfide, Water - n-Pentane, Water - Methane - n-Pentane, *GPA Res. Rep.* (1982) 1–73.

- [977] Y. Liu, M. Hou, H. Ning, D. Yang, G. Yang, B. Han, Phase Equilibria of CO<sub>2</sub> + N<sub>2</sub> + H<sub>2</sub>O and N<sub>2</sub> + CO<sub>2</sub> + H<sub>2</sub>O + NaCl + KCl + CaCl<sub>2</sub> Systems at Different Temperatures and Pressures, *J. Chem. Eng. Data.* 57 (2012) 1928–1932. <https://doi.org/10.1021/je3000958>.
- [978] G. Ferrentino, D. Barletta, M.O. Balaban, G. Ferrari, M. Poletto, Measurement and prediction of CO<sub>2</sub> solubility in sodium phosphate monobasic solutions for food treatment with high pressure carbon dioxide, *J. Supercrit. Fluids.* 52 (2010) 142–150. <https://doi.org/10.1016/j.supflu.2009.10.005>.
- [979] Y. Liu, M. Hou, G. Yang, B. Han, Solubility of CO<sub>2</sub> in aqueous solutions of NaCl, KCl, CaCl<sub>2</sub> and their mixed salts at different temperatures and pressures, *J. Supercrit. Fluids.* 56 (2011) 125–129. <https://doi.org/10.1016/j.supflu.2010.12.003>.
- [980] M.B. King, A. Mubarak, J.D. Kim, T.R. Bott, The mutual solubilities of water with supercritical and liquid carbon dioxides, *J. Supercrit. Fluids.* 5 (1992) 296–302. [https://doi.org/10.1016/0896-8446\(92\)90021-B](https://doi.org/10.1016/0896-8446(92)90021-B).
- [981] S.D. Zaalishvili, Solubility of carbon dioxide from its mixtures with hydrogen and nitrogen in water under pressure, *Zh Fiz Khim.* 14 (1940) 413–417.
- [982] R. Dohrn, A.P. Bünz, F. Devlieghere, D. Thelen, Experimental measurements of phase equilibria for ternary and quaternary systems of glucose, water, CO<sub>2</sub> and ethanol with a novel apparatus, *Fluid Phase Equilibria.* 83 (1993) 149–158. [https://doi.org/10.1016/0378-3812\(93\)87017-U](https://doi.org/10.1016/0378-3812(93)87017-U).
- [983] R. D'souza, J.R. Patrick, A.S. Teja, High Pressure Phase Equilibria in the Carbon Dioxide - n-Hexadecane and Carbon Dioxide - Water Systems, *Can. J. Chem. Eng.* 66 (1988) 319–323. <https://doi.org/10.1002/cjce.5450660221>.
- [984] J.A. Briones, J.C. Mullins, M.C. Thies, B.-U. Kim, Ternary phase equilibria for acetic acid-water mixtures with supercritical carbon dioxide, *Fluid Phase Equilibria.* 36 (1987) 235–246. [https://doi.org/10.1016/0378-3812\(87\)85026-4](https://doi.org/10.1016/0378-3812(87)85026-4).
- [985] A. Bamberger, G. Sieder, G. Maurer, High-pressure (vapor+liquid) equilibrium in binary mixtures of (carbon dioxide+water or acetic acid) at temperatures from 313 to 353 K, *J. Supercrit. Fluids.* 17 (2000) 97–110. [https://doi.org/10.1016/S0896-8446\(99\)00054-6](https://doi.org/10.1016/S0896-8446(99)00054-6).
- [986] O. Pfohl, P. Avramova, G. Brunner, Two- and three-phase equilibria in systems containing benzene derivatives, carbon dioxide, and water at 373.15 K and 10–30 MPa, *Fluid Phase Equilibria.* 141 (1998) 179–206. [https://doi.org/10.1016/S0378-3812\(97\)00210-0](https://doi.org/10.1016/S0378-3812(97)00210-0).
- [987] S. Takenouchi, G.C. Kennedy, The binary system H<sub>2</sub>O-CO<sub>2</sub> at high temperatures and pressures, *Am. J. Sci.* 262 (1964) 1055–1074. <https://doi.org/10.2475/ajs.262.9.1055>.
- [988] A. Zawisza, B. Malesinska, Solubility of carbon dioxide in liquid water and of water in gaseous carbon dioxide in the range 0.2–5 MPa and at temperatures up to 473 K, *J. Chem. Eng. Data.* 26 (1981) 388–391. <https://doi.org/10.1021/je00026a012>.
- [989] K. Tödheide, E.U. Franck, Das Zweiphasengebiet und die kritische Kurve im System Kohlendioxid–Wasser bis zu Drucken von 3500 bar, *Z. Für Phys. Chem.* 37 (1963) 387–401. [https://doi.org/10.1524/zpch.1963.37.5\\_6.387](https://doi.org/10.1524/zpch.1963.37.5_6.387).
- [990] E. Pérez, Y. Sánchez-Vicente, A. Cabañas, C. Pando, J.A.R. Renuncio, Excess molar enthalpies for mixtures of supercritical carbon dioxide and water+ethanol solutions, *J. Supercrit. Fluids.* 36 (2005) 23–30. <https://doi.org/10.1016/j.supflu.2005.03.006>.
- [991] Xuemin Chen, S.E. Gillespie, J.L. Oscarson, R.M. Izatt, Calorimetric determination of thermodynamic quantities for chemical reactions in the system CO<sub>2</sub>-NaOH-H<sub>2</sub>O from 225 to 325°C, *J. Solut. Chem.* 21 (1992) 825–848. <https://doi.org/10.1007/BF00651511>.
- [992] C.J. Wormald, N.M. Lancaster, A.J. Sellars, The excess molar enthalpies of {xH<sub>2</sub>O + (1 - x)CO}(g) and {xH<sub>2</sub>O + (1 - x)CO<sub>2</sub>}(g) at high temperatures and pressures, *J. Chem. Thermodyn.* 18 (1986) 135–147. [https://doi.org/10.1016/0021-9614\(86\)90128-X](https://doi.org/10.1016/0021-9614(86)90128-X).
- [993] L. Guo, X.-H. Wu, D.-X. Zheng, W. Deng, Measurement and Correlation of Vapor–Liquid Equilibrium for the Carbon Dioxide + 1-Butoxy Butane System, *J. Chem. Eng. Data.* 55 (2010) 476–478. <https://doi.org/10.1021/je900231r>.
- [994] C. Secuianu, V. Feroiu, D. Geană, Phase behavior for carbon dioxide+ethanol system: Experimental measurements and modeling with a cubic equation of state, *J. Supercrit. Fluids.* 47 (2008) 109–116. <https://doi.org/10.1016/j.supflu.2008.08.004>.
- [995] C.-Y. Day, C.J. Chang, C.-Y. Chen, Phase Equilibrium of Ethanol + CO<sub>2</sub> and Acetone + CO<sub>2</sub> at Elevated Pressures, *J. Chem. Eng. Data.* 41 (1996) 839–843. <https://doi.org/10.1021/je960049d>.
- [996] S. Yao, F. Liu, Z. Han, Z. Zhu, Vapor-liquid equilibria of binary systems of alcohols, water-carbon dioxide at supercritical or near critical condition, *Gaoxiao Huaxue Gongcheng Xuebao.* 3 (1989) 9–15.
- [997] H. Tanaka, M. Kato, Vapor-liquid equilibrium properties of carbon dioxide + ethanol mixture at high pressures., *J. Chem. Eng. Jpn.* 28 (1995) 263–266. <https://doi.org/10.1252/jcej.28.263>.
- [998] K. Tochigi, T. Namae, T. Suga, H. Matsuda, K. Kurihara, M.C. dos Ramos, C. McCabe, Measurement and prediction of high-pressure vapor–liquid equilibria for binary mixtures of carbon dioxide+n-octane,

- methanol, ethanol, and perfluorohexane, *J. Supercrit. Fluids.* 55 (2010) 682–689. <https://doi.org/10.1016/j.supflu.2010.10.016>.
- [999] S.N. Joung, C.W. Yoo, H.Y. Shin, S.Y. Kim, K.-P. Yoo, C.S. Lee, W.S. Huh, Measurements and correlation of high-pressure VLE of binary CO<sub>2</sub>–alcohol systems (methanol, ethanol, 2-methoxyethanol and 2-ethoxyethanol), *Fluid Phase Equilibria.* 185 (2001) 219–230. [https://doi.org/10.1016/S0378-3812\(01\)00472-1](https://doi.org/10.1016/S0378-3812(01)00472-1).
- [1000] L. Brandt, Einsatz überkritischer Fluide für die Trenntechnik, Thesis. (2011) 1–128.
- [1001] L.A. Galicia-Luna, A. Ortega-Rodriguez, D. Richon, New Apparatus for the Fast Determination of High-Pressure Vapor–Liquid Equilibria of Mixtures and of Accurate Critical Pressures, *J. Chem. Eng. Data.* 45 (2000) 265–271. <https://doi.org/10.1021/je990187d>.
- [1002] Yi-Ling Tian, Ming Han, Li Chen, Ji-Jun Feng, Ying Qin, Study on Vapor-Liquid Phase Equilibria for CO<sub>2</sub>-C<sub>2</sub>H<sub>5</sub>OH System, *Wuli Huaxue Xuebao.* 17 (2001) 155–160.
- [1003] J.L. Mendoza de la Cruz, L.A. Galicia-Luna, High-pressure vapor-liquid equilibria for the carbon dioxide + ethanol and carbon dioxide + 1-propanol systems at temperatures from 322.36 K to 391.96 K, *ELDATA Int Electron J Phys Chem Data.* 5 (1999) 157–164.
- [1004] R.A. Hauser, J.P. Zhao, P.R. Tremaine, A.E. Mather, Excess molar enthalpies of six (carbon dioxide + a polar solvent) mixtures at the temperatures 298.15 K and 308.15 K and pressures from 7.5 MPa to 12.6 MPa, *J. Chem. Thermodyn.* 28 (1996) 1303–1317. <https://doi.org/10.1006/jcht.1996.0115>.
- [1005] D.R. Cordray, R.M. Izatt, J.J. Christensen, J.L. Oscarson, The excess enthalpies of (carbon dioxide + ethanol) at 308.15, 325.15, 373.15, 413.15, and 473.15 K from 5.00 to 14.91 MPa, *J. Chem. Thermodyn.* 20 (1988) 655–663. [https://doi.org/10.1016/0021-9614\(88\)90016-X](https://doi.org/10.1016/0021-9614(88)90016-X).
- [1006] M. Sun, R. Ye, T. Liu, H. Liu, Measurements of the Critical Temperature and Pressure of Ethylene+ Benzene+ Ethylbenzene Mixture, *Chin J Chem Eng.* 10 (2002) 469–472.
- [1007] S.-D. Yeo, S.-J. Park, J.-W. Kim, J.-C. Kim, Critical Properties of Carbon Dioxide + Methanol, + Ethanol, + 1-Propanol, and + 1-Butanol, *J. Chem. Eng. Data.* 45 (2000) 932–935. <https://doi.org/10.1021/je000104p>.
- [1008] A. Mejía, H. Segura, M. Cartes, Vapor–Liquid Equilibria and Interfacial Tensions of the System Ethanol + 2-Methoxy-2-methylpropane, *J. Chem. Eng. Data.* 55 (2010) 428–434. <https://doi.org/10.1021/je9004068>.
- [1009] A. Arce, J. Martínez-Ageitos, A. Soto, VLE Measurements of Binary Mixtures of Methanol, Ethanol, 2-Methoxy-2-methylpropane, and 2-Methoxy-2-methylbutane at 101.32 kPa, *J. Chem. Eng. Data.* 41 (1996) 718–723. <https://doi.org/10.1021/je950323o>.
- [1010] T.M. Letcher, P.U. Govender, Excess Molar Enthalpies of an Alkanol + a Branched Chain Ether at the Temperature 298.15 K, *J. Chem. Eng. Data.* 40 (1995) 997–1000. <https://doi.org/10.1021/je00020a060>.
- [1011] S.M. Cebreiro, M. Illobre, M.M. Mato, P.V. Verdes, J.L. Legido, M.I. Paz Andrade, Excess molar enthalpies at 298.15 K of the binary mixtures. tert-butyl methyl ether + alcohol (n = 1,2,3,5), *J Therm Anal Calorim.* 70 (2002) 251–254. <https://doi.org/10.1023/A:1020634507355>.
- [1012] M.M. Mato, M. Illobre, P.V. Verdes, J.L. Legido, M.I.P. Andrade, Study on the effect of increasing the chain length of the alkanol in excess molar enthalpies of mixtures containing 2-methoxy-2-methylpropane, 1-alkanol, decane, *Fluid Phase Equilibria.* 296 (2010) 37–41. <https://doi.org/10.1016/j.fluid.2010.02.012>.
- [1013] Z. Yun, M. Shi, J. Shi, High Pressure Vapor-Liquid Phase Equilibrium For Carbon Dioxide-n-Butanol And Carbon Dioxide-i-Butanol, *Ranliao Huaxue Xuebao.* 24 (1996) 87–92.
- [1014] M.V. da Silva, D. Barbosa, High pressure vapor–liquid equilibrium data for the systems carbon dioxide/2-methyl-1-propanol and carbon dioxide/3-methyl-1-butanol at 288.2, 303.2 and 313.2 K, *Fluid Phase Equilibria.* 198 (2002) 229–237. [https://doi.org/10.1016/S0378-3812\(01\)00766-X](https://doi.org/10.1016/S0378-3812(01)00766-X).
- [1015] J.E. Gutiérrez, A. Bejarano, J.C. de la Fuente, Measurement and modeling of high-pressure (vapour+liquid) equilibria of (CO<sub>2</sub>+alcohol) binary systems, *J. Chem. Thermodyn.* 42 (2010) 591–596. <https://doi.org/10.1016/j.jct.2009.11.015>.
- [1016] H.-I. Chen, P.-H. Chen, H.-Y. Chang, High-Pressure Vapor-Liquid Equilibria for CO<sub>2</sub> + 2-Butanol, CO<sub>2</sub> + Isobutanol, and CO<sub>2</sub> + tert-Butanol Systems, *J. Chem. Eng. Data.* 48 (2003) 1407–1412. <https://doi.org/10.1021/je020214r>.
- [1017] A.I. Semenova, E.A. Emel'yanova, S.S. Tsimmerman, D.S. Tsiklis, Phase equilibriums in the isobutyl alcohol-carbon dioxide system, *Russ J Phys Chem.* 52 (1978) 1149–1152.
- [1018] K. Ochi, W. Dai, Y. Wada, H. Hayashi, K. Kurihara, K. Kojima, Measurement and correlation of excess molar enthalpies for the systems containing supercritical carbon dioxide and alcohols, *Fluid Phase Equilibria.* 194–197 (2002) 919–928. [https://doi.org/10.1016/S0378-3812\(01\)00704-X](https://doi.org/10.1016/S0378-3812(01)00704-X).
- [1019] E. Brunner, W. Hültenschmidt, G. Schlichthärle, Fluid mixtures at high pressures IV. Isothermal phase equilibria in binary mixtures consisting of (methanol + hydrogen or nitrogen or methane or carbon

- monoxide or carbon dioxide), *J. Chem. Thermodyn.* 19 (1987) 273–291. [https://doi.org/10.1016/0021-9614\(87\)90135-2](https://doi.org/10.1016/0021-9614(87)90135-2).
- [1020] N. Li, P. Ma, S. Xia, Determination of Solubility of Carbon Monoxide in Methanol-Dimethyl Carbonate under High Pressure, *Shiyou Huagong*. 34 (2005) 60–64.
- [1021] I.R. Krichevskii, N.M. Zhavoronkov, D.S. Tsiklis, Solubility of hydrogen, carbon monoxide and of their mixtures in methanol at high pressures, *Zh Fiz Khim*. 9 (1937) 317–328.
- [1022] C. Secuianu, V. Feroiu, D. Geană, Measurements and Modeling of High-Pressure Phase Behavior of the Carbon Dioxide + Pentan-1-ol Binary System, *J. Chem. Eng. Data*. 56 (2011) 5000–5007. <https://doi.org/10.1021/je200867n>.
- [1023] C. Secuianu, V. Feroiu, D. Geană, High-Pressure Vapour-Liquid Equilibria of Carbon Dioxide + I-Pentanol System. Experimental Measurements and Modelling, *Rev. Chim.-Buchar*. 58 (2007) 1176–1181.
- [1024] A. Staby, J. Mollerup, Measurement of mutual solubilities of 1-Pentanol and supercritical carbon dioxide, *J. Supercrit. Fluids*. 6 (1993) 15–19. [https://doi.org/10.1016/0896-8446\(93\)90005-I](https://doi.org/10.1016/0896-8446(93)90005-I).
- [1025] G. Silva-Oliver, L.A. Galicia-Luna, S.I. Sandler, Vapor–liquid equilibria and critical points for the carbon dioxide +1-pentanol and carbon dioxide +2-pentanol systems at temperatures from 332 to 432 K, *Fluid Phase Equilibria*. 200 (2002) 161–172. [https://doi.org/10.1016/S0378-3812\(02\)00024-9](https://doi.org/10.1016/S0378-3812(02)00024-9).
- [1026] H.J. Bittrich, E. Kauer, Thermodynamics of the system diethylamine-triethylamine. I. The liquid-vapor equilibrium, *Z Phys Chem Leipz*. 219 (1962) 224–238.
- [1027] H.J. Bittrich, M. Kulaneck, G. Duering, Thermodynamics of the system diethylamine-triethylamine. Enthalpies of mixing at 14, 18, and 25°, *Z Phys Chem Leipz*. 219 (1962) 387–395.
- [1028] F. Ratkovics, J. Liszi, M. Laszlo-Parragi, B. Szeiler, J. Devay, Mixing properties of the ethanol-diethylamine-triethylamine system, *Acta Chim Acad Sci Hung*. 77 (1973) 249–265.
- [1029] E. Kauer, L. Grote, H.-J. Bittrich, Zur Thermodynamik des Systems Diäthylamin-Triäthylamin. IV, *Z. Für Phys. Chem.* 232O (1966). <https://doi.org/10.1515/zpch-1966-23231>.
- [1030] S. Fuangfoo, M. Kersting, D.S. Viswanath, Isothermal Vapor–Liquid Equilibria for Methyl-2,2-dimethylethyl Ether + 2-Methylpropan-2-ol, Diethyl Ether + Ethyl-2,2-dimethylethyl Ether, 2-Methyl-2-butene + (2-Methylbutan-2-ol), and Diisopropyl Ether + Octane, *J. Chem. Eng. Data*. 44 (1999) 405–410. <https://doi.org/10.1021/je980248s>.
- [1031] S. Bernatová, I. Wichterle, Isothermal vapour–liquid equilibria in the ternary system tert-butyl methyl ether + tert-butanol + 2,2,4-trimethylpentane and the three binary subsystems, *Fluid Phase Equilibria*. 180 (2001) 235–245. [https://doi.org/10.1016/S0378-3812\(01\)00349-1](https://doi.org/10.1016/S0378-3812(01)00349-1).
- [1032] S. Loras, A. Aucejo, R. Muñoz, Isobaric Vapor–Liquid Equilibrium in the Systems Methyl 1,1-Dimethylethyl Ether + 2-Methyl-2-propanol and Methyl 1,1-Dimethylethyl Ether + 2-Methylpentane + 2-Methyl-2-propanol, *J. Chem. Eng. Data*. 44 (1999) 1169–1174. <https://doi.org/10.1021/je990095o>.
- [1033] T. Hiaki, K. Tatsuana, T. Tsuji, M. Hongo, Vapor–liquid equilibria for binary and ternary systems composed of 2-methoxy-2-methyl propane, 2-methyl-2-propanol, and octane at 101.3 kPa, *Fluid Phase Equilibria*. 156 (1999) 161–171. [https://doi.org/10.1016/S0378-3812\(99\)00026-6](https://doi.org/10.1016/S0378-3812(99)00026-6).
- [1034] F. Davolio, G.C. Pedrosa, M. Katz, Vapor-liquid equilibrium for the p-dioxane-acetonitrile system at 298.15 K, *J. Chem. Eng. Data*. 26 (1981) 26–27. <https://doi.org/10.1021/je00023a011>.
- [1035] R. Francesconi, F. Comelli, Excess thermodynamic properties for the binary system 1,4-dioxane-acetonitrile at 40.degree.C, *J. Chem. Eng. Data*. 33 (1988) 80–83. <https://doi.org/10.1021/je00052a004>.
- [1036] J.-P.E. Grolier, G. Roux-Desgranges, M. Berkane, E. Wilhelm, Heat capacities and densities of mixtures of very polar substances 1. Mixtures containing acetonitrile, *J. Chem. Thermodyn.* 23 (1991) 421–429. [https://doi.org/10.1016/S0021-9614\(05\)80130-2](https://doi.org/10.1016/S0021-9614(05)80130-2).
- [1037] H.J. Song, H.T. Zhang, W.Y. Ying, Study on vapor-liquid equilibrium for dimethyl ether/methanol binary system, *Tianranqi Huagong*. 30 (2005) 67–71.
- [1038] M.E. Pozo, W.B. Streett, Fluid phase equilibria for the system dimethyl ether/water from 50 to 220.degree.C and pressures to 50.9 MPa, *J. Chem. Eng. Data*. 29 (1984) 324–329. <https://doi.org/10.1021/je00037a030>.
- [1039] H. Holldorff, H. Knapp, Binary vapor-liquid-liquid equilibrium of dimethyl ether - water and mutual solubilities of methyl chloride and water: Experimental results and data reduction, *Fluid Phase Equilibria*. 44 (1988) 195–209. [https://doi.org/10.1016/0378-3812\(88\)80111-0](https://doi.org/10.1016/0378-3812(88)80111-0).
- [1040] S.-J. Park, K.-J. Han, J. Gmehling, Isothermal Phase Equilibria and Excess Molar Enthalpies for Binary Systems with Dimethyl Ether at 323.15 K, *J. Chem. Eng. Data*. 52 (2007) 1814–1818. <https://doi.org/10.1021/je700174h>.
- [1041] J.H. Hong, R. Kobayashi, Vapor–liquid equilibrium studies for the carbon dioxide—methanol system, *Fluid Phase Equilibria*. 41 (1988) 269–276. [https://doi.org/10.1016/0378-3812\(88\)80011-6](https://doi.org/10.1016/0378-3812(88)80011-6).

- [1042] K. Ohgaki, T. Katayama, Isothermal vapor-liquid equilibrium data for binary systems containing carbon dioxide at high pressures: methanol-carbon dioxide, n-hexane-carbon dioxide, and benzene-carbon dioxide systems, *J. Chem. Eng. Data.* 21 (1976) 53–55. <https://doi.org/10.1021/je60068a015>.
- [1043] T. Katayama, K. Ohgaki, G. Maekawa, M. Goto, T. Nagano, Isothermal Vapor-Liquid Equilibria Of Acetone-Carbon Dioxide And Methanol-Carbon Dioxide Systems At High Pressures, *J. Chem. Eng. Jpn.* 8 (1975) 89–92. <https://doi.org/10.1252/jcej.8.89>.
- [1044] C.J. Chang, C.-Y. Day, C.-M. Ko, K.-L. Chiu, Densities and P-x-y diagrams for carbon dioxide dissolution in methanol, ethanol, and acetone mixtures, *Fluid Phase Equilibria.* 131 (1997) 243–258. [https://doi.org/10.1016/S0378-3812\(96\)03208-6](https://doi.org/10.1016/S0378-3812(96)03208-6).
- [1045] D. Kodama, N. Kubota, Y. Yamaki, H. Tanaka, M. Kato, High Pressure Vapor-Liquid Equilibria and Density Behaviors for Carbon Dioxide+Methanol System at 313.15 K., *Netsu Bussei.* 10 (1996) 16–20. <https://doi.org/10.2963/jjtp.10.16>.
- [1046] A.I. Semenova, E.A. Emel'yanova, S.S. Tsimmerman, D.S. Tsiklis, Phase equilibriums in the methanol-carbon dioxide system, *Zh Fiz Khim.* 53 (1979) 2502–2505.
- [1047] A.-D. Leu, S.Y.-K. Chung, D.B. Robinson, The equilibrium phase properties of (carbon dioxide + methanol), *J. Chem. Thermodyn.* 23 (1991) 979–985. [https://doi.org/10.1016/S0021-9614\(05\)80178-8](https://doi.org/10.1016/S0021-9614(05)80178-8).
- [1048] Zhu Hu-Gang, Tian Yi-Ling, Chen Li, Feng Ji-Jun, Fu Hua-Feng, Studies on vapor-liquid phase equilibria for SCF CO<sub>2</sub>+ CH<sub>3</sub>OH and SCF CO<sub>2</sub>+ C<sub>2</sub>H<sub>5</sub>OH systems, *Gaodeng Xuexiao Huaxue Xuebao.* 23 (2002) 1588–1591.
- [1049] W. Dai, K. Kojima, K. Ochi, Measurement and Correlation of Excess Molar Enthalpies of CO<sub>2</sub> + CH<sub>3</sub>OH System in the Vicinity of Critical Point of Carbon Dioxide, *J Chem Eng Data.* 44 (1999) 161–164. <https://doi.org/10.1021/je980191+>.
- [1050] W. Dai, K. Ochi, K. Kurihara, K. Kojima, M. Hongo, Measurement and Correlation of Excess Enthalpy for the System(CO<sub>2</sub>+CH<sub>3</sub>OH) Containing Supercritical Carbon Dioxide., *Netsu Bussei.* 12 (1998) 64–69. <https://doi.org/10.2963/jjtp.12.64>.
- [1051] J.. Christensen, D.. Cordray, J.. Oscarson, R.. Izatt, The excess enthalpies of four (carbon dioxide + an alkanol) mixtures from 308.15 to 573.15 K at 7.50 to 12.50 MPa, *J. Chem. Thermodyn.* 20 (1988) 867–875. [https://doi.org/10.1016/0021-9614\(88\)90076-6](https://doi.org/10.1016/0021-9614(88)90076-6).
- [1052] J. Staroske, G. Figurski, Vapor-liquid equilibrium of the ternary system furfural - ethyl acetate - methanol and its binary subsystems at 298.15 K, *Chem Tech Leipz.* 44 (1992) 64–66.
- [1053] P. Murti, M. Van Winkle, Vapor-Liquid Equilibria for Binary Systems of Methanol, Ethyl Alcohol, 1-Propanol, and 2-Propanol with Ethyl Acetate and 1-Propanol-Water., *Ind. Eng. Chem. Chem. Eng. Data Ser.* 3 (1958) 72–81. <https://doi.org/10.1021/i460003a016>.
- [1054] I. Nagata, T. Yamada, S. Nakagawa, Excess Gibbs free energies and heats of mixing for binary systems ethyl acetate with methanol, ethanol, 1-propanol, and 2-propanol, *J. Chem. Eng. Data.* 20 (1975) 271–275. <https://doi.org/10.1021/je60066a007>.
- [1055] P. Susial, A. Sosa-Rosario, R. Rios-Santana, Vapor-Liquid Equilibria for Ethyl Acetate + Methanol at (0.1, 0.5, and 0.7) MPa. Measurements with a New Ebulliometer, *J. Chem. Eng. Data.* 55 (2010) 5701–5706. <https://doi.org/10.1021/je100614r>.
- [1056] A.M. Blanco, J. Ortega, Densities and Vapor-Liquid Equilibrium Values for Binary Mixtures Composed of Methanol + an Ethyl Ester at 141.3 kPa with Application of an Extended Correlation Equation for Isobaric VLE Data, *J. Chem. Eng. Data.* 43 (1998) 638–645. <https://doi.org/10.1021/je980012o>.
- [1057] J. Ortega, Excess enthalpy. Ethanol-ethyl ethanoate system, *Int Data Ser Sel Data Mix. Ser A.* 23 (1995) 161.
- [1058] R. Zhang, W. Yan, X. Wang, R. Lin, Molar excess enthalpies of ethyl acetate+alkanols at T=298.15K, p=10.0MPa, *Thermochim. Acta.* 429 (2005) 155–161. <https://doi.org/10.1016/j.tca.2005.03.009>.
- [1059] M. Rajendran, S. Renganarayanan, P.R. Madhavan, D. Srinivasan, Effect Of Dissolved Inorganic Salts On The Vapor-Liquid Equilibria And Enthalpy Of Mixing Of The Methanol-Ethyl Acetate System, *Chem. Eng. Commun.* 74 (1988) 179–193. <https://doi.org/10.1080/00986448808940458>.
- [1060] E. Lladosa, J.B. Montón, M. Burguet, R. Muñoz, Effect of pressure and the capability of 2-methoxyethanol as a solvent in the behaviour of a diisopropyl ether–isopropyl alcohol azeotropic mixture, *Fluid Phase Equilibria.* 262 (2007) 271–279. <https://doi.org/10.1016/j.fluid.2007.09.014>.
- [1061] Z. Zhang, L. Yang, Y. Xing, W. Li, Vapor-Liquid Equilibrium for Ternary and Binary Mixtures of 2-Isopropoxypropane, 2-Propanol, and N,N-Dimethylacetamide at 101.3 kPa, *J. Chem. Eng. Data.* 58 (2013) 357–363. <https://doi.org/10.1021/je300994y>.
- [1062] L. Sieg, J.L. Cruetzen, W. Jost, Zur Thermodynamik von Mischphasen VIII. Über das Verdampfungsgleichgewicht Methanol-n-Butylazetat, *Z Elektrochem Angew Phys Chem.* 55 (1951) 199–201. <https://doi.org/10.1002/bbpc.19510550307>.
- [1063] W.K. Park, Vapor-liquid equilibriums of ester-alcohol systems. III, *Hwahak Konghak.* 9 (1971) 181–190.

- [1064] F. Espiau, J. Ortega, E. Penco, J. Wisniak, Advances in the Correlation of Thermodynamic Properties of Binary Systems Applied to Methanol Mixtures with Butyl Esters, *Ind. Eng. Chem. Res.* 49 (2010) 9548–9558. <https://doi.org/10.1021/ie101165r>.
- [1065] J. Nagai, N. Isii, Volatility of fuels containing ethyl alcohol. I. Partial pressures of ethyl alcohol and ethyl ether in their mixtures and calculation of heat of mixture, *J Soc Chem Ind Jpn.* 38 (1935) 8B-12B.
- [1066] A.R. Gordon, E.J. Hornibrook, Liquid-Vapor Equilibrium for the System Ethanol - Diethyl - Ether, *Can J Res Sect B.* 24 (1946) 263–267.
- [1067] M.A. Villamañan, C. Casanova, A.H. Roux, J.-P.E. Grolier, Calorimetric investigation of the interactions between oxygen and hydroxyl groups in (alcohol+ether) at 298.15 K, *J. Chem. Thermodyn.* 14 (1982) 251–258. [https://doi.org/10.1016/0021-9614\(82\)90015-5](https://doi.org/10.1016/0021-9614(82)90015-5).
- [1068] G. Kortüm, V. Valent, Thermodynamische Mischungseffekte der Systeme Wasser(1)-1,4-Dioxan(2) und Methanol(1)-1,4-Dioxan(2); ein Vergleich, *Berichte Bunsenges. Für Phys. Chem.* 81 (1977) 752–761. <https://doi.org/10.1002/bbpc.19770810811>.
- [1069] J. Ortega, M. Chaar, J. Placido, Excess enthalpies of 72 binary liquid mixtures of methyl n-alkanoates (C4 - C16) + alkan-1-ols (C2 - C10) at 298.15 K, *ELDATA Int Electron J Phys Chem Data.* 1 (1995) 139–166.
- [1070] K. Tamura, M.M.H. Bhuiyan, Excess molar enthalpies of (methanol+1-propanol)+oxane or 1,4-dioxane mixtures at the temperature 298.15 K, *J. Chem. Thermodyn.* 35 (2003) 1657–1669. [https://doi.org/10.1016/S0021-9614\(03\)00150-2](https://doi.org/10.1016/S0021-9614(03)00150-2).
- [1071] I.B. Sitnyakovskii, A.A. Gaile, L.V. Semenov, L.L. Koldobskaya, O.S. Chupyra, Intermolecular interactions in dilute solutions of methanol in non-electrolytes, *Zh Obshch Khim.* 61 (1991) 2405–2410.
- [1072] E. Calvo, P. Brocos, Á. Piñeiro, M. Pintos, A. Amigo, R. Bravo, A.H. Roux, G. Roux-Desgranges, Heat Capacities, Excess Enthalpies, and Volumes of Mixtures Containing Cyclic Ethers. 4. Binary Systems 1,4-Dioxane + 1-Alkanols, *J. Chem. Eng. Data.* 44 (1999) 948–954. <https://doi.org/10.1021/je990078z>.
- [1073] P.P. Singh, D.V. Verma, P.S. Arora, Thermodynamics of binary methanol solutions, *Thermochim. Acta.* 15 (1976) 267–280. [https://doi.org/10.1016/0040-6031\(76\)85080-0](https://doi.org/10.1016/0040-6031(76)85080-0).
- [1074] J. Gmehling, VLE data for the design of separation processes, *AIChE Symp Ser.* 81 (1985) 121–129.
- [1075] M.-G. Kim, S.-J. Park, I.-C. Hwang, Excess molar enthalpies for the binary and ternary mixtures of ether compounds (di-isopropyl ether, di-butyl ether, propyl vinyl ether) with ethanol and isooctane at 298.15 K, *Korean J. Chem. Eng.* 25 (2008) 1160–1164. <https://doi.org/10.1007/s11814-008-0191-2>.
- [1076] R. Tanaka, S. Toyama, Excess Molar Volumes and Excess Molar Heat Capacities for Binary Mixtures of Ethanol with Chlorocyclohexane, 1-Nitropropane, Dibutyl Ether, and Ethyl Acetate at the Temperature of 298.15 K, *J. Chem. Eng. Data.* 41 (1996) 1455–1458. <https://doi.org/10.1021/je960179m>.
- [1077] P. Reddy, T.P. Benecke, D. Ramjugernath, Isothermal (vapour+liquid) equilibria for binary mixtures of diisopropyl ether with (methanol, or ethanol, or 1-butanol): Experimental data, correlations, and predictions, *J. Chem. Thermodyn.* 58 (2013) 330–339. <https://doi.org/10.1016/j.jct.2012.11.005>.
- [1078] J. Fárková, J. Linek, I. Wichterle, Isothermal vapour-liquid equilibria and excess volumes in the methanol-aliphatic ether systems, *Fluid Phase Equilibria.* 109 (1995) 53–65. [https://doi.org/10.1016/0378-3812\(95\)02710-V](https://doi.org/10.1016/0378-3812(95)02710-V).
- [1079] Á. Piñeiro, Excess volumes and isobaric heat capacities of diisopropyl ether with several alkanols at 298.15K, *Fluid Phase Equilibria.* 216 (2004) 245–256. <https://doi.org/10.1016/j.fluid.2003.11.003>.
- [1080] R.K. Toghiani, H. Toghiani, G. Venkateswarlu, Vapor-liquid equilibria for methyl tert-butyl ether + methanol and tert-amyl methyl ether + methanol, *Fluid Phase Equilibria.* 122 (1996) 157–168. [https://doi.org/10.1016/0378-3812\(96\)03043-9](https://doi.org/10.1016/0378-3812(96)03043-9).
- [1081] S. Loras, A. Aucejo, R. Muñoz, J. Wisniak, Azeotropic Behavior in the System Methanol + Methyl 1,1-Dimethylethyl Ether, *J. Chem. Eng. Data.* 44 (1999) 203–208. <https://doi.org/10.1021/je9801563>.
- [1082] Y. Wang, A. Tong, Y. Su, Z. Yang, Isobaric Vapor-Liquid Equilibrium for the System MTBE-Methanol, *Shiyou Huagong.* 18 (1989) 442–446.
- [1083] A. Westerholt, Weiterentwicklung der Gruppenbeitragszustandsgleichung VTPR zur Beschreibung der TAME-Synthese und Spaltung durch systematische Messung fehlender Phasengleichgewichtsdaten und Anpassung der erforderlichen Parameter, *Masters Thesis.* (2010) 1–113.
- [1084] J. Gmehling, S.J. Park, K. Fischer, B. Meents, Excess enthalpies of tert-butyl methyl ether, methanol, or ethanol+ butane or+ 2-methylpropene, *Int DATA Ser Sel Data Mix. Ser A.* 20 (1992) 146–152.
- [1085] I. Mertl, Liquid-vapour equilibrium. II. Phase equilibria in the ternary system ethyl acetate-ethanol-water, *Collect. Czechoslov. Chem. Commun.* 37 (1972) 366–374. <https://doi.org/10.1135/cccc19720366>.
- [1086] J. Pavlíček, G. Bogdanić, I. Wichterle, Vapour-liquid and chemical equilibria in the ethyl ethanoate+ethanol+propyl ethanoate+propanol system accompanied with transesterification reaction, *Fluid Phase Equilibria.* 328 (2012) 61–68. <https://doi.org/10.1016/j.fluid.2012.05.016>.

- [1087] Q. Li, J. Zhang, Z. Lei, J. Zhu, F. Xing, Isobaric Vapor-Liquid Equilibrium for Ethyl Acetate + Ethanol + 1-Ethyl-3-methylimidazolium Tetrafluoroborate, *J. Chem. Eng. Data.* 54 (2009) 193–197. <https://doi.org/10.1021/je800175s>.
- [1088] P. Susial, J.J. Rodriguez-Henriquez, A. Sosa-Rosario, R. Rios-Santana, Vapor-Liquid Equilibrium of Ethyl Acetate + C<sub>n</sub>H<sub>2n</sub>+1OH (n= 1,2,3) Binary Systems at 0.3 MPa, *Chin. J. Chem. Eng.* 20 (2012) 723–730. [https://doi.org/10.1016/S1004-9541\(11\)60241-3](https://doi.org/10.1016/S1004-9541(11)60241-3).
- [1089] P. Susial, A. Sosa-Rosario, J.J. Rodríguez-Henríquez, R. Rios-Santana, Vapor Pressure and VLE Data Measurements on Ethyl Acetate/Ethanol Binary System at 0.1, 0.5, and 0.7 MPa, *J. Chem. Eng. Jpn.* 44 (2011) 155–163. <https://doi.org/10.1252/jcej.10we176>.
- [1090] J. Hu, K. Tamura, S. Murakami, Excess thermodynamic properties of binary mixtures of ethyl acetate with benzene, ethanol, and 2,2,2-trifluoroethan-1-ol at 298.15 K, *Fluid Phase Equilibria.* 134 (1997) 239–253. [https://doi.org/10.1016/S0378-3812\(97\)00015-0](https://doi.org/10.1016/S0378-3812(97)00015-0).
- [1091] F. Wen-jun, Y. Qing-sen, L. Rui-sen, Z. Han-xing, Vapor heat capacity of binary and ternary systems, *Thermochim. Acta.* 299 (1997) 43–47. [https://doi.org/10.1016/S0040-6031\(97\)00135-4](https://doi.org/10.1016/S0040-6031(97)00135-4).
- [1092] T. Hu, Z. Qin, G. Wang, X. Hou, J. Wang, Critical Properties of the Reacting Mixture in the Esterification of Acetic Acid with Ethanol, *J. Chem. Eng. Data.* 49 (2004) 1809–1814. <https://doi.org/10.1021/je049771z>.
- [1093] G.J. Pierotti, C.H. Deal, E.L. Derr, Activity Coefficients and Molecular Structure, *Ind. Eng. Chem.* 51 (1959) 95–102. <https://doi.org/10.1021/ie50589a048>.
- [1094] J.N. Im, S.S. Park, H.O. Lee, Isothermal vapor-liquid equilibrium for the binary system acetone-water by the total pressure method, *Korean Chem. Eng. Res.* 12 (1974) 179–187.
- [1095] C. Treiner, P. Tzias, Standard Gibbs Free Energy of Transfer of n-Bu<sub>4</sub>NBr from Water to Water-Organic Solvent Mixtures as Deduced from Precise Vapor Pressure Measurements at 298.15°K, in: *Thermodyn. Behav. Electrolytes Mix. Solvents*, 1976: pp. 303–317.
- [1096] I. Lieberwirth, H. Schuberth, Das isotherme Dampf-Flüssigkeits-Phasengleichgewichtsverhalten des Systems Aceton/Wasser bei 35° C, *Z. Für Phys. Chem.* 260O (1979). <https://doi.org/10.1515/zpch-1979-26090>.
- [1097] E.P. Sokolova, A.G. Morachevskii, Thermodynamic properties of the acetone-water system, *Vestn Lenin U Fiz Kh.* (1967) 110–115.
- [1098] J. Griswold, S.Y. Wong, Phase-equilibria in the acetone-methanol-water system from 100° into the critical region, *Chem. Eng. Prog. Symp. Ser.* 48 (1952) 18–34.
- [1099] L. Verhoeve, H. De Schepper, The vapour-liquid equilibria of the binary, ternary and quaternary systems formed by acetone, methanol, propan-2-ol, and water, *J. Appl. Chem. Biotechnol.* 23 (2007) 607–619. <https://doi.org/10.1002/jctb.5020230807>.
- [1100] K. Ochi, K. Kojima, Vapor-liquid equilibriums for the system acetone + methanol + water, *Kagaku Kogaku.* 35 (1971) 583–586. <https://doi.org/10.1252/kakoronbunshu1953.35.583>.
- [1101] K. Kojima, K. Tochigi, H. Seki, K. Watase, Determination of vapor-liquid equilibriums from boiling point curves, *Kagaku Kogaku.* 32 (1968) 149–153. <https://doi.org/10.1252/kakoronbunshu1953.32.149>.
- [1102] D.F. Othmer, M.M. Chudgar, S.L. Levy, Binary and Ternary Systems of Acetone, Methyl Ethyl Ketone, and Water, *Ind. Eng. Chem.* 44 (1952) 1872–1881. <https://doi.org/10.1021/ie50512a042>.
- [1103] H.. French, Excess enthalpies of (acetone + water) at 278.15, 288.15, 298.15, 308.15, 318.15, and 323.15 K, *J. Chem. Thermodyn.* 21 (1989) 801–809. [https://doi.org/10.1016/0021-9614\(89\)90026-8](https://doi.org/10.1016/0021-9614(89)90026-8).
- [1104] M. Costas, D. Patterson, Heat capacities of water + organic-solvent mixtures, *J. Chem. Soc. Faraday Trans. 1 Phys. Chem. Condens. Phases.* 81 (1985) 2381. <https://doi.org/10.1039/f19858102381>.
- [1105] C. Narasigadu, P. Naidoo, C. Coquelet, D. Richon, D. Ramjugernath, Isothermal Vapor–Liquid Equilibrium Data for the Butan-2-one + Methanol or Ethanol Systems Using a Static-Analytic Microcell, *J. Chem. Eng. Data.* 58 (2013) 1280–1287. <https://doi.org/10.1021/je400065j>.
- [1106] N.F. Martínez, E. Lladosa, M. Burguet, J.B. Montón, Isobaric vapour–liquid equilibria for binary systems of 2-butanone with ethanol, 1-propanol, and 2-propanol at 20 and 101.3 kPa, *Fluid Phase Equilibria.* 270 (2008) 62–68. <https://doi.org/10.1016/j.fluid.2008.06.004>.
- [1107] C.-C. Wen, C.-H. Tu, Vapor–liquid equilibria for binary and ternary mixtures of ethanol, 2-butanone, and 2,2,4-trimethylpentane at 101.3kPa, *Fluid Phase Equilibria.* 258 (2007) 131–139. <https://doi.org/10.1016/j.fluid.2007.06.005>.
- [1108] J.-P. Chao, M. Dai, Studies of thermodynamic properties of binary mixtures containing an alcohol, *Thermochim. Acta.* 179 (1991) 257–264. [https://doi.org/10.1016/0040-6031\(91\)80355-M](https://doi.org/10.1016/0040-6031(91)80355-M).
- [1109] J. Iñarrea, J. Valero, P. Pérez, M. Gracia, C. Gutiérrez Losa, H<sub>m</sub>E and V<sub>m</sub>E of some (butanone or dipropylether + an alkanol) mixtures, *J. Chem. Thermodyn.* 20 (1988) 193–199. [https://doi.org/10.1016/0021-9614\(88\)90154-1](https://doi.org/10.1016/0021-9614(88)90154-1).
- [1110] I. Nagata, T. Ohta, S. Nakagawa, Excess Gibbs Free Energies And Heats Of Mixing For Binary Alcoholic Liquid Mixtures, *J. Chem. Eng. Jpn.* 9 (1976) 276–281. <https://doi.org/10.1252/jcej.9.276>.

- [1111] I. Nagata, O. Tago, T. Takahashi, Heats of Mixing for Binary Methyl Ethyl Ketone, Methyl Acetate-Alcohol Systems, *Chem. Eng.* 34 (1970) 1107-1112,a1. <https://doi.org/10.1252/kakoronbunshu1953.34.1107>.
- [1112] L. Pikkarainen, Excess enthalpies of binary solvent mixtures of 2-butanone with aliphatic alcohols, *Thermochim. Acta.* 114 (1987) 239-244. [https://doi.org/10.1016/0040-6031\(87\)80044-8](https://doi.org/10.1016/0040-6031(87)80044-8).
- [1113] I.G. Vinichenko, M.P. Susarev, Study and calculation of the liquid-vapor equilibrium in the acetone-ethanol-hexane system, *J Appl Chem USSR.* 39 (1966) 1475-1478.
- [1114] M.-J. Lee, C.-H. Hu, Isothermal vapor-liquid equilibria for mixtures of ethanol, acetone, and diisopropyl ether, *Fluid Phase Equilibria.* 109 (1995) 83-98. [https://doi.org/10.1016/0378-3812\(95\)02705-J](https://doi.org/10.1016/0378-3812(95)02705-J).
- [1115] S.W. Campbell, R.A. Wilsak, G. Thodos, Vapor-liquid equilibrium measurements for the ethanol-acetone system at 372.7, 397.7, and 422.6 K, *J. Chem. Eng. Data.* 32 (1987) 357-362. <https://doi.org/10.1021/je00049a021>.
- [1116] H.-C. Ku, C.-H. Tu, Isobaric vapor-liquid equilibria for mixtures of acetone, ethanol, and 2,2,4-trimethylpentane at 101.3kPa, *Fluid Phase Equilibria.* 231 (2005) 99-108. <https://doi.org/10.1016/j.fluid.2005.01.007>.
- [1117] S. Shen, Y. Wang, J. Shi, Determination of Excess Enthalpies and the Prediction of Vapor - Liquid Equilibria for Some Ketone Alcohol Systems, *Gaoxiao Huaxue Gongcheng Xuebao.* 4 (1990) 1-7.
- [1118] P.-J. Lien, H. Lin, M.-J. Lee, Excess Molar Enthalpies for Binary Mixtures of Ethanol + Acetone, + Octane, + Cyclohexane and 1-Propanol + Acetone, + Octane, + Heptane at 323.15 K, *J. Chem. Eng. Data.* 48 (2003) 359-361. <https://doi.org/10.1021/je020149l>.
- [1119] A. Tamir, A. Apelblat, M. Wagner, An evaluation of thermodynamic analyses of the vapor-liquid equilibria in the ternary system acetone-chloroform-methanol and its binaries, *Fluid Phase Equilibria.* 6 (1981) 113-139. [https://doi.org/10.1016/0378-3812\(81\)80007-6](https://doi.org/10.1016/0378-3812(81)80007-6).
- [1120] R.A. Wilsak, S.W. Campbell, G. Thodos, Vapor-liquid equilibrium measurements for the methanol-acetone system at 372.8, 397.7 and 422.6 K, *Fluid Phase Equilibria.* 28 (1986) 13-37. [https://doi.org/10.1016/0378-3812\(86\)85066-X](https://doi.org/10.1016/0378-3812(86)85066-X).
- [1121] D.C. Botía, D.C. Riveros, P. Ortiz, I.D. Gil, O.F. Sánchez, Vapor-Liquid Equilibrium in Extractive Distillation of the Acetone/Methanol System Using Water as Entrainer and Pressure Reduction, *Ind. Eng. Chem. Res.* 49 (2010) 6176-6183. <https://doi.org/10.1021/ie901702h>.
- [1122] D.S.M. Constantino, C.S.M. Pereira, S.P. Pinho, V.M.T.M. Silva, A.E. Rodrigues, Isobaric Vapor-Liquid Equilibrium Data for Binary System of Glycerol Ethyl Acetal and Acetonitrile at 60.0 kPa and 97.8 kPa, *J. Chem. Eng. Data.* 58 (2013) 1717-1723. <https://doi.org/10.1021/je400138m>.
- [1123] W. Li, D. Sun, T. Zhang, S. Dai, F. Pan, Z. Zhang, Separation of acetone and methanol azeotropic system using ionic liquid as entrainer, *Fluid Phase Equilibria.* 383 (2014) 182-187. <https://doi.org/10.1016/j.fluid.2014.10.011>.
- [1124] A.N. Campbell, E.M. Kartzmark, Thermodynamic and other properties of methanol + acetone, carbon disulphide + acetone, carbon disulphide + methanol, and carbon disulphide + methanol + acetone, *J. Chem. Thermodyn.* 5 (1973) 163-172. [https://doi.org/10.1016/S0021-9614\(73\)80076-X](https://doi.org/10.1016/S0021-9614(73)80076-X).
- [1125] J. Schmelzer, K. Quitzsd, Isobare Flüssigkeit-Dampfgleichgewichte der binären Systeme Benzol-Äthylendiamin und Wasser-Äthylendiamin, *Z. Für Phys. Chem.* 252O (1973). <https://doi.org/10.1515/zpch-1973-25231>.
- [1126] F. Rivenq, Ebulliometry of water-ethylenediamine mixtures, *Bull Soc Chim Fr.* 8-9 (1963) 1606-1608.
- [1127] V. Ragaini, L. Zanderighi, R. Santi, The liquid-vapor equilibrium of the ethylenediamine-water system, *Atti Soc Peloritana Sci Fis Mat Nat.* 14 (1968) 537-548.
- [1128] M. Bahlmann, Evaluation and revision of the modified UNIFAC (Dortmund) approach for alcohol systems, Master, Universität Oldenburg, 2010.
- [1129] T.H. Cho, K. Ochi, K. Kojima, Isobaric vapor-liquid equilibria for binary systems with limited miscibility, water-n-amyl alcohol and water-isoamyl alcohol, *Kagaku Kogaku Ronbunshu.* 10 (1984) 181-183.
- [1130] B. Marongiu, I. Ferino, R. Monaci, V. Solinas, S. Torrazza, Thermodynamic properties of aqueous non-electrolyte mixtures. Alkanols + water systems., *J. Mol. Liq.* 28 (1984) 229-247. [https://doi.org/10.1016/0167-7322\(84\)80027-6](https://doi.org/10.1016/0167-7322(84)80027-6).
- [1131] M.-J. Lee, L.-H. Tsai, G.-B. Hong, H. Lin, Multiphase Coexistence for Aqueous Systems with Amyl Alcohol and Amyl Acetate, *Ind. Eng. Chem. Res.* 41 (2002) 3247-3252. <https://doi.org/10.1021/ie0105371>.
- [1132] J. Polák, S. Murakami, V.T. Lam, H.D. Pflug, G.C. Benson, Molar excess enthalpies, volumes, and Gibbs free energies of methanol - isomeric butanol systems at 25 °C, *Can. J. Chem.* 48 (1970) 2457-2465. <https://doi.org/10.1139/v70-417>.

- [1133] A. Arce, J. Martínez-Ageitos, E. Rodil, A. Soto, Phase equilibria involved in extractive distillation of 2-methoxy-2-methylpropane+methanol using 1-butanol as entrainer, *Fluid Phase Equilibria*. 171 (2000) 207–218. [https://doi.org/10.1016/S0378-3812\(00\)00364-2](https://doi.org/10.1016/S0378-3812(00)00364-2).
- [1134] W.B. Kay, W.E. Donham, Liquid-vapour equilibria in the iso-butanol—n-butanol, methanol—n-butanol and diethyl ether—n-butanol systems, *Chem. Eng. Sci.* 4 (1955) 1–16. [https://doi.org/10.1016/0009-2509\(55\)85001-4](https://doi.org/10.1016/0009-2509(55)85001-4).
- [1135] R.. Stokes, Excess enthalpies of (butan-1-ol + methanol) at 278.15, 298.15, and 318.15 K, *J. Chem. Thermodyn.* 20 (1988) 1349–1352. [https://doi.org/10.1016/0021-9614\(88\)90172-3](https://doi.org/10.1016/0021-9614(88)90172-3).
- [1136] H. Ogawa, S. Murakami, Excess volumes, isentropic compressions, and isobaric heat capacities for methanol mixed with other alkanols at 25°C, *J. Solut. Chem.* 16 (1987) 315–326. <https://doi.org/10.1007/BF00646123>.
- [1137] E.H.M. Wright, B.A. Akhtar, Soluble surface films of short-chain monocarboxylic acids on organic and aqueous substrates, *J. Chem. Soc. B Phys. Org.* (1970) 151. <https://doi.org/10.1039/j29700000151>.
- [1138] S. Miyamoto, S. Nakamura, Y. Iwai, Y. Arai, Measurement of Isothermal Vapor–Liquid Equilibria for Binary and Ternary Systems Containing Monocarboxylic Acid, *J. Chem. Eng. Data*. 46 (2001) 1225–1230. <https://doi.org/10.1021/je0003849>.
- [1139] A. Reichl, U. Daiminger, A. Schmidt, M. Davies, U. Hoffmann, C. Brinkmeier, C. Reder, W. Marquardt, A non-recycle flow still for the experimental determination of vapor–liquid equilibria in reactive systems, *Fluid Phase Equilibria*. 153 (1998) 113–134. [https://doi.org/10.1016/S0378-3812\(98\)00409-9](https://doi.org/10.1016/S0378-3812(98)00409-9).
- [1140] J. Zhao, J. Bao, Y. Hu, Excess molar enthalpies of (an alkanol + a carboxylic acid) at 298.15 K measured with a Picker calorimeter, *J. Chem. Thermodyn.* 21 (1989) 811–818. [https://doi.org/10.1016/0021-9614\(89\)90027-X](https://doi.org/10.1016/0021-9614(89)90027-X).
- [1141] Z. Kooner, D. Fenby, Vapour pressure study of the deuterium exchange reaction in methanol-ethanol systems: equilibrium constant determination, *Aust. J. Chem.* 33 (1980) 1943. <https://doi.org/10.1071/CH9801943>.
- [1142] D.J. Hall, C.J. Mash, R.C. Pemberton, Vapor liquid equilibria for the systems water-methanol, water-ethanol, methanol-ethanol, and water-methanol-ethanol at 298.15 K determined by a rapid transpiration method, 1979.
- [1143] S.-K. Oh, S.W. Campbell, Total Pressure Measurements for Copper(II) Chloride + Methanol + Ethanol at 303.15 K, *J. Chem. Eng. Data*. 40 (1995) 504–508. <https://doi.org/10.1021/je00018a033>.
- [1144] K.L. Butcher, W.I. Robinson, An apparatus for determining high-pressure liquid-vapour equilibrium data. I. The methanol-ethanol system, *J. Appl. Chem.* 16 (2007) 289–292. <https://doi.org/10.1002/jctb.5010161003>.
- [1145] A. Arce, J. Martínez-Ageitos, E. Rodil, A. Soto, Measurement and prediction of isobaric vapour–liquid equilibrium data of the system ethanol+methanol+2-methoxy-2-methylpropane, *Fluid Phase Equilibria*. 146 (1998) 139–153. [https://doi.org/10.1016/S0378-3812\(98\)00227-1](https://doi.org/10.1016/S0378-3812(98)00227-1).
- [1146] H.D. Pflug, A.E. Pope, G.C. Benson, Heats of mixing of normal alcohols at 25.deg., *J. Chem. Eng. Data*. 13 (1968) 408–410. <https://doi.org/10.1021/je60038a032>.
- [1147] D.M. Trampe, C.A. Eckert, Calorimetric measurement of partial molar excess enthalpies at infinite dilution, *J. Chem. Eng. Data*. 36 (1991) 112–118. <https://doi.org/10.1021/je00001a033>.
- [1148] G. Geiseler, K. Sühnel, K. Quitzsch, Exzeßigenschaften der binären Mischsysteme aus den isomeren Butanolen, *Z. Für Phys. Chem.* 254O (1973). <https://doi.org/10.1515/zpch-1973-25425>.
- [1149] K. Quitzsch, S. Köhler, K. Taubert, G. Geiseler, Isobare Flüssigkeit-Dampf-Gleichgewichte der „quasi-idealen“ binären Systeme n-Butanol/sek.-Butanol und n-Butanol/tert.-Butanol, *J. Für Prakt. Chem.* 311 (1969) 429–437. <https://doi.org/10.1002/prac.19693110312>.
- [1150] S. Murakami, G.C. Benson, Thermodynamic Properties of Some Isomeric Butyl Alcohol Mixtures, *Bull. Chem. Soc. Jpn.* 46 (1973) 74–79. <https://doi.org/10.1246/bcsj.46.74>.
- [1151] J.A. Duran, F.P. Córdoba, I.D. Gil, G. Rodríguez, A. Orjuela, Vapor–liquid equilibrium of the ethanol+3-methyl-1-butanol system at 50.66, 101.33 and 151.99kPa, *Fluid Phase Equilibria*. 338 (2013) 128–134. <https://doi.org/10.1016/j.fluid.2012.11.004>.
- [1152] L. Gay, Distillation and rectification of complex mixtures. II, *Chim Ind Genie Chim.* 18 (1927) 187–203.
- [1153] V.V. Udovenko, T.B. Frid, Heats of vaporization of binary mixtures. II, *Zh Fiz Khim.* 22 (1948) 1135–1145.
- [1154] J.S. Kim, J.M. Lee, The prediction of vapor-liquid equilibrium data for methanol/3-methyl-1-butanol system at constant temperature, *Kongop Hwahak.* 16 (2005) 749–754.
- [1155] J. Resa, C. González, B. Moradillo, A. Ruiz, Isobaric vapor-liquid equilibria of 3-methyl-1-butanol with methanol and vinyl acetate at 101.3 kPa, *Fluid Phase Equilibria*. 132 (1997) 205–213. [https://doi.org/10.1016/S0378-3812\(97\)00027-7](https://doi.org/10.1016/S0378-3812(97)00027-7).
- [1156] H. Yamamoto, K. Fukase, J. Shibata, Vapor–Liquid Equilibria for Alcohol + Alcohol + Sodium Iodide at 298.15 K, *J. Chem. Eng. Data*. 41 (1996) 1066–1070. <https://doi.org/10.1021/je9600966>.

- [1157] C. Berro, R. Deyrieux, A. Peneloux, An Ebulliometer for Rapid and Precise Determination of the Vapor-Liquid Equilibrium of Solutions. The Binary System Methanol - 1-Propanol at 60.02 °C, *J Chim Phys Phys Chim Biol.* 72 (1975) 1118–1123.
- [1158] N. Gultekin, Vapor-liquid equilibria at 1 atm for ternary and quaternary systems composed of acetone, methanol, 2-propanol, and 1-propanol, *J. Chem. Eng. Data.* 35 (1990) 132–136. <https://doi.org/10.1021/je00060a010>.
- [1159] J.R. Khurma, D.V. Fenby, Thermochemical study of deuterium exchange reactions in water-alcohol and alcohol-alcohol systems, *J. Phys. Chem.* 83 (1979) 2443–2447. <https://doi.org/10.1021/j100482a004>.
- [1160] T.A. Wilson, The total and partial vapor pressures of aqueous ammonia solutions, *Univ Ill. Eng Exp Stand Bull.* 146 (1925).
- [1161] P.C. Gillespie, W.V. Wilding, G.M. Wilson, Vapor-liquid equilibrium measurements on the ammonia-water system from 313 K to 589 K, *AIChE Symp Ser.* 83 (1987) 97–127.
- [1162] H. Inomata, N. Ikawa, K. Arai, S. Saito, Vapor-liquid equilibria for the ammonia-methanol-water system, *J. Chem. Eng. Data.* 33 (1988) 26–29. <https://doi.org/10.1021/je00051a010>.
- [1163] I.I. Clifford, E. Hunter, The System Ammonia–Water at Temperatures up to 150°C. and at Pressures up to Twenty Atmospheres., *J. Phys. Chem.* 37 (1932) 101–118. <https://doi.org/10.1021/j150343a014>.
- [1164] S.S.H. Rizvi, R.A. Heidemann, Vapor-liquid equilibria in the ammonia-water system, *J. Chem. Eng. Data.* 32 (1987) 183–191. <https://doi.org/10.1021/je00048a017>.
- [1165] J.C. Chu, R.J. Getty, L.F. Brennecke, R. Paul, *Distillation Equilibrium Data*, 1950.
- [1166] J. Wucherer, Measurement of the pressure, temperature and composition of the liquid and vapor phases of ammonia-water mixtures in the saturated state, *Z Gesamte Kaelte-Ind.* 39 (1932) 136–140.
- [1167] A. Sakabe, D. Arai, H. Miyamoto, M. Uematsu, Measurements of the critical parameters for  $\{x\text{NH}_3+(1-x)\text{H}_2\text{O}\}$  with  $x=(0.9098, 0.7757, 0.6808)$ , *J. Chem. Thermodyn.* 40 (2008) 1527–1530. <https://doi.org/10.1016/j.jct.2008.05.017>.
- [1168] N.G. Polikhronidi, I.M. Abdulagatov, R.G. Batyrova, G.V. Stepanov, PVT measurements of water-ammonia refrigerant mixture in the critical and supercritical regions, *Int. J. Refrig.* 32 (2009) 1897–1913. <https://doi.org/10.1016/j.ijrefrig.2009.07.008>.
- [1169] C.L. Sassen, R.A.C. Van Kwartel, H.J. Van der Kooi, J. De Swaan Arons, Vapor-liquid equilibria for the system ammonia + water up to the critical region, *J. Chem. Eng. Data.* 35 (1990) 140–144. <https://doi.org/10.1021/je00060a013>.
- [1170] T.N. Tyvina, A.A. Naumova, V.V. Fokina, Liquid-gas equilibrium in an acetonitrile-ammonia system, *J Appl Chem USSR.* 52 (1979) 2458–2460.
- [1171] M. Ewert, Theory of concentrated solutions. XIII. Aqueous solutions of organic compounds, *Bull Soc Chim Belg.* 45 (1936) 493–515.
- [1172] A. Aucejo, S. Loras, J.B. Monton, Isobaric vapor-liquid equilibria of prop-2-en-1-ol (allyl alcohol) + water system at 30, 60, and 100 kPa, *ELDATA Int. Electron. J. Phys.-Chem. Data.* 2 (1996) 1–4.
- [1173] R. Weller, H. Schubert, E. Leibnitz, Phasengleichgewichtsmessungen. IV. Die Phasengleichgewichte dampfförmig/flüssig des Systems Phenol/n-Butylacetat/Wasser bei 44,4°C, *J. Für Prakt. Chem.* 21 (1963) 234–249. <https://doi.org/10.1002/prac.19630210502>.
- [1174] V. Kliment, V. Fried, J. Pick, Liquid-vapor equilibrium. XXXIII. The systems butyl acetate-phenol and water-phenol, *Collect Czech Chem Commun.* 29 (1964) 2008–2015.
- [1175] C.H. Chou, J.L. Perng, M.D. Lee, Y.P. Chen, Vapor-liquid equilibrium measurements of the ternary system of ethanol, water and phenol at 760mmHg, *J Chin Inst Chem Eng.* 18 (1987) 393–399.
- [1176] L. von Erichsen, E. Dobbert, The mutual solubility behavior of alkylphenols and water, *Brennst.-Chem.* 21–22 (1955) 338–345.
- [1177] E. Schuermann, R. Diederichs, Heats of mixing of phenol-water systems, *Ber Bunsen-Ges Phys Chem.* 68 (1964) 429–434.
- [1178] J.B. Ferguson, The System Water-Phenol, *J. Phys. Chem.* 31 (1926) 757–763. <https://doi.org/10.1021/j150275a013>.
- [1179] A.N. Campbell, A.J.R. Campbell, Concentrations, Total and Partial Vapor Pressures, Surface Tensions and Viscosities, in the Systems Phenol—Water and Phenol—Water—4% Succinic Acid, *J. Am. Chem. Soc.* 59 (1937) 2481–2488. <https://doi.org/10.1021/ja01291a001>.
- [1180] J. Polak, B.C.-Y. Lu, Excess Gibbs free energies and excess volumes of methyl formate + methanol and methyl formate + ethanol at 298.15 K, *J. Chem. Thermodyn.* 4 (1972) 469–476. [https://doi.org/10.1016/0021-9614\(72\)90031-6](https://doi.org/10.1016/0021-9614(72)90031-6).
- [1181] N. Kozub, H. Schubert, E. Leibnitz, Phasengleichgewichtsuntersuchungen dampfförmig-flüssig am System Methanol/Methylformiat unter Verwendung einer gaschromatographischen Analysenmethode, *J. Für Prakt. Chem.* 17 (1962) 282–292. <https://doi.org/10.1002/prac.19620170505>.

- [1182] A.T. Sundberg, P. Uusi-Kyyny, M. Pakkanen, V. Alopaeus, Vapor–Liquid Equilibrium for Methoxymethane + Methyl Formate, Methoxymethane + Hexane, and Methyl Formate + Methanol, *J. Chem. Eng. Data.* 56 (2011) 2634–2640. <https://doi.org/10.1021/je200140m>.
- [1183] J. Zeng, C. Fu, W.L. Hu, Study on the VLE for methyl formate-methanol system, *Tianranqi Huagong.* 25 (2000) 54–56.
- [1184] M. López, J. Fernández, F. Sarmiento, J.L. Legido, L. Romani, E. Jiménez, M.I. Paz Andrade, Excess molar enthalpies at the temperature 298.15 K of (an n-alkyl formate + an n-alkanol) IV.  $\{x\text{HCO}_2(\text{CH}_2)_i\text{CH}_3 + (1-x)\text{C}_j\text{H}_{2j+1}\text{OH}\}$  ( $i = 0$  to 3 and  $j = 1$  and 2), *J. Chem. Thermodyn.* 24 (1992) 809–814. [https://doi.org/10.1016/S0021-9614\(05\)80225-3](https://doi.org/10.1016/S0021-9614(05)80225-3).
- [1185] J. Linek, I. Wichterle, K.N. Marsh, Vapor–Liquid Equilibria for Water + Diacetone Alcohol, Ethyl Methanoate + Water, and Ethyl Methanoate + Phenol, *J. Chem. Eng. Data.* 41 (1996) 1219–1222. <https://doi.org/10.1021/je960183y>.
- [1186] R. Wittig, J. Lohmann, R. Joh, S. Horstmann, J. Gmehling, Vapor–Liquid Equilibria and Enthalpies of Mixing in a Temperature Range from 298.15 to 413.15 K for the Further Development of Modified UNIFAC (Dortmund), *Ind. Eng. Chem. Res.* 40 (2001) 5831–5838. <https://doi.org/10.1021/ie010444j>.
- [1187] I. Nagata, T. Ohta, M. Ogura, S. Yasuda, Excess Gibbs free energies and heats of mixing for binary systems: ethyl formate with methanol, ethanol, 1-propanol, and 2-propanol, *J. Chem. Eng. Data.* 21 (1976) 310–313. <https://doi.org/10.1021/je60070a020>.
- [1188] A. Soto, P. Hernández, J. Ortega, Experimental VLE at 101.32 kPa in binary systems composed of ethyl methanoate and alkan-1-ols or alkan-2-ols and treatment of data using a correlation with temperature-dependent parameters, *Fluid Phase Equilibria.* 146 (1998) 351–370. [https://doi.org/10.1016/S0378-3812\(98\)00193-9](https://doi.org/10.1016/S0378-3812(98)00193-9).
- [1189] J. Hu, K. Tamura, S. Murakami, Excess thermodynamic properties of binary mixtures of ethyl formate with benzene, ethanol, and 2,2,2-trifluoroethan-1-ol at 298.15 K, *Fluid Phase Equilibria.* 131 (1997) 197–212. [https://doi.org/10.1016/S0378-3812\(96\)03230-X](https://doi.org/10.1016/S0378-3812(96)03230-X).
- [1190] V.P. Sazonov, V.V. Filippov, Study of the thermodynamic properties of the nitromethane-butyl alcohol system, *Vestn Leningr Univ Ser 4 Fiz Khim.* 2 (1977) 151–153.
- [1191] C.A. Cerdeiriña, C.A. Tovar, D. González, E. Carballo, L. Romani, Thermodynamics of the nitromethane + 1-butanol system near the upper critical point, *Fluid Phase Equilibria.* 179 (2001) 101–115. [https://doi.org/10.1016/S0378-3812\(00\)00485-4](https://doi.org/10.1016/S0378-3812(00)00485-4).
- [1192] H. Feng, Y. Wang, J. Shi, G.C. Benson, B.C.-Y. Lu, Excess enthalpies of (methyl formate or nitroethane + an n-alkane) and of (nitromethane + butan-1-ol or hexan-1-ol or ethan-1,2-diol), *J. Chem. Thermodyn.* 23 (1991) 169–174. [https://doi.org/10.1016/S0021-9614\(05\)80294-0](https://doi.org/10.1016/S0021-9614(05)80294-0).
- [1193] L.P.N. Rebelo, V. Najdanovic-Visak, Z.P. Visak, M. Nunes da Ponte, J. Troncoso, C.A. Cerdeiriña, L. Romani, Two ways of looking at Prigogine and Defay's equation, *Phys. Chem. Chem. Phys.* 4 (2002) 2251–2259. <https://doi.org/10.1039/b200292b>.
- [1194] V.K. Sharma, J. Singh, Thermodynamics of molecular interactions in binary mixtures containing nitromethane: Molar excess volumes and molar excess enthalpies, *Indian J Chem Sect A.* 38 (1999) 65–69.
- [1195] G. Scatchard, G.M. Wilson, Vapor-Liquid Equilibrium. XIII. The System Water-Butyl Glycol from 5 to 85°, *J. Am. Chem. Soc.* 86 (1964) 133–137. <https://doi.org/10.1021/ja01056a004>.
- [1196] O. Chiavone-Filho, P. Proust, P. Rasmussen, Vapor-liquid equilibria for glycol ether + water systems, *J. Chem. Eng. Data.* 38 (1993) 128–131. <https://doi.org/10.1021/je00009a031>.
- [1197] G.N. Escobedo-Alvarado, S.I. Sandler, Vapor–Liquid Equilibrium of Two Aqueous Systems that Exhibit Liquid–Liquid Phase Separation, *J. Chem. Eng. Data.* 44 (1999) 319–322. <https://doi.org/10.1021/je980228q>.
- [1198] A.G. Aizpiri, F. Monroy, C. del Campo, R.G. Rubio, M. Díaz Peña, Range of simple scaling and critical amplitudes near a LCST. The 2-butoxyethanol + water system, *Chem. Phys.* 165 (1992) 31–39. [https://doi.org/10.1016/0301-0104\(92\)80040-3](https://doi.org/10.1016/0301-0104(92)80040-3).
- [1199] U. Onken, Die thermodynamischen Funktionen des Systems Wasser/Butylglykol, *Z Elektrochem.* 63 (1959) 321–327.
- [1200] K.-H. Lim, W.B. Whiting, D.H. Smith, Excess Enthalpies and Liquid-Liquid Equilibrium Phase Compositions of the Nonionic Amphiphile 2-Butoxyethanol and Water, *J. Chem. Eng. Data.* 39 (1994) 399–403. <https://doi.org/10.1021/je00014a048>.
- [1201] H.J.E. Dobson, CCCXCVII.—The partial pressures of aqueous ethyl alcohol, *J Chem Soc Trans.* 127 (1925) 2866–2873. <https://doi.org/10.1039/CT9252702866>.
- [1202] R.. Pemberton, C.. Mash, Thermodynamic properties of aqueous non-electrolyte mixtures II. Vapour pressures and excess Gibbs energies for water + ethanol at 303.15 to 363.15 K determined by an accurate static method, *J. Chem. Thermodyn.* 10 (1978) 867–888. [https://doi.org/10.1016/0021-9614\(78\)90160-X](https://doi.org/10.1016/0021-9614(78)90160-X).

- [1203] D.T. Vu, C.T. Lira, N.S. Asthana, A.K. Kolah, D.J. Miller, Vapor-Liquid Equilibria in the Systems Ethyl Lactate + Ethanol and Ethyl Lactate + Water, *J. Chem. Eng. Data.* 51 (2006) 1220–1225. <https://doi.org/10.1021/je050537y>.
- [1204] K. Kurihara, T. Minoura, K. Takeda, K. Kojima, Isothermal Vapor-Liquid Equilibria for Methanol + Ethanol + Water, Methanol + Water, and Ethanol + Water, *J. Chem. Eng. Data.* 40 (1995) 679–684. <https://doi.org/10.1021/je00019a033>.
- [1205] V. Niesen, A. Palavra, A.J. Kidnay, V.F. Yesavage, An apparatus for vapor-liquid equilibrium at elevated temperatures and pressures and selected results for the water-ethanol and methanol-ethanol systems, *Fluid Phase Equilibria.* 31 (1986) 283–298. [https://doi.org/10.1016/0378-3812\(86\)87013-3](https://doi.org/10.1016/0378-3812(86)87013-3).
- [1206] F. Barr-David, B.F. Dodge, Vapor-Liquid Equilibrium at High Pressures. The Systems Ethanol-Water and 2-Propanol-Water., *J. Chem. Eng. Data.* 4 (1959) 107–121. <https://doi.org/10.1021/je60002a003>.
- [1207] E.C. Voutsas, C. Pamouktsis, D. Argyris, G.D. Pappa, Measurements and thermodynamic modeling of the ethanol-water system with emphasis to the azeotropic region, *Fluid Phase Equilibria.* 308 (2011) 135–141. <https://doi.org/10.1016/j.fluid.2011.06.009>.
- [1208] C.A. Jones, E.M. Schoenborn, A.P. Colburn, Equilibrium Still for Miscible Liquids, *Ind. Eng. Chem.* 35 (1943) 666–672. <https://doi.org/10.1021/ie50402a009>.
- [1209] H.E. Hughes, J.O. Maloney, Application of radioactive tracers to diffusional operations. Binary and ternary equilibrium data, *Chem Eng Progr.* 48 (1952) 192–200.
- [1210] C.H. Bloom, C.W. Clump, A.H. Koeckert, Simultaneous Measurement of Vapor-Liquid Equilibria and Latent Heats of Vaporization, *Ind. Eng. Chem.* 53 (1961) 829–832. <https://doi.org/10.1021/ie50622a029>.
- [1211] V.N. Stabnikov, B.Z. Matyushev, T.B. Protsyuk, N.M. Yushchenko, Equilibrium in the ethyl alcohol-water system at atmospheric pressure, *Pishch Promst Kiev.* 15 (1972) 49–56.
- [1212] H. Otsuki, F.C. Williams, Effect of pressure on vapor-liquid equilibria for the system ethyl alcohol-water, *Chem Eng Progr Symp Ser.* 49 (1953) 55–67.
- [1213] T. Friese, P. Ulbig, S. Schulz, K. Wagner, Effect of NaCl or KCl on the Excess Enthalpies of Alkanol + Water Mixtures at Various Temperatures and Salt Concentrations, 44 (1999) 701–714. <https://doi.org/10.1021/je980303x>.
- [1214] J.B. Ott, C.E. Stouffer, G.V. Cornett, B.F. Woodfield, R.C. Wirthlin, J.J. Christensen, U.K. Deiters, Excess enthalpies for (ethanol + water) at 298.15 K and pressures of 0.4, 5, 10, and 15 MPa, *J. Chem. Thermodyn.* 18 (1986) 1–12. [https://doi.org/10.1016/0021-9614\(86\)90036-4](https://doi.org/10.1016/0021-9614(86)90036-4).
- [1215] J.B. Ott, G.V. Cornett, C.E. Stouffer, B.F. Woodfield, C. Guanquan, J.J. Christensen, Excess enthalpies of (ethanol+water) at 323.15, 333.15, 348.15, and 373.15 K and from 0.4 to 15 MPa, *J. Chem. Thermodyn.* 18 (1986) 867–875. [https://doi.org/10.1016/0021-9614\(86\)90121-7](https://doi.org/10.1016/0021-9614(86)90121-7).
- [1216] J.. Ott, C.. Stouffer, G.. Cornett, B.. Woodfield, C. Guanquan, J.. Christensen, Excess enthalpies for (ethanol + water) at 398.15, 423.15, 448.15, and 473.15 K and at pressures of 5 and 15 MPa. Recommendations for choosing (ethanol + water) as an HmE reference mixture, *J. Chem. Thermodyn.* 19 (1987) 337–348. [https://doi.org/10.1016/0021-9614\(87\)90115-7](https://doi.org/10.1016/0021-9614(87)90115-7).
- [1217] C.J. Wormald, M.J. Lloyd, Excess enthalpies for (water + ethanol) at  $T = 398$  K to  $T = 548$  K and  $p = 15$  MPa, *J. Chem. Thermodyn.* 28 (1996) 615–626. <https://doi.org/10.1006/jcht.1996.0058>.
- [1218] G.C. Benson, P.J. D'Arcy, Excess isobaric heat capacities of water-n-alcohol mixtures, *J. Chem. Eng. Data.* 27 (1982) 439–442. <https://doi.org/10.1021/je00030a021>.
- [1219] H. Ogawa, S. Murakami, Excess isobaric heat capacities for water + alkanol mixtures at 298.15 K, *Thermochim. Acta.* 109 (1986) 145–154. [https://doi.org/10.1016/0040-6031\(86\)85016-X](https://doi.org/10.1016/0040-6031(86)85016-X).
- [1220] J.-P.E. Grolier, E. Wilhelm, Excess volumes and excess heat capacities of water + ethanol at 298.15 K, *Fluid Phase Equilibria.* 6 (1981) 283–287. [https://doi.org/10.1016/0378-3812\(81\)85011-X](https://doi.org/10.1016/0378-3812(81)85011-X).
- [1221] A.R. Bazaev, I.M. Abdulgatov, E.A. Bazaev, A. Abdurashidova, (p,v,T,x) Measurements of  $\{(1-x)\text{H}_2\text{O}+x\text{C}_2\text{H}_5\text{OH}\}$  mixtures in the near-critical and supercritical regions, *J. Chem. Thermodyn.* 39 (2007) 385–411. <https://doi.org/10.1016/j.jct.2006.08.002>.
- [1222] A.-L. Vierk, Experimentelle Untersuchungen an den Zweistoffsystemen: Wasser-Acetonitril, Wasser-Dioxan, Äthanol-Acetonitril und Cyclohexan-Dioxan, *Z. Für Anorg. Chem.* 261 (1950) 283–296. <https://doi.org/10.1002/zaac.19502610504>.
- [1223] S.-J. Park, H.-J. Oh, H.-J. Choi, S.-K. Peak, K. Fischer, J. Gmehling, Phase equilibrium and excess molar volume for systems acrylonitrile+water, acetonitrile+water, and acrylonitrile+acetonitrile, *Hwahak Konghak.* 35 (1997) 678–683.
- [1224] H. Sugi, T. Katayama, Ternary Liquid-Liquid And Miscible Binary Vapor-Liquid Equilibrium Data For The Two Systems n-Hexane Ethanol Acetonitrile And Water Acetonitrile-Ethyl Acetate, *J. Chem. Eng. Jpn.* 11 (1978) 167–172. <https://doi.org/10.1252/jcej.11.167>.
- [1225] J. Szydłowski, M. Szykuła, Isotope effect on miscibility of acetonitrile and water, *Fluid Phase Equilibria.* 154 (1999) 79–87. [https://doi.org/10.1016/S0378-3812\(98\)00438-5](https://doi.org/10.1016/S0378-3812(98)00438-5).

- [1226] R.. Stokes, Excess partial molar enthalpies for (acetonitrile + water) from 278 to 318 K, *J. Chem. Thermodyn.* 19 (1987) 977–983. [https://doi.org/10.1016/0021-9614\(87\)90044-9](https://doi.org/10.1016/0021-9614(87)90044-9).
- [1227] M. Nakamura, K. Tamura, S. Murakami, Isotope effects on thermodynamic properties: mixtures of  $x(\text{D}_2\text{O or H}_2\text{O}) + (1 - x)\text{CH}_3\text{CN}$  at 298.15 K, *Thermochim. Acta.* 253 (1995) 127–136. [https://doi.org/10.1016/0040-6031\(94\)02086-4](https://doi.org/10.1016/0040-6031(94)02086-4).
- [1228] A. Schedemann, Weiterentwicklung von thermodynamischen Vorhersagemethoden als Grundlage für die Lösungsmittelauswahl bei der Flüssig-Flüssig-Extraktion und der Absorption, 2013.
- [1229] J. Acosta, A. Arce, E. Rodil, A. Soto, A thermodynamic study on binary and ternary mixtures of acetonitrile, water and butyl acetate, *Fluid Phase Equilibria.* 203 (2002) 83–98. [https://doi.org/10.1016/S0378-3812\(02\)00171-1](https://doi.org/10.1016/S0378-3812(02)00171-1).
- [1230] C. De Visser, W.J.M. Heuvelsland, L.A. Dunn, G. Somsen, Some properties of binary aqueous liquid mixtures. Apparent molar volumes and heat capacities at 298.15 K over the whole mole fraction range, *J. Chem. Soc. Faraday Trans. 1 Phys. Chem. Condens. Phases.* 74 (1978) 1159. <https://doi.org/10.1039/f19787401159>.
- [1231] G.C. Benson, P.J. D’Arcy, Y.P. Handa, Thermodynamics of aqueous mixtures of nonelectrolytes. V. Isobaric heat capacities and ultrasonic speeds for water + ethanenitrile mixtures at 25°C, *Thermochim. Acta.* 46 (1981) 295–301. [https://doi.org/10.1016/0040-6031\(81\)80328-0](https://doi.org/10.1016/0040-6031(81)80328-0).
- [1232] Jinyan Fu, Kun Wang, Ying Hu, Studies on the Vapor-Liquid Equilibrium and Vapor-Liquid-Liquid Equilibrium for a Methanol-Methyl Methacrylate-Water Ternary System (I) Three Different Binary Systems, *Huagong Xuebao.* 39 (1988) 64–76.
- [1233] G.J. Maximo, A.J.A. Meirelles, E.A.C. Batista, Boiling point of aqueous d-glucose and d-fructose solutions: Experimental determination and modeling with group-contribution method, *Fluid Phase Equilibria.* 299 (2010) 32–41. <https://doi.org/10.1016/j.fluid.2010.08.018>.
- [1234] M.L. McGlashan, A.G. Williamson, Isothermal liquid-vapor equilibria for system methanol-water, *J. Chem. Eng. Data.* 21 (1976) 196–199. <https://doi.org/10.1021/je60069a019>.
- [1235] J. Yao, H. Li, S. Han, Vapor-liquid equilibrium data for methanol-water-NaCl at 45°C, *Fluid Phase Equilibria.* 162 (1999) 253–260. [https://doi.org/10.1016/S0378-3812\(99\)00204-6](https://doi.org/10.1016/S0378-3812(99)00204-6).
- [1236] K.A. Dulitskaya, Vapor pressure of binary systems. I, *Zh Obschch Khim.* 15 (1945) 9–21.
- [1237] M. Nagatani, K. Fujino, Measurement of isothermal vapor-liquid equilibria for methanol-water system, *Fukuoka Daigaku Kogaku Shuho.* 64 (2000) 147–152.
- [1238] Z. Bao, M. Liu, J. Yang, N. Wang, Measurement and Correlation of Moderate Pressure Vapor-Liquid Equilibrium Data for Methanol - Water Binary System, *Huagong Xuebao.* 46 (1995) 230–233.
- [1239] W. Schröder, Messungen von Siedegleichgewichten bei Überdruck: Messungen von Siedegleichgewichten bei Überdruck, *Chem. Ing. Tech.* 30 (1958) 523–525. <https://doi.org/10.1002/cite.330300809>.
- [1240] R.O. Pryanikova, G.D. Efremova, Liquid-vapor equilibrium and volume behavior of the methanol-water system at high temperatures and pressures, *Fiz Khim Rastvorov.* (1972) 228–233.
- [1241] C. Yang, F. Sun, S. Ma, X. Yin, H. Zeng, Organic Salt Effect on Vapor-Liquid Equilibrium of the Methanol + Water System at Subatmospheric Pressure, *J. Chem. Eng. Data.* 57 (2012) 2696–2701. <https://doi.org/10.1021/je300613v>.
- [1242] T.M. Lesteva, S.K. Ogorodnikov, S.V. Kazakova, Liquid-vapor equilibrium in the trimethylcarbinol-methanol-water system at a pressure of 760 mm. V, *J Appl Chem USSR.* 43 (1970) 1582–1586.
- [1243] M. Hirata, S. Suda, Vapor-liquid equilibrium under pressurized conditions; experimental apparatus and methanol-water system, *Kagaku Kogaku.* 31 (1967) 759–766. <https://doi.org/10.1252/kakoronbunshu1953.31.759>.
- [1244] E. Bose, Remarks on thermochemical statement of Julius Thomsens, *Phys Z.* 7 (1906) 503–505.
- [1245] S.W. Cochran, J.C. Holste, K.N. Marsh, B.E. Gammon, K.R. Hall, Enthalpies of water + methanol mixtures between 180 K and 320 K, *Fluid Phase Equilibria.* 88 (1993) 171–181. [https://doi.org/10.1016/0378-3812\(93\)87110-M](https://doi.org/10.1016/0378-3812(93)87110-M).
- [1246] I. Tomaszkiwicz, S.L. Randzio, P. Gierycz, Excess enthalpy in the methanol-water system at 278.15, 298.15 and 323.15 K under pressures of 0.1, 20 and 39 mpa, *Thermochim. Acta.* 103 (1986) 281–289. [https://doi.org/10.1016/0040-6031\(86\)85164-4](https://doi.org/10.1016/0040-6031(86)85164-4).
- [1247] V. Hynek, S. Degrange, M. Polednicek, V. Majer, J. Quint, J.P.E. Grolier, Combined flow-mixing power-compensation calorimeter and vibrating tube densimeter for measurements at superambient condition, *J Solut. Chem.* 28 (1999) 631–666. <https://doi.org/10.1023/A:1021759810070>.
- [1248] G.C. Benson, P.J. D’Arcy, O. Kiyohara, Thermodynamics of aqueous mixtures of nonelectrolytes II. Isobaric heat capacities of water-n-alcohol mixtures at 25°C, *J. Solut. Chem.* 9 (1980) 931–938. <https://doi.org/10.1007/BF00646404>.

- [1249] A.R. Bazaev, I.M. Abdulagatov, J.W. Magee, E.A. Bazaev, A.E. Ramazanova, A.A. Abdurashidova, PVTx Measurements for a H<sub>2</sub>O + Methanol Mixture in the Subcritical and Supercritical Regions, *Int. J. Thermophys.* 25 (2004) 805–838. <https://doi.org/10.1023/B:IJOT.0000034238.64651.32>.
- [1250] V.P. Sazonov, Isothermal liquid-liquid-vapor equilibrium of nitromethane - isopropanol - water, *Zh Prikl Khim.* 59 (1986) 1451–1456.
- [1251] V.V. Udovenko, T.F. Mazanko, Liquid-Vapor Equilibrium in the Propan-2-ol - Water and Propan-2-ol - Benzene Systems, *Zhurnal Fiz. Khimii.* 41 (1967) 1615–1620.
- [1252] E. Sada, T. Morisue, ISOTHERMAL VAPOR-LIQUID EQUILIBRIUM DATA OF ISOPROPANOL-WATER SYSTEM, *J. Chem. Eng. Jpn.* 8 (1975) 191–195. <https://doi.org/10.1252/jcej.8.191>.
- [1253] H.S. Wu, D. Hagewiesche, S.I. Sandler, Vapor—liquid equilibria of 2-propanol + water + N,N-dimethyl formamide, *Fluid Phase Equilibria.* 43 (1988) 77–89. [https://doi.org/10.1016/0378-3812\(88\)80073-6](https://doi.org/10.1016/0378-3812(88)80073-6).
- [1254] A. Wilson, E.L. Simons, Vapor-Liquid Equilibria. 2-Propanol - Water System, *Ind. Eng. Chem.* 44 (1952) 2214–2219. <https://doi.org/10.1021/ie50513a063>.
- [1255] P. Marzal, J.B. Montón, M.A. Rodrigo, Isobaric Vapor–Liquid Equilibria of the Water + 2-Propanol System at 30, 60, and 100 kPa, *J. Chem. Eng. Data.* 41 (1996) 608–611. <https://doi.org/10.1021/je9503113>.
- [1256] A. Arce, A. Arce, J. Martínez-Ageitos, E. Rodil, A. Soto, (Vapour+liquid) equilibrium of (DIPE+IPA+water) at 101.32kPa, *J. Chem. Thermodyn.* 35 (2003) 871–884. [https://doi.org/10.1016/S0021-9614\(03\)00018-1](https://doi.org/10.1016/S0021-9614(03)00018-1).
- [1257] R. Privat, J.-N. Jaubert, Y. Privat, A simple and unified algorithm to solve fluid phase equilibria using either the gamma-phi or the phi-phi approach for binary and ternary mixtures, *Comput. Chem. Eng.* 50 (2013) 139–151. <https://doi.org/10.1016/j.compchemeng.2012.11.006>.
- [1258] J.-W. Qian, R. Privat, J.-N. Jaubert, P. Duchet-Suchaux, Enthalpy and heat capacity changes on mixing: fundamental aspects and prediction by means of the PPR78 cubic equation of state, *Energy Fuels.* 27 (2013) 7150–7178. <https://doi.org/10.1021/ef401605c>.
- [1259] L. Avaullee, L. Trassy, E. Neau, J.N. Jaubert, Thermodynamic modeling for petroleum fluids I. Equation of state and group contribution for the estimation of thermodynamic parameters of heavy hydrocarbons, *Fluid Phase Equilibria.* 139 (1997) 155–170. [https://doi.org/10.1016/S0378-3812\(97\)00168-4](https://doi.org/10.1016/S0378-3812(97)00168-4).
- [1260] S. Vitu, R. Privat, J.-N. Jaubert, F. Mutelet, Predicting the phase equilibria of CO<sub>2</sub> + hydrocarbon systems with the PPR78 model (PR EoS and  $k_{ij}$  calculated through a group contribution method), *J. Supercrit. Fluids.* 45 (2008) 1–26. <https://doi.org/10.1016/j.supflu.2007.11.015>.
- [1261] J.-N. Jaubert, R. Privat, F. Mutelet, Predicting the phase equilibria of synthetic petroleum fluids with the PPR78 approach, *AIChE J.* 56 (2010) 3225–3235. <https://doi.org/10.1002/aic.12232>.
- [1262] X. Xu, J.-N. Jaubert, R. Privat, P. Arpentiner, Prediction of thermodynamic properties of alkyne-containing mixtures with the E-PPR78 model, *Ind. Eng. Chem. Res.* 56 (2017) 8143–8157. <https://doi.org/10.1021/acs.iecr.7b01586>.
- [1263] J.-N. Jaubert, L. Coniglio, The group contribution concept: a useful tool to correlate binary systems and to predict the phase behavior of multicomponent systems involving supercritical CO<sub>2</sub> and fatty acids, *Ind. Eng. Chem. Res.* 38 (1999) 5011–5018. <https://doi.org/10.1021/ie990544d>.
- [1264] J.-N. Jaubert, R. Privat, Relationship between the binary interaction parameters ( $k_{ij}$ ) of the Peng–Robinson and those of the Soave–Redlich–Kwong equations of state: Application to the definition of the PR2SRK model, *Fluid Phase Equilibria.* 295 (2010) 26–37. <https://doi.org/10.1016/j.fluid.2010.03.037>.
- [1265] T. Holderbaum, J. Gmehling, PSRK: a group contribution equation of state based on UNIFAC, *Fluid Phase Equilibria.* 70 (1991) 251–265. [https://doi.org/10.1016/0378-3812\(91\)85038-V](https://doi.org/10.1016/0378-3812(91)85038-V).
- [1266] J. Chen, K. Fischer, J. Gmehling, Modification of PSRK mixing rules and results for vapor–liquid equilibria, enthalpy of mixing and activity coefficients at infinite dilution, *Fluid Phase Equilibria.* 200 (2002) 411–429. [https://doi.org/10.1016/S0378-3812\(02\)00048-1](https://doi.org/10.1016/S0378-3812(02)00048-1).
- [1267] J. Ahlers, J. Gmehling, Development of an universal group contribution equation of state, *Fluid Phase Equilibria.* 191 (2001) 177–188. [https://doi.org/10.1016/S0378-3812\(01\)00626-4](https://doi.org/10.1016/S0378-3812(01)00626-4).
- [1268] J. Ahlers, J. Gmehling, Development of a universal group contribution equation of state. 2. Prediction of vapor–liquid equilibria for asymmetric systems, *Ind. Eng. Chem. Res.* 41 (2002) 3489–3498. <https://doi.org/10.1021/ie020047o>.
- [1269] E. Voutsas, V. Louli, C. Boukouvalas, K. Magoulas, D. Tassios, Thermodynamic property calculations with the universal mixing rule for EoS/G<sup>E</sup> models: Results with the Peng–Robinson EoS and a UNIFAC model, *Fluid Phase Equilibria.* 241 (2006) 216–228. <https://doi.org/10.1016/j.fluid.2005.12.028>.
- [1270] J.-N. Jaubert, P. Borg, L. Coniglio, D. Barth, Phase equilibria measurements and modeling of EPA and DHA ethyl esters in supercritical carbon dioxide, *J. Supercrit. Fluids.* 20 (2001) 145–155. [https://doi.org/10.1016/S0896-8446\(01\)00062-6](https://doi.org/10.1016/S0896-8446(01)00062-6).

- [1271] J.-N. Jaubert, R. Privat, Y. Le Guennec, L. Coniglio, Note on the properties altered by application of a Péneloux–type volume translation to an equation of state, *Fluid Phase Equilibria*. 419 (2016) 88–95. <https://doi.org/10.1016/j.fluid.2016.03.012>.
- [1272] R. Privat, J.-N. Jaubert, Y. Le Guennec, Incorporation of a volume translation in an equation of state for fluid mixtures: which combining rule? which effect on properties of mixing?, *Fluid Phase Equilibria*. 427 (2016) 414–420. <https://doi.org/10.1016/j.fluid.2016.07.035>.
- [1273] A. Piña-Martinez, R. Privat, J.-N. Jaubert, Use of 300 000 experimental data over 1800 pure fluids to assess the performance of 4 CEoS: SRK, PR, *tc*-RK, *tc*-PR., *AIChE J.* (2021) (in press).
- [1274] O. Redlich, J.N.S. Kwong, On the thermodynamics of solutions. V. An equation of state. Fugacities of gaseous solutions, *Chem. Rev.* 44 (1949) 233–244.
- [1275] G.M. Kontogeorgis, P. Coutsikos, Thirty years with EoS/ $g^E$  models—what have we learned?, *Ind. Eng. Chem. Res.* 51 (2012) 4119–4142. <https://doi.org/10.1021/ie2015119>.
- [1276] M.-J. Huron, J. Vidal, New mixing rules in simple equations of state for representing vapour-liquid equilibria of strongly non-ideal mixtures, *Fluid Phase Equilibria*. 3 (1979) 255–271. [https://doi.org/10.1016/0378-3812\(79\)80001-1](https://doi.org/10.1016/0378-3812(79)80001-1).
- [1277] M.L. Michelsen, A modified Huron-Vidal mixing rule for cubic equations of state, *Fluid Phase Equilibria*. 60 (1990) 213–219. [https://doi.org/10.1016/0378-3812\(90\)85053-D](https://doi.org/10.1016/0378-3812(90)85053-D).
- [1278] M.L. Michelsen, A method for incorporating excess Gibbs energy models in equations of state, *Fluid Phase Equilibria*. 60 (1990) 47–58. [https://doi.org/10.1016/0378-3812\(90\)85042-9](https://doi.org/10.1016/0378-3812(90)85042-9).
- [1279] S. Dahl, M.L. Michelsen, High-pressure vapor-liquid equilibrium with a UNIFAC-based equation of state, *AIChE J.* 36 (1990) 1829–1836. <https://doi.org/10.1002/aic.690361207>.
- [1280] G.M. Kontogeorgis, R. Privat, J.-N. Jaubert, Taking another look at the Van der Waals equation of state—almost 150 years later, *J. Chem. Eng. Data*. 64 (2019) 4619–4637. <https://doi.org/10.1021/acs.jced.9b00264>.
- [1281] J.-N. Jaubert, R. Privat, SAFT and cubic EoS: Type of deviation from ideality naturally predicted in the absence of BIPs. Application to the modelling of athermal mixtures, *Fluid Phase Equilibria*. 533 (2021) 112924. <https://doi.org/10.1016/j.fluid.2020.112924>.
- [1282] Y. Le Guennec, Développement d'équations d'état cubiques adaptées à la représentation de mélanges contenant des molécules polaires (eau, alcools, amines ...) et des hydrocarbures, Ph.D. thesis, Université de Lorraine, 2018. <http://www.theses.fr/2018LORR0245> (accessed September 25, 2021).
- [1283] G.M. Wilson, Vapor-liquid equilibrium. XI. A new expression for the excess free energy of mixing, *J. Am. Chem. Soc.* 86 (1964) 127–130. <https://doi.org/10.1021/ja01056a002>.
- [1284] J.M. Smith, H.C. Van Ness, M.M. Abbott, M.T. Swihart, Introduction to chemical engineering thermodynamics, Eighth edition, McGraw-Hill Education, New York, NY, 2018.
- [1285] T. Tsuboka, T. Katayama, Modified Wilson equation for vapor-liquid and liquid-liquid equilibria, *J. Chem. Eng. Jpn.* 8 (1975) 181–187. <https://doi.org/10.1252/jcej.8.181>.
- [1286] I.K. Nikolaidis, R. Privat, J.-N. Jaubert, I.G. Economou, Assessment of the perturbed chain-statistical associating fluid theory equation of state against a benchmark database of high-quality binary-system data, *Ind. Eng. Chem. Res.* 60 (2021) 8935–8946. <https://doi.org/10.1021/acs.iecr.1c01234>.
- [1287] R. Privat, J.-N. Jaubert, Discussion around the paradigm of ideal mixtures with emphasis on the definition of the property changes on mixing, *Chem. Eng. Sci.* 82 (2012) 319–333. <https://doi.org/10.1016/j.ces.2012.07.030>.
- [1288] J.-W. Qian, R. Privat, J.-N. Jaubert, P. Duchet-Suchaux, Enthalpy and Heat Capacity Changes on Mixing: Fundamental Aspects and Prediction by Means of the PPR78 Cubic Equation of State, *Energy Fuels*. 27 (2013) 7150–7178. <https://doi.org/10.1021/ef401605c>.
- [1289] P.H. Van Konynenburg, R.L. Scott, Critical Lines and Phase Equilibria in Binary Van Der Waals Mixtures, *Philos. Trans. R. Soc. Lond. Ser. Math. Phys. Sci.* 298 (1980) 495–540.
- [1290] R. Privat, J.-N. Jaubert, Classification of global fluid-phase equilibrium behaviors in binary systems, *Chem. Eng. Res. Des.* 91 (2013) 1807–1839. <https://doi.org/10.1016/j.cherd.2013.06.026>.
- [1291] D. Maraver, S. Quoilin, J. Royo, Optimization of Biomass-Fuelled Combined Cooling, Heating and Power (CCHP) Systems Integrated with Subcritical or Transcritical Organic Rankine Cycles (ORCs), *Entropy*. 16 (2014) 2433–2453. <https://doi.org/10.3390/e16052433>.
- [1292] I.H. Bell, J. Wronski, S. Quoilin, V. Lemort, Pure and Pseudo-pure Fluid Thermophysical Property Evaluation and the Open-Source Thermophysical Property Library CoolProp, *Ind. Eng. Chem. Res.* 53 (2014) 2498–2508. <https://doi.org/10.1021/ie4033999>.
- [1293] E.W. Lemmon, M.L. Huber, M.O. McLinden, NIST Standard Reference Database 23: Reference Fluid Thermodynamic and Transport Properties-REFPROP, Version 9.1, (2013). <https://www.nist.gov/publications/nist-standard-reference-database-23-reference-fluid-thermodynamic-and-transport> (accessed April 13, 2021).

- [1294] S. Quoilin, M.V.D. Broek, S. Declaye, P. Dewallef, V. Lemort, Techno-economic survey of Organic Rankine Cycle (ORC) systems, *Renew. Sustain. Energy Rev.* 22 (2013) 168–186. <https://doi.org/10.1016/j.rser.2013.01.028>.
- [1295] J. Bao, L. Zhao, A review of working fluid and expander selections for organic Rankine cycle, *Renew. Sustain. Energy Rev.* 24 (2013) 325–342. <https://doi.org/10.1016/j.rser.2013.03.040>.
- [1296] A. Mota-Babiloni, P. Makhnatch, R. Khodabandeh, Recent investigations in HFCs substitution with lower GWP synthetic alternatives: Focus on energetic performance and environmental impact, *Int. J. Refrig.* 82 (2017) 288–301. <https://doi.org/10.1016/j.ijrefrig.2017.06.026>.
- [1297] K.G. Joback, Designing molecules possessing desired physical property values, Thesis, Massachusetts Institute of Technology, 1989. <https://dspace.mit.edu/handle/1721.1/14191> (accessed March 4, 2021).
- [1298] K. Joback, G. Stephanopoulos, Designing Molecules Possessing Desired Physical Property-Values, Elsevier Science Publ B V, Amsterdam, 1990.
- [1299] R. Gani, B. Nielsen, A. Fredenslund, A group contribution approach to computer-aided molecular design, *AIChE J.* 37 (1991) 1318–1332. <https://doi.org/https://doi.org/10.1002/aic.690370905>.
- [1300] A.P. Duvedi, L.E.K. Achenie, Designing environmentally safe refrigerants using mathematical programming, *Chem. Eng. Sci.* 51 (1996) 3727–3739. [https://doi.org/10.1016/0009-2509\(96\)00224-2](https://doi.org/10.1016/0009-2509(96)00224-2).
- [1301] J.E. Ourique, A. Silva Telles, Computer-aided molecular design with simulated annealing and molecular graphs, *Comput. Chem. Eng.* 22 (1998) S615–S618. [https://doi.org/10.1016/S0098-1354\(98\)00108-2](https://doi.org/10.1016/S0098-1354(98)00108-2).
- [1302] E.C. Marcoulaki, A.C. Kokossis, On the development of novel chemicals using a systematic optimisation approach. Part II. Solvent design, *Chem. Eng. Sci.* 55 (2000) 2547–2561. [https://doi.org/10.1016/S0009-2509\(99\)00523-0](https://doi.org/10.1016/S0009-2509(99)00523-0).
- [1303] N.V. Sahinidis, M. Tawarmalani, M.R. Yu, Design of alternative refrigerants via global optimization, *Aiche J.* 49 (2003) 1761–1775. <https://doi.org/10.1002/aic.690490714>.
- [1304] A. Kazakov, M.O. McLinden, M. Frenkel, Computational Design of New Refrigerant Fluids Based on Environmental, Safety, and Thermodynamic Characteristics, *Ind. Eng. Chem. Res.* 51 (2012) 12537–12548. <https://doi.org/10.1021/ie3016126>.
- [1305] A.I. Papadopoulos, M. Stijepovic, P. Linke, On the systematic design and selection of optimal working fluids for Organic Rankine Cycles, *Appl. Therm. Eng.* 30 (2010) 760–769. <https://doi.org/10.1016/j.applthermaleng.2009.12.006>.
- [1306] O. Palma-Flores, A. Flores-Tlacuahuac, G. Canseco-Melchor, Optimal molecular design of working fluids for sustainable low-temperature energy recovery, *Comput. Chem. Eng.* 72 (2015) 334–349. <https://doi.org/10.1016/j.compchemeng.2014.04.009>.
- [1307] M. Lampe, M. Stavrou, J. Schilling, E. Sauer, J. Gross, A. Bardow, Computer-aided molecular design in the continuous-molecular targeting framework using group-contribution PC-SAFT, *Comput. Chem. Eng.* 81 (2015) 278–287. <https://doi.org/10.1016/j.compchemeng.2015.04.008>.
- [1308] E.E. Bolton, Y. Wang, P.A. Thiessen, S.H. Bryant, Chapter 12 - PubChem: Integrated Platform of Small Molecules and Biological Activities, in: R.A. Wheeler, D.C. Spellmeyer (Eds.), *Annu. Rep. Comput. Chem.*, Elsevier, 2008: pp. 217–241. [https://doi.org/10.1016/S1574-1400\(08\)00012-1](https://doi.org/10.1016/S1574-1400(08)00012-1).
- [1309] Directive 2014/34/EU of the European Parliament and of the Council of 26 February 2014 on the harmonisation of the laws of the Member States relating to equipment and protective systems intended for use in potentially explosive atmospheres (recast) Text with EEA relevance, 2014. <http://data.europa.eu/eli/dir/2014/34/oj/eng> (accessed March 15, 2021).
- [1310] Ø. Hodnebrog, M. Etminan, J.S. Fuglestedt, G. Marston, G. Myhre, C.J. Nielsen, K.P. Shine, T.J. Wallington, Global warming potentials and radiative efficiencies of halocarbons and related compounds: A comprehensive review, *Rev. Geophys.* 51 (2013) 300–378. <https://doi.org/10.1002/rog.20013>.
- [1311] W.M. Organization (WMO), (NOAA) National Oceanic and Atmospheric Administration, (UNEP) United Nations Environment Programme, (NASA) National Aeronautics and Space Administration, E. Commission, World Meteorological Organization (WMO), GORMP, 58. Scientific Assessment of Ozone Depletion: 2018, WMO, Geneva, 2018.
- [1312] The European Parliament and the Council of the European Union, Regulation (EU) No 517/2014 of the European Parliament and the Council of 16 April 2014 on fluorinated greenhouse gases and repealing Regulation (EC) No 842/2006, *J Eur Union.* (2014) 195–230.
- [1313] Regulation (EC) No 1005/2009 of the European Parliament and of the Council of 16 September 2009 on substances that deplete the ozone layer (Text with EEA relevance), 2009. <http://data.europa.eu/eli/reg/2009/1005/oj/eng> (accessed February 22, 2021).
- [1314] S. Eyerer, F. Dawo, J. Kaindl, C. Wieland, H. Spliethoff, Experimental investigation of modern ORC working fluids R1224yd(Z) and R1233zd(E) as replacements for R245fa, *Appl. Energy.* 240 (2019) 946–963. <https://doi.org/10.1016/j.apenergy.2019.02.086>.

- [1315] A. Piña-Martinez, R. Privat, S. Lasala, G. Soave, J.-N. Jaubert, Search for the optimal expression of the volumetric dependence of the attractive contribution in cubic equations of state, *Fluid Phase Equilibria*. 522 (2020) 112750. <https://doi.org/10.1016/j.fluid.2020.112750>.
- [1316] Commission Delegated Regulation (EU) 2015/2402 of 12 October 2015 reviewing harmonised efficiency reference values for separate production of electricity and heat in application of Directive 2012/27/EU of the European Parliament and of the Council and repealing Commission Implementing Decision 2011/877/EU, 2015. [http://data.europa.eu/eli/reg\\_del/2015/2402/oj/eng](http://data.europa.eu/eli/reg_del/2015/2402/oj/eng) (accessed April 6, 2021).
- [1317] Commission Regulation (EU) 2016/2281 of 30 November 2016 implementing Directive 2009/125/EC of the European Parliament and of the Council establishing a framework for the setting of ecodesign requirements for energy-related products, with regard to ecodesign requirements for air heating products, cooling products, high temperature process chillers and fan coil units (Text with EEA relevance ), 2016. <http://data.europa.eu/eli/reg/2016/2281/oj/eng> (accessed April 6, 2021).
- [1318] E. Macchi, S. Campanari, P. Silva, *La microgenerazione a gas naturale*, Polipress, 2005.
- [1319] M. Compton, S. Willis, B. Rezaie, K. Humes, Food processing industry energy and water consumption in the Pacific northwest, *Innov. Food Sci. Emerg. Technol.* 47 (2018) 371–383. <https://doi.org/10.1016/j.ifset.2018.04.001>.



**Appendix**



## Appendix A : Supporting Information of Publication I

The Supporting Information is available free of charge on the ACS Publications website at DOI: [10.1021/acs.iecr.9b04660](https://doi.org/10.1021/acs.iecr.9b04660).

- Appendix A1: Compound-by-compound analysis of the PC-SAFT and SRK performances for the three considered parameterizations and values of all the corresponding parameters (PDF).
- Appendix A2: Experimental data temperature-range selected to regress pure-component parameters and to calculate MAPE (PDF).

## Appendix B : Supporting Information of Publication II

The Supporting Information is available free of charge on the ACS Publications website at DOI: [10.1021/acs.jced.8b00640](https://doi.org/10.1021/acs.jced.8b00640).

- The updated parameter values for the translated-consistent  $tc$ -PR and  $tc$ -RK cubic equations of state.

## Appendix C : Supplementary data of Publication III

Supplementary material related to this article that includes optimized  $m_{PR}$  and  $m_{RK}$  parameters for each of the 1721 compounds considered in this study along with the MAPE on  $P^{sat}$  and/or  $\Delta_{vap}H$  and/or  $c_{P,liq}^{sat}$  and/or  $v_{liq}^{sat}$  and/or  $v_c$  calculated with the generalized updated  $\alpha$ -functions and the reported volume-translation parameter  $c$ , is provided in the enclosed document (**SI\_PIII.pdf**) accompanying the manuscript.

## Appendix D : Supporting Information of Publication V

Additional Supporting Information may be found in the online version of the article at: <https://doi.org/10.1002/aic.17518>.

- Appendix D1: Determination of the associating character of a pure component.
- Appendix D2: Temperature ranges used for the generation of pseudo-experimental data.
- Appendix D3: Pure-compound database.
- Appendix D4: Parameter values for the translated-consistent  $tc$ -RK and  $tc$ -PR cubic equations of state.
- Appendix D5: Compound by compound results for the four investigated CEoS.

## Appendix E : Supporting Information of Publication VI

The Supporting Information is available free of charge at: <https://pubs.acs.org/doi/10.1021/acs.iecr.0c01734>.

- Appendix E1: List of the 107 pure compounds included in the proposed database with their corresponding *associating character*. NA = Non-Associating, HA = Hydrogen-Acceptor, HD = Hydrogen-Donor, SA = Self-Associating (PDF).

- Appendix E2: System-by-system analysis of the {PR EoS + classical mixing rules with a T-dependent  $k_{ij}$ } performances to correlate the data included in the proposed database (PDF).
- Appendix E3: Numerical values of the experimental data included in the proposed database with the corresponding references (*light* Excel file named: **database.xlsx**).
- Appendix E4: Numerical values of the experimental data included in the proposed database with the corresponding references and with a visualization of the experimental data through graphs (nine *large size* Excel files named: **BACi\_with visualization of the data.xlsx** (i=1 to 9)).

## Appendix F : Supporting Information of Publication VII

The Supporting Information is available free of charge at:  
<https://pubs.acs.org/doi/10.1021/acs.iecr.1c03003>.

- Appendix F1: Derivation of mixing rules for  $a_m/b_m$  at infinite or zero pressure.
- Appendix F2: Combining rule for  $b_{ij}$ .
- Appendix F3: Binary interaction parameters for three  $tc$ -PR- $a_{res}^{E,\gamma}$  and the PR-Van-Laar models.

## Appendix G : Supporting Information of Publication VIII

The Supporting Information is available free of charge at:  
<https://pubs.acs.org/doi/10.1021/acssuschemeng.1c03362>.

- Appendix G1: Derivation of the efficiency of the Carnot cycle.
- Appendix G2: The effect of lowering the vapor quality at the exit of the vapor generator on the thermal efficiency of an ideal Rankine cycle.

**Résumé en français des travaux menés et des résultats obtenus**



## Contexte

Selon l'Agence Internationale de l'Énergie (AIE), "les économies modernes sont tributaires de la fourniture d'électricité qui doit être fiable et d'un prix abordable" [1]. La forme d'énergie la plus consommée dans le monde est la chaleur ; elle représente la moitié de la consommation totale d'énergie. La demande en réfrigération et surtout en climatisation n'a cessé de croître depuis la moitié du siècle dernier. Il est donc indéniable que la satisfaction des besoins de la société actuelle dépend profondément de l'approvisionnement en froid, en chaleur et en électricité. Ainsi, l'un des principaux défis de ce siècle est de rendre cet approvisionnement en énergie plus efficace, respectueux de l'environnement et durable.

En général, l'électricité est produite dans des centrales électriques qui utilisent diverses sources d'énergie telles que le charbon, l'énergie nucléaire et le gaz naturel. S'y ajoutent les sources d'énergie renouvelables (SER) telles que les énergies hydraulique, éolienne, solaire et géothermique. Une quantité beaucoup plus faible mais croissante d'électricité est produite par des systèmes décentralisés, faisant référence à une variété de technologies qui produisent de l'électricité à l'endroit ou près de l'endroit où elle sera utilisée.

La chaleur et le froid sont quant à eux souvent produits sur site. Bien que la taille des installations puisse varier d'un usage industriel à un usage résidentiel, les systèmes de chauffage et de refroidissement se trouvent au même endroit que les utilisateurs finaux.

La majeure partie de l'énergie primaire nécessaire à la fourniture d'électricité, de chaleur et de froid provient de sources non renouvelables ce qui représente un obstacle majeur à l'atteinte de la neutralité en carbone. Ces dernières années, la législation de l'Union Européenne (UE) sur la promotion des SER a considérablement évolué [2]. En 2009, les responsables politiques de l'UE ont fixé comme objectif que 20 % de la consommation énergétique de l'UE proviendrait des SER en 2020. Récemment, en 2018, l'objectif que 32 % de la consommation énergétique de l'UE proviendrait des SER d'ici 2030 a été acté [3].

Comme le montre la [Figure F.1](#), la part de la consommation énergétique de l'UE provenant de sources renouvelables était de 19,7 % en 2019. L'une des stratégies pour atteindre l'objectif de 32 % en 2030 consiste à accroître l'utilisation des systèmes énergétiques décentralisés (SED). Ce type de systèmes permet non seulement de réduire les pertes d'électricité le long des lignes de transmission et de distribution qui apparaissent lorsque la production d'électricité est centralisée, mais il est également adapté à l'inclusion des SER dans le « mix » énergétique d'un pays ou d'une région. La production décentralisée peut desservir une structure unique, comme une maison ou une entreprise, ou faire partie d'un micro-réseau (un réseau plus petit qui est également relié au système de distribution d'électricité plus large), comme dans une grande installation industrielle, une base militaire ou un grand campus universitaire [4].

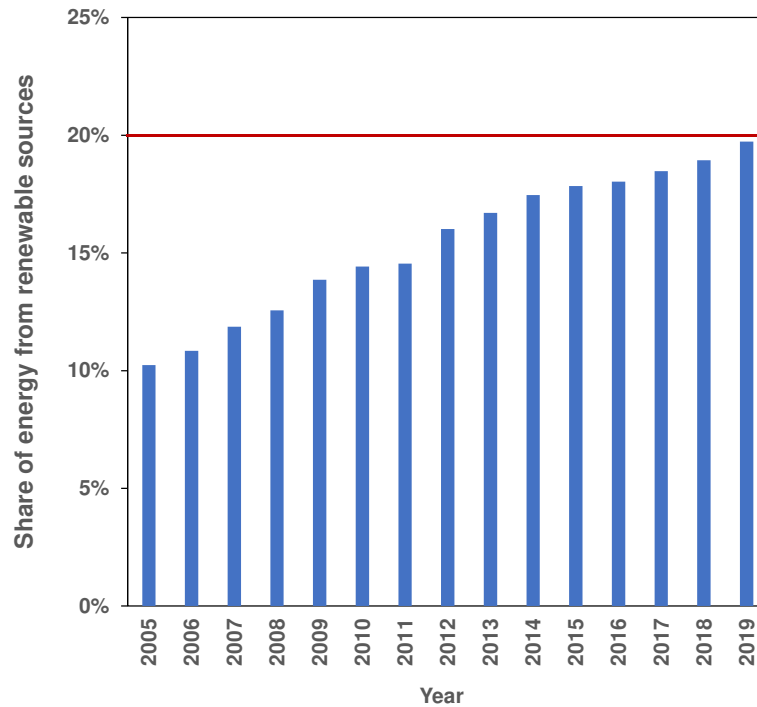


**Figure F.1 .** Évolution de la part de la consommation énergétique de l'UE provenant de sources renouvelables depuis 2005. Données fournies par l'Agence européenne pour l'environnement [5].

La promotion des SED a ouvert la voie à différentes technologies telles que la production combinée de chaleur et d'électricité (CHP, en anglais « Combined Heat and Power ») ou la production conjointe de froid, de chaleur et d'électricité (CCHP, en anglais « Combined Cooling, Heating and Power »). Les systèmes conventionnels de CHP/CCHP sont constitués de différents sous-systèmes : un cycle moteur pour la production d'électricité, un système de fourniture de chaleur et un système de production de froid. Ces différentes entités fonctionnent chacune avec un fluide de travail et un cycle thermodynamique différent et sont équipées de turbines et/ou de compresseurs parcourus par des fluides monophasiques. Récemment, Briola [5] et Briola et al. [6] ont présenté un cycle CCHP innovant, inspiré des brevets de Mokadam [7] et Fabris [9], fonctionnant avec des turbines et des compresseurs qui admettent des fluides diphasiques. Un tel cycle permet le développement d'un dispositif tout-en-un capable de produire de l'énergie électrique, de la chaleur et du froid avec un seul fluide de travail. Parmi les défis de conception de ce nouveau système CCHP, la sélection du fluide de travail apparaît comme une étape clé de son développement.

Le travail de recherche de cette thèse est consacré à relever ce défi en proposant une méthodologie de sélection de fluides de travail prometteurs pour les systèmes CCHP innovants, de type tout-en-un.

## Motivations et objectifs

Plusieurs travaux ont été consacrés à la sélection des fluides de travail pour les systèmes CCHP conventionnels ou de nouvelle génération [9]-[13]. Néanmoins, il est possible d'identifier des points faibles dans les divers travaux relatifs à la conception de fluides de travail pour des systèmes CCHP :

- le nombre de fluides de travail pris en compte est souvent faible et le choix souvent influencé par des études antérieures réalisées sur des Cycles Organiques de Rankine (ORC).
- une évaluation systématique de critères techniques, thermodynamiques, toxicologiques, d'inflammabilité et environnementaux n'a en général pas été réalisée pour les systèmes CCHP (par critères techniques, on entend ici les limitations techniques dues à la construction des unités d'exploitation; dans le cas présent, il s'agit essentiellement de la pression maximale autorisée avant la défaillance des matériaux et la gestion de l'entrée d'air dans les systèmes à basse pression).

L'objectif principal de cette thèse est de développer une méthodologie reposant sur une approche « product-design » afin de concevoir le fluide de travail le mieux adapté pour une machine de type CCHP. Plusieurs milliers de fluides différents ont été testés et l'approche développée prend en compte des critères thermodynamiques, techniques, environnementaux, d'inflammabilité et de toxicité dans le processus de sélection du fluide et donc dans l'évaluation des performances du cycle.

Afin d'évaluer les performances des cycles thermodynamiques, il est nécessaire d'établir des bilans de matière et d'énergie. Par exemple, l'application du premier principe à un système ouvert, renfermant plusieurs constituants et fonctionnant en régime permanent s'écrit :

$$\dot{W} + \dot{Q} = \sum \dot{m}_s \left( h_s + \frac{v_s^2}{2} + gz_s \right) - \sum \dot{m}_e \left( h_e + \frac{v_e^2}{2} + gz_e \right) \quad (\text{F.1})$$

où  $\dot{W}$  et  $\dot{Q}$  sont les puissances mécanique et calorifique échangées avec le milieu extérieur;  $\dot{m}$  est le débit massique tandis que  $h$ ,  $v$  et  $z$  désignent respectivement l'enthalpie spécifique, la vitesse et l'altitude d'un courant de matière. Les indices  $e$  et  $s$  désignent les courants d'entrée et de sortie. D'après l'équation précédente, il est possible de constater que ce bilan d'énergie repose sur l'estimation des enthalpies et donc sur la connaissance de l'état physique du courant qui va à son tour nécessiter la résolution des conditions d'équilibre entre phases et une estimation fine des pressions de vapeur des corps purs. Les entropies sont également requises car elles interviennent dans les définitions des rendements isentropiques des opérations de compression et de détente. Enfin, la densité qui intervient dans la conception du système de canalisation et dans le dimensionnement d'équipements tels que les turbines, les compresseurs, les pompes et les échangeurs de chaleur doit également être déterminée avec soin.

En résumé, les propriétés clés qui doivent être correctement estimées dans le cadre de cette thèse sont : la pression de vapeur, la densité, l'enthalpie et l'entropie. Cette tâche peut être assurée par un modèle thermodynamique. Dans cette thèse, les équations d'état cubiques sont retenues en raison de leur précision, du faible nombre de paramètres expérimentaux requis, de leur facilité de mise en œuvre et de leur robustesse.

Afin de s'assurer de la précision d'un modèle quelconque, il est nécessaire de comparer les valeurs calculées à des données expérimentales. Dans le cas de la pression de vapeur, de la densité et de l'enthalpie, de nombreuses données sont disponibles dans les bases de données de corps purs. Dans le cas de l'enthalpie et de l'entropie, les données d'enthalpie et d'entropie de vaporisation sont privilégiées.

La mise en œuvre de la méthodologie « product-design », requérant au préalable de développer une équation d'état cubique précise et performante, ce travail a été décomposé en trois étapes de manière à essayer de répondre aux trois questions de recherche fondamentales (RQs) suivantes :

**RQ1 :** Quelles modifications doivent être apportées aux équations d'état cubiques afin de reproduire avec précision les pressions de vapeur, les densités, les enthalpies de vaporisation et les capacités calorifiques des corps purs ?

**RQ2 :** Comment étendre efficacement les équations d'état cubiques aux mélanges ?

**RQ3 :** Comment des critères thermodynamiques, de construction, toxicologiques, d'inflammabilité et environnementaux peuvent-ils être inclus dans une approche « product-design » destinée à sélectionner le meilleur fluide de travail pour une machine de type CCHP ?

## Plan de la thèse

Cette thèse est composée de quatre chapitres qui situent le travail de recherche dans son contexte et qui résument les principaux résultats acquis. Ces derniers ont fait l'objet de plusieurs publications qui à leur tour constituent l'ossature de cette thèse. Le contenu des chapitres se décompose comme suit :

**Chapitre 1** Il donne un bref aperçu du problème lié à la résolution des conditions d'équilibre entre phases ainsi que des outils dont dispose la thermodynamique des procédés pour le résoudre, notamment les équations d'état et les modèles d'énergie de Gibbs d'excès.

**Chapitre 2** Il présente le travail de recherche consacré à la réponse à la question RQ1, c'est-à-dire à l'étude et à l'amélioration des équations d'état cubiques (CEoS) pour les corps purs. Dans ce chapitre, les différentes modifications apportées aux CEoS au cours des années afin d'améliorer leur précision sont discutées. Enfin, le modèle de Peng-Robinson *translaté et cohérent* (*tc-PR*) retenu pour ce travail, est présenté.

**Chapitre 3** En réponse à la question RQ2, il décrit l'extension des équations d'état cubiques aux mélanges. En particulier, la façon dont le modèle *tc-PR* a été étendu aux mélanges est décrite. L'extension proposée repose sur un couplage innovant de l'équation d'état avec un modèle de coefficient d'activité. Trois modèles de coefficients d'activité sont testés et leurs performances sont comparées en s'appuyant sur des données expérimentales contenues dans une base de données de référence développée à cette fin.

**Chapitre 4** Il aborde la question RQ3 et commence par présenter la machine de type CCHP qui a été retenue pour cette thèse. Ensuite, la méthodologie de type « product-design » sélectionnée pour cette étude est décrite et mise en œuvre. Les résultats de la sélection du fluide de travail sont discutés.

Le manuscrit se termine alors par des conclusions générales sur les travaux de recherche décrits dans cette thèse, ainsi que par quelques perspectives relatives aux équations d'état cubiques et à l'application de la méthodologie de sélection du fluide de travail à des systèmes énergétiques plus sophistiqués.

## Principaux résultats obtenus

La contribution de cette thèse à la réponse aux trois questions de recherche fondamentales (RQs) exposées précédemment est maintenant discutée.

### **RQ1. Quelles modifications doivent être apportées aux équations d'état cubiques afin de reproduire avec précision les pressions de vapeur, les densités, les enthalpies de vaporisation et les capacités calorifiques des corps purs ?**

L'équation d'état de Van der Waals (VdW) [63], proposée en 1873, est la première, la plus simple et la plus connue des équations d'état cubiques (CEoS). Elle s'écrit :

$$P(T, v) = \frac{RT}{v-b} - \frac{a_c}{v^2} \quad \text{with:} \quad \begin{cases} a_c = \frac{27}{64} \frac{R^2 T_{c,\text{exp}}^2}{P_{c,\text{exp}}} \\ b = \frac{1}{8} \frac{RT_{c,\text{exp}}}{P_{c,\text{exp}}} \end{cases} \quad (\text{F.2})$$

où  $a_c$  et  $b$  sont respectivement le paramètre attractif critique et le covolume. Il s'agit d'une CEoS dite à 2 paramètres car son application à un corps pur nécessite la connaissance préalable de deux propriétés caractéristiques du composé étudié (la température critique  $T_{c,\text{exp}}$  et la pression critique  $P_{c,\text{exp}}$ ).

L'un des points forts de la théorie proposée par Van der Waals est le traitement indépendant des forces **répulsives** et **attractives**, identifiées respectivement par les termes et  $P_{rep}$  et  $P_{att}$  dans l'Eq. (F.2). En outre, l'EoS de VdW est capable de représenter la coexistence des phases liquide et vapeur et de prédire le comportement des fluides subcritiques et supercritiques.

Malgré de nombreux atouts qualitatifs, l'EoS de VdW n'est pas considérée comme suffisamment précise pour des applications de conception de procédés et différentes modifications ont été introduites au fil des années. Sous une forme générale, les CEoS modernes peuvent être écrites selon :

$$P = \frac{RT}{v-b} - \frac{a(T)}{v^2 + ubv + wb^2} \quad (\text{F.3})$$

où les constantes  $u$  et  $w$  sont soit des constantes universelles (les mêmes valeurs s'appliquent à tous les composés), soit des quantités spécifiques à chaque corps purs. Le paramètre  $a(T)$  dépendant de la température se décompose classiquement selon :

$$a(T) = a_c \cdot \alpha(T) \quad (\text{F.4})$$

Il est le produit de la valeur du paramètre attractif déterminé à la température critique ( $a_c$ ) par une quantité appelée « fonction  $\alpha$  ». Cette dernière a une grande influence sur les propriétés d'équilibre liquide-vapeur calculées, comme la pression de vapeur, l'enthalpie de vaporisation et la capacité calorifique du liquide à saturation. D'autre part, la fonction volumique du terme attractif ( $v^2 + ubv + wb^2$ ) et, en particulier, les valeurs numériques attribuées à  $u$  et  $w$ , régissent essentiellement la précision des propriétés volumétriques prédites.

Tout au long de ce travail, il a été démontré que la prise en compte de deux concepts majeurs était nécessaire pour améliorer la précision des CEOs : la *cohérence thermodynamique* d'une part et la *translation volumique* d'autre part. En effet, en définissant une méthode de paramétrage fiable s'appuyant sur ces concepts, il a été possible de définir des CEOs très précises telle que l'EoS de Peng-Robinson *translatée-cohérente* (*tc-PR*) :

$$P(T, v) = \frac{RT}{v + c - b} - \frac{a_c \cdot \alpha(T_r)}{(v + c)(v + c + b) + b(v + c - b)}$$

$$\text{with: } \begin{cases} \alpha(T_r) = T_r^{N(M-1)} \exp[L(1 - T_r^{MN})] \\ c = v_{liq}^{sat, u-PR}(T_r = 0.8) - v_{liq, exp}^{sat}(T_r = 0.8) \\ \eta_c = \left[1 + \sqrt[3]{4 - 2\sqrt{2}} + \sqrt[3]{4 + 2\sqrt{2}}\right]^{-1} \approx 0.25308 \\ a_c = \frac{40\eta_c + 8}{49 - 37\eta_c} \frac{R^2 T_{c, exp}^2}{P_{c, exp}} \approx 0.45724 \frac{R^2 T_{c, exp}^2}{P_{c, exp}} \\ b = \frac{\eta_c}{\eta_c + 3} \frac{RT_{c, exp}}{P_{c, exp}} \approx 0.07780 \frac{RT_{c, exp}}{P_{c, exp}} \end{cases} \quad (F.5)$$

En se concentrant sur le paramétrage, le travail de recherche décrit dans cette thèse a permis d'améliorer les capacités du modèle *tc-PR*, initialement développé par Le Guennec et al. [146], pour aboutir à une équation d'état cubique très précise qui pourrait être utilisée non seulement dans le domaine des applications liées à l'énergie mais aussi lors de la conception de procédés assistée par ordinateur impliquant des entrées et sorties de matière fluide. Avant cette étude, le modèle *tc-PR* avait montré un potentiel prometteur en termes de précision sur les pressions de vapeur, les densités liquides, les enthalpies de vaporisation et les capacités thermiques. Cependant le modèle *tc-PR* souffrait de l'absence d'une méthode universelle de paramétrage permettant de savoir sur quelles données expérimentales les paramètres de la fonction  $\alpha$  et la translation volumique devaient être déterminés. Cette thèse a montré que des paramètres fiables pouvaient être obtenus mais à condition qu'ils soient ajustés – au moins – sur des données de pression de vapeur.

Cette thèse a également contribué à la constitution d'une base de données de référence adaptée à l'identification des forces et des faiblesses d'un modèle thermodynamique lors de son application à des corps purs. Elle répertorie 1800 molécules pour lesquelles, en plus des coordonnées critiques ( $T_c$ ,  $P_c$  et  $v_c$ ), des corrélations précises pour  $P^{sat}$  et  $\rho_{liq}^{sat}$  sont disponibles. Parmi les 1800 molécules présentes, 1536 fluides possèdent également une corrélation précise pour l'enthalpie de vaporisation ( $\Delta_{vap}H$ ) et 890 pour la capacité calorifique du liquide ( $c_{P, liq}^{sat}$ ). Au final, cette base de données renferme 306 700 données pseudo-expérimentales de haute qualité.

Les études présentées dans les **Publications I à V** soulignent que l'utilisation de la fonction  $\alpha$  de Twu91, très flexible et spécifique à chaque corps pur, améliore considérablement la reproduction des pressions de vapeur, des enthalpies de vaporisation et des capacités calorifiques des liquides. En outre, ces mêmes publications mettent en évidence l'amélioration spectaculaire de la reproduction des densités liquides lorsqu'un paramètre de translation de volume est utilisé. Au final, l'EoS *tc-PR* est capable de reproduire les 306 700 points expérimentaux de la banque de données de corps purs avec une déviation globale

moyenne inférieure à 2%. En particulier, un tel modèle est capable de corrélérer les pressions de vapeur avec une erreur de 1% alors que les erreurs sur  $\Delta_{vap}H$ ,  $c_{p,liq}^{sat}$  et  $v_{liq}^{sat}$  sont proches de 2%.

## **RQ2. Comment étendre efficacement les équations d'état cubiques aux mélanges ?**

Afin d'étendre efficacement les CEoS aux mélanges, il est essentiel d'aborder la question des règles de mélange. Les travaux de recherche de cette thèse ont démontré l'avantage d'utiliser des règles de mélange avancées (de type EoS/ $a_{res}^{E,\gamma}$ ) dérivant de l'égalisation de la partie résiduelle de l'énergie d'Helmholtz d'excès calculée par l'EoS et de la même quantité provenant d'un modèle de coefficient d'activité (ACM). La mise en œuvre de telles règles de mélange semble particulièrement pertinent car il permet non seulement de s'affranchir du choix de la pression de raccordement des deux contributions mais également de corriger tous les écueils décrits dans la littérature à propos des anciennes règles de mélange avancées.

L'étape suivante consistait à utiliser ces règles de mélange pour étendre le modèle *tc-PR* aux systèmes multi-constituants. À cette fin, trois modèles de coefficient d'activité ont été testés : Wilson, UNIQUAC et NRTL. À la lumière des résultats obtenus, il est possible de conclure que le meilleur choix pour étendre le modèle *tc-PR* EoS aux systèmes renfermant plusieurs constituants avec des règles de mélange de type EoS/ $a_{res}^{E,\gamma}$  est d'utiliser la partie résiduelle du modèle de Wilson  $a_{res}^{E,\gamma}$ . Le modèle correspondant a été simplement appelée *tc-PR-Wilson*. Pour résumer, lorsqu'elle est appliquée à un mélange, l'EoS *tc-PR* s'écrit :

$$P(T, v, z) = \frac{RT}{v + c_m - b_m} - \frac{a_m(T, z)}{(v + c_m)(v + c_m + b_m) + b_m(v + c_m - b_m)}$$

$$with: \begin{cases} b_m = \sum_i^{n_c} \sum_j^{n_c} z_i z_j \left( \frac{b_i^{2/3} + b_j^{2/3}}{2} \right)^{3/2} \\ a_m = b_m \left[ \sum_i^{n_c} z_i \frac{a_i}{b_i} + \frac{a_{res}^{E,\gamma}}{\Lambda_{PR}} \right] \text{ with } \Lambda_{PR} = -\sqrt{2}/2 \cdot \ln(1 + \sqrt{2}) \\ c_m = \sum_i^{n_c} z_i \cdot c_i \end{cases} \quad (F.6)$$

Un tel modèle se distingue particulièrement dans la prédiction des compositions des phases liquide et vapeur, des points azéotropiques et des pressions triphasiques.

De la même manière que pour les composés purs, une base de données de référence renfermant des données de haute qualité pour 200 systèmes binaires a été construite. Elle permet d'évaluer la précision d'un modèle thermodynamique ou de comparer les performances de différents modèles lorsqu'ils sont appliqués à des systèmes multi-constituants. Une procédure spécifique pour le calcul des déviations entre les valeurs calculées par le modèle et les données expérimentales a été mise au point. Il s'est ensuivi une méthodologie pour la notation d'un modèle thermodynamique. Au total, les 200 systèmes binaires sélectionnés couvrent toutes les catégories de mélanges. Ils ont été répartis en 9 familles en fonction du caractère *associé* des deux constituants, c'est-à-dire de leur capacité à être impliqués dans

une liaison hydrogène. En général, pour chaque système binaire de la base de données, dix propriétés ont été déterminées expérimentalement : composition de la phase liquide  $x$ , composition de la phase gazeuse  $y$ , pression triphasique  $P_{LLV}$ , composition triphasique  $z_{LLV}$ , pression critique  $P_c$ , composition critique  $x_c$ , pression azéotrope  $P_{azeo}$ , composition azéotrope  $x_{azeo}$ , enthalpie de mélange  $h^M$  et capacité calorifique de mélange  $c_p^M$ .

**RQ3. Comment des critères thermodynamiques, de construction, toxicologiques, d'inflammabilité et environnementaux peuvent-ils être inclus dans une approche « product-design » destinée à sélectionner le meilleur fluide de travail pour une machine de type CCHP ?**

COGEN Europe, l'Association européenne pour la promotion de la cogénération, définit la cogénération comme la production simultanée de chaleur utile et d'électricité à partir d'une seule source d'énergie primaire [134]. Il convient de noter que les systèmes CHP (également appelés de cogénération) ont plus de 100 ans et peuvent atteindre des rendements allant de 70 à 90 % [135]. Ils se composent d'un cycle moteur principal, qui produit de l'énergie électrique, et d'un système de récupération de chaleur permettant de fournir de l'énergie sous forme de chaleur à différentes températures. Maintenant, si une partie de l'énergie mécanique/électrique produite ou de la chaleur résiduelle d'un système CHP est ensuite utilisée pour le refroidissement des locaux ou des procédés, il devient un système de CCHP. Les technologies de base pour les applications typiques de CHP/CCHP sont les turbines à gaz et les moteurs alternatifs pour les grandes installations, et les micro-turbines, ORC, moteurs Stirling et même les piles à combustible pour les utilisateurs de petite échelle. Les technologies de production de froid, quant à elles, comprennent les unités activées thermiquement telles que les pompes à chaleur à absorption, ainsi que les systèmes de réfrigération décrivant un cycle de compression de vapeur [136,137].

Dans cette thèse, une version simplifiée du cycle CCHP proposé par Briola [7] dans son brevet est considérée. Ce cycle fonctionne avec un seul fluide de travail et tolère que les détentes et compressions soient effectuées dans le domaine diphasique. La configuration du CCHP retenu dans cette étude est représentée dans la [Figure F.2](#).

Le fluide de travail à l'état de liquide bouillant est comprimé de manière isentropique par une pompe (1-2), chauffé à pression constante dans un évaporateur (2-3), et détendu de manière isentropique dans une turbine (3-4). Ensuite, la condensation partielle de la vapeur 4 (procédé 4-5) est destinée à libérer la puissance calorifique spécifique ( $q_M$ ) requise à  $T_M$ . Elle est suivie d'une détente isentropique (5-6) et d'une condensation à pression constante (6-7). Ensuite, le fluide est détendu de façon isentropique (7-8), chauffé à pression constante dans un évaporateur (8-9) où il absorbe la puissance calorifique  $q_C$ , comprimé de façon isentropique (9-10), et enfin condensé à pression constante (10-1) jusqu'à l'état initial. La quantité de chaleur spécifique absorbée à température constante par le fluide de travail à partir de la source à basse température ( $T_C$ ) représente un effet de refroidissement ( $q_C$ ) dans l'environnement.

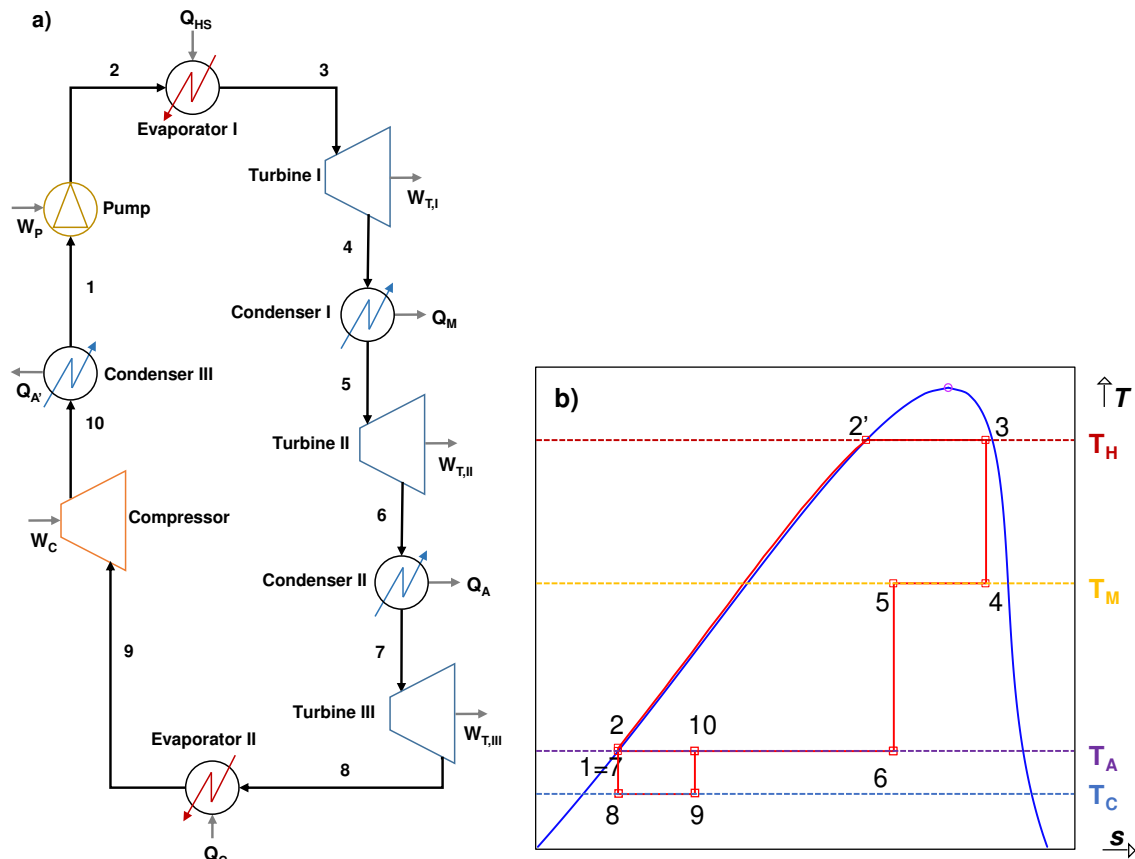


**Figure F.2 .** a) Vue schématique d'un cycle CCHP idéal. b) Esquisse du diagramme température-entropie correspondant.

Un des enjeux de cette thèse était de trouver le fluide de travail optimal pour une machine semblable à celle représentée sur la [Figure F.2](#).

Une étude bibliographique a permis de conclure que les méthodes reposant sur la recherche d'un fluide dont les propriétés étaient disponibles dans les bases de données thermodynamiques offrait le meilleur compromis entre la définition d'espace de conception acceptable et les propriétés cibles considérées.

La méthodologie de recherche dans les bases de données a été mise en œuvre pour cribler environ 60000 espèces incluses dans les bases de données DDB, DIPPR et NIST TDE 103b.

L'approche de criblage a pris en compte des contraintes thermodynamiques, techniques, de sécurité et environnementales. Le criblage couplé à l'évaluation des performances ont démontré que les fluides inflammables tels que le vinylacétylène ou le HFC-152 ont un bon potentiel pour les applications de type CCHP. Dans le cas où des restrictions de sécurité très contraignantes sont imposées, le HCFO-1233zd(E) pourrait être un candidat intéressant puisqu'il est ininflammable et non toxique.

## Perspectives

Au cours de l'élaboration de cette thèse, plusieurs hypothèses ont été formulées et différentes questions ont été soulevées. Elles amènent à considérer les différentes pistes de recherches futures :

- **Étude de l'inclusion d'un terme d'association pour les composés purs :** Il est possible de remarquer que toutes les molécules non auto-associées ne sont pas parfaitement modélisées par des équations d'état cubiques comme SRK, PR, *tc-RK* et *tc-PR*, et que près de 2/3 des composés auto-associés de la base de données des corps purs sont représentés avec une grande précision par les mêmes équations d'état. À ce stade, on peut légitimement se demander si l'ajout d'un terme d'association est la bonne solution pour améliorer la précision des équations d'état cubiques.
- **Étude du phénomène d'auto-association pour les mélanges :** Malgré le potentiel prometteur du modèle *tc-PR-Wilson*, des améliorations doivent être apportées en termes de prédictions du comportement des systèmes dans lesquels des liaisons hydrogène sont rompues sans possibilité d'en former de nouvelles. C'est par exemple le cas des systèmes eau + hydrocarbure.
- **Étude de la dépendance en température des paramètres d'interaction binaire du modèle *tc-PR-Wilson* :** L'étape suivante consiste à étudier l'influence de la dépendance en température des paramètres d'interactions binaires du modèle *tc-PR-Wilson* sur la reproduction des données d'équilibre de phases (VLE, LLE, VLLE) et des propriétés énergétiques (comme  $h^M$ ).

**Développement d'un modèle prédictif *tc-PR-Wilson* basé sur le concept de contributions de groupes :** Disposer d'un modèle prédictif serait un atout indéniable. Afin de définir les interactions entre groupes, il faut pouvoir disposer de milliers de données expérimentales d'équilibre entre phases. Bien que l'équipe de thermodynamique possède les banques DDB et TDE, des données demeurent manquantes pour certains systèmes. Pour cette raison, des travaux récents ont été consacrés à la détermination expérimentale et à la modélisation du comportement à haute pression des systèmes binaires tels que CO<sub>2</sub> + cyclooctane ([Publication X](#)), et CO<sub>2</sub> + 2,3-diméthylbutane ([Publication XI](#)). Ces efforts sont à poursuivre.

**Mise en œuvre d'une approche holistique pour la conception de procédés et de produits :** En suivant la méthodologie proposée par Bowskill et al. [147], il serait intéressant de développer une méthode informatique pour la conception intégrée du procédé et du fluide de travail pour les applications de type CCHP. Parallèlement aux calculs thermo-physiques effectués avec le modèle *tc-PR*, il serait souhaitable de mettre en œuvre des méthodes fiables pour l'estimation de l'inflammabilité ou de la toxicité de ces molécules pour lesquelles ces propriétés sont encore manquantes.

**Résumé**



## **Équations d'état cubiques et modèles d'ordre supérieur pour décrire les mélanges fluides : Développement, paramétrage et validation sur des procédés industriels de conversion d'énergie.**

---

L'une des stratégies visant à atteindre l'objectif de 32 % de la consommation d'énergie de l'UE provenant de sources d'énergies renouvelables d'ici 2030 consiste à accroître l'utilisation des systèmes énergétiques décentralisés (DES). La promotion des DES a ouvert la voie à différentes technologies telles que la production combinée de chaleur et d'électricité (CHP) ou les systèmes de production simultanée de froid, de chaleur et d'électricité (CCHP). Récemment, un nouveau cycle CCHP pour lequel les turbines et les compresseurs ont été conçus de manière à ce que le fluide de travail puisse opérer dans le domaine diphasique, a été développé. L'avantage de ce cycle est qu'il permet de produire simultanément les trois formes d'énergie souhaitées (chaleur, froid et électricité) avec un unique fluide de travail. Parmi les défis scientifiques liés à la conception de ce nouveau système CCHP, la sélection du fluide de travail apparaît comme une étape décisive expliquant pourquoi dans cette thèse, une méthodologie permettant l'optimisation du fluide de travail pour des machines complexes a été mise au point. Les résultats obtenus ont permis de mettre en évidence des fluides de travail conduisant à de hauts rendements et pourraient, en outre, servir de base à de futurs développements théoriques et expérimentaux. Un élément clé du développement de la méthodologie proposée repose sur l'utilisation des équations d'état cubiques pour les composés purs et les mélanges dans le but d'estimer avec précision les propriétés d'équilibre entre phases et les propriétés thermiques. Tout au long de ce travail, la prise en compte de deux concepts majeurs était nécessaire pour améliorer la précision des équations d'état cubiques (CEoS) : la *cohérence thermodynamique* d'une part et la *translation volumique* d'autre part. En effet, en définissant une méthode de paramétrage fiable s'appuyant sur ces concepts, il a été possible de définir des CEoS très précises telle que l'EoS de Peng-Robinson *translatée-cohérente* (tc-PR). Afin d'étendre efficacement les CEoS aux mélanges, il est essentiel d'aborder la question des règles de mélange. Les travaux de recherche de cette thèse ont démontré l'avantage d'utiliser des règles de mélange avancées (de type EoS/ $a_{res}^{E,\gamma}$ ) dérivant de l'égalisation de la partie résiduelle de l'énergie d'Helmholtz d'excès calculée par l'EoS et de la même quantité provenant d'un modèle de coefficient d'activité. Enfin, à partir de bases de données commerciales telles que la DDB, la DIPPR ou la NIST TDE 103b, une méthodologie de recherche multicritères de fluides de travail a été mise en œuvre et a permis de passer en revue plus de 60 000 espèces différentes. Cette approche par criblage a tenu compte de diverses contraintes thermodynamiques, techniques, de sécurité et environnementales. Le criblage couplé à l'évaluation des performances a démontré que les fluides tels que le HFC-152 ou le HCFO-1233zd(E) ont un fort potentiel pour les applications de type CCHP.

## **Cubic and higher order equations of state for fluid mixtures: Development, parameterization and validation through industrial energy conversion applications.**

---

One of the strategies to achieve the target of 32% share of EU energy consumption coming from renewable energy sources (RES) by 2030 is to increase the use of distributed energy systems (DES). The promotion of DES has opened the way to different technologies such as combined heat and power (CHP) or combined cooling, heating and power (CCHP) systems. Recently, a novel CCHP cycle, operating with two-phase expanders and compressors, has been designed. Such a cycle enables the development of an all-in-one device capable of producing electric, heating and cooling power with a single working fluid. Among the design challenges of this novel CCHP system, the working fluid selection appears as a key stage of its development. In this thesis, a methodology for the selection of promising working fluids for Combined Cooling, Heating and Power (CCHP) applications has been presented. This study has intended to provide an insight about working fluids that should be considered for further theoretical and experimental investigations. A key stage of the development of the proposed methodology relied on the study of cubic equations of state for pure compounds and mixtures in with the purpose of enhancing their accuracy on the estimation of saturation and caloric properties. Throughout this work it has been showed that two major concepts are necessary for the development of cubic equations of state (CEoS): the consistency and volume-translation concepts. Their implementation along with a sound parameterization method leads to highly accurate CEoS such as the *translated-consistent* Peng-Robinson (tc-PR) EoS. In order to safely extend CEoS to mixtures addressing the question of mixing rules is capital. The research work of this thesis introduced advanced mixing rules (EoS/ $a_{res}^{E,\gamma}$ ) derived by equating the residual part of the excess Helmholtz energy from an EoS and from an explicit activity-coefficient model. Finally, a database search methodology has been implemented to screen about 60 000 species included in the DDB, the DIPPR and the NIST TDE 103b databases. The screening approach considered thermodynamic, process-related, constructional, safety and environmental constraints. The screening coupled with the performance evaluation have demonstrated that fluids such as HFC-152 or HCFO-1233zd(E) have a good potential for CCHP applications.